EVOLUÇÃO GEODINÂMICA DOS SECTORES SETENTRIONAIS DA ZONA DE OSSA-MORENA NO CONTEXTO DO VARISCO IBÉRICO

GEODYNAMIC EVOLUTION OF NORTHERNMOST SECTORS OF OSSA-MORENA ZONE IN IBERIAN VARISCIDES CONTEXT

Noel Alexandre Fontes Moreira

Tese apresentada à Universidade de Évora
para obtenção do Grau de Doutor em Ciência da Terra e do Espaço
Especialidade: Processos Geológicos

ORIENTADORES: *Rui Manuel Soares Dias*
Jorge Manuel Costa Pedro
José Manuel Correia Romão

ÉVORA, DEZEMBRO DE 2017

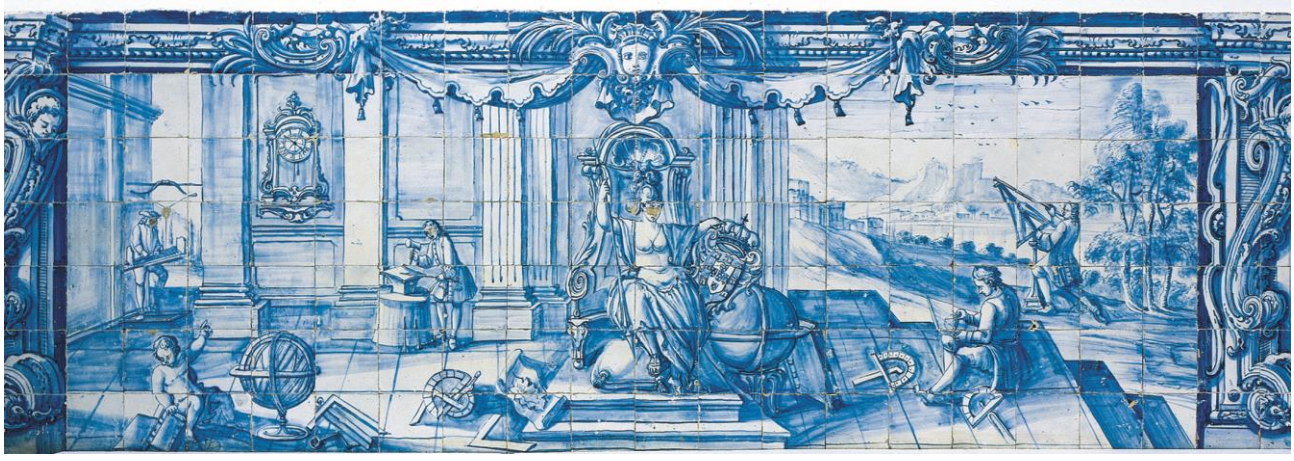

INSTITUTO DE INVESTIGAÇÃO E FORMAÇÃO AVANÇADA

EVOLUÇÃO GEODINÂMICA DOS SECTORES SETENTRIONAIS DA ZONA DE OSSA-MORENA NO CONTEXTO DO VARISCO IBÉRICO

GEODYNAMIC EVOLUTION OF NORTHERNMOST SECTORS OF OSSA-MORENA ZONE IN IBERIAN VARISCIDES CONTEXT

Noel Alexandre Fontes Moreira

Tese apresentada à Universidade de Évora
para obtenção do Grau de Doutor em Ciência da Terra e do Espaço
Especialidade: Processos Geológicos

ORIENTADORES: *Rui Manuel Soares Dias*
Jorge Manuel Costa Pedro
José Manuel Correia Romão

POPH QUALIFICAR É CRESCER.
QREN QUADRO DE REFERÊNCIA ESTRATÉGICO NACIONAL PORTUGAL 2007.2013
GOVERNO DA REPÚBLICA PORTUGUESA
UNIÃO EUROPEIA Fundo Social Europeu

Às mulheres da minha vida -

a minha Mãe e a minha Irmã -

e à Mariana

Índice

Evolução Geodinâmica dos sectores setentrionais da Zona de Ossa-Morena no contexto do Varisco Ibérico

Resumo

Os estudos levados a cabo na região Abrantes-Tomar permitiram reconhecer dois domínios distintos: um domínio Este com claras afinidades litoestratigráficas, estruturais e geoquímicas com a Zona de Ossa-Morena (ZOM) e um domínio a Oeste com características tectonoestratigráficas, metamórficas e magmáticas próprias que permitem a sua distinção do restante Terreno Varisco Ibérico.

O domínio Este apresenta uma sucessão litoestratigráfica com afinidades à transição Neoproterozóico-Câmbrico da ZOM. Aqui distinguiram-se duas sequências distintas, que colocam em evidência a presença de uma evolução policíclica. Com efeito, a sequência Neoproterozóica mostra o desenvolvimento de um arco vulcânico, ao qual se associa a génese de uma bacia de *back-arc*. Esta bacia poderá apresentar oceanização incipiente, encontrando-se materializada na Zona de Cisalhamento Tomar-Badajoz-Córdoba. Estes dados são compatíveis com os modelos propostos para a ZOM durante o Ciclo Cadomiano, tendo esta zona de cisalhamento sido reactivada como um importante cisalhamento intraplaca durante o Ciclo Varisco. A sequência Câmbrica apresenta claras afinidades litoestratigráficas e geoquímicas com as sucessões sin-*rift* intra-continental que caracterizam o início do Ciclo Varisco na ZOM.

O domínio Oeste é caracterizado pela presença de unidades tectono-estratigráficas com características metamórficas e magmáticas distintas no contexto do Maciço Ibérico, sendo a sua evolução geodinâmica condicionada pela Zona de Cisalhamento Porto-Tomar-Ferreira do Alentejo, que delimita o bordo Este deste domínio. A comparação com os sectores de Coimbra, Porto-Albergaria e Berlengas permitiu a caracterização de um terreno com características tectono-estratigráficas próprias (Terreno Finisterra), que apresenta características análogas ao Bloco de Léon (Maciço Armoricano) e ao Mid-German Crystalline Rise, permitindo a sua correlação à escala do Varisco Europeu.

A integração dos dados do sector de Abrantes-Tomar nos modelos geodinâmicos propostos para o Maciço Ibérico, implicou a realização de estudos pontuais noutras regiões, como sejam Almograve, Ponta Ruiva e Vila Boim.

Palavras-Chave

Maciço Ibérico, Zona de Ossa-Morena, Ciclo Varisco, Zona de Cisalhamento Porto-Tomar-Ferreira do Alentejo, Terreno Finisterra

Geodynamic Evolution of northernmost sectors of Ossa-Morena Zone in Iberian Variscides context

Abstract

The studies in the Abrantes-Tomar region allowed to recognize two distinct domains: an eastern one with clear lithostratigraphic, structural and geochemical affinities with the Ossa-Morena Zone (OMZ) and a western domain which has its own tectonostratigraphic, metamorphic and magmatic features, allowing its individualization from the Iberian Variscan Terrane.

The eastern domain presents a lithostratigraphic succession with affinities to the Neoproterozoic-Cambrian of the OMZ. Two sequences were distinguished, highlighting the presence of a polycyclic geodynamic evolution. Indeed, the Neoproterozoic sequence shows the development of a volcanic arc and a coeval back-arc basin. This basin may present incipient oceanization, being materialized in the Tomar-Badajoz-Córdoba Shear Zone. These data are compatible with the models proposed for the OMZ during the Cadomian Cycle. This shear zone was reactivated as an intraplate shear zone during the Variscan Cycle. The Cambrian sequence presents lithostratigraphic and geochemical affinities with the intra-continental sin-rift successions that typify the beginning of the Variscan Cycle in the OMZ.

The western domain is characterized by the presence of tectonostratigraphic units with particular tectonostratigraphic, metamorphic and magmatic features in the context of the Iberian Massif. Its geodynamic evolution was controlled by the Porto-Tomar-Ferreira do Alentejo Shear Zone, which delimits its eastern boundary. The comparison with the sectors of Coimbra, Porto-Albergaria and Berlengas sectors allowed the characterization of the Finisterra Terrane. The geological features of this Terrane are similar to those exhibited in the Léon Block (Armorican Massif) and Mid-German Crystalline Rise ones. Such behaviour allows their correlation in the European Variscan Belt context.

The obtained data in Abrantes-Tomar region was integrated into the geodynamic models proposed for the Iberian Massif. In order to strengthen the proposed geodynamic models, new data were obtained in other regions, as in the Almograve, Ponta Ruiva and Vila Boim regions.

Keywords

Iberian Massif, Ossa-Morena Zone, Variscan Cycle, Porto-Tomar-Ferreira do Alentejo Shear Zone, Finisterra Terrane

Agradecimentos

Bem chegado o momento mais pessoal da dissertação, tentarei de alguma forma enfatizar todas as pessoas e instituições que tiveram um papel preponderante neste percurso, nesta fase angustiante e de contrarrelógio que é o doutoramento e que termina como este manuscrito. Agradeço desde já a todas as pessoas que se cruzaram comigo, que partilharam histórias, momentos mais ou menos felizes e que por vezes até partilharam experiências similares. Agradeço desde já a todos; contudo não poderia deixar de enfatizar algumas destas pessoas.

Quem me conhece esperaria, e bem, que a primeira palavra fosse para a minha Mãe; uma mulher que é bem mais do que isso é uma guerreira incansável procurando sempre o melhor para os seus e consequentemente para si. A Ela agradeço desde logo todos os ensinamentos e modo de estar vida que me passou; coragem, esforço, ética, camaradagem e optimismo são alguns dos valores que me transmitiu e foi com eles que cresci. Ela quis dar-me aquilo que nunca teve possibilidade de ter, uma educação superior, uma vida melhor e para isso esforçou-se ao máximo para que isso fosse possível. Trabalhou intensamente para que nada nos faltasse e isso é de formalizar por escrito aqui; é uma força singela de dizer OBRIGADO.

Da minha irmã só posso sentir orgulho e é nela que vejo o excelente trabalho como educadora que a minha mãe fez. É íntegra, correcta e trabalhadora, tendo como principal objectivo ser feliz! A ela devo um agradecimento, pois nela vejo uma mulher batalhadora, dócil e carinhosa, que apesar de todas as adversidades lutou e consegui atingir o seu sonho! Sei que terá um excelente futuro à tua frente e isso tranquiliza-me!

Agradeço também à toda a minha família, a todos (e são muitos) sem excepção, mas seria injusto se não enfatizasse:

- a minha avó uma mulher quase centenária que lutou e deu tudo aos seus filhos e netos, uma mulher que colheu da terra aquilo que a terra lhe deu;
- a minha Juca e meu tio Nuno (e consequentemente ao Sérgio e ao Pedro), que estiveram ali sempre, com um papel por vezes quase invisível durante uma fase essencial no crescimento de qualquer criança e que sempre me proporcionaram o melhor;
- os meus primos Andreia, Diana, Inês, Gonçalo e Daniel com os quais partilhei milhares de momentos únicos e que não são descritíveis;

- os meus tios São, Carmo, Augusta, Luz, Rogério, Zé e Celestino que para além de tudo sempre me apoiaram em tudo e que sempre mas sempre me motivaram, me deram aquilo que não tem valor.

Agora, e depois desta descrição e agradecimento a um décimo da minha família, é inevitável agradecer à Mariana. Bem aqui não há muito a dizer… Ela foi sem dúvida um pilar, um alicerce para mim. Uma mulher, uma amiga, uma companheira, uma conselheira… Ela foi o meu Xanax, a minha adrenalina, cafeina e nicotina, foi uma brisa no verão e o saco de água quente no inverno; ela foi peça chave neste desfecho. Não me interessa minimamente o que acontecerá, sei o que aconteceu e como tal é mais do que justo que esta tese te seja dedicada a ti também. Por tudo obrigado! É óbvio que com uma pessoa como a Mariana vêm de arraste todos os seus familiares e amigos, a quem deixo nesta linha uma palavra singela mas sincera, pois não é todos os dias que ouvimos "eu admiro-te" vindo do nada.

Agora à pessoa que toda a gente agradece numa tese, mas neste caso isto vai muito para lá do cliché típico de umas palavras nas páginas de agradecimentos de uma tese: ao meu orientador Rui Dias. O Rui é um exemplo para qualquer um. É um poço de sabedoria (e de trabalho também), mas foi com ele que muitas das portas se abriram para mim e foi com ele que aprendi muito. Sempre acreditou no meu trabalho, sempre me deu autonomia e liberdade para fazer aquilo que me dava gozo, puxando-me para terra de vez em quando para que não deixasse de ter os pés assentes em solo firme. Ele é um exemplo a seguir na dinâmica que imprime, na forma como vê o mundo e a ciência e seja qual for o meu percurso é e será sempre um prazer trabalhar contigo! A ti também um MUITO OBRIGADO!

Aos meus amigos de longa data deixo um abraço firme, pois eles mesmo sem estarem fisicamente presentes em todos os momentos, eles estiveram sempre que precisei. Ao Patrício, Eliana, Santa Barbara, Francisco (Xisco), Inácio, Diana, Cunha, Santos, César e *Manel Bar* um obrigado e uma cerveja para vocês zequinhas! Ao Nuno, ao Rafa (amigos de infância), ao Pedro, à Ana Rita e à Inês Damas que apesar de tudo e da distância me mostraram que a amizade é muito mais que estar é ser… Ao Torreense e ao TopoSCUT que me serviu de escape em alguns dos momentos de stress e que fez (re)ver e (re)encontrar algumas das características mais distintivas das pessoas de Torres Vedras. E aqui destacado pelos motivos óbvios, o Marco Martins, ele que é meu ouvinte e conselheiro desde há muitos anos a esta parte. Ele sabe quem sou, conhece os meus meandros tão bem como eu (às vezes melhor). Esteve nos picos, altos e baixos, para me ouvir, para me escutar e aconselhar, para me dar na cabeça e para me incentivar mesmo quando as vontades se esmorecem… Há uma parte disto que também é tua!

Ao José Romão (meu co-orientador) por todo o apoio científico e logístico, mas também pela confiança que sempre depositou em mim, no meu trabalho. Foi ouvido atento e voz critica nas

discussões que tivemos que sem dúvida muito incrementaram a qualidade do trabalho. Há que dar uma palavra de apreço. Ao António Ribeiro devo sem a mínima dúvida um obrigado; ele é o PAI da geologia de Portugal sem qualquer dúvida. As discussões com ele são sempre profícuas apesar dos gritos e discordâncias. São nestas discussões que percebemos os lapsos e pontos fortes das hipóteses que colocamos. Ao Jorge Costa Pedro (co-orientador) deixo também palavras de agradecimento. A exactidão, minuciosidade e rigor do seu trabalho são de ressalvar. Há sempre algo a dizer e há sempre algo a melhorar, mesmo quando já está bom. Agradeço assim aos três todas as discussões e partilha de ideias! E é claro, ao Esperancinha!!

E como falamos em partilha de ideias e discussões deixo aqui uma lista de pessoas com quem tive o prazer de trabalhar durante este tempo e com os quais discuti, resultando daí uma quantidade apreciável das minhas interpretações: Gil Machado, Telmo Bento dos Santos, António Mateus, João Mata, José Piçarra e Alexandre Araújo. Uma palavra também para um segundo núcleo com quem discuti os dados, observações e interpretações: Luís Lopes, Fernando Noronha, Maria dos Anjos Ribeiro, Nuno Inês, Carlos Ribeiro, Pedro Nogueira, Pedro Farias e Patrícia Moita (eu sei que me vou esquecer de alguém). A todos eles agradeço a paciência, a abertura e a possibilidade para discutirmos as mais diversas temáticas.

Quero também agradecer ao Centro Ciência Viva de Estremoz e claramente a toda a sua equipa (Patrícia, Alexis, Susana, André, Flor, Sandra, Isabel, Vânia, Eduardo, Maneta, Alice, Rute, Cristina, Rosário, Ana Jacinto, Nuno, Francisco, Raquel, Carla). Foram vários os momentos passados em equipa; momentos bons, momentos menos bons, mas nunca mas nunca me senti sozinho aqui. Sempre me apoiaram em todos os momentos com preocupação pelo meu trabalho, com o meu bem-estar e com que tudo corresse bem. Foram um apoio inegável!

Agora a todos os ocupas André Vinhas, Fábio Amaral, Carla Pacheco, Pedro Almeida, João Correia e Caterina Basile, pois aqui eramos quase como uma família italiana, mas daquelas meio destruturadas. Um agradecimento especial para a Inês Pereira, pois várias conversas, angústias, confidências e momentos foram partilhados e discutidos sempre com amizade e respeito mútuo. Foram momentos incríveis vividos neste espaço! São memórias que não se esquecem.

Ao pessoal de Estremoz que me acolheu nesta Terra belíssima e com os quais partilhei momentos divertidos e, alguns dos quais, inesquecíveis: Gimbra, Andreia, Joaquim, Manuela, Pardal, Vasco, Mourinha, Peralta, Ana Vieira, Gato, Marta, Maria João, Paulo Gonçalves; obrigado por me fazerem sentir-me em casa.

Finalizando, e porque não me quero esquecer de ninguém, à Idalinda e Teresa do Secretariado do Departamento de Geociências que sempre me facilitaram e ajudaram, descomplicando o burocrático. Quero agradecer ao Jorge Velez e à Sandra Velez, pois com eles passei horas sem fim no Laboratório de Geociências durante a manufacturação lâminas delgadas e polidas, bem

como na preparação e moagem de amostras para geoquímica. À Sandra um abraço especial pois no fundo ainda me teve de ouvir umas quantas vezes a desabafar, pois claramente o laboratório não é vida para mim!

Quero agradecer ao Instituto de Investigação e Formação Avançada da Universidade de Évora e em especial à Engenheira Cláudia Marques, que agilizou todos os procedimentos aquando da obtenção da bolsa e entrada no 3º Ciclo de Estudo, à Escola de Ciências e Tecnologia da UÉvora, e em especial ao Professor Doutor Mourad Bezzeghoud que não só me proporcionou todos os materiais e espaços de que necessitei, mas também por ter agilizado todos os procedimentos burocráticos e ainda ao Instituto de Ciências da Terra (ICT), minha instituição de acolhimento, o qual sempre me proporcionou todas as condições de trabalho necessárias à realização da dissertação. Queria também agradecer à Câmara Municipal de Abrantes pela disponibilização da base topográfica para os trabalhos realizadas, ainda durante a tese de mestrado e que também foram utilizados durante este 3º Ciclo de Estudos e aos Bombeiros de Abrantes que me salvaram de passar uma noite ao relento no Tejo.

Queria ainda agradecer ao Laboratório Hércules, através do Professor Doutor José Mirão, e ao Laboratório de Geologia Isotópica da Universidade de Aveiro (LGI-UA), através do Professor Doutor José Francisco Santos e da Doutora Sara Ribeiro, pela disponibilidade e apoio ao meu projecto de doutoramento, agilizando a utilização de equipamentos e obtenção de dados. Agradeço ainda ao Laboratório de Isótopos Estáveis do Departamento de Geologia da FCUL, e em especial à Doutora Ana Isabel Janeiro e ao Professor Doutor Miguel Gaspar, a disponibilidade e esforço para obtenção de dados de isótopos estáveis em carbonatos, que, contudo, se revelaram não esclarecedores e daí não se ter avançado para estudos mais aprofundados. Contudo agradece-se a oportunidade e esforço.

Finalmente, agradeço à Fundação Calouste Gulbenkian (Prémio Estimulo à Investigação 2011) e à Fundação para a Ciência e Tecnologia (Bolsa de Doutoramento de referência: SFRH/BD/80580/2011 e o apoio financeiro ao ICT), pelo financiamento disponibilizado e que me permitiram levar a cabo uma boa parte das campanhas de campo realizadas, bem como a generalidade das análises geoquímicas efectuadas.

Por fim, deixo aqui um pedido de desculpas a todos aqueles que esperavam mais de mim, aos quais eu não pude dar mais e aqueles com quem falhei, mas como penso que sempre compreenderam, numa fase conturbada da vida como esta, em que todos os minutos contam e em que, infelizmente, o tempo não se multiplica eu não consegui dar mais de mim. Multipliquei-me, tentei não falhar com ninguém mas era-me impossível. Como tal um pedido de desculpas sem referir nomes, pois sei que se o fizesse, com certeza a lista era grande e me iria esquecer de alguém.

Prefácio

Serve a presente secção para explanar e enquadrar o conteúdo e organização da presente dissertação. Após anos de trabalho, que se iniciam em 2009 com a minha Dissertação de Mestrado (entregue em 2012), vários problemas e questões se foram levantando não só sobre a região inicialmente proposta como foco de estudo durante o Doutoramento (Tomar-Abrantes), mas também sobre a sua ligação com outros sectores do Orógeno Varisco.

A temática inicialmente definida aquando do concurso à Bolsa de Doutoramento da Fundação para a Ciência e a Tecnologia da qual fui alvo enquadrava-se no estudo d'"*A zona de cisalhamento de Tomar - Badajoz - Córdova no contexto das suturas variscas ibéricas*". Contudo, o avançar dos trabalhos, o aparecimento de questões diversas, as discussões calorosas e desafiantes com diversos investigadores e a tentativa de interdisciplinaridade nas diversas áreas da Geologia levaram a que o objectivo inicialmente traçado fosse sendo alterado, integrando um conjunto de dados que vão para além do estudo da Zona de Cisalhamento Tomar-Badajoz-Córdova.

Assim a actual temática da dissertação ("*Evolução Geodinâmica dos sectores setentrionais da Zona de Ossa-Morena no contexto do Varisco Ibérico*") procurou integrar de forma abrangente uma parte significativa dos dados adquiridos durante o período deste 3º Ciclo de Estudos, enquadrando e discutindo-os, sempre que possível, no contexto do Varisco Ibérico. Este acabou por ser um dos alicerces da minha formação durante este percurso conducente à obtenção do grau e consequentemente à elaboração desta dissertação. A tentativa da percepção da geologia regional, enquadrando os dados da meso- e microescala obrigaram desde logo não só a fazer um esforço por conhecer os dados e ideias já publicadas por outros autores, mas também a observar, conhecer, percorrer, avaliar e estudar áreas externas ao foco de estudo inicial. É desta forma que surgem os trabalhos realizados em diversos sectores não só na Zona de Ossa-Morena, mas também nas Zonas Centro Ibérica, Galiza-Trás-os-Montes e Sul Portuguesa. Uma parte destes trabalhos não se encontram reflectidos nesta tese, pois foram selecionados os que melhor tipificam a temática da dissertação.

No que respeita à organização da dissertação, a avaliação de um qualquer investigador nos dias que correm está totalmente focalizada nas métricas de publicações com impacto científico em revistas indexadas e nos mais diversos parâmetros que as avaliam, deixando na maioria dos casos os perfis dos investigadores de parte. Desta forma, aquando da idealização da organização

interna da dissertação, procurou-se conciliar esta premissa com as imposições da instituição que me confere o grau. Desta forma, optou-se pela elaboração de um conjunto de capítulos independentes *per si*, com organização interna própria e que permitissem reavaliação rápida e posterior submissão a revistas que cumpram os parâmetros supra mencionados. Uma parte dos capítulos aqui presentes foram já alvo de avaliação por pares e publicados em revistas indexadas, sendo que uma parte considerável dos dados e interpretações aqui contidas se encontram ainda por publicar. Nalguns casos encontram-se em fase de maturação no que respeita ao enquadramento no contexto do Orógeno Varisco e, consequentemente, na elaboração de um modelo geodinâmico que permita não só explicar os dados obtidos, como também os já publicados por outros autores.

Na realidade, esta dissertação representa a minha visão actual e "inexperiente" do Varisco Ibérico e que poderá (e deverá) sofrer modificações ao longo do meu percurso (sim tenho esperança de ter um percurso) como investigador, até porque

"Não há factos, apenas interpretações."

"Tudo evolui; não há realidades eternas: tal como não há verdades absolutas.".

in: Humano, demasiado Humano

Friedrich Wilhelm Nietzsche

(Filósofo Alemão, 1844-1900)

Se esta dissertação é na verdade o meu "estado actual dos conhecimentos" e embora tenha dúvidas sobre as temáticas e modelos propostos/abordados na dissertação, há também aqui uma tentativa de olhar para a geologia regional de forma integrada, evolutiva e inclusiva, tentando acreditar que todos os dados existentes resultam de trabalhos fidedignos e éticos, o que nos dias que correm é algo que começo a não acreditar; são os benefícios e malefícios das métricas cegas que avaliam sem olhar para o perfil. Dito de outra forma, "não interessa o que digo, interessa dizer diferente, publicar e ser citado" e infelizmente esta parece-me ser a tendência geral da ciência/geologia actual. Para que fique claro, neste momento não falo de ninguém em particular (grupo de investigadores ou investigador individual), apenas aproveito esta secção de cariz aberto e menos científico para "desabafar" sobre o estado actual das coisas. Não querendo parecer presunçoso, deixo uma citação que me parece de alguma forma retratar o que foi supra mencionado.

"O problema do mundo de hoje é que as pessoas inteligentes estão cheias de dúvidas, e as pessoas idiotas estão cheias de certezas..."

Bertrand Russell

(Matemático e Filósofo Britânico, 1872-1970)

Para finalizar, enfatizo a necessidade da aquisição de novo conhecimento, principalmente no que respeita à cartografia geológica, que tem sido cada vez mais vista como o parente pobre da geologia nos últimos anos, mesmo por geólogos, o que é desde logo um erro crasso, pois a cartografia geológica é, e deve ser vista como, a base de qualquer trabalho geológico. Os métodos analíticos têm limitações inerentes à própria metodologia e apenas com um constrangimento que resulta da colecta de dados de campo, os restantes dados passam a ter representatividade. Esta visão da cartografia geológica como "parente pobre" resulta em grande parte da dualidade entre o tempo necessário para a obtenção de dados capazes de serem publicáveis com impacto e a própria necessidade selvática de publicação. Assim, e propositadamente, termino com uma citação de um dos vários filósofos gregos, homens que tinham tempo para pensar não só sobre a sociedade em que se inseriam mas também sobre os eventos naturais que os envolviam (percursora da ciência moderna), o que permitiu a elevação deste império para além da história.

"*Existe apenas um bem, o saber, e apenas um mal, a ignorância.*"

in: *Vidas e Doutrinas dos Filósofos Ilustres*, Diógenes Laérico

Socrates

(Filósofo Grego, 469 a.C.-399 a.C.)

Espero assim que esta dissertação seja assim um contributo para a geologia, em particular para a discussão e avanço do conhecimento geológico nacional, ibérico e europeu. Espero que esta dissertação não seja o fim, mas sim o início, pois se alguma coisa ficou clara para mim durante este percurso, é que foram mais as perguntas que se levantaram do que as que foram respondidas.

I.

Introdução e enquadramento das áreas em Estudo

A compreensão da evolução geodinâmica da Zona de Ossa-Morena (ZOM) é fulcral no contexto do Varisco Ibérico, tendo implicações claras na geodinâmica da Cadeia Orogénica Varisca Europeia. Existem diversas sínteses recentes sobre a evolução geodinâmica do Varisco Europeu; a leitura destes trabalhos expõe a controvérsia existente no que respeita ao número de placas envolvidas na colisão que origina a Pangeia e consequentemente no número de oceanos Variscos. Enquanto Dias *et al*. (2016) referem a presença de dois oceanos Variscos principais no segmento europeu, nomeadamente o Oceano Rheic e o Galiza-Maciço Central separando os Terrenos Gondwanicos da Avalónia e Armorica (Fig. 1A), outros autores (e.g. Faure *et al*., 2005; Ribeiro *et al*., 2007; Franke e Dulce, 2016; Pérez-Cáceres *et al*., 2016) mencionam a presença de outras suturas Variscas quer no Maciço Ibérico, quer nos restantes Maciços Variscos Europeus (Fig. 1B); estas suturas delimitariam blocos continentais menores. Durante o Carbónico-Pérmico, estes blocos continentais menores, a Gondwana e Avalónia-Laurentia colidiriam entre si, resultando do fecho dos oceanos Variscos e dando origem ao supercontinente Pangeia.

Por isso, é fundamental analisar o número de suturas Variscas existentes no Maciço Ibérico. Uma das possíveis suturas apontadas por diversos autores (e.g. Franke e Dulce, 2016; Pérez-Cáceres *et al*., 2016) fica localizada na zona de cisalhamento de Tomar-Badajoz-Córdova (ZCTBC), que se prolonga desde a região de Abrantes-Tomar (Portugal) até Córdoba (Espanha), apresentando uma orientação WNW-ESE, sub-paralela à orientação geral do Orógeno no Maciço Ibérico (Fig. 1B). Esta estrutura marca o contacto entre duas das zonas paleogeográficas do Maciço Ibérico (Fig. 2), nomeadamente a Zona Centro Ibérica e a ZOM (e.g. Ribeiro *et al*, 1979; 2007). Contudo, a presença de uma sutura Varisca nesta zona de cisalhamento não é de todo consensual, sendo que vários autores interpretam esta estrutura como uma estrutura herdada do ciclo Cadomiano, reactivada durante o Orógeno Varisco como um importante cisalhamento intraplaca. Mas mesmo aqui modelos opostos são propostos:

- Alguns autores (Ribeiro *et al*., 2007; 2009; Romão *et al*., 2010) interpretam esta zona de cisalhamento como uma sutura cadomiana, contendo um conjunto de rochas

metamórficas de alto grau de idade Cadomiana (Henriques *et al*., 2015; 2016), posteriormente retrabalhadas durante o ciclo Varisco;

- Enquanto outros evidenciam a presença de um domínio orogénico na ZCTBC associado à génese de um arco vulcânico e uma bacia de *back-arc* resultantes da subducção Cadomiana localizada no bordo Norte da Gondwana, tendo sido posteriormente invertidos durante as fases terminais do mesmo ciclo orogénico (Eguiluz *et al*., 2000; Sanchez-Lorda *et al*., 2014).

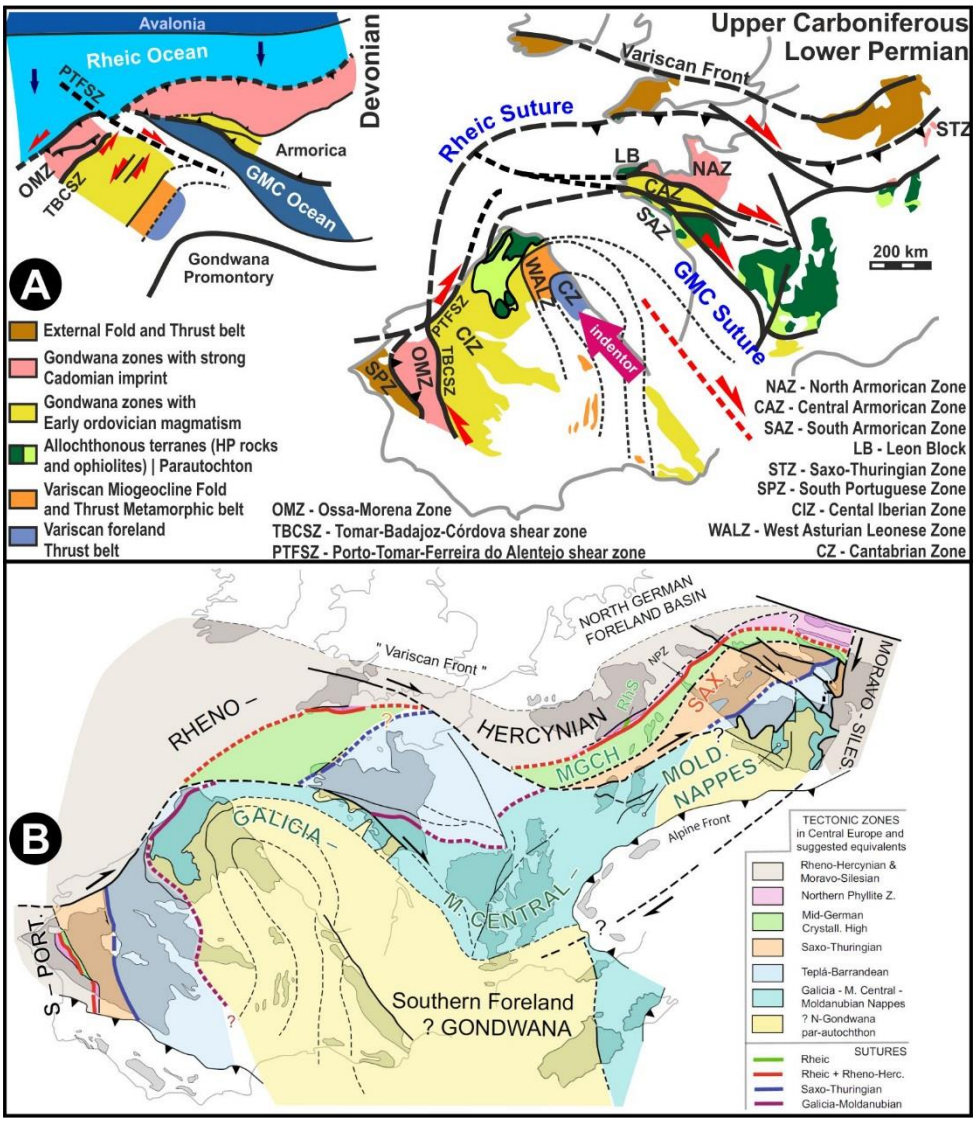

Figura 1 – Reconstituições paleogeográficas para o Varisco Europeu:

A – Proposta de Dias *et al*. (2016) onde se destaca a presença dois oceanos principais separando três placas distintas – Gondwana, Armorica e Avalónia;

B – Proposta de organização com várias Suturas Variscas, evidenciando a presença de um conjunto de blocos continentais menores (em Franke e Dulce, 2016).

O facto de existirem rochas máficas e ultramáficas, algumas com evidências de alta pressão (Eguiluz *et al*., 1990; Ordóñez Casado, 1998; Pinto *et al*., 2006; Pereira *et al*., 2010a), associadas a esta estrutura de primeira ordem, tendo em conta o conhecimento das cadeias orogénicas recentes, indiciam a presença de uma sutura. A interpretação geodinâmica destas rochas de alta pressão seria linear, se esta zona de cisalhamento não contivesse rochas proterozóicas com indícios de sobreposição de episódios tectono-metamórficos anteriores ao ciclo Varisco (e.g. Abalos e Cusí, 1995; Ribeiro *et al*, 2009). Com efeito, alguns autores consideram o metamorfismo de alta pressão como sendo de idade Cadomiana (e.g. Ribeiro *et al*., 2009) enquanto outros consideram-nas Variscas (Ordóñez Casado, 1998; Pereira *et al*., 2010a). Os dados geocronológicos obtidos nestas da zona axial da ZCTBC (e.g. Ordóñez Casado, 1998; Pereira *et al*., 2010a) não são totalmente esclarecedores quanto à idade deste metamorfismo de alta pressão, embora pareçam apontar idades Paleozóicas. A interpretação geodinâmica desta zona de cisalhamento torna-se ainda mais complexa devido aos intensos episódios tectonometamórficos Variscos que retrabalham as estruturas de idade Cadomiana (e.g. Dallmeyer e Quesada, 1992; Ribeiro *et al*, 2007).

A região de Abrantes-Tomar representa os sectores mais ocidentais da ZCTBC e da ZOM, sendo a compreensão desta região essencial para o entendimento da evolução geodinâmica desta estrutura de primeira ordem à escala do Orógeno e consequentemente desta zona paleogeográfica. Esta região ganha ainda maior preponderância pois neste local surge a interferência entre a zona de cisalhamento previamente referida e uma outra zona de cisalhamento de primeira ordem à escala do Orógeno, a Zona de Cisalhamento Porto-Tomar-Ferreira do Alentejo (ZCPTF). Também neste caso não há consenso quanto à evolução e significado geodinâmico da ZCPTF:

- Pereira *et al*. (2010b) considera que a ZCPTF se desenvolve durante o Carbónico terminal (Pensilvaniano) como uma zona de intensa deformação cisalhante direita desenvolvida em regime de deformação não-coaxial frágil-dúctil e afectando um conjunto de alto grau metamórfico (fácies anfibolítica) de idade Mississipiana geneticamente associado à ZCTBC;
- Outros autores consideram esta zona de cisalhamento uma paleotransformante activa pelo menos desde o início das fases convergentes do Ciclo Varisco, mas que poderá ser herdada pelo menos desde as fases precoces deste Ciclo Orogénico (Dias e Ribeiro, 1993; Chaminé, 2000; Ribeiro *et al*., 2007; 2013).

Segundo Ribeiro *et al*. (2007; 2013), esta paleotransformante conecta as suturas do NW e SW Ibérico, levando assim a propor a presença de um novo Terreno Tectonoestratigráfico na

Ibéria, delimitado a Este pela ZCPTF, o qual foi denominado de Terreno Finisterra. Este terreno apresentaria uma evolução geodinâmica distinta das restantes zonas do Terreno Ibérico durante o Paleozóico, sendo necessária a sua diferenciação dos demais.

Se tivermos em conta a interpretação de Pereira *et al* (2010b), a deformação cisalhante direita da ZCPTF, com orientação geral N-S e de carácter frágil-dúctil, afecta as unidades tectono-metamórficas e magmáticas associadas à ZCTBC, transportando fragmentos dos sectores setentrionais da ZOM, em particular dos domínios associados à ZCTBC (que os autores denominam de Coimbra-Córdoba), até à região do Porto. Este modelo dá pouco enfase ao papel da ZCPTF na estruturação do Orógeno durante as suas fases precoces, atribuindo-lhe um carácter tardio em relação à edificação do orógeno, referindo ainda que não existem evidências para considerar esta zona de cisalhamento como uma falha transformante activa durante a evolução Paleozóica no Norte da Gondwana.

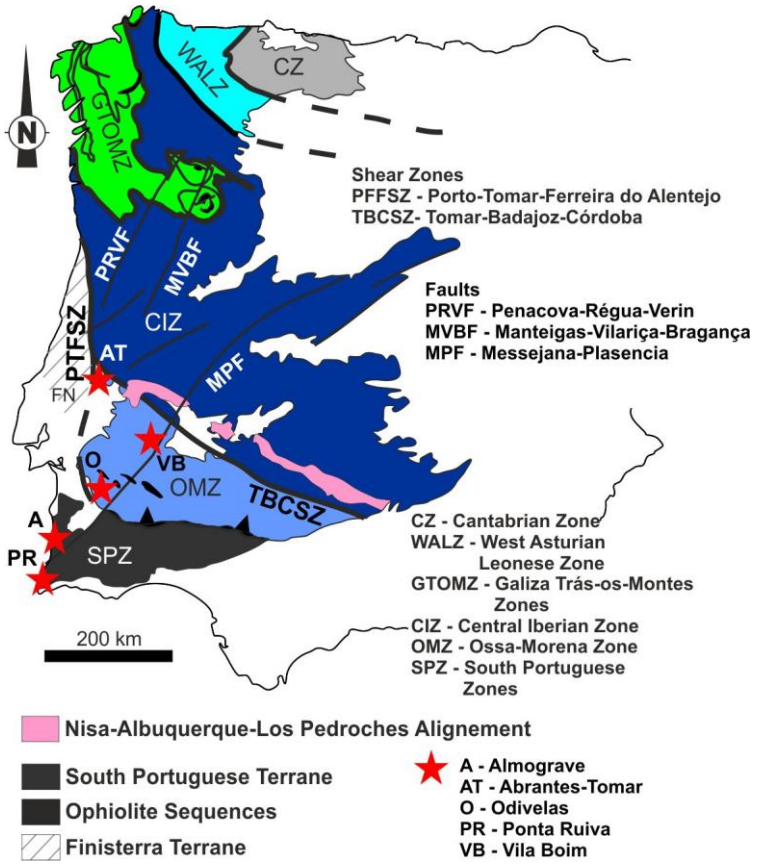

Figura 2 – Organização tectonoestratigráfica do Maciço Ibérico, pondo em evidência a localização das áreas de estudo (estrelas).

Como é evidente, diferentes visões/interpretações destas estruturas implicam mudanças drásticas na dinâmica da Tectónica de Placas Paleozóica em torno do sector Ibérico, traduzindo-se em modelos geodinâmicos totalmente distintos, quer em termos do número de blocos

continentais quer em oceanos envolvidos na génese do Orógeno Varisco Europeu e consequentemente do Maciço Ibérico.

De facto, a importância destas zonas de cisalhamento à escala do Orógeno é inegável, mas a caracterização geológica de pormenor da região de Abrantes-Tomar, e consequentemente da interferência entre estas duas zonas de cisalhamento, talvez pela complexidade estrutural, metamórfica e estratigráfica, não tem sido alvo de trabalhos de pormenor que permitam o entendimento desta interferência. Merecem destaque os trabalhos pioneiros de Gonçalves *et al*. (1979) e Teixeira (1981) que realizaram a cartografia na região de Abrantes, sendo que os trabalhos posteriormente realizados são, na sua grande maioria, trabalhos pontuais de índole diversa e a uma escala de menor pormenor (*e.g.* Conde, 1984; Pereira *et al*., 1998; Ribeiro *et al*., 2009; 2013; Pereira *et al*., 2010b; Romão *et al*., 2010; Henriques *et al*., 2015; 2016).

Os trabalhos conducentes à dissertação de Mestrado (Moreira, 2012) revelaram características particulares do ponto de vista geodinâmico na região de Abrantes. Aqui, o autor descreve uma interacção entre estas duas zonas de cisalhamento: a ZCPTF impede a propagação para Oeste da ZCTBC, gerando um padrão estrutural que é compatível com a presença de uma dobra em bainha, como previamente proposto por Ribeiro *et al*. (2009) para a região. Isto revela que durante a primeira fase de deformação a ZCPTF deveria estar activa, algo que já havia sido proposto por Dias e Ribeiro (1993) com base no padrão dos elipsoides de deformação finita obtidos nos quartzitos do ordovício na região do Buçaco, servindo assim de barreira à propagação da ZCTBC para Oeste.

Com o intuito de compreender melhor não só a estrutura mas também a estratigrafia (lito- ou tectono-) desta região, possibilitando assim a correlação entre esta região e as zonas circundantes, selecionaram-se duas áreas de trabalho distintas, ambas consideradas como contidas nos sectores setentrionais da ZOM:

- A região de Abrantes foi alargada para Oeste, para os sectores de Constância-Tomar, onde, de acordo o modelo proposto por Pereira *et al*. (2010b), deveriam surgir as unidades com afinidades à ZOM (Fig. 2). Contudo, outros autores (e.g. Romão *et al*., 2014) consideram que este sector já se enquadra no Terreno Finisterra;
- Um sector externo à região de Abrantes-Tomar, que apresentasse um menor grau metamórfico e menor complexidade estrutural, permitindo assim um maior controle a nível (lito)estratigráfico, como seja o sector de Torre de Cabedal (Vila Boim; Fig. 2), localizado no sector de Alter-do-Chão-Elvas (Oliveira *et al*., 1991; Moreira *et al*, 2014).

O estudo comparado destes sectores permite um melhor conhecimento dos sectores setentrionais da ZOM, em particular da região de Abrantes-Tomar, nomeadamente do ponto de vista geoquímico e litoestratigráfico, possibilitando assim o refinamento dos modelos

geodinâmicos propostos para a ZOM, não só no ciclo Varisco, mas também no ciclo Cadomiano (e.g. Ribeiro *et al*., 2007; 2009; 2010; Azor *et al*., 2008; Linnemann *et al*., 2008; Pereira *et al*., 2010b).

Contudo, só por si, esta comparação não permite o entendimento da interacção entre as duas zonas de cisalhamento previamente referidas. Com efeito, levantamentos geológicos recentes realizados por Romão e colaboradores na região de Tomar-Ferreira do Zêzere, conducentes à realização da Carta Geológica de Tomar à escala 1:50.000, demonstraram a presença de unidades tectonoestratigráficas com orientação N-S a NNW-SSE (Romão *et al*., 2013), o que é anómalo em relação à estruturação NW-SE geral da ZOM e do restante Maciço Ibérico. Esta interpretação está de acordo com os trabalhos realizados por Moreira (2012), que define na região de Abrantes uma unidade "exótica" no que respeita à estratigrafia típica da transição Neoproterozóico-Câmbrico desta Zona. Desta forma, o alargamento da área de trabalho para as regiões a Oeste de Abrantes, mais especificamente para o sector de Constância-Tomar, permitiu ainda a definição de um conjunto de unidades tectonoestratigráficas que parecem estar geneticamente relacionadas com a ZCPTF e que não apresentam afinidades tectonoestratgráficas com a ZOM. Ribeiro *et al*. (2013) compara levantamentos preliminares realizados na região, com os sectores de Porto-Albergaria-Espinho, propondo a definição do Terreno Finisterra, algo que os trabalhos realizados pretendem testar.

Os trabalhos realizados na região de Abrantes-Tomar, durante o período respeitante à obtenção do grau de doutor, apenas têm preponderância se devidamente enquadrados e integrados no contexto do Varisco Ibérico, embora com especial enfase no SW Ibérico. Desde os processos que levam à edificação da Cadeia Cadomiana no Neoproterozóico, passando pela compreensão do episódio de *rifting* iniciado no Paleozóico inferior (Câmbrico), por estiramento do bordo Norte da Gondwana, até ao episódio de colisão continental no Paleozóico superior que termina com a formação do supercontinente Pangeia, muitas questões permanecem em aberto, algumas das quais com discussões que parecem não ter solução próxima. Tentar-se-á assim, sempre que possível, integrar os dados agora obtidos com os dados publicados em trabalhos prévios de outros autores, refinando-se assim os modelos propostos para o Orógeno Varisco Europeu, e em particular para o SW Ibérico, durante os Ciclos Cadomiano e Varisco (e.g. Ribeiro *et al*., 2007; 2009; Linnemann *et al*., 2008; Nance *et al*., 2012; 2015).

Qualquer modelo geodinâmico proposto terá de ter em conta a totalidade de dados existentes/publicados para a região. Para que o modelo proposto seja robusto, este deverá não só explicar os novos dados, como também englobar os dados previamente publicados, sejam eles de carácter estratigráfico, geoquímico, geofísico, petrográfico ou geocronológico. É

fundamental que qualquer modelo proposto seja capaz de explicar as relações/observações de campo, pois são estas que confirmam e constrangem os restantes dados analíticos e/ou laboratoriais. A título de exemplo, a existência de um processo de *rifting* intracontinental gerará uma sucessão sedimentar com características próprias, acompanhado por um conjunto de rochas magmáticas com características geoquímicas próprias e um processo colisional associado a uma zona de subducção implicará necessariamente a génese de um conjunto de rochas metamórficas e a deformação das sucessões previamente geradas.

Todas estas alterações dos processos geodinâmicos actuantes e consequentemente dos ambientes geotectónicos dominantes num determinado instante espácio-temporal deverão estar representadas no registo geológico. É neste sentido que se dá importância à evolução Devónica da Zona de Ossa-Morena. Trabalhos levados a cabo ao longo dos anos na região SW de Portugal, com especial enfase na região de Odivelas (Ferreira do Alentejo; Fig. 2), mostram a presença de um importante episódio carbonatado no SW da ZOM. Embora a sua caracterização estratigráfica e cronológica tenha sido já realizada em trabalhos prévios (e.g. Boogaard, 1972; 1983; Machado *et al*., 2009; 2010), a sua compreensão/interpretação do ponto de vista geodinâmico enquadrando os restantes dados de relativos à evolução Devónica da ZOM não tinha sido ainda efectuada. A análise dos dados estratigráficos, paleoambientais, magmáticos e tectono-metamórficos desta idade mostram claramente a mudança dos processos geodinâmicos actuantes durante na transição Silúrico-Devónico inferior e posteriormente durante o Devónico terminal-Carbónico. Estes dois momentos parecem ser fundamentais para a evolução da ZOM e consequentemente para a edificação do Orógeno Varisco, algo que se explanará em capítulos próprios (capítulos V e VI).

Durante o Carbónico, os processos de colisão continental resultante do fecho do(s) Oceano(s) Varisco(s) gera/acentua uma das estruturas mais significativas do Orógeno, o denominado Arco-Ibero-Armoricano. Esta estrutura arqueada de primeira ordem, foi desde muito cedo identificada (Schulz; 1858; Bertrand, 1887; Suess, 1888), embora recentemente vários trabalhos tenham gerado um conjunto de novos dados que levaram à proposta de modelos alternativos para a sua explicação. Desde os modelos clássicos de indentação (e.g. Matte e Ribeiro, 1975; Dias e Ribeiro, 1995), aos de arco controlados por grandes cisalhamentos variscos (e.g. Brun and Burg, 1982; Martínez Catalán, 2011a), vários modelos tinham sido propostos. Na última década foi dada muita ênfase a um modelo, e as suas variantes, que propõem o buckling de toda a litosfera, gerando a sua delaminação (Gutiérrez-Alonso *et al*., 2004; Weil *et al*., 2013). Este último modelo defende ainda que todo o arco é gerado durante o Carbónico terminal, o que é incongruente com os dados que mostram um regime transpressivo esquerdo na Ibéria desde as etapas iniciais das fases convergentes do Ciclo de Wilson, que se

inicia durante o Devónico ou até Silúrico (e.g. Ribeiro *et al*., 2010). Para além disso, mais recentemente foi proposta a existência de uma nova estrutura arqueada na Ibéria, o denominado Arco Centro-Ibérico (Martínez Catalán, 2011b), também ela interpretada como resultante do buckling litosférico (Johnston *et al*. 2013). Também em capítulo próprio (capítulo IX) se discutirá a génese destas estruturas arqueadas na Ibéria, não só enquadrando e discutindo os dados publicados, mas também propondo um modelo que os integre.

O sobreespessamento da cadeia resultante do processo de colisão continental dá origem a abundantes corpos magmáticos, maioritariamente localizados nas zonas internas do Maciço Ibérico. Após este sobreespessamento e a génese do Arco Ibero-Armoricano, a colisão obliqua entre os blocos continentais a Norte (Laurentia-Báltica-Avalónia) e a Sul (Gondwana e outros blocos continentais) do(s) oceano(s) Varisco(s) gera um regime de deformação intracontinental transcorrente dominantemente direito e que é responsável pela génese de diversos cisalhamentos E-W de primeira ordem à escala do Orógeno (Fig. 3; e.g. Arthaud e Matte, 1977; Ribeiro, 2002).

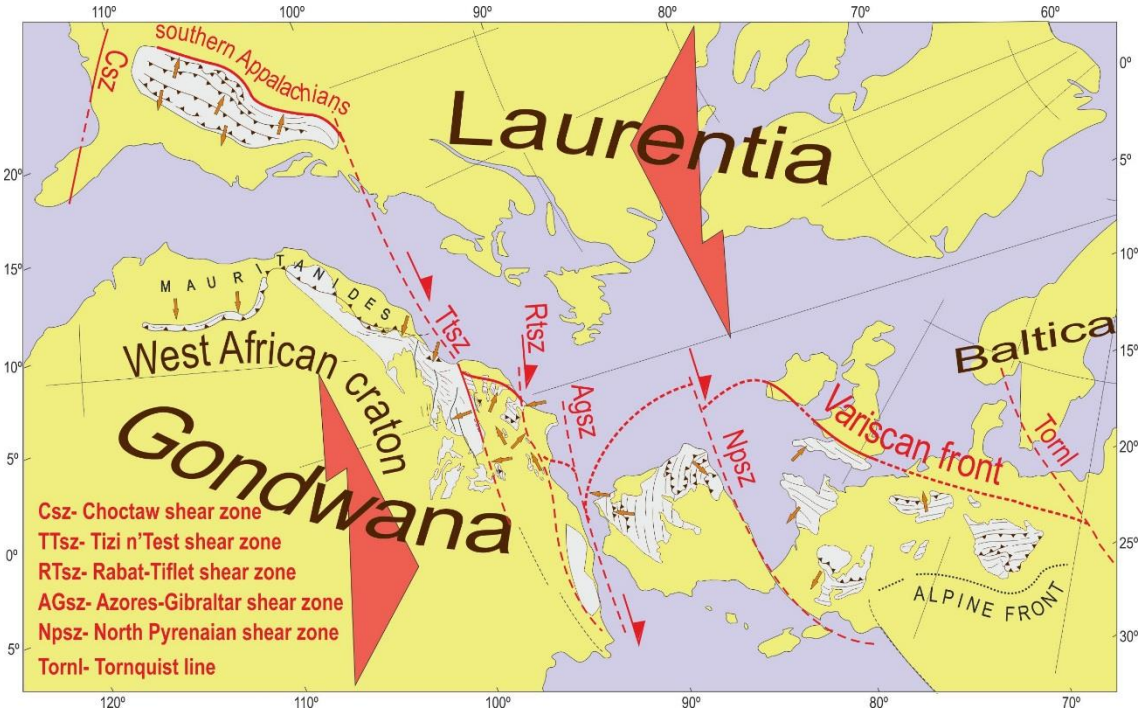

Figura 3 – Modelo de colisão final para o Ciclo Varisco pondo em evidência a presença de grandes cisalhamentos E-W direitos resultantes da colisão obliqua direita Varisca (adaptado de Arthaud e Matte, 1977).

Nesse período, usualmente denominado de Tardi-Varisco, o Maciço Ibérico apresenta características singulares no Orógeno Varisco Europeu, desenvolvendo um padrão de

fracturação caracterizado pela sua extrema homogeneidade geométrica. Esta fase tardia de deformação é caracterizada por um padrão de estruturas de carácter frágil a frágil-dúctil com uma direcção predominantemente NNE-SSW a NE-SW, o denominado sistema Régua-Vilariça-Messejana (Fig. 2), que afectam todas as zonas paleogeográficas do Maciço Ibérico. No entanto, interpretações díspares têm vindo a ser propostas no que diz respeito à cinemática destas estruturas:

- Em trabalhos clássicos (Ribeiro *et al*., 1979; Iglésias e Ribeiro 1981; Choukhroune e Iglésias 1980; Pereira *et al*. 1993) e em outros mais recentes (e.g. Ribeiro, 2002; Moreira *et al*., 2010; Dias e Basile, 2013), a grande maioria dos autores consideram que estas estruturas apresentam cinemática esquerda durante o Ciclo Varisco;
- Contudo, outros autores consideram uma cinemática direita para estas estruturas durante os episódios tardios do Orógeno Varisco, sendo que a cinemática esquerda observada resultaria do seu re-jogo durante o Alpino (Lourenço, 2002; Marques *et al*., 2002; 2010).

A presença e abundância destas estruturas NNE-SSW com cinemática esquerda quer na região de Abrantes, quer na região de Vila Boim e a impossibilidade de constranger temporalmente a sua génese nestes locais, levou ao seu estudo noutro local do Maciço Ibérico, onde fosse possível constranger a idade da cinemática esquerda. Desta forma, selecionaram-se dois locais, nomeadamente Almograve e Ponta Ruiva (Fig. 2), ambos na Zona Sul-Portuguesa onde para além de constranger a cinemática e a geometria das Falhas Tardi-Variscas era também possível constranger a idade desta cinemática devido à existência de depósitos associados de idade Triásica.

Tendo em conta o que foi previamente exposto, cada um dos capítulos (e subcapítulos) seguintes apresentará uma organização interna própria, com introdução, desenvolvimento e conclusões, onde se abordará isoladamente cada uma das temáticas desenvolvidas durante este ciclo de estudos. Esta estrutura conduziu à opção de elaborar a maior parte destes capí,tulos sob a forma de artigos a serem apresentados a revistas científicas da especialidade. Tendo em vista os constrangimentos temporais inerentes a uma tese de doutoramento, estes artigos encontram-se em diversos estádios; alguns encontram-se já publicados, outros estão aceites mas em fase de revisão, enquanto outros irão ser submetidos em breve. A finalizar a dissertação, é apresentada uma conclusão sucinta dos principais resultados obtidos e os “desafios futuros” (capitulo XI) resultantes dos trabalhos realizados.

Referências

Abalos, B., Díaz Cusí, J. (1995). Correlation between seismic anisotropy and major geological structures in SW Iberia: a case study on continental lithosphere deformation. Tectonics, 14, 1021–1040.

Arthaud, F., Matte, P. (1977). Late paleozoic strike-slip faulting in southern Europe and northern Africa; Result of a right-lateral shear zone between the Appalachians and the Urals. Geological Society America Bulletin, 88, 130.

Azor, A., Rubatto, D., Simancas, J.F., González Lodeiro, F., Martínez Poyatos, D., Martín Parra, L.M., Matas, J. (2008). Rheic Ocean ophiolitic remnants in southern Iberia questioned by SHRIMP U-Pb zircon ages on the Beja-Acebuches amphibolites. Tectonics, 27.

Bertrand, M. (1887). La Chaîne des Alpes et la formation du continent européen. Bull. Soc. Geol. Fr. 15 (3), 423-447.

Boogaard, M. (1972). Conodont faunas from Portugal and Southwestern Spain. Part 1: A Middle Devonian fauna from near Montemor-o-Novo. Scripta Geologica, 13, 1-11.

Boogaard, M. (1983). Conodont faunas from Portugal and southwestern Spain. Part 7. A Frasnian conodont fauna near the Estação de Cabrela (Portugal). Scripta Geologica, 69, 1-17.

Brun, J., Burg, J. (1982). Combined thrusting and wrenching in the Ibero-Armorican Arc – a corner effect during continental collision. Earth Planet. Sci. Lett., 61, 319-332.

Chaminé, H. (2000). Estratigrafia e estrutura da Faixa Metamórfica de Espinho – Albergaria-a-Velha (Zona de Ossa Morena: Implicações geodinâmicas). Tese de Doutoramento, Universidade do Porto, 497 p.

Choukhroune, P., Iglésias, M. (1980). Zonas de cisalla dúctil en el NW de la Peninsula Ibérica. Cuad. Lab. Xeol. Laxe, 1, 163-164.

Conde, L. (1984). Excursão geológica na região de Ferreira do Zêzere-Abrantes. VI Reunião do Grupo de Ossa Morena, Livro-guia, Universidade de Coimbra, 1-8.

Dallmeyer, R.D., Quesada, C. (1992). Cadomian vs. Variscan evolution of the Ossa-Morena Zone (SW Iberia): field and 40Ar/39Ar mineral age constraints. Tectonophysics, 216, 339-364.

Dias, R., Ribeiro, A. (1993). Porto-Tomar shear zone, a major structure since the begining of the Variscan orogeny. Comun. Inst. Geol. Mineiro, 79, 29-38.

Dias, R., Ribeiro, A. (1995). The Ibero-Armorican arc: a collisional effect against an irregular continent? Tectonophysics, 246 (1–3), 113–128.

Dias, R., Basile, C. (2013). Estrutura dos sectores externos da Zona Sul Portuguesa; implicações geodinâmicas. In: Dias R, Araújo A, Terrinha P, Kullberg JC (ed), Geologia de Portugal, vol. 1, Escolar Editora, 787-807.

Dias, R., Ribeiro, A., Romão, J., Coke, C., Moreira, N. (2016). A review of the arcuate structures in the Iberian Variscides; constraints and genetical models. Tectonophysics, 681, 170–194. DOI:10.1016/j.tecto.2016.04.011

Eguiluz, L., Abalos, B., Gil Ibarguchi, J.I., (1990). Eclogitas de la Banda de Cizalla Badajoz-Córdoba (Suroeste de España). Geogaceta, 7, 28-31.

Eguíluz L., Gil Ibarguchi J.I., Abalos B., Apraiz A. (2000). Superposed Hercynian and Cadomian orogenic cycles in the OssaMorena zone and related areas of the Iberian Massif. Geol. Soc. Am. Bull., 112, 1398-1413.

Faure, M., Bé Mézème, E., Duguet, M., Cartier, C., Talbot, J. (2005). Paleozoic tectonic evolution of Medio-europa from the example of the French Massif Central and Massif Armoricain. In: Carosi R, Dias R, Iacopini D, Rosenbaum G (eds) The southern Variscan belt. J Virt Explor, 19, 5. DOI: 10.3809/jvirtex.2005.00120

Franke, W., Dulce, J-C. (2016). Back to sender: tectonic accretion and recycling of Baltica‐derived Devonian clastic sediments in the Rheno‐Hercynian Variscides. Int J Earth Sci (Geol Rundsch). DOI: 10.1007/s00531-016-1408-y

Gonçalves, F., Zbyszewski, G., Carvalhosa, A., Coelho, A. (1979). Carta Geológica de Portugal 1:50.000, folha 27-D (Abrantes). Serv. Geol. Portugal, Lisboa.

Gutiérrez-Alonso, G., Fernández-Suárez, J., Weil, A. (2004). Orocline triggered lithospheric delamination. Geol. Soc. Am. Spec. Pap., 383, 121–131.

Henriques, S.B.A., Neiva, A.M.R., Ribeiro, M.L., Dunning, G.R., Tajčmanová, L., (2015). Evolution of a Neoproterozoic suture in the Iberian Massif, Central Portugal: New U-Pb ages of igneous and metamorphic events at the contact between the Ossa Morena Zone and Central Iberian Zone. Lithos, 220-233, 43-59. DOI:10.1016/j.lithos.2015.02.001

Henriques, S.B.A., Neiva, A.M.R., Tajčmanová, L., Dunning, G.R. (2016). Cadomian magmatism and metamorphism at the Ossa Morena/Central Iberian zone boundary, Iberian Massif, Central Portugal: Geochemistry and P–T constraints of the Sardoal Complex. Lithos, 268–271, 131–148. DOI:10.1016/j.lithos.2016.11.002

Iglesias, M., Ribeiro, A. (1981). Zones de cisaillement ductile dans l'arc ibéro-armoricain. Comun. Serv. Geol.Portugal, 67, 85-87.

Johnston, S.,Weil, A., Gutiérrez-Alonso, G. (2013). Oroclines: thick and thin. Geol. Soc. Am. Bull., 125 (5–6), 643–663.

Linnemann, U., Pereira, M.F., Jeffries, T., Drost, K., Gerdes, A. (2008). Cadomian Orogeny and the opening of the Rheic Ocean: new insights in the diacrony of geotectonic processes constrained by LA–ICP–MS U–Pb zircon dating (Ossa-Morena and Saxo-Thuringian Zones, Iberian and Bohemian Massifs). Tectonophysics 461, 21–43.

Lourenço, J., Mateus, A., Coke, C., Ribeiro, A. (2002). A zona de falha Penacova-Régua-Verín na região de Telões (Vila Pouca de Aguiar); alguns elementos determinantes da sua evolução em tempos tardivariscos. Comum. Inst. Geol. Mineiro, 89, 105-122.

Machado, G., Hladil, J., Koptikova, L., Fonseca, P., Rocha, F.T., Galle, A. (2009). The Odivelas Limestone: Evidence for a Middle Devonian reef system in western Ossa-Morena Zone. Geol Carpath, 60(2), 121-137.

Machado, G., Hladil, J., Koptikova, L., Slavik, L., Moreira, N., Fonseca, M., Fonseca, P. (2010). An Emsian-Eifelian Carbonate-Volcaniclastic Sequence and the possible Record of the basal choteč event in western Ossa-Morena Zone, Portugal (Odivelas Limestone). Geol Belgica, 13, 431-446.

Marques, F., Mateus, A., Tassinari, C. (2002). The Late-Variscan fault network in central-northern Portugal (NW Iberia): a re-evaluation. Tectonophysics, 359, 255-270. DOI:10.1016/S0040-1951(02)00514-0

Marques, F., Burg, J., Lechmann, S., Schmalholz, S. (2010). Fluid-assisted particulate flow of turbidites at very low temperature: A key to tight folding in a submarine Variscan foreland basin of SW Europe. Tectonics, 29. DOI:10.1029/2008TC002439

Martínez Catalán, J. (2011a). Are the oroclines of the Variscan belt related to late Variscan strike-slip tectonics? Terra Nova, 23, 241–247.

Martínez Catalán, J. (2011b). The Central Iberian arc: implications for the Iberian Massif. Geogaceta, 50 (1), 7–10.

Matte, Ph., Ribeiro, A. (1975). Forme et orientation de l'ellipsoïde de déformation dans la virgation hercynienne de Galice. Relations avec le plissement et hypothèses sur la genèse de l'arc ibéro-armoricain. C. R. Acad. Sci. Paris D 280, 2825–2828.

Moreira, N. (2012). Caracterização estrutural da zona de cisalhamento Tomar-Badajoz-Córdova no sector de Abrantes. Tese de Mestrado (não publicada), Universidade de Évora, 225 p.

Moreira, N., Dias, R., Coke, C., Búrcio, M. (2010). Partição da deformação Varisca nos sectores de Peso da Régua e Vila Nova de Foz Côa (Autóctone da Zona Centro Ibérica); Implicações Geodinâmicas. Comunicações Geológicas, 97, 147-162.

Moreira, N., Dias, R., Pedro, J.C., Araújo, A. (2014). Interferência de fases de deformação Varisca na estrutura de Torre de Cabedal; sector de Alter-do-Chão – Elvas na Zona de Ossa-Morena. Comunicações Geológicas, 101(I), 279-282.

Nance, R.D., Gutiérrez-Alonso, G., Keppie, J.D., Linnemann, U., Murphy, J.B., Quesada, C., Strachan, R.A., Woodcock, N.H. (2012). A brief history of the Rheic Ocean. Geoscience Frontiers, 3, 125-135.

Nance, R.D., Neace, E.R., Braid, J.A., Murphy, J.B., Dupuis, N., R.K. Shail, R.K. (2015). Does the Meguma Terrane extend into SW England? Geoscience Canada, 42, 61-76.

Oliveira, J.T., Oliveira, V., Piçarra, J.M. (1991). Traços gerais da evolução tectono-estratigráfica da Zona de Ossa Morena, em Portugal: síntese crítica do estado actual dos conhecimentos. Comun. Serv. Geol. Port., 77, 3-26.

Ordóñez-Casado, B. (1998). Geochronological studies of the Pre-Mesozoic basement of the Iberian Massif: the Ossa-Morena Zone and the Allochthonous Complexes within the Central Iberian Zone. PhD dissertation, ETH, Switzerland, 235p.

Pereira, E., Ribeiro, A., Meireles, C. (1993). Cisalhamentos hercínicos e controlo das mineralizações de Sn-W, Au e U na Zona Centro-Ibérica em Portugal. Cuaderno Lab. Xeolóxico de Laxe, 18, 89-119.

Pereira, E., Romão, J., Conde, L. (1998). Geologia da Transversal de Tomar-Mação Sutura entre a Zona Centro-Ibérica (ZCI) e Zona de Ossa-Morena (ZOM). In: Oliveira, J. T., Pereira, R. (Eds.) Livro guia das excursões do V Congresso Nacional de Geologia, 159-188.

Pereira, M.F., Apraiz, A., Chichorro, M., Silva, J.B., Armstrong. R.A. (2010a). Exhumation of high-pressure rocks in northern Gondwana during the Early Carboniferours (Coimbra–Cordoba shear zone, SW Iberian Massif): Tectonothermal analysis and U–Th–Pb SHRIMP in-situ zircon geochronology. Gondwana Research, 17, 440-460. DOI:10.1016/j.gr.2009.10.001

Pereira, M.F., Silva, J.B., Drost, K., Chichorro, M., Apraiz, A. (2010b). Relative timing of the transcurrent displacements in northern Gondwana: U-Pb laser ablation ICP-MS zircon and monazite geochronology of gneisses and sheared granites from the western Iberian Massif (Portugal). Gondwana Research, 17(2-3), 461-481. DOI:10.1016/j.gr.2009.08.006

Pérez-Cáceres, I., Poyatos, D.M., Simancas, J.F., Azor, A. (2016). Testing the Avalonian affinity of the South Portuguese Zone and the Neoproterozoic evolution of SW Iberia through detrital zircon populations, Gondwana Research. DOI:10.1016/j.gr.2016.10.010

Pinto, L.B., Pedro, J.C., Araújo, A., Inverno, C., Oliveira, V.M.J., Munhá, J. (2006). Retrogradação de eclogitos e mineralizações auríferas em Algueireiras-Algueireirinhas, Assumar, zona de cisalhamento Tomar-Córdova. VII Congresso Nacional de Geologia, Livro de Resumos I, 25-28.

Ribeiro, A. (2002). Soft Plate Tectonics. Springer-Verlag, Berlin.

Ribeiro, A., Antunes, M.T., Ferreira, M.P., Rocha, R.B., Soares, A.F., Zbyszewski, G., Moitinho de Almeida, F., Carvalho, D., Monteiro, J.H. (1979). Introduction à la Géologie Générale du Portugal. Serviços Geológicos de Portugal.

Ribeiro, A., Munhá, J., Dias, R., Mateus, A., Pereira, E., Ribeiro, L., Fonseca, P., Araújo, A., Oliveira, T., Romão, J., Chaminé, H., Coke, C., Pedro, J. (2007). Geodynamic evolution of the SW Europe Variscides. Tectonics, 26(6), TC6009. DOI: 10.1029/2006TC002058

Ribeiro, A., Pereira, E., Fonseca, P., Mateus, A., Araújo, A., Munhá, J., Romão, J., Rodrigues, J.F. (2009). Mechanics of thick-skinned Variscan overprinting of Cadomian basement (Iberian Variscides). C. R. Geosciences, 341(2-3), 127-139. DOI:10.1016/j.crte.2008.12.003

Ribeiro, A., Munhá, J., Fonseca, P.E., Araújo, A., Pedro, J.C., Mateus, A., Tassinari, C., Machado, G., Jesus, A. (2010). Variscan ophiolite belts in the Ossa-Morena Zone (Southwest Iberia): geological characterization and geodynamic significance. Gondwana Res, 17, 408–421

Ribeiro, A., Romão, J., Munhá, J., Rodrigues, J., Pereira, E., Mateus, A., Araújo, A. (2013). Relações tectonostratigráficas e fronteiras entre a Zona Centro-Ibérica e a Zona Ossa-Morena do Terreno Ibérico e do Terreno Finisterra. In: R. Dias, A. Araújo, P. Terrinha, J.C. Kullberg (Eds), Geologia de Portugal, vol. 1, Escolar Editora, 439-481.

Romão, J., Ribeiro, A., Munhá, J., Ribeiro, L. (2010). Basement nappes on the NE boundary the Ossa-Morena Zone (SW Iberian Variscides). European Geosciences Union, General Assembly, Vienna, Austria (Abstract).

Romão, J., Moreira, N., Pedro, J., Mateus, A., Dias, R., Ribeiro, A. (2013). Contribution to the knowledge of the tectono-stratigraphic units of the Finisterra Terrane in the Tomar region. *In*: N. Moreira, R. Dias, A Araújo, (Eds). *Geodinâmica e Tectónica Global; a importância da cartografia geológica*. 9ª Conferência Anual do GGET-SGP, Estremoz, 87-91. ISBN: 978-989-95398-3-9.

Romão, J., Moreira, N., Dias, R., Pedro, J., Mateus, A., Ribeiro, A. (2014). Tectonoestratigrafia do Terreno Ibérico no sector Tomar-Sardoal-Ferreira do Zêzere e relações com o Terreno Finisterra. Comunicações Geológicas, 101(I), 559-562.

Sanchez-Lorda, M.E., Sarrionandia, F., Ábalos, B., Carrracedo, M., Eguíluz, L., Gil Ibarguchi, J.I. (2014). Geochemistry and paleotectonic setting of Ediacaran metabasites from the Ossa-Morena Zone (SW Iberia). Int J Earth Sci (Geol Rundsch), 103, 1263–1286 DOI:10.1007/s00531-013-0937-x

Schulz, G., 1858. Atlas geológico y topográfico de Asturias. Lit. de G. Pfeiffer (2 Maps +1 Plate).

Suess, E., 1888. Das Antlitz der Erde, Vol. II. Vol. IV. F. Tempsky, Prag and Wien, and G.Freytag, Leipzig (704 p).

Teixeira, C. (1981). Geologia de Portugal. Precâmbrico-Paleozóico. Lisboa, Fundação Calouste Gulbenkian. 629p

Weil, A., Gutiérrez-Alonso, G., Johnston, S., Pastor-Galán, D. (2013). Kinematic constraints on buckling in a lithospheric-scale orocline along the northernmargin of Gondwana: a geologic synthesis. Tectonophysics, 582, 25–49.

II.

O Limite NW da Zona de Ossa-Morena; Lito-estratigrafia e Geoquímica da Região de Abrantes

A Zona de Ossa-Morena é uma das zonas paleogeográficas definidas no Terreno Ibérico, contactando nos seus domínios setentrionais com a Zona Centro Ibérica. A definição dos seus limites é um dos pontos fulcrais na evolução deste terreno tectonoestratigráfico.

A cartografia geológica da região Tomar-Sardoal-Ferreira do Zêzere e a caracterização de unidades lito e tectonoestratigráficas destintas nesta região, agora considerada como o limite NW da Zona de Ossa-Morena, permitiu individualizar sucessões com afinidades, quer à Zona Centro-Ibérica quer à Zona Ossa Morena, as quais anteriormente tinham sido todas elas consideradas como integrantes na Zona de Ossa-Morena (Pereira *et al*., 1998; Romão *et al*., 2013; 2014). Estas sucessões são separadas entre si pelo Carreamento de Ortiga-Torrão. Para além disso, nas regiões a Oeste da Zona de Cisalhamento Porto-Tomar-Ferreira do Alentejo, anteriormente também considerada como integrante na Zona Ossa-Morena, caracteriza-se uma outra sucessão com características tectonoestratigráficas próprias, agora englobados no Terreno Finisterra, que será abordado num capítulo próprio (capítulo VII). A presença de um terreno com características distintas nesta região havia sido já proposta por outros autores (*e.g.* Ribeiro *et al*., 2007; 2013; Romão *et al*., 2013), contudo nesta dissertação define-se e caracteriza-se esta sucessão.

Na região Tomar-Sardoal-Ferreira do Zêzere foram definidas três sucessões do Terreno Ibérico, apresentando afinidades distintas:

- Uma sucessão com afinidades à Zona Centro-Ibérica. A sucessão é monometamórfica e considerada como sendo do Neoproterozóico ao (?)Silúrico (Romão *et al*., 2014; Romão (coord.), 2016). A sucessão foi definida para o sector de Ferreira do Zêzere, apresentando similaridades com as sucessões típicas desta zona paleogeográfica definidas por exemplo para a região de Mação (Romão, 2000), localizada a Oeste do Carreamento de Ortiga-Torrão (Romão *et al*., 2014).
- Sucessões com afinidades à Zona de Ossa-Morena. As sucessões são compostas por um conjunto de rochas metamórficas que apresentam evidências de metamorfismo

Cadomiano e Varisco (Pereira *et al*., 2010; Henriques *et al*., 2015). Estas unidades apresentam características metamórficas distintas, o que levou Romão *et al*. (2010) a propor uma organização tectonoestratigráfica, que separa quatro "grupos tectonoestratigráficos" distintos, compostos por três fragmentos de crusta Cadomiana retrabalhada durante o Ciclo Varisco, sobre a qual se sobrepõe por uma sucessão atribuída ao Paleozóico inferior.

Estudos prévios na região de Abrantes (localizado a sul do domínio previamente descrito) conducentes à dissertação de Mestrado (Moreira, 2012) permitiram identificar a presença de um conjunto de unidades litoestratigráficas que mostram afinidades com as sucessões típicas da transição Neoproterozóico-Câmbrico da Zona de Ossa-Morena, incluindo unidades vulcano-sedimentares Cadomianas sobre as quais se sobrepõe uma sequência atribuída ao Paleozóico inferior, seguindo a organização proposta por Romão *et al*. (2010). Contudo, a intensa deformação, da qual resulta um complexo padrão estrutural, e o elevado grau metamórfico resultantes do Ciclo de Wilson Varisco dificultam a percepção das relações espaciais e, consequentemente, temporais/estratigráficas entre as diversas unidades definidas.

Esta sucessão foi alvo de reavaliação durante a tese agora apresentada. Esta reavaliação não só teve como base as relações de campo, como também adicionou um conjunto de dados de cariz petrográfico e geoquímico que permitiram não só refinar mas também suportar as correlações previamente propostas. Tal facto ganha maior importância uma vez que os contactos entre as sucessões definidas são na maioria dos casos separadas entre si por cisalhamentos resultantes das fases de deformação de idade Varisca.

A sequência estratigráfica agora definida para a região de Abrantes é assim composta por duas sucessões distintas:

- A sucessão basal é composta por três unidades com similaridades às sucessões Neoproterozóicas da Zona de Ossa-Morena. Esta sucessão de natureza siliciclástica contém um conjunto de rochas vulcânicas intercaladas, na sua maioria nas duas unidades inferiores, que apresentam características geoquímicas compatíveis com um episódio magmático de carácter anorogénico. As unidades basais desta sucessão são intruídas por um batólito granítico de idade Ediacariana intensamente deformado durante o Orógeno Varisco (Granito de Maiorga; Mateus *et al*., 2015). Este batólito é considerado como resultante dos processos colisionais associados ao Ciclo Cadomiano.

- A sucessão de topo, aqui denominada de Grupo de Abrantes, é caracterizada por um conjunto de três unidades com claras afinidades ao Câmbrico inferior da Zona de Ossa-Morena. Estas unidades apresentam uma componente não negligenciável de rochas

vulcânicas associadas à componente meta-sedimentar. Também neste caso, a assinatura geoquímica das rochas orto-derivadas é compatível com a presença de um evento de *rifting* intracontinental durante o Câmbrico inferior. A unidade basal da sequência inclui um conjunto de rochas de natureza félsica com assinatura orogénica, possivelmente resultantes da fusão da crusta Cadomiana, enquanto as duas unidades de topo contêm um conjunto de rochas básicas que mostram a presença de um evento anorogénico temporalmente concordante com a deposição destas unidades.

A sequência definida apresenta, como previamente referido, claras similaridades com as sucessões da Zona de Ossa-Morena, o que está de acordo com a localização do limite entre as duas zonas paleogeográficas do Terreno Ibérico anteriormente proposto.

Desta forma, o capítulo em causa incluirá duas secções distintas. A primeira (capítulo II.1) onde se apresenta a organização do Terreno Ibérico para o sector de Tomar-Sardoal-Ferreira do Zêzere; o texto aqui contido representará na íntegra o texto que se encontra publicado na revista *Comunicações Geológicas* em 2014, no volume especial relativo ao IX Congresso Nacional de Geologia, realizado no Porto no mesmo ano (vide referência abaixo). A segunda secção (capítulo II.2), que inclui um trabalho ainda por submeter a uma revista da especialidade, define a sucessão litoestratigráfica para a região de Abrantes, onde se apresentaram os dados cartográficos, petrográficos e geoquímicos das rochas orto-derivadas contidas nas unidades definidas. Este trabalho inclui ainda um ensaio de correlação da sucessão definida com as sucessões do Neoproterozóico-Câmbrico dos restantes sectores da Zona de Ossa-Morena.

A totalidade dos dados apresentados permitiram a conceptualização de um modelo geodinâmico evolutivo para Zona de Ossa-Morena durante o Neoproterozóico e o Câmbrico inferior. A evolução Neoproterozóica integra, para além de dados inéditos obtidos durante a elaboração desta tese, um vasto conjunto de dados previamente publicados por outros autores para a Zona de Ossa-Morena (*e.g*. Eguiluz *et al*., 2000; Linnemann *et al*., 2008; Sanchez-Lorda *et al*., 2014; Henriques *et al*., 2015) e que revelam a génese de um arco vulcânico e uma bacia de *back-arc* relacionada com a subducção Ediacariana associada ao bordo Norte da Gondwana (Ciclo Cadomiano). A sequência Câmbrica representa uma sequência sin-*rift* intracontinental, resultante do início dos processos extensivos actuantes sobre o bordo Norte da Gondwana e que leva à génese dos oceanos Variscos; esta sequência Câmbrica marca o início do Ciclo Varisco.

Abaixo menciona-se as referências específicas aos subcapítulos apresentados seguidamente, que, quando publicados, apresentam a sua referência completa:

- *Capítulo II.1*

ROMÃO, J., MOREIRA, N., DIAS, R., PEDRO, J., MATEUS, A., RIBEIRO, A. (2014), Tectonoestratigrafia do Terreno Ibérico no sector Tomar-Sardoal-Ferreira do Zêzere e relações com o Terreno Finisterra. Comunicações geológicas, 101 (Vol. Especial I), 559-562.

- *Capítulo II.2*

MOREIRA, N. *et al* (em preparação), Lithostratigraphic characterization of the Abrantes region (Central Portugal); the Cadomian to Variscan Cycle transition in the Ossa-Morena Zone.

De referir ainda que o Capítulo II.1, sendo a publicação um artigo curto publicado num volume especial no âmbito do congresso, como previamente referido, esta publicação acarreta limitações de espaço que impossibilitaram a citação de todos os trabalhos pertinentes para o efeito. Desta forma, e seguindo na íntegra o trabalho publicado, alguns trabalhos com indubitável pertinência não foram citados.

Referências

Eguíluz L., Gil Ibarguchi J.I., Abalos B., Apraiz A. (2000). Superposed Hercynian and Cadomian orogenic cycles in the OssaMorena zone and related areas of the Iberian Massif. Geol. Soc. Am. Bull., 112: 1398-1413.

Henriques, S.B.A., Neiva, A.M.R., Ribeiro, M.L. Dunning, G.R. Tajčmanová, L. (2015). Evolution of a Neoproterozoic suture in the Iberian Massif, Central Portugal: New U-Pb ages of igneous and metamorphic events at the contact between the Ossa Morena Zone and Central Iberian Zone. Lithos, 220–223, 43–59. DOI:10.1016/j.lithos.2015.02.001

Linnemann, U., Pereira, M.F., Jeffries, T., Drost, K., Gerdes, A. (2008). Cadomian Orogeny and the opening of the Rheic Ocean: New insights in the diacrony of geotectonic processes constrained by LA-ICP-MS U-Pb zircão dating (Ossa-Morena and Saxo-Thuringian Zones, Iberian and Bohemian Massifs)". Tectonophysics, 361, 21-43. DOI:10.1016/j.tecto.2008.05.002

Mateus, A., Mata, J., Tassinari, C., Rodrigues, P., Ribeiro, A., Romão, J., Moreira, N., (2015). Conciliating U-Pb SHRIMP Zircon Dating with Zircon Saturation and Ti-in-Zircon Thermometry in the Maiorga and Endreiros Granites (Ossa-Morena Zone, Portugal). X Congresso Ibérico de Geoquímica, Laboratório Nacional de Energia e Geologia, Lisboa, 38-41.

Moreira, N. (2012). Caracterização estrutural da zona de cisalhamento Tomar-Badajoz-Córdova no sector de Abrantes. Tese de Mestrado (não publicada), Universidade de Évora, 225 p.

Pereira, E., Romão, J., Conde, L. (1998). Geologia da Transversal de Tomar-Mação Sutura entre a Zona Centro-Ibérica (ZCI) e Zona de Ossa-Morena (ZOM). In: Oliveira, J. T., Pereira, R. (Eds.) Livro guia das excursões do V Congresso Nacional de Geologia, 159-188.

Pereira, M.F., Silva, J.B., Drost, K., Chichorro, M., Apraiz, A. (2010). Relative timing of the transcurrent displacements in northern Gondwana: U-Pb laser ablation ICP-MS zircon and monazite geochronology of gneisses and sheared granites from the western Iberian Massif (Portugal). Gondwana Research, 17(2-3), 461-481. DOI: 10.1016/j.gr.2009.08.006

Ribeiro, A., Munhá, J., Dias, R., Mateus, A., Pereira, E., Ribeiro, L., Fonseca, P., Araújo, A., Oliveira, T., Romão, J., Chaminé, H., Coke, C., Pedro, J. (2007). Geodynamic evolution of the SW Europe Variscides. Tectonics, 26(6), TC6009. DOI: 10.1029/2006TC002058

Ribeiro, A., Romão, J., Munhá, J., Rodrigues, J., Pereira, E., Mateus, A., Araújo, A. (2013). Relações tectonostratigráficas e fronteiras entre a Zona Centro-Ibérica e a Zona Ossa-Morena do Terreno Ibérico e do Terreno Finisterra. In: R. Dias, A. Araújo, P. Terrinha, J.C. Kullberg (Eds), Geologia de Portugal, vol. 1, Escolar Editora, 439-481.

Romão, J. (2000). Estudo Tectono-estratigráfico de um segmento do bordo SW da Zona Centro-Ibérica (ZCI) e as suas relações com a Zona de Ossa Morena (ZOM). Tese de Doutoramento (não publicada), Universidade de Lisboa, 322 p.

Romão, J. (coord; 2016), Carta Geológica à escala 1/50 000, Folha 27D – Tomar, LNEG.

Romão, J., Ribeiro, A., Munhá, J., Ribeiro, L. (2010). Basement nappes on the NE boundary the Ossa-Morena Zone (SW Iberian Variscides). European Geosciences Union, General Assembly, Vienna, Austria (Abstract).

Romão, J., Moreira, N., Pedro, J. C., Mateus, A., Dias, R., Ribeiro, A. (2013). Contribuição para o conhecimento das unidades tectono-estratigráficas do Terreno Finisterra na região de Tomar. In: Moreira, N., Dias, R., Araújo, A. (eds.), Geodinâmica e Tectónica Global; a Importância da cartografia geológica, Livro de actas da 9ª Conferência Anual do GGET-SGP, Estremoz, 87-91.

Romão, J., Moreira, N., Dias, R., Pedro, J., Mateus, A., Ribeiro, A. (2014). Tectonoestratigrafia do Terreno Ibérico no sector Tomar-Sardoal-Ferreira do Zêzere e relações com o Terreno Finisterra. Comunicações geológicas, 101(I), 559-562.

Sanchez-Lorda, M.E., Sarrionandia, F., Ábalos, B., Carrracedo, M., Eguíluz, L., Gil Ibarguchi, J.I. (2014). Geochemistry and paleotectonic setting of Ediacaran metabasites from the Ossa-Morena Zone (SW Iberia). Int J Earth Sci (Geol Rundsch), 103, 1263–1286 DOI:10.1007/s00531-013-0937-x

II.1

Tectonoestratigrafia do Terreno Ibérico no sector Tomar-Sardoal-Ferreira do Zêzere e relações com o Terreno Finisterra

Index

II.1.1. Introdução

O Terreno Autóctone Ibérico (TAI) constitui uma unidade estrutural de primeira ordem que faz parte do zonamento geotectónico da Cadeia Varisca Ibérica e compreende as zonas Centro-Ibérica (ZCI) e Ossa Morena (ZOM). É limitado a ocidente pelo Terreno Finisterra que se estende a W da zona de cisalhamento Porto-Tomar-Ferreira do Alentejo, ZCPTFA (Ribeiro *et al.,* 2007; Romão *et al*., 2013).

A região em estudo localiza-se na confluência das zonas de cisalhamento de primeira ordem: Tomar-Badajoz-Córdova, ZCTBC (WNW-ESE, cinemática esquerda, transpressiva e vergente para E) e ZCPTFA (NNW-SSE a N-S e cinemática dextra). A primeira constitui uma mega estrutura em flor, cuja zona axial ocidental constitui uma megadobra deitada em bainha vergente para WNW, resultante do efeito barreira da ZCPTFA. A outra tem sido interpretada como uma falha transformante durante o ciclo Varisco, que conecta a sutura do SW-Ibérica com a sutura NW-Ibérica, sendo uma estrutura eventualmente herdada do ciclo Cadomiano (Ribeiro *et al.*, 2007; Ribeiro *et al.*, 2013).

A cartografia geológica detalhada na região de Tomar-Sardoal-Ferreira do Zêzere (Fig. 1) permitiu reconhecer sucessões tectono-metamórficas no Terreno Finisterra com características próprias, que não são correlacionáveis com unidades da ZCI e ZOM (Romão *et al*., 2013).

O objectivo deste estudo é caracterizar as sucessões tectono-estratigráficas representativas do TAI, nas ZCI e ZOM, e referir sumariamente as relações geométricas e cinemáticas já obtidas na região que serão objecto de futuras publicações.

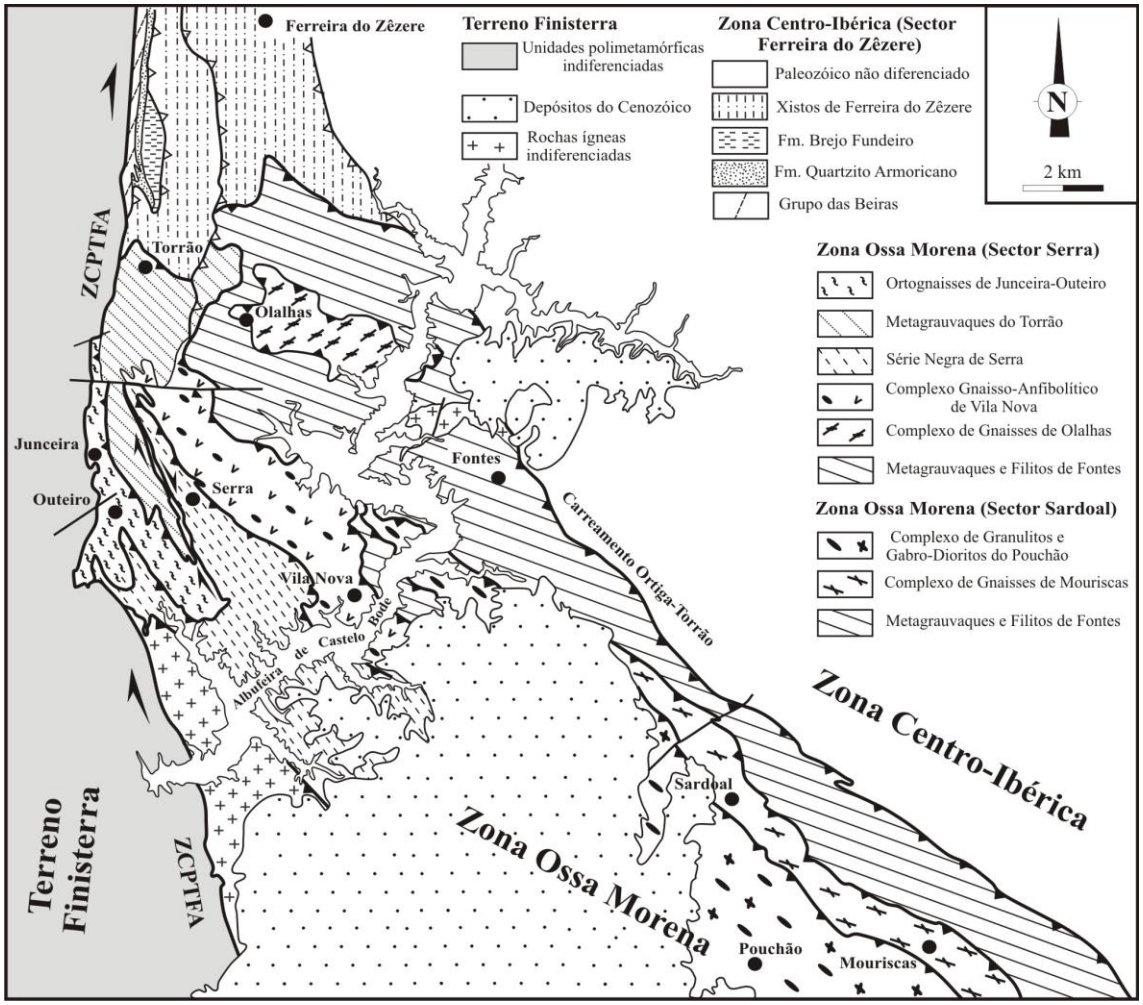

Figura 1 – Esboço do mapa geológico da região de Sardoal - Serra (Tomar) - Ferreira do Zêzere.

II.1.2. Caracterização das sucessões tectonoestratigráficas no TAI

Trabalhos de cartografia geológica recentes evidenciaram elevada complexidade nas relações entre as unidades que integram o TAI e o Terreno Finisterra.

O traçado do contacto entre a ZOM e ZCI corresponde ao carreamento de Ortiga – Torrão, de orientação geral WNW-ESE, cuja cinemática gera a sobreposição para NE de litologias da ZOM sobre sucessões litológicas imbricadas da ZCI (Fig. 1). Porém, a continuidade deste acidente e da sucessão de unidades que integram o TAI é impedida para ocidente, devido à presença da ZCPTFA, que delimita o Terreno Finisterra a oriente (Romão *et al*., 2013). Em trabalhos anteriores, o traçado deste acidente estava localizado mais a NE; a ocidente deste as unidades representadas cartograficamente eram consideradas litologias da ZOM (Pereira *et al*., 1998).

Estudos geológicos recentes permitiram estabelecer uma sucessão tectono-estratigráfica de afinidades com a ZCI na área entre o acidente que era considerado o limite entre a ZOM e a

ZCI, que designamos actualmente por cavalgamento de ribeira de S. Silvestre - ribeira de Lameirão, e a ZCPTFA. Esta sucessão é constituída, da base para o topo, por (Fig. 2A):

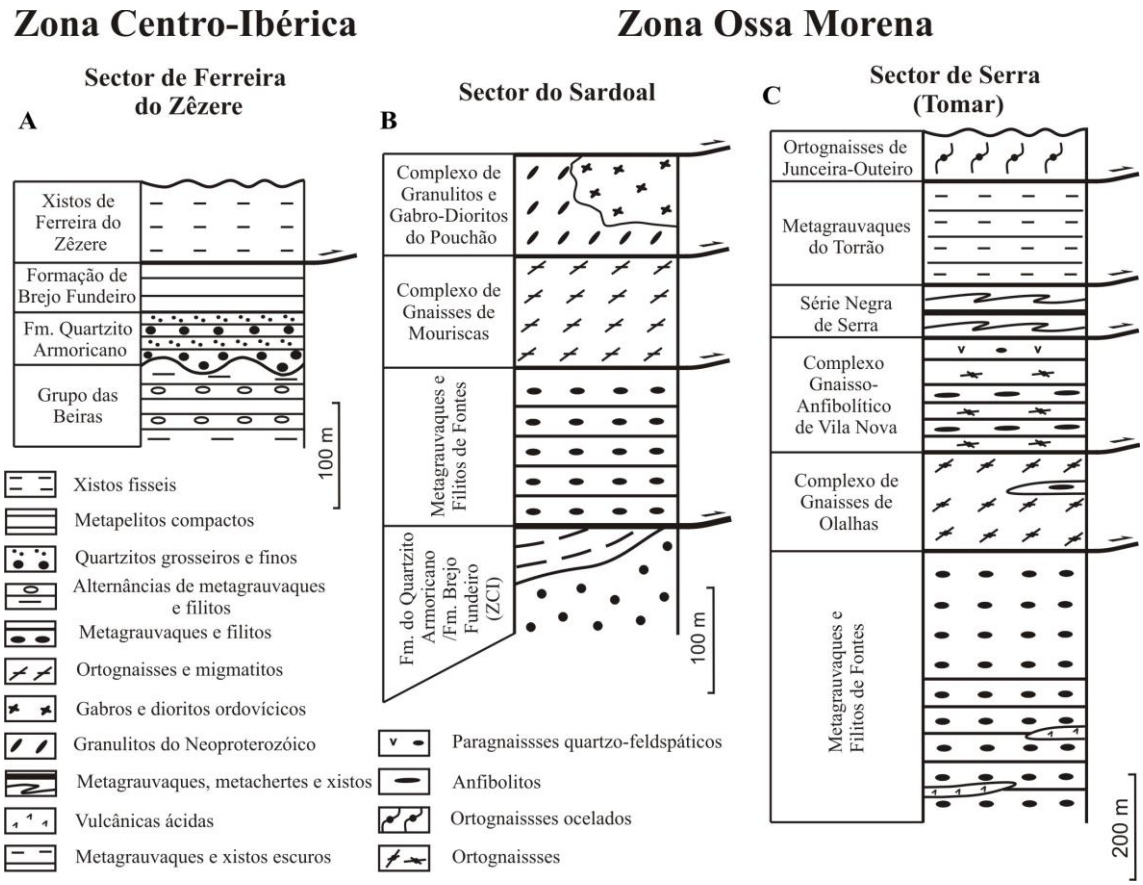

Figura 2 – Colunas tectono-estratigráficas representativas das sucessões dos sectores Sardoal e Serra (Tomar) na Zona Ossa Morena e Ferreira do Zêzere da Zona Centro-Ibérica (nomenclatura de acordo com a utilizada na Carta Geológica à escala 1:50.000, folha 27-B Tomar, LNEG).

- *Grupo das Beiras*. É limitado a ocidente pelos Ortognaisses de Couço dos Pinheiros que integram o Terreno Finisterra (Romão *et al.*, 2013) e constituído por alternâncias de filitos escuros, muitas vezes laminados, e bancadas de metagrauvaques normalmente com geometria lenticular (±100m de espessura). O Grupo das Beiras tem sido datado do Ediacariano terminal na sua base, mas o topo pode subir até ao Câmbrico (Jensen *et al.*, 2007). Sobre esta unidade surgem, em discordância, quartzitos recristalizados da unidade subsequente.

- *Formação do Quartzito Armoricano*. Aflora com particular relevância na serra de Santa Catarina e é constituída por bancadas de quartzitos, por vezes micáceos, que no geral não ultrapassam 1m de espessura, intercaladas de finos estratos de metassiltitos quartzosos e micáceos. Foram identificados icnofósseis das quais se destaca o

icnogénero *Cruziana*. A espessura estimada é de ±40m, tendo sido apontada uma idade do Câmbrico Superior ao Tremadociano (Romão *et al*., 2010).

- *Formação de Brejo Fundeiro*. É constituída por bancadas compactas e espessas de metapelitos de cor escura, intercaladas de metassiltitos milimétricos a centimétricos mais claros (±60m de espessura). Não foram encontrados fósseis que permitam datar a unidade com precisão, porém as litologias e a presença de briozoários sugerem correlações com unidades do Ordovícico Médio.

- *Xistos de Ferreira do Zêzere*. É limitada por cavalgamentos, sendo caracterizada por alternâncias de bancadas de xisto, no geral, de cor escura, e metassiltitos mais claros; ambos os litótipos apresentam espessuras milimétricas a centimétricas, cuja espessura aproximada é de ±100m. A sua idade é desconhecida; contudo, por correlação com outras unidades paleozóicas da ZCI, sugere-se que possam ser do Silúrico ou mesmo do Devónico.

A sucessão tectono-estratigráfica da ZOM foi subdividida em duas megassequências localizadas nas regiões do Sardoal e Serra (Tomar), respectivamente. A sucessão do Sardoal, com orientação NW-SE e transporte para NE, imbrica no carreamento de Ortiga–Torrão. Da base para ao topo, é constituída por (Fig. 2B):

- *Metagrauvaques e Filitos de Fontes.* Contacta a N e NE com a ZCI através do carreamento de Ortiga – Torrão e a S e SW com o Complexo de Gnaisses de Mouriscas através do cavalgamento de Casal da Igreja – Sardoal. É composta por alternâncias de metagrauvaques, muitas vezes grosseiros e quartzosos, e filitos micáceos escuros, interestratificados localmente de horizontes vulcânicos félsicos (a espessura não deverá ser inferior a 200-300m). Dados geocronológicos recentes, obtidos a partir de populações de zircões detríticos (U-Pb, LA-ICP-MS), sugerem idade criogeniana-neoproterozóica (Henriques, 2013).

- *Complexo de Gnaisses de Mouriscas*. Contacta com o Complexo Granulítico e Gabro-Diorítico de Pouchão, sendo constituído por gnaisses graníticos de granularidade fina a grosseira que passam localmente a gnaisses mais ou menos migmatizados, no geral muito deformados; interdigitados nesta unidade ocorrem pegmatitos estirados. A idade radiométrica U-Pb (método ID-TIMS) dos gnaisses finos, obtida a partir zircões ígneos, correspondeu a 569±3Ma e as monazites metamórficas produziram 540±5Ma (Henriques, 2013).

- *Complexo de Granulitos e Gabro-Dioritos de Pouchão*. É constituída por corpos de granulitos anfibolitizados, finos a grosseiros, e de gabro-dioritos indiferenciados; como

se encontram interdigitados não foi possível separá-los cartograficamente. Os primeiros corpos foram datados de 544±2Ma e 544,3±2,5Ma e os gabro-dioritos de 483±1,5Ma e 477±2Ma a partir de zircões ígneos por Henriques (2013).

As unidades estabelecidas na região de Serra (Tomar) fazem parte de uma sucessão tectono-estratigráfica alóctone, que sofreu transporte para N-NE; contactam entre si por acidentes tangenciais de baixo ângulo. Esta sucessão é constituída, da base para o topo, pelas seguintes unidades (Fig. 2C):

- *Metagrauvaques e Filitos de Fontes*. Já descrita na sucessão do Sardoal, embora mostre neste sector uma espessura acima dos 1000m, sendo que a parte superior é caracterizada por cerca de 250m de bancadas possantes de metarenitos, no geral micáceos.

- *Complexo de Gnaisses de Olalhas*. Corresponde a um *klippe,* que se sobrepõe estruturalmente à unidade já descrita no parágrafo anterior. É constituído maioritariamente por ortognaisses, por vezes ocelados, e mais subordinadamente por granulitos anfibolitizados e paragnaisses fortemente estirados (±150 a 200m de espessura). Henriques (2013) datou os ortognaisses de 590±3Ma a partir de zircões ígneos, indicando que ocorreu um pico metamórfico aos cerca de 540Ma com base nas idades de zircões metamórficos nos anfibolitos e de monazites metamórficas em ortognaisses.

- *Complexo Gnaisso-Anfibolítico de Vila Nova*. É limitada superiormente pelo cavalgamento de Casa Nova que a sobrepõe aos Metagrauvaques e Filitos de Fontes; o seu contacto inferior corresponde ao cavalgamento de Serra, responsável pelo transporte da Série Negra sobre o referido complexo. Este complexo é constituído por bandas de paragnaisses quartzo-feldspáticos de grão fino, ortognaisses, metadioritos, epidositos e anfibolitos, no geral bandados (possança de ±200 a 300m). Dados geocronológicos apontam para um pico metamórfico responsável pela génese de anfibolitos aos 540Ma (monazites) e a cristalização dos ortognaisses aos 592-603Ma em zircões ígneos (Henriques, 2013).

- *Série Negra de Serra*. É limitada pelo granito de Alverangel a SW e pela unidade Ortognaisses ocelados de Junceira - Outeiro a W; todos os limites entre as unidades referidas são efectuados por acidentes. A Série Negra é constituída por alternâncias de xistos negros e metagrauvaques escuros com intercalações de metachertes e metavulcanitos bimodais. Tem sido datada do Ediacariano, quer pelo conteúdo

fossilífero (Gonçalves & Palácios, 1984), quer por datações de zircões detríticos (Pereira *et al*., 2010).

- *Metagrauvaques do Torrão*. Limitados a N pelo carreamento Ortiga-Torrão que a coloca em contacto com a unidade Xistos de Ferreira do Zêzere da ZCI e a W pelos Ortognaisses de Junceira – Outeiro (ZCPTFA). É composta por alternâncias de bancadas de metagrauvaques e de xistos escuros, no geral micáceos (espessura estimada de ±200m). A idade é desconhecida.

- *Ortognaisses de Junceira - Outeiro*. Estão limitados a ocidente pela ZCPTFA e a oriente pelas unidades Metagrauvaques do Torrão e Série Negra de Serra, sendo os contactos efectuados por acidentes tectónicos. Esta unidade é constituída por ortognaisses no geral ocelados, com granularidade variável, de fina a média. A sua mineralogia é monótona e marcada por quartzo e feldspatos (plagioclase abundante), apresentando-se a biotite e moscovite como minerais acessórios. A idade é desconhecida, possivelmente correlacionável com os ortognaisses de Olalhas ou de Vila Nova.

II.1.3. Considerações finais

Os resultados aqui apresentados permitiram estabelecer sucessões tectono-estratigráficas em terrenos anteriormente incluídos na ZOM. De facto, foi identificada uma estrutura triangular entre o limite da ZCPTFA e o antigo cavalgamento que separava a ZOM da ZCI, onde foi identificada uma sucessão tectono-estratigráfica do Neoproterozóico ao Silúrico (?), formada por unidades caracteristicas da ZCI.

Esta sequência é truncada pelo carreamento Ortiga-Torrão, responsável pelo transporte de unidades da ZOM sobre as da ZCI. Na ZOM estabeleceram-se duas megassequências tectono-estratigráficas: uma, constituída por unidades de um autóctone relativo (região do Sardoal) e outra, onde as unidades são completamente alóctones (região de Serra, Tomar). A sucessão do Sardoal apresenta-se altamente tectonizada com critérios de transporte tangencial para NE, cavalgando sobre o autóctone Centro-Ibérico, sendo composta por unidades com caracteristicas de crosta intermédia a superior, de idade cadomiana. A megassequência de Serra (Tomar), com as mesmas tipicidades e idade similar, constitui uma sucessão alóctone imbricada, marcada por transporte para N-NE.

As sucessões monometamórfica da ZCI e polimetamórficas da ZOM e o carreamento de Ortiga-Torrão são interrompidos por efeito barreira em consequência do movimento dextro da ZCPTFA que coloca a sequência neoproterozóica do Terreno Finisterra em contacto com as sequências anteriores.

A geometria da estrutura e a síntese da evolução cinemática, prova que há duas gerações de acidentes tangenciais, em eventual continuidade; na primeira geração ocorre transporte dúctil a frágil para NE e na segunda geração, ao transporte dúctil para NW (dobra bainha na zona axial de ZCTBC, seguem-se cavalgamentos frágeis para NW e N que deslocam os acidentes para NE, quer na região de Serra quer na de Ferreira do Zêzere.

Referências

Gonçalves, F., Palácios, T. (1984). Novos elementos paleontológicos e estratigráficos sobre o Proterozóico português na Zona Ossa Morena. *Mem. Acad. Cienc. Lisboa*, 15, 225-235.

Henriques, S.A. (2013). Magmatitos e metamorfitos de alto grau no contacto entre as zonas de Ossa Morena e Centro-Ibérica: significado geodinâmico. Tese Univ. Coimbra (não publicada), 249p.

Jensen, S., Palacios, T., Marti Mus, M. (2007). A brief review of the fossil record of the Ediacaran – Cambrian transition in the area of Montes de Toledo – Guadalupe, Spain. In: P. Vickers-Rich (Eds.). The rise and fall of the Ediacaran biota. Geological Society of London, 286, 223-235.

Pereira, E., Romão, J., Conde, L. (1998). Geologia da Transversal de Tomar-Mação: Sutura entre a Zona Centro-Ibérica (ZCI) e Zona de Ossa Morena (ZOM). In: J.T. Oliveira, R. Dias (Eds.). Livro guia das excursões V Cong. Nac. Geol., IGM, 159-190.

Pereira, M.F., Silva, J.B., Drost, K., Chichorro, M., Apraiz, A. (2010). Relative timing of the transcurrent displacements in northern Gondwana: U-Pb laser ablation ICP-MS zircon and monazite geochronology of gneisses and sheared granites from the western Iberian Massif (Portugal). Gondwana Research, 17(2-3), 461-481. DOI:10.1016/j.gr.2009.08.006

Ribeiro, A., Munhá, J., Dias, R., Mateus, A., Pereira, E., Ribeiro, L., Fonseca, P., Araújo, A., Oliveira, T., Romão, J., Chaminé, H., Coke, C., Pedro, J. (2007). Geodynamic evolution of SW Europe Variscides. *Tectonics*, 26, TC6009.

Ribeiro, A., Romão, J., Munhá, J., Rodrigues, J., Pereira, E., Mateus, A., Araújo, A. (2013). Relações tectonostratigráficas e fronteiras entre a Zona Centro-Ibérica e a Zona Ossa-Morena do Terreno Ibérico e do Terreno Finisterra. *In*: R. Dias, A. Araújo, P., Terrinha, J.C. Kulberg, (*Eds*.). *Geologia de Portugal,* Vol. I. Escolar Editora, 439-481.

Romão, J., Dunning, G., Marcos, A., Dias, R., Ribeiro, A. (2010). O lacólito granítico de Mação-Penhascoso: idade e as suas implicações (SW da Zona Centro-Ibérica). *Livro de resumos do VIII Cong. Nac. Geol.* Universidade de Minho, Braga, IX-5.

Romão, J., Moreira, N., Pedro, J., Mateus, A., Dias, R., Ribeiro, A. (2013). Contribution to the knowledge of the tectono-stratigraphic units of the Finisterra Terrane in the Tomar region. *In*: N. Moreira, R. Dias, A Araújo (*Eds*.). *Geodinâmica e Tectónica Global; a importância da cartografia geológica.* 9ª Conferência Anual do GGET-SGP, Estremoz, 87-91. ISBN: 978-989-95398-3-9.

II.2

Lithostratigraphic characterization of the Abrantes region (Central Portugal); the Cadomian to Variscan Cycle transition in the Ossa-Morena Zone

Index

II.2.1. Introduction

The Iberian Massif (IM) represents the western edge of the European Variscan Chain and the lithostratigraphic record, from Neoproterozoic to Palaeozoic, reflecting a long-lasting geodynamic evolution correlative of two orogenic cycles: Cadomian and Variscan (*e.g.* Eguíluz *et al.*, 2000; Simancas *et al.*, 2004; Ribeiro *et al.*, 2007; 2009). The recognition of stratigraphic, structural, magmatic and metamorphic contrasting features allowed the subdivision of IM into different tectonostratigraphic zones. The early IM subdivision proposal is due by Lötze (1945) and afterwards other proposals are established (*e.g.* Julivert *et al.*, 1974; Ribeiro *et al.*, 1979; 1990; Quesada, 1991), however, no significantly changes for the foremost boundaries are done (Fig. 1A).

During Upper Neoproterozoic times, the Ossa-Morena Zone (OMZ) and Central Iberian Zone (CIZ) underwent distinct geodynamic evolution, as recorded by its distinct geological record. The boundary between these tectonostratigraphic zones is marked by a lithospheric shear zone, known as the Tomar-Badajoz-Cordoba Shear Zone (TBCSZ; Fig. 1A), which some authors consider a Cadomian suture (*e.g*. Ribeiro *et al.*, 2007; 2009). This shear zone includes strongly dismembered and retrograded eclogite lenses, granulites and gneisses with Neoproterozoic age (Quesada, 1991; Abalos *et al.*, 1992; Pereira *et al.*, 2006; 2010a; Ribeiro *et al.*, 2009; Henriques *et al.*, 2015), recording its polycyclic evolution. Although other authors (e.g. Linnemann *et al.*, 2008; Sanchez-Lorda *et al.* 2014; Eguiluz *et al.*., 2016) propose that the Cadomian suture was located at south of the OMZ (current coordinates), removing importance to the TBCSZ during Cadomian Cycle.

During Early Cambrian times, the OMZ and CIZ shared a common geodynamic evolution, controlled by the first stages of Variscan Cycle, however with their own features (*e.g.* Pereira *et al.*, 2006; Ribeiro *et al.*, 2007; 2009; Linnemann *et al.*, 2008; Sanchez-Garcia *et al.*, 2010). The intracontinental rifting onset, which culminate with a Variscan Ocean opening at southwest of OMZ (*e.g.* Ribeiro *et al.*, 2007; Pedro *et al.*, 2010; Sanchez-Garcia *et al.*, 2010; Moreira *et al.*, 2014a), led to the development of a set of individual basins with peculiar stratigraphic features (Oliveira *et al.*, 1991; Etxebarria *et al.*, 2006; Araújo *et al.*, 2013).

The Abrantes region was affected by intense tectono-metamorphic events during Variscan and Cadomian Cycles and the reconstruction of lithostratigraphic succession is crucial to understand the geodynamical evolution of these area. In addition, the relevance of this region relies on its location, neighbouring the OMZ and CIZ. In fact, the detailed characterization of the lithostratigraphic succession recognised in the Abrantes region supports its affinity with the OMZ sequences developed throughout the Neoproterozoic-Cambrian transition. There is no evidence to support any kind of correlation with geological units of the CIZ. This study shows the lithostratigraphic affinity of defined succession with the Neoproterozoic-Cambrian successions of OMZ, based on comprehensive lithostratigraphic and geochemical characterization, extending the OMZ until Abrantes region as initially proposed by Romão *et al.* (2010; 2014).

II.2.2. Geological setting

The Abrantes region is a key sector of the SW Iberian Variscides, offering the possibility to characterize in detail the spatial arrangement and the interference patterns related to the convergence of two first-order shear zones: the Porto-Tomar-Ferreira do Alentejo (PTFASZ), with right-lateral kinematics, and the TBCSZ, described as a sinistral transpressive shear zone

(Fig. 1). The comprehensive lithostratigraphic succession analysis is a critical step to improve significantly the current understanding of the role played by PTFASZ and TBCSZ during decisive timeframes of the geodynamic evolution occurred in Neoproterozoic-Cambrian transition times, but also during the Upper Palaeozoic times.

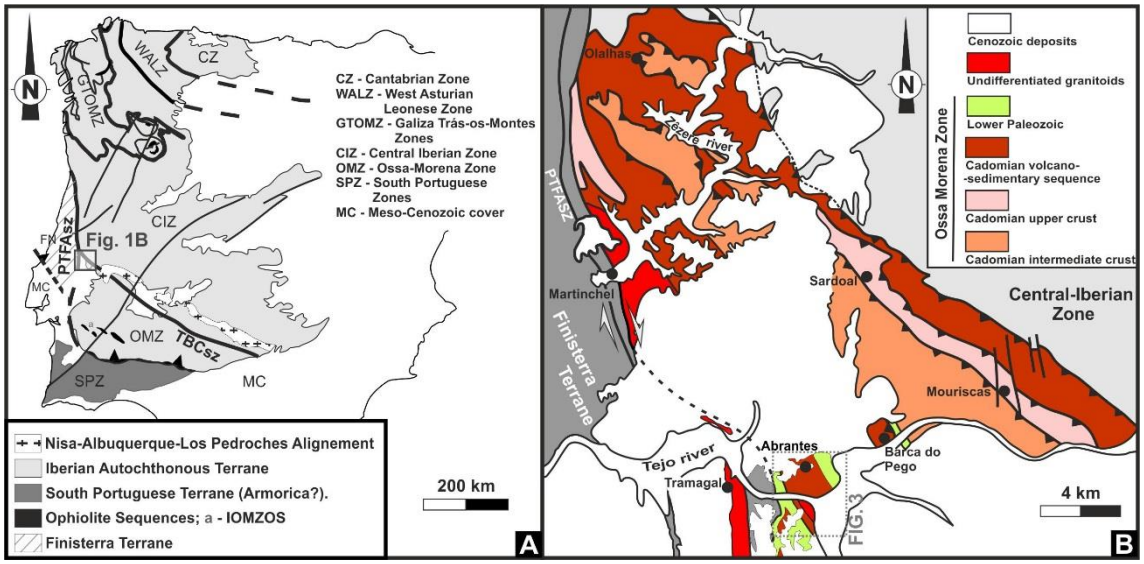

Figure 1 – Geographic and geological settings:

A – Subdivision of the Iberian Massif in tectonostratigraphic zones (modified from, e.g., Julivert *et al.*, 1974; Ribeiro *et al.*, 1990; Quesada, 1991);

B – Simplified geological map of the Tomar-Abrantes region, showing the fundamental tectonostratigraphic succession proposed by Romão *et al.* (2010), with the location of study area.

The stratigraphic sequence observed in Abrantes, devoid of fossil content and recrystallized under Greenschist to Amphibolitic metamorphic conditions (Moreira, 2012), was early considered as Proterozoic (Gonçalves *et al.,* 1979; Teixeira, 1981). The authors highlights its macroscopic resemblance with the *Série Negra* (Black Series) of OMZ. However, preliminary works (e.g. Romão *et al.,* 2010; Moreira *et al.*, 2015) show that it is possible to distinguish a typical OMZ Neoproterozoic-Cambrian succession. A tectonostratigraphic succession was proposed by Romão *et al.* (2010) for the Tomar-Abrantes region (Fig. 1B):

- A Cadomian Middle Crust composed of retrogressed granulites developed in the course of a high grade metamorphic event peaking at 539 ± 3 Ma (Henriques *et al.*, 2009) and involving a Neoproterozoic protolith;

- A Cadomian Upper Crust composed of gneissic granites with Neoproterozoic age (569±3 Ma, U-Pb in zircons; Henriques *et al.*, 2015) and metamorphosed during the Neoproterozoic-Cambrian times (ca. 545 Ma, U-Pb in monazites; Henriques *et al.*, 2015);

- A Cadomian volcano-sedimentary sequence composed of phyllites and meta-greywackes recrystallized under greenschist facies conditions, interbedded with black cherts and bimodal meta-volcanic rocks, included in the *Série Negra* Group;

- An Early Palaeozoic succession (Cambrian to Silurian) composed of bimodal meta-volcanic rocks, marbles and meta-arkoses, presenting similarities with the OMZ successions.

According to Romão *et al.* (2010), the stratigraphic succession observed in Abrantes region is composed of a Cadomian volcano-sedimentary sequence overlaid by an Early Palaeozoic cover (Fig. 1B). The lowermost units, representing the Cadomian Middle and Upper crust, only can be observed in the eastern sections of the study area (Fig. 1B).

II.2.3. Synopsys of Neoproterozoic-Cambrian successions of OMZ

The OMZ stratigraphy is usually organized in domains or sectors, emphasizing the particular stratigraphic features presented by small basins generated during the early Palaeozoic crustal thinning (e.g. Liñan and Quesada, 1990; Oliveira *et al.*, 1991; Gozalo *et al.*, 2003; Etxebarria *et al.*, 2006; Araújo *et al.*, 2013). Following, a summary of the regional Neoproterozoic and Cambrian stratigraphic characteristics can be attempted, highlighting, when necessary, the specific features recognized in some domains (Fig. 2).

II.2.3.1. Neoproterozoic succession

The OMZ stratigraphic succession begins with units assigned to the Neoproterozoic, usually forming the core of NW-SE oriented structures. From north to south, these units have been described: (1) the northern edge of the OMZ, outlined by TBCSZ and the Obejo-Valsequillo-Puebla de la Reina Domain (Apalategui *et al.*, 1990); (2) the core of the Estremoz, Olivenza-Monesterio and Vila Boim-Elvas Antiforms located in Central OMZ; and (3) in the Almadén de la Plata-Aracena and Montemor-o-Novo regions and in the core of the Moura, Viana do Alentejo and Serpa Antiforms, in the OMZ Southern Domains (*e.g.* Quesada *et al.*, 1990; Oliveira *et al.*, 1991; Eguilluz *et al.*, 2000; Lopes, 2003; Pereira *et al.*, 2006; 2012a; Araújo *et al.*, 2013; Moreira *et al.*, 2014b). Despite of local labelling, all these units are commonly included the *Série Negra* Group, formally described in Portugal by Carvalhosa (1965) and in Spain by Alia (1963) and Vegas (1968).

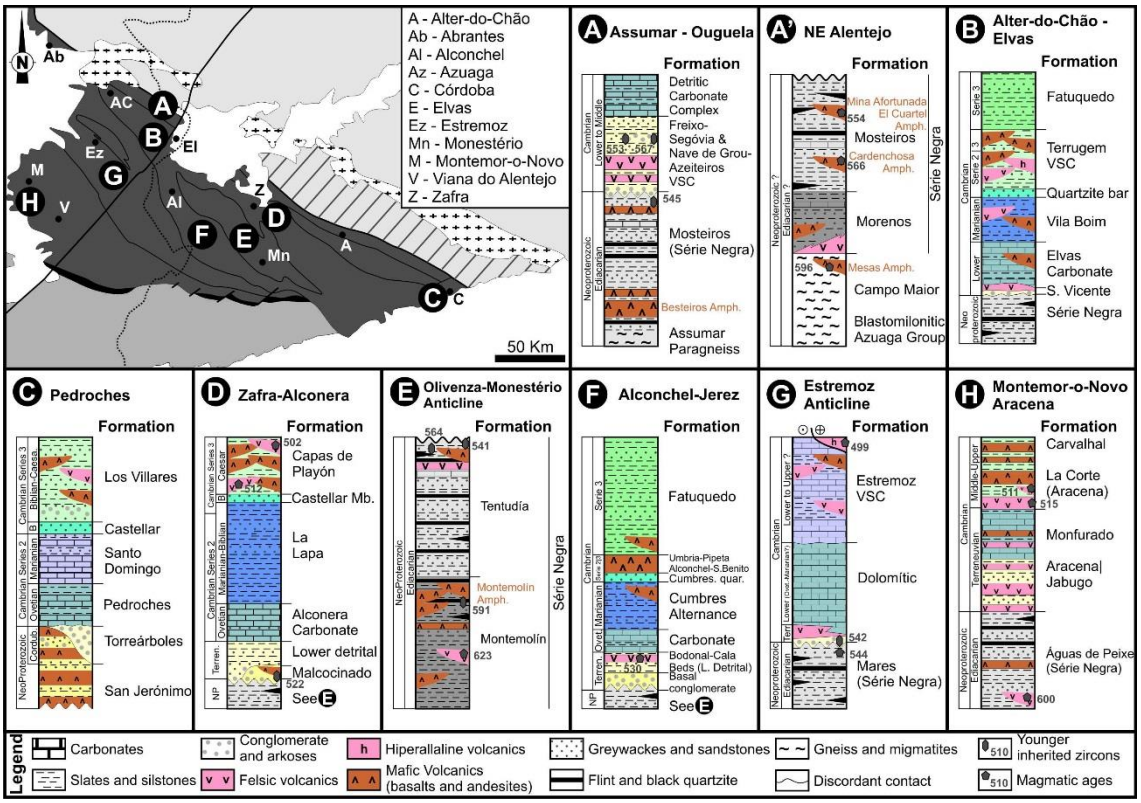

Figure 2 – Neoproterozoic-Cambrian lithostratigraphic columns of the OMZ and their location in a simplified subdivision map of OMZ proposed by Apalategui *et al.* (1990) (Columns and geochronological data adapted from: (A) Pereira *et al.*, 2006; Linnemann *et al.*, 2008; (A') – Oliveira *et al.*, 1991; Ordóñez-Casado, 1998; (B) Oliveira *et al.*, 1991; Moreira *et al.*, 2014b; (C) Ordóñez-Casado, 1998; Gozalo *et al.*, 2003; Creveling *et al.*, 2013; (D) Gozalo *et al.*, 2003; Vera, 2004; Etxebarria *et al.*, 2006; Sanchez-Gárcia *et al.*, 2010; (E) Eguíluz *et al.*, 1990; Schafer *et al.*, 1993; Fernandez-Suarez *et al.*, 2002; Vera, 2004; Sanchez-Garcia *et al.*, 2007; Ordoñez-Casado *et al.*, 2009; (F) Etxebarria *et al.*, 2006; Romeo *et al.*, 2006; Sanchez-Gárcia *et al.*, 2010; (G) Coelho and Gonçalves, 1970; Oliveira *et al.*, 1991; Pereira *et al.*, 2012a (H) Oliveira *et al.*, 1991; Ordóñez-Casado, 1998; Pereira *et al.*, 2006; Chichorro *et al.*, 2008).

In the Portuguese segment of the TBCSZ (NE Alentejo), Oliveira *et al.* (1991) describe a basal unit, beneath *Série Negra* Group, comprising moderately to strongly retrograded high-grade metamorphic rocks, namely felsic (ortho)gneisses and migmatites, associated with mafic granulites and locally including eclogite lenses (Campo Maior Formation; Fig. 2). Recent geochronological data (Pereira *et al.*, 2012b) were interpreted as indicative of an Ordovician age for the protolith of some of this (ortho)gneisses (465 ± 14 Ma; SHRIMP U-Pb in zircon). However, similar high-grade rocks, as Cerro Muriano gneiss (595 ± 30 Ma; K-Ar in feldspar – Bellon *et al.*, 1979), associated to Neoproterozoic ortho-amphibolites are also observed in the Central Unit (*e.g.* Abalos, 1989; 1992; Abalos *et al.*, 1990; 1991), being the age of high-grade metamorphic rocks dubious.

In NE Alentejo, over the basal high-grade unit, two distinct metasedimentary Formations, both included in *Série Negra* Group and recording metamorphic recrystallization under greenschist to amphibolite facies conditions (Fig. 2), was described, from bottom to top (Oliveira *et al.,* 1991):

- Morenos Formation: comprises felsic and mafic meta-volcanic rocks, black metacherts, siliceous shales, meta-arkoses and metapsammites; the top of this sequence is locally traced by calc-silicate rocks and garnet-bearing micaschists.
- Mosteiros Formation: includes a monotonous sequence of black schists, metagreywackes and metapsammites interlayered with black siliceous chemiogenic (metacherts/flints) or siliciclastic fine-grained quartzites and amphibolites (*e.g.* Oliveira *et al.*, 1991; Eguíluz *et al.*, 2000; Oliveira *et al.*, 2003; Araújo *et al.*, 2013; Fig. 2). The bottom of Mosteiros Formation succession comprises a mafic meta-volcanic member with sub-alkaline tholeiitic geochemical signature, labelled as the Besteiros Amphibolites (Ribeiro *et al.*, 2003; Pereira *et al.*, 2006).

Also in the Olivenza-Monesterio Anticline, two distinct lithostratigraphic sequences were identified (*e.g.* Eguíluz *et al.*, 1990; 2000; Vera, 2004; Ordoñez-Casado *et al.*, 2009; Fig. 2), from bottom to top:

- Montemolín Succession: composed of graphite-rich metapelites, meta-quartzwackes and biotite-bearing metapsammites, sometimes also including metagreywackes and meta-arkoses, with lenticular black quartzites, metacarbonates and amphibolites (Eguíluz *et al.*, 1990; 2000; Ordoñez-Casado *et al.*, 2009). The abundance of amphibolites increases to the top of the succession, where an important amphibolite member, with less significant metapelite and metagreywacke series, occurs (the Montemolín Amphibolites; Eguíluz *et al.*, 1990; 2000). Geochemical data in these amphibolites point to a tholeiitic affinity (Eguíluz *et al.*, 1990; Gómez-Pugnaire *et al.*, 2003; Sanchez Lorda *et al.*, 2014). The youngest age of detrital zircons extracted from metapelites on top of the Montemolín Succession indicates a maximum deposition time span around 590-580 Ma (591 ± 11; SHRIMP U-Pb in zircon, Ordoñez-Casado *et al.*, 2009), therefore constraining the depositional age of the this succession.
- Tentudía Succession: apparently in stratigraphic continuity with the Montemolín succession, but records metamorphic recrystallization under lower grade conditions. It comprises essentially a monotonous sequence of black shales, metagreywackes and black quartzites, sporadically with amphibolite lenses and metacarbonates (Eguíluz *et al.*, 1990; 2000; Quesada *et al.*, 1990; Sanchez Lorda *et al.*, 2014). A maximum deposition

age around 540-545 Ma (Ediacarian-Cambrian transition) point to the top of the *Série Negra* Group (*e.g.* Schäfer *et al.*, 1993; Fernandez-Suarez *et al.*, 2002; Chichorro *et al.*, 2008; Linnemann *et al.*, 2008; Pereira *et al.*, 2012a).

The basal section of the Olivenza-Monestério Anticline is rooted in a migmatitic core whose early (prograde) metamorphic path has been assigned to the Lower Palaeozoic geodynamic evolution (Eguíluz *et al.*, 2000; Simancas *et al.*, 2004 and references therein).

The amphibolites within Neoproterozoic successions present tholeiitic (N/E-MORB) to calc-alkaline geochemical affinity and they are interpreted as resulting from volcanic-arc development during Cadomian Cycle (Eguíluz *et al.*, 1990; Gómez-Pugnaire *et al.*, 2003; López-Guijarro *et al.*, 2008; Sanchez Lorda *et al.*, 2014). The available geochronological data for these amphibolites and other volcanic rocks apparently show two distinct steps of volcanic activity:

- ca. 630-600 Ma: 617 ± 6 Ma (U-Pb in zircon; Schäfer *et al.*, 1989) for amphibolites from TBCSZ; 645 ± 17 Ma, 610 ± 13 Ma and 585 ± 8,9 Ma (LA-ICPMS U-Pb in zircon; Sanchez-Lorda *et al.*, 2016), from El Cuartel calc-alkaline amphibolite (northern OMZ); 611 +17/-12 Ma (U-Pb in zircon; Schäfer, 1990) from the Cardenchosilla amphibolites (northern OMZ); 596 ± 14 and 577 ± 26 Ma (SHRIMP U-Pb in zircon; Ordóñez-Casado, 1998) from Las Mesas amphibolites (northern OMZ); 623 ± 3 Ma (TIMS U-Pb zircon; Sanchez-Garcia *et al.*, 2007) from meta-rhyolites of Loma del Aire; 600 ± 13 Ma (SHRIMP U-Pb zircon; Ordóñez-Casado, 1998) from granodiorites in the Lora del Rio region
- ca. 580-545 Ma: 566 ± 9 Ma (SHRIMP U-Pb in zircon, Ordóñez-Casado, 1998) and 567 ± 3 Ma (U-Pb in zircon, Schäfer *et al.*, 1988) and 580 ± 1,4 Ma (LA-ICPMS U-Pb in zircon; Sanchez-Lorda *et al.*, 2016) from La Cardenchosilla E-MORB amphibolites; 554 ± 16 Ma and 549 ± 16 Ma (SHRIMP U-Pb in zircon; Ordóñez-Casado, 1998) from El Cuartel and Calera de León amphibolites respectively; 544.2 ± 1.7 Ma, 544.3 ± 2.5 Ma and 544 ± 2 Ma (SHRIMP U-Pb in zircon; Henriques *et al.*, 2015) from Mouriscas amphibolites; 573 ± 14 Ma (SHRIMP U-Pb zircon; Bandrés *et al.*, 2004) from subvolcanic rocks related to Valle de la Serena granitic porphyry.

Unconformably on top of the Tentudía Succession, it occurs a meta-volcanoclastic sequence comprising andesites, conglomerates, psammites and pellites (Malcocinado and San Jerónimo Formations), being assigned to the Lower Cambrian age (522 ± 8 Ma; maximum age of deposition of siliciclastic series, SHRIMP U-Pb in zircons; Ordonez Casado *et al.*, 1998). The volcanic lithotypes show a calc-alkaline geochemical affinity (Sánchez-Carretero *et al.*, 1990; Pin *et al.*, 2002; Lopez Guijarro *et al.*, 2008). So far, successions alike of the Malcocinado and San Jerónimo Formations were not identified in the OMZ Portuguese segment

Considering the geochronological constraints so far determined, all the aforementioned lithostratigraphic sequences should be developed in the course of the Cadomian Cycle, thus recording the main evolving stages of OMZ during Neoproterozoic times, roughly from 630-530 Ma (Quesada *et al.*, 1990; Eguilluz *et al.*, 2000; Pereira *et al.*, 2006; 2011; Ribeiro *et al.*, 2009; Sanchez Lorda *et al.*, 2014; Henriques *et al.*, 2015).

II.2.3.2. Cambrian succession

The Cambrian succession is unconformably over the Neoproterozoic succession. This succession comprises felsic meta-volcanic rocks, metaconglomerates (including pebbles of early deformed rocks from the *Série Negra* Group), arkosic metasandstones and metapelites (*e.g.* Basal Cambrian Conglomerate, Bodonal-Cala Beds, Torreárboles, S. Vicente, Nave de Grou-Azeiteiros and Freixo-Segóvia Formation; Mata and Munhá 1990; Oliveira *et al.*, 1991; Pereira *et al.*, 2006a; 2012a; Chichorro *et al.*, 2008; Sánchez-García *et al.*, 2010; Fig. 2). Occasionally, some interbedded carbonate rocks occur within sequence, becoming progressively more abundant to the top of the sequence. Geochronological data for detrital zircons from siliciclastic horizons in the Estremoz Anticline and other correlative lithostratigraphic units in the OMZ North domains indicate maximum deposition ages around 530 Ma (Pereira *et al.*, 2006; 2012a; Linnemann *et al.*, 2008). The obtained detrital ages is consistent with magmatic ages obtained in interbedded felsic meta-volcanic rocks ages (530 $\pm$ 3 Ma, U-Pb in zircons; Romeo *et al.*, 2006). These felsic meta-volcanic rocks presents calc-alkaline geochemistry (*e.g.* Ordoñez-Casado *et al.*, 1998; Sanchez-Garcia *et al.*, 2010).

Over the previous described detrital-felsic succession, without stratigraphic unconformity, an extensive carbonate succession comprising a minor volcanic component was developed during Early Cambrian (*e.g*. Mata and Munhá, 1990; Oliveira *et al.*, 1991; Simancas *et al.*, 2004; Etxebarria *et al.*, 2006; Sánchez-García *et al.*, 2010; Moreira *et al.*, 2014b). The carbonate succession (Pedroches, Estremoz Dolomitic, Elvas Carbonated, Alconera and Carvalhal Formations; Fig. 2) includes dolomite-rich and calcite marbles and limestones, besides with occasional siliciclastic beds (*e.g.* Oliveira *et al.*, 1991; Pereira *et al.*, 2006; Chichorro *et al.*, 2008; Creveling *et al.*, 2013). These successions are assigned to Lower Ovetian to Lower Marianian (Cambrian Series 2), based on faunistic associations (*e.g.* Liñan and Quesada, 1990; Oliveira *et al.*, 1991; Gozalo *et al.*, 2003; Creveling *et al.*, 2013). Sometimes, the succession contacts directly with the *Série Negra* Group, without the basal Cambrian clastic units and the contact is an angular unconformity.

Overlapping the Lower Cambrian carbonate succession, a siliciclastic sequence with flysch characteristics is usually recognized (*e.g.* Cumbres alternances, Vila Boim and Lapa Formation; Fig. 2), with metasandstones, metapelites and rare metaconglomerates (Oliveira *et al.*, 1991; Gozalo *et al.*, 2003). Metapelites become significant to the top of sequence. Acritarch and trilobite faunas indicate a Marianian-Biblian age (Lower Cambrian; Delgado, 1905; Oliveira *et al.*, 1991; Gozalo *et al.*, 2003). Interbedded bimodal meta-volcanic rocks with tholeiitic geochemical signature occur in these siliciclastic sequence (*e.g.* Mata and Munhá, 1990; Etxebarria *et al.*, 2006; Sanchez-Garcia *et al.*, 2008; 2010). Over the Marianian-Biblian siliciclastic sequence, a micaceous quartzite package with metric thickness assigned to the Biblian period is described (Quartzite Bar and Castellar Formation; Oliveira, 1984; Oliveira *et al.*, 1991; Liñan *et al.*, 1995; Gozalo *et al.*, 2003; Araújo *et al.*, 2013).

In Middle Cambrian (Fig. 2), the deposition of siliciclastic series (metapelites, metapsammite and metagreywackes) continues, but the bimodal (subaerial and underwater) volcanic component becomes further important (Terrugem Volcano-Sedimentary Complex, Capas de Playón, Umbria-Pipeta Basalts, Los Villares and Alcoches-S. Benito Formation; Oliveira *et al.*, 1991; Sánchez-García *et al.*, 2010; Araújo *et al.*, 2013). The meta-volcanic rocks show an alkaline to alkaline-transitional composition while some felsic terms reveal a peralkaline geochemical affinity (Mata and Munhá 1990; Sanchez-Garcia *et al.*, 2010). The preserved paleontological record (trilobites, brachiopods and Acritarchs) indicates a Middle Cambrian age, ranging from Biblian to Caesarautian (Oliveira *et al.*, 1991; Gozalo *et al.*, 2003; Vera, 2004). Geochronological data in the meta-volcanic rocks are compatible with this temporal window (515-500Ma; Cambrian series 2/3; Sanchez-Garcia *et al.,* 2008; 2010).

To the top of the sequence, as volcanic component gradually decreases, meta-pelites become dominant notwithstanding the sporadic development of thick metagreywacke beds (Fatuquedo and Ossa (?) Formations; Oliveira *et al.*, 1991; Sánchez-García *et al.*, 2010; Araújo *et al.*, 2013). The Fatuquedo Formation is Middle-Upper Cambrian in age, based in acritarch faunas (Mette, 1989). The mafic meta-volcanic rocks contained in the Ossa Formation display alkaline to alkaline transitional features (Mata and Munhá, 1990).

On top of the aforementioned successions an unconformity (paraconformity?) is described, sometimes outlined by a metaconglomerate with decimetre clasts of quartzites, quartz, mafic and felsic magmatic rocks (Oliveira, 1984; Oliveira *et al.*, 1991; Sanchez-Garcia *et al.*, 2010) denoting a sedimentation (or erosional) gap. The absence of the Upper Cambrian sedimentation is a typical feature all over OMZ.

However, in Pedroches, Estremoz and Moura-Ficalho sections (Fig. 2), the Marianian-Biblian unit, or even all the Cambrian clastic units as in Estremoz and Moura-Ficalho, do not appear. In Pedroches section, a sequence of metalimestones (Santo Domingo Formation) of Marianian age with abundant interbedded siliciclastic rocks is described (Gozalo *et al.* 2003; Creveling *et al.*, 2013). In Estremoz and Ficalho-Moura section, over the Lower Cambrian Dolomite Formation, a continuous siliceous horizon is observed, being interpreted as a record of an episode of sub-aerial exposure (Oliveira, 1984; Carvalhosa *et al.*, 1987; Oliveira *et al.*, 1991) that precede the development of volcano-sedimentary complexes with abundant calcite marbles, calc-schists and interlayered bimodal meta-volcanic rocks (Mata and Munhá, 1985; Oliveira *et al.*, 1991; Araújo *et al.*, 2013).

The age of Estremoz and Ficalho-Moura volcano-sedimentary complexes is controversial, with assigned ages ranging from Cambrian to Devonian (Perdigão, 1967; Carvalho *et al.*, 1971; Oliveira, 1984; Carvalhosa *et al.*, 1987; Oliveira *et al.*, 1991). Crinoids fragments and conodonts from Ferrarias marbles (considered by some authors as stratigraphic equivalent to the Estremoz Anticline Marbles; Piçarra, 2000) seems to show an Upper Silurian-Devonian age (Piçarra and Le Menn, 1994; Piçarra, 2000; Sarmiento *et al.*, 2000). Some authors (*e.g.* Lopes, 2003; Pereira *et al.*, 2012a) argue that these ages do not correspond to the depositional age, but the presence of sub-aerial exposure and remobilization of Devonian faunal material. Recently, Pereira *et al.* (2012a) obtained a radiometric age 499.4 ± 3.3 (U-Pb, LA-ICP-MS in zircons) in rhyolites intercalated in the Estremoz marbles, proposing a Guzhangian-Paibian age (Middle-Upper Cambrian). However, the stratigraphic position of the rhyolite sample is uncertain with regard to Estremoz marbles and it is not interbedded in marble sequence (Coelho and Gonçalves, 1970), remaining the age unknown.

II.2.4. Lithostratigraphy of Abrantes region

The work performed in the Abrantes region allows to identify and characterize several lithostratigraphic units (Fig. 3 and 4), which include various rock types distinguishable on the basis of their meso-mircroscopic petrographic features.

The structure of Abrantes region is highly complex due the action of two high-strain deformation episodes (Fig. 3B; Moreira, 2012). The first one (D_1) is poorly preserved and spatially heterogeneous: in axial zone, where the older units outcrops (considered as Neoproterozoic), a low dipping foliation was generated, showing tangential transport to NW. The axial structure is poorly preserved due the action of the second deformation episode (D_2), being well-preserved in Maiorga Granite, Neoproterozoic in age (Mateus *et al.*, 2015). In both limbs of structure,

where outcrops the early units (Paleozoic related), the D_1 folds show opposite geometrical vergence, i.e. to SW in SW limb and to NE in NE limb. The D_1 episode was interpreted as result from a kilometric sheath fold associated to TBCSZ NW termination. The D_2 affects and almost totally transposes all previous structures, being associated with a high-strain dextral non-coaxial deFormation regime, induced by PTFASZ kinematics. The D_2 is characterized by the development of dextral shear zones, with intense strain partition, which rework, reorient, refold and dismember the earliest structure.

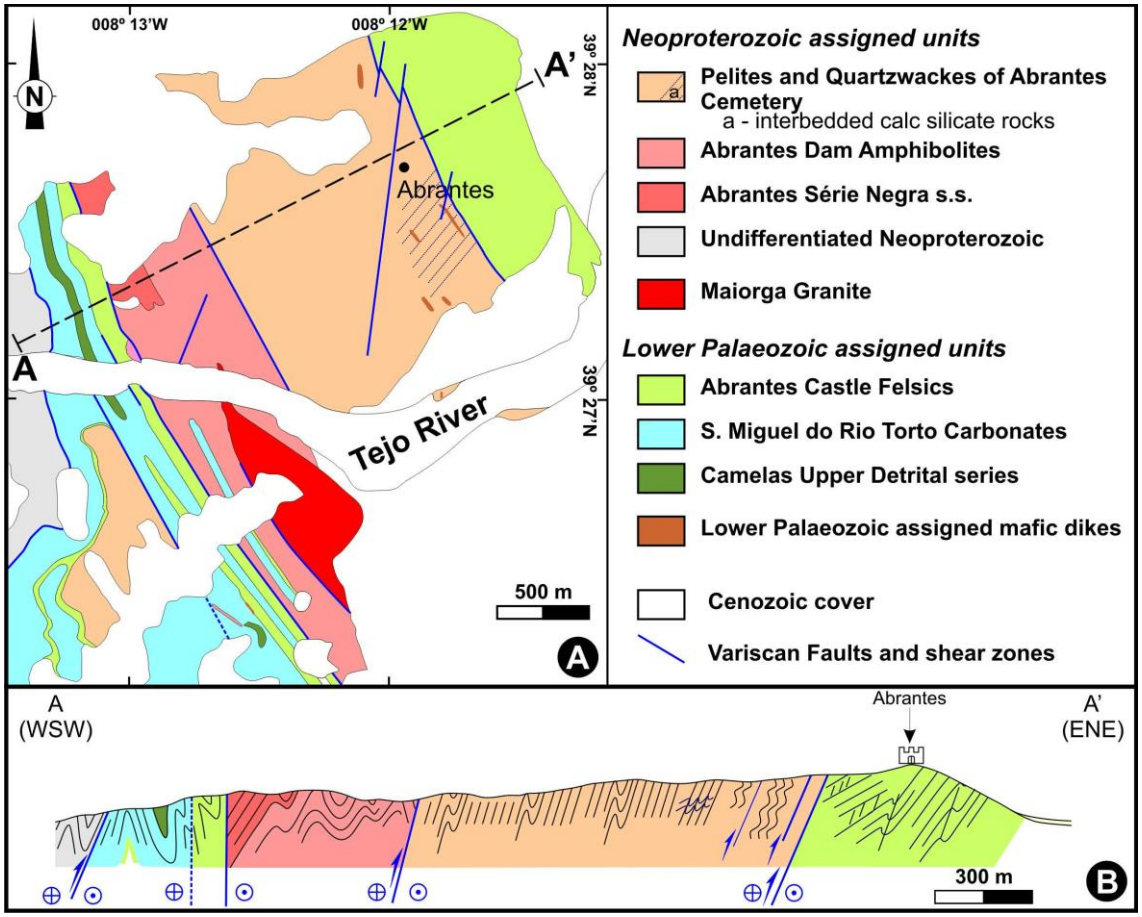

Figure 3 – Simplified geological map of Abrantes (A) and representative cross-section (B), disclosing the spatial relationship between units ascribed to Neoproterozoic and Palaeozoic (map geographic coordinates – WGS 84).

II.2.4.1. Axial zone units – Neoproterozoic related

Three distinct units were recognized in axial zone of Abrantes (Fig. 3), showing strong lithological and petrographic similarities with the Neoproterozoic sections of OMZ (Fig. 2, 4). From the apparent bottom to the top, these units were labelled as: (1) *Abrantes Cemetery Pelites and Quartzwackes,* (2) *Abrantes Dam Amphibolites* and (3) *Abrantes Série Negra s.s.*

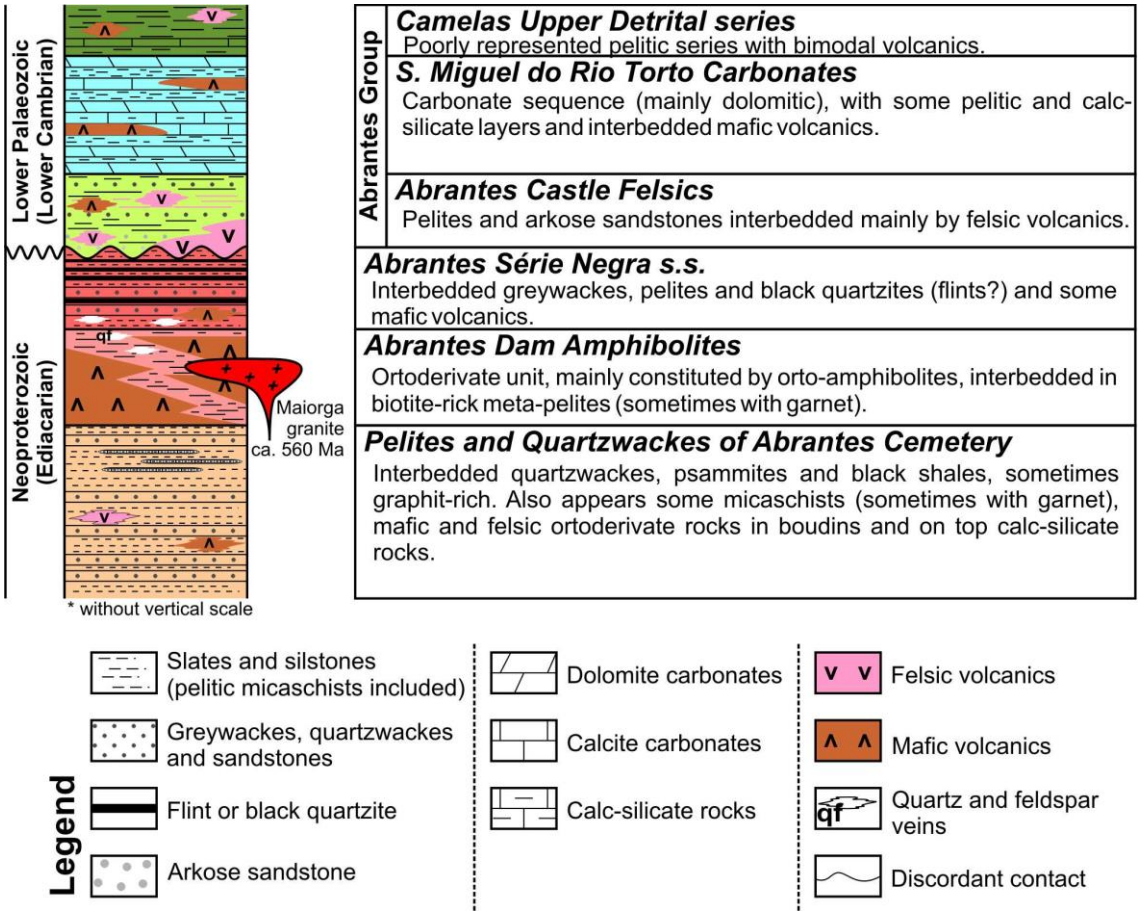

Figure 4 – Lithostratigraphic column proposal for the Abrantes region.

Abrantes Cemetery Pelites and Quartzwackes

This unit is preserved at the eastern sectors of the study area (Fig. 3). The unit is well exposed in Francisco Sá Carneiro Avenue (near Abrantes Cemetery) and in north margin of Tejo River near the Abrantes Dam.

It contacts at East with the Abrantes Castle Felsics (see section 4.2.) and at West with the Abrantes Dam Amphibolites, in both cases through Variscan shear zones. This unit is mostly composed of a siliciclastic succession (Fig. 5A and 5B), which includes decametric thick meta-quartzwackes, metagreywackes, metapsammites, dark phyllites and micaschists (both occasionally hosting thin beds of carbonate beds); heterometric quartz veins preserving evidence of multiphase deformation are present.

Micaschists are usually fine-grained and composed of quartz + biotite ± chlorite ± opaque minerals phases (Fig. 6A), sometimes involving garnet (millimetre-centimetre) porphyroblasts, possibly resulting from Variscan metamorphism blasthesis. To the East, these rocks include intercalations of carbonate beds, sometimes preserving evidences of previous deformation prior

to the Variscan Cycle (Fig. 5C). Similar carbonates also occurs disseminated within phyllites (Fig. 6B), suggesting a silicate protolith with disseminated carbonates. The carbonate features are clearly distinguished from the carbonates assigned to the Lower Palaeozoic (see description below).

In addition, the dark colours displayed by some sections of the metagreywacke/slate succession can be taken as a marker of local enrichments in carbonaceous matter, part of it possibly lately recrystallized as tiny graphite plates (Fig. 6C).

The *Abrantes Cemetery Pelites and Quartzwackes* includes lenses (often boudin-type structures) of felsic and mafic derived rocks (Fig. 5D, 6D and 6E), namely:

- very fine-grained amphibolitic schist (Fig. 6D; sample GQAB 20), with mafic nature, whose grano-nematoblastic matrix comprises strips enriched in preferentially oriented green (to bluish) amphibole interspersed with bands composed of plagioclase, quartz, muscovite and opaque mineral phases; garnet and plagioclase porphyroblasts reaching centimetre dimensions (1-2 cm; Fig. 5D) and commonly rimmed by late chlorite.
- fine-grained meta-volcanic felsic rock (Fig. 6E; sample GQAB 18) with nodular texture, presenting abundant garnet (sometimes elliptical in shape) and prismatic andalusite porphyroblasts. The matrix includes quartz + feldspar + biotite + opaque mineral phases ± muscovite. Garnet is millimetric in size and associated with green amphibole; late developed rims of biotite and chlorite outline the metamorphic retrogression path.

Abrantes Dam Amphibolites

The best unit cross-section is in the southern bank of Tejo River, near Abrantes Dam. The Abrantes Dam Amphibolites represents a volcano-sedimentary sequence, mostly composed of mafic ortho-derived rocks (Fig. 5E), being interbedded with a minor siliciclastic component (Fig. 4 and 5F).

Abundant quartz ribbons with millimetre to centimetric thick are usual; quartz display evidence of significant dynamic recrystallization leading to polygonal arrangements that preserve grains with wavy-undulatory extinction. Centimetre to decimetre lenses of quartz-feldspathic rocks can be occasionally recognized.

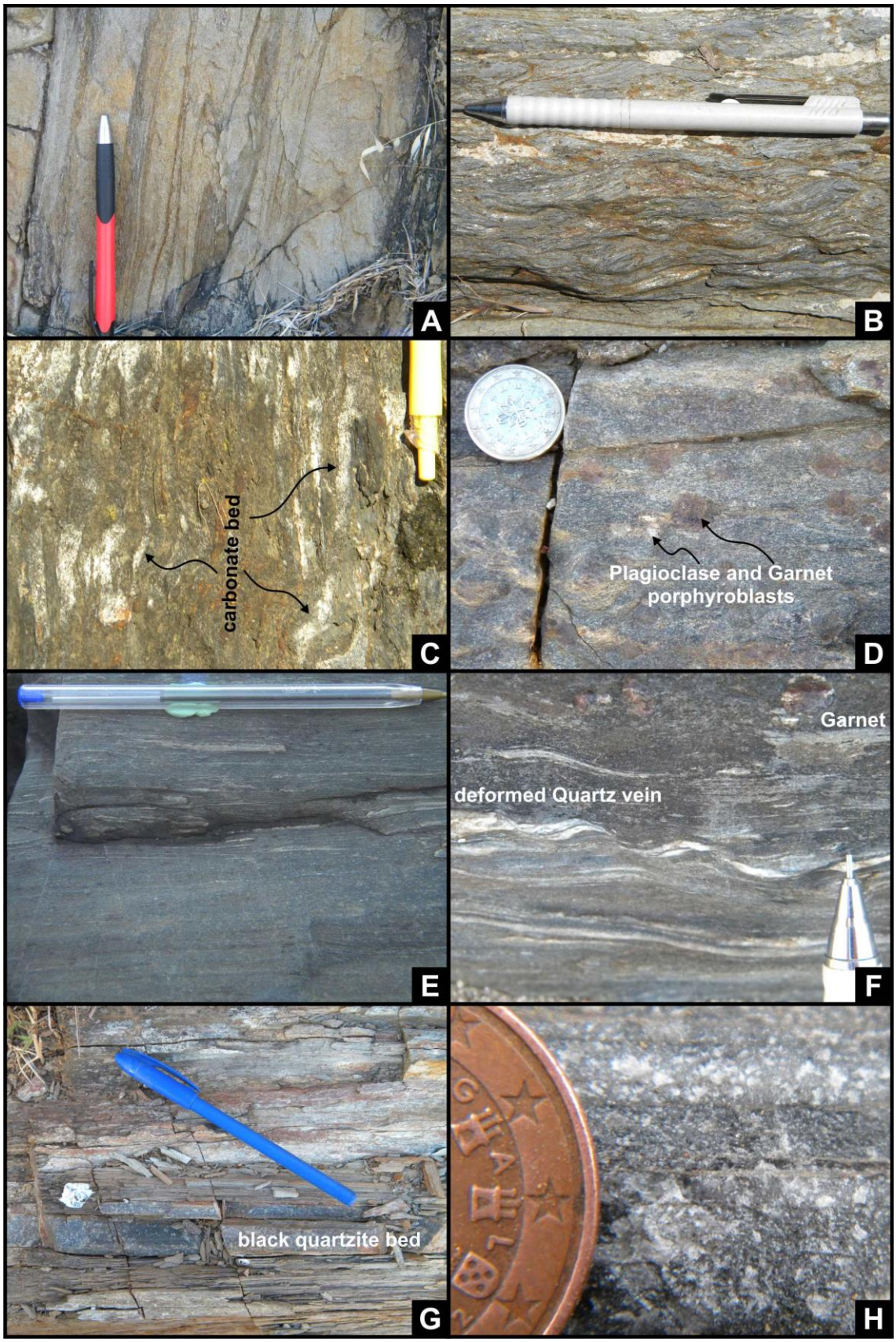
A
B
carbonate bed
C
Plagioclase and Garnet
porphyroblasts
D
E
Garnet
deformed Quartz vein
F
black quartzite bed
G
H

Figure 5 – Macroscopic features displayed by rocks types forming the Neoproterozoic assigned units:

Pellites and Quartzwackes of Abrantes Cemetery

A – Typical showing of meta-(quartz)greywacke and metapellite sequence.

B – Sheared micaschist.

C – Typical showing of micaschist interbedded with calcite metalimestone beds.

D – Typical showing of mafic/intermediate ortho-derived rock (amphibole schist), preserved in a boudin-type structure developed within siliciclastic series – Sample GQAB 20.

Abrantes Dam Amphibolites

E – Representative specimen of amphibolite – Similar to samples GQAB 5A and 5B.

F – Distinctive biotite-rich metapellite with garnet and deformed quartz veins.

Abrantes Série Negra s.s.

G – Interbedded black quartzites in black metapelites (here, the characteristic black colour is partially modified by chemical weathering).

H – Textural detail of a recrystallized black quartzite.

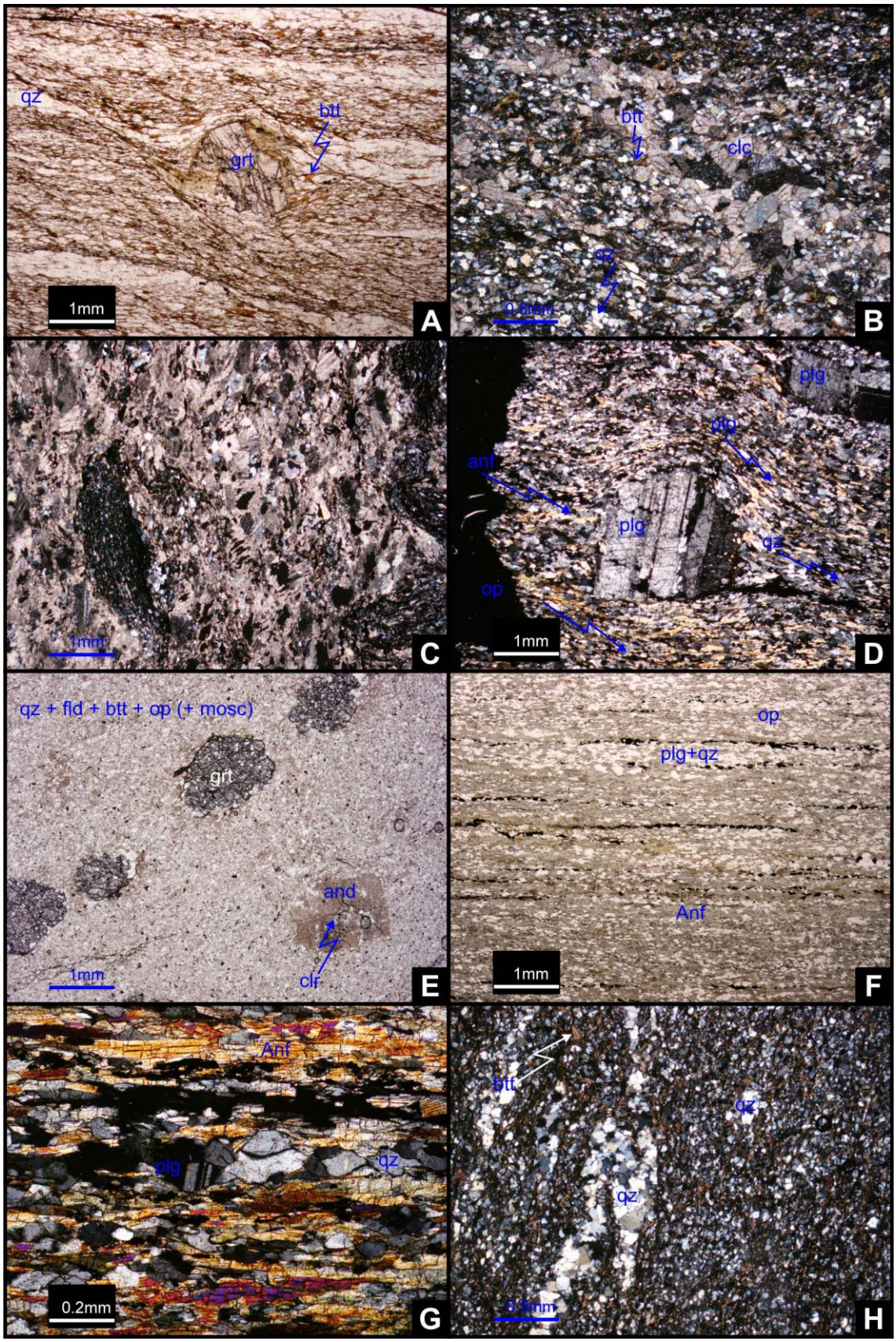
qz
btt
grt
1mm
A
btt
clc
qz
0.5mm
B
1mm
C
plg
plg
anf
plg
qz
op
1mm
D
qz + fld + btt + op (+ mosc)
grt
and
cl
1mm
E
op
plg+qz
Anf
1mm
F
Anf
plg
qz
0.2mm
G
btt
qz
qz
0.5mm
H

Figure 6 – Microscopic features displayed by rocks types forming the Neoproterozoic assigned units (mineral abbreviations according to Whitney and Evans, 2010: grt – garnet; qz – quartz; bt – biotite; cal – calcite; amp – amphibole; op – opaque minerals; pl – plagioclase; fsp – undifferentiated feldspar; ms – muscovite; and – andaluzite; chl – chlorite; zrn – zircon; dol – dolomite; gr – graphite; ep – epidote):

Pellites and Quartzwackes of Abrantes Cemetery

A – Fine-grained biotite-rich micaschist with garnet porphiroblast (parallel nicols).

B – Common carbonate matrix of micaschist, showing calcite grains dispersed in silicate minerals (crossed nicols).

C – Calcite-rich cataclastic rock, including fragments of a previous deformed graphite-rich metapelites (crossed nicols).

D – Plagioclase porphiroblast in a quatz-feldspar-amphibole matrix of a mafic ortho-derived rock (amphibole schists) interspersed in siliciclastic series as boudin-type structures (crossed nicols) – Sample GQAB 20.

E – Textural and mineralogical features of fine-grained felsic ortho-derived rock interspersed in siliciclastic series as boudin-type structure (parallel nicols) – Sample GQAB 18.

Abrantes Dam Amphibolites

F – Fine-grained oriented nematoblastic texture, showing interleaves of amphibole rich and quartz-plagioclase rich bands (parallel nicols) – Sample GQAB 5A.

G – Textural detail of a representative amphibolite (crossed nicols) – Sample GQAB 5A.

H – Fine-grained biotite-rich pelitic schist, representative of metapelites which forming this unit, showing also a deformed quartz vein (crossed nicols).

The amphibolites (Fig. 6F and 6G) comprise medium to fine-grained green amphibole + plagioclase + quartz + opaque minerals phases ± feldspar (± fine-grained, secondary muscovite related with feldspar alteration; samples GQAB 5A and 5B). The texture is strongly oriented, nematoblastic to granonematoblastic, with the development of amphibole (± opaque mineral phases) bands alternating with quartz + feldspar s.l. ones. The intense S-L fabric presented in these amphibolites and its medium to fine-grained texture seems to show the mylonitic processes associated to metamorphism. The metamorphic mineralogical assemblage, under amphibolite facies metamorphism, seems to show a mafic origin to these ortho-derived rocks. The primary texture was totally obliterates.

The siliciclastic component is represented by fine-grained biotite-rich black phyllites/schists, essentially comprising quartz + biotite ± opaque minerals phases ± undifferentiated feldspar ± garnet (Fig. 6H). It is also possible to highlight the presence of deformed quartz ribbons, exhibiting granolepidoblastic texture, polygonal textures and wavy-undulatory extinction.

Abrantes Série Negra

The Abrantes *Série Negra* ("*Black Series*") contact the Abrantes Dam Amphibolites in stratigraphic continuity. This succession are poorly outcropping and the best section to see its lithostratigraphic features is on hillside at south of Abrantes Municipal Pool Complex, in north margin of Tejo River.

The former unit includes a siliciclastic succession mainly composed of metagreywackes, metapsammites, metapellites and black slates (some of them graphite-rich); occasionally interlayered bimodal meta-volcanics can be seen.

Within this siliciclastic succession with black colours, it was recognized millimetre to centimetre thick black quartzites (or flints?; Fig. 5G and 5H). This lithotype and the low abundance of amphibolites were used as distinguish criteria between this unit and the Abrantes Dam Amphibolite Unit, which do not contain black quartzites.

4.2. Abrantes Group – Paleozoic related units

The Abrantes Group expression was firstly used by Conde (1984), although, not providing its comprehensive characterization. The same label is here reused to encompass the volcano-sedimentary units with Paleozoic litostratigraphic affinities.

Abrantes Castle Felsics

The unit cropping out in East and West of study area and it contacts with the Neoproterozoic related units through shear zones, being its stratigraphic positioning complex. The best cross-sections for this unit are, to the East, in Francisco Sá Carneiro Avenue and in northern bank of Tejo River, at West section.

This succession comprises a meta-volcano-sedimentary sequence where siliciclastic layers (psammites, pelites and arkoses), with bright colours, enclose volcanic-derived levels with rhyodacitic nature (Fig. 7); syn-metamorphic centimetre quartz veins are common. At NE, near Barca do Pego (Fig. 1B), the sequence also includes metaconglomerates.

In the eastern section of the study area (Fig. 3) the unit thickness is higher than at west and the volcanic component is more significant, locally preserving features compatible with a volcaniclastic origin (Fig. 7B; samples GQAB 17 and 28), as primary layering. The prevalent quartz-feldspar mineral assemblage is complemented by large amounts of chlorite + epidote + biotite + opaque mineral phases (mainly pyrite; Fig. 7B to 7D), which compose the thin-grained matrix. The systematic presence of preferentially oriented biotite and chlorite (+ epidote) in rock matrix indicates progression of metamorphic recrystallization under greenschist facies conditions (transitional of chlorite-biotite zones), somewhat below those achieved in axial sectors (amphibolite-greenshist transitional facies). Epidote occurs as disseminated grains within the fine-grained matrix, as well in late narrow bands/veins together with non-deformed chlorite and pyrite, cutting across early structures, possibly reflecting the retrogression path evolution or hydrothermal processes (Fig. 7C, 7D).

In the western section, the rhyodacites display an evident granoblastic equigranular texture, usually with submillimetre dimensions, and comprise abundant quartz and feldspar (along with plagioclase; Fig. 7E; sample GQAB 26), besides accessory amounts of biotite + fine-grained muscovite + zircon + opaque mineral phases (Fig. 7E). Some of these bodies are stratified, with intense dynamic recrystallization, possibly related with the Variscan metamorphic event. Locally, some amphibolite dykes are also identified (sample AB 41).

In addition, a decametric sub-volcanic rhyodacite body occurs within this unit. This body presents fine-grained equigranular mosaic texture, being composed of abundant quartz + feldspar + plagioclase, occasionally with biotite + amphibole ± muscovite (Fig. 7F).

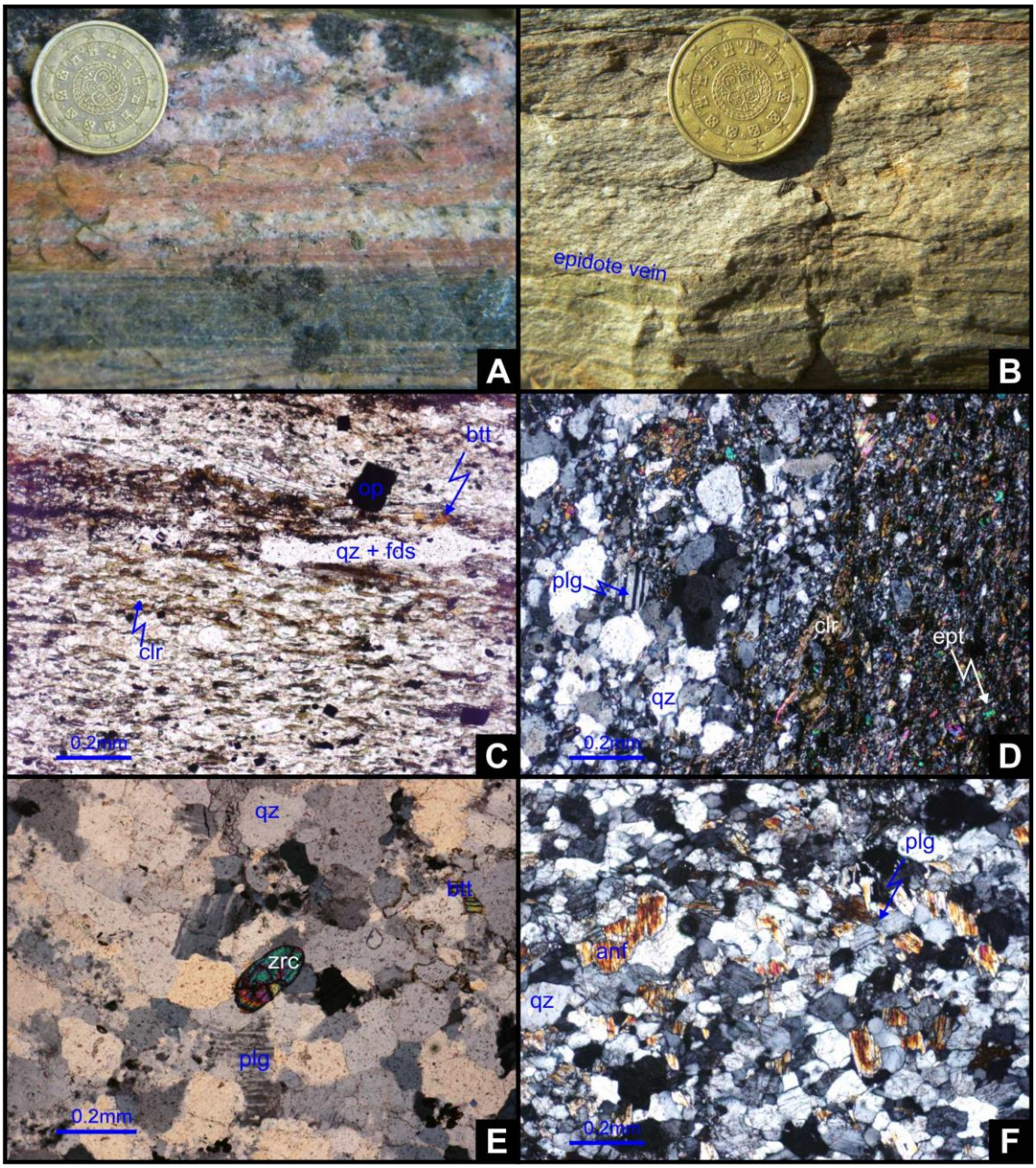
A
epidote vein
B
btt
op
qz + fds
clr
0.2mm
C
plg
clr
ept
qz
0.2mm
D
qz
btt
zrc
plg
0.2mm
E
plg
ant
qz
0.2mm
F

Figure 7 – Macro and microscopic features of Abrantes Castel Felsics (Abrantes Group – assigned to Lower Palaeozoic; mineral abbreviations as in Fig. 6):

A – Felsic banded rock cropping out at the western sector of the study area.

B – Meta-volcanic stratified rock representative of east section of the study area; note the development of epidote-bearing veins sub parallel to the primary planar structure.

C – Eastern sector meta-volcanic stratified rock, displaying late disturbance of the early oriented texture by opaque cubic minerals (pyrite), formed during the retrogression path (parallel nicols).

D – Epidote-chlorite late-developed vein cutting the meta-volcanoclastic rock in eastern sector of the study area (crossed nicols).

E – Textural and mineralogical features of a rhyo-dacite recrystallized body interbedded in volcaniclastic series (crossed nicols) – Sample GQAB 26.

F – Decametric rhyo-dacite body preserved in the eastern sector of the study area (crossed nicols).

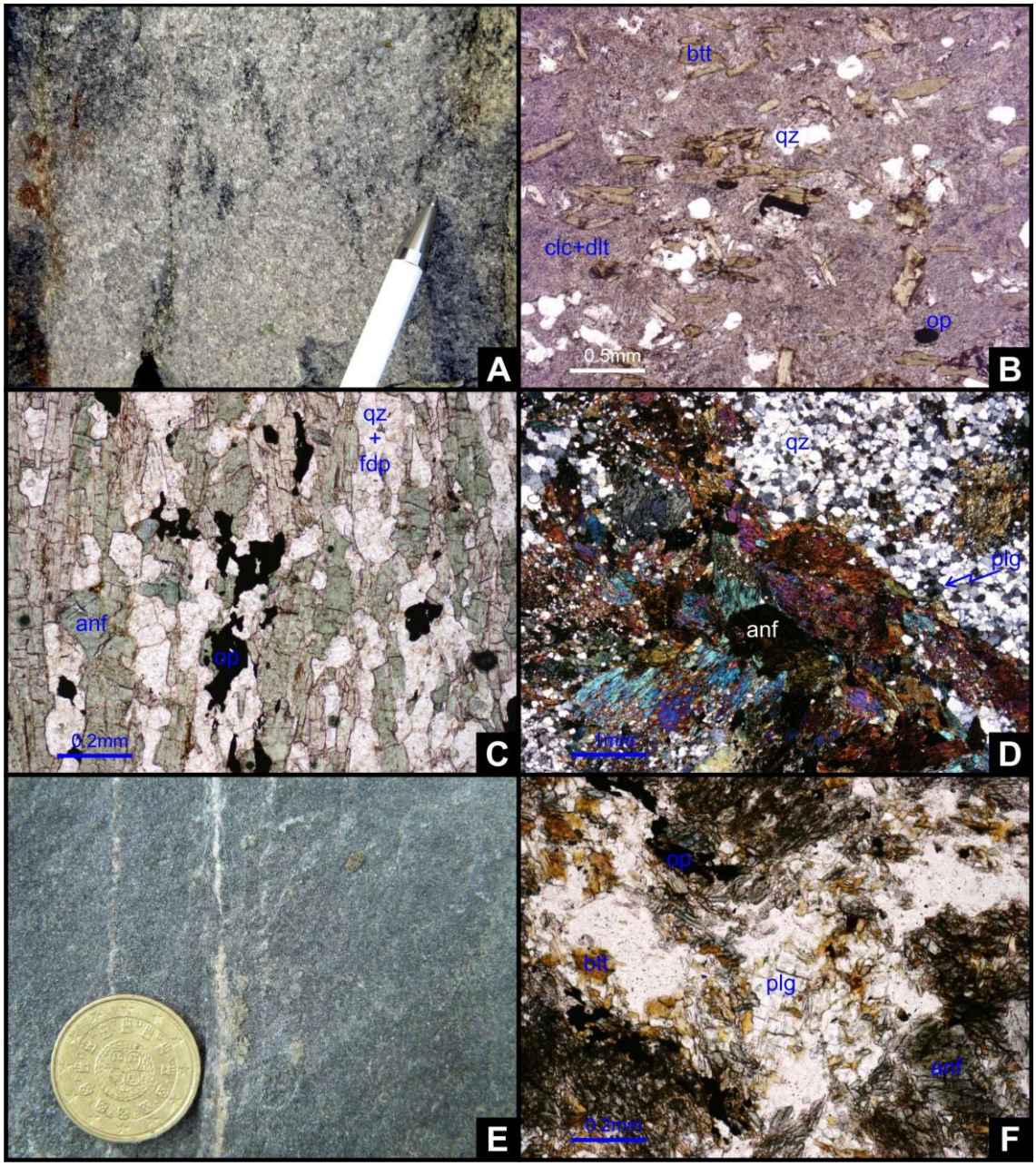
A
btt
qz
clc+dlt
op
0.5mm
B
qz
+
fdp
anf
op
0.2mm
C
qz
plg
anf
1mm
D
E
op
btt
plg
anf
0.2mm
F

Figure 8 – Macro and microscopic features of the S. Miguel do Rio Torto Carbonates and the Camelas Upper Detrital series (Abrantes Group – assigned to Lower Palaeozoic; mineral abbreviations as in Fig. 6):

A – Dolomite-rich marbles representative of the S. Miguel do Rio Torto Carbonates.

B – Typical silicate minerals (quartz and biotite) in a carbonate (calcite and dolomite) matrix (parallel nicols).

C – Nematoblastic texture of green amphibole arrays forming the mafic/intermediate ortho-derived rocks observed in the Camelas Upper Detrital series (parallel nicols) – Sample AB 46.

D – Main mineralogical constituents of mafic/intermediate ortho-derived rocks observed in the Camelas Upper Detrital series; note the evident quartz polygonal texture (crossed nicols).

E – Representtie ortho-derived fine-grained textured grey-greenish body interlayered in the S. Miguel do Rio Torto Carbonates.

F – Mafic dyke with coarse-grained texture attributed to Lower Palaeozoic, cutting the Neoproterozoic assigned units. The magmatic mineral assemblage and textures are completely obliterated by Variscan metamorphic products (crossed nicols) – Sample GQAB 14.

S. Miguel do Rio Torto Carbonates

Overlying the Abrantes Castle Felsics, a (siliciclastic-)carbonate unit is developed, being its transition gradual. The unit comprises dominant dolomite-rich marbles (Fig. 8A) with intercalations of calcite marbles and, ocassionally, calc-schists and metapelites. Evidences of secondary late dolomitization can be observed (Moreira *et al.* 2016). Usually these marbles displays pink to whitish colours but the relative abundance of disseminated epidote within the carbonate matrix may generate greenish marbles.

Carbonate rocks include a significant siliciclastic component (Fig. 8B) mainly composed of quartz (grain sizes up to centimetre) + feldspar *s.l.* + micas (biotite > muscovite); occasionally opaque mineral phases are also recognised. The abundant siliciclastic component is interpreted as a result of a proximal (continental) source. Calc-shist rocks (quartz + mica > carbonates) interbedded with marbles are scarce and display grey colours. They may represent either (felsic) volcanic-derived products highly modified by metasomatic process, or sedimentary-derived (marly limestones) products.

Commonly, black-greenish rocks within the siliciclastic sequence (Fig. 8E) are observed, forming sill-like or boudin-like bodies interpreted as (mafic) meta-volcanic-derived products synchronous of carbonate sedimentation (samples AB 40, AB 48, AB 77-A, GQAB 19). These rocks display fine-grained grano-nematoblastic texture and comprise plagioclase + amphibole + biotite + opaque mineral phases ± chlorite ± quartz ± titanite. Similar bodies intrude the Neoproterozoic assigned sequence of Abrantes Cemetery Pelites and Quartzwackes unit (sample GQAB 14), possibly representing dykes feeding the volcanic products included in the Palaeozoic assigned units. Their textures are coarse-grained and the mineral assemblage is consistent with a dolerite protolith (Fig. 8F).

Camelas Upper Detrital series

The sequence assigned to the Early Palaeozoic culminates with a late and poorly represented volcano-siliciclastic succession, occupying synfom cores (Fig. 3). The transition between this unit and the S. Miguel do Rio Torto Carbonates appears to be gradual; the basal succession also includes carbonate-rich layers that fade towards the succession's top.

The siliciclastic components prevail over those volcano-derived and comprise fine-grained rocks, namely dark-grey to black phyllites. The amphibolites display strongly oriented nematoblastic (due to amphibole grains stretching) to grano-nematoblastic (evident polygonal/mosaic of plagioclase/feldspar±quartz) textures and are composed of green to

brownish prismatic amphibole + plagioclase + opaque mineral phases + feldspar ± quartz (Fig. 8C and 8D), suggesting a mafic volcanic protolith (samples AB 46 and GQAB 25).

II.2.4.3. Geochemical data of (meta)volcanic lithotypes

In this study, for the litostratigraphic correlation between Abrantes region and the other OMZ litostratigraphic sequences, 16 samples from Abrantes were selected for whole-rock geochemical analyses: (1) two felsic rocks and two amphibolite from the Abrantes Cemetery Pelites and Quartzwackes Unit (one is considered a Cambrian dyke as previously mentioned), (2) two amphibolites from the Abrantes Dam Amphibolites Unit; (3) three felsic rocks and one amphibolite from Abrantes Castle Felsics Unit; (4) four amphibolites interbedded in S. Miguel do Rio Torto Carbonates Unit; and, finally, (5) two amphibolites from the Camelas Upper Detrital series. Join to these samples, seven samples from Alter-do-Chão-Elvas sector, near Vila Boim village, are also collected: (1) two felsic rocks from basal Cambrian Unit, (2) 4 mafic to intermediate meta-volcanic rocks interbedded in Elvas Carbonated Formation and (1) one mafic rock from Vila Boim Formation. The Vila Boim volcanic rocks was selected because in this sector the Cambrian stratigraphy was well constrained by several studies (Oliveira *et al.*, 1991; Gozalo *et al.*, 2003; Moreira *et al.*, 2014b) and it is possible to compare the geochemical fingerprint of interbedded volcanic rocks, allowing a stronger correlation.

Major and trace elements were analyzed at the Activation Laboratories - ACTLABS (Canada) using the lithium metaborate/tetraborate fusion for ICP (WRA Code 4B) and ICP-MS (WRA Code 4B2). Samples were fused with a flux of lithium metaborate and lithium tetraborate in an induction furnace. The melt mixed with 5% nitric acid containing an internal standard until completely dissolved. The samples were run for major and trace elements on a combination of simultaneous/sequential Thermo Jarrell-Ash ENVIRO II ICP. Calibration was performed using seven USGS and Canmet certified reference materials. One of the seven standards is used during the analysis for every group of samples. The sample solution prepared under Code 4B is spiked with internal standards to cover the entire mass range, is further diluted and is introduced into a Perkin Elmer Sciex ELAN 6000, 6100 or 9000 ICP-MS using a proprietary (ACTLABS) sample introduction methodology. Analytical precision and accuracy for major elements are 1 to 2% and better than 5% for trace elements. Whole-rock geochemical data and analytical methods are summarized in Table I (Abrantes) and II (Vila Boim).

II.2.4.3.1. Abrantes magmatic rocks

Besides the variation in LOI contents (Loss on Ignition; 0,43-5,31%), major element compositions and Alkalis (Na_2O+K_2O) contents vs SiO_2 (Le Maitre *et al.*, 1989; Fig. 9A1) recognize the previous subdivision in felsic and mafic rocks. The felsic rocks (two metadacites and three metarhyolites; Le Maitre *et al.*, 1989) display high contents in SIO_2 (65,54-81,50%) and lower in TiO_2 (0,25-0,71%), $Fe_2O_{3(tot)}$ (0,88-6,93%) and MgO (0,10-2,19%), while the mafic rocks (amphibolites corresponding to basalts and one trachy-basalt; Le Maitre *et al.*, 1989) display SiO_2 values lower than 51% (45,99-50,85%) and higher values in TiO_2 (1,73-3,85%), $Fe_2O_{3(tot)}$ (9,98-16,11%) and MgO (3,67-9,71%) when compared to the felsic rocks. The Al_2O_3 is homogeneous (13,38-16,11%) in mafic rocks and more variable in felsic ones (9,85-16,66%).

The data show that the felsic rocks are subalkaline with homogenous Alkalis content (5,55-6,40%; Fig. 9A1) and the projection in AFM diagram (Fig. 9A2) shows a dispersion between the tholeiitic and calk-alkaline series. Mafic rocks are plotted on alkaline and subalkaline fields with Alkalis ranging from 2,78 to 6,84% (Fig. 9A1). The data projection from mafic rocks in the AFM diagram (Fig. 9A2) shows a tholeiitic features for all samples, being projected near the Irvine and Baragar (1971) curve, exception for sample AB 46 projected in calk-alkaline series field duo to the high Alkalis content, although very closed from the curve, being an exception.

The metadacites with SiO_2 ranging between 66,08 and 67,00% and Alkalis between 5,60-6,40% are distinguish from the three metarhyolites with high silica content (77,18-81,93%) and persistent Alkalis percentage (5,55-5,72%). The metarhyolite GQAB 26 presents higher content in Na_2O (5,65%) and lower K_2O (0,07%), while the two metarhyolites (GQAB 17 and GQAB 28) presents similar contents in K_2O and Na_2O (2,20-3,23% and 2,32-3,39%, respectively).

The metadacites with Alumina Saturation Index (ASI; Frost *et al.* 2001) between 3,47 and 3,88 (Fig. 9B) are peraluminous (GQAB 16 is a ferroan-dacite and sample GQAB 18 is a magnessian-dacite). The metarhyolites have considerable contents in Al_2O_3 (9,9-11,0%) and its ASI are also consistent with peraluminous nature (1,79-2,86; Fig. 9B), although lower than the determinate in metadacites. Nevertheless, the sample GQAB 26 is more magnesian (MgO 0,93%), whereas the other two (GQAB 17 and GQAB 28) are ferriferous ($Fe_2O_{3(tot)}$ 1,8-3,2%; Fig. 9B).

As mentioned, the mafic rocks are amphibolites, corresponding to ten basalts and one trachy-basalt (GQAB 19). The amphibolites (metabasalts) present typical major elements values for mafic rocks (Al_2O_2 13,44-16,24%; K_2O 0,24-1,14%; Na_2O 2,19-4,32%; CaO 7,45-10,66%). The $Fe_2O_{3(tot)}$ (10,51-16,24%) and MgO (3,70-10,22%) values vary significantly. The samples GQAB 5B and GQAB 20 present lower contents in MgO (4,88 and 3,70% respectively) and higher $Fe_2O_{3(tot)}$

contents (14,61 and 16,24% respectively), while in the other samples the MgO (5,88-10,22%) and $Fe_2O_{3(tot)}$ contents (10,51-13,66%) are quite homogeneous. Consequently, the GQAB 5B and GQAB 20 samples presents lower #Mg (23,00-30,47) compared with the other ones (36,97-56,06). The TiO_2 content also shows this separation with higher values in GQAB 5B and GQAB 20 (3,53-3,86%) and lower ones in other samples (1,76-2,92%). Finally, the outlier amphibolite GQAB 19 (metatrachy-basalt) is distinguish from the other amphibolites because have high values of K_2O (3,10%), lower CaO content (5,09%) and in the #Mg (27,29), which reflect the higher content in $Fe_2O_{3(tot)}$ (15,96%) relatively to MgO (4,57%).

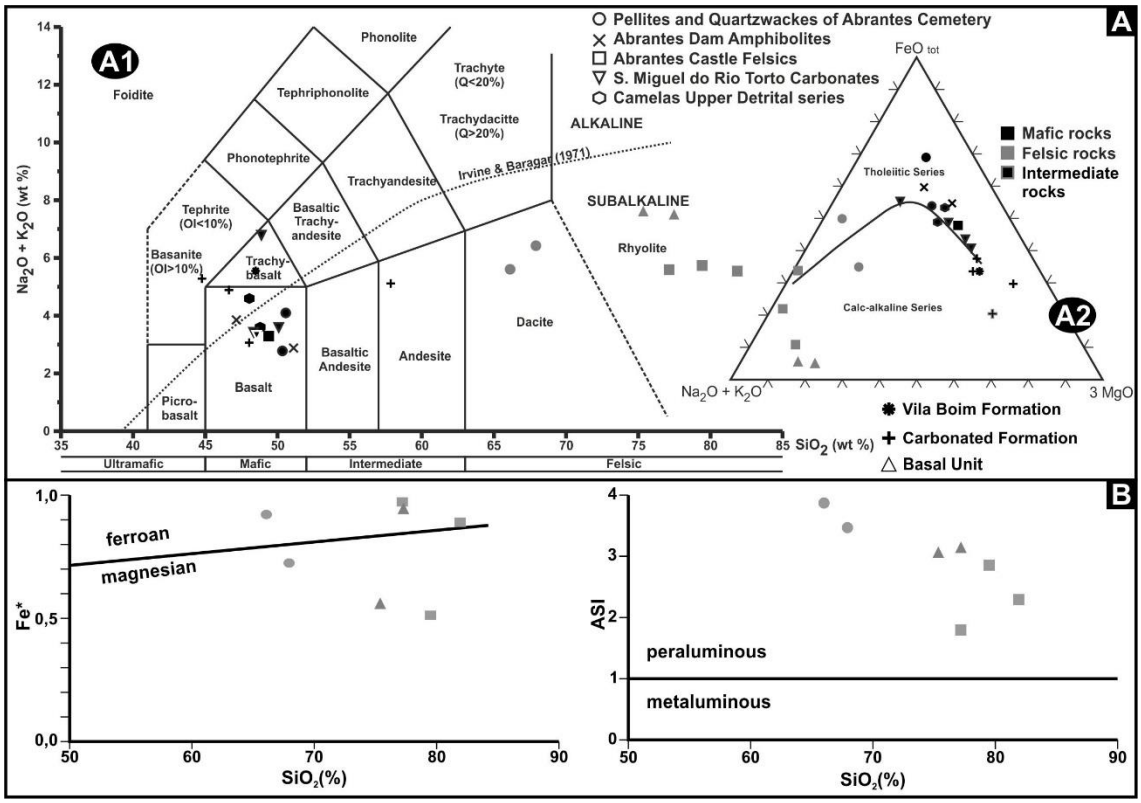

Figure 9 – Geochemical features of analysed volcanic derived rock from Abrantes and Vila Boim:

A – Total Alkalis vs. Silica diagram (A1; adapted from Le Maitre *et al.*, 1989) and AFM diagram (A2; adapted from Irvine and Baragar, 1971)

B – Fe* and ASI vs Silica diagrams applied to felsic rocks (adapted from Frost *et al.*, 2001).

Due to metamorphism and/or weathering processes the variations in the HFSE (High Field Strength Elements) like REE, Th, Nb, Ta, Zr, Hf, Ti, Y, etc. seem more reliable indicators of the igneous petrogenesis (e.g. Pearce, 1982; Rollinson, 1993), and should reflect the primary igneous features. Therefore, the geochemical data analysis and the subsequent petrogenetic interpretation will be based in the trace element geochemical variations and according with litostratigraphic correlation of units which they are sampled.

Rocks from Neoproterozoic assigned Litostratigraphic Units

This sample group includes: (1) two metadacites (GQAB16 and GQAB 18) and one amphibolite (GQAB 20) from the Abrantes Cemetery Pelites and Quartzwackes Unit and (2) two amphibolites from the Abrantes Dam Amphibolites Unit (GQAB 5A and GQAB 5B). The amphibolite interpreted as a Cambrian metadolerite dyke sampled in Abrantes Cemetery Pelites and Quartzwackes Unit will be analysed joint to the samples from Cambrian related litostratigraphic units.

The REE contents plotted in a normalized primitive mantle diagram (Fig. 10A) shows similar patterns for metadacites, nevertheless the sample GQAB18 is somewhat enriched in REE contents. Both samples present negative Eu anomalies (Eu/Eu* 0,67-0,78) and are enriched in LREE relatively to MREE and HREE ($[La/Sm]_n$ = 3,49 to 2,83; $[La/Yb]_n$ = 8,06 to 5,33). The normalized ratios between LREE and HFSE, like Nb and Th, shows a slightly to moderate enrichment in La relative to Nb ($[La/Nb]_n$ = 1,05 to 2,51) and depleted La relative to Th ($[La/Th]_n$ = 0,32 to 0,83; Fig. 10B).

The more enriched feature of sample GQAB 18, relatively to GQAB 16 (Fig. 10B), revelled by REE contents is also present in other incompatible elements like Nb, Ta, La, Sm, Zr, Tb, Y, Tm and Yb. However, Ti have lower values in GQAB 18 (3209 ppm) than in GQAB 16 (4275 ppm) and Th presents similar values (10,95±0,35ppm).

The sample GQAB 16 presents higher Th/Ta ratios (11,2), while sample GQAB 18 have lower ratio value (2,1), attributing an orogenic affinity to GQAB 16 and anorogenic features to GQAB 18 (Fig. 11A; Gordon and Schandl, 2000). A similar behaviour is also revealed by Nb-Y and Ta-Yb diagrams (Fig. 11B; Pearce *et al.*, 1984), suggesting that the ferroan-dacite (GQAB 16) can be related with orogenic magmatism, whereas the magnessian-dacite (GQAB 18) show affinities with within-plate magmatism.

The three amphibolites display variable values in REE. The REE and HSFE normalized primitive mantle plots (Fig. 10A and 10B) define two distinct patterns:

(1) Amphibolite GQAB 5A: the sample is depleted in LREE relatively to MREE and HREE ($[La/Sm]_n$ = 0,50; $[La/Yb]_n$ = 0,51), with enrichment in La relative to Nb and Th ($[La/Nb]_n$ = 2,16; $[La/Th]_n$ = 3,17) and show affinities with the HFSE patterns presented by N-MORB (Sun *et al.*, 1979; Sun and McDonough, 1989).

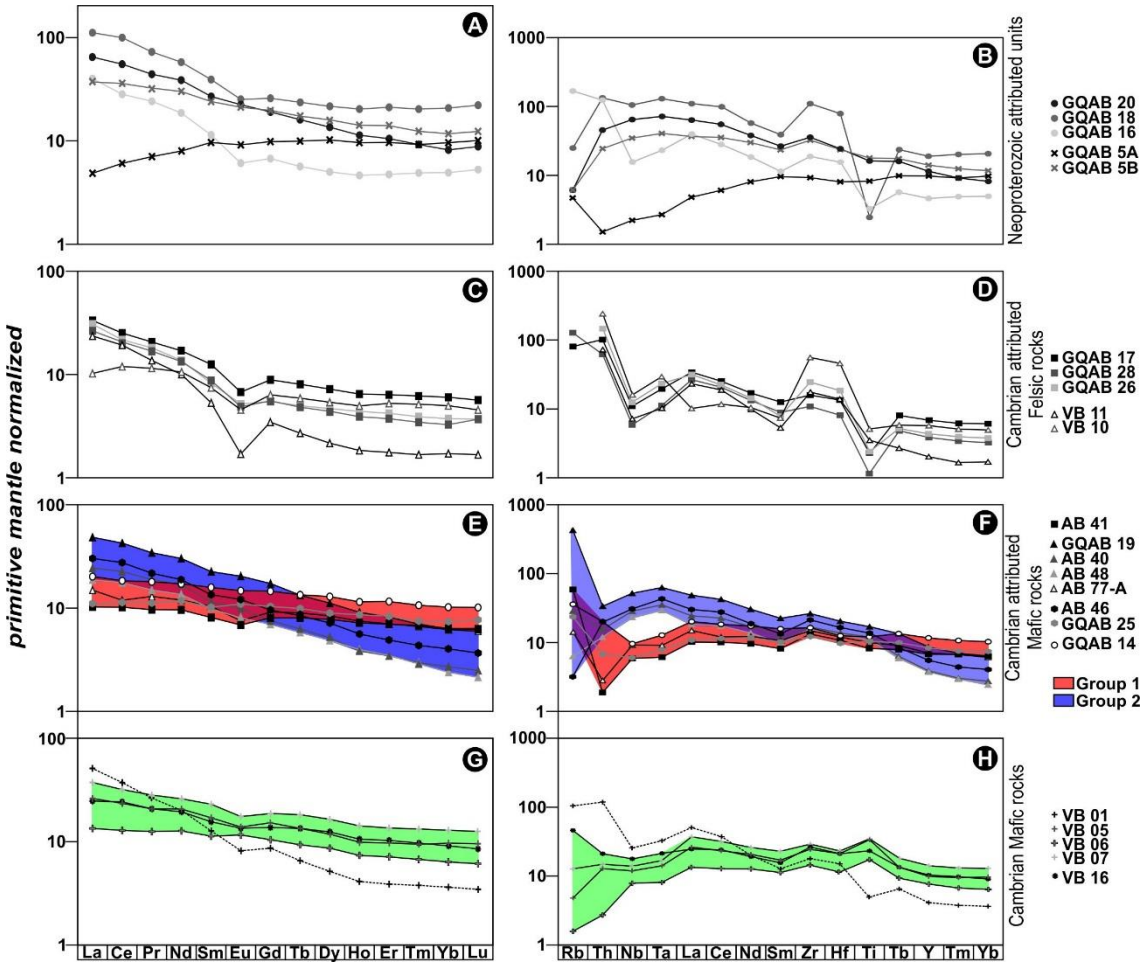

Figure 10 – Primitive mantle-normalized REE and HFSE diagrams (primitive mantle values according to Sun and McDonough, 1989).

(2) Amphibolites GQAB 5B and GQAB 20: these samples are enriched in LREE with respect to MREE and HREE ($[La/Sm]_n$ = 1,55 to 2,40; $[La/Yb]_n$ = 3,17 to 7,87). The LREE shows similar content relatively to Nb and Th ($[La/Nb]_n$ = 0,99 to 1,06; $[La/Th]_n$ = 1,42 to 1,51). However, despite the general highest values in REE in GQAB 20 sample the similar REE and HFSE patterns between these two samples, shows similarities with anorogenic basalts such as OIB and E-MORB (Sun *et al.*, 1979; Sun and McDonough, 1989).

These amphibolites do not present anomalies in Eu ([Eu/Eu*] 0,94 to 0,97). Amphibolite GQAB 5A presents [Zr/Y] = 2,3, and [Hf/Ta] = 22,7, while amphibolites GQAB 5B and GQAB 20 have higher values of [Zr/Y] (5,8 to 7,7) and lower [Hf/Ta] (2,5 to 4,4). The variations in HFSE ratios and data plot in Zr/Y vs Zr (Fig. 12A; Pearce and Gale, 1977; Pearce, 1982; 1983), Th/Yb vs Ta/Yb (Fig. 12B; Pearce, 1982) and Hf-Th-Ta (Fig. 12C; Wood, 1980) diagrams are in agreement with the REE patterns and suggest anorogenic tholeiitic fingerprints such as N-MORB (GQAB 5A) to within-plate tholeiitic to alkali-tholeiitic basalts (GQAB 5B and GQAB 20).

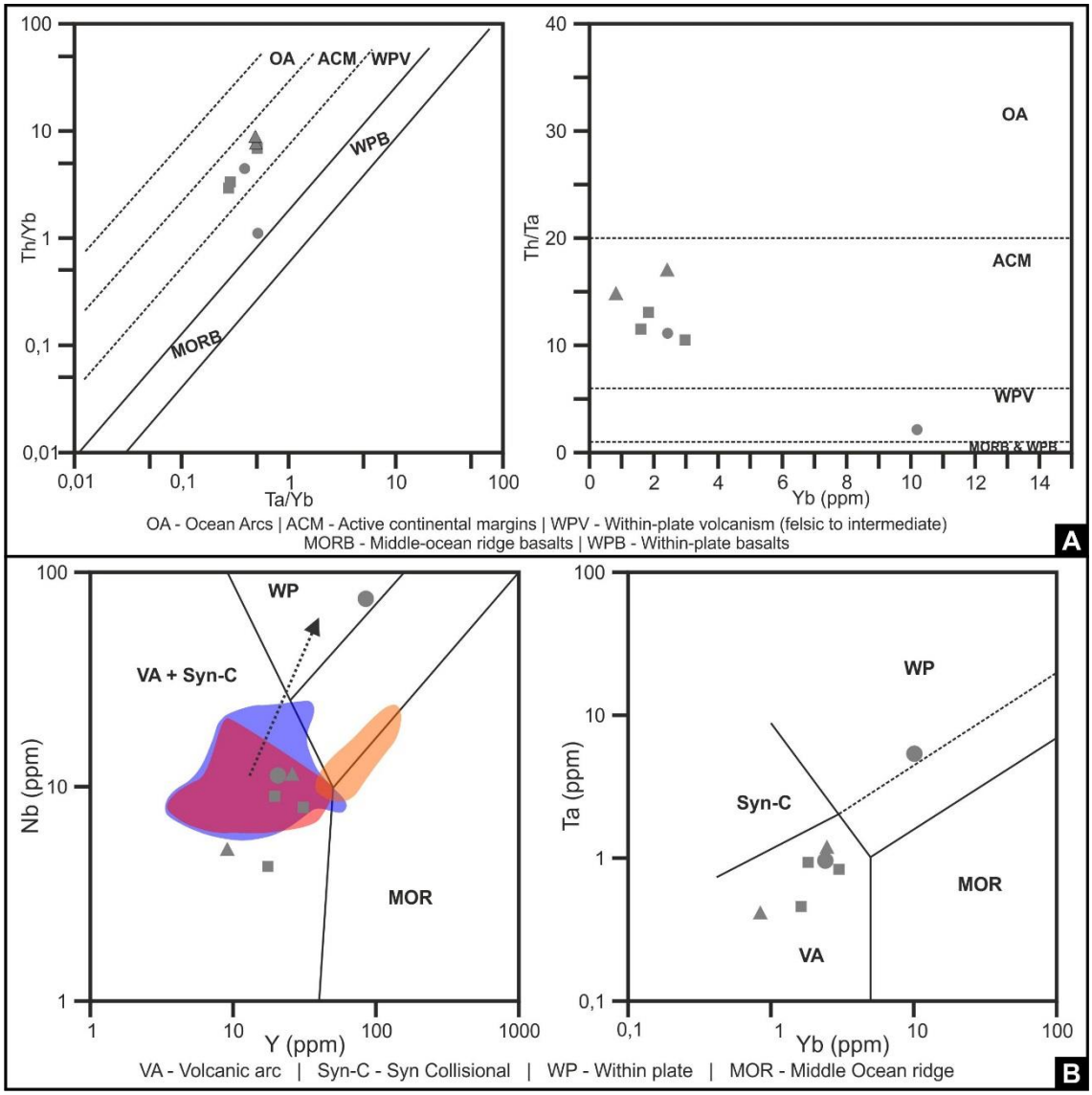

Figure 11 – Discriminant diagrams for the felsic derived volcanic rocks:

A – Th, Ta and Yb relations diagrams (adapted from Gordon and Schandl, 2000);

B – Nb vs Y and Ta vs Yb diagrams (adapted from Pearce *et al.*, 1984).

Rocks from Cambrian assigned Litostratigraphic Units

This sample group is composed of eleven samples: (1) one amphibolite (GQAB 14) considered a Cambrian dyke from the Abrantes Cemetery Pelites and Quartzwackes Unit, (2) three metarhyolites (GQAB 17, GQAB 26, GQAB 28) and one amphibolite (AB 41) from Abrantes Castle Felsics Unit; (3) four amphibolites (GQAB 19, AB 40, AB48, AB 77-A) interbedded in S. Miguel do Rio Torto Carbonates Unit; and (4) two amphibolites (GQAB 25, AB 46) from the Camelas Upper Detrital series.

The REE contents of metarhyolites, plotted in a normalized primitive mantle diagram (Fig. 10C), display patterns with negative anomalies in Eu (Eu/Eu* = 0,63-0,76), being enriched in LREE with respect to MREE and HREE ($[La/Sm]_n$ = 2,66 to 3,74; $[La/Yb]_n$ = 5,53 to 8,23). The LREE are enriched relatively to Nb ($[La/Nb]_n$ = 2,46 to 4,47) and depleted relative to Th ($[La/Th]_n$ = 0,21 to 0,42). The HFSE normalized primitive mantle diagram (Fig. 10D) display similar patterns for the three metarhyolite samples with enrichments in the more incompatible HFSE (i.e. Th, Ta, La) relatively to the less incompatible HFSE (i.e. Tb, Y, Tm, Yb) coupled with negative Ti and Nb anomalies.

The metarhyolites show a Th/Ta ratio range between 10,5 and 13,1, which are common in active continental margins (Fig. 11A; Gordon and Schandl, 2000). The same geochemical feature are assigned by Nb-Y and Ta-Yb discriminant diagrams (Fig. 11B; Pearce *et al.*, 1984), being projected in volcanic-arc volcanism field.

The amphibolites (metabasalts and metatrachy-basalt) data plot in a primitive mantle normalized REE and HSFE diagrams (Fig. 10E and 10F) display two distinct patterns:

(1) Amphibolites GQAB 14, GQAB 25, AB 41 and AB 77-A: these samples are slightly enriched in LREE with respect to MREE ($[La/Sm]_n$ = 1,07-1,43) and a little more relative to HREE ($[La/Yb]_n$ = 1,46-2,42). Two subgroup patterns can be highlighted, based in Eu contents and LREE/HFSE ratios:

(1A) The samples AB 41 and AB 77-A present negative anomalies in Eu ([Eu/Eu*] = 0,76-0,85), possibly due to fractionation of plagioclase. The LREE is slightly enriched relative to Nb ($[La/Nb]_n$ = 1,62-1,75) and highly enriched in LREE relatively to Th ($[La/Th]_n$ = 5,31-5,46).

(1B) The samples GQAB 14 and GQAB 25 do not present negative anomalies in Eu ([Eu/Eu*] = 0,97-1,07). The LREE is slightly enriched relative to Nb ($[La/Nb]_n$ = 1,80-2,11) and Th ($[La/Th]_n$ = 1,01-1,62).

In general, all the samples are depleted in more incompatible HFSE as Th, Nb and Ta (GQAB 14 presents Th, La and Ce contents slightly higher) relatively to less incompatible HFSE (Y, Tm, Yb), presenting REE patterns similar with those mentioned for anorogenic basalts such as N-MORB to T-MORB (Sun *et al.*, 1979; Sun and McDonough, 1989).

(2) Amphibolites GQAB 19, AB 40, AB 46 and AB 48: these samples do not present negative anomalies in Eu (Eu/Eu*] = 0,96-1,05). They are enriched in LREE with respect to MREE ($[La/Sm]_n$ = 1,90-2,24) and highly enriched in LREE and MREE relatively to HREE ($[La/Yb]_n$ = 7,50-9,00; $[Sm/Yb]_n$ = 3,35-422). As respect to the LREE and other HFSE relation, the LREE are slightly depleted relative to Nb ($[La/Nb]_n$ = 0,81-0,97) and slightly enriched relative to Th ($[La/Th]_n$ =

1,45-1,57). These samples present a similar pattern of incompatible elements being enriched in more incompatible HFSE (Th, Nb, Ta, La, Ce) relatively to the less incompatible (Ti, Tb, Y, Tm, Yb), which are similar to the E-MORB and OIB patterns (e.g. Sun *et al.*, 1979; Sun and McDonough, 1989).

The discrimination between these two groups is also clear in Zr/Y and Ti/Y ratios (Fig. 12A): group (1) has Zr/Y = 3,44-5,27 and Ti/Y = 293,28-413,82, while group (2) has Zr/Y = 7,65-10,81 and Ti/Y = 575,96-911,30. The Pearce and Gale (1977) and Pearce (1982; 1983) diagrams (Fig. 12A), based on previous mentioned ratios, assign the group (1) to plate margin basalts, while the group (2) are associated with within-plate magmatism.

The group (1) samples also show the previous subdivision based on Eu anomaly and LREE/HFSE ratios: the subgroup (1A), with Zr/Y = 4,84-5,27, is projected in within-plate basalts field, near the MORB field, while subgroup (1B), with Zr/Y = 3,44-3,60, is projected within MORB field (Fig. 12A). The group (2) shows higher values of Zr/Y (7,65-10,81), being projected in within-plate basalts field (Fig. 12A). Despite these variations, the data plot of the analysed mafic rocks in the Ti-Zr diagram (Pearce, 1982; Fig. 12A) show a tholeiitic trend ([Ti/Zr] = 81±9), between MORB and within plate component.

The ratios Th/Yb vs Ta/Yb discriminant diagram (Fig. 12B; Pearce, 1982) also show the two mentioned groups: the group (1) presents lower values of Ta/Yb (0,08-0,12) and Th/Yb (0,05-0,34) being projected in MORB field (subgroup (1A): [Ta/Yb] = 0,08-0,12; [Th/Yb] =0,05-0,08) and in volcanic arc-basalts near from MORB and within plate tholeiites fields (subgroup (1B): [Ta/Yb] = 0,09-0,10; [Th/Yb] = 0,16-0,34), while the group (2) samples presents higher values of Ta/Yb (0,82-1,08) and Th/Yb (0,86-0,99), being plotted in the within-plate magmatism field (Fig. 12B).

The Hf-Th-Ta (Wood, 1980) ternary discriminant diagrams allows to a better characterization of tectonic setting (Fig. 12C). The amphibolites from group (1) have a Hf/Ta = 7,50-13,60. The subgroup (1A) with highest values of Hf/Ta (10,00-13,60) is projected in the N-MORB field, while the subgroup (1B), with Hf/Ta=7,50-9,38, is plotted within N-MORB field, near the boundary with volcanic-arc basalts, and in the volcanic-arc basalts field. The samples from group (2) have a Hf/Ta ratio ranging between 2,46 and 3,25, being projected in E-MORB to within-plate tholeiites fields (Fig. 12C).

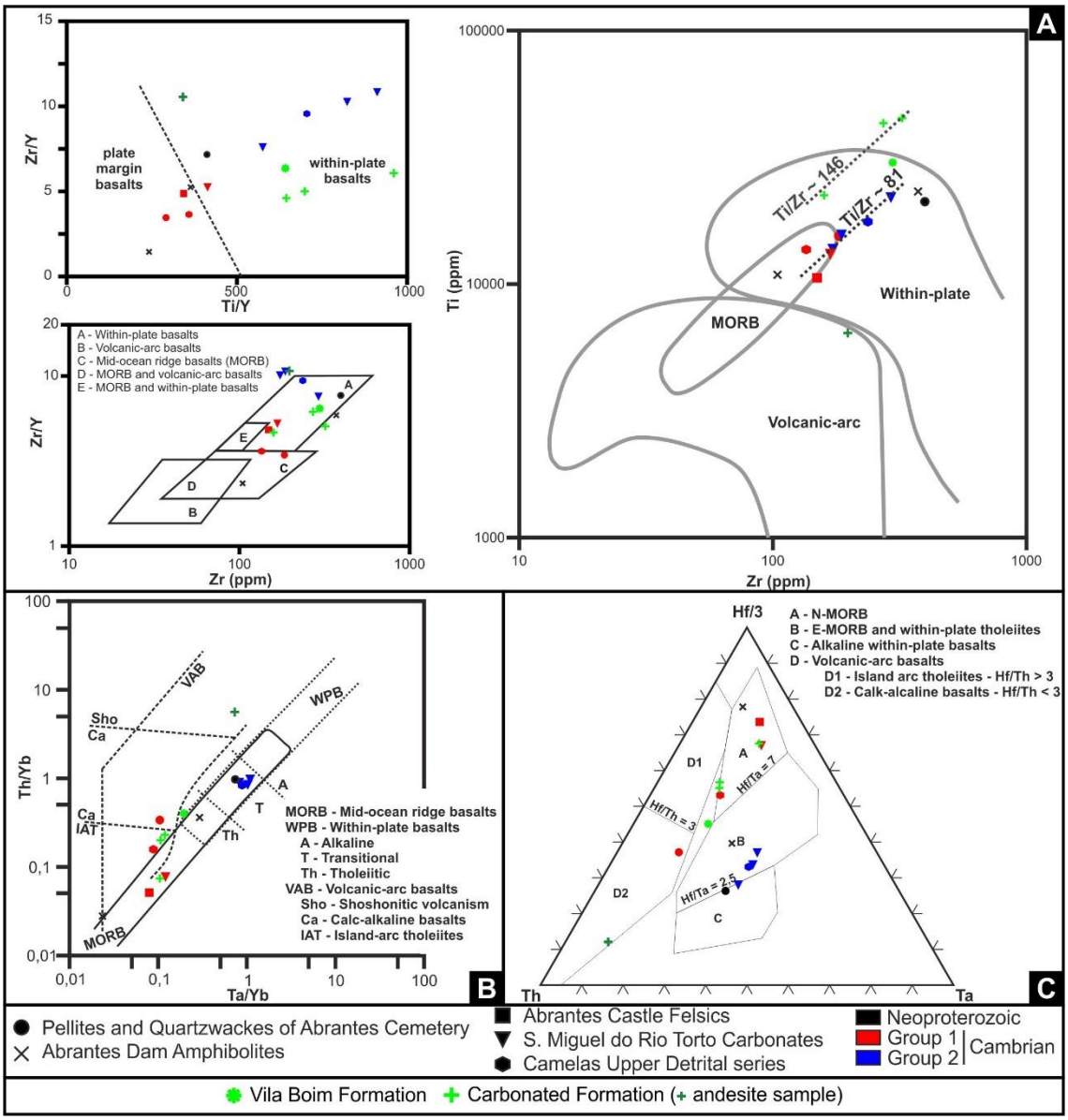

Figure 12 – Discriminant diagrams used to mafic derived volcanic rocks:

A – Ti, Zr and Y relation diagrams (adapted from Pearce and Gale, 1977; Pearce, 1982; 1983);

B – Th/Yb vs Ta/Yb diagram (adapted from Pearce, 1982);

C – Hf-Th-Ta ternary diagram (adapted from Wood, 1980).

II.2.4.3.2. Vila Boim volcanic rocks

The Vila Boim samples show higher dispersion in its geochemical nature. The Alkalis contents vs SiO_2 (Le Maitre *et al.*, 1989; Fig. 9A1) recognize two felsic (rhyolites - VB 10, VB 11), one intermediate (andesite - VB 01) and four mafic rocks (two basalts – VB 06, VB 07 –, one tephrite-basanite – VB 05 – and one trachy-basalt – VB 16). The rhyolites display high contents in SiO_2 (75,40-77,30%) and lower TiO_2 (0,45-0,67%), $Fe_2O_{3(tot)}$ (0,71-0,77%), MgO (0,05-0,68%) and Al_2O_3 (13,32-14,40%) when compared with intermediate (SIO_2 57,84%; TiO_2 0,64%; $Fe_2O_{3(tot)}$ 6,83%;

MgO 5,12%; Al_2O_3 16,99%) and mafic ones (SIO_2 44,77-48,53%; TiO_2 2,25-4,52%; $Fe_2O_{3(tot)}$ 12,27-15,32%; MgO 4,57-6,63%; Al_2O_3 14,67-15,66%). The rhyolites presents high content in Na_2O (7,36-7,54%) and lower K_2O (0,02-0,03%) and CaO (0,36-0,60%), when compared with intermediate (Na_2O 2,39%; K_2O 2,72%; CaO 7,24%) and mafic (Na_2O 2,94-5,18%; K_2O 0,09-0,71%; CaO 7,29-13,43%) volcanics,

The obtained data shows that felsic rocks are subalkaline with homogeneous Alkalis contents (7,38-7,57%; Fig. 9A1), being projected in calc-alkaline series in AFM diagram (Fig. 9A2). Mafic rocks are plotted on alkaline and subalkaline fields with Alkalis ranging from 3,06-5,56% and the intermediate rock is projected in alkaline field, showing 5,11% of Alkalis content (Fig. 9A1). The mafic and intermediate rocks are projected near the Irvine and Baragar (1971) curve in the AFM diagram (Fig. 9A2), being clearly enriched in MgO, specially the samples VB 01 and VB 06. The samples VB 01, VB 05 and VB 16 are projected in calk-alcaline field while the samples VB 06 and VB 07 are projected in tholeiitic field.

The rhyolites are peraluminous, presenting ASI between 3,06 and 3,16. Nevertheless, the sample VB10 is a ferroan-rhyolite and the VB11 is a magnessian-rhyolite, being clearly enriched in MgO when compared with VB10 (table II).

Although the mafic rocks presents distinct geochemical nature, there are no substantial variations on major elements contents. The tephrite-basanite is quite similar to basalts, with higher content in $Fe_2O_{3(tot)}$ (12,27-15,32%), CaO (8,30-13,43%), MgO (4,57-6,63%), TiO_2 (2,25-4,52), being poor in K_2O (0,09-0,12). The trachy-basalt from Vila Boim Formation (VB 16) is only distinguish from the other mafic samples because have higher K_2O values (0,71%) and lower CaO content (7,29%), being the other major elements clear similar.

The #Mg for the mafic samples range between 29,59-32,84 (VB05, VB07 and VB16) and 40,45 (VB 06), which reflect the higher content in MgO (6,63%) relatively to Fe2O3(tot) (12,80%) in VB 06 basalt. The enrichment in MgO is accompanied by a depletion in Na_2O and TiO_2 contents in this sample, which is the main distinctive feature of VB 06 basalt.

The REE patterns of Vila Boim rhyolites, plotted in a normalized primitive mantle diagram (Fig. 10C), display negative anomalies in Eu (Eu/Eu* = 0,38-0,66). They are enriched in LREE with respect to MREE and HREE ($[La/Sm]_n$ = 1,38 to 4,35; $[La/Yb]_n$ = 2,06 to 13,58).

The sample VB 11 is enriched in LREE relatively to Nb ($[La/Nb]_n$ =3,24) and depleted relative to Th ($[La/Th]_n$ = 0,32), while in the VB 10, LREE is depleted relative to Nb and highly depleted relative to Th ($[La/Nb]_n$ = 0,63, $[La/Th]_n$ =0,04). The HFSE normalized primitive mantle diagram (Fig. 10D) display similar patterns for the rhyolite samples with enrichments in the more incompatible HFSE (i.e. Th, Ta) relatively to the less incompatible HFSE (i.e. Tb, Y, Tm, Yb). It must

to be emphasized the presence of Nb and Sm negative anomaly in both samples and an enrichment in Zr and Hf. Some distinctive features are identified in rhyolite samples: the sample VB 10 is generally more enriched in HFSE elements, with exception to La and Ce, showing positive anomaly in Ta and negative anomaly in La and Ti, which are not identified in sample VB 11.

The rhyolites show a Th/Ta ratio range between 14,8 and 17,0, similar to those observed in the rhyolites from the active continental margins (Fig. 11A; Gordon and Schandl, 2000). Similar features are assigned by Nb-Y and Ta-Yb discriminant diagram (Fig. 11B; Pearce *et al.*, 1984).

The mafic and intermediate volcanic rocks data are plotted in a primitive mantle normalized REE and HSFE diagrams (Fig. 10G and 10H) display two distinct patterns:

(1) Andesite (VB 01): it is enriched in LREE with respect to MREE and to HREE ($[La/Sm]_n$ = 3,96; $[La/Yb]_n$ = 13,94). The sample present negative anomaly in Eu ([Eu/Eu*] = 0,76), possibly due to fractionation of plagioclase, being enriched in LREE relative to Nb ($[La/Nb]_n$ = 1,99) and depleted relative to Th ($[La/Th]_n$ = 0,42). The sample is enriched in Th, Ta and La relatively to less incompatible HFSE (Tb, Y, Tm, Yb). The HFSE pattern shows negative anomalies in Nd, Sm and Ti.

(2) Mafic rocks (VB 05, VB 06, VB 07 and VB 16): although the REE patterns are quite similar, two distinct behaviours are identified as respect to Eu anomaly: the sample VB-06 do not present Eu anomaly Eu ([Eu/Eu*] = 1,06) while the other samples presents a slightly negative anomaly (Eu (Eu/Eu*] =0,84-0,92). The VB 06 sample do not shows clear enrichement of LREE relative to MREE ($[La/Sm]_n$ = 1,18), being enriched relative to HREE ($[La/Yb]_n$ = 2,01), while the samples with Eu negative anomaly are slightly enriched in LREE with respect to MREE and to HREE ($[La/Sm]_n$ = 1,53-1,63; $[La/Yb]_n$ = 2,70-2,90), being slightly enriched in MREE relatively to HREE ($[Sm/Yb]_n$ = 1,70-1,78). This slightly differentiation is also clear in LREE-HFSE relation: the sample VB 06 are slightly enriched in LREE relatively to Nb ($[La/Nb]_n$ = 1,69) and highly enriched in Th ($[La/Th]_n$ =4,91) while the other samples are equally enriched in LREE relatively to Nb and Th ($[La/Nb]_n$ = 1,39-2,70; $[La/Th]_n$ = 1,17-2,50). The diagram are uniform for all the mafic rocks, presenting a horizontal pattern, being slightly enrichment in more incompatible HFSE (i.e. Th, Nb, Ta) relatively to the less incompatible HFSE (i.e. Y, Tm, Yb). The sample VB 06 presents clear depletion in Th relatively to less incompatible HFSE (Tb, Y, Tm, Yb). The patterns also show slightly positive anomalies in La and Zr, slightly negative anomalies in Sm and Hf, and clear positive anomaly in Ti. The general patterns are similar with the N-MORB to T-MORB patterns (e.g. Sun *et al.*, 1979; Sun and McDonough, 1989).

The projection of mafic rocks in the discriminant diagrams of Pearce and Gale, (1977) and Pearce (1982; 1983) indicates a within plate origin for these mafic rocks (Fig. 12A). As in Abrantes samples, also here a linear trend is defined in the Ti-Zr diagram ([Ti/Zr] = 146±3; Pearce, 1982), although in this case the ratio is higher, resulting from Ti enrichement in this samples. The Th/Yb vs Ta/Yb discriminant diagram (Fig. 12B; Pearce, 1982) show a slightly distinct geochemical fingerprint: the sample VB-06 is projected in MORB field (Ta/Yb = 0,11 and Th/Yb= 0,07), while the other samples are projected in volcanica-arc basalts field, near the boundary of MORB (VB 05 and VB 07) and within plate basalts (VB 16) fields (Ta/Yb = 0,11-0,19 and Th/Yb= 0,20-0,40). Similar behaviour is also identified in Hf-Th-Ta ternary discriminant diagram (Wood, 1980): sample VB 06 is projected in N-MORB field, the samples VB 05 and VB 07 are projected in N-MORB field, near the boundary with volcanic-arc basalts, and the sample VB 16 projected near the boundary between N-MORB, E-MORB - within-plate tholeiites and volcanic-arc fields (Fig. 12C). All the samples presents a Hf/Ta higher than 7 (7,46-11,40) typical of N-MORB's. The andesite sample present a discrepant behaviour, being generally projected in volcanic-arc fields (Fig. 12).

II.2.4.3.3. Discussion of geochemical data

The mafic and one of the felsic rocks sampled in Neoproterozoic assigned units from Abrantes presents anorogenic features. Exception to GQAB 16 metadacite, which present higher values of Th/Ta ratio, presenting an orogenic fingerprint (Gordon and Schandle, 2000).

According to Gordon and Schandl (2000), the increase of Th in felsic rocks is attributed to the contribution of a volcanic-arc component related with convergent margins (i.e. volcanic rocks are more enriched in Th with respect to Ta in subduction zones than in within-plate and mid-oceanic ridge volcanism). The enrichment in Th/Ta ratios in GQAB 16 could be interpreted by two distinct ways:

- the two dacite samples are related with the same anorogenic process and the differences can be explained due by heterogeneities in magmatic sources. According to this possibility, the GQAB 16 metadacite melting source could be a subtract with orogenic features, being enriched in Th relative to Ta, or
- the samples represents two distinct geodynamical processes acting during the Neoproterozoic times, firstly anorogenic followed by an orogenic process.

Although the amphibolites present uniform geochemical features, with anorogenic tholeiitic features, the sample GQAB 5A presents N-MORB features and the other two samples a tholeiitic (to transitional) within-plate basalts. This fact seems to show the presence of crustal stretching

processes during Neoproterozoic times, possibly related to Cadomian Cycle. Similar features are also described in other ortho-derived amphibilites as in Montemolín (Eguíluz *et al.*, 1990; Gómez-Pugnaire *et al.*, 2003; Sanchez Lorda *et al.*, 2014) and Besteiros (Ribeiro *et al.*, 2003), also attributed to Neoproterozoic.

The mafic and felsic samples sampled in Cambrian attributed units from Abrantes and from Vila Boim show geochemical features which seems to display that they are linked to continental rifting processes.

The rhyolites present higher values of Th/Ta, typical of active continental margins (Gordon and Schandle, 2000), which is also compatible with the relations between Nb-Y and Yb-Ta proposed by Pearce *et al.* (1984). However, the geological setting of these samples is not compatible with this geological ambience.

The application of discrimination diagram to first steps of Cambrian felsic volcanism is complex, since the melts generated by continental crust melting depends on the thickness and sources of continental crust composition and also the incompatibility of Th, Nb, Ta, Y and Yb, as reported by Pearce *et al.* (1984). Indeed, these kind of behaviour were also reported by Mata and Munhá, (1990) and Sánchez-Garcia *et al.*, (2008; 2010) for cambrian metarhyollites in other sectors of OMZ (Fig. 11B), being also interpreted as relate to the first steps of Variscan Cambrian extension.

The spatial (and temporal) association between felsic and mafic volcanic rocks shows a possible relation to the same geodynamic process. Indeed, all the mafic rocks, sampled in Cambrian attributed units from Abrantes and Vila Boim, present anorogenic fingerprints. The mafic rocks samples from Abrantes and Vila Boim show typical tholeiitic trend, with association between within-plate and MORB-like basalts. This trend is evident in Th/Yb-Ta/Yb, Zr/Y-Ti/Y and Ti-Zr diagram of Pearce (1982; 1983) and Pearce and Gale (1977), which seems to show that they are co-genetic.

The geochemical data shows two distinct groups in mafic rocks based in REE content:

- N-MORB to T-MORB, sometimes with negative anomalies in Eu and a slightly enrichment in Th. This fact could result from the magma migration process, followed by a differentiation process with crystallization of plagioclase. During the migration process, the magma could have contamination with continental crust rocks, which could explain the enrichment in Th. This possibility could explain the projection of some samples within or near from volcanic-arc basalts field on Wood (1980) and Pearce (1982) diagrams (Fig. 12), and

- a group more enriched in LREE relative to previously mentioned, that contain a REE and HFSE patterns similar to E-MORB/OIB. The discriminant diagrams corroborate its tholeiitic anorogenic fingerprint, attributing a within-plate nature to these mafic rocks.

In summary, the samples collected in Cambrian attributed units from both localities presents tholeiitic anorogenic features, presenting bimodal nature, emphasizing the continental stretching during Cambrian times, compatible with Variscan Ocean opening during Ordovician Times (Pedro *et al.*, 2010; Sánchez-Garcia *et al.*, 2010).

II.2.5. Stratigraphic Correlation Analysis

The stratigraphic succession described for the Abrantes region shows similarities with the Neoproterozoic-Cambrian sequences defined for diverse sectors of the OMZ, such as the Alter-do-Chão-Elvas domain, where Vila Boim samples are provided. Due to the absence of geochronological and paleontological data supporting the stratigraphic correlations, the proposal assigning ages for the units forming the Abrantes stratigraphic succession will be based on standard lithostratigraphic relationships with Neoproterozoic-Lower Cambrian stratigraphic sequences established for other sectors of this paleogeographic zone (*e.g.* Liñan and Quesada, 1990; Oliveira *et al.*, 1991; Gozalo *et al.*, 2003; Etxebarria *et al.*, 2006; Pereira *et al.*, 2006; Araújo *et al.*, 2013; Fig. 13 and 14), also using the geochemical data from volcanic rocks to strengthen this correlation.

The Abrantes Neoproterozoic assigned units could be correlate with units included in the Neoproterozoic *Série Negra* Group of the NE Alentejo sector (*e.g.* Quesada *et al.*, 1990; Oliveira *et al.*, 1991; Eguíluz *et al.*, 1995) and the Olivenza-Monesterio Antiform (*e.g.* Eguíluz *et al.*, 1990; 1995; 2000; Schäfer *et al.*, 1993; Quesada *et al.*, 1990;. Ordoñez-Casado *et al.*, 2009). Indeed, the general features displayed by the Abrantes Cemetery Pelites and Quartzwackes are similar to those typifying the basal units of *Série Negra*, such as the Morenos and Montemolín Formations (Fig. 9 and 10).

The Abrantes Dam Amphibolites, with a geochemistry from the N-MORB's to the within plate tholeiitic basalts, should trace an important episode of mafic volcanism in Abrantes region during Neoproterozoic times. Similar lithostratigraphic and geochemical features are also described in the Neoproterozoic sections forming the OMZ northern sectors, either in Portugal (Besteiros Amphibolites; *e.g.* Ribeiro *et al.*, 2003; Pereira *et al.*, 2006) or in Spain (Las Mesas, El Cuartel and Montemolin Amphibolites; Abalos and Eguíluz, 1989; Eguíluz *et al.*, 1990; 1995; 2000; Ordoñez-Casado, 1998; Sanchez Lorda *et al.*, 2014; 2016). Although in some places in

Northern OMZ, basalts with volcanic-arc geochemistry are also identified associated to N-MORB's to the within plate tholeiitic basalts (Sanchez Lorda *et al.*, 2014).

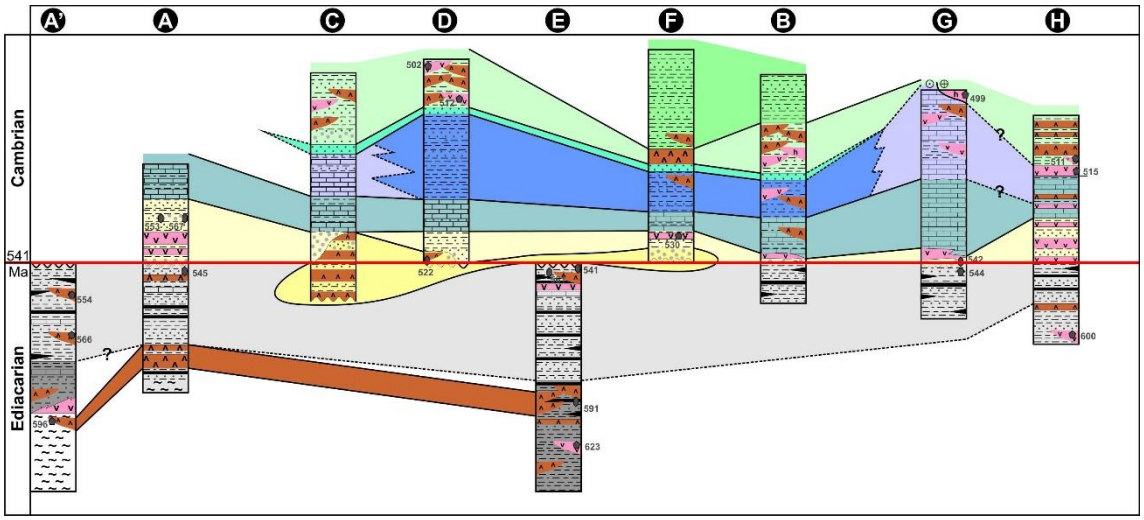

Figure 13 – Stratigraphic correlation diagram of the Neoproterozoic and Cambrian lithostratigraphic units in the OMZ (see Fig. 2 for the legend and location of stratigraphic charts).

As in Abrantes, the Montemolin amphibolites are interspersed in metapelite series (Sanchez Lorda *et al.*, 2014). In Olivença-Monestério Anticline, a maximum deposition time span around 590-580 Ma is proposed, thus constraining the age of the amphibolite sequence (Schafer *et al.*, 1989; 1990; Ordoñez-Casado, 1998). In addition to the previously mentioned data it should be noted that the Abrantes Dam Amphibolites is intruded by a gneissic granite (Maiorga Granite; Fig. 14) dated of 482±79 Ma (Rb-Sr, whole rock; Serrano Pinto, 1984) and, more recently, of 569±6 Ma (SHRIMP U-Pb in zircon; Mateus *et al.*, 2015), attesting its possible age.

Over the amphibolite-dominant unit and in apparent stratigraphic continuity, the Abrantes *Série Negra s.s.* are deposited, being characterized by the presence of flints (sometimes named as black metacherts or black quartzites in other sections), within dark-coloured metapelites and metagreywackes series, occasionally with subordinate amphibolites.

This lithological diversity is described in classical works (Alia, 1963; Carvalhosa, 1965; Vegas, 1968) as one of the main lithological features in the *Série Negra* succession. Thus, the Abrantes *Série Negra s.s.* could be correlated with the Mosteiros and Tentudia Formations (*e.g.* Eguíluz *et al.*, 1990; 1995; 2000; Quesada *et al.*, 1990; Oliveira *et al.*, 1991; Schäfer *et al.*, 1993).

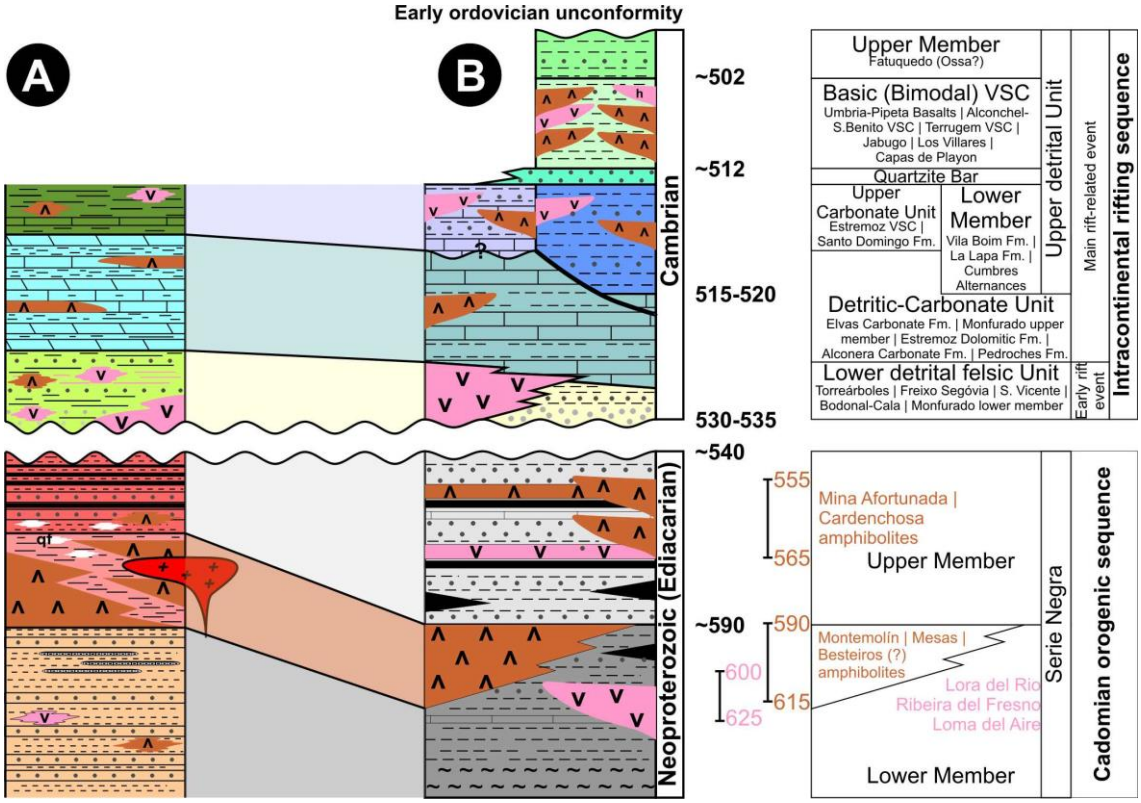

Figure 14 – Proposed general lithostratigraphic column for the Neoproterozoic-Cambrian of OMZ (adapted from Pereira *et al.*, 2011 and Nance *et al.*, 2012) and the correlation with lithostratigraphic column preserved in the Abrantes region.

As respect to the Cambrian related units, geochemical, petrologic, petrographic and stratigraphic features displayed by the Abrantes Castle Felsics support its correlation with S. Vicente, Freixo-Segovia and Nave de Grou-Azeiteiros volcano-sedimentary complexes (Pereira and Silva, 2006; Pereira *et al.*, 2006; 2011; Sanchez-Garcia *et al.*, 2010), as well with the lower member of the Monfurado Formation (Montemor-Ficalho sector; Chichorro *et al.*, 2008; Fig. 13) and the Torreárboles Formation and the Bodonal-Cala volcano-sedimentary complex (Quesada *et al.*, 1990; Eguíluz *et al.*, 2000; Gozalo *et al.*, 2003; Sanchez-Garcia *et al.*, 2003; 2008; 2010). Geochronological studies indicates a Lower Cambrian for these units, scattered in the 530-520 Ma time window (Pereira *et al.*, 2006;. 2012a; Romeo *et al.*, 2006; Chichorro *et al.*, 2008; Linnemann *et al.*, 2008; Alvaro *et al.*, 2014; Fig. 13 and 14).

The OMZ Early Cambrian felsic volcanism presents volcanic-arc signature (Mata and Munhá, 1990; Sanchez-Garcia *et al.*, 2008) that is also reported in studied felsic samples, resulting from its orogenic melting sources. The coarse-grained lithotypes, typical of Cambrian basal units, are poorly preserved in study area, excepting in its eastern sectors (near the Barca Pego; Fig. 1B) where levels of meta-arkoses and meta-conglomerates can be observed without ambiguity (Fig.

13). The discontinuous character of the basal conglomerate is reported in other OMZ sectors and, in these cases, the Carbonated Units are deposited directly over the Neoproterozoic succession (*e.g.* Liñan and Quesada, 1990; Oliveira *et al.*, 1991; Gozalo *et al.*, 2003; Creveling *et al.*, 2013).

Geological mapping (Fig. 3) shows that Abrantes Castel Felsics contact with all Neoproterozoic assigned units, which seems to be symptomatic of a deformation episode affecting only the Neoproterozoic assigned units in Abrantes region (possibly resulting from Cadomian orogeny), which is also emphasized by early deformation episodes noted in Abrantes Cemetery Pelites and Quartzwackes Unit. However, this assumption needs to be seen with caution, since the contacts between Cambrian and the Neoproterozoic units are structural demarked by Variscan shear zones.

The S. Miguel do Rio Torto Carbonates, developed over the previous volcano-sedimentary sequence in apparent stratigraphic continuity, correlates suitably with the Elvas Carbonated and Estremoz Dolomite Formations and the Assumar and Ouguela Detrital-Carbonate Complexes (Oliveira *et al.*, 1991; Pereira *et al.*, 2006; 2012a; Moreira *et al.*, 2014b; 2016), as well as with the Detrital-Carbonated Unit present in Alconchel, Alconera and Pedroches (*e.g.* Gozalo *et al.*, 2003; Sanchez-Garcia *et al.*, 2010; Creveling *et al.*, 2013; Fig. 13 and 14). These units are composed of crystalline dolomite and calcite marbles and limestones, which are interbedded with mafic volcanic rocks. The analysed mafic rocks in the S. Miguel do Rio Torto Carbonates unit display geochemical features compatible with within plate to MORB geochemistry, which is in accordance with the geochemical fingerprints identified in similar units, such as in Alter-do-Chão-Elvas, in Zafra-Alconera or in Alconchel-Jerez successions (Mata and Munhá, 1990; Sanchez-Garcia *et al.*, 2008; 2010). These carbonate-rich units are assigned to the Lower Cambrian (Ovetian-Lower Marianian, Series 2), based on its fossiliferous content (*e.g.* Liñan and Quesada, 1990; Gozalo *et al.*, 2003; Creveling *et al.*, 2013). Recent isotopic studies also indicate similar $^{87}Sr/^{86}Sr$ ratios for the Abrantes and other Cambrian carbonates from OMZ (Moreira *et al.*, 2016).

Overlaying the S. Miguel do Rio Torto Carbonates, also in stratigraphic continuity, a poorly represented upper siliciclastic unit with interleaved bimodal meta-volcanic rocks (mafic prevailing over felsic terms) can be observed and the mafic rocks also present tholeiitic fingerprint. This upper unit presents some similarities with the top detrital(-carbonate) sequence reported in Pedroches succession (NE Spain; Santo Domingo Formation; *e.g.* Liñan and Quesada, 1990; Gozalo *et al.*, 2003; Creveling *et al.*, 2013; Fig. 13 and 14). However, it is not reported the presence of significant volcanic rocks in Santo Domingo Formation, which also

present a higher abundance of carbonate layers. Accepting this correlation, the age of the Camelas Upper Detrital Series should be ascribed to Marianian. Note that equivalent time span is represented in basal sections of siliciclastic successions overlapping the carbonate-rich units cropping out in the Alter-do-Chão-Elvas-Cumbres Mayores Domain (Vila Boim, La Lapa Formations and Cumbres Alternances; Delgado, 1905; Liñan and Quesada, 1990; Oliveira *et al.*, 1991; Gozalo *et al.*, 2003; Creveling *et al.*, 2013). In these siliciclastic Formations, also with Marianian age, the bimodal volcanic rocks are recognized (Oliveira *et al.*, 1991; Gozalo *et al.*, 2003), showing that volcanic processes are active during sedimentation of Camelas Upper Detrital Series, which could explain the presence of bimodal volcanic rocks in this unit.

II.2.6. Geodynamic evolution

This section propose a model for the Neoproterozoic and Cambrian evolution of OMZ, which try to integrate the new Abrantes data with previous models of the Iberian Variscides.

The generation of a Neoproterozoic volcanic-arc in the northern margin of Gondwana induced by the subduction of Iapetus below the southern continent is consensual (Fig. 15A; Eguilluz *et al*., 2000; Ballèvre *et al*., 2001; Ribeiro *et al*., 2007; Linnemann *et al*., 2008). However, its location is debatable. While some consider it was developed south (in current coordinates) of the OMZ, resulting from Iapetus subduction (Ballèvre *et al*., 2001; Murphy *et al*., 2004; Linnemann *et al*., 2008; Sanchez-Lorda *et al*., 2014), the presence of Neoproterozoic HT and HP metamorphic rocks along the TBCSZ led others to considered this first other structure as the Cadomian suture (Ribeiro *et al*., 2009). The Neoproterozoic sequence, included in Série Negra Group, with a lower member formed by siliciclastic rocks with some calco-silicate and limestone layers, suggests a deposition in a relatively energetic shallow marine environment. The younger zircons find in this member suggests a maximum deposition around 590-580 Ma (Ordoñez-Casado *et al*., 2009).

The volcanic-arc magmatism is sometimes considered to be represented in Northern OMZ, by the calc-alkaline basalts with Early Ediacarian age (ca. 630-590 Ma; Sanchez-Lorda *et al*., 2014). These conclusion seems incongruent with a passive margin environment of the Série Negra lower member, indicated by its anorogenic bimodal volcanism typical from a within-plate magmatic settings. An alternative proposal consider the deposition of this member in the back-arc basin developed over the the thinned Gondwana margin, which may contain evidences of calc-alkaline magmatism related to volcanic-arc magmatism (Fig. 16A). This environment could also explain the anorogenic bimodal volcanic rocks enclosed in this member, that could result from the beginning of continental stretching related with this back-arc basin (Fig. 16B).

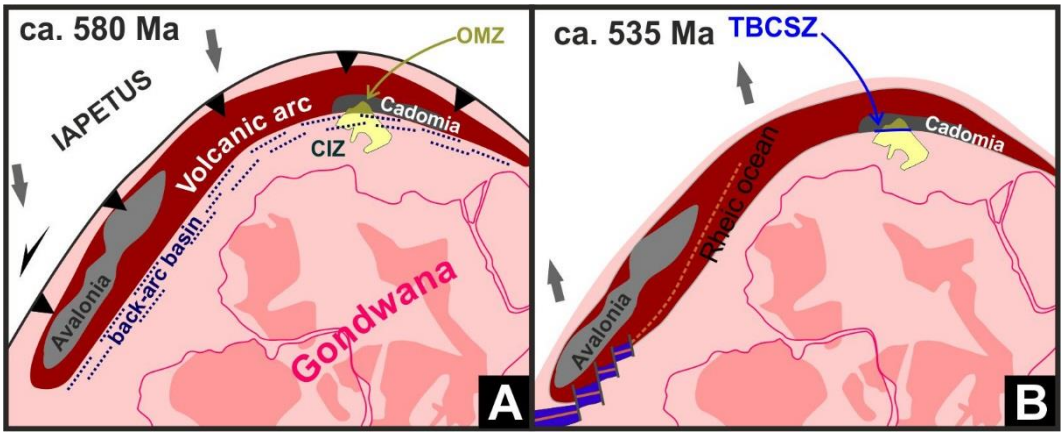

Figure 15 – Proposal of paleogeographic reconstitution of North-Gondwana margin during (A) Neoproterozoic and (B) Lower Cambrian times (adapted from Murphy *et al*., 2004; Pereira *et al.*, 2006; Linnemann *et al*., 2008).

This is compatible with the association between the volcanic arc calc-alkaline basalts with N-MOR and E-MOR basalts with a 580 Ma age (Lorda-Sanchez *et al*., 2014). Such age is in accordance, not only with the time span for the back-arc-basin formation (ca. 590-550 Ma; Linnemann *et al*., 2008), but also with the presence of dioritic and granitic plutonism with similar ages (ca. 580-570Ma; Ordoñez-Casado, 1998; Bandrés *et al*., 2004).

The progression of the back-arc stretching led to the overlap of the previous shallow and energetic marine sequence by a significant tholeiitic volcanism. Such volcanism induced the formation of abundant mafic rocks, now represented by the amphibolites of Abrantes Dam, Besteiros, Las Mesas and Montemolín (Eguíluz *et al*., 1990; Quesada *et al*., 1990; Ribeiro *et al*., 2003; Sanchez-Lorda *et al*., 2014). These amphibolites could represent the evolution of the anorogenic magmatism related with the back-arc lithospheric stretching (Fig. 16B), which is supported by their E-MORB to N-MORB signature. This process could have generated oceanization in the back-arc basin (Fig. 16C). This small ocean were developed in the northern domain of OMZ, separating two distinct basements in Iberia: the OMZ one, with a strong Cadomian imprint, and the CIZ one, where Cadomian magmatism and deformation is negligible.

The oceanization in back-arc basins, with generation of MORB-like basalts is observed in relation to the Mariana Trough induced by the Pacific subduction (Gribble *et al*., 1998; Pearce and Stern, 2006; Oakley *et al*., 2009).

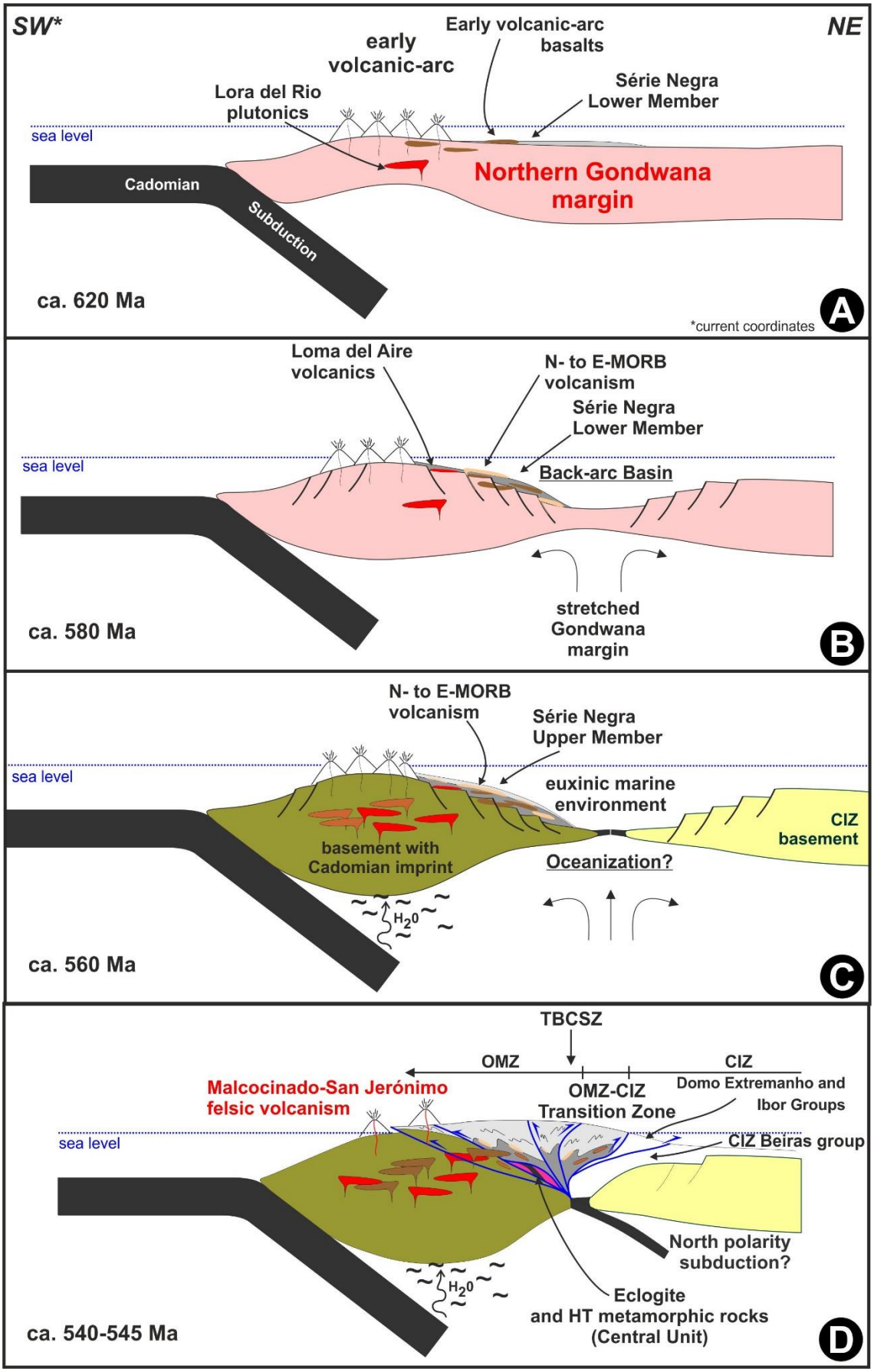
SW*
NE
early volcanic-arc
Early volcanic-arc basalts
Série Negra Lower Member
Lora del Rio plutonics
sea level
Cadomian
Subduction
Northern Gondwana margin
ca. 620 Ma
*current coordinates
A
Loma del Aire volcanics
N- to E-MORB volcanism
Série Negra Lower Member
sea level
Back-arc Basin
stretched Gondwana margin
ca. 580 Ma
B
N- to E-MORB volcanism
Série Negra Upper Member
sea level
euxinic marine environment
CIZ basement
basement with Cadomian imprint
Oceanization?
H2O
ca. 560 Ma
C
TBCSZ
OMZ
CIZ
Malcocinado-San Jerónimo felsic volcanism
OMZ-CIZ Transition Zone
Domo Extremanho and Ibor Groups
sea level
CIZ Beiras group
North polarity subduction?
H2O
Eclogite and HT metamorphic rocks (Central Unit)
ca. 540-545 Ma
D

Figure 16 – Main stages in the Ediacarian evolution of OMZ (includes data from Abalos *et al*., 1991; Linnemann *et al*., 2008; Ribeiro *et al*., 2007; Sanchez-Lorda *et al*., 2014; Jensen and Palacios, 2016):

A – Generation of an early volcanic-arc, associated to plutonism;

B – Beginning of the back-arc basin opening, with generation of MORB-like volcanic rocks;

C – Oceanization of the back-arc basin, related with Cadomian subduction;

D – Upper Ediacarian inversion of the back-arc, with the development of a cryptic structure along the TBCSZ, and the last pulses of Cadomian magmatism.

Above this OMZ magmatic event, begins the deposition of the Upper Member of Série Negra Group, a flyschoid sequence of greywackes interlayered with black shales and black quartzites (flints). These features indicate a deeper marine euxinic environment (continental slope or transition continental shelf-slope; Walker, 1976; Stow and Shanmugam, 1980) compatible with the deposition of Série Negra Upper Member in a confined back-arc basin (Fig. 16C).

During Upper Ediacarian times (ca. 545-540 Ma), the inversion of the back-arc basin deformed previous succession giving rise to the Cadomian Orogeny (Fig. 15B and 16D). The Malcocinado and San Jerónimo Formations, could represent the last pulses of the Cadomian chain volcanism, which was accompanied between 550 and 530 Ma by plutonism (Fig. 16D; Salman, 2004; Simancas *et al*., 2004). This inversion also deformed the Ediacarian Units from the southern CIZ domains that have been deposit in the back-arc basin (Domo Extremanho and Ibor Groups; Palacios *et al*., 2013; Eguiluz *et al*., 2015; 2016; Jensen and Palacios, 2016; Fig. 16D).

Although the presence of a back-arc basin between OMZ and CIZ, with possible small oceanization, during the Ediacarian seems inescapable, it should have been very narrow, as shown by the isotopic similarities between the Ediacarian detrital successions of both zones, proving that they have never been substantially separated during that time (Lopez-Guijarro *et al*., 2008).

The inversion of the back-arc basin also explains, not only the presence of Late Ediacarian granulites but also Cadomian HP rocks associated to the TBCSZ. This lithospheric structure are reactivated during the Variscan Cycle as an intraplate shear zone, controlling the Early Variscan structure of OMZ (Fig. 16D; Abalos, 1992; Abalos *et al*., 1992; Ribeiro *et al*., 2009; Romão *et al*., 2010; Henriques *et al*., 2015).

During the Lower Cambrian (ca. 525 Ma), began the crustal stretching related with the early stages of the Variscan Cycle and the coeval deposition of the OMZ Cambrian sequence, which includes the Abrantes Group succession. During the early intracontinental rifting, occurs

the deposition of a detrital volcano-sedimentary complex with arkoses and conglomerates, which corresponds to the molasses of the Cadomian Orogenic Chain (Fig. 17A). Associated to these clastic deposits an intense calc-alkaline felsic magmatism are produced (Mata and Munhá, 1990; Ordoñez-Casado *et al*., 1998; Pereira *et al*., 2006; López-Guijarro *et al*., 2008; Sanchez-Garcia *et al*., 2010), due to the melting of the Cadomian lithosphere. This geochemical signature emphasize the orogenic nature of the Cadomian melted crust and not the temporal extension of orogenic processes.

The transition from the late stages of the Cadomian Cycle to the early steps of the Variscan intracontinental rifting seems to be almost continuous (Simancas *et al*., 2004). This could indicate that the beginning of the Variscan Cycle might be related with the Cadomian high heat flow, due to the asthenospheric upwelling associated with the Cadomian slab break-off (?). Such process could explain, both the emplacement of mantle derived magmatic rocks during lower Cambrian (Culebrín tonalite, 532 ± 4 Ma Pb-Pb in zircon; Salman, 2004) and the Late Cadomian ages of the HT metamorphism (ca. 540-510 Ma; Eguíluz *et al*., 2000 and references therein; Henriques *et al*., 2015).

After the deposition of the Lower Cambrian (Ovetian-Marianian) volcano-siliciclastic complexes, a wide marine carbonate platform were established, from the region of Abrantes-Assumar-Pedroches region, towards the southern domains of OMZ (Montemor-Ficalho-Aracena; Fig. 17B). Locally, in the carbonate shelf a mafic volcanism with within-plate to MORB geochemistry is found. This shows that the crustal thinning related with the continental rifting continues during the carbonated sedimentation. Moreover, the presence of limestones emphasizes the continuity of marine environment in the syn-rift basins. The abundance of impure dolomite-rich limestones bellow the shallow carbonated shelf is recognize in several syn-rift succession (e.g. Kullberg *et al*., 2013; Martín-Martín e al., 2013; Ershova *et al*., 2016).

After the deposition of the carbonate dolomite-rich sediments, the progression of the intracontinental rifting develops two distinct depositional environments in the OMZ (Fig. 17C):

- In Alter-do-Chão-Elvas-Cumbres Mayores domain predominate the deep facies represented by flysch-type lithotypes, associated to bimodal volcanism (ca. 515-510 Ma);
- In the northern (Abrantes-Pedroches) and southern domains (Estremoz-Ficalho-Escoural) the shallow marine sedimentation were dominant. In Estremoz and Ficalho a second carbonated unit were formed, while in Escoural and Abrantes-Pedroches a gradual transition between carbonated and siliciclastic sedimentation is found. In both domains the sedimentation is coeval of a bimodal volcanism.

Previous zoning seems to indicate the presence of two distinct marine sedimentary environments during this stage (Fig. 17C): in the deepest, the clastic flyschoid sedimentation prevails, while in the shallow one the carbonated and thin-grained sedimentation is pervasive.

The MORB-like mafic dykes in the Neoproterozoic and Lower Cambrian units are related to the Lower Palaeozoic intracontinental rifting (Oliveira *et al*., 1991; Sanchez-Garcia *et al*., 2003; 2008; 2010; Etxebarria *et al*., 2006; Lopez-Guijarro *et al*., 2008). These volcanic rocks dykes, intruding the Neoproterozoic units, represent the Cambrian volcanism feeding channels.

The intracontinental rifting process culminates in the Upper-Cambrian-Lower Ordovician with the opening of a Variscan Ocean in the southwest of the OMZ margin (Pedro *et al*., 2010; Sanchez-Garcia *et al*., 2010; Moreira *et al*., 2014a). This tectonic environment is compatible with the Upper Cambrian sedimentary unconformity pervasive in the OMZ (Oliveira *et al*., 1991; Gozalo *et al*., 2003).

It should be emphasized that the recognition of a typical OMZ Neoproterozoic-Cambrian transition sequence in the Abrantes region is of major importance, because it allows to place the OMZ-CIZ boundary to the NE of Olalhas-Sardoal-Mouriscas sector, as already proposed by Romão *et al*. (2014).

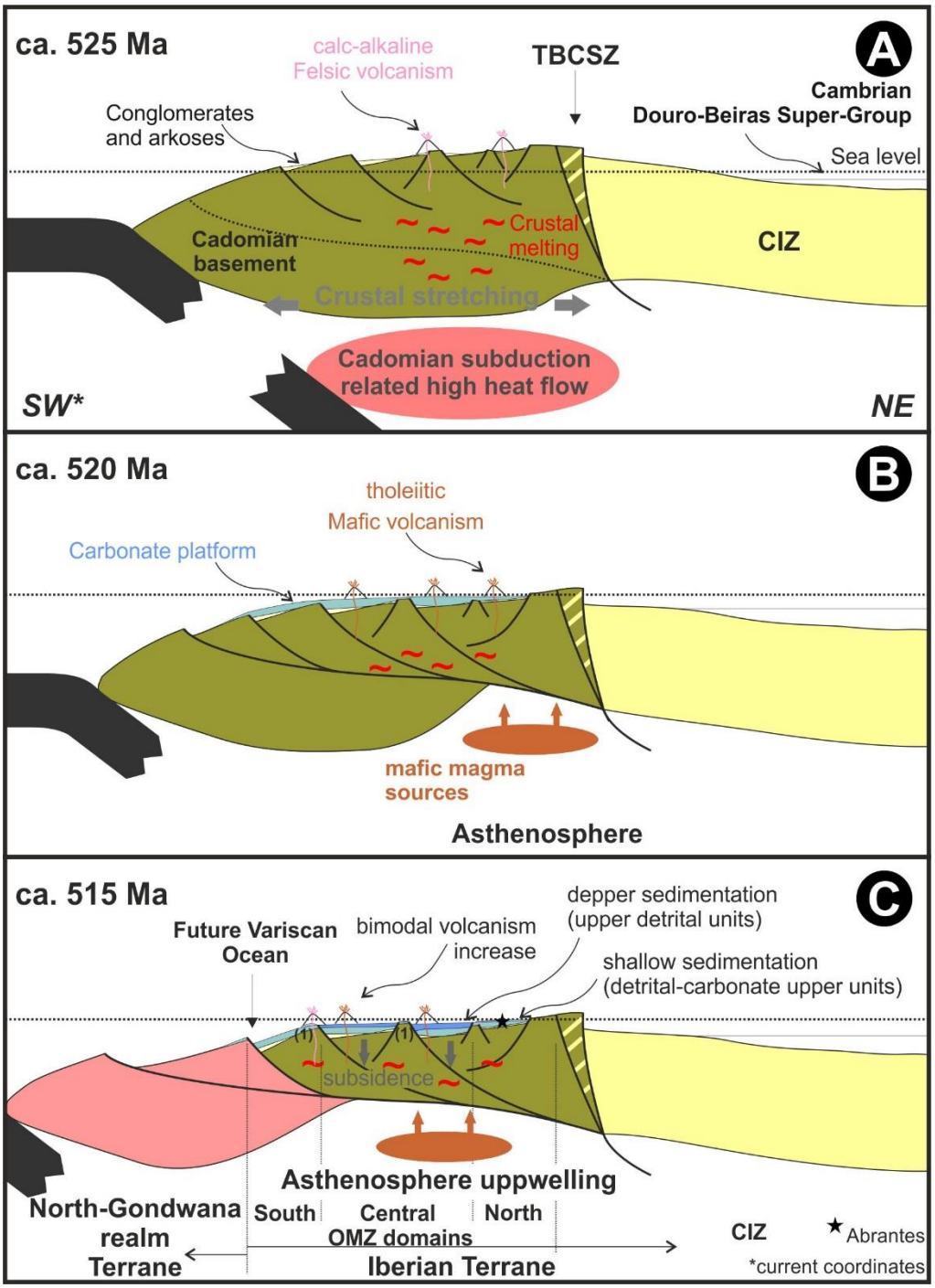

Figure 17 – Proposed Lower to Middle Cambrian evolution of OMZ, emphasising the beginning of North Gondwana lithosphere stretching related to the onset of the Variscan Cycle (includes data from Linnemann *et al*., 2008; Ribeiro *et al*., 2007; Moreira *et al*., 2014b; Jensen and Palacios, 2016):

A – The early felsic magmatic pulse, with calc-alkaline signature resulting from melting of the Cadomian crust;

B – Tholeiitic magmas are related to asthenospheric sources contemporaneous shallow carbonated sedimentation;

C – The lateral and vertical variations of the stratigraphic sequence due the depth of basin related with its subsidence during crustal stretching.

References

Abalos, B. (1992). Variscan shear-zone deFormation of a late Precambrian basement in SW Ibéria: implications for Circum-Atlantic Pre-Mesozoic tectonics. Journal of Structural Geology 14(7), 807-823. DOI: 10.1016/0191-8141(92)90042-U

Abalos, B., Eguíluz, L. (1989). Structural analysis and deformed early lineations in Black quartzites from the central Badajoz-Cordoba shear zone (Iberian Variscan Fold Belt), Rev. Soc. Gel. España, 2 (1-2), 95-102.

Abalos, B., Eguíluz, L., Apalategui, O. (1990). Constituición ectono-estratigráfica del Corredor Blastomilonítico de Badajoz-Córdoba: nueva proposta de subdivicion. Geogaceta, 7, 71-72.

Abalos, B., Gil Ibarguchi, J.I., Eguíluz, L. (1991). Cadomian subduction/collision and Variscan transpression in the Badajoz-Córdoba shear belt, southwest Spain. Tectonophysics 199, 51-72. DOI: 10.1016/0040-1951(91)90118-C

Alía, M. (1963): Rasgos estructurales de la Baja Extremadura. Bol Real Soc Esp Hist Nat 61:247–262

Álvaro, J.J., Bellido, F., Gasquet, D., Pereira, M.F., Quesada, C., Sánchez-García, T., (2014). Diachronism in the late Neoproterozoic–Cambrian arc-rift transition of North Gondwana: A comparison of Morocco and the Iberian Ossa-Morena Zone. Journal of African Earth Sciences, 98, 113-132. DOI: 10.1016/j.jafrearsci.2014.03.024

Apalategui, O., Eguíluz, L., Quesada, C. (1990). Ossa-Morena zone: structure. In: Dallmeyer, R.D., Martínez-García, E. (Eds.), Pre-Mesozoic Geology of Iberia. Springer-Verlag, Berlin-Heidelberg, Germany, pp. 280–292.

Araújo, A., Piçarra de Almeida, J., Borrego, J., Pedro, J., Oliveira, J.T. (2013). As regiões central e sul da Zona de Ossa-Morena, in: Dias, R., Araújo, A., Terrinha, P., Kullberg, J.C. (Eds.), Geologia de Portugal (Vol. I), Escolar Editora, Lisboa, 509-549.

Ballèvre, M., Le Goff, E., Hébert, R. (2001). The tectonothermal evolution of the Cadomian beld of Northern Britanny, France: Neoproterozoic volcanic arc. Tectonophisics, 331, 19-43. DOI: 10.1016/S0040-1951(00)00234-1

Bandrés, A., Eguíluz, L., Pin, C., Paquette, J.L., Ordónez-Casado, B., Le Fèvre, B., Ortega, L.A., Gil Ibarguchi, J.I. (2004). The northern Ossa-Morena Cadomian batholith (Iberian Massif): magmatic arc origin and early evolution. International Journal of Earth Sciences 93, 860–885. DOI: 10.1007/s00531-004-0423-6

Bellon, H., blachere, H., Crousilles, M., Deloche, C., Dixsaut, C., Hertricht, B., Prostdame, V., Rossi, Ph., Simon, D., Tamain, G. (1979). Radiochronologie, évolution tectono-magmatique et implications métallogénetiques dans les Cadomo-Variscides du Sud-Est hespérique. Bulletin Societé Géologique France, 21, 113-120.

Carvalho, D., Goínhas, J., Oliveira, V., Ribeiro, A. (1971). Observações sobre a geologia do Sul de Portugal e consequências metalogenéticas. Est. Not. Trabalhos, Serv. Fom. Mineiro, 20, 1-2, 153-199.

Carvalhosa, A. (1965). Contribuição para o conhecimento geológico da região entre Portel e Ficalho (Alentejo). Memorias dos Serviços Geológicos de Portugal 11, 1-130.

Carvalhosa, A., Gonçalves, F., Oliveira, V. (1987). Notícia explicativa da folha 36-D, Redondo. Serviços Geológicos de Portugal.

Chichorro, M., Pereira, M.F., Díaz-Azpiroz, M., Williams, I.S., Fernandez, C., Pin, C., Silva, J.B. (2008). Cambrian ensialic rift-related magmatism in the Ossa-Morena Zone (Évora-Aracena metamorphic belt, SW Iberian Massif): Sm-Nd isotopes and SHRIMP zircão U-Th-Pb geochronology. Tectonophysics 461, 91-113. DOI:10.1016/j.tecto.2008.01.008

Coelho, A., Gonçalves, F. (1970). Rocha hiperalcalina de Estremoz. Bol. Soc. Geol. Portugal, XVII, 181-185.

Conde, L. (1984). Excursão geológica na região de Ferreira do Zêzere-Abrantes. VI Reunião do Grupo de Ossa Morena, Livro-guia, 1-8, Universidade de Coimbra.

Creveling, J.R., Fernández-Remolar, D., Rodríguez-Martínez, M., Menéndez, S., Bergmann, K.D., Gill, B.C., Abelson, J. Amils, R., Ehlmann, B.L., García-Bellido, D.C, Grotzinger, J.P., Hallmann, C., Stack, K.M., Knoll, A.H. (2013). Geobiology of a Lower Cambrian Carbonate Platform, Pedroche Formation, Ossa Morena Zone, Spain. Palaeogeography, Palaeoclimatology, Palaeoecology 386, 459-478. DOI:10.1016/j.palaeo.2013.06.015

Delgado, J.F.N. (1905). Contribuições para o estudo dos terrenos paleozóicos. I. Precâmbrico e Arcaico; II. Câmbrico. Com. Serv. Geol. Portugal 7, 56-122.

Eguíluz L., Gil Ibarguchi J.I., Abalos B., Apraiz A. (2000). Superposed Hercynian and Cadomian orogenic cycles in the OssaMorena zone and related areas of the Iberian Massif. Geol. Soc. Am. Bull., 112: 1398-1413.

Eguíluz, L., Abalos, B., Ortega, L.A. (1990). Anfibolitas proterozoicas del sector central de la zona de Ossa Morena. Geoquímica e implicaciones geodinâmicas. Cuaderno Lab. Xeolóxico de Laxe. 15, 119-131

Eguíluz. L., Apraiz, A., Abalos, A., Martinez-Torres, L.M. (1995). Evolution de la zone d'Ossa Morena (Espegne) au cous du proterozoique superior: corrélations acec l'orogène cadomien nord armoricain. Geológie de la France, 3, 35-47.

Eguiluz L. Martinez-Torres L.M., Sarrionadia F., Carracedo M., Gil-Ibarguchi J.I. (2015). The Ibero-Armorican Belt: an evolving island-arc along northern Gondwana between ca. 650 and 480 Ma. Geólogie de la France, 2015(1), 58-59.

Eguiluz, L., Palacios, T., Jensen S., Sarrionandia, F. (2016). La Zona Centro Iberica Meridional: Cuenca tras-arco del orogeno cadomiense del Norte de Gondwana. Geoguias, 10, 55-88

Ershova, V.B., Prokopiev, A.V., Khud, A.K. (2016). Devonian–Permian sedimentary basins and paleogeography of the Eastern Russian Arctic: An overview. Tectonophysics 691(A), 234-255. DOI: 10.1016/j.tecto.2016.03.026

Etxebarria M., Chalot-Prat F., Apraiz A., Eguíluz L. (2006). Birth of a volcanic passive margin in Cambrian time: Rift paleogeography of the Ossa-Morena Zone, SW Spain. Precamb. Res., 147: 366-386. DOI:10.1016/j.precamres.2006.01.022

Fernández-Suárez, J., Gutiérrez-Alonso, G., Jeffries, T.E. (2002). The importance of along margin terrane transport in northern Gondwana: insights from detrital zircon parentage in Neoproterozoic rocks from Iberia and Brittany. Earth and Planetary Science Letters 204, 75–88. DOI:10.1016/S0012-821X(02)00963-9

Frost, B.R., Barnes, C.G., Collins, W.J., Arculus, R.J., Ellis, D.J., Frost, C.D. (2001). A Geochemical Classification for Granitic Rocks. J. Petrol., 42 (11), 2033-2048. DOI: 10.1093/petrology/42.11.2033

Gómez-Pugnaire, M., Azor, A., Fernández-Soler, J., Sánchez Vizcaíno, V. L. (2003). The amphibolites from the Ossa-Morena/Central Iberian Variscan suture (Southwestern Iberian Massif): Geochemistry and tectonic interpretation, Lithos, 68, 23 – 42. DOI:10.1016/S0024-4937(03)00018-5

Gonçalves, F., Zbyszewski, G., Carvalhosa, A., Coelho, A. (1979). Carta Geológica de Portugal 1:50 000, folha 27-D (Abrantes). Serv. Geol. Portugal, Lisboa.

Gorton M.P., Schandl E.S. (2000). From continents to island arcs: a geochemical index of tectonic setting for arc-related and within-plate felsic to intermediate volcanic rocks. The Canadian Mineralogist, 38, 1065-1073. DOI: 10.2113/gscanmin.38.5.1065

Gozalo, R., Liñán, E., Palacios, T., Gámezvintaned, J.A., Mayoral, E. (2003). The Cambrian of the Iberian Peninsula: an overview. Geologica Acta 1, 103–112.

Gribble R.F., Stern, R.J. Newman, S., Bloomer, S.H, O'hearn, T. (1998). Chemical and Isotopic Composition of Lavas from the Northern Mariana Trough: Implications for Magmagenesis in Back-arc Basins. Journal of Petrology 39(1), 125–154. DOI: 10.1093/petroj/39.1.125

Henriques, S.B.A., Neiva, A.M.R., Ribeiro, M.L., Dunning, G.R., Tajčmanová, L., (2015). Evolution of a Neoproterozoic suture in the Iberian Massif, Central Portugal: New U-Pb ages of igneous and metamorphic events at the contact between the Ossa Morena Zone and Central Iberian Zone. Lithos 220-233, 43-59. DOI:10.1016/j.lithos.2015.02.001

Irvine, T.N., Baragar, W.R.A. (1971). A guide to the chemical classification of the common volcanic rocks: Canadian Journal of Earth Sciences, 8, 523-548. DOI: 10.1139/e71-055

Jensen, S., Palacios, T. (2016). The Ediacaran-Cambrian trace fossil record in the Central Iberian Zone, Iberian Peninsula. Comunicações Geológicas, 103(I), 83-92.

Julivert, M., Fontboté, J.M., Ribeiro, A., Conde, L.E. (1974). Memória Explicativa del Mapa Tectónico de la Península Ibérica y Baleares. Instituto Geológico y Minero de España, Madrid, 113 pp.

Kullberg, J. C., Rocha, R. B., Soares, A. F., Rey, J., Terrinha, P., Azerêdo, A. C., Callapez, P., Duarte, L. V., Kullberg, M. C., Martins, L., Miranda, J. R., Alves, C., Mata, J., Madeira, J., Mateus, O., Moreira, M., Nogueira, C. R. (2013). A Bacia Lusitaniana: Estratigrafia, Paleogeografia e Tectónica. In: R. Dias, A. Araújo, P. Terrinha, J.C. Kullberg (Eds), Geologia de Portugal, vol. 2, Escolar Editora, 195-347.

Le Maitre, R. W. (Editor), Bateman, P,, Dudek, A., Keller, J. Er Al. (1989). A Classification of Igneous rocks and Glossary of Term: Recommendations of the International Union of Geological Sciences Subcommission on the Systematics of Igneous Rocks. Blackwell Scientific Publications, Oxford

Liñán, E., Álvaro, J., Gozalo, R., Gámez-Vintaned, J.A., Palacios, T. (1995). El Cámbrico Medio de la Sierra de Córdoba (Ossa-Morena, S de España): trilobites y paleoicnología. Implicaciones bioestratigráficas y paleoambientales. Revista Española de Paleontología, 10 (2), 219-238.

Liñán, E., Quesada, C. (1990). Ossa-Morena Zone: Stratigraphy, in: Dallmeyer, R.D., Martinez Garcia, E. (Eds.) Pre-Mesozoic Geology of Iberia. Springer-Verlag, Berlin, 229–266.

Linnemann, U., Pereira, M.F., Jeffries, T., Drost, K., Gerdes, A. (2008). Cadomian Orogeny and the opening of the Rheic Ocean: New insights in the diacrony of geotectonic processes constrained by LA-ICP-MS U-Pb zircão dating (Ossa-Morena and Saxo-Thuringian Zones, Iberian and Bohemian Massifs)". Tectonophysics 361, 21-43. DOI:10.1016/j.tecto.2008.05.002

Lopes, J.L. (2003). Contribuição para o conhecimento Tectono-Estratigráfico do Nordeste Alentejano, transversal Terena-Elvas. Implicações económicas no aproveitamento de rochas ornamentais existentes na região (Mármores e Granitos). PhD Thesis (unpublished), Évora University, Portugal 568 pp.

López-Guijarro, R., Armendáriz M., Quesada C., Fernández-Suárez J., Murphy, J. B, Pin,C., Bellido, F. (2008). Ediacaran–Palaeozoic tectonic evolution of the Ossa Morena and Central Iberian zones (SW Iberia) as revealed by Sm–Nd isotope systematics. Tectonophysics 461, 202–214. DOI:10.1016/j.tecto.2008.06.006

Lötze, F. (1945): Zur Gliederung der Varisciden der Iberishen Meseta. Geoteckt Forsch, vol. 6, pp.78-92.

Martín-Martín, J.D., Gomez-Rivas, E., Bover-Arnal, T., Travéa, A., Salas, R., Moreno-Bedmar, J.A., Tomás, S., Corbella, M., Teixell, A., Vergés, J., Stafford, S.L. (2013). The Upper Aptian to Lower Albian syn-rift carbonate succession of the southern Maestrat Basin (Spain): Facies architecture and fault-controlled stratabound dolostones. Cretaceous research 41, 217-236. DOI: 10.1016/j.cretres.2012.12.008

Mata, J., Munhá, J. (1985). Geochemistry of mafic volcanic rocks from the Estremoz region (South Central Portugal). Comunicações dos Serviços geológicos de Portugal, 71(2), 175-185.

Mata, J., Munhá, J., (1990). Magmatogénese de metavulcanitos câmbricos do nordeste alentejano: os estádios iniciais de "rifting" continental. Comun. Serv. Geol. Portugal 76, 61-89.

Mateus, A., Mata, J., Tassinari, C., Rodrigues, P., Ribeiro, A., Romão, J., Moreira, N., (2015). Conciliating U-Pb SHRIMP Zircon Dating with Zircon Saturation and Ti-in-Zircon Thermometry in the Maiorga and Endreiros Granites (Ossa-Morena Zone, Portugal). X Congresso Ibérico de Geoquímica, Laboratório Nacional de Energia e Geologia, Lisboa, 38-41.

Mette, W. (1989). Acritarchs from Lower Paleozoic rocks of the Western Sierra Morena (SW Spain) and biostratigraphic results. Geologica et Paleontologica, Merburg, 53: 1-19.

Moreira, N. (2012). Caracterização estrutural da zona de cisalhamento Tomar-Badajoz-Córdova no sector de Abrantes. Unpublished MsC thesis, University of Évora, 225 p.

Moreira, N., Araújo, A., Pedro, J.C., Dias, R. (2014a). Evolução geodinâmica da Zona de Ossa-Morena no contexto do SW Ibérico durante o Ciclo Varisco. Comunicações geológicas 101 (Vol. Especial I), 275-278.

Moreira, N., Dias, R., Pedro, J.C., Araújo, A. (2014b). Interferência de fases de deformação Varisca na estrutura de Torre de Cabedal; sector de Alter-do-Chão – Elvas na Zona de Ossa-Morena. Comunicações geológicas 101 (Vol. Especial I), 279-282.

Moreira, N., Pedro, J., Romão, J., Dias, R., Araújo, A. Ribeiro A. (2015). The Neoproterozoic-Cambrian transition in Abrantes Region (Central Portugal); Litostratigraphic correlation with Cambrian Series of Ossa-Morena Zone. The Variscan belt: correlations and plate dinamics. Géologie de la France (Variscan 2015 special issue, Rennes), 2015(1), 101-102. ISBN:978-2-7159-2612-7.

Moreira, N., Pedro, J., Santos, J.F., Araújo, A., Romão, J., Dias, R., Ribeiro, A., Ribeiro, S., Mirão, J. (2016). $^{87}Sr/^{86}Sr$ ratios discrimination applied to the main Paleozoic carbonate sedimentation in Ossa-Morena Zone. In: IX Congreso Geológico de España (special volume). Geo-Temas, 16(1), 161-164. ISSN 1576-5172.

Murphy , J. B., Pisarevsky, S. A., Nance, R. D., Keppie, J. D. (2004). Neoproterozoic–Early Palaeozoic evolution of peri-Gondwanan terranes: implications for Laurentia–Gondwana connections. International Journal of Earth Sciences 93, 659–82. DOI: 10.1007/s00531-004-0412-9

Nance, R.D., Gutiérrez-Alonso, G., Keppie, J.D., Linnemann, U., Murphy, J.B., Quesada, C., Strachan, R.A., Woodcock, N.H. (2012). A brief history of the Rheic Ocean. Geoscience Frontiers 3, 125-135. DOI:10.1016/j.gsf.2011.11.008

Oakley, A. J., Taylor, B., Moore, G. F., Goodliffe, A. (2009). Sedimentary, volcanic, and tectonic processes of the central Mariana Arc: Mariana Trough back-arc basin Formation and the West Mariana Ridge. Geochemistry Geophysics Geosystems, 10(8), Q08X07, DOI:10.1029/2008GC002312

Oliveira, D. P. S., Reed, R. M., Milliken, K. L., Robb, L. J., Inverno, C. M. C., D'Orey, F. L. C. (2003). *Série Negra* black quartzites – Tomar Cordoba Shear Zone, E Portugal: mineralogy and cathodoluminescence studies. Cadernos Lab. Xeolóxico de Laxe, 28, 193-211.

Oliveira, J.T., Oliveira, V., Piçarra, J.M. (1991). Traços gerais da evolução tectono-estratigráfica da Zona de Ossa Morena, em Portugal: síntese crítica do estado actual dos conhecimentos. Comun. Serv. Geol. Port. 77, 3-26.

Oliveira, V.M. (1984). Contribuição para o conhecimento geológico-mineiro da regiao de Alandroal-Juromenha (Alto Alentejo). Est. Not. Trab., Serv. Fom. Mineiro XXVI (1-4): 103-126.

Ordóñez Casado, B. (1998). Geochronological studies of the Pre-Mesozoic basement of the Iberian Massif: the Ossa-Morena Zone and the Allochthonous Complexes within the Central Iberian Zone. PhD Thesis ETH Zurich, 235 p.

Ordoñez-Casado, B., Gebauer, D., Eguíluz, L. (1998). SHRIMP age-constraints for the calc-alkaline volcanism in the Olivenza-Monesterio Antiform (Ossa Morena, SW Spain). Goldschmidt Conference, Toulouse. Mineralogical Magazine, 62A, 1112-1113.

Ordoñez-Casado, B., Gebauer, D., Eguíluz, L. (2009). Zircão Ion-Probe Dating the Maximum Age of Deposition of the Montemolín Succession (Lower *Série Negra*) in the Ossa Morena Zone, Spain. Macla, 11, 137-138

Palacios, T. Eguiluz, L., Apalategui, A. (2013). Geological Map of Estremadura (1:350.000) and descriptive memory. UPV-EHU, Bilbao, 222p.

Pearce, J.A. (1982). Trace element characteristics of lavas from destructive plate boundaries. In: Thorpe, R. S. (ed.), Andesites. New York: John Wiley & Sons, 525-548.

Pearce, J.A. (1983). Role of the sub-continental lithosphere in magma genesis at active continental margins. In: Hawkesworth, C.J. and Norry, M.J. eds.Continental basalts and mantle xenoliths, Nantwich, Cheshire: Shiva Publications, pp. 230-249.

Pearce, J.A., Gale, G. H. (1977). Identification of ore-deposition environment from trace element geochemistry of associated igneous host rocks. In: Volcanic Processes in Ore Genesis. Spec. Publ. Inst. Min. Metall. And Geol. Soc. London, 14-24. 10.1144/GSL.SP.1977.007.01.03

Pearce, J.A., Stern R.J. (2006). Origin of Back-Arc Basin Magmas: Trace Element and Isotope Perspectives. Geophysical Monograph Series 166, 63-86. DOI: 10.1029/166GM06

Pearce, J.A., Harris, N.B.W., Tindle, A.G. (1984). Trace element discrimination diagrams for the tectonic interpretation of granitic rocks. J. Petrol., 25 (4), 956-983. DOI: 10.1093/petrology/25.4.956

Pedro, J. C., Araújo, A., Tassinari, C., Fonseca, P. E., Ribeiro, A. (2010). Geochemistry and U-Pb zircão age of the Internal Ossa-Morena Zone Ophiolite Sequences: a remnant of Rheic Ocean in SW Iberia, Ofioliti 35 (2), 117-130. WOS:000285862100004.

Perdigão, J. (1967). Estudos geológicos na Pedreira de Mestre André (Barrancos). Comun. Serv. Geol. Portugal 52.

Pereira, M.F., Silva, J.B. (2006). Nordeste Alentejano, In R. Dias, A. Araújo, P. Terrinha, J. Kullberg (Eds.) Geologia de Portugal no Contexto da Ibéria. Uni. Evora, Evora, p. 145-150

Pereira, M.F., Chichorro, M., Linnemann, U., Eguíluz, L., Silva, J.B. (2006). Inherited arc signature in Ediacaran and Early Cambrian basins of the Ossa-Morena Zone (Iberian Massif, Portugal): paleogeographic link with European and North African Cadomian correlatives. Precambrian Research, 144, 297-315. DOI:10.1016/j.precamres.2005.11.011

Pereira, M.F., Apraiz, A., Chichorro, M., Silva, J.B., Armstrong, R.A. (2010a). Exhumation of high-pressure rocks in northern Gondwana during the Early Carboniferours (Coimbra-Cordoba shear zone, SW Iberian Massif): tectonothermal analysis and U-Th-Pb SHRIMP in-situ zircon geochronology. Gondwana Research, 17(2), 440-460. DOI:10.1016/j.gr.2009.10.001

Pereira, M.F., Silva, J.B., Drost, K., Chichorro, M., Apraiz, A. (2010b). Relative timing of transcurrent displacements in northern Gondwana: U–Pb laser ablation ICP-MS zircão and monazite geochronology of gneisses and sheared granites from the western Iberian Massif (Portugal). Gondwana Research, 17, 461–481. DOI:10.1016/j.gr.2009.08.006

Pereira, M.F., Chichorro, M., Sola, A.R., Silva, J.B., Sanchez-Garcia, T., Bellido, F., (2011). Tracing the Cadomian magmatism with detrital/inherited zircão ages by in-situ U-Pb SHRIMP geochronology (Ossa-Morena Zone, SW Iberian Massif).Lithos 123(1-4), 204-217. DOI: 10.1016/j.lithos.2010.11.008

Pereira, M.F., Solá, A.R., Chichorro, M., Lopes, L., Gerdes, A., Silva, J.B., (2012a). North-Gondwana assembly, break up and paleogeography: U–Pb isotope evidence from detrital and igneous zircãos of Ediacaran and Cambrian rocks of SW Iberia. Gondwana Research 22(3–4), 866-881. DOI:10.1016/j.gr.2012.02.010

Pereira, M.F., Silva, J.B., Chichorro, M., Ordóñez-Casado, B., Lee, J.K.W., Williams, I.S., (2012b). Early Carboniferous wrenching, exhumation of high-grade metamorphic rocks and basin instability in SW Iberia: constraints

derived from structural geology and U-Pb and 40Ar-39Ar geochronology. Tectonophysics 558-559, 28-44 DOI:10.1016/j.tecto.2012.06.020

Piçarra, J.M. (2000). Estudo estratigráfico do sector de Estremoz-Barrancos, Zona de Ossa Morena, Portugal. Vol. I - .Litoestratigrafia do intervalo Câmbrico médio?-Devónico inferior, Vol. II - Bioestratigrafia do intervalo Ordovícico-Devónico inferior. PhD Thesis (unpublished), Évora University, Portugal.

Piçarra, J.M., Le Meen, J. (1994). Ocorrência de crinóides em mármores do Complexo Vulcano-Sedimentar Carbonatado de Estremoz: implicações estratigráficas. Comunicações do Instituto Geológico e Mineiro 80, 15-25

Pin, Ch., Liñán, E., Pascual, E., Donaire, T., Valenzuela, A. (2002). Late Neoproterozoic crustal growth in the European variscides: Nd isotope and geochemical evidence from the Sierra de Córdoba andesites (Ossa-Morena Zone, Southern Spain). Tectonophysics 352, 133-151. DOI:10.1016/S0040-1951(02)00193-2

Quesada, C. (1991). Geological constraints on the Palaeozoic tectonic evolution of tectonostratigraphic terranes in the Iberian Massif. Tectonophysics 185, 225-245. DOI: 10.1016/0040-1951(91)90446-Y

Quesada, C., Apalategui, O., Eguíluz, L., Liñan, E., Palácios, T. (1990). Ossa-Morena Zone. Precambrian. In R. D. Dallmeyer, E. Martinez (Eds.). Pre-Mesozoic Geology of Iberia. Springer Verla, Berlin, pp. 252- 258.

Ribeiro, A., Antunes, M. T., Ferreira, M. P., Rocha, R. B., Soares, A. F., Zbyszewski, G., Moitinho de Almeida, F., Carvalho, D., Monteiro, J. H. (1979). Introduction à la géologie générale du Portugal. Serviços Geológicos de Portugal, 114 p.

Ribeiro, A., Munhá, J., Dias, R., Mateus, A., Pereira, E., Ribeiro, L., Fonseca, P., Araújo, A., Oliveira, T., Romão, J., Chaminé, H., Coke, C., Pedro, J. (2007). Geodynamic evolution of SW Europe Variscides. Tectonics 26, TC6009. DOI: 10.1029/2006TC002058

Ribeiro, A., Pereira, E., Fonseca, P., Mateus, A., Araújo, A., Munhá, J., Romão, J. Rodrigues, J. F., Castro, P., Meireles, C., Ferreira, N. (2009). Mechanics of thick-skinned Variscan overprinting of Cadomian basement (Iberian Variscides). C. R. Geosciences, Paris 341 (2-3), 127-139. DOI: 10.1016/j.crte.2008.12.003

Ribeiro, A., Quesada, C., Dallmeyer, R. D. (1990). Geodynamic evolution of the Iberian Massif. In R. D. Dallmeyer, E. Martínez García (Eds.) Pre- Mesozoic Geology of Iberia. Springer-Verlag, pp. 397-410.

Ribeiro, M.L., Pereira, M.F., Solá, A.R. (2003). O ciclo Cadomiano na ZOM: Evidências geoquímicas. Congresso Ibérico de Geoquimica. Universidade de Coimbra, Portugal, 102–104.

Rollinson, H. (1993). Using Geochemical Data: evaluation, presentation, interpretation, p. 102-212

Romão, J., Ribeiro, A., Munhá, J., Ribeiro, L. (2010). Basement nappes on the NE boundary the Ossa-Morena Zone (SW Iberian Variscides). European Geosciences Union, General Assembly, Vienna, Austria (Abstract).

Romão, J., Moreira, N., Dias, R., Pedro, J., Mateus, A., Ribeiro, A. (2014). Tectonoestratigrafia do Terreno Ibérico no sector Tomar-Sardoal-Ferreira do Zêzere e relações com o Terreno Finisterra. Comunicações Geológicas 101 (Vol. Especial I), 559-562

Romeo, I., Lunar, R., Capote, R., Quesada, C., Dunning, G.R., Piña, R., Ortega, L., (2006). U/Pb age constraints on Variscan Magmatism and Ni-Cu-PGE metallogeny in the Ossa-Morena Zone (SW Iberia). Journal of the Geological Society of London 163, 837-846. DOI: 10.1144/0016-76492005-065

Salman, K. (2004). The timing of the Cadomian and Variscan cycles in the Ossa-Morena Zone, SW Iberia: granitic magmatism from subduction to extension. Journal of Iberian Geology 30, 119-132.

Sánchez Carretero, R., Eguíluz, L., Pascual, E., Carracedo, M. (1990). Ossa-Morena Zone: Igneous rocks. In: Dallmeyer, R. D. and Martínez García, E., (eds.), Pre-Mesozoic Geology of Iberia, Springer Verlag, Berlin: 292-313.

Sánchez-García, T., Bellido, F., Pereira, M.F., Chichorro, M., Quesada, C., Pin, C., Silva, J.B. (2010). Rift-related volcanism predating the birth of the Rheic Ocean (Ossa-Morena zone, SW Iberia). Gondwana Research 17, 392–407. DOI:10.1016/j.gr.2009.10.005

Sánchez-García, T., Bellindo, F., Quesada, C. (2003). Geodynamic setting and geochemical signatures of Cambrian-Ordovician rift-related igneous rocks (Ossa-Morena Zone, SW Iberia). Tectonophysics 365, pp. 233-255. DOI:10.1016/S0040-1951(03)00024-6

Sánchez-García, T., Quesada, C., Bellido, F., Dunning, G.R., González de Tánago, J. (2008). Two-step magma flooding of the upper crust during rifting: the Early Palaeozoic of the Ossa Morena Zone (SW Iberia). Tectonophysics 461, 72–90.

Sánchez-García, T., Quesada, C., Dunning, G.R., Perejón, A., Bellido, F., Moreno-Eiris, E. (2007). New geochronological and geochemical data of the Loma del Aire Unit, Ossa- Morena Zone. IGCP 497-Galicia Meeting 2007. Publicaciones del IGME, 164–165. DOI:10.1016/j.tecto.2008.03.006

Sanchez-Lorda, M.E., Sarrionandia, F., Ábalos, B., Carrracedo, M., Eguíluz, L., Gil Ibarguchi, J.I. (2014). Geochemistry and paleotectonic setting of Ediacaran metabasites from the Ossa-Morena Zone (SW Iberia). Int J Earth Sci (Geol Rundsch), 103, 1263–1286 DOI:10.1007/s00531-013-0937-x

Sánchez-Lorda, M.E., Ábalos, B., García de Madinabeitia, S., Eguíluz, L., Gil Ibarguchi, J.I., Paquette, J.L. (2016). Radiometric discrimination of pre-Variscan amphibolites in the Ediacaran *Série Negra* (Ossa-Morena Zone, SW Iberia). Tectonophysics, 681, 31–45. DOI: 10.1016/j.tecto.2015.09.020

Sarmiento, G.N., Piçarra, J.M., Oliveira, J.T. (2000). Conodontes do Silúrico (Superior?)-Devónico nos "Mármores de Estremoz", Sector de Estremoz-Barrancos (Zona de Ossa Morena, Portugal). Implicações estratigráficas e estruturais a nível regional. I Congresso Ibérico de Paleontologia/VIII International Meeting of IGCP 421 (abstract book), Évora, 284-285.

Schäfer, H. J. (1990): Geochronological investigations in the Ossa-Morena Zone, SW Spain. Ph. D. ETH, Zurich: 153 p.

Schäfer, H.J., Gebauer, D., Nägler, Th.F., Von Quadt, A. (1988). U–Pb zircon and Sm–Nd studies of various rock-types of the Ossa-Morena Zone (Southwest Spain). Simposio sobre cinturones orogénicos. I Congreso Español de Geologíapp. 51–57.

Schäfer, H. J., Gebauer, D. Ynagler, Th. F. (1989). Pan-African and Caledonian ages in the Ossa-Morena Zone (Southwest Spain): a U-Pb zircão and Sm-Nd study. Terra Abstracts, 1, 350-351.

Schäfer, H.J., Gebauer, D., Nagler T.F., Eguíluz, L. (1993). Conventional and ion-microprobe U-Pb dating of detrital zircãos of the Tentudía Group (*Série Negra*, SW Spain): implications for zircão systematics, stratigraphy, tectonics and the Precambrian/Cambrian boundary. Contrib Mineral Petrol, 113, 289-299.

Serrano Pinto, M. (1984). Granitóides Caledónicos e Hercínicos na Zona de Ossa-Morena (Portugal) – Nota sobre aspectos geocronológicos. Memórias e Notícias – Universidade de Coimbra, 97, 81-94.

Simancas, J.F., Expósito, I., Azor, A., Martínez Poyatos, D.J., González Lodeiro, F., (2004). From the Cadomian orogenesis to the Early Palaeozoic Variscan rifting in southwest Iberia. Journal of Iberian Geology 30, 53–71.

Stow, D.A.V., Shanmugam, G. (1980). Sequences of structures in finegrained turbidites: comparison of recent deep-sea and ancient flysch sediments. Sediment. Geol., 25 (1-2), 23-42. DOI:10.1016/0037-0738(80)90052-4

Sun S.S., McDonough W.F. (1989). Chemical and isotopic systematics of oceanic basalts: implications for mantle composition and processes. In Magmatism in the Ocean Basins (eds. A. D. Saunders and M. J. Norry, vol. 42.). The Geological Society, 313–345. DOI:10.1144/GSL.SP.1989.042.01.19

Sun, S.S., Nesbht, R. W.Sharaskin, A. Y. (1979). Geochemical characteristics of mid-ocean ridge basalts. Earth and Planetary Science Letters, 44, 119-138. DOI: 10.1016/0012-821X(79)90013-X

Teixeira, C. (1981). Geologia de Portugal. Precâmbrico-Paleozóico. Lisboa, Fundação Calouste Gulbenkian. 629p

Vegas, K. (1968). Sobre la existencia de Precambrico en la Baja Extremadura, Estud, GeoL 24, 85-89.

Vera, J.A., (Eds.), (2004). Geología de España. Sociedad Geológica de España e Instituto Geológico y Minero de España, 884 p.

Walker, R.G. (1976). Facies Models 2. Turbidites and Associated Coarse Clastic Deposits. GeoscienceCanada, 3 (1), 25-36.

Whitney, D.L., Evans, B.W. (2010). Abbreviations for names of rock-forming minerals. American Mineralogist, 95 (1), 185-187. DOI: 10.2138/am.2010.3371

Wood, D.A (1980). The application of a Th-Hf-Ta diagram to problems of tectono-magmatic classification and to establishing the nature of crustal contamination of basaltic lavas of the British Tertiary volcanic province. Earth and Planetary Science Letters, 50, 11–30. DOI: 10.1016/0012-821X(80)90116-8

III.

Isótopos de Estrôncio e a correlação dos Eventos Carbonatados da Zona de Ossa-Morena

Como referido, a sucessão litoestratigráfica previamente definida para região de Abrantes apresenta claras afinidades litoestratigráficas e geoquímicas com as sucessões típicas da transição Neoproterozóico-Câmbrico inferior da Zona de Ossa-Morena (capítulo II.2). Contudo, os episódios tectono-metamórficos Variscos, que afectam a sequência ali presente, obliteram por completo o conteúdo fossilífero das unidades que constituem esta sucessão. Com a finalidade de fortalecer a correlação entre estas unidades meta-sedimentares ou vulcano-sedimentares da região de Abrantes e as sucessões estratigráficas dos restantes domínios da Zona de Ossa-Morena, algumas das quais com idades constrangidas pelo conteúdo fossilífero (como seja por exemplo a região de Vila Boim, sector de Alter-do-Chão-Elvas), foram aplicadas metodologias alternativas, como sejam as assinaturas isotópicas de Estrôncio (Sr).

Esta tentativa de correlação isotópica resulta da razão $^{87}Sr/^{86}Sr$ ser considerada constante em todos os oceanos num dado momento e, por outro lado, ter variado nos oceanos ao longo do tempo (e.g. McArthur *et al*., 2012 e referências inclusas). A uniformidade num dado momento resulta do tempo de residência de Sr no oceano ser maior que o tempo mistura dos próprios oceanos. O facto de se considerar que o oceano é uniforme quanto à sua mistura, faz com que em qualquer momento e em qualquer local do oceano a razão $^{87}Sr/^{86}Sr$ seja igual (McArthur, 1994).

Desta forma, selecionaram-se um conjunto de locais nesta zona paleogeográfica onde as sucessões da transição Neoproterozóico-Câmbrico inferior estivessem definidas. Em cada um destas sucessões, a unidade carbonatada típica do Câmbrico inferior, mais propriamente de idade Ovetiana-Marianiana, seria o foco de estudo. Esta unidade é interpretada como resultante da precipitação de carbonatos em ambiente de plataforma continental durante as fases iniciais do *rifting* Varisco. Daqui resulta que cada cristal de calcite precipitado neste período fornecer-nos-ia a assinatura da razão isotópica no oceano da altura, uma vez que os processos de fraccionação isotópica não são actuantes no momento da génese do cristal de calcite. Esperar-

se-ia que as amostras desta idade fornecessem no seu conjunto um *cluster* de assinaturas similares, podendo assim correlacionar-se.

Com objectivo de constranger a aplicabilidade do método, optou-se também por adicionar um segundo conjunto de amostras de carbonatos representativos de um segundo episódio de sedimentação carbonatada da Zona de Ossa-Morena. Este episódio teve lugar no Devónico inferior a médio, sendo característico dos domínios meridionais desta zona paleogeográfica. Estes carbonatos encontrarem-se muito bem constrangidos do ponto de vista cronológico devido ao seu conteúdo fossilífero (idade variável entre o Emsiano a Givetiano; Moreira e Machado, *in press* e referências inclusas) e apresentam um grau e metamorfismo extremamente baixo.

Os valores da razão isotópica $^{87}Sr/^{86}Sr$ obtidos para as amostras de carbonatos da Zona de Ossa-Morena serão comparados com as curvas da razão isotópica definidas para o Fanerozóico (e.g. McArthur *et al*., 2012). Os valores desta razão isotópica são significativamente distintos para o Devónico inferior a médio e para o Câmbrico. Desta forma, e se a metodologia aplicada fosse significativa, obter-se-iam dois *clusters* distintos de assinaturas, um composto pelos carbonatos Devónicos e o outro pelos carbonatos Câmbricos ou atribuídos ao Câmbrico.

Foram colectadas 37 amostras em toda a Zona de Ossa-Morena, incluindo essencialmente amostras dos sectores Portugueses, com excepção para uma amostra colectada em Espanha. Esta amostra foi selecionada uma vez que se encontrava num alinhamento de rochas carbonatadas (alinhamento Bencatel-Ferrarias-Cheles-Barrancos) com génese e idade dúbia, tendo sido alvo de discussão intensa ao longo dos últimos anos. Sumariamente, a região do Anticlinal de Ferrarias forneceu crinóides e outro conteúdo fossilífero que apontam uma idade Silúrica superior a Devónica inferior para esses carbonatos (Piçarra e Sarmiento, 2006). Também na região de Bencatel (sul do Anticlinal de Estremoz) e Barrancos revelaram a presença fósseis que são compatíveis com a idade proposta, sendo que alguns autores extrapolaram os dados paleontológicos para a restante sequência dos Mármores de Estremoz que apresenta um grau metamórfico mais alto e que até ao momento se tem revelado azóica (e.g. Piçarra, 2000; Piçarra e Sarmiento, 2006). Os dados isotópicos obtidos não excluem a idade Câmbrica para os carbonatos em causa sendo compatível também com a idade Silúrica superior (Pridoli) pelo menos para alguns dos carbonatos deste alinhamento; esta idade é compatível com um outro episódio carbonatado descrito na Zona de Ossa-Morena. Contudo, a assinatura destes carbonatos é significativamente distinta da assinatura do episódio Devónico, mostrando que estes carbonatos não seriam resultantes deste mesmo episódio.

Por fim, com intuito de constranger o efeito dos processos metamórficos e meteóricos na assinatura em causa, colheram-se também amostras que revelassem claras evidências

macroscópicas da actuação destes processos, nomeadamente dolomitos secundários e mármores com paragéneses metamórficas diversificadas. Desta forma, para além de se conseguir estabelecer a assinatura dos carbonatos Câmbricos, ou atribuídos ao Câmbrico, e Devónicos, seria possível também perceber o efeito destes processos na razão $^{87}Sr/^{86}Sr$ inicial.

De referir ainda que as análises contidas neste trabalho resultam de um protocolo de colaboração científica com os colegas José Francisco Santos e Sara Ribeiro do Laboratório de Geologia Isotópica da Universidade de Aveiro, onde foram realizadas as análises das razões isotópicas de Estrôncio, e com José Mirão do Laboratório Hércules (Universidade de Évora), onde se realizaram as difrações de Raio-X. Os dados em causa foram parcialmente apresentados no IX Congreso Geológico de España, resultando daí um resumo alargado sobre os dados isotópicos em causa. Seguidamente, no subcapítulo II.1 apresenta-se a totalidade dos dados obtidos e que ainda não foram alvo de publicação em revistas da especialidade, sendo espectável a sua submissão breve.

- *Capítulo III.1*

MOREIRA, N. *et al*. (em preparação), $^{87}Sr/^{86}Sr$ ratios discrimination applied to the Palaeozoic carbonates of the Ossa-Morena Zone

Referências

McArthur, J.M. (1994). Recent trends in strontium isotope stratigraphy. Terra Nova 6: 331-358. DOI: 10.1111/j.1365-3121.1994.tb00507.x

McArthur, J.M., Howarth, R.J., Shields, G.A. (2012). Strontium Isotope Stratigraphy. In: Gradstein F.M., Ogg J.G., Schmotz M.D., Ogg G.M. (Eds.), A Geologic Time Scale 2012 (Chapter 7), Elsevier, 127-144.

Moreira, N., Machado, G. (in press). Devonian sedimentation in Western Ossa-Morena Zone and its geodynamic significance. In Quesada. C., Oliveira, J.T. (Eds.), The Geology of Iberia: a geodynamic approach. Springer (Berlin), Regional Geology Review series.

Piçarra, J.M. (2000). Estudo estratigráfico do sector de Estremoz-Barrancos, Zona de Ossa Morena, Portugal. Vol. I - Litoestratigrafia do intervalo Câmbrico médio?-Devónico inferior, Vol. II - Bioestratigrafia do intervalo Ordovícico-Devónico inferior. PhD Thesis (unpublished), Évora University, Portugal.

Piçarra, J.M., Sarmiento, G. (2006). Problemas de posicionamento estratigráfico dos Calcários Paleozóicos da Zona de Ossa Morena (Portugal). In: J. Mirão & A. Balbino (Eds.), VII Congresso Nacional de Geologia abstract book (vol. II), Estremoz, 657-660.

III.1

$^{87}Sr/^{86}Sr$ ratios discrimination applied to the Palaeozoic carbonates of the Ossa-Morena Zone

Index

III.1.1. Introduction

The definition of lithostratigraphic successions in metamorphic and strongly deformed domains is essential to constrain its geodynamical evolution. However, in these cases, the paleontological data are often scarce and the chronological establishment of a local lithostratigraphic succession is dependent of the correlation with well-defined lithostratigraphic successions with fossiliferous data or, in some cases, using the geochronological data to constrain the age of the lithostratigraphic successions.

In Abrantes, despite the greenschist-amphibolite metamorphic recrystallization and the strong variscan deformation (Romão et al., 2010; Moreira, 2012; Moreira et al., 2015), structural and petrological data show a lithostratigraphic succession similar to the Neoproterozoic-Cambrian series of Ossa-Morena Zone (OMZ; e.g. Oliveira et al., 1991; Gozalo et al., 2003). One of the Abrantes lithostratigraphic units is a carbonated succession (S. Miguel do Rio Torto

Carbonates), mainly composed of dolomite and calcite marbles interbedded with mafic volcanic rocks and calc-schists (Moreira et al., 2015). The litostratigraphic and petrographic features of this unit are similar to the Lower Cambrian carbonated successions of OMZ (Oliveira et al., 1991; Gozalo et al., 2003; Araújo et al., 2013). Nevertheless, not only the carbonate sedimentation in OMZ is not exclusive of Lower Cambrian, but often its age is highly debatable in some sectors, as in Estremoz Anticline and in Ficalho (Piçarra, 2000; Piçarra and Sarmiento, 2006; Pereira et al., 2012).

The determination of the $^{87}Sr/^{86}Sr$ of the OMZ carbonates could help to constrain the lithostratigraphic correlations between them. Indeed, by comparing the $^{87}Sr/^{86}Sr$ ratios in marbles and limestones from different domains of OMZ, with available chronological and isotopic data, it is possible to establish strontium isotopic signatures for the Cambrian and Devonian carbonated episodes. This methodology allows a coherent correlation between OMZ carbonates.

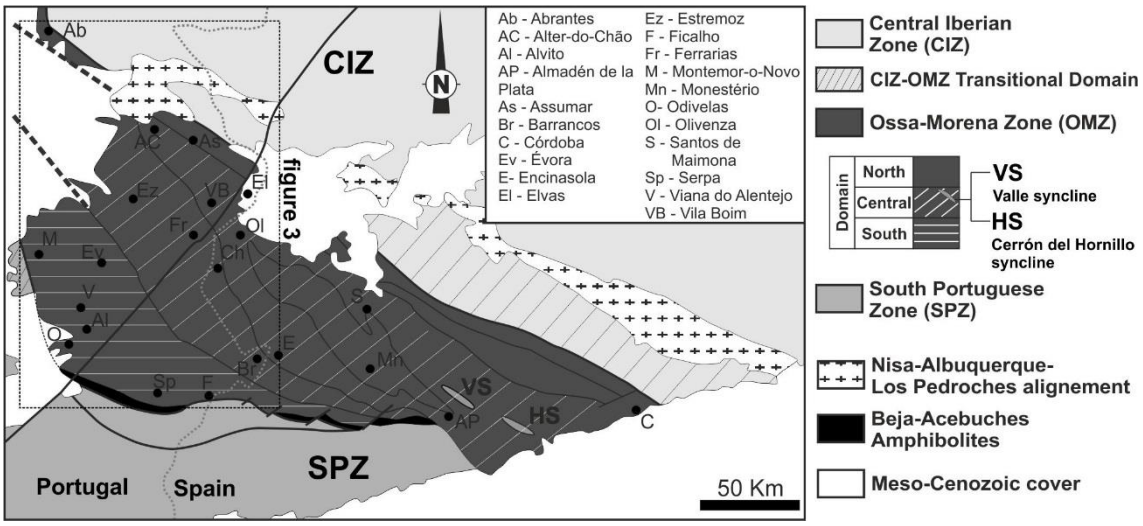

Figure 1 – Geological sketch of the OMZ in the context of neighboring tectonostratigraphic Variscan Zones text (adapted from Oliveira et al., 1991 and Robardet and Gutierrez-Marco, 2004).

III.1.2. The Ossa-Morena Zone Carbonates

The stratigraphic successions defined for OMZ show the presence of four regional distinct carbonate sedimentation episodes:

(i) The first episode, Cambrian in age (Ovetian-Marianian – Cambrian Stage 2; Oliveira et al., 1991; Gozalo et al., 2003, Alvaro et al., 2014), is related with the first pulses of Variscan Cycle during the continental rifting process (Sánchez-Gárcia et al., 2008; 2010; Moreira et al., 2014a). This episode is characterized by sequences of dolomite and calcite marbles or limestones, sometimes with siliciclastic beds and interbedded

metavolcanic rocks (Oliveira et al., 1991; Vera, 2004; Sánchez-Gárcia et al., 2008; 2010; Pereira et al., 2012; Araújo et al., 2013; Moreira et al., 2014a). The Ovetian-Marianian age is constrained by paleontological data in Spain (Gozalo et al., 2003; Vera, 2004 and included references) and in Portugal (Alter-do-Chão-Elvas Domain; Oliveira et al., 1991; Araújo et al., 2013). In the successions with no biostratigraphic data, the age is based on lithostratigraphic correlations, such as in the Abrantes, Estremoz, Ficalho and Viana do Alentejo successions (Fig 1; Oliveira et al., 1991; Moreira et al., 2015; 2016);

(ii) An Upper Ordovician episode (Kralodvorian – Ka3 and Ka4; Robardet and Gutierez-Marco, 2004; Sarmiento et al., 2008; 2011), the Pelmatozoan Limestone, is preserved in Valle and Cerrón del Hornillo synclines (Fig. 1; Robardet and Gutierrez-Marco, 1990; 2004; Sarmiento et al., 2008; 2011). This unit is characterized by massive limestones, sometimes bioclastic (Sarmiento et al., 2008; 2011), with evidences of dolomitization. The massive features are less evident on top and bottom of the sequence, where laminated textures were developed. On top of the limestones succession, karstified morphology was described (Robardet and Gutierez-Marco, 2004).

(iii) Also in Valle and Cerrón del Hornillo synclines, the Scyphocrinites Limestone has an Upper Silurian age, with the bottom of sequence could be Late Ludlow or early Pridoli (Robardet and Gutierez-Marco, 1990; 2004). This unit consists in dark limestones interbedded with calcareous shales. These limestones are not represented in Silurian succession of Barrancos area (temporally similar to Xistos Raiados Formation; Piçarra, 2000). Although, in Murtiga Formation (Encinasola area), considered equivalent of the Xistos Raiados Formation, Pridoli limestones have been mentioned (Robardet and Gutierez-Marco, 2004).

(iv) The fourth episode is Lower-Middle Devonian in age, being represented in the SW domains of the OMZ (Machado et al., 2009; 2010; Moreira et al., 2010; Moreira and Machado, in press). Machado et al. (2009; 2010) described a calciturbiditic sequence (Odivelas Limestone), recently interpreted as a reef system (Moreira and Machado, in press), spatially associated to basaltic rocks with low-K tholeiitic to calc-alkaline geochemical signatures (Rebolado Basalts; Santos et al., 1990; 2013; Silva et al., 2011). The paleontological data from the Odivelas limestones provides Emsian to Givetian ages (Conde and Andrade, 1974; Oliveira et al., 1991; Machado et al., 2009; 2010). Similar facies and ages (Eifelian to Frasnian) are also described in limestones associated to the Toca da Moura and Cabrela Carboniferous basins (Pena and

Pedreira de Engenharia Limestones near Montemor-o-Novo; Boogard, 1972; 1983; Machado and Hladil, 2010). These limestones are interpreted, at least in part, as Devonian olistoliths within the previous mentioned basins (Pereira and Oliveira, 2003; Pereira et al., 2006; Oliveira et al., 2013).

In addition, in some Carboniferous basins located in the Central and North domains of the OMZ (Robardet and Gutierez-Marco, 1990; Palácios Gonzalez et al., 1990; Medina-Varea et al., 2005; Armendáriz, 2006), some limestones are also described interbedded in siliciclastic sequences, however some of these limestones are not marine limestones.

Although the age of the Palaeozoic carbonated sedimentation in OMZ is usually well constrained, in the Estremoz-Barrancos sector and in Ficalho succession it is a highly debatable subject (Oliveira et al., 1991; Piçarra, 2000; Pereira et al., 2012; Araújo et al., 2013 and references therein). In these cases, overlying the basal carbonated unit (mostly dolomitic marbles – the Dolomitic Formation), a volcano-sedimentary complex with abundant calcite marbles is found (Oliveira et al., 1991; Araújo et al., 2013). The presence of crinoid fragments and conodonts in the calcite limestones of Ferrarias (which according to Piçarra, 2000 is equivalent of the neighbouring Estremoz Marbles), Barrancos and Ficalho, assigning at least an Upper Silurian to Devonian age to these limestones (Piçarra and Le Menn, 1994; Sarmiento et al., 2000; Piçarra and Sarmiento, 2006). These fossiliferous limestones are contained in the volcano-sedimentary complexes developed over the basal Cambrian Carbonated Units (Piçarra, 2000).

However, some authors argue that these ages could not be considered the depositional ages of the limestones, but results from mixing younger materials due to sub-aerial exposure and remobilization of faunal material (Pereira et al., 2012). The same authors obtain a 499.4 ± 3.3 Ma age (SHRIMP U-Pb zircon) in meta-rhyolites, that they considered intercalated into marbles from the Estremoz sequence, proposing a Middle-Upper Cambrian transition age for the Estremoz volcano-sedimentary complex. Nevertheless, field relations of these meta-rhyolites (Coelho and Gonçalves, 1970; Gonçalves, 1972) precludes such conclusion (see chapter V.2 for a discussion).

III.1.3. The $^{87}Sr/^{86}Sr$ Ratio Approach

As the isotopic ratio $^{87}Sr/^{86}Sr$ of oceanic waters has varied over the time (Fig. 2), its determination could be used in the correlation and, in some cases, dating the marine carbonates that preserve the seawater $^{87}Sr/^{86}Sr$ fingerprint (Burke et al., 1982; Veizer, 1989; Veizer et al., 1999; McArthur et al., 2012 and included references).

The $^{87}Sr/^{86}Sr$ variation has been due by changing the fluxes of Sr to the ocean, from the two main sources: mantle and continental crust (McArthur, 1994; Veizer et al., 1999). In middle ocean ridges, the hydrothermal circulation induces the interaction between oceanic crust and seawater, generates a modification of strontium isotopic ratio in seawater: the loss of Sr from seawater is replaced by leached Sr from middle ocean ridge rocks, decreasing the $^{87}Sr/^{86}Sr$ of marine seawater (McArthur, 1994). On the other hand, the continental weathering supplies are higher than that of marine Sr. Indeed, addition of continental crust Sr to the ocean, therefore increases the marine $^{87}Sr/^{86}Sr$ ratio (McArthur, 1994). Nowadays, the $^{87}Sr/^{86}Sr$ ratio in seawater is always higher than 0.703 (minimum value of mid ocean ridge rocks) and usually lower than 0.713 (best estimated value of modern rivers; McArthur, 1994).

The analytical precision of the $^{87}Sr/^{86}Sr$ ratio that can be measured is ± 0.00002 (McArthur, 1994). This precision makes analytically indistinguishable the ratio variation in seawater from worldwide localities. This uniformity is resulted from the residence time of Sr in the Ocean that is far longer than the time it takes currents to mix the oceans, so the oceans are thoroughly mixed on time scale that are short relative to the rates of gain and loss of Sr (McArthur, 1994; McArthur et al., 2012). As such, it is assumed that the ocean has always been well mixed, as in present, and consequently is isotopically uniform with respect to $^{87}Sr/^{86}Sr$. This fact allows to correlate and even date some marine rocks and minerals.

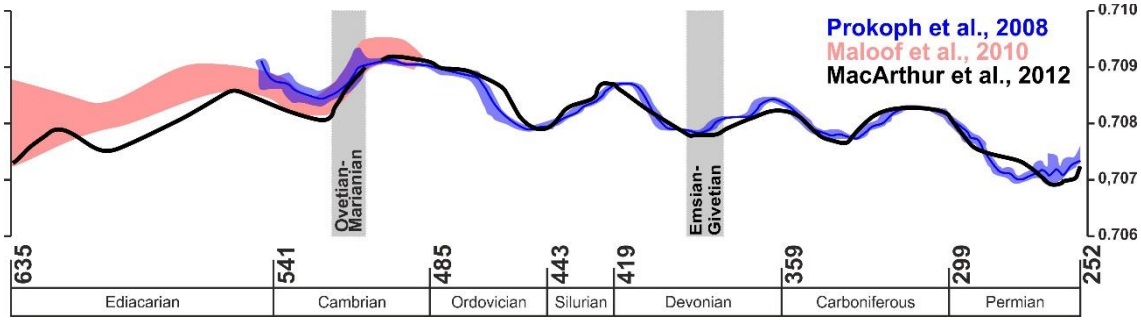

Figure 2 – Variation of $^{87}Sr/^{86}Sr$ through the Ediacarian and Palaeozoic times (curves adapted from Prokoph et al., 2008; Maloof et al., 2010; MacArthur et al., 2012).

III.1.4. Sample preparation and methods

37 samples of OMZ carbonate rocks were collected. After sample characterization by conventional petrographic techniques, they underwent specific preparation, such as cleaning and removing meteoric surface alteration followed by crushing, gridding and sieving, in order to obtain powdered carbonate samples smaller than 63 µm, enriched in carbonate specimens. The used methodology allow to concentrate the carbonated phases in powdered samples.

The detailed mineralogical composition of carbonates was analysed in a X-Ray difractometer (XRD – Bruker D8 Discover with DaVinci geometry) and using a Lynxeye linear detector (Hercules Laboratory, University of Évora). The scans was collected from 2θ 3º to 75º, with steps of 0.005º and one second by step. The semi quantification of the phases abundances were done using the DIFFRAC.SUITE software from Bruker by the RIR-Reference Intensity Ratio (Hubbard et al., 1976; 1988 and included references).

The strontium isotope analyses were done using a Mass Spectrometer Thermal Ionization (TIMS) with a VG Sector 54 spectrometer (Isotopic Geology Laboratory, University of Aveiro). The main procedure involve a first stage of rocks sample dissolution with HCl with some drops of HF and HNO_3 for the carbonates. Afterwards, the remaining solutions, including the carbonate leachated samples, were dried and re-dissolved in HCl and subject to a conventional two-stage ion chromatography separation with cation exchange resins for Sr purification. This methodology should guarantee the non-carbonate fraction separation from the whole sample. After the carbonate concentration and purification in each sample the isotopic measurements of $^{87}Sr/^{86}Sr$ ratios were performed by means of a thermal ionization mass spectrometry (VG Sector 54).

III.1.5. Geological framework, Petrography and XRD analysis of OMZ Carbonates

The 37 carbonate samples from the OMZ Paleozoic Carbonates were characterized by conventional petrographic techniques, with special attention to textural, mineralogical and metasomatic (i.e. secondary dolomitization) features and by XRD analyses. The samples includes marbles and limestones, with calcite and dolomite as the main mineral carbonate specimens, and one sandstone with calcite cement. Some dolomite carbonates show macro and microscopic textural evidences of secondary dolomitization, while in others the dolomitization is interpreted as “primary” and/or diagenetic.

A short general framework for the collected samples and the main petrographic features of analysed samples are summarized below according to the geographic sectors of samples provenience.

III.1.5.1. Northern OMZ Carbonates (Abrantes, Assumar)

From the northern OMZ domains, 7 samples were collected, 6 from Abrantes and 1 from Assumar regions (table 1; Fig. 3A and 3B). The Abrantes samples are from S. Miguel do Rio Torto Carbonates, characterized by dolomite and calcite marbles interbedded with mafic volcanic rocks, which have been correlated with the Lower Cambrian carbonated units of the OMZ (Moreira et al., 2015; 2016). This unit was affected by Variscan greenschist to amphibolite

metamorphic recrystalization. The Assumar carbonates are included in a Detrital-Carbonated Complex, also attributed to Lower Cambrian (Pereira and Silva, 2001).

The XRD analyses (table 2) reveals a variable carbonate content in carbonates in these marbles, with three samples containing more than 95% of carbonates (GQAB-3, GQAB-7, ASS-1), three ranges between 95-80% (GQAB-4, GQAB-13, GQAB-27) and one between 80-60% (GQAB-37). Two samples are calcite marbles (GQAB-3 and GQAB-4), while the others are dolomitic (the sample GQAB-27 has a small proportion of calcite). The non-carbonate fraction in mainly composed of quartz and micas, although in some samples clay minerals (GQAB-13, GQAB-27, GQAB-37), orthose (GQAB-37) and titanite (GQAB-4) are identified. In the Assumar sample (ASS-1), the presence of chlorite is also substantial.

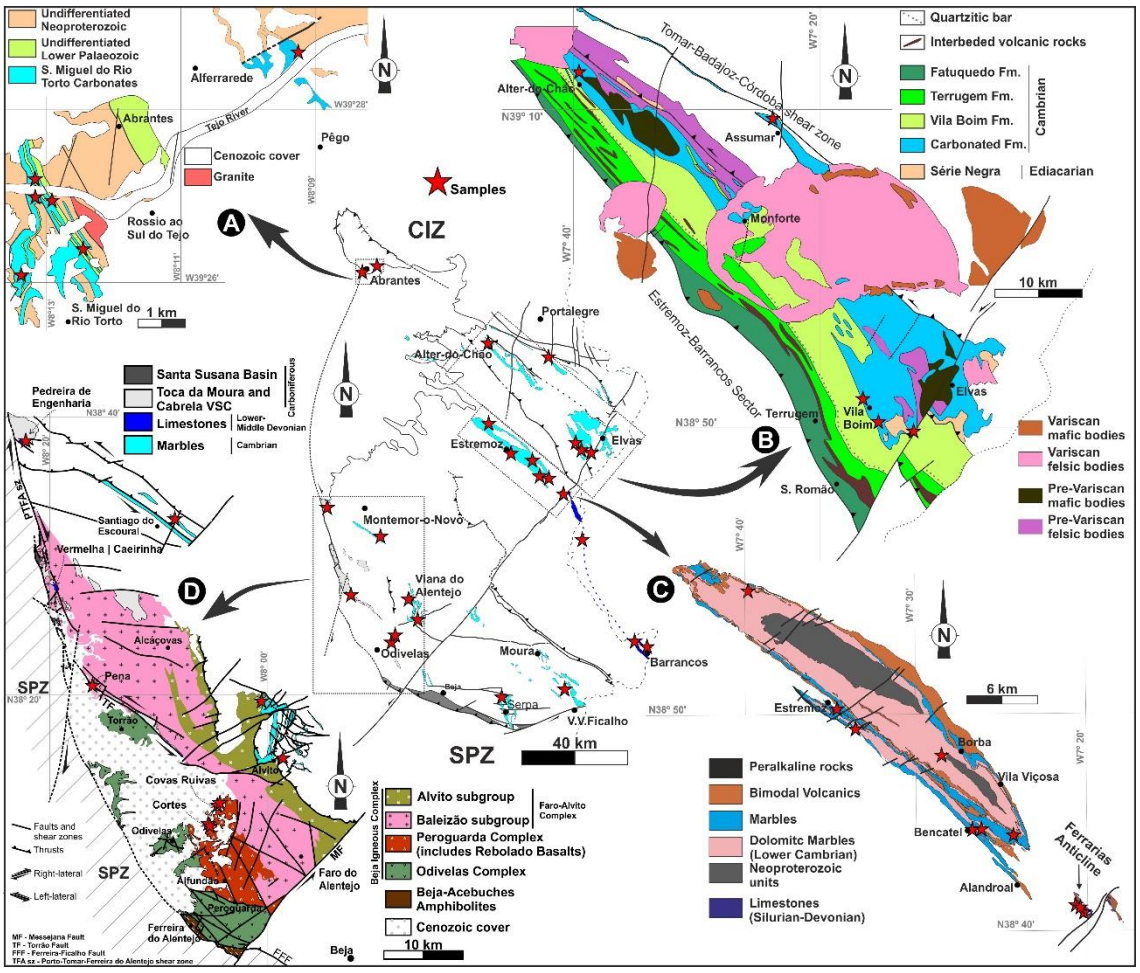

Figure 3 – Geological context of the OMZ carbonate samples:

A – Abrantes region geological map (adapted from Moreira, 2012);

B – Alter-do-Chão-Elvas sector geological map, also showing the location of the Assumar sample location (adapted from LNEG, 2010);

C – Estremoz Anticline (adapted from Piçarra, 2000; LNEG, 2010);

D – Southwest sectors of OMZ (adapted from LNEG, 2010; Moreira and Machado, in press).

The macroscopic and conventional petrographic characterization shows four distinct lithofacies of Northern OMZ carbonates (table 1):

- Samples GQAB-3 and GQAB-4 are extremely pure calcite marbles (calcite ~90%), presenting granoblastic inequigranular textures (calcite with millimetre dimensions). The non-carbonated component is mostly composed of significant quartz (5-10%) and opaque minerals.

- Sample GQAB-27 is a dolomite marble (dolomite > 80%; Fig. 4A) with granoblastic inequigranular texture, with dolomite from millimetre to submillimetre dimension. The dolomite predates metamorphism (possibly diagenetic), presenting type II (and IV?) twins (Passchier and Trouw, 2005), which shows metamorphic recrystallization of dolomite. Significant quartz (~10%) and muscovite (5-10%) and few opaque minerals compose the non-carbonated content.

- Samples ASS-1 and GQAB-7 are dolomite marbles (dolomite > 85%), with substantial quartz content (~10%). Some vestigial opaque minerals, micas (biotite or muscovite) and epidote are also identified. Two generations of dolomite are clear identified: one previous to metamorphism, with recrystallization evidences (type II twins in crystal), and a second one characterized by fine-grained turbid/cloudy dolomite (sometimes euhedral and zoned), being associated to dissolution and growing over the previous dolomite generation. The macroscopic evidences of dissolution and late dolomite precipitation was removed during sample preparation.

- Samples GQAB-13 and GQAB-37 are mainly dolomitic (>80%), characterized by pervasive dissolution and late dolomitization with abundant cloudy euhedral dolomite. The sample GQAB-13 preserves some earlier recrystallized dolomite with millimetre size, although the secondary late dolomitization is dominant (Fig. 5A). The non-carbonate fraction presents significative quartz content (5-10%), but also biotite, muscovite, amphibole, feldspars, chlorite and opaque minerals (~10%). The pervasive dolomitization is also visible at mesoscale.

III.1.5.2. Alter-do-Chão – Elvas Sector Limestones

In the Alter-do-Chão – Elvas sector, 4 samples are collected (table 1; Fig. 3B). The samples present very low-grade metamorphism and a fine-grain (submillimetric) texture, belonging to the Elvas Carbonated Unit (Oliveira et al., 1991; Moreira et al., 2014b). This unit is mainly composed of Ovetian-Marianian dolomite (and calcite) limestones, which are overlapped by the

Vila Boim Formation, with a Marianian-Biblian age based on trilobite, acritarchs and brachiopods faunas (Oliveira et al., 1991; Gozalo et al., 2003).

Table 1 – Main geographic, stratigraphic and macroscopic features of analysed samples.

		Stratigraphic features					Macroscopic features		
		Unit / Formation	Lithology	Age			Main carbonate	Secundary Dolomitization	Granularity
				Cambrian	Devonian	Silurian-Devonian			
GQAB-3	Abrantes	São Miguel do Rio Torto Carbonates	Marble	X			C	-	+++
GQAB-4	Abrantes	São Miguel do Rio Torto Carbonates	Marble	X			C	-	+++
GQAB-7	Abrantes	São Miguel do Rio Torto Carbonates	Dolomite marble	X			D	+	+++
GQAB-13	Abrantes	São Miguel do Rio Torto Carbonates	Dolomite marble	X			D	++	+++
GQAB-27	Abrantes	São Miguel do Rio Torto Carbonates	Dolomite marble	X			D	+	++
GQAB-37	Abrantes	São Miguel do Rio Torto Carbonates	Dolomite marble	X			D	++	++
ASS-1	Assumar	Assumar detrital-carbonated Complex	Dolomite marble	X			D	+	++
VB-2	Vila Boim	Elvas Carbonated Formation	Limestone	X			C	-	+
VB-12	Vila Boim	Elvas Carbonated Formation	Dolostone	X			D	+	+
VB-18	Vila Boim	Elvas Carbonated Formation	Limestone	X			C	-	+
ALT-1	Alter-do-Chão	Elvas Carbonated Formation	Dolostone	X			D	+	+
ETZ-2	Estremoz	Estremoz volcano-sedimentary Complex	Marble	X		X?	C	-	+++
ETZ-3	Vila Viçosa-Pardais	Estremoz volcano-sedimentary Complex	Marble	X		X?	C	-	+++
ETZ-5	Bencatel	Estremoz volcano-sedimentary Complex	Marble	X		X?	C	-	+++
ETZ-6A	Borba	Dolomitic Formation	Dolostone	X			D	++	++
ETZ-7	Estremoz	Estremoz volcano-sedimentary Complex	Marble	X		X?	C	-	+++
ETZ-9	Sousel	Dolomitic Formation	Dolomite marble	X			D	-	++
FER-1	Ferrarias	Ferrarias Limestone	Limestone			X?	C and D	++	++
FER-2	Ferrarias	Ferrarias Limestone	Dolosone			X?	D and C	++	++
FER-3	Ferrarias	Ferrarias Limestone	Limestone			X?	C	-	++
BA-3	Barrancos	Monte das Russianas Formation	Sandstone, calcite cement		X		C	-	+
BA-4	Barrancos	Barrancos Igneous Complex	Limestone			X?	C	-	+
BEN-1	Bencatel	-	Dolostone			X?	D and C	-	+
BEN-2	Bencatel	-	Limestone			X?	C	-	++
CHE-1	Cheles (SPN)	-	Marble	X			C	-	++
OD-1	Odivelas	Odivelas Limestone (Covas Ruivas)	Limestone		X		C	-	+
OD-2	Odivelas	Odivelas Limestone (Covas Ruivas)	Limestone		X		C	-	+
OD-4	Monte da Pena	Toca da Moura Complex (Pena Limestones)	Limestone		X		C	-	+
OD-5A	Odivelas	Odivelas Limestone (Cortes)	Limestone		X		C	-	++
OD-6	Odivelas	Odivelas Limestone (Cortes)	Bioclastic limestone		X		C	-	++
CAB-1	Cabrela	Cabrela Complex (Pedreira da Engenharia Limestone)	Dolostone		X		D	+	+
VIA-1	Viana do Alentejo	Viana-Alvito volcano-sedimentary Complex	Marble	X			C	-	+++
VIA-2	Viana do Alentejo	Viana-Alvito volcano-sedimentary Complex	Secondary dolostone	X			D	+++	+
ALV-1	Alvito	Viana-Alvito volcano-sedimentary Complex	Marble	X			D	++	+++
SRP-1	Serpa	Moura-Ficalho volcano-sedimentary Complex	Marble	X			D and C	-	+++
FIC-2	Ficalho	Moura-Ficalho volcano-sedimentary Complex	Limestone	X?		X?	C	-	+
ESC-1	Escoural	Monfurado Formation	Marble	X			C	+	+++

(C) Calcite
(D) Dolomite

(-) absente
(+) present
(++) intense
(+++) prevasive

(+) fine-grained
(++) intermediate
(+++) coarse-grained

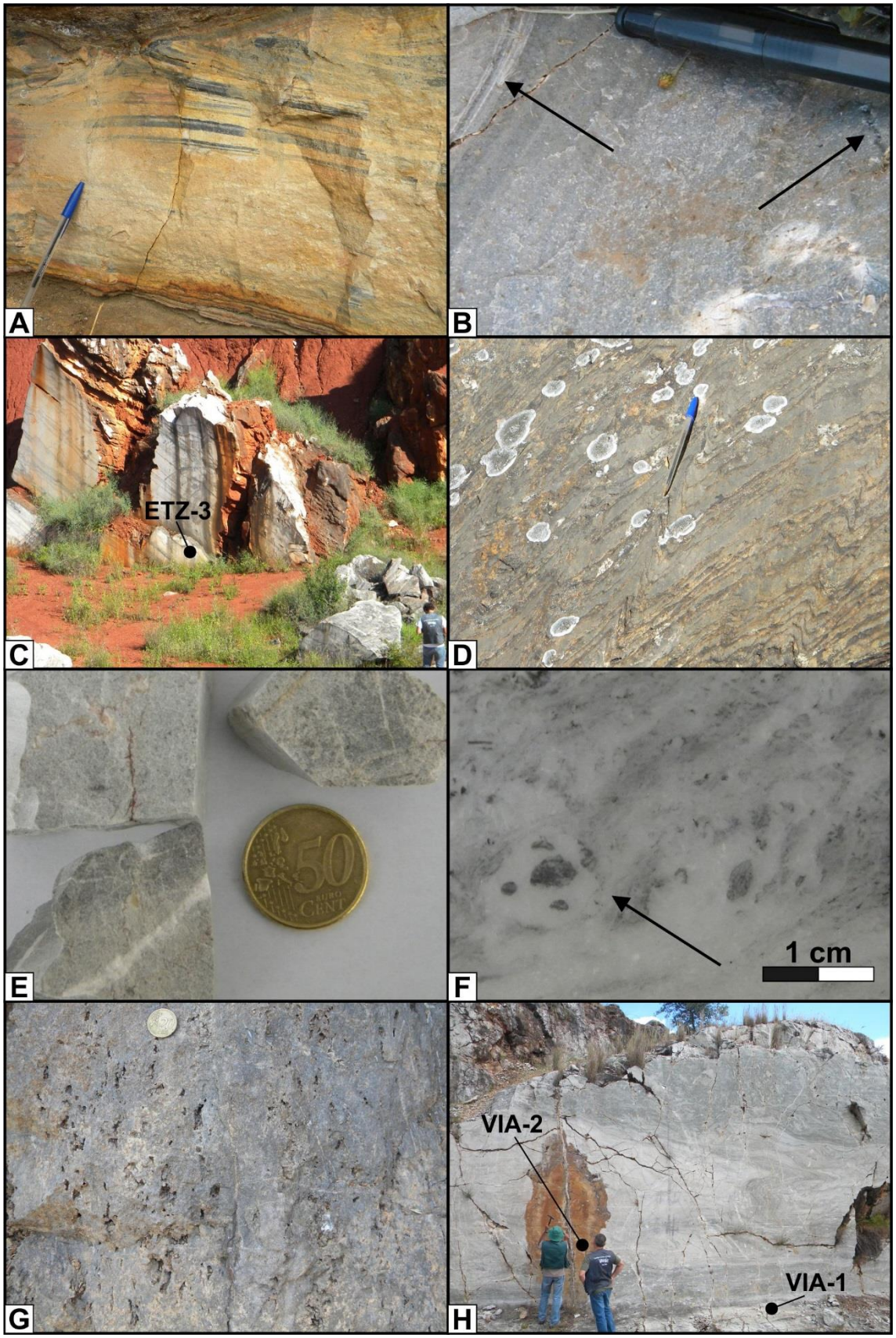
A
B
ETZ-3
C
D
50
EURO
CENT
E
1 cm
F
G
VIA-2
VIA-1
H

Figure 4 – Main macroscopic features of selected samples:

A – Dolomite marble from Abrantes sector, showing the presence of Dolomite recrystallization (AB-27 sample);

B – Fine-grained grey limestone from the Alter-do-Chão-Elvas sector, showing quartz-rich layers (VB-2 sample);

C – Sample location of the white marble from southern limb of the Estremoz anticline (ETZ-3 sample), showing the intense karstification;

D – Impure limestone from Barrancos sector (BA-4 sample). This locality provides some unclassified crinoid fragments (Piçarra and Sarmiento, 2006);

E – Macroscopic features of the Pena limestones, showing evidences of fluid interaction with late calcite veins (OD-4 sample);

F – Transverse or slightly oblique sections of (?) *cupressocrinitids* columnals from the Odivelas Limestones, typical of Middle Devonian age (OD-6 sample);

G – Macroscopic evidences of secondary late dolomitization and dissolution (CAB-1 sample);

H –Viana do Alentejo carbonates, showing the relation between VIA-1 (calcite marbles) and VIA-2 (late dolostone vein) samples.

The XRD analyses (table 2) shown that these limestones are impure, presenting more than 23% of non-carbonate mineral (Fig. 6A). Two samples (VB-2, VB-18) are calcite-rich, with a small dolomite content (lower than 1%; Fig. 6A1), and two are dolomitic (VB-12, ALT-1; Fig. 6A2). The non-carbonate fraction is composed of quartz, micas and chlorite (in one sample albite is also identified).

Petrography studies indicates two distinct lithotypes:

- Samples VB-2 and VB-18 are fine-grained impure grey calcite limestones (calcite=60-70%; Fig. 4B), with significant quartz, chlorite and epidote content (25-35%) and some sericite, amphibole, feldspars and opaque minerals (Fig. 5B). The sample VB-2 also presents some dolomite.
- Samples VB-12 and ALT-1 are fine-grained impure dolostones (dolomite=65-75%), but do not present pervasive late dolomitization at mesoscale. The dolomite is considered syn-diagenetic (or primary?) and macroscopic secondary dolomitization evidences were removed during sample preparation. Occasionally, some dissolution are recognized at thin-section scale, with generation of fine-grained cloudy late dolomite (sometimes euhedral). The first generation of dolomite sometimes presents type I twins, suggesting weak recrystallization (Passchier and Trouw, 2005). The non-carbonated content (25-30% of the sample) are mostly composed of quartz and some (chloritized) biotite, sericite, chlorite, amphibole, feldspar and opaque minerals.

III.1.5.3. Estremoz Anticline

In the Estremoz Anticline, 6 carbonates samples were collected (table 1; Fig. 3C). The Estremoz Anticline have a Neoproterozoic core, below a Cambrian sequence composed of arkosic sandstones at the base, overlapped by dolomite marbles unit (Dolomitic Formation; e.g. Oliveira et al., 1991), where the samples ETZ-6A and ETZ-9 have been collected. On top of the Dolomitic Formation, it is developed the Estremoz Volcano-Sedimentary Complex, mainly composed of calcite marbles (where the samples ETZ-2, ETZ-3, ETZ-5 and ETZ-7 have been collected) interbedded with mafic and felsic volcanic rocks (Oliveira et al., 1991). All these succession were deformed and metamorphosed under greenschist metamorphic conditions during the Variscan orogeny (Pereira et al., 2012).

The XRD analysis (table 2) indicates that the samples ETZ-2, ETZ-3, ETZ-5 and ETZ-7 are extremely pure, with a calcite content higher than 95%, while the silicate component is composed of quartz and micas (Fig. 6B). The other samples (ETZ-6A and ETZ-9) are dolomitic presenting a significant content in non-carbonate minerals (36 and 11% respectively). The non-

carbonated content is mostly composed of micas and quartz, although orthose and chlorite were also identified in sample ETZ-9.

The petrographic studies identifies four distinct lithotypes:

- Samples ETZ-2 and ETZ-3 are white marbles (Fig. 4C) with no evidences of secondary dolomitization. The marbles present a granoblastic inequigranular texture. Both samples are extremely pure, being composed of calcite (>95%) and some quartz clasts. The calcite is pervasively recrystallized, showing type II twins (Fig. 5C).

- Samples ETZ-5 and ETZ-7 are dark to grey marbles, with dispersed organic matter. The marbles present granoblastic inequigranular texture, showing slightly oriented calcite crystals in ETZ-5 sample. The sample ETZ-5 is extremely pure, being mostly composed of calcite (~90%). The sample ETZ-7 is slightly more impure (calcite 80-85%), showing some layers composed of fine-grained calcite with abundant quartz (~15%) interbedded with medium-grained calcite ones. Both samples presents type I and II twins in calcite crystals, showing some recrystallization.

- Sample ETZ-6A is an impure dolostone (dolomite=60-75%), containing abundant quartz and sericite (25-30%) and some chlorite and opaque minerals. It shows clear evidences of late secondary dolomitization and dissolution from macro to microscale (Fig. 5D). The dolomite, frequently with euhedral to sub-euhedral shape, has no evidences of recrystallization, with internal zonation showing more than one episode of dolomitization (Fig. 5D).

- Sample ETZ-9 is a dolomite marble, with recrystallized dolomite crystals (~90%) and a granoblastic texture. There is no evidences of dissolution or late dolomitization, showing that the dolomite is previous to the metamorphic event (possibly diagenetic or primary?). The dolomite shows type I to type II twins, as in calcite marbles.

III.1.5.4. Bencatel-Ferrarias-Cheles-Barrancos Alignment

The presence of dolostones and limestones, spatially associated with bimodal magmatic rocks and breccias, defines the here named Bencatel-Ferrarias-Cheles-Barrancos alignment (Fig. 3; Oliveira, 1984; Araújo et al., 2013). However, the geodynamic meaning of this NW-SE to N-S alignment, which follows the general structural trend of OMZ (Fig. 3), is poorly understood. In Barrancos region (Fig. 3) these alignment was named Barrancos Igneous Complex (Araújo et al., 2013 and references therein).

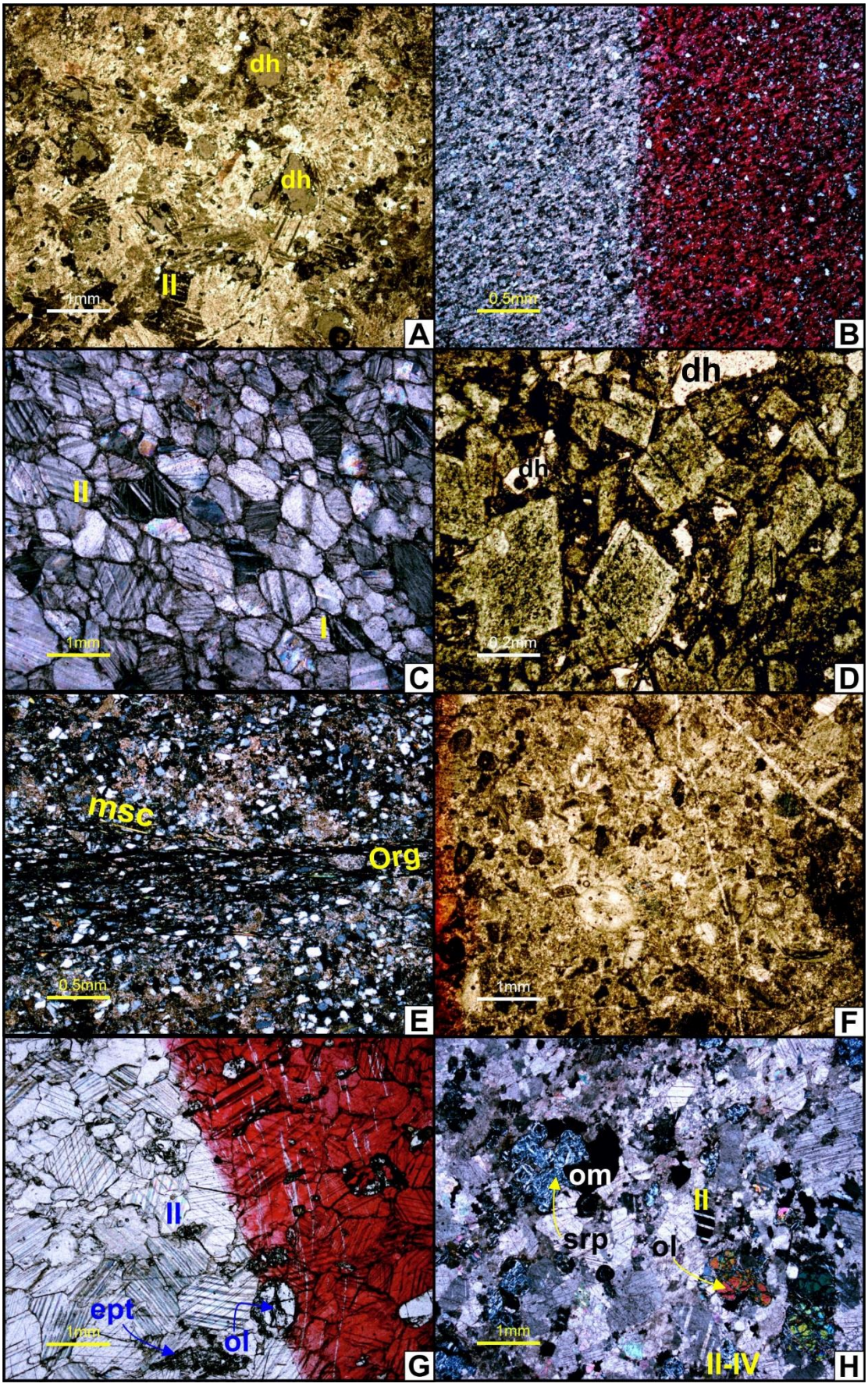
dh
dh
II
1mm
A
0.5mm
B
II
I
1mm
C
dh
dh
0.2mm
D
msc
Org
0.5mm
E
1mm
F
II
ept
ol
1mm
G
om
srp
II
ol
1mm
II-IV
H

Figure 5 – Main petrographic features of selected carbonated samples (dh – dissolution hole; msc – muscovite; org – organic matter; ept – epidote; ol – olivine; I – type I twin; II – Type II twin; IV – type IV twin; srp – serpentine; om – opaque minerals):

A – Two generations of dolomite, the first one previous to metamorphism showing recrystallized type II twins: the second one overgrowing and partially substituting the first generation (GQAB-13 sample);

B – Fine-grained calcite limestone, coloured by Alizarin Red Solution. The picture show the presence of fine-grained quartz+feldspar, muscovite and epidote (VB-18 sample);

C – Extremely pure marble from Estremoz Anticline, showing type I and II twins in calcite (ETZ-2 sample);

D – Dolostone resulting from the total substitution of primary carbonate structure, showing dissolution holes and euhedral zoned crystals of dolomite, with cloudy core and clear edges (ETZ-6A sample);

E – Sandstone with calcite cement from Monte das Russianas Formation (BA-3 sample), showing the presence of organic matter rich layers;

F – Bioclastic Devonian limestone from Odivelas Limestone (OD-1 sample);

G – Calcite marble from Viana do Alentejo, with epidote and olivine crystals in a granoblastic texture with type II twins in calcite (VIA-1 sample);

H – Serpa marble (SRP-1 sample), showing the association substitution of olivine crystal by serpentine group minerals. The carbonates are highly recrystallized with type II and IV twins.

The Barrancos and Ferrarias limestones, considered equivalent by some authors of the Estremoz Volcano-Sedimentary Complex (Piçarra, 2000), have locally Upper Silurian to Devonian fossils (Piçarra and Le Menn, 1994; Sarmiento et al., 2000; Piçarra and Sarmiento, 2006). This alignment intercepts the Cheles Limestones (Spain), considered a structural klippe structure of Lower Cambrian carbonates over the Ordovician-Silurian successions developed during the early Variscan events (Moreno and Vegas, 1976; Vegas and Moreno, 1973). The Bencatel carbonates are located in southern limb of Estremoz Anticline (Fig. 3C), presenting clear distinguish features as respect to the previously described Estremoz marbles. Seven samples are collected in this alignment (table 1): two near Bencatel (BEN-1, BEN-2), three from Ferrarias Anticline (FER-1, FER-2, FER-3), one from Cheles structure (CHE-1) and two near Barrancos (BA-3, BA-4).

The XRD analyses (table 2) indicate a strong heterogeneity in the carbonates content: more than 95% in two samples (FER-2, BEN-2), between 90 and 80% in two samples (FER-1, FER-3; Fig. 7A), between 80 and 70% in another two samples (BEN-1, CHE-1) and 57% in the last sample (BA-4). Concerning the dominant carbonate specimen: two samples are calcitic (FER-3, CHE-1), two are calcite-dominant (FER-1, BA-4), one presents similar proportion of calcite and dolomite (BEN-2), one is dolomite-dominant (BEN-1) and one is dolomitic with vestiges of calcite (FER-2). The non-carbonate content is mainly composed of quartz and micas, although some samples also present feldspars (FER-1, CHE-1) and clay minerals (BEN-1, CHE-1). The sample BA-3 presents a clearly distinct XRD pattern, with more than 80% of non-carbonated minerals (mainly composed of quartz, micas, chlorite and goethite) and the remaining 19% being composed of calcite (Fig. 7B).

The macroscopic features of samples FER-3, BA-4, BEN-1 and BEN-2 have strong similarities, being characterized by laminated dark-grey limestones, which is clearly distinct from other samples. Macro- and microscopic features allow to identify distinct lithofacies:

- Sample FER-1 have some evidences of a not pervasive late dolomitization. It is characterized by submillimetric calcite and dolomite (60%) with abundant quartz (30-35%) and some muscovite and opaque minerals. The sample contains quartz-rich layers, as well as some organic matter parallel to bedding. Some calcite veins are also identified and recrystallization are recognized. After the crushing the fragments with clear late dolomitization and late calcite veins were eliminated by visual inspection.
- Sample FER-2 is mostly composed of dolomite (70%) and abundant quartz (25%), complemented by muscovite and opaque minerals. Macro and microscale evidences of pervasive dolomitization and dissolution, with generation of euhedral cloudy late dolomite, are recognized.

- Samples FER-3 and BA-4 are impure calcite limestones (Fig. 4D) without evidences of secondary dolomitization (calcite ranges between 65 and 80%). The non-carbonated content is composed of quartz (10-30%), fine-grained muscovite (<5%), opaque minerals (~5%) and organic matter remnants. The calcite crystals presents type I twins that shows a slightly recrystallization. It is important to emphasize the presence of some hydrothermal evidences observed near the FER-3 locality.

- Samples CHE-1 is a pure calcite carbonate (~80%) with a fine-grained submillimetric granoblastic texture and no evidences of secondary dolomitization. The non-carbonated component is composed of quartz, fine-grained mica and opaque minerals and organic matter remains. The calcite shows type I twins, revealing weak recrystallization.

- Samples BEN-1 and BEN-2 are dolomite-calcite limestones (circa of 70-85%), containing abundant quartz (10-30%) and also opaque minerals and muscovite. Evidences of organic matter are clear in both samples. In samples BEN-1 dolomite seems to show some recrystallization with type I twins. Some veins of calcite are identified and it is not evident the presence of a pervasive late dolomitization at meso- and microscale.

- Sample BA-3 is a sandstone with calcite cement. The sample shows abundant quartz (60-70%), muscovite (10-15%), and opaque minerals (~5%), as well evidences of organic matter (Fig. 5E). The cement is composed of submillimetric calcite, which represents 10-15% of sample content. Although the sample was included in this sample group, it is clearly distinct, being collected in the siliciclastic Monte das Russianas Formation (Lower Devonian; Oliveira, 1984; Araujo et al., 2013).

III.1.5.5. Odivelas Limestone and Cabrela-Toca da Moura Complexes

This group includes 6 samples of Devonian grey to dark limestones *s.l.* (table I; Boogard, 1972; Machado et al., 2009; 2010; Machado and Hladil, 2010) with very low-grade metamorphism. Four samples are from Odivelas Limestones (two from Covas Ruivas locality - OD-1, OD-2 - and two from Cortes - OD-5A, OD-6) and two were collected in Toca da Moura (Pena Limestones; OD-4) and Cabrela (Pedreira da Engenharia Limestones; CAB-1) Carboniferous Basins (Fig. 3D).

The XRD analyses (table 2) emphasises the presence of the highly pure limestones, usually with carbonate content higher than 88%. One sample (CAB-1) is a dolostone, being the most impure carbonate with 11% of non-carbonate content (Fig. 7D), while the other samples are limestones, containing more than 92% of calcite (Fig. 7C). The non-carbonated content is mainly composed of quartz with some chlorite and mica.

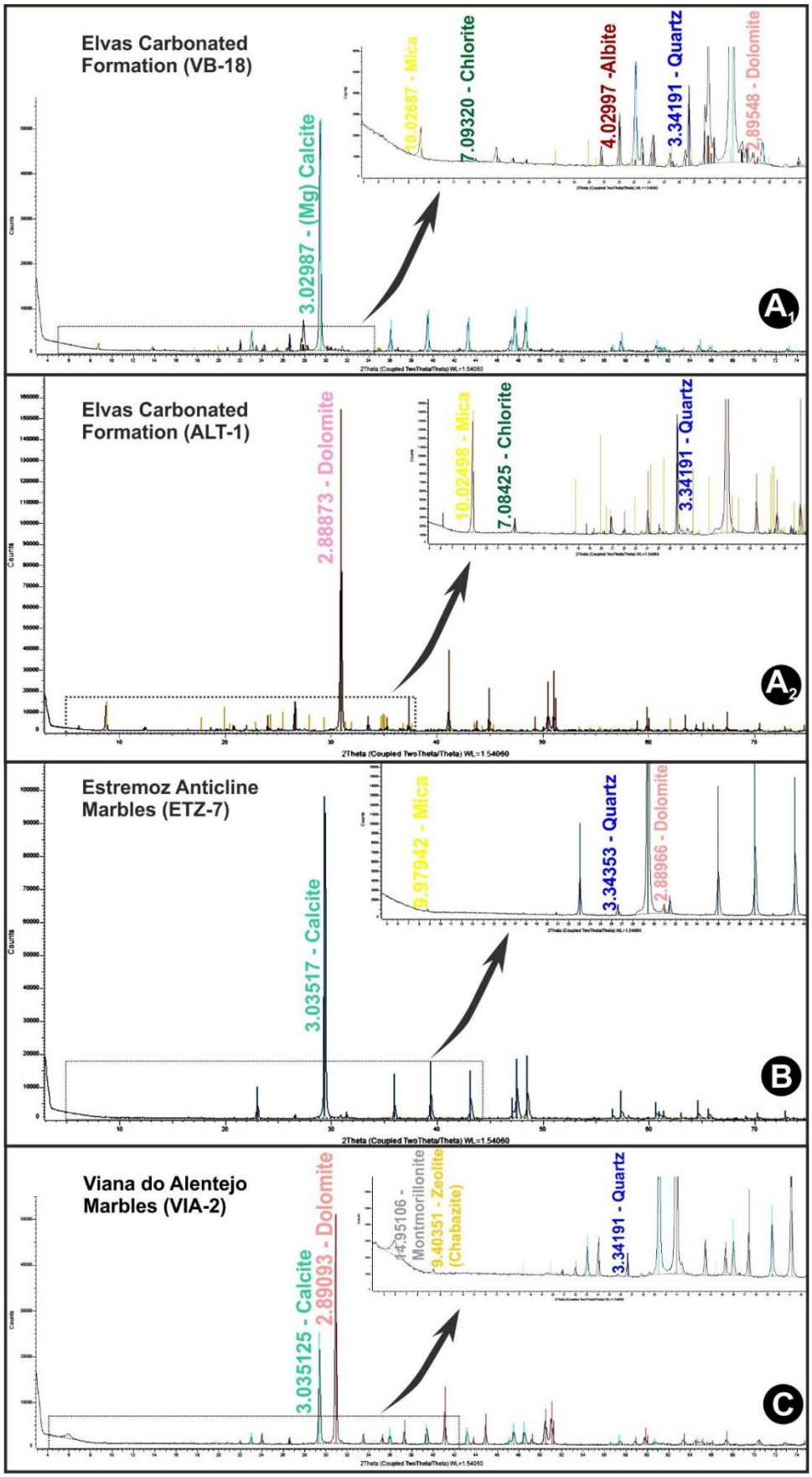

Figure 6 – XRD pattern of the Cambrian limestones (A1 and A2), the Cambrian attributed marbles (B) and a late dolostone growing in a fracture (C).

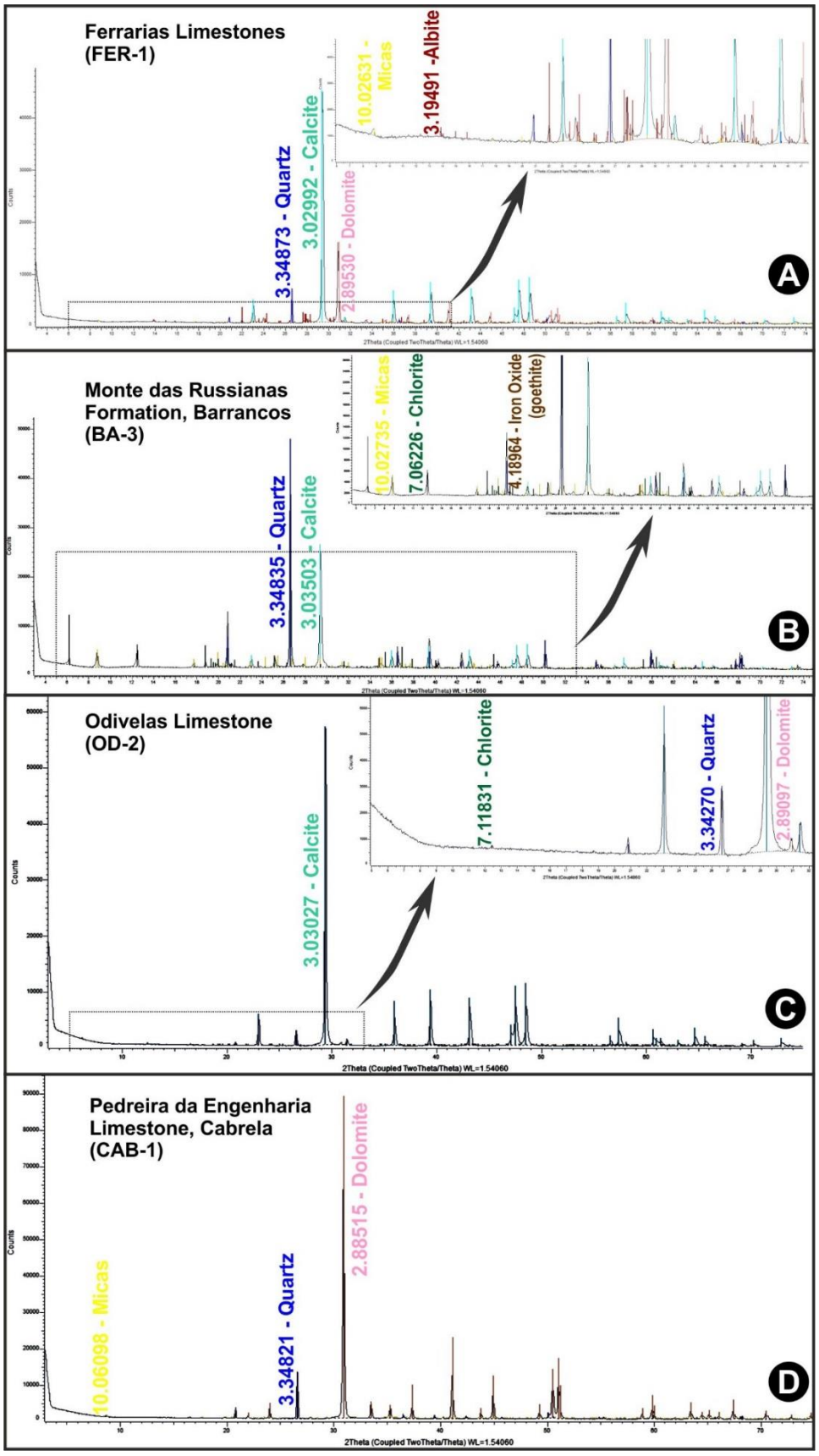

Figure 7 – XRD pattern of the Late Silurian-Early Devonian(?) limestones from Ferrarias (A), Early Devonian Sandstone with calcite cement from Barrancos (B) and Early Devonian Limestones (C) and Dolostones (D) from Odivelas and Cabrela respectively.

Table 2 – Semi quantitative results obtained by XRD analyses for the analysed samples.

	Calcite	Dolomite	Ankerite	Quartz	Mica	Chlorite	Others		obs.	Carbonates (%)	Others (%)
GQAB-3	96.17	0.00	0.00	1.42	2.42	0.00	0.00			96.17	3.83
GQAB-4	92.13	0.00	0.00	3.05	4.14	0.00	0.67	Titanite		92.13	7.87
GQAB-7	0.00	96.81	0.00	1.28	1.92	0.00	0.00			96.81	3.19
GQAB-13	0.00	94.25	0.00	1.52	0.88	0.00	3.35	Montmorillonite		94.25	5.75
GQAB-27	0.44	84.21	0.00	5.28	9.39	0.00	0.67	Kaolinite		84.65	15.35
GQAB-37	0.00	67.75	0.00	8.41	16.30	0.00	1.09 + 6.46	Kaolinite + Orthose		67.75	32.25
ASS-1	0.00	95.05	0.00	0.78	1.05	3.12	0.00			95.05	4.95
VB-2	67.74	0.23	0.00	12.31	13.93	5.79	0.00			67.97	32.03
VB-12	0.37	76.13	0.00	2.37	3.52	17.61	0.00			76.50	23.50
VB-18	74.05	0.89	0.00	5.01	14.43	0.59	5.03	Albite	Mg Calcite	74.94	25.06
ALT-1	0.00	62.06	0.00	4.16	30.80	2.98	0.00			62.06	37.94
ETZ-2	96.77	0.00	0.00	1.99	1.24	0.00	0.00			96.77	3.23
ETZ-3	95.91	0.72	0.00	0.58	2.79	0.00	0.00			96.63	3.37
ETZ-5	95.83	0.00	0.00	0.33	3.82	0.00	0.00			95.83	4.17
ETZ-6A	0.00	63.53	0.00	1.96	34.50	0.00	0.00			63.53	36.47
ETZ-7	95.52	1.22	0.00	1.07	2.19	0.00	0.00			96.74	3.26
ETZ-9	0.00	89.00	0.00	1.88	5.95	1.36	1.82	Orthose		89.00	11.00
FER-1	57.57	25.49	0.00	8.62	2.31	0.00	6.00	Albite		83.06	16.94
FER-2	0.09	95.00	0.00	2.98	1.93	0.00	0.00		Mg Calcite	95.09	4.91
FER-3	81.18	0.00	0.00	7.87	10.95	0.00	0.00			81.18	18.82
BA-3	19.25	0.00	0.00	34.70	20.07	25.35	0.63	Goethite		19.25	80.75
BA-4	55.48	1.52	0.00	15.60	27.39	0.00	0.00		Fe Dolomite	57.00	43.00
BEN-1	7.82	64.37	0.00	14.31	7.88	0.00	0.53 + 5.09	Kaolinite + Microcline		72.19	27.81
BEN-2	49.86	46.45	0.00	0.84	2.85	0.00	0.00			96.31	3.69
CHE-1	77.69	0.00	0.00	0.45	19.92	0.00	1.29 + 0.65	Kaolinite + Montmorillonite		77.69	22.31
OD-1	92.41	0.89	0.00	3.04	0.00	3.18	0.48	Hematite		93.30	6.70
OD-2	93.75	1.05	0.00	4.19	0.00	1.00	0.00			94.80	5.20
OD-4	99.53	0.00	0.00	0.47	0.00	0.00	0.00			99.53	0.47
OD-5A	96.54	0.00	0.00	0.66	0.00	0.00	2.80	Talc		96.54	3.46
OD-6	99.69	0.00	0.00	0.31	0.00	0.00	0.00			99.69	0.31
CAB-1	0.00	88.41	0.00	9.54	2.05	0.00	0.00			88.41	11.59
VIA-1	98.25	0.00	0.00	0.36	0.00	0.00	0.33 + 1.07	Titanite + Montmorillonite		98.25	1.75
VIA-2	26.02	68.95	0.00	1.48	0.00	0.00	0.63 + 2.92	Zeolite group (Chabazite) + Montmorillonite		94.97	5.03
ALV-1	8.20	0.00	82.01	0.47	0.00	9.31	0.00		or Fe Dolomite	90.21	9.79
SRP-1	8.07	88.80	0.00	0.00	0.00	1.19	1.93	Serpentine Group (Lizardite or Chrysotil)		96.87	3.13
FIC-2	64.33	0.00	0.00	31.80	3.87	0.00	0.00			64.33	35.67
ESC-1	44.90	35.56	0.00	0.13	1.15	12.00	5.52 + 0.84	Tremolite-Actinolite + Talc		80.46	19.54

The petrographic studies allow to recognize three distinct lithofacies in these limestones:

- Samples OD-1, OD-2, OD4 and OD-5A are almost composed of calcite (90-95%; Fig. 5F). Some opaque minerals and abundant organic matter were also identified. In sample OD-1 quartz is also recognized while in sample OD-5A fibrous talc is identified. The sample OD-4 has some evidences of recrystallization coupled with hydrothermal fluid interaction (Fig. 4E), while in samples OD-1, OD-2 and OD-5A, the recrystallization is less intense. Nevertheless, type I twins are present in all samples. In sample OD-1 fossil fragments were recognized (Fig. 5F).
- Sample OD-6 is a rudstone with abundant fragments of crinoids and other bioclastic material (Fig. 4F). This sample is mostly composed of calcite (>95%), some opaque minerals and frequent organic matter. The sedimentary texture presents some recrystallization with type I twins developed in the calcite.
- Sample CAB-1 is an impure dolostone (dolomite 85-90%), with frequent quartz layers. There is a secondary dolomitization associated to intense dissolution (Fig. 4G), generating a pervasive generation of cloudy euhedral dolomite, sometimes zoned, possibly replacing the initial calcite content. Some levels rich in organic matter were identified.

III.1.5.6. Southern OMZ Carbonates (Escoural, Viana-Alvito, Serpa, Ficalho)

In the southernmost sectors of the OMZ, 6 carbonate samples were collected (table 1; Fig. 3). These carbonates outcrop in antiformal structures (Araújo et al., 2013), being attributed to Cambrian based on lithostratigraphic correlation with the northern and central domains of the OMZ (Oliveira et al., 1991; Araújo et al., 2013). Two carbonated units are usually considered in this area: the basal unit composed of dolomite marbles/limestones, sometimes poorly represented (Oliveira et al., 1991), and the upper one (where all samples are collected) characterized by marbles/limestones associated with bimodal magmatism (Ribeiro et al., 1992; Oliveira et al., 1991; Araújo et al., 2013). However, in the Ficalho region, dark-grey limestones generally included in upper unit, present Silurian-Devonian conodonts (Piçarra and Sarmiento, 2006).

The XRD studies (table 2) show the presence of highly variable contents in carbonates: 2 samples with more than 95% (SRP-1 and VIA-1), 3 samples with 95-80% (VIA-2, ALV-1 and ESC-1) and one sample with significant lower values (~65%; FIC-2). The main carbonate are also heterogeneous: calcite is the only identified carbonate in VIA-1 and FIC-2 samples, while in VIA-2, SRP-1 and ESC-1, dolomite and calcite were identified, being the dolomite dominant in sample VIA-2 (Fig. 6C) and SRP-1. The sample ALV-1 also contain calcite, although the dominant carbonate is Ankerite. Concerning the non-carbonate content, quartz is present in all samples,

although a greater diversity of phases is described: zeolite (VIA-2), clay minerals (VIA-1, VIA-2), chlorite (ALV-1), micas (FIC-2, ESC-1), serpentine (SRP-1), amphibole – tremolite-actinolite – and talc (ESC-1).

This group is heterogeneous, including several differential features that will be described below:

- Samples VIA-1 and VIA-2 are sampled in the same old marble quarry (Fig. 4H). The sample VIA-1 is a calcite marble (85-90%), with intense recrystalization, type II and III (and IV?) twins, and a coarse-grained (centimetric to millimetric) granoblastic texture (Fig. 5G). Olivine (forsterite?), epidote and brucite(?), but also some K-Feldspar and quartz, are recognized. The sample VIA-2 is a secondary dolostone (dolomite=60-70%) contained in a vein controlled by a fracture zone within calcite marbles. This dolostone has no evidences of recrystallization, also presenting submillimetric late calcite veins. Quartz, chlorite, opaque minerals, amphibole, feldspar and muscovite(?) compose the non-carbonated fraction. Several dissolution indications are recognized and secondary dolomite, sometimes euhedral and zoned, is pervasive.
- Sample ALV-1 is a fine-grained ankerite (85-90%) marble, with granoblastic texture, also containing quartz, chlorite, amphibole, feldspar and muscovite (?). A significant content of opaque minerals phases (iron oxides?; 2-5%) were also identified. The carbonates present type IV twins, emphasizing an intense recrystallization. Late sub-millimetric calcite veins without recrystallization were identified.
- Sample SRP-1 is mostly composed of dolomite (~70%), presenting granoblastic inequigranular (centimetric to millimetric) texture. The dolomite is considered as diagenetic (or primary?) or syn-metamorphic, showing evidences of deeply recrystallization with type II and IV twins (Fig. 5H). The non-carbonated content (20-25%) is dominated by serpentine and olivine (forsterite?), coupled with some spinel and opaque minerals (Fig. 5H). The presence of olivine relics indicates high-temperature metamorphism (Bucher and Grapes, 2011), while the serpentine is result of retrograde metamorphism. Sub-millimetric calcite (~5%), with no evidences of recrystallization, was identified, which seems to be synchronous (or later?) to the retro-metamorphism.
- Sample ESC-1 has an equigranular medium-grained granoblastic polygonal texture. It is composed of calcite and dolomite (~85%), tremolite-actinolite (5-10%), opaque minerals and talc. The carbonates show type II twins, denoting some recrystallization. There is no evidences of late dolomitization and dissolution. The tremolite should result from metamorphism under amphibolite facies conditions, while the talc could be related to the retrograde metamorphism (Bucher and Grapes, 2011).

- Sample FIC-2 is a fine-grained (submillimeric) impure limestone (calcite 65-70%), with abundant quartz (30-35%), some muscovite and dispersed organic matter. The sample do not shows evidences of late dolomitization and dissolution.

III.1.6. $^{87}Sr/^{86}Sr$ Ratio of the Carbonated Rocks

The projection of $^{87}Sr/^{86}Sr$ ratio of the OMZ carbonated rocks shows the presence of two distinct clusters (table 3; Fig. 8).

The first cluster is composed of the Odivelas and Pena limestones (OD-1, OD-2, OD-4, OD-5A, OD-6), which present $^{87}Sr/^{86}Sr$ ratio lower than 0.70800 with a very small dispersion, ranging between 0.707680 and 0.70778. However, the dolostones associated to the Cabrela Carboniferous Basin (Oliveira et al., 1991; 2013; Moreira and Machado, in press), with similar age (and genesis?), presents significant higher $^{87}Sr/^{86}Sr$ values (CAB-1; 0.70972), when compared with the Odivelas and Pena limestones (Fig. 8).

The Sr fingerprint of CAB-1 could be influenced by the interaction between the original $^{87}Sr/^{86}Sr$ ratio in limestones and the meteoric fluids (which usually have higher 87Sr/86Sr ratios; McArthur, 1994) and its "anomalous" higher value could be explained by the pervasive secondary dolomitization and dissolution (Fig. 4G). As the age of dolomitization is unknown, two hypothesis can be considered: (1) the dolomitization took place during the re-sedimentation of limestones within the intracontinental Caberla Basin (if it is considered the olistolith nature to these limestones; Oliveira et al., 2013 and references therein) or (2) the dolomitization results from recent interaction with meteoric fluids.

When comparing the Odivelas and Pena limestones it should be emphasized their similar $^{87}Sr/^{86}Sr$ fingerprint, nevertheless the presence of silicification, the oxide mineral phases and hydrothermal activity in the Pena Limestones (Machado and Hladil, 2010). Although, it must to be emphasized that only the most preserved lithofacies were analysed in Pena Limestone (OD-4 sample). This seems to indicate that, in this case, the hydrothermal interaction do not change the primary Sr ratio.

The other cluster is composed of calcite and dolomite limestones and marbles, presenting higher $^{87}Sr/^{86}Sr$ values and ranging between 0.7083 and 0.7093 (table 3). In this cluster, where there is no evidences of pervasive late dolomitization, two groups are recognized in this cluster (Fig. 8):

(1) A lower group, with ratios ranging between 0.7073 and 0.7078, is mostly composed of calcite carbonates (ETZ-2, ETZ-3, ETZ-5, ETZ-7, FIC-1, VB-2, VB-18, GQAB-3, GQAB-4) and

two dolomite carbonates affected by a pervasive metamorphic recrystallization of dolomite (ETZ-9, GQAB-27);

(2) An upper group (0.7090-0.7093) mainly composed of dolomite-rich carbonates with some evidences of late dolomitization (ALT-1, VB-12, GQAB-7 and ASS-1) and two calcite-rich marbles (VIA-1 and ESC-1), with no evidences of secondary dolomitization.

The lower group comprises Abrantes-Assumar and Estremoz marbles. Their values are similar to most of the previous published data from Estremoz marbles affected by medium grade metamorphism (Fig. 8; Marinelli et al., 2007; Taelman et al., 2013). The previous data is totally corroborant with $^{87}Sr/^{86}Sr$ ratios obtained for Alter-do-Chão – Elvas limestones (VB-2, VB-18), which have very low metamorphic grade and a well constrained age (Ovetian-Marianian; Gozalo et al., 2003). The upper group, with slightly higher ratios, contains not only the South OMZ marbles from Viana do Alentejo and Escoural (VIA-1, ESC-1; Fig. 3D), with medium to high temperature paragenesis, but also the dolomite-rich carbonates with some evidences of late dolomitization from Northern OMZ sectors (ASS-1, GQAB-7) and from Alter-do-Chão-Elvas Domain (ALT-1, VB-12).

The Serpa marble (SRP-1) presents an extremely anomalous high $^{87}Sr/^{86}Sr$ ratio (0.711052), clearly higher than the previous reported cluster, although the sample shares clear similarities with VIA-1 sample. In SRP-1 sample, the dolomite is highly recrystallized, showing that this dolomitization should be contemporaneous or previous to the metamorphic episode. Indeed, the dolomitization could be related to the interaction with hydrothermal high temperature metamorphic and/or magmatic fluids (Bucher and Grapes, 2011) during Variscan Cycle. The presence of serpentine in SRP-1 dolomite marble, resulting from retrogradation of olivine, indicates either a regional metamorphism under granulite facies or intense high temperature hydrothermal activity (Bucher and Grapes, 2011; Winter, 2013).

Thus, it could be considered that the anomalous higher values is resulted from the interaction between the high-temperature (metamorphic) fluids with Serpa Marbles, thus increasing the $^{87}Sr/^{86}Sr$ ratio. This could also explain the slightly higher values obtained to Viana do Alentejo and Escoural samples, which also presents higher metamorphic grade. Previous data from Viana do Alentejo marble had already shown higher $^{87}Sr/^{86}Sr$ values when compared with Estremoz marbles (Morbidelli et al., 2007). This possibility is in accordance with the presence of Carboniferous thermal metamorphism described in the Viana do Alentejo marbles (Gomes and Fonseca, 2006) and the presence of a high temperature event in Escoural marbles country rocks (Chichorro, 2006; Chichorro et al., 2008; Moita et al., 2009). A similar behaviour also explains the higher values obtained in Almaden de la Plata marbles (Fig. 1 and 8; Morbidelli et al., 2007), where a high temperature metamorphism is observed (Ábalos et al., 1991).

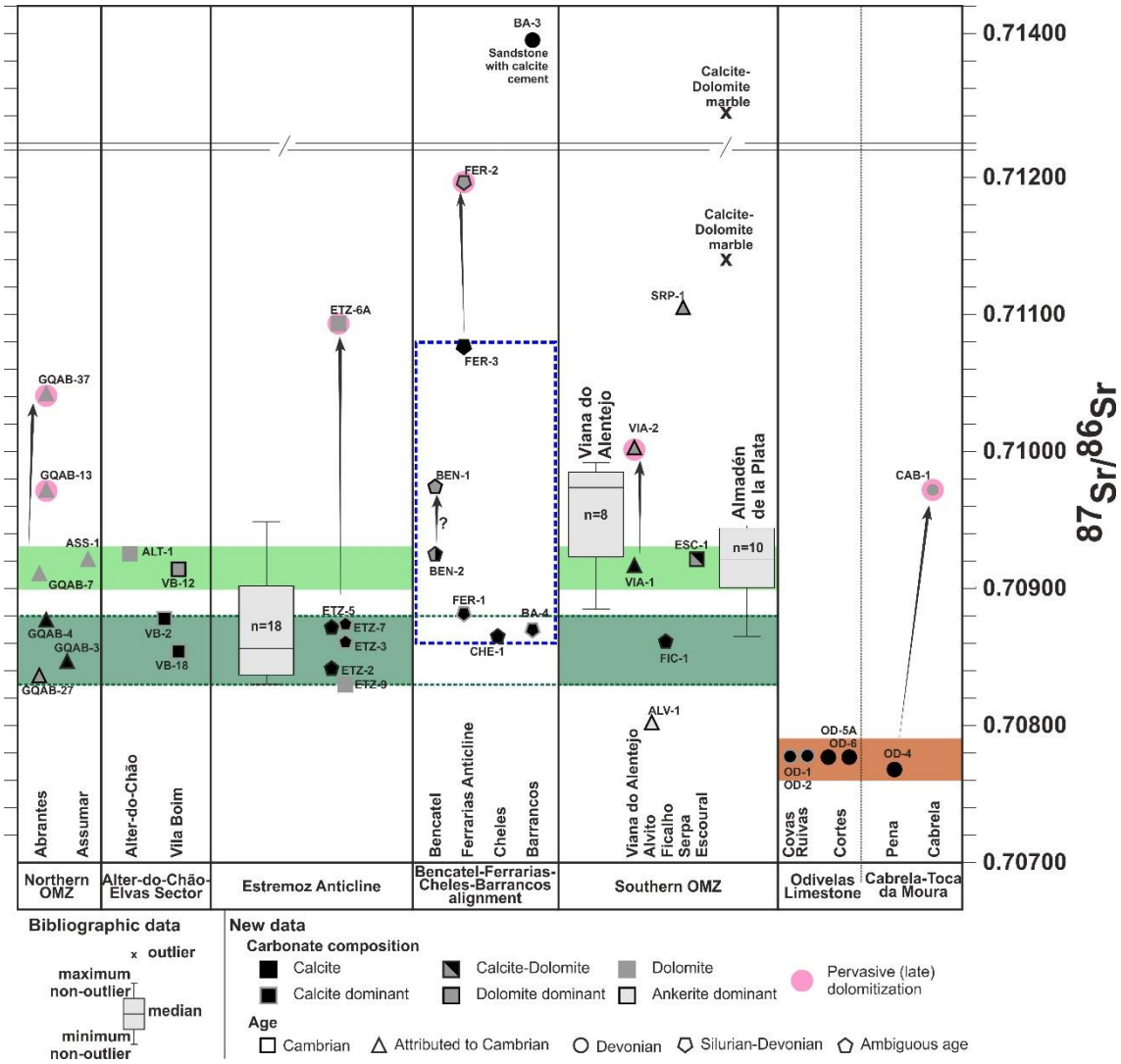

Figure 8 – Projection of $^{87}Sr/^{86}Sr$ values ratios of Palaeozoic OMZ carbonates, emphasizing the presence of different clusters (see text for more details). The arrows represents the effect of secondary/meteoric dolomitization. In the box-plots, are represented the published $^{87}Sr/^{86}Sr$ data from Viana do Alentejo, Estremoz Anticline and Almandén de la Plata marbles (adapted from Morbidelli et al., 2007; Taelman et al., 2013).

Therefore, the increase of $^{87}Sr/^{86}Sr$ values in the high-temperature metamorphic marbles (VIA-1, ESC-1 and SRP-1) is compatible with the interaction between primary $^{87}Sr/^{86}Sr$ marbles signatures and the higher $^{87}Sr/^{86}Sr$ values typical of the high temperature (metamorphic) fluids derived from upper crust (Rollinson, 1993). High $^{87}Sr/^{86}Sr$ values were obtained in OMZ Neoproterozoic-Cambrian siliciclastic rocks and in rocks resulting from anatexis of Ediacaran metasediments in the Évora Massif (Pereira et al., 2006; Moita et al., 2009). Thus, the current strontium ratio signature of these marbles (VIA-1, ESC-1 and SRP-1) could result from the mixing between primary signature and the metamorphic fluids fingerprint. This seems to show that the

low to medium metamorphic grade do not change significantly the primary signature of $^{87}Sr/^{86}Sr$, contrary to what happens with high-temperature metamorphism.

The samples with pervasive secondary late dolomitization (VIA-2, ETZ-6A, GQAB-13, GQAB-37) present higher values of $^{87}Sr/^{86}Sr$, comparatively to the calcitic and dolomitic limestones/marbles without or with insipient evidences of pervasive secondary late dolomitization collected in the same sectors (Fig. 8). Similar behaviour has been reported previously to the Cabrela dolostones (Fig. 8), being interpreted as the result from the interaction between meteoric fluids and carbonated rocks.

The Alvito Fe-rich carbonate (ALV-1) despite has textural evidences of metasomatic process, shows the lowest $^{87}Sr/^{86}Sr$ value (0.708023) and is regarded as an outlier (Fig. 8). Such anomalous ratio in an ankerite-rich marble require more data in order to understand the influence of ankeritic or dolomite Fe-rich fluids in the $^{87}Sr/^{86}Sr$ ratio during the metasomatism.

The samples from Bencatel-Ferrarias-Cheles-Barrancos alignment are analysed separately because its behaviour is slightly random. Indeed, the $^{87}Sr/^{86}Sr$ data for the limestones and dolostones collected in this alignment are clearly distinct from the data for the Odivelas-Pena limestones cluster (Fig. 8). These carbonates usually presents $^{87}Sr/^{86}Sr$ values similar to those obtained in the limestones/marbles from the second cluster, ranging between 0.70860 and 0.71200, however, as mentioned the data dispersion is higher (Fig. 8):

- Samples from Cheles (CHE-1), Barrancos (BA-4) and one from Ferrarias (FER-1) presents clear similarities with the primary limestone signature of second cluster (0.708655-0.708812). Although doubts remain in relation to its age, lithostratigraphic and geodynamical significance (see discussion below);
- The Bencatel samples (BEN-1, BEN-2) presents $^{87}Sr/^{86}Sr$ values compatible with the upper group of the second cluster (0.709743 and 0.709255 respectively). Both samples contain dolomite, but is debatable the temporal relation between the dolomitization and the metamorphic processes. The strontium ratio increase could reflect the effect of secondary dolomitization on a primary Sr ratio that may be similar to CHE-1, BAR-4 and FER-1. Both samples were collected in the SW limb of Estremoz Anticline, presenting dubious position in relation to Estremoz Volcano-Sedimentary Complex.
- Ferrarias samples (FER-2 and FER-3) present significant higher values of $^{87}Sr/^{86}Sr$ (0.711960 and 0.710761 respectively; Fig. 8). As mentioned, this sector is affected by intense fracturing with evidences of intense rock/fluid interaction. This may justify the high values observed in FER-3 calcite limestone. The sample FER-2 presents a pervasive secondary dolomitization, which should increase the $^{87}Sr/^{86}Sr$ ratio;

Table 3 – $^{87}Sr/^{86}Sr$ isotopic data from studied samples (results obtained in Isotopic Geology Laboratory of Aveiro University).

Sector	Sample	$^{87}Sr/^{86}Sr$	2σ
Northern OMZ Carbonates	GQAB-3	0.708471	0.000014
	GQAB-4	0.708773	0.000026
	GQAB-7	0.709106	0.000014
	GQAB-13	0.709716	0.000024
	GQAB-27	0.708366	0.000021
	GQAB-37	0.710410	0.000017
	ASS-1	0.708866	0.000024
Alter-Do-Chão – Elvas Sector Limestones	VB-2	0.708777	0.000013
	VB-12	0.709136	0.000030
	VB-18	0.708538	0.000021
	ALT-1	0.709227	0.000024
Estremoz Anticline	ETZ-2	0.708420	0.000033
	ETZ-3	0.708610	0.000033
	ETZ-5	0.708716	0.000027
	ETZ-6A	0.710933	0.000021
	ETZ-7	0.708741	0.000027
	ETZ-9	0.708299	0.000023
Bencatel-Ferrarias-Cheles-Barrancos Alignment	FER-1	0.708812	0.000013
	FER-2	0.711960	0.000016
	FER-3	0.710761	0.000018
	BA-3	0.714002	0.000021
	BA-4	0.708694	0.000018
	BEN-1	0.709743	0.000021
	BEN-2	0.709255	0.000031
	CHE-1	0.708655	0.000021
Odivelas Limestone and Cabrela-Toca da Moura Complexes	OD-1	0.707775	0.000020
	OD-2	0.707784	0.000016
	OD-4	0.707680	0.000023
	OD-5A	0.707774	0.000017
	OD-6	0.707772	0.000016
	CAB-1	0.709720	0.000020
Southern OMZ Carbonates	VIA-1	0.709169	0.000023
	VIA-2	0.710030	0.000021
	ALV-1	0.708023	0.000025
	SRP-1	0.711052	0.000020
	FIC-2	0.708617	0.000018
	ESC-1	0.709016	0.000014

- The BA-3 sample displays the most anomalous higher $^{87}Sr/^{86}Sr$ value (0.714002; Fig. 8). This sandstone with calcite cement is composed of significant amounts of siliciclastic components. The obtained ratio should be the result either from the interaction between the silicate and carbonate components during the diagenetic process or from the interaction rock/fluid dominated by crustal fluids (Rollinson, 1993), not representative of strontium isotopic signature of seawater during the limestone precipitation.

III.1.7. $^{87}Sr/^{86}Sr$ and the age of OMZ Carbonated Episodes; a Discussion

The variation of $^{87}Sr/^{86}Sr$ ratio during the Phanerozoic times is generally well constrained (Fig. 2; McArthur et al., 2012). This could be used to have discuss or even constrain of the possible ages of the OMZ carbonated episodes.

However, the Cambrian worldwide curve of the $^{87}Sr/^{86}Sr$ values is not well constrained, due to the lack of precise biostratigraphic age of world Cambrian successions, coupled with the scarcity of well-preserved material that could be used for strontium studies (McArthur et al., 2012). Thus, several curves were proposed (Fig. 9A; Derry et al., 1994, Brasier et al., 1996, Nicholas, 1996 and Denison et al., 1998).

The Ovetian-Marianian Alter-do-Chão-Elvas limestones (Oliveira et al., 1991), with no evidences of late dolomitization, present a $^{87}Sr/^{86}Sr$ (VB-2 and VB-8; 0.708538 and 0.708777) with a very good correlation with most of the proposed worldwide seawaters values for this age (Fig. 9A; Derry et al., 1994; Brasier et al., 1996; Nicholas, 1996). Similar Sr ratio values (0.7083-0.7088) were obtained for the Ficalho limestone (FIC-2) and to the dolomite and calcite marbles from Estremoz (ETZ-2, ETZ-3, ETZ-5, ETZ-7, ETZ-9) and Abrantes (GQAB-3, GQAB-4, GQAB-27), which also have no secondary dolomitization although present an higher metamorphic-grade (greenschists to amphibolite). Such similarities support the attribution of these formations to the Ovetian-Marianian (Oliveira et al., 1991; Moreira et al., 2015; 2016), although some care should be used because similar strontium ratios are also found in some Silurian and Devonian periods (Fig. 9B and 9C).

Some Abrantes-Assumar (GQAB-7, ASS-1), Alter-do-Chão-Elvas (ALT-1, VB-12) and Southern OMZ (VIA-1, ESC-1) samples, also attributed to the same Cambrian carbonate event (Oliveira et al., 1991; Pereira and Silva, 2001; Moreira et al., 2015; 2016), present slightly higher $^{87}Sr/^{86}Sr$ values (0.7090-0.7093), that should represent the balance between the primary Sr signature with the higher strontium values provided by:

(1) The high temperature metamorphic fluids in the Viana do Alentejo and Escoural marbles;

(2) The meteoric fluids in the Abrantes-Assumar and Alter-do-Chão-Elvas carbonates.

Although it could be considered that the higher values of this sample group are compatible with the Cambrian $^{87}Sr/^{86}Sr$ worldwide curve proposed by Denison et al. (1998), we didn't support this hypothesis, which led all the other samples with lower ratios unexplained.

However, doubts still remain in Bencatel-Ferrarias-Cheles-Barrancos alignment and consequently its relation with Estremoz marbles stay debatable. Indeed, although some of these samples have $^{87}Sr/^{86}Sr$ ratios similar to those obtained to Cambrian and Cambrian attributed carbonates, they have a more complex geodynamic significance:

- The Ferrarias samples (FER-1, FER-3) are from the localities whre crinoids fragments and conodonts are found in dark limestones (Piçarra and Le Meen, 1994; Piçarra and Sarmiento, 2006), being sometimes slightly recrystallized. Locally these limestones present conglomeratic features and some limestone boulders are also found in clastic sequence. Although sample FER-3 have no evidences of dolomitization, it exhibit an anomalous higher $^{87}Sr/^{86}Sr$ values, clear dissimilar from the one of FER-1 sample. Near the FER-3 location, evidences of hydrothermal processes were identified, which could explain this value. The FER-1 $^{87}Sr/^{86}Sr$ signature is similar to those obtained in some Estremoz dark marbles (ETZ-5 and ETZ-7).

- The Bencatel samples (BEN-1 and BEN-2) are also dark calcite-dolomite limestones, collected near the fossiliferous locality of Piçarra and Sarmiento (2006). The samples are located in the southern limb of Estremoz anticline, being locally associated to some conglomeratic features. The $^{87}Sr/^{86}Sr$ values are slightly higher than Estremoz marbles.

- The Cheles sample (CHE-1) is from an isolate calcite limestone outcrop interpreted as a a klippe structure considered as Cambrian, but with no biostratigraphic data (Moreno and Vegas, 1976; Vegas and Moreno, 1973). The strontium ratios are similar to the Estremoz dark marbles.

- The Barrancos sample (BA-4) was been collected where unclassified crinoid fragments were described (Piçarra and Sarmiento, 2006), being spatially associated to breccias and bimodal volcanic rocks. Its strontium ratio is similar to the Estremoz dark marbles values.

The presence of crinoids in localities where some of the samples were collected implies, at least, an Ordovician age for these limestones (Guensburg and Sprinkle, 2001; Ausich et al., 2015), which is compatible with the considered Late Silurian to Early Devonian age based in their conodonts content (Piçarra and Sarmiento, 2006). The possible Upper Silurian age raises the possibility of correlation with Pridoli Scyphocrinites Limestone from Valle and Cerrón del Hornillo (Spain; Robardet and Gutiérrez-Marco, 2004), although this carbonate episode has not been described in Portugal (e.g. Piçarra, 2000; Piçarra and Sarmiento, 2006). The Pridoli $^{87}Sr/^{86}Sr$ signatures ranges between 0.70865 and 0.70885 (Fig. 9B; Azmy et al., 1999; McArthur et al., 2012), being concordant not only with some of the samples contained in this alignment (BA-4, FER-1 and CHE-1), but also with the dark marbles from the southern limb of Estremoz anticline (ETZ-5 and ETZ-7). In fact, the Estremoz dark marbles present a slightly higher values than the Estremoz white marbles (ETZ-2 and ETZ-3), thus being totally compatible with the strontium ratio Pridoli values. To clarify the possible existence of two distinct episodes fact it will be necessary a wider sampling in black limestones and marbles from Estremoz and Bencatel-Ferrarias-Cheles-Barrancos alignment.

The strontium ratio of the Cheles sample (0.708655) fits within the group range defined by the samples attributed to Cambrian (0.7083 and 0.7088; Fig. 9A). Nevertheless, the absence of bio- and lithostratigraphic control in these limestones prevnt a definitive conclusion.

Thus the geodynamic meaning of this alignment is still poorly known and it is possible that the two carbonate episodes are represented. In fact, the presence of carbonates associated with breccias and magmatic rocks involved by a siliciclastic matrix could indicate the presence of a syn-orogenic deposit contained boulders (olistoliths) of magmatic and carbonated rocks, with different provenances and ages.

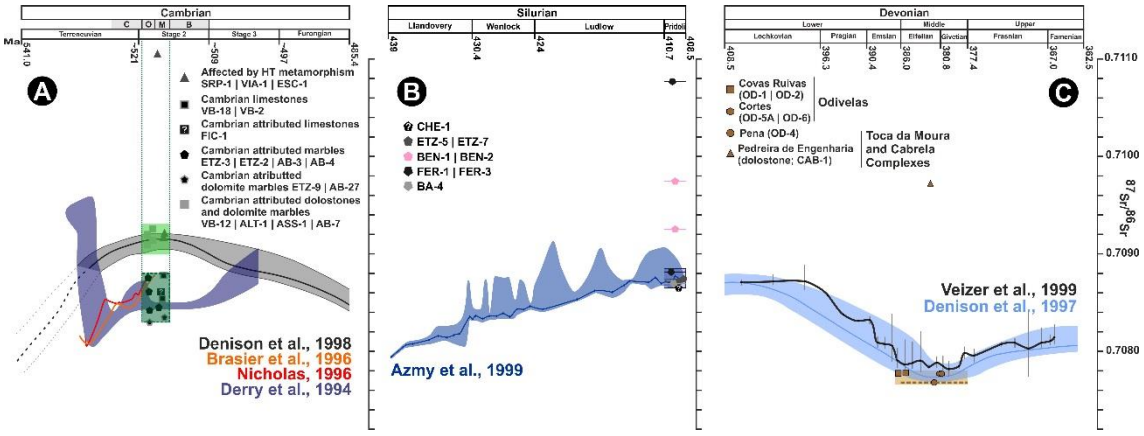

Figure 9 – Projection of OMZ data in the proposed $^{87}Sr/^{86}Sr$ curves for worldwide seawater during:

A – Cambrian (C – Corduban; O – Ovetian M – Marianian, B – Bilbilian; seawater curves adapted from Derry et al., 1994, Brasier et al., 1996, Nicholas, 1996 and Denison et al., 1998);

B – Silurian (seawater curve adapted from Azmy et al., 1999);

C – Devonian (seawater curves adapted from Denison et al., 1997 and Veizer et al., 1999).

Finally, the $^{87}Sr/^{86}Sr$ signatures of Lower-Middle Devonian Limestones not only have a very low dispertion, ranging between 0.70770 and 0.70780, but are also totally concordant with the lower $^{87}Sr/^{86}Sr$ values proposed for the worldwide seawater trend from this age (Fig. 9C; Denison et al., 1997 and Veizer et al., 1999), which is totally distinct from Cambrian and Silurian ones. Concerning the Odivelas limestones (Cortes and Covas Ruivas localities; Fig. 9C), the obtained values, ranging between 0.707784 and 0.707772, could also be explained by the interaction between the seawater and the host volcanic rocks ($^{87}Sr/^{86}Sr$ ranges between 0.7038 and 0.7066; Santos et al., 2013). However, in Pena Limestones (OD-4 sample), although the host volcanic rocks have not been identified (Moreira and Machado, in press), the isotopic ratio values remain similar (0.707680), which seems to show that such values represent the primary strontium signature of the seawater. The strong accuracy observed in all the Lower-Middle Devonian

limestones also indicates that the Bencatel-Ferrarias-Cheles-Barrancos alignment limestones should not be Emsian-Givetian in age.

III.1.8. Final Remarks

This work helps to highlight some constrains in the use of $^{87}Sr/^{86}Sr$ ratios as a method to correlate the carbonated sedimentation in sedimentary and metamorphic lithostratigraphic successions.

One of the major limitations is their use in rocks with intense dolomitization related to meteoric fluids, because such process increases the $^{87}Sr/^{86}Sr$ values, due the interaction with upper crustal fluids characterized by higher strontium ratios. A similar behaviour is also expected in carbonated rocks that have interacted with high temperature metamorphic and/or hydrothermal fluids.

Nevertheless its limitation, the $^{87}Sr/^{86}Sr$ data clearly emphasize at least two events of carbonate sedimentation in the OMZ: the Lower-Middle Devonian carbonates have lower values (0.70770-0.70780), than the ratios observed in Cambrian carbonates and, perhaps, also some Silurian limestones. The Devonian data are totally corroborant with global values obtained to Emsian-Givetian worldwide Sr curve (Veizer et al., 1999).

However, the available $^{87}Sr/^{86}Sr$ ratio available are still insufficient to constrain the age and origin of the Bencatel-Ferrarias-Cheles-Barrancos carbonates and its relation with Estremoz marbles. Indeed, although the Cambrian limestones from Alter-do-Chão-Elvas (Ovetian-Marianian in age) have $^{87}Sr/^{86}Sr$ signatures similar to those obtained to Abrantes and Estremoz marbles, they are also similar to some Upper Silurian-Lower Devonian limestones from Bencatel-Ferrarias-Cheles-Barrancos alignment.

Concerning the carbonates with a possible Cambrian and Silurian ages, they present some $^{87}Sr/^{86}Sr$ ratios overlap. Thus, more studies are needed in Estremoz and Ferrarias anticlines and in Barrancos, which also should include the Scyphocrinites Limestones (Pridoli; Robardet and Gutiérrez-Marco, 2004), in order to define their distinctive $^{87}Sr/^{86}Sr$ ratio. Nevertheless, it is clear that these limestones are not from the Lower-Middle Devonian times.

The strontium studies of the OMZ carbonates prove to be adequate to the Lower-Middle Devonian and Cambrian rocks, nevertheless some doubts still remain regarding the age and origin of the from Bencatel-Ferrarias-Cheles-Barrancos carbonates and its relation with Estremoz marbles. Thus, this methodology is suitable to other OMZ carbonates without biostratigraphic data, but could also be useful in the Silurian and Ordovician marine limestones with biostratigraphic control, helping to characterize and correlate the different carbonates events based on their $^{87}Sr/^{86}Sr$ fingerprint.

References

Ábalos, B., Ibarguchi, G., Eguiluz, L. (1991). Structural and metamorphic evolution of the Almaden de la Plata Core (Seville, Spain) in relation to syn-metamorphic shear between the Ossa-Morena and South Portuguese zones of the Iberian Variscan fold belt. Tectonophysics, 191, 365-387. DOI: 10.1016/0040-1951(91)90068-4

Álvaro, J.J., Bellido, F., Gasquet, D., Pereira, M.F., Quesada, C., Sánchez-García, T., (2014). Diachronism in the late Neoproterozoic–Cambrian arc-rift transition of North Gondwana: A comparison of Morocco and the Iberian Ossa-Morena Zone. Journal of African Earth Sciences. DOI: 10.1016/j.jafrearsci.2014.03.024

Araújo, A., Piçarra de Almeida, J., Borrego, J., Pedro, J., Oliveira, J.T. (2013). As regiões central e sul da Zona de Ossa-Morena, In: Dias, R., Araújo, A., Terrinha, P., Kullberg, J.C. (Eds.), Geologia de Portugal (Vol. I), Escolar Editora, Lisboa, 509-549.

Armendáriz, M. (2006). Los depósitos carbonatados de la cuenca carbonífera del Guadiato (Córdoba, SO del Macizo Ibérico). Boletín Geológico y Minero, 117, 513-518

Ausich, W.I., Kammer, T.W., Rhenberg, E.C., Wright, D.F. (2015). Early phylogeny of crinoids within the pelmatozoan clade. Palaeontology, 58, 937-952. DOI: 10.1111/pala.12204

Azmy, K., Veizer, J., Wenzal, B., Bassett, M., Cooper, P. (1999). Silurian strontium isotope stratigraphy. Geological Society of America Bulletin, 111, 475-483. DOI: 10.1130/0016-7606(1999)111<0475:SSIS>2.3.CO;2

Boogard, M. (1972). Conodont faunas from Portugal and Southwestern Spain. Part 1: A Middle Devonian fauna from near Montemor-o-Novo. Scripta Geologica, 13, 1-11.

Boogard, M. (1983). Conodont faunas from Portugal and southwestern Spain. Part 7. A Frasnian conodont fauna near the Estação de Cabrela (Portugal). Scripta Geologica, 69, 1-17.

Brasier, M.D., Shields, G.A., Kuleshov, V.N., Zhegallo, E.A. (1996). Integrated chemo- and biostratigraphic calibration of early animal evolution: Neoproterozoic-early Cambrian of southwest Mongolia. Geological Magazine, 133, 445-485. DOI: 10.1017/S0016756800007603

Bucher, K., Grapes, M. (2011). Petrogenesis of Metamorphic Rocks. Springer-Verlag, 8th Edition, 428 p.

Burke W. H., Denison, R. E., Hetherington, E. A., Koepnick, R. B., Nelson, H. F., Otto, J. B. (1982): Variation of seawater $^{87}Sr/^{86}Sr$ throughout Phanerozoic time. Geology, 10, 516-519. DOI: 10.1130/0091-7613(1982) 10<516:VOSSTP>2.0.CO;2

Chichorro, M. (2006). Estrutura do Sudoeste da Zona de Ossa-Morena: Área de Santiago de Escoural – Cabrela (Zona de Cisalhamento de Montemor-o-Novo, Maciço de Évora). Unpublished PhD thesis, Universidade de Évora, Portugal, 502p.

Chichorro, M., Pereira, M.F., Diaz-Azpiroz, M., Williams, I.S., Fernandez, C., Pin, C., Silva, J.B., (2008). Cambrian ensialic rift-related magmatism in the Ossa-Morena Zone (Évora-Aracena metamorphic belt, SW Iberian Massif): Sm–Nd isotopes and SHRIMP zircon U–Th–Pb geochronology. Tectonophysics, 461, 91–113. DOI: 1016/j.tecto.2008.01.008

Coelho, A., Gonçalves, F. (1970): Rocha hiperalcalina de Estremoz. Bol. Soc. Geol. Portugal, XVII, 181-185.

Conde, L.N., Andrade, A.A.S. (1974). Sur la faune meso et/ou néodévonienne des calcaires du Monte das Cortes, Odivelas (Massif de Beja). Memórias e Notícias, Univ. Coimbra, 78, 141-146.

Denison, R.E., Koepnick, R.B., Burke, W.H., Hetherington, E.A., Fletcher, A. (1997). Construction of the Silurian and Devonian seawater $^{87}Sr/^{86}Sr$ curve. Chemical Geology, 140, 109-121. DOI: 10.1016/S0009-2541(97)00014-4

Denison, R.E., Koepnick, R.B., Burke, W.H., Hetherington, E.A. (1998). Construction of the Cambrian and Ordovician seawater $^{87}Sr/^{86}Sr$ curve. Chemical Geology, 152, 325-340. DOI: 10.1016/S0009-2541(98)00119-3

Derry, L.A., Brasier, M.D., Corfield, R.M., Rozanov, A.Y., Zhuravlev, A.Y. (1994). Sr and C isotope in Lower Cambrian carbonates from the Siberian craton: A paleoenvironmental record during the 'Cambrian explosion'. Earth and Planetary Science Letters, 128, 671-681. DOI: 10.1016/0012-821X(94)90178-3

Guensburg T.E, Sprinkle, J. (2001). Earliest crinoids: New evidence for the origin of the dominant Paleozoic echinoderms. Geology 29(2): 131–134. DOI: 10.1130/0091-7613(2001)029<0131:ECNEFT>2.0.CO;2

Gomes, E.M.C., Fonseca, P.E. (2006). Eventos metamórfico/metassomáticos tardi-variscos na região de Alvito (Alentejo, sul de Portugal). Cadernos Lab. Xeolóxico de Laxe, 31, 67 - 85.

Gonçalves, F. (1972). Geological Map of Portugal, scale 1:50 000, 36-B (Estremoz), Serviços Geológicos de Portugal, Lisboa.

Gozalo, R., Liñán, E., Palacios, T., Gámez-Vintaned, J.A., Mayoral, E. (2003). The Cambrian of the Iberian Peninsula: an overview. Geologica Acta, 1, 103–112.

Hubbard C. R., Snyder, R.L. (1988). RIR-Measurement and Use in Quantitative XRD, Powder Diffraction, 3(2), 74-77. DOI: 10.1017/S0885715600013257

Hubbard, C. R., Evans, E. H., Smith, D. K. (1976). The Reference Intensity Ratio, I/Ic, for Computer simulated Powder Patterns. J. Appl. Cryst., 9, 169-174. DOI: 10.1107/S0021889876010807

LNEG (2010). Geological map of Portugal at 1:1.000.000, 3rd edition, Laboratório Nacional de Energia e Geologia, Lisboa.

Machado, G., Hladil, J. (2010). On the age and significance of the limestone localities included in the Toca da Moura volcano-sedimentary Complex: preliminary results. In: Santos A, Mayoral E, Melendez G, Silva CMD, Cachão M (Ed), III Congresso Iberico de Paleontologia / XXVI Jornadas de la Sociedad Espanola de Paleontologia, Lisbon, Portugal. Publicaciones del Seminario de Paleontologia de Zaragoza (PSPZ), 9, 153-156.

Machado, G., Hladil, J., Koptikova, L., Fonseca, P., Rocha, F.T., Galle, A. (2009). The Odivelas Limestone: Evidence for a Middle Devonian reef system in western Ossa-Morena Zone. Geol Carpath, 60(2), 121-137. DOI: 10.2478/v10096-009-0008-1

Machado, G., Hladil, J., Koptikova, L., Slavik, L., Moreira, N., Fonseca, M., Fonseca, P. (2010). An Emsian-Eifelian Carbonate-Volcaniclastic Sequence and the possible Record of the basal choteč event in western Ossa-Morena Zone, Portugal (Odivelas Limestone). Geol Belg, 13, 431-446.

Maloof, A.C., Porter, S.M., Moore, J.L., Dudás, F.O., Bowring, S.A., Higgins, J.A., Fike, D.A., Eddy, M.P. (2010). The earliest Cambrian record of animals and ocean geochemical change. GSA Bulletin, 122 (11-12), 1731–1774. doi: 10.1130/B30346.1

McArthur, J.M. (1994). Recent trends in strontium isotope stratigraphy. Terra Nova, 6, 331-358. DOI: 10.1111/j.1365-3121.1994.tb00507.x

McArthur, J.M., Howarth, R.J., Shields, G.A. (2012). Strontium Isotope Stratigraphy. In: Gradstein F.M., Ogg J.G., Schmotz M.D., Ogg G.M. (Eds.), A Geologic Time Scale 2012 (Chapter 7), Elsevier, 127-144

Medina-Varea, P., Sarmiento, G.N., Rodríguez, S., Cózar, P. (2005). Early Serpukhovian conodonts from the Guadiato Area (Córdoba, Spain). Coloquios de Paleontología, 55, 21-50.

Moita, P., Santos, J.F., Pereira, M.F. (2009). Layered granitoids: interaction between continental crust recycling processes and mantle-derived magmatism. Examples from the Évora Massif (Ossa-Morena Zone, southwest Iberia, Portugal). Lithos, 111(3–4), 125–141. DOI: 10.1016/j.lithos.2009.02.009

Morbidelli, P., Tucci, P., Imperatori, C., Polvorinos, A., Preite Martinez, M., Azzaro, E., Hernandez, M. J. (2007). Roman quarries of the Iberian peninsula: "Anasol" and "Anasol"-type. Eur. J. Mineral, 19, 125–135. DOI: 10.1127/0935-1221/2007/0019-0125

Moreira, N. (2012). Caracterização estrutural da zona de cisalhamento Tomar-Badajoz-Córdova no sector de Abrantes. Unpublished MsC thesis, University of Évora, 225 p.

Moreira, N., Machado, G. (in press). Devonian sedimentation in Western Ossa-Morena Zone and its geodynamic significance. In Quesada. C., Oliveira, J.T. (Eds.), The Geology of Iberia: a geodynamic approach. Springer (Berlin), Regional Geology Review series.

Moreira, N., Machado, G., Fonseca, P.E., Silva, J.C., Jorge, R.C.G.S., Mata, J. (2010). The Odivelas Palaeozoic volcano-sedimentary sequence: Implications for the geology of the Ossa-Morena Southwestern border. Comunicações Geológicas, 97, 129-146

Moreira, N., Araújo, A., Pedro, J.C., Dias, R. (2014a). Evolução geodinâmica da Zona de Ossa-Morena no contexto do SW Ibérico durante o Ciclo Varisco. Comunicações Geológicas 101(I), 275-278.

Moreira, N., Dias, R., Pedro, J.C., Araújo, A. (2014b). Interferência de fases de deformação Varisca na estrutura de Torre de Cabedal; sector de Alter-do-Chão – Elvas na Zona de Ossa-Morena. Comunicações Geológicas, 101(I), 279-282.

Moreira, N., Pedro, J., Romão, J., Dias, R., Araújo, A., Ribeiro A. (2015). The Neoproterozoic-Cambrian transition in Abrantes Region (Central Portugal); Litostratigraphic correlation with Cambrian Series of Ossa-Morena Zone. The Variscan belt: correlations and plate dinamics. Géologie de la France (Variscan 2015 special issue, Rennes), 2015(1), 101-102. ISBN: 978-2-7159-2612-7.

Moreira, N., Pedro, J., Santos, J.F., Araújo, A., Romão, J., Dias, R., Ribeiro, A., Ribeiro, S., Mirão, J. (2016). $^{87}Sr/^{86}Sr$ ratios discrimination applied to the main Paleozoic carbonate sedimentation in Ossa-Morena Zone. In: IX Congreso Geológico de España (special volume). Geo-Temas, 16(1), 161-164. ISSN 1576-5172.

Moreno, F., Vegas, R. (1976). Tectónica de las séries ordovícias y siluricas en la región de Villanueva del Fresno. Estudios geológicos, 32, 47-52.

Nicholas, C.J. (1996). The Sr isotopic evolution of the oceans during the 'Cambrian explosion'. Journal of the Geological Society, 153, 243-254. DOI: 10.1144/gsjgs.153.2.0243

Oliveira, J.T. (1984). Transversal Barrancos-Ficalho. Cadernos do Laboratorio Xeolóxico de Laxe, 8, 347-357

Oliveira, J.T., Relvas, J., Pereira, Z., Munhá, J., Matos, J., Barriga, F., Rosa, C. (2013). O Complexo Vulcano-Sedimentar de Toca da Moura-Cabrela (Zona de Ossa Morena): evolução tectono-estratigráfica e mineralizações associadas. In: Dias, R., Araújo, A., Terrinha, P., Kullberg, J.C. (Eds.), Geologia de Portugal (Vol. I), Escolar Editora, Lisboa, 621-645.

Oliveira, J.T., Oliveira, V., Piçarra, J.M. (1991). Traços gerais da evolução tectono-estratigráfica da Zona de Ossa Morena, em Portugal: síntese crítica do estado actual dos conhecimentos. Comun. Serv. Geol. Port. 77, 3-26.

Palácios Gonzalez, M.J. Palacios, T., Valenzuela, J.M.G (1990). Trilobites y Goniatites de la cuenca carbonífera de los Santos de Maimona: deducciones bioestratigráficas. Geogaceta, 8, 66-67.

Passchier, C.W., Trouw, R.A.J. (2005). Microtectonics. 2nd Edition, Springer, 382P..

Pereira. Z., Oliveira, J.T. (2003). Estudo palinostratigráfico do sinclinal da Estação de Cabrela. Implicações tectonostratigráficas. Cienc. Terra UNL Lisboa, 5, 118–119.

Pereira, Z., Oliveira, V., Oliveira, J.T. (2006). Palynostratigraphy of the Toca da Moura and Cabrela Complexes, Ossa Morena Zone, Portugal. Geodynamic implications. Rev Palaeobot Palyno, 139, 227-240. DOI: 10.1016/j.revpalbo.2005.07.008

Pereira, M.F., Silva, J.B. (2001). The Northeast Alentejo Neoproterozoic-Lower Cambrian succession (Portugal): implications for regional correlations in the Ossa morena Zone (Iberian Massif). Geogaceta, 30, 106-111.

Pereira, M.F., Medina, J., Chichorro, M., Linnemann, U. (2006). Preliminary Rb-Sr and Sm-Nd isotope geochemistry on Ediacaran and Early Cambrian Sediments from the Ossa-Morena Zone (Portugal). In: J. Mirão & A. Balbino (Eds.), VII Congresso Nacional de Geologia abstract book (vol. I), Estremoz, 213–215.

Pereira, M.F., Solá, A.R., Chichorro, M., Lopes, L., Gerdes, A., Silva, J.B. (2012). North-Gondwana assembly, break up and paleogeography: U–Pb isotope evidence from detrital and igneous zircons of Ediacaran and Cambrian rocks of SW Iberia. Gondwana Research, 22(3-4), 866-881. DOI: 1016/j.gr.2012.02.010

Piçarra, J.M. (2000). Estudo estratigráfico do sector de Estremoz-Barrancos, Zona de Ossa Morena, Portugal. Vol. I - Litoestratigrafia do intervalo Câmbrico médio?-Devónico inferior, Vol. II - Bioestratigrafia do intervalo Ordovícico-Devónico inferior. PhD Thesis (unpublished), Évora University, Portugal.

Piçarra, J.M., Le Meen, J. (1994). Ocorrência de crinóides em mármores do Complexo Vulcano-Sedimentar Carbonatado de Estremoz: implicações estratigráficas. Comunicações do Instituto Geológico e Mineiro, 80, 15-25.

Piçarra, J.M., Sarmiento, G. (2006). Problemas de posicionamento estratigráfico dos Calcários Paleozóicos da Zona de Ossa Morena (Portugal). In: J. Mirão & A. Balbino (Eds.), VII Congresso Nacional de Geologia abstract book (vol. II), Estremoz, 657-660.

Prokoph, A., Shields, G.A., Veizer, J. (2008). Compilation and time-series analysis of a marine carbonate $\delta^{18}O$, $\delta^{13}C$, $^{87}Sr/^{86}Sr$ and $\delta^{34}S$ database through Earth history. Earth-Science Reviews, 87, 113-133. DOI: 10.1016/j.earscirev.2007.12.003

Ribeiro, M.L., Mata, J., Piçarra, J.M. (1992). Vulcanismo bimodal da região de Ficalho: características geoquímicas. Comunicações Serviços Geológicos de Portugal, 78(2), 75-85.

Robardet, M., Gutiérrez-Marco, J.C. (1990). Passive margin phase (Ordovician-Silurian-Devonian). In: Dallmeyer RD, Martínez García E (Ed), Pre-Mesozoic geology of Iberia, Springer-Verlag, Berlin, 249-251.

Robardet, M., Gutiérrez-Marco, J.C. (2004). The Ordovician, Silurian and Devonian sedimentary rocks of the Ossa-Morena Zone (SW Iberian Peninsula, Spain). J Iber Geol, 30, 73-92

Rollinson, H.R. (1993). Using geochemical data: evaluation, presentation, interpretation, Addison-Wesley Longman Ltd, Singapore, 352p.

Romão, J., Ribeiro, A., Munhá, J., Ribeiro, L. (2010). Basement nappes on the NE boundary the Ossa-Morena Zone (SW Iberian Variscides). European Geosciences Union, General Assembly, Vienna, Austria (Abstract).

Sánchez-García, T., Quesada, C., Bellido, F., Dunning, G.R., González de Tánago, J. (2008). Two-step magma flooding of the upper crust during rifting: the Early Palaeozoic of the Ossa Morena Zone (SW Iberia). Tectonophysics, 461, 72–90. DOI: 10.1016/j.tecto.2008.03.006

Sánchez-García, T., Bellido, F., Pereira, M.F., Chichorro, M., Quesada, C., Pin, C., Silva, J.B. (2010). Rift-related volcanism predating the birth of the Rheic Ocean (Ossa-Morena zone, SW Iberia). Gondwana Research, 17, 392-407. DOI: 10.1016/j.gr.2009.10.005

Santos, J.F., Andrade, A., Munhá, J. (1990). Magmatismo orogénico varisco no limite meridional da Zona de Ossa-Morena. Comun. Serv. Geol. Portugal, 76, 91-124.

Santos, J.F., Mata, J., Ribeiro, S., Fernandes, J., Silva, J. (2013). Sr and Nd isotope data for arc-related (meta) volcanics (SW Iberia), Goldschmidt Conference Abstracts, 2132.

Sarmiento, G.N., Piçarra, J.M., Oliveira, J.T. (2000). Conodontes do Silúrico (Superior?)-Devónico nos "Mármores de Estremoz", Sector de Estremoz-Barrancos (Zona de Ossa Morena, Portugal). Implicações estratigráficas e estruturais a nível regional. I Congresso Ibérico de Paleontologia/VIII International Meeting of IGCP 421 (abstract book), Évora, 284-285.

Sarmiento, G.N., Gutiérrez-Marco, J.C., Del Moral, B. (2008). Conodontos de la "Caliza de Pelmatozoos" (Ordovícico Superior), Norte de Sevilla, Zona de Ossa-Morena (España). Coloquios de Paleontología, 58, 73-99.

Sarmiento, G.N., Gutiérrez-Marco, J.C., Rodríguez-Cañero, R., Martín Algarra, A., Navas-Parejo, P. (2011). A Brief Summary of Ordovician Conodont Faunas from the Iberian Peninsula. In: Gutiérrez-Marco, J.C., Rábano, I. and García-Bellido, D. (eds.), Ordovician of the World. Cuadernos del Museo Geominero, IGME, 14, 505-514. ISBN 978-84-7840-857-3

Silva, J.C., Mata, J., Moreira, N., Fonseca, P.E., Jorge, R.C.G.S., Machado, G. (2011). Evidence for a Lower Devonian subduction zone in the southeastern boundary of the Ossa-Morena-Zone. In: Absctracts of the VIII Congresso Ibérico de Geoquímica, Castelo Branco, 295-299.

Taelman, D., Elburg, M., Smet, I., Paepe, P., Lopes, L., Vanhaecke, F., Vermeulen, F. (2013). Roman marble from Lusitania: petrographic and geochemical characterization. Journal of Archaeological Science, 40, 2227-2236. DOI: 10.1016/j.jas.2012.12.030

Vegas, R., Moreno, R. (1973). Sobre la tectónica del flanco meridional de la Antiforma de Burgillos (sur de la provincia de Badajoz). Estudios Geologicos, 29, 513-517.

Veizer, J., Ala, D., Azmy, K., Bruckschen, P., Buhl, D., Bruhn, F., Carden, G.A.F., Diener, A., Ebneth, S., Godderis, Y., Jasper, T., Korte, C., Pawellek, F., Podlaha, O.G., Strauss, H. (1999). $^{87}Sr/^{86}Sr$, δ13C and δ18O evolution of Phanerozoic seawater. Chemical Geology, 161, 59-88. DOI: 10.1016/S0009-2541(99)00081-9

Veizer, J. (1989). Strontium Isotopes in Seawater through Time. Ann. Rev. Earth Planet. Sci., 17, 141-167. DOI: 10.1146/annurev.earth.17.1.141

Vera, J.A., (Eds., 2004). Geología de España. SGE and IGME, 884p.

Winter, J.D. (2013). Principles of igneous and metamorphic petrology. 2nd edition, Pearson New International Edition. ISBN13: 9781292021539

IV

Estrutura de Torre de Cabedal

A necessidade de enquadramento e compreensão da estrutura da região de Abrantes no contexto da estruturação dos domínios setentrionais da Zona de Ossa-Morena, mas principalmente a análise e correlação da sua sucessão litoestratigrafica com os restantes domínios desta zona paleogeográfica, levou à escolha de uma área localizada nos domínios proximais à Zona de Cisalhamento Tomar-Badajoz-Córdoba, mas onde o grau metamórfico fosse menos intenso. Foi então seleccionada uma janela de Neoproterozoico no sector de Alter-do-Chão-Elvas, onde era possível observar as características litoestratigráficas da sequência típica do Neoproterozóico-Câmbrico inferior. Esta janela, denominada de Estrutura de Torre de Cabedal, fica localizada na região a SE da povoação de Vila Boim (Fig. 1).

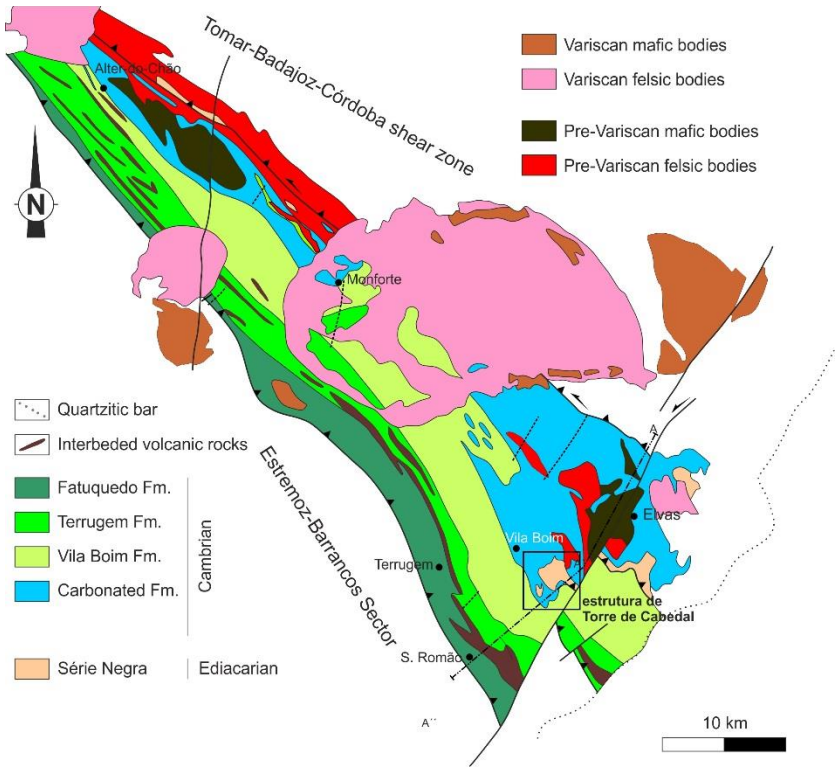

Figura 1 – Carta Geológica simplificada do sector de Alter-d-Chão-Elvas (adaptado de Carta Geológica de Portugal à Escala 1:50.000, folhas 32-B, 32-D, 33-C, 36-B, 37-A e 37-C, e Carta Geológica de Portugal à Escala 1:500.000, folha Sul).

Para além da caracterização e comparação das lito-facies da sequência estratigráfica desta região, os trabalhos aí realizados pretendiam também a compreensão das relações geométricas entre as rochas magmáticas de idade câmbrica com o encaixante sedimentar. No capítulo referente à Litoestratigrafia e Geoquímica da sucessão Neoproterozóico-Câmbrico inferior de Abrantes (capítulo II.2), as amostras analisadas e referidas como pertencentes ao sector de Alter-do-Chão-Elvas, provêm deste sector, permitindo assim uma melhor caracterização do magmatismo câmbrico representante das fases iniciais do Ciclo de Wilson Varisco na Zona de Ossa-Morena.

Contudo, para a compreensão da sequência litoestratigráfica da região, foi necessária uma caracterização estrutural preliminar da região, o que originou o capítulo que se segue. Os levantamentos de campo realizados na região mostraram a presença de duas fases de deformação Varisca, de carácter frágil-dúctil, seguida por uma terceira fase de deformação, mais frágil, com características similares ao Tardi-Varisco. As duas fases mais precoces são responsáveis pela inversão da sequência estratigráfica deste sector, sendo que a elaboração de um corte geológico simplificado neste sector (Fig. 2) mostra que as unidades mais recentes (localizadas mais a sul) são sobrepostas pelas unidades mais antigas de idade compreendida entre o Neoproterozóico e o Câmbrico inferior, mais concretamente a Série Negra e a Unidade Carbonatada de Elvas. É do resultado da interferência destas duas fazes de deformação que surgem as diversas janelas de Neoproterozóico cartografadas neste sector (Fig. 1).

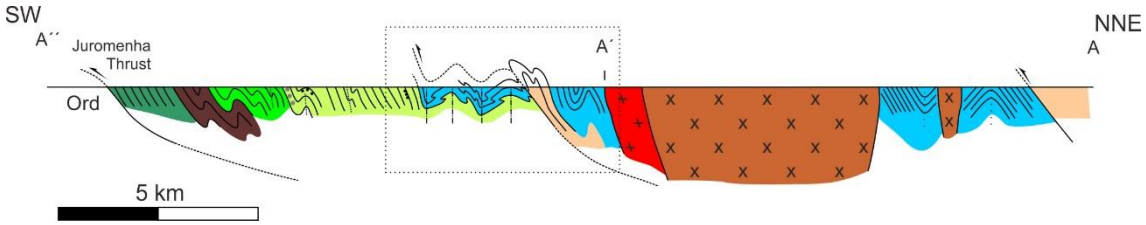

Figura 2 – Corte geológico simplificado do sector de Alter-do-Chão-Elvas (vide localização do corte e legenda na Fig. 1)

Este capítulo apresenta os dados estruturais desta estrutura e que possibilitaram a melhor compreensão da estratigrafia da região. O texto apresentado neste capítulo segue na íntegra o artigo com o mesmo título publicado na revista Comunicações Geológicas em 2014, no volume especial relativo ao IX Congresso Nacional de Geologia, realizado no Porto no mesmo ano. Contudo, apresenta-se sempre que necessário, para além das figuras publicadas no referido artigo, figuras adicionais que permitem a melhor compreensão do capítulo em causa.

- Capítulo IV.1.

MOREIRA, N., DIAS, R., PEDRO, J.C., ARAÚJO, A. (2014), Interferência de fases de deformação Varisca na estrutura de Torre de Cabedal; sector de Alter-do-Chão – Elvas na Zona de Ossa-Morena. Comunicações geológicas, 101 (Vol. Especial I), 279-282.

De referir ainda que, sendo a publicação um artigo curto publicado num volume especial no âmbito do congresso, como previamente referido, esta publicação acarreta limitações de espaço que impossibilitaram a citação de todos os trabalhos pertinentes para o efeito. Desta forma, e seguindo na íntegra o trabalho publicado, alguns trabalhos com indubitável pertinência não foram citados.

Referências

Gonçalves, F. (1971). Carta Geológica de Portugal à escala 1: 50.000, folha 33-C (Campo Maior). Serviços Geológicos de Portugal.

Gonçalves, F. (1972). Carta Geológica de Portugal à escala 1: 50.000, olha 36-B (Estremoz). Serviços Geológicos de Portugal.

Gonçalves, F. (1972). Carta Geológica de Portugal à escala 1: 50.000, folha 32-B (Portalegre). Serviços Geológicos de Portugal.

Gonçalves, F., Perdigão, J.C., Carvalho, S., Teixeira, C. (1969). Carta Geológica de Portugal à escala 1: 50.000, folha 37-A (Elvas). Serviços Geológicos de Portugal.

Gonçalves, F., Ladeira F. L., Joaquim, A. N. (1973). Carta Geológica de Portugal à escala 1: 50.000, folha 32-D (Sousel). Serviços Geológicos de Portugal.

Oliveira, J. T., Pereira, E. (Coord. Soco Hercínico); Almeida, J. P., Carvalhosa, D., Carvalhosa, A., Ferreira, J. N. Ferreira, Gonçalves, F., Oliveira, V., Ribeiro, A., Ribeiro, M. L., Silva, A. F., Noronha, F., Young, T. (Colaboradores Soco Herecínico) (1992), Carta Geológica de Portugal à escala 1/500 000, folha Sul. Serviços Geológicos de Portugal.

Perdigão, J. C. (1974), Carta Geológica de Portugal à escala 1: 50.000, folha 37-C (Juromenha). Serviços Geológicos de Portugal.

IV.1

Interferência de fases de deformação Varisca na estrutura de Torre de Cabedal; sector de Alter-do-Chão – Elvas na Zona de Ossa-Morena

Índice

IV.1.1. Introdução e Enquadramentos Geológico

A Zona de Ossa-Morena (ZOM) foi tradicionalmente subdividida em zonas e sub-zonas ou domínios tectonoestratigráficos essencialmente com base na sua estratigrafia (*e.g.* Apalategui *et al*., 1990). Oliveira *et al.* (1991) propôs o conceito de sector que visa a melhor compreensão das várias secções desta zona paleogeográfica, não atribuindo conotação tectónica aos limites entre os diversos sectores; os autores dividem o domínio português da ZOM em cinco sectores com características próprias.

O Sector Alter-do-Chão-Elvas (Fig. 1) é limitado a norte pelo Cavalgamento de Alter do Chão (Pereira & Silva, 2006), sendo que a interpretação do limite sul, com o sector de Estremoz-Barrancos não é consensual. Alguns autores (*e.g.* Oliveira *et al.*, 1991) consideram que o limite, no domínio português, é marcado pela presença de uma discordância cambro-ordovícica, enquanto para outros (*e.g.* Araújo *et al.,* 1994) o limite é interpretado como uma estrutura à escala regional, com cinemática cavalgante, designado Cavalgamento da Juromenha.

O presente trabalho pretende ser uma primeira aproximação à estruturação deste sector da ZOM, tendo como base de trabalho um domínio restrito onde toda a estratigrafia da região se encontra exposta (estrutura de Torre de Cabedal; Lopes, 2003) e onde as relações estratigráficas são bem conhecidas.

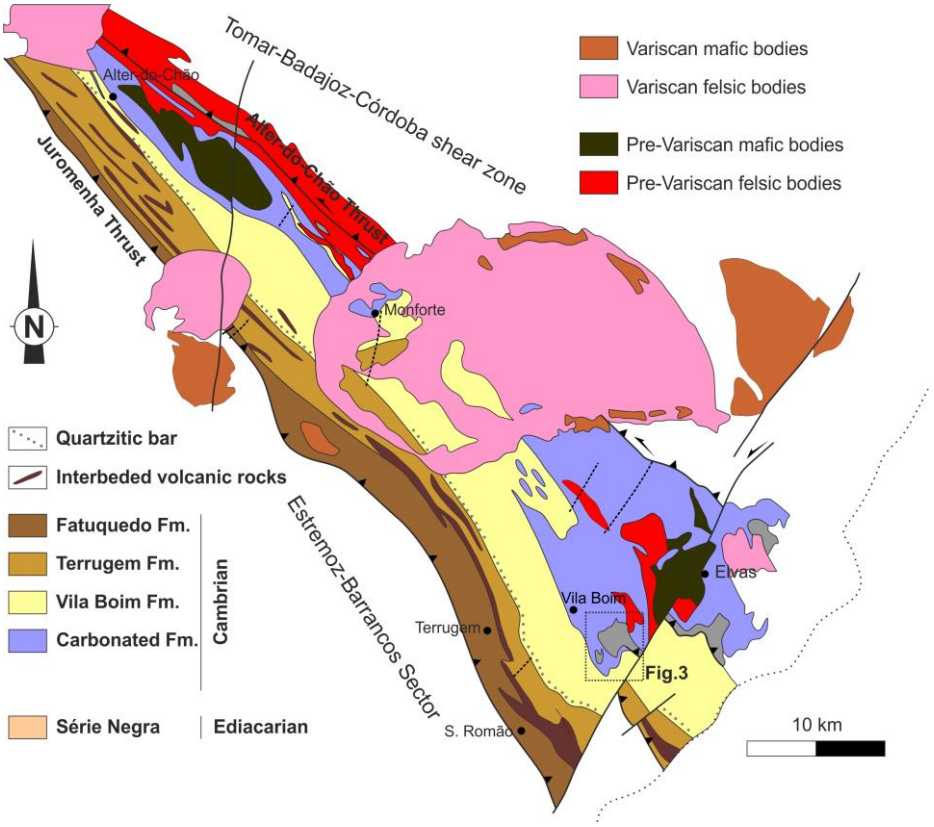

Figura 1 – Esboço geológico do Sector Alter-do-Chão-Elvas, com referência à localização da estrutura de Torre de Cabedal (adaptado de Carvalho et al., 1992).

IV.1.2. Síntese Estratigráfica do Sector de Alter-do-Chão-Elvas

O sector de Alter-do-Chão – Elvas é caracterizado por uma espessa sequência de unidades atribuídas ao Câmbrico (Fig. 2), ostentando um metamorfismo regional de baixo grau, pontualmente com evidências de metamorfismo de contacto associado à instalação de corpos magmáticos do Ordovícico e Carbónico (Pereira & Silva, 2006). Estas unidades assentam sobre o soco Neoproterozóico da ZOM, classicamente denominado de Série Negra (*e.g.* Oliveira *et al.*, 1991; Fig. 2), que aflora pontualmente em "janelas" (Fig. 1). Esta unidade é constituída por uma intercalação de xistos negros e metagrauvaques, com liditos e carbonatos subordinados.

Sobre a unidade neoproterozóica ocorre, discordantemente, uma série clástica (com conglomerados e arcoses) do Câmbrico inferior (*ca.* 540-520 Ma) com intercalações de rochas ortoderivadas félsicas (tufos félsicos e riólitos), com espessura variável (*e.g.* Oliveira *et al.*, 1991; Pereira & Silva, 2006; Fig. 2). Esta unidade clástica passa progressivamente a uma série constituída por carbonatos (maioritariamente dolomíticos), com intercalações de rochas siliciclásticas, a Formação Carbonatada de Elvas (Oliveira *et al.,* 1991). Esta formação tem sido correlacionada com a Formação de Alconera em Espanha, onde surgem faunas de trilobites e arqueociatas, que datam a unidade do Câmbrico inferior (Gozalo *et al.,* 2003). Por vezes, as

unidades carbonatadas contactam directamente com a Série Negra de forma discordante, sem existência da unidade clástica na sua base.

A topo da unidade carbonatada surge uma sequência *flychóide* constituída por uma alternância de metagrauvaques, psamitos e metapelitos, designada por Formação de Vila Boim (*e.g.* Oliveira *et al*., 1991: Fig. 2). Esta formação é atribuída ao Câmbrico inferior (Marianiano-Bibliano), com base em faunas de trilobites, acritarcos e braquiópodes (Gozalo *et al.,* 2003). Intercalados na Formação de Vila Boim, ocorrem vulcanitos de natureza toleítica, interpretados como resultantes do processo de *rifting* intracontinental associado aos estádios iniciais do ciclo varisco (Mata & Munhá, 1990). A sequência anteriormente descrita termina, com o aparecimento de bancadas quartzíticas-conglomeráticas métricas datadas do Câmbrico médio (Barra Quartzítica; Oliveira *et al.,* 1991). Sobre a Barra Quartzítica sobrepõe-se, concordantemente, o Complexo Vulcano-Sedimentar de Terrugem (Oliveira et al., 1991; Araújo *et al.*, 2013 e referências inclusas; Fig. 2). Este é constituído por uma sequência terrígena com pelitos, arenitos e grauvaques, onde surgem intercaladas possantes massas de rochas vulcânicas bimodais com quimismo alcalino-transicional, semelhante ao exibido pelos basaltos intraplaca, muito embora nalguns casos surjam padrões geoquímicos típicos de E-MORB e N-MORB, correlacionáveis com basaltos de crista oceânica (Mata & Munhá, 1990; Sánchez-Gárcia *et al*., 2010). Este complexo é atribuído ao Câmbrico médio-superior por correlação com as Camadas de Playon e com os Basaltos de Umbria-Pipeta (Sánchez-Gárcia *et al.,* 2010) onde foram identificados braquiópodes, trilobites e acritarcas dessa idade (Gozalo *et al.,* 2003). Dados radiométricos recentes em rochas pertencentes aos Basaltos de Umbria-Pipeta forneceram idades entre os 505-515 Ma (Sánchez-Gárcia *et al.,* 2010).

Este complexo passa gradualmente a um conjunto terrígeno constituído por alternâncias milimétricas a centimétricas de pelitos, siltitos e bancadas mais espessas de grauvaques (Formação de Fatuquedo; Oliveira *et al.,* 1991). Esta formação é considerada do Câmbrico médio, por correlação com unidades semelhantes, em Espanha, onde foram identificados acritarcas. Referência ainda para a presença de intercalações de basaltos alcalinos-transicionais (Mata & Munhá, 1990) riólitos e tufos félsicos.

No topo desta série surge em discordância um conglomerado com calhaus decimétricos de quartzito e quartzo (por vezes com fragmentos de vulcanitos ácidos, básicos e granitos); este conglomerado tem sido mencionado como marcador da discordância Câmbrico-Ordovícico (*e.g.* Oliveira *et al.*, 1991; Fig. 2). Contudo, esta interpretação não é de todo consensual. Alguns autores consideram que o conglomerado em causa marca um acidente de 1ª ordem no limite entre os sectores Alter-do-Chão-Elvas e Estremoz-Barrancos, o designado Cavalgamento da Juromenha (*e.g.* Araújo *et al.,* 1994; Fig. 2).

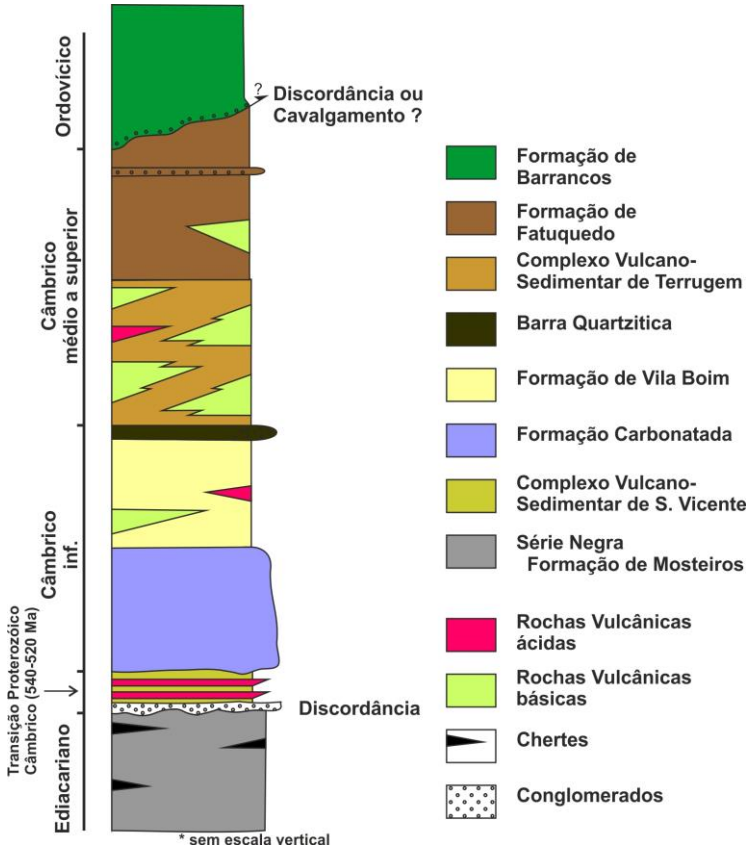

Figura 2 – Coluna estratigráfica do sector de Alter-do-Chão-Elvas (adaptado de Oliveira et al., 1991; Pereira e Silva, 2006; Sánchez-García et al., 2010).

IV.1.3. Caracterização Estrutural da Estrutura de Torre de Cabedal

A deformação Varisca no sector em estudo é resultante da sobreposição de duas fases de deformação principais, à qual se junta uma fase de deformação tardia com características mais frágeis (Fig. 3). Seguidamente apresenta-se uma descrição de cada um dos episódios de deformação presentes numa janela estratigráfica, onde é possível observar toda a sequência estratigráfica deste sector e que se denominou Estrutura de Torre de Cabedal (Lopes, 2003).

IV.1.3.1. *Primeira Fase de Deformação*

A primeira fase de deformação Varisca (D_1) desenvolve-se em andar estrutural superior, em condições de baixo grau metamórfico. Esta fase de deformação é caracterizada pelo desenvolvimento de dobras cilíndricas fechadas a isoclinais, de plano axial sub-horizontal a pouco inclinado. As dobras apresentam diferentes amplitudes (desde a centimétrica à hectométrica) ostentando geralmente assimetria, que é variável tendo em conta a sua posição relativamente às dobras de 1ª ordem (Fig. 4A.1 E A.2). Estas dobras apresentam frequentemente espessamento da charneira e flancos laminados (Fig. 4A.1). A clivagem S_1

associada ao processo de dobramento é incipiente, desenvolvendo-se pontualmente nos níveis mais pelíticos.

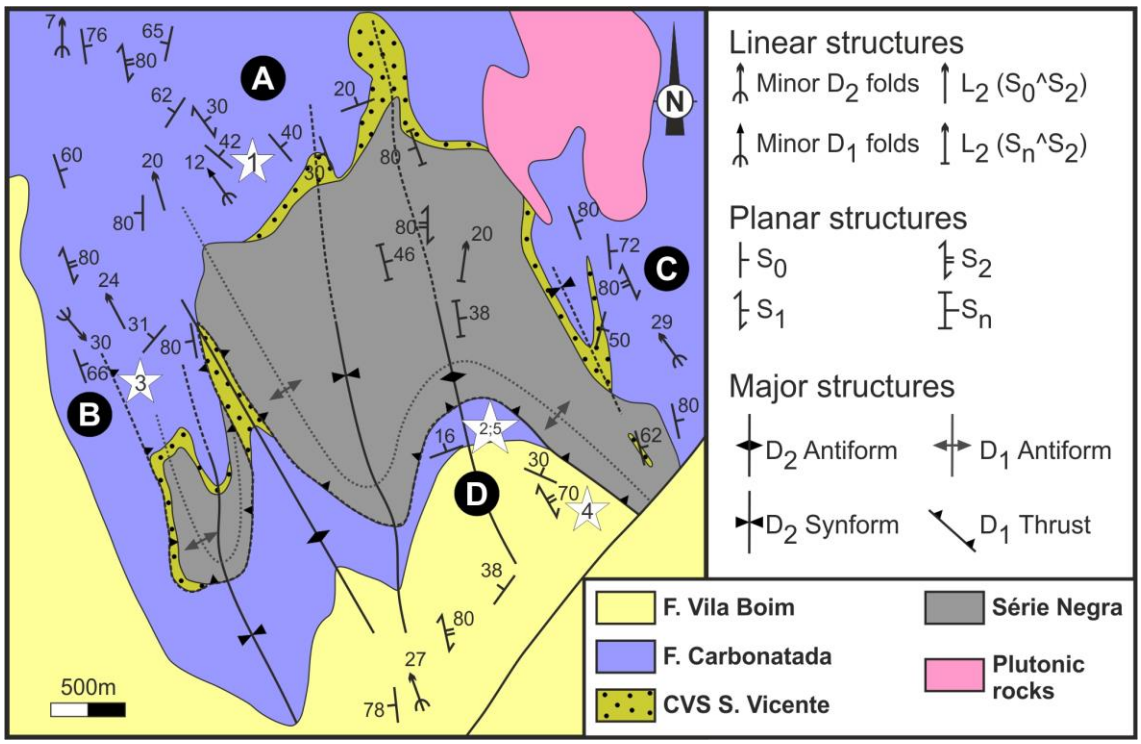

Figura 3 – Mapa geológico e estrutural simplificado da estrutura de Torre de Cabedal (limites geológicos parcialmente adaptados de Gonçalves & Assunção, 1970).

Os eixos das dobras D_1 apresentam grande dispersão na sua orientação, apresentando sentidos de mergulho variáveis entre NW-SE (mergulhantes geralmente para NW) e E-W. Esta variação na orientação dos eixos das dobras D_1 pode ser resultado da actuação da segunda fase de deformação, não sendo de excluir a possibilidade de uma variação na sua orientação inicial, eventualmente associada a mantos dobras primeira ordem com eixos ondulados, como descrito para outras regiões da ZOM (*e.g.* Araújo *et al.*, 2013). No que respeita à vergência das dobras D_1, a análise da assimetria de dobras de 2ª ordem parecem mostrar que a vergência para o quadrante S-SW (Fig. 4A.2).

Este processo de dobramento é responsável pela inversão da estratigrafia da região, sendo possível observar, critérios de polaridade invertida nos litótipos típicos da Formação de Vila Boim, mas também nos níveis pelíticos intercalados na Formação Carbonatada. Esta inversão é bem evidente no sul da área em estudo onde é possível observar a inversão completa da estrutura, com a Formação Carbonatada a sobrepor-se à Formação de Vila Boim.

O regime de deformação progressiva durante a D_1 leva à laminação dos flancos inversos das dobras deitadas, gerando cavalgamentos com vergência geométrica idêntica à evidenciada

nos dobramentos (Fig. 4A.3). Como seria de esperar, os cavalgamentos D_1 apresentam orientações variáveis, resultantes da actuação da segunda fase de deformação, que os redobram. Muito embora a superfície destes acidentes geralmente não aflorem, os mesmos são postos em evidência pelo padrão de afloramento.

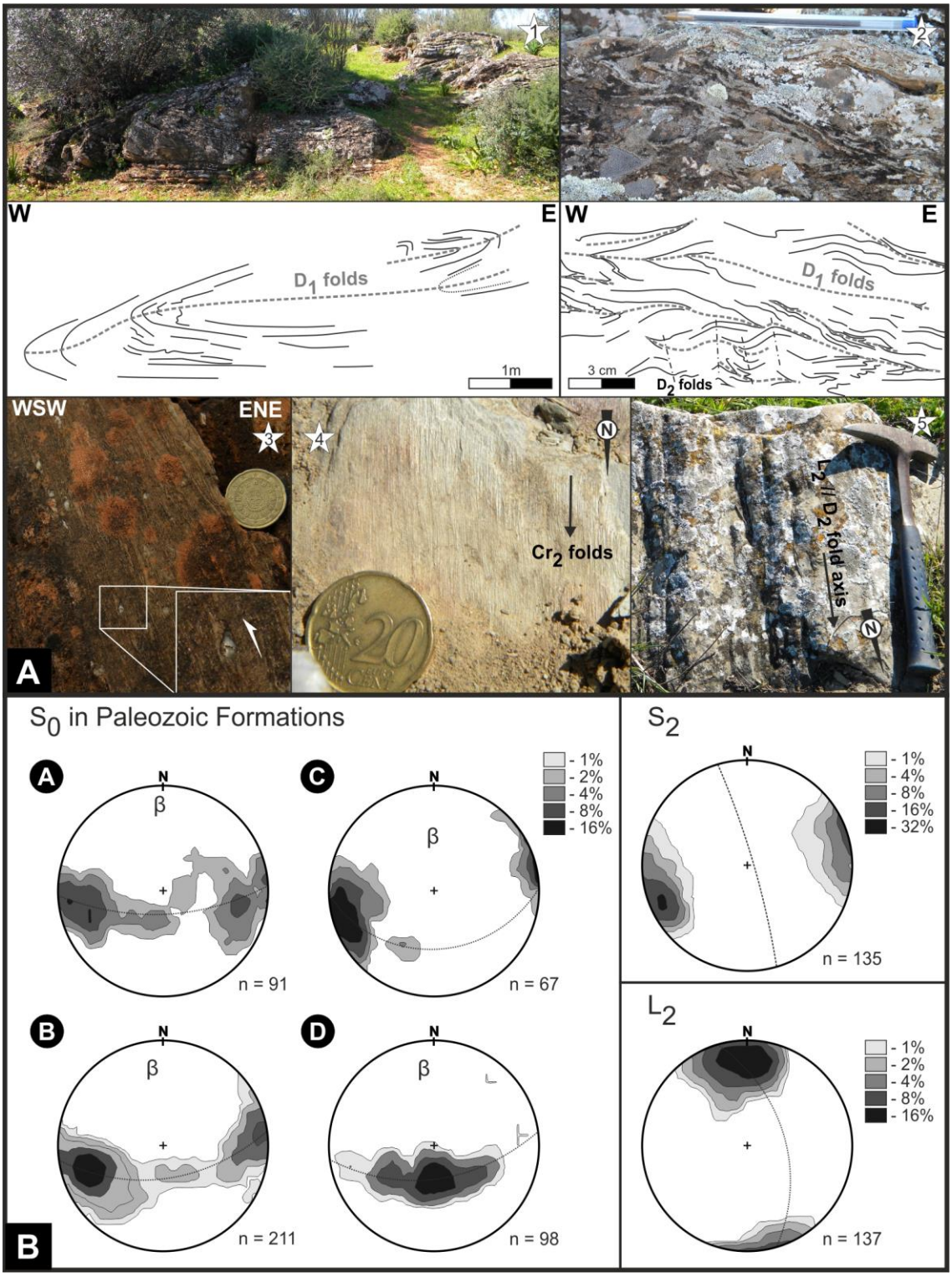

Figura 4 – Caracterização estrutural da Estrutura de Torre de Cabedal:

A – Estruturas observadas na estrutura de Torre de Cabedal: 1 e 2 – dobras deitadas D_1 na Fm. Carbonatada, 3 – critérios de cavalgamento para SW associado à D_1, 4 – clivagem de crenulação D_2 afectando pelitos da Fm. Vila Boim, 5 – dobras abertas D_2 na Fm. Carbonatada (localização na Fig. 3);

B – Diagramas de densidades de pontos referentes a pólos dos planos de estratificação (S_0) para quatro secções da estrutura (ver localização na fig. 3), clivagem de segunda fase (S_2) e lineações de intersecção (L_2) – rede de Schmidt, hemisfério inferior.

IV.1.3.2. *Segunda Fase de Deformação*

A segunda fase de deformação Varisca (D_2) oblitera parcialmente a estrutura prévia associado à D_1 Varisca. A D_2 é responsável pela geração de dobramentos de orientação NNW-SSE, com planos axiais verticais, muito embora, estas estruturas apresentem por vezes clara vergência geométrica para WSW. As dobras D_2 são também elas cilíndricas, muito embora a sua geometria seja variável no que respeita ao ângulo de abertura, sendo possível evidenciar dobras abertas a fechadas.

As dobras apresentam uma clivagem S_2 de plano axial (que por vezes é de crenulação; Fig. 4A.4, A.5 e B), geralmente em leque. Esta apresenta uma orientação NNW-SSE, ostentando elevados pendores para E (N16ºW, 85ºE; Fig. 4B), atitude que está de acordo com a vergência geométrica referida para as dobras D_2. Pontualmente, é possível evidenciar a presença de critérios cinemáticos esquerdos associados às estruturas D_2.

A lineação de intersecção L_2 (S_0^S_2) apresenta grande uniformidade, mergulhando levemente para N-NNW (19º, N05ºW; Fig. 4B). Esta lineação é sub-paralela às dobras associadas a esta fase de deformação, muito embora os eixos das dobras apresentem um ligeiro ângulo no que respeita ao sentido de mergulho e pendores ligeiramente superiores (27º, N07ºE). A variação entre a atitude da lineação de intercepção e dos eixos das dobras D_2 pode ser resultante da estruturação prévia D_1 que é posteriormente redobrada durante esta fase de deformação.

Esta fase de deformação é gerada em níveis estruturais intermédios, sendo o metamorfismo incipiente. O pico metamórfico desta região dá-se durante esta fase de deformação, atingindo a zona da clorite (Pereira & Silva, 2006).

IV.1.3.3. *Deformação Tardia*

Em regime frágil, mas ainda associado às fases tardias do ciclo Varisco, surgem duas famílias de fracturação principais, uma de orientação NE-SW (N40ºE a N53ºE) e uma segunda

E-W (E-W a S75ºE), ambas verticalizadas. A primeira família apresenta evidências de cinemática esquerda, com desenvolvimento pontual de bandas *kink* centimétricas. Esta família, apresenta por vezes uma componente vertical, com abatimento do bloco sudoeste. É desta fase de deformação a falha que limita a este a área em estudo (Fig. 3), pondo em contacto directo a Formação de Vila Boim com a Série Negra.

IV.1.4. Considerações Finais

O padrão de afloramento presente na estrutura de Torre de Cabedal é resultante da presença de duas fases de deformação Varisca principais (Fig. 5). A primeira fase é responsável pela génese de dobras deitadas, associadas a cavalgamentos, com vergência para S-SW e que são responsáveis pela inversão da estratigrafia da região, colocando as unidades basais do Câmbrico sobre unidades mais recentes (Fm. Vila Boim), seguindo-se uma fase de deformação com geração de dobras de plano axial vertical, a ligeiramente vergente para WSW, acentuando a inversão da estratigrafia. O padrão de interferência exibido (Fig. 3 e 5) parece mostrar características intermédias entre tipo 2 e 3 de Ramsay & Huber (1987). Esta mudança de geometria no dobramento poderá ser resultante da mudança nos processos geodinâmicos actuantes na ZOM durante o Ciclo Varisco.

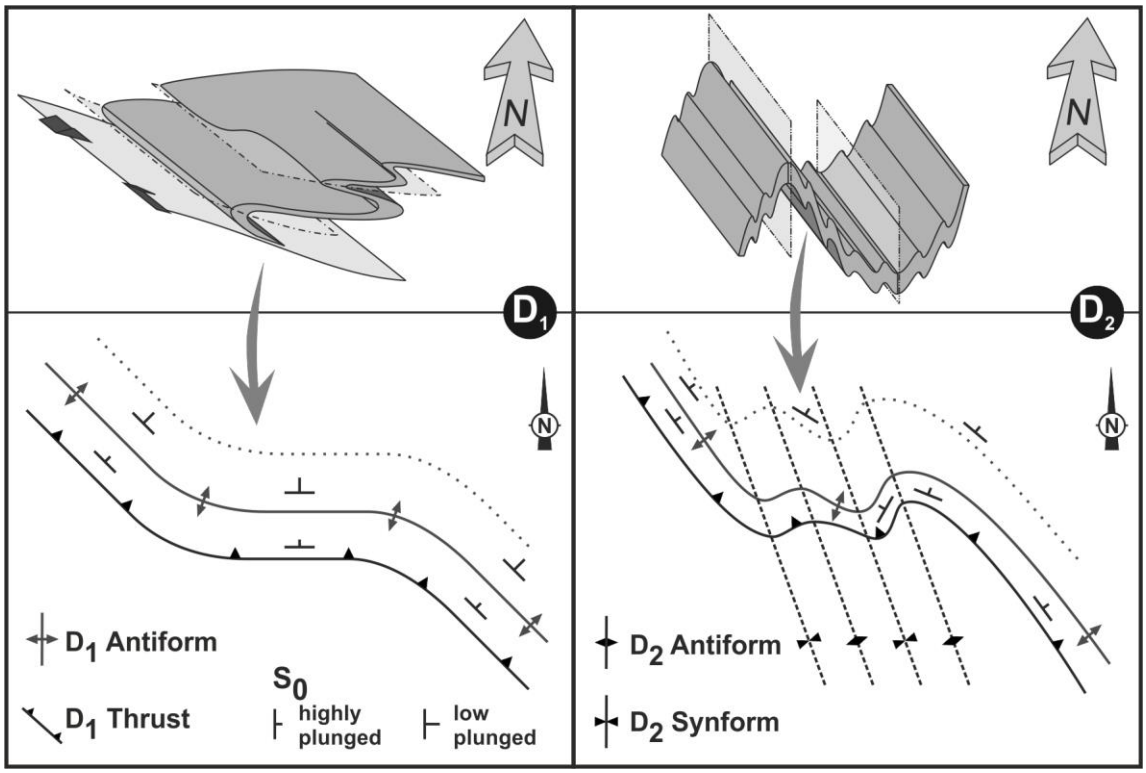

Figura 5 – Características geométricas e cinemáticas dos episódios de deformação e modelo interpretativo para o padrão de interferência para a Estrutura de Torre de Cabedal.

Referências

Apalategui, O., Eguiluz, L., Quesada, C. (1990). Ossa Morena Zone, Structure. In: R.D. Dallmeyer and E. Martínez-García (Eds.): Pre-Mesozoic Geology of Iberia, Springer-Verlag, 2, 80-219.

Araújo, A., Lopes, L., Pereira, M. F., Gonçalves, F., Silva, J. B., Ribeiro, A. (1994). Novos elementos sobre a Carreamento da Juromenha (Elvas). *Anais da Universidade de Évora*, 105-109.

Araújo, A., Piçarra de Almeida, J., Borrego, J., Pedro, J., Oliveira, J. T. (2013). As regiões central e sul da Zona de Ossa-Morena. In: R. Dias, A. Araújo, P. Terrinha, J.C. Kullberg (Eds.), Geologia de Portugal, vol. 1, Escolar Editora, 509-549.

Carvalho, D., Oliveira, J. T., Pereira, E., Ramalho, M., Antunes, M. T., Monteiro, J. H. (1992). Carta Geológica de Portugal na escala 1:500.000 (Folha Sul). Serv. Geol. Portugal, Lisboa.

Gonçalves, F., Assunção, C.T. (1970). Notícia explicativa da folha 37-A (Elvas) da Carta Geológica de Portugal à escala 1:50 000, Serv. Geol. Portugal, Lisboa.

Gozalo, R., Liñán, E., Palacios, T., Gámezvintaned, J.A. & Mayoral, E. (2003). The Cambrian of the Iberian Peninsula: an overview. *Geologica Acta* 1, 103–112. DOI:10.1344/105.000001596.

Lopes, L. (2003). Contribuição para o conhecimento Tectono – Estratigráfico do Nordeste Alentejano, transversal Terena – Elvas. Implicações económicas no aproveitamento de rochas ornamentais existentes na região (Mármores e Granitos). Tese de Doutoramento (não publicada), Universidade de Évora, 568 p.

Mata, J., Munhá, J. (1990). Magmatogénese de metavulcanitos câmbricos do nordeste alentejano: os estádios iniciais de "rifting" continental. *Comun. Serv. Geol. Portugal,* 76, 61-89.

Oliveira, J. T., Oliveira, V., Piçarra, J.M. (1991). Traços gerais da evolução tectono-estratigráfica da Zona de Ossa morena, em Portugal: síntese critica do estado actual dos conhecimentos. *Comun. Serv. Geol. Portugal,* 77, 3-26.

Pereira, M.F., Silva, J.B. (2006). Nordeste Alentejano, In: R. Dias, A. Araújo, P. Terrinha, J.C. Kullberg (Eds.). Geologia de Portugal no Contexto da Ibéria. Uni. Évora, Évora, 145-150.

Ramsay, J. G., Huber, M. I. (1987). The Techniques of Modern Structural Geology (vol.2): Folds and Fractures. London, Academic Press, 278 p.

Sánchez-García, T., Bellido, F., Pereira, M.F., Chichorro, M., Quesada, C., Pin, C., Silva, J.B. (2010). Rift related volcanism predating the birth of the Rheic Ocean (Ossa-Morena Zone, SW Iberia). *Gondwana Research*, 17 (2–4), 392–407.

V.

Evolução Devónica da Zona de Ossa-Morena; uma proposta

O início dos processos que levam à edificação da Cadeia Varisca e consequentemente à génese da Pangeia são essenciais nos modelos para reconstituição paleogeográfica do Paleozóico. Esta problemática ganha ainda maior importância uma vez que o número de blocos continentais envolvidos, e consequentemente o número de oceanos Variscos, não é totalmente claro, dando origem a um conjunto de modelos díspares. Contudo, a Zona de Ossa-Morena apresenta evidências de que o início dos processos relacionados com o início da subducção Varisca do SW da Ibéria se encontrava activo pelo menos desde o Emsiano. A análise dos dados de cariz estratigráfico, metamórfico, estrutural e magmático mostram que este processo se inicia muito provavelmente durante o Devónico inferior (Pragiano-Emsiano), não sendo até de excluir que se possa ter iniciado um pouco mais cedo, na transição Silúrico-Devónico.

A análise das sucessões estratigráficas Devónicas da Zona de Ossa-Morena mostra um hiato de sedimentação durante o Devónico médio, com excepção para a região de Odivelas, onde surge uma sucessão Carbonatada de idade Emsiana-Givetiana, localizada no bordo sul desta zona paleogeográfica. Este episódio de sedimentação carbonatada associa-se à presença de vulcanismo activo, evidente na presença de tufitos intercalados na sucessão. Este hiato deverá representar o início do levantamento generalizado da Zona de Ossa-Morena, que se deverá ter iniciado previamente. De facto, as sucessões do Devónico inferior mostram evidências de deformação sin-sedimentar, em especial a sucessão da Bacia de Terena interpretada como um fosso sin-tectónico, onde é possível evidenciar uma sucessão que inclui o *flysch* de Terena a Sul, passando lateralmente a uma sequência siliciclástica de cimento carbonatado, e os calcários Eifelianos-Emsianos da região de Odivelas.

A presença de uma sedimentação Devónica condicionada pela tectónica está de acordo com a presença de um evento de deformação anterior ao Carbónico. Na verdade, as bacias de idade Carbónica assentam em discordância sobre um substrato previamente estruturado, sendo que esta fase de deformação é considerada Devónica, possivelmente associada ao processo de subducção activa no SW da Zona de Ossa-Morena. Os dados geocronológicos existentes expõem a presença de um episódio de metamorfismo de alta pressão de idade Devónica supeior, sendo

que o conjunto de dados é totalmente concordante com a presença de um processo de subducção activo durante grande parte do Devónico.

Este capítulo surge na sequência dos trabalhos realizados ao longo dos anos, desde 2009 até à actualidade, nas sucessões Devónicas do bordo sul da Zona de Ossa-Morena, mais propriamente na região de Odivelas, onde surgem evidências de sedimentação contemporânea dos episódios vulcânicos e de deformação precoces. Este capítulo incluirá assim dois subcapítulos que incidirão sobre as seguintes temáticas:

- O trabalho realizado com o colega Gil Machado a convite dos editores do Livro da Geologia da Ibéria que irá ser editado pela *Springer*, Doutores José Tomás Oliveira e Cecílio Quesada, sobre a sedimentação Devónica do SW Ibérico e as suas implicações geodinâmicas. Este capítulo, já aceite para publicação, inclui também uma pequena secção sobre as implicações geodinâmicas destes carbonatos para a evolução da Ossa-Morena, o qual será exposto e refinado no subcapítulo seguinte (capítulo V.2).
- No segundo subcapítulo inclui-se um trabalho de revisão exaustiva das características gerais da estratigrafia, metamorfismo, magmatismo e estruturação Devónica da Zona de Ossa-Morena. O capítulo em causa foi construído com intuito de submissão a uma revista da especialidade. Este assunto é perfeitamente actual, uma vez que os trabalhos recentemente publicados pelos mais diversos autores sobre a Zona de Ossa-Morena, geralmente enfatizam a evolução Carbónica, menosprezando geralmente a evolução geodinâmica desta zona paleogeográfica durante o Devónico. Contudo, os dados existentes claramente indicam um processo de convergência com uma evolução prolongada no tempo, que se inicia durante o Devónico inferior e se prolonga até ao Fameniano terminal, altura em que se terão iniciado os processos de colisão continental.

Abaixo mencionam-se as referências específicas dos subcapítulos apresentados seguidamente:

- *Capítulo V.1*

MOREIRA, N., MACHADO, G. (in press). Devonian sedimentation in Western Ossa-Morena Zone and its geodynamic significance. In Quesada. C., Oliveira, J.T. (Eds.), The Geology of Iberia: a geodynamic approach. Springer (Berlin), Regional Geology Review series.

- *Capítulo V.2*

MOREIRA, N. et al (em preparação). From the Devonian evolution of Ossa-Morena Zone (SW Iberian Variscides) to the SW Iberian Variscan Ocean subduction in the Early Devonian.

V.1

Devonian sedimentation in Western Ossa-Morena Zone and its geodynamic significance

Index

V.1.1. Introduction

Devonian carbonate sediments are poorly developed in Ossa-Morena Zone (OMZ). In the south-west branch of this zone, several Devonian limestone occurrences are known and its description, regional framework and significance are the subject of this subsection.

V.1.1.1. Regional overview of Devonian sedimentary rocks in OMZ and neighboring regions

From the Ordovician to the Early Devonian the sedimentation in the OMZ was generally occurring in a passive margin setting (Quesada 1990; Robardet and Gutiérrez-Marco 1990; 2004). This is recorded in metasedimentary rocks cropping out in areas from Portalegre to Cordoba and more to the south in the Barrancos-Estremoz area (Robardet and Gutiérrez-Marco 1990; 2004; Oliveira *et al*. 1991; Piçarra 2000), Terena syncline (Piçarra 2000) and Valle, Venta de Ciervo and Cerron del Hornillo synclines in Spain (Robardet and Gutiérrez-Marco 1990; 2004). Most of the

paleozoic rocks are siliciclastics, composed of proximal deposits to deep fan turbidites (Oliveira *et al*. 1991; Piçarra 2000; Borrego *et al*. 2005). Lower Devonian reefal and other carbonate sedimentation in the OMZ is rare, but reported by May (1999) and Rodríguez *et al*. (2007) in Spain and Piçarra (2000) and Piçarra and Sarmiento (2006) in Portugal. Middle Devonian (meta)sedimentary rocks are very rare in the OMZ. This has been explained by a generalized uplift of this area during the Middle Devonian, creating a regional scale hiatus, as a consequence of the first pulses of the Hercynian orogeny (Robardet and Gutiérrez-Marco 1990; 2004; Oliveira *et al*. 1991). In Western OMZ, several scattered occurrences of reefal and peri-reefal carbonates were described near Cabrela (Boogaard 1972; 1983; Ribeiro 1983; Pereira and Oliveira 2003a; 2006), and within the Beja Igneous Complex (BIC) around the Odivelas water reservoir (Conde and Andrade 1974; Machado *et al*. 2009; 2010; Fig.1). Other rare occurrences of limestones in the same domain are reported near the contact area with the South Portuguese Zone (SPZ) around the Caeirinha mine and Pena (Pereira *et al*. 2006; Oliveira *et al*. 2013), shown to be Middle Devonian in age (Machado and Hladil 2010).

Together with the reefal and peri-reefal sediments, these occurrences frequently have interbedded or spatially related black cherts (with radiolarite lenses), tuffites and marly limestones.

During the Late Devonian and Carboniferous, the sedimentation is controlled by the pulses and geometry of the oblique collision occurring between the SPZ and the OMZ in a synorogenic phase (Quesada *et al*. 1990).

V.1.1.2. Magmatism in Western boundary of OMZ

In the southwesternmost domains of the OMZ, a suite of magmatic rocks is present, generally included in the BIC (e.g. Andrade 1983; Oliveira *et al*. 1991; Jesus *et al*. 2007; 2016). This igneous Complex includes plutonic (*e.g.* Beja Layered Gabbroic Sequence) and volcanic rocks (*e.g.* Toca da Moura and Cabrela volcano-sedimentary Complexes) related with different stages of a convergent process between OMZ and the South Portuguese Zone (*e.g.* Jesus *et al*. 2007; Ribeiro *et al*. 2010; Fig. 1). This suite presents a Devonian-Carboniferous range of ages, distinct magmatic natures and consequently distinctive geodynamic significances.

The description of the magmatism is not the objective of this work, thus only two distinct volcanic units will be briefly described because they present key features of the western OMZ carbonate sedimentation general framework:

- Rebolado basalts (Peroguarda Unit; e.g. Andrade *et al*. 1976; Santos *et al*. 1990);

- Toca da Moura and Cabrela Volcano-Sedimentary Complexes (e.g. Oliveira *et al*. 2013).

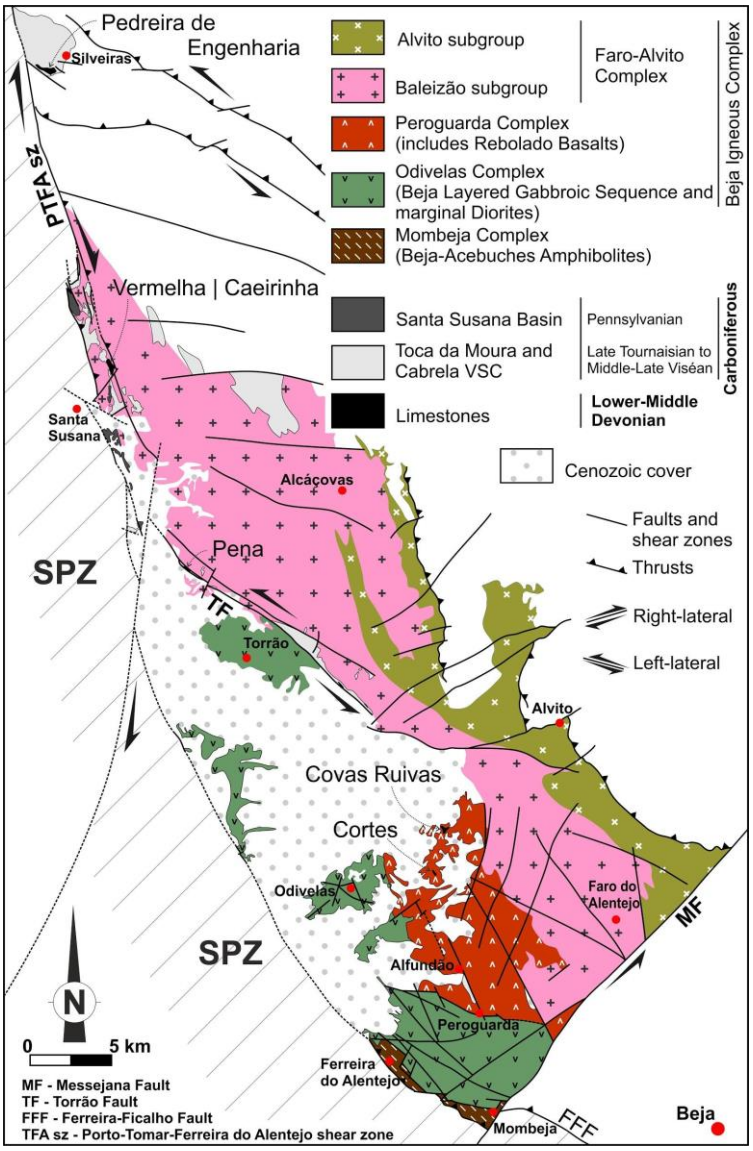

Figure 1 – Simplified geological sketch of western OMZ emphasizing magmatic and Late Paleozoic sedimentary rocks (adapted from Geological map of Portugal at 1:500.000 scale (1992); Andrade *et al*. 1976; Santos *et al*. 1990; Oliveira *et al*. 2013; Machado *et al*. 2013; Jesus *et al*. 2016).

Andrade *et al*. (1976) divide the magmatic rocks in the Odivelas-Alvito cross section in three distinct Complexes: Odivelas, Peroguarda and Faro-Alvito. The Odivelas and Faro-Alvito Complexes are mainly composed of plutonic rocks, with gabbro-diorite or granitic composition and a Carboniferous age (Andrade *et al*. 1976; Pin *et al*. 2008; Jesus *et al*. 2007; 2016). In turn, the Peroguarda Complex is mainly composed of mafic to intermediate volcanic rocks. This Complex is

subdivided in three units, among which the Rebolado Basalts (OD-6 in Santos *et al*. 1990 nomenclature). This unit is spatial and stratigraphically associated with the (Lower-)Middle Devonian limestones in Covas Ruivas and Cortes locations (Conde and Andrade 1974; Andrade *et al*. 1976; Machado *et al*. 2009; 2010; Moreira *et al*. 2010; Fig. 1 and 2), presenting a mafic to intermediate nature with abundant effusive lithotypes and tephra rocks (Santos *et al*. 1990; Silva *et al*. 2011). These basalts exhibit low grade hydrothermal metamorphism (Andrade *et al*. 1976; Santos *et al*. 1990; Silva *et al*. 2011), which does not obliterate the original volcanic textures.

Santos *et al*. (1990) refers a spatial association between Peroguarda and Odivelas Complex, showing plutonic facies in SW border (Odivelas Complex) which laterally pass to the volcanic ones in NE branch (Peroguarda Complex). Recent studies (Jesus *et al*. 2016) also show a NW-SE to WNW-ESE magmatic layering in the Odivelas Complex (designated as Layered Gabbroic Sequence by the authors), which is congruent with Santos *et al*. (1990) data. However, the Odivelas Complex is Carboniferous in age (Jesus *et al*. 2007; 2016; Pin *et al*. 2008). Geochemical data suggests that the mafic-intermediate sub-alkaline volcanic rocks contained in the Rebolado Basalts unit present significant similarities with the typical orogenic volcanic arc magmatism, exhibiting a low-K tholeiitic to calc-alkaline signature (Santos *et al*. 1990; Silva *et al*. 2011). However, Santos *et al*. (1990) remark a slight difference between two sectors: the Odivelas-Penique, in the North, where the calc-alkaline signature is more pronounced, while the Alfundão-Peroguarda sector presents a predominant tholeiitic nature. Recently, Santos *et al*. (2013) supported this distinction based in isotopic data (Sm-Nd and Rb-Sr isotope pairs). The data provide evidences of common mantle (or very similar) sources for the mafic magmas in both sectors, although the Odivelas-Penique group shows some evidences of crustal assimilation.

The Toca da Moura and Cabrela Volcano-Sedimentary Complexes are located in the southwestern border of the OMZ (Fig. 1). These Complexes are composed of a sequence of slightly deformed pelites, siltstones and greywackes, interbedded with felsic, intermediate and basic volcanic rocks, although felsic volcanics are predominant in the Cabrela Basin (e.g. Oliveira *et al*. 2013). At the base of the sequence, conglomeratic levels are identified (Ribeiro 1983; Oliveira *et al*. 1991). In both Complexes, Devonian limestones (Boogaard 1983; Machado and Hladil 2010) are also present. However, its geometric and stratigraphic relation with the siliciclastic sedimentation is poorly constrained (Oliveira *et al*. 1991; 2013). Pereira and Oliveira (2003a) suggest these limestones are, at least in part, olistoliths. The Toca da Moura and Cabrela Complexes are coeval, providing miospore associations which indicate a late Tournaisian to Middle-Late Viséan age

(Pereira and Oliveira 2003b; Pereira *et al*. 2006; Oliveira *et al*. 2013; Lopes *et al*. 2014). These complexes are deposited over a well-structured Silurian(?) basement defining an angular unconformity (Pereira and Oliveira 2003a; Pereira *et al*. 2006).

In the Toca da Moura Complex, Santos *et al*. (1987) characterize basalts, dolerites, andesites and rhyodacite rocks. All these rocks present a low grade metamorphism related to late Variscan deformation episodes. The same authors argue the orogenic calc-alkaline geochemical signature of these volcanic series, explaining the diversity of lithotypes with fractional crystallization processes. The Cabrela felsic volcanics (rhyodacites; Chichorro 2006) present geochemical similarities with the previously described Toca da Moura volcanics and some felsic and intermediate dykes intruded in the Évora Massif (Chichorro 2006), also showing a calc-alkaline signature. According to Chichorro (2006), this volcanism can represent the effusive member of the Évora Massif magmatism.

V.1.2. Lower-Middle Devonian rocks in Western OMZ

Despite the relevance of the initial paleontological work carried out by Boogaard (1972; 1983) and Conde and Andrade (1974) who studied the limestone occurrences in western OMZ, there was still a big gap on the knowledge of these units, notably on the range of the sedimentation ages, integration with other occurrences in neighboring regions and especially their geodynamic significance.

V.1.2.1. Geographic distribution

The Odivelas Limestone and correlatable units are presently found scattered in from the Odivelas reservoir area (Ferreira do Alentejo) in the South to the Cabrela village in the North (Vendas Novas and Montemor-o-Novo). Most of the known occurrences are aligned NNW-SSE close to the OMZ-SPZ boundary (Fig. 1). Other, spatially restricted occurrences of carbonate rocks, cherts, tuffites and marls are known further to the East (to Vidigueira area), but these may represent older Cambrian(?) rocks.

Each of the occurrences is composed of loose boulders, small quarries and natural outcrops spanning in areas usually less than $1km^2$. They are found interbedded or spatially associated with the Rebolado basalts (see below) or Toca da Moura-Cabrela Complex rocks which are volumetrically much more important (Fig. 2).

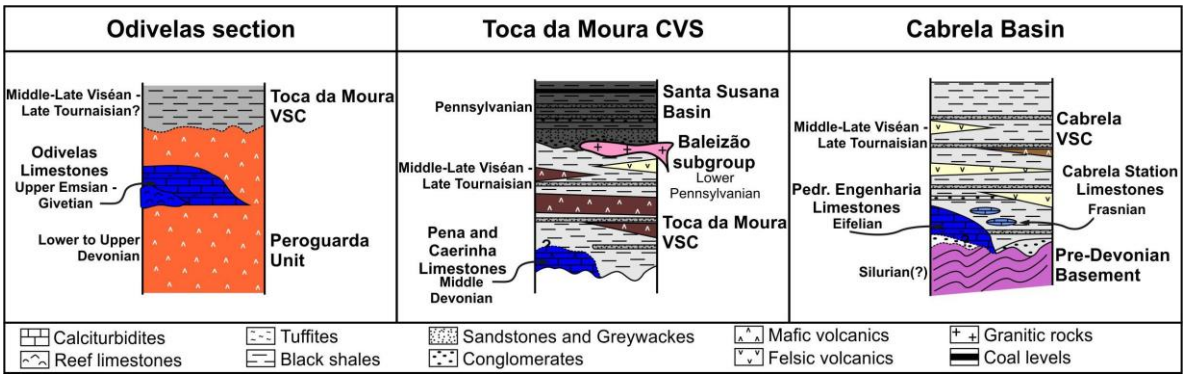

Figure 2 – Schematic stratigraphic sections on the Odivelas, Toca da Moura and Cabrela areas (based on data from Carvalhosa 1977; Ribeiro 1983; Oliveira *et al*. 1991; 2013; Chichorro 2006; Pereira *et al*. 2006; Machado *et al*. 2009; 2010; Machado and Hladil 2010; Moreira *et al*. 2010).

V.1.2.2. Brief description of facies and biostratigraphy

The vast majority of the known limestone occurrences are composed of crinoidal wackestones (up to 90% crinoidal fragments) with subordinate proportions of other bioclasts such as forams, tentaculites, ostracods, bryozoans, corals and stromatoporoids (Fig. 3B, G, I). Associated with this lithofacies fine-grained calcimudstones with abundant peloids (up to 75 %) occur. These have occasional mixing of coarser grains such as crinoidal fragments, tentaculites and radiolarians. These two lithofacies are interbedded (dm to m-thick beds) and generally interpreted as calciturbidites, in more distal (calcimudstones) or more proximal (wackestones) settings. While this is clear in continuous outcrops such as Covas Ruivas (Machado *et al*. 2010) the interpretation is only tentative in localities with small discontinuous outcrops, as Pena and Caeirinha. The origin of the carbonate material is most likely a reef system updip. This is corroborated by the highly diversified reef fauna found in the few, very coarse carbonate breccias. The only locality with bioherm/biostromal facies (Fig. 3H) is Cortes, where very coarse grained packstone-grainstones (locally rudstones and boundstones) with abundant crinoids, rugose and tabulate corals, brachiopods and stromatoporoids occur in the central part of the outcrop area and indicative of latest Eifelian to earliest Givetian ages (Machado *et al*. 2009). Unpublished conodont work by the authors confirms the age determination. This central area is surrounded by calciturbidite facies (Machado *et al*. 2009). Cortes and Covas Ruivas occurrences constitute the Odivelas Limestone s.s.

In some of the localities (Pena, Caerinha, Cabrela) these lithofacies are overprinted by intense dolomitization and/or silicification (Machado and Hladil 2010; Moreira *et al*., 2016). Nevertheless,

crinoid columnal sections and remnants of the original facies are partially preserved and allow petrographic and biostratigraphical work to be conducted (Fig. 3I).

Other notable lithofacies present are tuffites interbedded with the calciturbidites. These form cm-thick beds, frequently cherty or with millimetric carbonate lenses, which in some levels have radiolarians, tentaculites and ostracod shells (Fig. 3B, C, D, E). These are always volumetrically less relevant than the carbonates and are interpreted as hemipelagic sediments. They also occur in the volcaniclastic sequences of the Rebolado basalts, that under and overlay the limestones (Fig. 3C). The tuffites have been described in detail in the Odivelas reservoir area (Machado *et al*. 2010). In the Cabrela area, both calciturbidite and (possible) tuffites seem macroscopically identical, but have not been studied petrographically (Fig. 3J).

As briefly described above, nearly all the known occurrences of the Odivelas Limestone and correlatable units are Middle Devonian in age. A notable exception is the very base of the sequence in Covas Ruivas which includes the youngest Emsian (Early Devonian) conodont biozone (*patulus*) and ranges to the *australis* biozone. The presence of crinoid ossicles of *Gasterocoma* sp. and *Cupressocrinities* sp. (and dominance over other crinoids) is quite distinctive of many of these localities (except in Covas Ruivas), indicating a late Eifelian to early Givetian age. The presence of large limestone boulders, Frasnian in age (Boogaard 1983), within the Mississippian Toca da Moura/Cabrela Complex and often spatially associated with Middle Devonian limestone outcrops (Eifelian; Boogaard 1972) is puzzling. Frasnian carbonate rocks are not known in the area, thus the source area of the boulders (likely olistoliths) is currently unknown. Possibly the carbonate sedimentation continued in some areas from the Early-Middle Devonian into the Frasnian. A reanalysis of the limestone boulders in the basal conglomerates and other scattered limestone occurrences in the Cabrela area is underway and will shed light on this subject.

Recent work performed by Moreira *et al*. (2016) also shows clear similarities between the $^{87}Sr/^{86}Sr$ ratio signature presented in Pena, Cortes and Covas Ruivas Limestones (ratio value lower than 0,70800) with the global values defined for Early-Middle Devonian times (Veizer *et al*. 1999; McArthur *et al*. 2012). However, the Pedreira da Engenharia dolomitized limestones, with similar age and genesis, presents higher $^{87}Sr/^{86}Sr$ values (0,70972), which, according to Moreira *et al*. (2016), could be the result of secondary dolomitization processes.

Thus the sedimentation of the Odivelas Limestone and correlatable units occurred in an interval between the latest Emsian to the Early Givetian, possibly extending into the Frasnian.

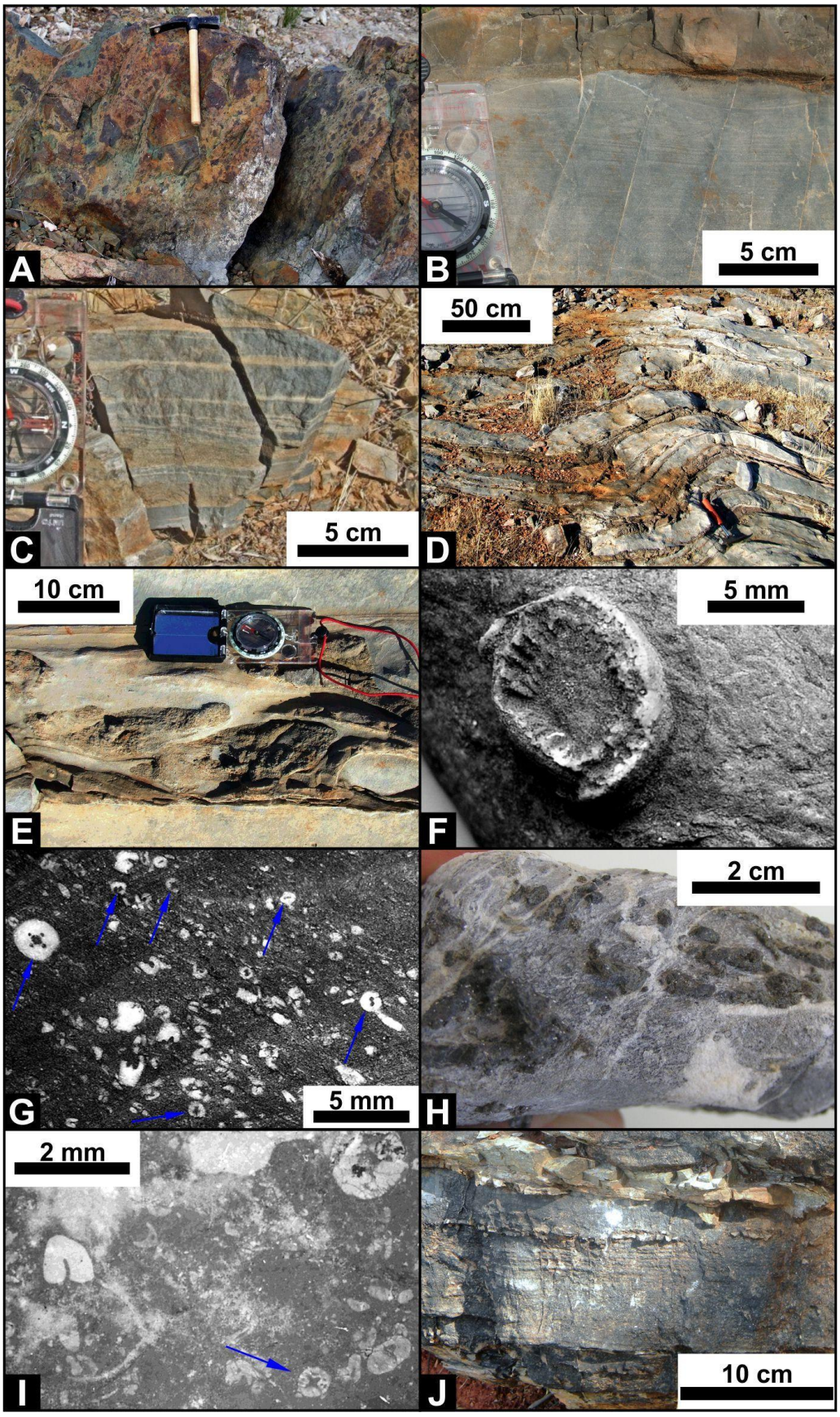
A
B
5 cm
C
5 cm
50 cm
D
10 cm
E
5 mm
F
G
5 mm
2 cm
H
2 mm
I
J
10 cm

Figure 3 – Outcrop and polished sections photographs of the Odivelas Limestone and correlatable units:

A-E Covas Ruivas locality: A - Pyroclastic rocks below the first calciturbidite beds; B - Detail of calciturbidite bed (note fining upward character and cross bedding on top) and sharp contact with the tuffite bed above (adapted from Machado *et al*. 2010); C - Thinly bedded tuffite near the base of the calciturbidite sequence (adapted from Machado *et al*. 2010); D - Alternation of calciturbidites (thicker lighter beds) and tuffites (thinner darker beds) gently folded; E - Convolute bedding showing a mix of tuffite material (darker) in a calciturbidite bed as evidence of slope syn-sedimentary deformation;

F-H Cortes locality: F - *Pseudamplexus* sp. coral weathered out in loose limestone boulder (adapted from Machado *et al*. 2009); G - Crinoidal limestone with small cupressocrinitid and gasterocomids columnals (arrows). Polished slab (adapted from Machado *et al*. 2009); H - Packstone with amphiporids (high relief) and crinoidal, brachiopod and ostracod fragments;

I - Caeirinha locality. Crinoidal limestone with small cupressocrinitid columnals (arrow). Thin section (adapted from Machado and Hladil 2010);

J - Cabrela locality. Pedreira de Engenharia Fm. Calciturbidite bed with fining upward trend and sharp contact with the (?)hemipelagic sediment above. Note similarity with B.

V.1.2.3. Post deposition evolution

The current distribution of Devonian limestones reflects their original disposition, but also post deposition processes, tectonic and possibly sedimentary. Their current small areal extent is likely a consequence of their original limited extent, but also the erosional processes of Devonian rocks (along with older and younger Paleozoic rocks) in the Alentejo peneplain.

While in Odivelas area the limestone rocks are clearly *in situ* (stratigraphically bounded by Rebolado volcanics; Fig. 3A), the other occurrences along the Western border of the OMZ may be tectonically displaced, as in the Cabrela and Toca da Moura Complexes. The limestones interpreted as olistoliths in these Complexes (which are at least partially Frasnian in age) and the limestone boulders in the basal conglomerate of the Toca da Moura complex show that during the Mississippian the Odivelas Limestone was being eroded.

Although the Devonian limestone outcrops are few and small, in Covas Ruivas two distinct episodes of folding can be discriminated (Moreira *et al*. 2010), which seem to represent the most recent (Carboniferous?) deformation events. However, the post-depositional tectonics in western OMZ are clearly dominated by brittle to brittle-ductile structures. Three main families can be highlighted: a N-S to NNW-SSE right-lateral faults, which also mark the limit between the OMZ and SPZ near Cabrela and in the Santa Susana Carboniferous Basin, the WNW-ESE to W-E ones, which include the Torrão and Ferreira-Ficalho Faults, and finally a NE-SW sinistral ones, genetically associated to Messejana Fault (Fig. 1). These faults were active during the Variscan Cycle (e.g. Moreira *et al*. 2010; 2014; Machado *et al*. 2012), and possibly some of them could control the Carboniferous sedimentation. However, some of these families have Meso-Cenozoic reactivation (e.g. Pimentel and Azevedo 1994; Cabral 2012), which further complicates the structural pattern and partially obliterates its kinematic record during post-Devonian evolution of Western OMZ.

V.1.3. Global events and intercontinental correlation

The Basal Choteč Event (BCE) is a global event which corresponds to a transgressive pulse just above the Emsian-Eifelian boundary. In carbonate slope conditions this is materialized by suboxic organic-rich sediments and lower carbonate sedimentation rates. These sediments are frequently overlain by coarse bioclastic calciturbidites or debris-flow carbonate breccias (e.g. Berkyová *et al*. 2008; Chlupáč and Kukal 1986). This sequence of lithologies is precisely what is observed in the Covas Ruivas section from upper *partitus* to *costatus* conodont biozones, consistent with the BCE ages of other localities around the World. The magnetic susceptibility record is also consistent and

correlatable with other sections such as Lone Mountain, Nevada USA; Issemour, Morocco; Red Quarry, Barrandian Czech Republic and Khoda-Kurgan Gorge, Uzbekistan (see Machado *et al*. 2010 and references therein for details).

The end-Eifelian Kačák-otomari Event is another anoxic event which is potentially recorded in a small (2m thick) calciturbidite section in the Cortes locality. The organic-rich limestones with chert nodules, low magnetic susceptibility magnitudes and pattern, correlatable with other sections in the Czech Republic (Hladil *et al*. 2006) are tentative, but not definitive indications of the record of this event (see Machado *et al*. 2009 for details).

Overall, the age, local paleogeographical setting associated with volcanic buildings, the reef fauna and even the timing and nature of the magmatism are strikingly similar to other areas in Variscan Europe, notably the Rhenish area (Braun *et al*. 1994; Konigshof *et al*. 2010) in Germany, Horní Benešov in Moravia; (Hladil *et al*. 1994; Galle *et al*. 1995) and neighboring regions (Krebs 1974). These occurrences are part of the peri-Laurussian realm of the inner side of the Variscan tectonic facies belt. In both Cortes (Late Eifelian-Early Givetian) and in Covas Ruivas (Early Eifelian) the reef fauna is particularly diversified, containing elements which are typical of the Rhenish area, but also Peri-Gondwana elements (Machado *et al*. 2009; 2010).

V.1.4. Geodynamic evolution; Implications to SW Iberia Variscisdes

V.1.4.1. Local and regional paleogeography

Considering the known lithofacies, both carbonate and volcaniclastic, the fossil content and their stratigraphic and spatial relationships, the local paleogeography can be modelled with significant detail. Reef systems developed around the top of volcanic edifices (Fig. 4) where their top would be close enough to the sea surface to allow colonization and development of reef building taxa. These were probably isolated reefs, not larger than a few km across, possibly forming atolls and perhaps small detached carbonate platforms where the seabed morphology allowed it. On the flanks of the volcanic edifices, coeval peri-reefal sedimentation occurred, essentially as calciturbidites, extending at least to the base of slope.

Volcanic and volcaniclastic rocks pre-date and post-date carbonate sedimentation and constitute the majority of the rocks filling the accommodation space in the basin, together with younger rocks (Toca da Moura/Cabrela Complex?). In the Cabrela area, the absence of direct evidence for coeval volcanic rocks suggests these reefs and consequent peri-reefal sedimentation could also develop in basement highs (Fig. 4).

According to Andersen *et al*. (2003), the formation of calciturbidites is influenced by several factors, among which stands out sea level fluctuations and local slope and seafloor topography, although some calciturbidite sequences are directly related to tectonic activity. In Devonian western OMZ, the tectonic environment and the seafloor topography seem to be coupled. The subduction process, which probably begins during Early Devonian (see below), generates a volcanic arc and seafloor elevations (basement highs) during the deformation process (Fig. 5A). Over these tectonic reliefs, under the previous mentioned favorable environmental conditions, reef systems could develop that would be eroded/dismantled along its edges, generating calciturbidite sequences on the slopes (Fig. 4), including occasional debris-flow breccias and syn-sedimentary deformation (Fig. 3E).

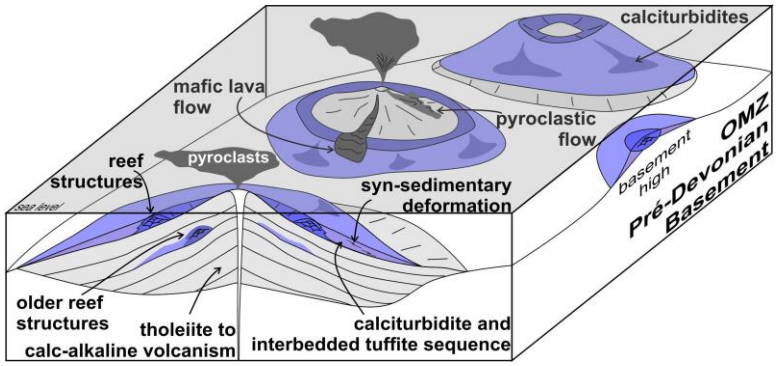

Figure 4 – Latest Early Devonian to Middle Devonian schematic model of the local/regional paleogeography of the Odivelas-Cabrela area in Western OMZ.

V.1.4.2. Subduction timing; a proposal to Devonian evolution of SW Iberia

The beginning of oblique subduction process of the Rheic Ocean under the OMZ is poorly constrained. Although it is considered that the process begins during the Devonian (e.g. Ribeiro 1983; Quesada, 1990; Oliveira *et al*. 1991; Moreira *et al*. 2014), some authors consider that it may even started at the time of the Silurian-Devonian boundary (e.g. Ribeiro *et al*. 2010). Stratigraphic (e.g. Oliveira *et al*. 1991; Machado *et al*. 2010; Araújo *et al*. 2013), magmatic (e.g. Costa *et al*. 1990; Santos *et al*. 1990; Moita *et al*. 2005a; Silva *et al*. 2011), metamorphic (e.g. Quesada and Dallmeyer 1994; Moita *et al*. 2005b; Pedro *et al*. 2013) and structural (e.g. Ribeiro 1983; Araújo *et al*. 2005; 2013) data clearly show the presence tectono-metamorphic events during Devonian times.

The sedimentary and biostratigraphic data are consistent with crustal uplift of the OMZ during Early Devonian (at least during the Emsian; circa 400 Ma) times, possibly related to the beginning of

the subduction process (Moreira *et al*. 2014). Indeed, the characteristic euxinic marine sedimentation of the Silurian times (Black Shale Series; e.g. Piçarra 2000; Araújo *et al*. 2013) is replaced by shallow carbonate sedimentation in central OMZ (Ferrarias and Barrancos) although here the age is poorly constrained (Late Silurian to Devonian), because the sedimentary record is fragmentary (e.g. Piçarra 2000; Piçarra and Sarmiento 2006; Araújo *et al*. 2013). This trend is possibly present in the in the Odivelas sector, but the sedimentary record is incomplete. The carbonate sedimentation in the SW branch of the OMZ seems to persist until the Frasnian, although only some remobilized limestones were found in the Cabrela Formation (Boogaard 1983; Pereira and Oliveira 2003a; 2003b; Pereira *et al*. 2006).

The Devonian magmatism, poorly represented in the OMZ, can be observed in the Peroguarda Unit. Although there are no geochronological data which supports its Devonian age, the presence of Lower-Middle Devonian limestones interbedded with the Rebolado Basalts (Oliveira *et al*. 1991; Moreira *et al*. 2010) constrains its age. The orogenic low-K tholeiitic to calc-alkaline geochemical signature of the Rebolado Basalts (e.g. Santos *et al*. 1990; 2013; Silva *et al*. 2011) seems to indicate that proximal volcanic arc magmatism is represented by this unit. With (Late) Devonian age and far from subduction (Central OMZ), a calc-alkaline to shoshonitic magmatism is developed in Veiros-Vale Maceira (Costa *et al*. 1990; Moita *et al*. 2005a). The geochemical and spatial arrangement of Devonian magmatism suggests that subduction related magmatic activity migrates to the north, assigning a north polarity to the Rheic subduction under the OMZ, extending up to 365 Ma - Famennian (e.g. Moita *et al*. 2005a; Araújo *et al*. 2013).

Recent geochronological studies (Braid *et al*. 2011; Pereira *et al*. 2012; Rodrigues *et al*. 2015; Pérez-Cáceres *et al*. 2016), based on detrital zircons content in OMZ and SPZ Carboniferous syn-orogenic sedimentary sequences, show large populations of Devonian inherited zircons, which may represent an indirect evidence of subduction-related magmatism during this period. The Mississippian Cabrela Basin siliciclastics provide two Devonian inherited zircons clusters, with Eifelian-Givetian and Famennian ages (Pereira *et al*. 2012). Similar clusters are also obtained in the SPZ Mississippian siliciclastic lithotypes of Mértola and Mira Formations (Pereira *et al*. 2012; Rodrigues *et al*. 2015), although in Mira Formation, only the latter cluster (Famennian) is present. These SPZ units possibly have a source area in SW OMZ (Jorge *et al*. 2013). In the Spanish sector of the SPZ, the Santa Iria Formation presents a Late Devonian cluster of inherited zircons (Braid *et al*. 2011; Pérez-Cáceres *et al*. 2016), while in Ribeira de Limas and Ronquillo Formations Early Devonian

(Emsian) inherited zircons are present, representing the youngest Devonian cluster of these units (Pérez-Cáceres *et al*. 2016).

The previous mentioned data are in agreement with ages attributed to Peroguarda Unit volcanism, which seems to represent a preserved section of volcanic arc magmatism in the SW branch of the OMZ, related with subduction processes, supporting the existence of a magmatic arc during Devonian times, eroded during the Mississippian, intruded by younger plutonic rocks composing the BIC and finally eroded by recent peneplanation.

Also the metamorphic ages obtained from HP-LT metamorphic rocks, in the SW border of the OMZ, are in agreement with a Devonian subduction process. Geochronological data indicate a Famennian age to the baric peak of this HP-LT metamorphism (371 ± 17 Ma; Sm/Nd isochronous whole rock-garnet; Moita *et al*. 2005b; Pedro *et al*. 2013), materializing the active subduction processes.

After the genesis and development of volcanic arc magmatism and the related carbonate sedimentation, the collision process between SPZ and the OMZ begins during the Mississippian (Tournaisian; e.g. Jesus *et al*. 2007; 2016; Ribeiro *et al*. 2010; Moreira *et al*. 2014; Fig. 5B). During this period, the magmatic activity became intense in the BIC (Pin *et al*., 2008; Jesus *et al*. 2007; 2016), but also in the Évora Massif (Chichorro, 2006; Pereira *et al*., 2015).

During the Mississippian (Fig. 5B) the accommodation space continues to be filled (probably controlled by active tectonism), dominated by turbidite sedimentation and volcaniclastics (Toca da Moura and Cabrela Complexes; e.g. Ribeiro 1983; Pereira *et al*. 2006). The previously deformed OMZ substrate is eroded, feeding these basins as indicated by the lenses of Frasnian limestones found in the western border of the Cabrela basin (Cabrela Station Limestones), which some authors interpret as olistholiths within Mississippian turbidites (Pereira and Oliveira 2003a; Pereira *et al*. 2006; Oliveira *et al*. 2013). In the Cabrela Complex, fragments of granites and slates are described in the basal conglomerate (Ribeiro 1983; Oliveira *et al*. 1991; Pereira *et al*. 2006), emphasizing the unconformity between the Cabrela Formation and the previous deformed sequence, consequently dating the first deformation episode as earlier than Late Devonian.

In turn, the Toca da Moura and Cabrela calc-alkaline Carboniferous volcanism may not represent the real volcanic arc magmatism, but the remains of the processes after the subduction stop, i.e. during the collision, as mentioned by Santos *et al*. (1987). This magmatism could be related with the BIC emplacement or the Évora Massif activity (Fig. 5B) as proposed by Chichorro (2006).

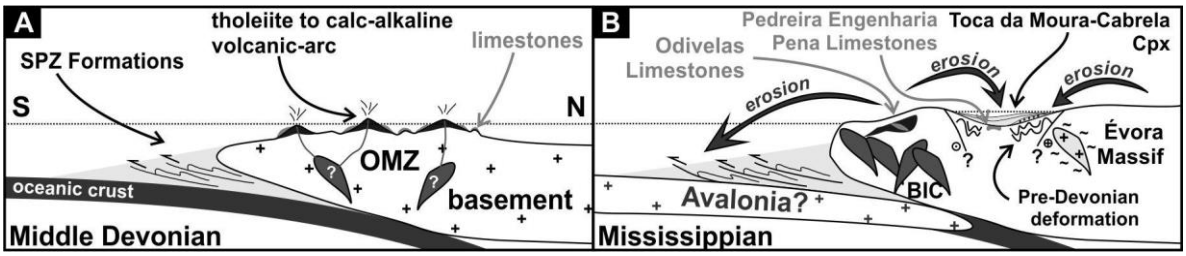

Figure 5 – Schematic model of Devonian-Mississippian evolution of the OMZ southwest branch. N and S are current coordinates:

A – Development of proximal volcanic arc with growth of reef structures, related to subduction during the Middle Devonian;

B – Beginning of continental collision process, with emplacement of large plutonic bodies (BIC). The Devonian volcanic arc and limestones are partially eroded, feeding the OMZ and SPZ syn-orogenic Mississippian basins.

References

Andrade, A.A.S. (1983). Contribution à l'analyse de la suture hercynienne de Beja (Portugal): perspectives métallogéniques. Laboratoire de Métallogénie I Nancy, Institut National Polytechnique de Lorraine. PhD thesis, 137 p.

Andrade, A., Pinto, A., Conde, L. (1976). Sur la géologie du Massif de beja: Observations sur la transversale d`Odivelas. Comun. Serv. Geol. Portugal, 60, 171-202.

Andresen, N., Reijmer, J.J.G., Droxler, A.W. (2003). Timing and distribution of calciturbidites around a deeply submerged carbonate platform in a seismically active setting (Pedro Bank, Northern Nicaragua Rise, Caribbean Sea). Int J Earth Sci (Geol Rundsch), 92, 573-592. DOI: 10.1007/s00531-003-0340-0

Araújo, A., Fonseca, P., Munhá, J., Moita, P., Pedro, J., Ribeiro, A. (2005). The Moura Phyllonitic complex: An accretionary complex related with obduction in the Southern Iberia Variscan Suture. Geodin Acta, 18(5), 375-388.

Araújo, A., Piçarra, J., Borrego, J., Pedro, J., Oliveira, J.T. (2013). As regiões central e sul da Zona de Ossa-Morena. In: Dias R, Araújo A, Terrinha P, Kullberg JC (Ed) Geologia de Portugal (Vol. I), Escolar Editora, Lisboa, 509-549.

Berkyová, S., Frýda, J., Koptíková, L. (2008). Environmental and biotic changes close to the Emsian/ Eifelian boundary in the Prague Basin, Czech Republic: paleontological, geochemical and sedimentological approach. In: Kim AI, Salimova FA, Meshchankina NA (Ed) International Conference Global Alignments of Lower Devonian Carbonate and Clastic Sequences, SDS/ IGCP Project 499 joint field meeting, 25.8.-3.9.2008, State Committee of the Republic of Uzbekistan on Geology and Resources & Kitab State Geological Reserve, Contributions, Taskhent-Novosibirsk, 18-19.

Boogard, M. (1972). Conodont faunas from Portugal and Southwestern Spain. Part 1: A Middle Devonian fauna from near Montemor-o-Novo. Scripta Geologica, 13, 1-11.

Boogard, M. (1983). Conodont faunas from Portugal and southwestern Spain. Part 7. A Frasnian conodont fauna near the Estação de Cabrela (Portugal). Scripta Geologica, 69, 1-17.

Borrego, J., Araújo, A., Fonseca, P.E. (2005). A geotraverse through the south and central sectors of the Ossa-Morena Zone in Portugal (Iberian Massif). In Carosi, R., Dias, R., Iacopini, D., Rosenbaum, G. (Eds.), The southern Variscan belt, J. Virtual Explorer, 19, paper 10. DOI: 10.3809/jvirtex.2005.00117

Braid, J.A., Murphy, J.B., Quesada, C., Mortensen, J. (2011). Tectonic escape of a crustal fragment during the closure of the Rheic Ocean: U–Pb detrital zircon data from the Late Palaeozoic Pulo do Lobo and South Portuguese zones, southern Iberia. J Geol Soc London, 168, 383-392. DOI: 10.1144/0016-76492010-104

Braun, R., Oetken, S., Königshof, P., Kornder, L., Wehrmann, A. (1994). Development and biofacies of reef-influenced carbonates (Lahn - syncline, Rheinisches Schieferge-birge). Courier Forschungsinstitut Senckenberg, 169, 351-386.

Cabral, J. (2012). Neotectonics of mainland Portugal: state of the art and future perspectives. J Iber Geol, 38(1), 71-84. DOI: 10.5209/rev_JIGE.2012.v38.n1.39206

Carvalhosa, A. (1977). Características geológicas do Maciço de Évora (Nota preliminar). Boletim da Sociedade Geológica de Portugal, Lisboa, 20, 283-312.

Chichorro, M. (2006). Estrutura do Sudoeste da Zona de Ossa-Morena: Área de Santiago de Escoural — Cabrela (Zona de Cisalhamento de Montemor-o-Novo, Maciço de Évora). Ph.D. thesis (unpublished), Évora University, 502 p.

Chlupáč, I., Kukal, Z. (1986). Reflection of possible global Devonian events in the Barrandian area, C.S.S.R.. In: Walliser OH (Ed) Global Bio-events, Lect Notes Earth Sci, Springer-Verlag, Berlin, 8, 169-179.

Conde, L.N., Andrade, A.A.S. (1974). Sur la faune meso et/ou néodévonienne des calcaires du Monte das Cortes, Odivelas (Massif de Beja). Memórias e Notícias, Univ. Coimbra, 78, 141-146.

Costa, D., Viana, A., Munhá, J. (1990). Petrologia e geoquímica dos maciços de Veiros e Vale Maceira. In: Abstrats of the VIII Semana de Geoquímica, Lisboa.

Galle, A., Hladil, J., Isaacson, P.E. (1995). Middle Devonian biogeography of closing South Laurussia to North Gondwana Variscides; examples from the Bohemian Massif, Czech Republic, with emphasis on Horni Benešov. Palaios, 10, 221-239. DOI: 10.2307/3515254

Hladil, J., Helešicová, K., Hrubanová, J., Müller, P., Ureš, M. (1994). Devonian island elevations under the scope - Central Europe, basement of the Carpathian Mountains in Moravia. Jahrbuch der Geologischen Bundesanstalt in Wien, 136(4), 741-750.

Hladil, J., Geršl, M., Strnad, L., Frána, J., Langrová, A., Spišiak, J. (2006). Stratigraphic variation of complex impurities in platform limestones and possible significance of atmospheric dust: a study with emphasis on gamma-ray spectrometry and magnetic susceptibility outcrop logging (Eifelian-Frasnian, Moravia, Czech Rep.). Int J Earth Sci, 95(4), 703-723. DOI: 10.1007/s00531-005-0052-8

Jesus, A.P., Munhá, J., Mateus, A., Tassinari, C., Nutman, A.P. (2007). The Beja layered gabbroic sequence (Ossa-Morena Zone, Southern Portugal): geochronology and geodynamic implications. Geodin Acta, 20, 139-157.

Jesus, A.P., Mateus, A., Munhá, J.M., Tassinari, C.G.C., Bento dos Santos, T.M., Benoit, M. (2016). Evidence for underplating in the genesis of the Variscan synorogenic Beja Layered Gabbroic Sequence (Portugal) and related mesocratic rocks. Tectonophysics, 683(30), 148-171. DOI: 10.1016/j.tecto.2016.06.001

Jorge, R.C.G.S., Fernandes, P., Rodrigues, B., Pereira, Z., Oliveira, J. (2013). Geochemistry and provenance of the Carboniferous Baixo Alentejo Flysch Group, South Portuguese Zone. Sediment Geol, 284, 133-148. DOI: 10.1016/j.sedgeo.2012.12.005.

Königshof, P., Nesbor, H.D., Flick, H. (2010). Volcanism and reef development in the Devonian: a case study from the Rheinisches Schiefergebirge (Lahn Syncline,Germany). Gondwana Res, 17(2–3), 264-280. DOI: 10.1016/j.gr.2009.09.006

Krebs, W, (1974). Devonian carbonate complexes of central Europe. In: Laporte LF (Ed), Reefs in time and space, Society Economic Paleontologists Mineralogists Special Publication, 18, 155-208.

Lopes, G., Pereira, Z., Fernandes, P., Wicander, R., Matos, J., Rosa, D., Oliveira, J.T. (2014). The significance of the reworked palynomorphs (Middle Cambrian to Tournaisian) in the Viséan Toca da Moura Complex (South Portugal). Implications for the geodynamic evolution of Ossa Morena Zone. Rev Palaeobot and Palyno, 200, 1-23. DOI: 10.1016/j.revpalbo.2013.07.003

Machado, G., Hladil, J. (2010). On the age and significance of the limestone localities included in the Toca da Moura volcano-sedimentary Complex: preliminary results. In: Santos, A., Mayoral, E., Melendez, G., Silva, C.M.D., Cachão, M. (Ed), III Congresso Iberico de Paleontologia / XXVI Jornadas de la Sociedad Espanola de Paleontologia, Lisbon, Portugal. Publicaciones del Seminario de Paleontologia de Zaragoza (PSPZ), 9, 153-156.

Machado, G., Hladil, J., Koptikova, L., Fonseca, P., Rocha, F.T., Galle, A. (2009). The Odivelas Limestone: Evidence for a Middle Devonian reef system in western Ossa-Morena Zone. Geol Carpath, 60(2), 121-137.

Machado, G., Hladil, J., Koptikova, L., Slavik, L., Moreira, N., Fonseca, M., Fonseca, P. (2010). An Emsian-Eifelian Carbonate-Volcaniclastic Sequence and the possible Record of the basal choteč event in western Ossa-Morena Zone, Portugal (Odivelas Limestone). Geol Belg, 13, 431-446.

Machado, G., Dias da Silva, I., Almeida, P. (2012). Palynology, Stratigraphy and Geometry of the Pennsylvanian continental Santa Susana Basin (SW Portugal). J. Iber. Geol., 38(2), 429–448. DOI: 10.5209/rev_JIGE.2012.v38.n2.40467

May, A. (1999). Stromatoporen aus dem Ober-Emsium (Unter-Devon) der Sierra Morena (Süd-Spanien). Münstersche Forsch. Geol. Paläont., 86, 97-105.

McArthur, J.M., Howarth, R.J., Shields, G.A. (2012). Strontium Isotope Stratigraphy. In: Gradstein FM, Ogg JG, Schmotz MD, Ogg GM (Ed), A Geologic Time Scale 2012 (Chapter 7), Elsevier, 127-144.

Moita, P., Munhá, J., Fonseca, P.E., Tassinari, C., Araújo, A., Palácios, T. (2005a). Dating orogenic events in Ossa-Morena Zone. In: Abstract of the XIV Semana de Gequimica/VIII Congresso de geoquimica dos Paises de Lingua Portuguesa, Aveiro, 2, 459-461.

Moita, P., Munhá, J., Fonseca, P., Pedro, J., Tassinari, C., Araújo, A., Palacios, T. (2005b). Phase equilibria and geochronology of ossa morena eclogites. In: Abstracts of the XIV Semana de Gequimica/VIII Congresso de geoquimica dos Paises de Lingua Portuguesa, Aveiro, 2, 471-474.

Moreira, N., Machado, G., Fonseca, P.E., Silva, J.C., Jorge, R.C.G.S., Mata, J. (2010). The Odivelas Palaeozoic volcano-sedimentary sequence: Implications for the geology of the Ossa-Morena Southwestern border. Comunicações Geológicas, 97, 129-146.

Moreira, N., Araújo, A., Pedro, J., Dias, R. (2014). Evolução geodinâmica da Zona de Ossa-Morena no contexto do SW Ibérico durante o Ciclo Varisco. Comunicações Geológicas, 101 (I), 275–278.

Moreira, N., Pedro, J., Santos, J.F., Araújo, A., Romão, J., Dias, R., Ribeiro, A., Ribeiro, S., Mirão, J. (2016). 87Sr/86Sr ratios discrimination applied to the main Paleozoic carbonate sedimentation in Ossa-Morena Zone. *In*: IX Congreso Geológico de España (special volume). Geo-Temas, 16(1), 161-164. ISSN 1576-5172.

Oliveira, J., Oliveira, V., Piçarra, J. (1991). Traços gerais da evolução tectono-estratigráfica da Zona de Ossa-Morena, em Portugal. Comun. Serv. Geol. Portugal, 77, 3-26.

Oliveira, J.T., Relvas, J., Pereira, Z., Munhá, J., Matos, J., Barriga, F., Rosa, C. (2013). O Complexo Vulcano-Sedimentar de Toca da Moura-Cabrela (Zona de Ossa Morena): evolução tectono-estratigráfica e mineralizações associadas. In: Dias, R., Araújo, A., Terrinha, P., Kullberg, J.C. (Ed.), Geologia de Portugal (Vol. I), Escolar Editora, Lisboa, 621-645.

Pedro, J., Araújo, A., Fonseca, P., Munhá, J., Ribeiro, A., Mateus, A. (2013). Cinturas Ofiolíticas e Metamorfismo de Alta Pressão no Bordo SW da Zona de Ossa-Morena. In: Dias, R., Araújo, A., Terrinha, P., Kullberg, J.C. (Ed.), Geologia de Portugal (Vol. I), Escolar Editora, Lisboa, 647-671.

Pereira, M.F., Chichorro, M., Johnston, S.T., Gutiérrez-Alonso, G., Silva, J.B., Linnemann, U., Drost, K. (2012). The missing Rheic Ocean magmatic arcs: Provenance analysis of Late Paleozoic sedimentary clastic rocks of SW Iberia. Gondwana Res, 22(3-4), 882-891. DOI: 10.1016/j.gr.2012.03.010

Pereira, M.F., Chichorro, M., Moita, P., Santos, J.F., Solá, A.M.R., Williams, I.S., Silva, J.B., Armstrong, R.A. (2015). The multistage crystallization of zircon in calc‑alkaline granitoids: U–Pb age constraints on the timing of Variscan tectonic activity in SW Iberia. Int J Earth Sci (Geol Rundsch), 104(5), 1167–1183. DOI 10.1007/s00531-015-1149-3

Pereira, Z., Oliveira, J.T. (2003a). Estudo palinostratigráfico do sinclinal da Estação de Cabrela. Implicações tectonostratigráficas. Cienc. Terra UNL Lisboa, 5, 118–119.

Pereira, Z., Oliveira, J.T. (2003b). Palinomorfos do Viseano do Complexo vulcânico da Toca da Moura, Zona de Ossa Morena. Cienc. Terra UNL Lisboa, 5, 120–121.

Pereira, Z., Oliveira, V., Oliveira, J.T. (2006). Palynostratigraphy of the Toca da Moura and Cabrela Complexes, Ossa Morena Zone, Portugal. Geodynamic implications. Rev Palaeobot Palyno, 139, 227-240. DOI: 10.1016/j.revpalbo.2005.07.008

Pérez-Cáceres, I., Martínez Poyatos, D., Simancas, J.F., Azor, A. (2016). Detrital zircon populations in the lower formations of the South Portuguese Zone (SW Iberia, Variscan Orogen). Geo-Temas, 16(1), 25-28. ISSN 1576-5172

Piçarra, J.M. (2000). Stratigraphical study of the Estremoz-Barrancos sector, Ossa-Morena Zone, Portugal. Middle Cambrian?-Lower Devonian Lithostratigraphy and Biostratigraphy. PhD Thesis (unpublished), Évora University, vol.1, 268p.

Piçarra, J.M., Sarmiento, G. (2006). Problemas de posicionamento estratigráfico dos Calcários Paleozóicos da Zona de Ossa Morena (Portugal). In: Abstract of the VII Congresso Nacional de Geologia, vol. II, 657-660.

Pimentel, N., Azevedo, T.M. (1994). Etapas e controlo Alpino da Sedimentação na bacia do Sado (SW de Portugal). Cuad. Lab. Xeol. de Laxe, 19, 229-238.

Pin, C., Fonseca, P.E., Paquette, J.L., Castro, P., Matte, Ph. (2008). The ca. 350 Ma Beja Igneous Complex: a record of transcurrent slab break-off in the Southern Iberia Variscan Belt? Tectonophysics, 461, 356–377. DOI: 10.1016/j.tecto.2008.06.001

Quesada, C. (1990). Introduction of the Ossa-Morena Zone (part V). In: Dallmeyer, R.D., Martínez García, E. (Ed.), Pre-Mesozoic geology of Iberia, Springer-Verlag, Berlin, 249-251.

Quesada, C., Dallmeyer, R.D. (1994). Tectonothermal evolution of the Badajoz-Cordóba shear zone (SW Iberia): characteristics and 40Ar/ 39Ar mineral age constraints. Tectonophysics, 231, 195-213. DOI: 10.1016/0040-1951(94)90130-9

Quesada, C., Robardet, M., Gabaldón, V. (1990). Synorogenic phase (Upper Devonian-Carboniferous- Lower Permian). In: Dallmeyer RD, Martínez García E (Ed), Pre-Mesozoic geology of Iberia, Springer-Verlag, Berlin, 249-251.

Ribeiro, A. (1983). Relações entre formações do Devónico superior e o Maciço de Évora na região de Cabrela (Vendas Novas). Comun. Serv. Geol. Portugal, 69(2), 267-269.

Ribeiro, A., Munhá, J., Fonseca, P.E., Araújo, A., Pedro, J., Mateus, A., Tassinari, C., Machado, G., Jesus, A., (2010). Variscan Ophiolite Belts in the Ossa-Morena Zone (Southwest Iberia): geological characterization and geodynamic significance. Gondwana Res, 17, 408-421. DOI: 10.1016/j.gr.2009.09.005

Robardet, M., Gutiérrez-Marco, J.C. (1990). Passive margin phase (Ordovician-Silurian-Devonian). In: Dallmeyer RD, Martínez García E (Ed), Pre-Mesozoic geology of Iberia, Springer-Verlag, Berlin, 249-251.

Robardet, M., Gutiérrez-Marco, J.C. (2004). The Ordovician, Silurian and Devonian sedimentary rocks of the Ossa-Morena Zone (SW Iberian Peninsula, Spain). J Iber Geol, 30, 73-92.

Rodrigues, B., Chew, D.M., Jorge, R.C.G.S., Fernandes, P., Veiga-Pires, C., Oliveira, J.T. (2015). Detrital zircon geochronology of the Carboniferous Baixo Alentejo Flysch Group (South Portugal); Constraints on the provenance and geodynamic evolution of the South Portuguese Zone, J. Geol. Soc. London. DOI: 10.1144/jgs2013-084.

Rodríguez, S., Fernández-Martínez, E., Cózar, P., Valenzuela-Ríos, J.I., Liao, J-Ch., Pardo, M.V., May, A. (2007). Emsian reefal development in Ossa-Morena Zone (SW Spain): Stratigraphic succession, microfacies, fauna and depositional environment. In: Abstracts of the X Internacional Congress on Fossil Cnidaria and Porifera, Saint Petersburg, 76-77.

Santos, J.F., Mata, J., Gonçalves, F., Munhá, J. (1987). Contribuição para o conhecimento geológico-petrológico da região de Santa Susana: o Complexo Vulcano-Sedimentar da Toca da Moura. Comun. Serv. Geol. Portugal, 73, 29-48.

Santos, J.F., Andrade, A., Munhá, J. (1990). Magmatismo orogénico varisco no limite meridional da Zona de Ossa-Morena. Comun. Serv. Geol. Portugal, 76, 91-124.

Santos, J.F., Mata, J., Ribeiro, S., Fernandes, J., Silva, J. (2013). Sr and Nd isotope data for arc-related (meta) volcanics (SW Iberia), Goldschmidt Conference Abstracts, 2132.

Silva, J.C., Mata, J., Moreira, N., Fonseca, P.E., Jorge, R.C.G.S., Machado, G. (2011). Evidence for a Lower Devonian subduction zone in the southeastern boundary of the Ossa-Morena-Zone. In: Absctracts of the VIII Congresso Ibérico de Geoquímica, Castelo Branco, 295-299.

Veizer, J., Ala, D., Azmy, K., Bruckschen, P., Buhl, D., Bruhn, F., Carden, G.A.F., Diener, A., Ebneth, S., Godderis, Y., Jasper, T., Korte, C., Pawellek, F., Podlaha, O.G., Strauss, H. (1999). 87Sr/86Sr, δ13C and δ18O evolution of Phanerozoic seawater. Chem Geol, 161, 59-88. DOI: 10.1016/S0009-2541(99)00081-9

V.2.

From the Devonian evolution of Ossa-Morena Zone (SW Iberian Variscides) to the SW Iberian Variscan Ocean subduction in the Early Devonian

Index

V.2.1. Introduction

The beginning of oblique subduction process of the SW Iberian Variscan Ocean under the Ossa-Morena Zone (OMZ) is poorly constrained. Although it is considered that the process began during Devonian times (e.g. Ribeiro 1983; Quesada, 1990; Oliveira *et al*. 1991; Moreira *et al*. 2010; 2014a; Nance *et al*., 2012; Dias *et al*., 2016; Pérez-Cáceres *et al*., 2016a), some authors consider that it may have started earlier, during the Silurian (e.g. Ribeiro *et al*. 2007; 2010). Thus, although the Silurian-Devonian age is generally accepted, the precise age to the beginning of subduction process is generally not mentioned.

Stratigraphic (e.g. Quesada *et al*., 1990; Oliveira *et al*. 1991; Robardet and Gutiérrez-Marco, 2004; Machado *et al*. 2010; Araújo *et al*. 2013), magmatic (e.g. Costa *et al*. 1990; Santos *et al*. 1990; Moita *et al*. 2005a; Silva *et al*. 2011), metamorphic (e.g. Quesada and Dallmeyer 1994; Moita *et al*. 2005b; Pedro *et al*. 2013) and structural (e.g. Ribeiro 1983; Araújo *et al*. 2005; 2013) data from OMZ show the existence of early tectono-metamorphic episodes during Devonian

times, which allow to constrain the first events correlated with the subduction of the SW Iberia Variscan Ocean.

The precise age of subduction onset is extremely important to the paleogeographic reconstruction models of Late Palaeozoic times and consequently for the correct evaluation of the geodynamic evolution of the Iberian and European Variscides. In the following sections the geological features of the OMZ are described, emphasizing the available tectono-metamorphic, magmatic and sedimentary data that allows to discuss the timing of the subduction onset and, consequently, its evolution during Devonian times.

V.2.2. Geological Setting

The Rheic Ocean was one of the most significant oceans of the Palaeozoic Era, developing between Gondwana and northern continental blocks, namely the Avalonia Continent (Nance *et al*., 2012; Matte, 2001; Ribeiro *et al*., 2007). Although it is generally considered that the SW Iberian suture represents the Rheic Ocean (e.g. Ribeiro *et al*., 2007; Nance *et al*., 2012), other authors considers that the suture between OMZ and South Portuguese Zone (SPZ) represents the Pulo do Lobo Ocean suture, closed during Famenian-Lower Carrboniferous times (Fig. 1A; Quesada, 1991; Oliveira *et al*., 2013a). It is unknown the basement of SPZ and, although it is possible that the SPZ basement is Avalonia Continental block, there is no data that makes it possible to affirm it. Thus, from now on, this ocean will be mentioned as SW Iberia Variscan Ocean.

Regardless of the ocean and continental blocks involved, during Late Neoproterozoic-Early Palaeozoic times, the Iberian Massif is part of Northern margin of Gondwana (Ribeiro *et al*., 2007; Linnemann *et al*., 2008; Nance *et al*., 2012). During Early Palaeozoic times, the continental stretching of the North Gondwana margin begins, possibly as a continuation of Neoproterozoic orogenic activity (Nance *et al*., 2012). During Cambrian times, the continental stretching generates a continental rifting process, which produces a syn-rift sedimentary succession (Sánchez-Gárcia *et al*., 2010) in OMZ, culminating with the SW Iberia Variscan Ocean opening during Early Ordovician times at South of OMZ (current coordinates; Fig. 1A; Ribeiro *et al*., 2007; Pedro *et al*., 2010; 2013; Nance *et al*., 2012; Sánchez-Gárcia *et al*., 2010). During Ordovician and Silurian times, the OMZ was located in thinned North Gondwana margin, with sedimentation typical of stable continental margins, until Lower Devonian times (Quesada 1990; Robardet and Gutiérrez-Marco 1990; 2004).

During Late Devonian-Early Carboniferous times, evidences of syn-tectonic sedimentation, generally with flyschoid and molassic features, is reported across the OMZ (Palacios González *et al*, 1990; Quesada *et al*., 1990; Oliveira *et al*., 1991; Armendariz *et al*., 2008). The age of these

syn-tectonic deposits is oldest in the southernmost domains of OMZ, being progressively younger to northeast, which has been interpreted as an indication that deformation migrates from the suture zone to the most internal domains of the hinterland (Apalategui and Quesada, 1987; Quesada *et al*., 1990).

Evidences of continental collision begin in Early Carboniferous (Jesus *et al*., 2007; Moreira *et al*., 2014a), which leads to consider that Early Carboniferous successions are already controlled by the collisional processes. This is also supported by the existence of an unconformity between the Carboniferous series and the older Palaeozoic ones, sometimes with conglomerates including deformed clasts derived from Early Palaeozoic successions (Quesada *et al*., 1990).

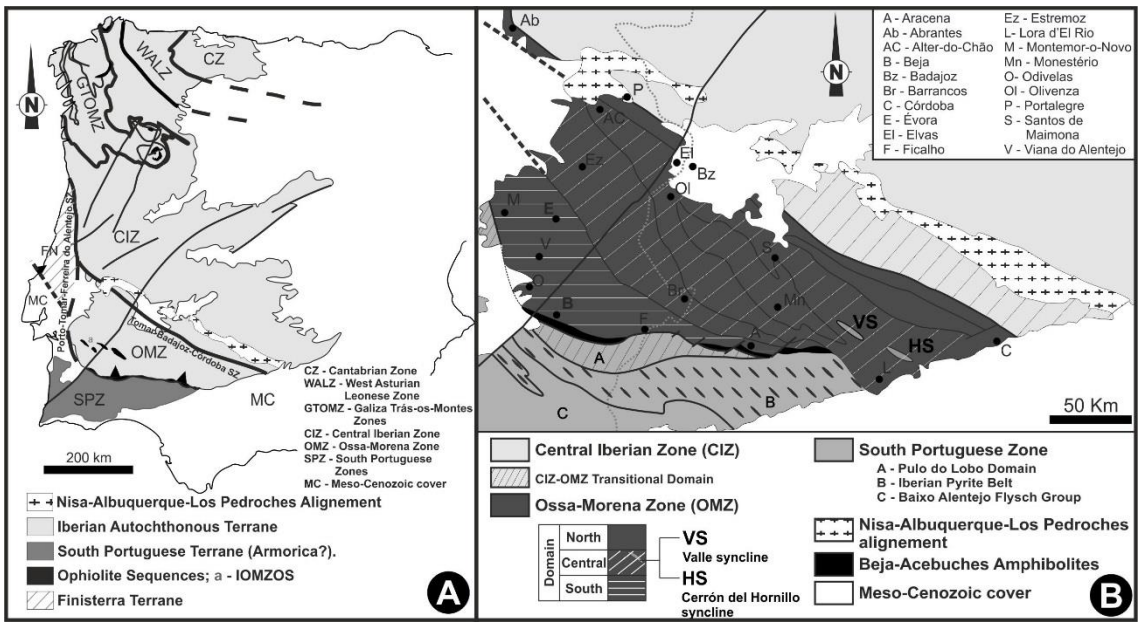

Figure 1 – (A) Main tectono-statigraphic zones of Iberian Variscan Massif (adapted from San-José *et al*., 2004; Ribeiro *et al*., 2007; 2010; Romão *et al*., 2014). (B) Subdivision of OMZ in North, Central and South domains based on geological features (adapted from Oliveira *et al*., 1991; San-José *et al*., 2004; Robardet and Gutierrez-Marco, 2004).

V.2.3. Stratigraphic Evidences; the Devonian Series

After the SW Iberia Variscan Ocean oceanization in the SW of the OMZ (Pedro *et al*., 2010; 2013; Sánchez-Gárcia *et al*., 2010), from the Ordovician to the Silurian-Early Devonian, passive margin sedimentation prevail in the OMZ (Quesada 1990; Robardet and Gutiérrez-Marco 1990; 2004; Sánchez-Gárcia *et al*., 2010).

The Silurian (Llandovery-Ludlow) sedimentation was characterized by great uniformity throughout the OMZ. The "Xistos com Nódulos", Papuda Formations and Lower Shales with

Graptolites Series (Central OMZ; Fig. 1B) are characterized by the presence of condensed sedimentation with very fine-grained facies (carbonaceous black shales and siltstones) and flints, typical of euxinic environments (Oliveira *et al*., 1991; Piçarra, 2000; Robardet and Gutierrez-Marco, 2004; Piçarra *et al*., 2009; Araújo *et al*., 2013), suggesting a stable tectonic framework, that is consistent with the absence of Silurian magmatism in OMZ (Fig. 2).

Overlying the Silurian euxinic sedimentation, two distinct Late Silurian-Early Devonian types of sedimentation are described in the OMZ, which will be described in the next sections.

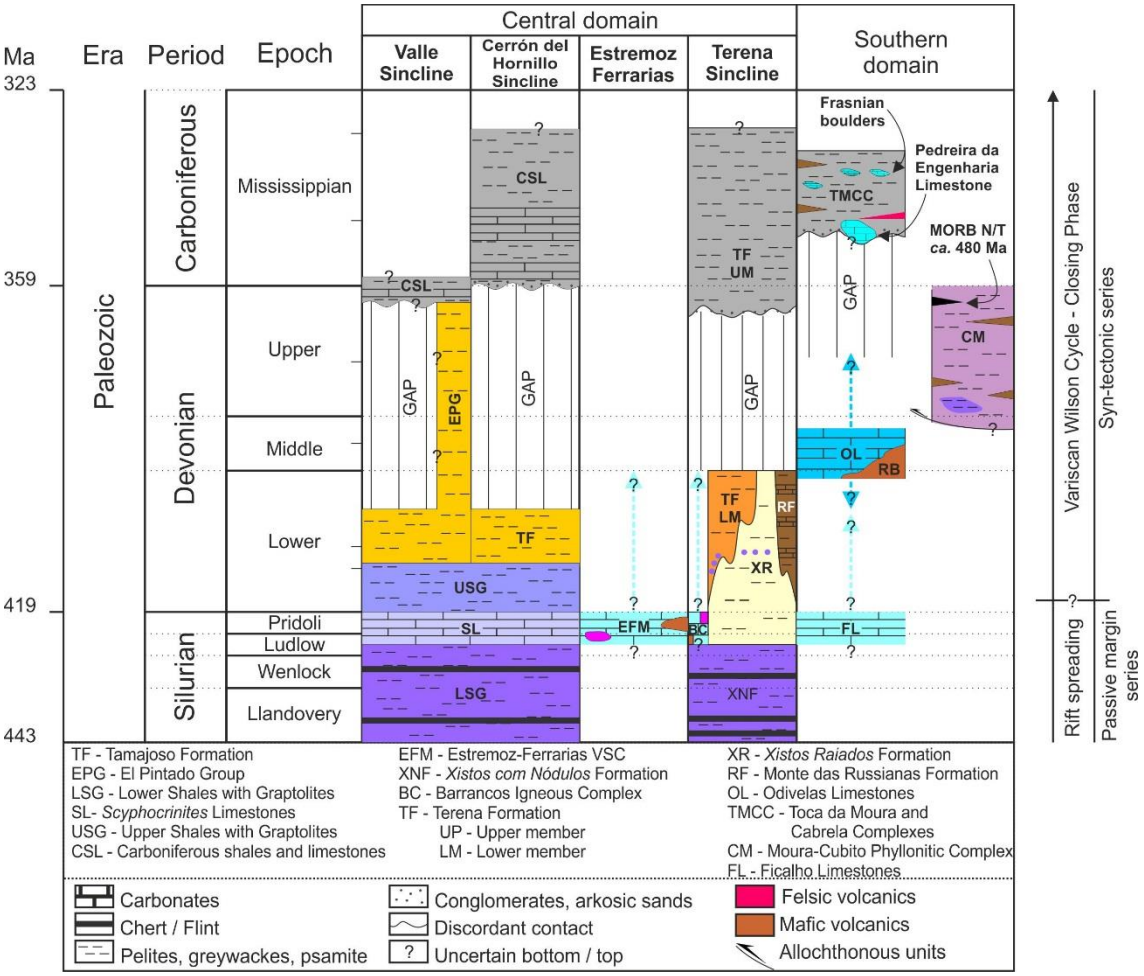

Figure 2 – Stratigraphic synopsis of Silurian to Carboniferous successions in Central and South Domains of the OMZ (see references on text).

V.2.3.1. Siliciclastic Sedimentation in the Terena Basin

In the Central Domains of the OMZ (Fig. 1B), after the deposition of the Silurian black shales, the sedimentation became progressively more shallow and energetic, marked by a prevalent environment oxidation with sedimentation of shales at the bottom, gradually with more sandstones and impure quartzites towards the top of the sequence (Xistos Raiados Formation -

Fig. 2 and 3A; Piçarra, 2000; Araújo *et al*, 2013). The sedimentation of Xistos Raiados Formation extends from Pridoli until the end of the Early Devonian (Emsian; Oliveira *et al*., 1991; Pereira *et al*., 1999; Piçarra, 2000; Gutiérrez-Marco and Robardet, 2004; Araújo *et al*, 2013). The top of the unit includes clasts of Early Silurian units, as well as gravitational landslides (Araújo *et al*., 2013).

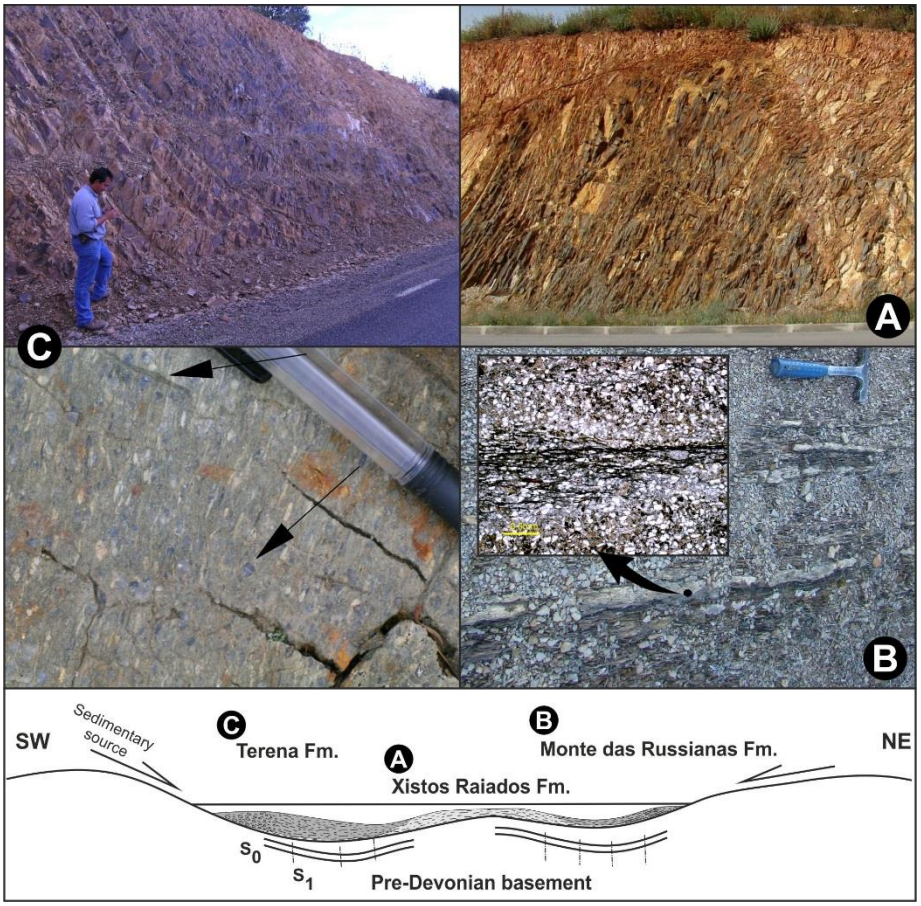

Figure 3 – Schematic interpretative sketch of the Terena Basin showing the lateral facies transition between Monte das Russianas (A), Xistos Raiados (B) and Terena Formations (C). The arrows indicates the Silurian flints contained in Terena Formation conglomerates.

Simultaneously to the deposition of the Xistos Raiados Formation, during Pragian-Emsian times a siliciclastic unit with black shales, siltstones and sandstones with calcite cement was deposited (Monte das Russianas Formation - Fig. 2 and 3B; Perdigão *et al*., 1982; Araújo *et al*., 2013). This formation presents many similarities with Xistos Raiados Formation and its lateral transition is gradual (Oliveira *et al*., 1991; Robardet and Gutiérrez-Marco, 2004; Araújo *et al*., 2013). With the same age, the Terena Formation was also deposited as a flysch sequence composed of shales and greywackes (Fig. 2 and 3C), occasionally with conglomeratic levels, mainly in the bottom of sequence (Pereira *et al*., 1999; Piçarra, 2000). The Terena Formation includes clasts of Silurian flints (Fig. 3C), as well as lithoclasts of the Devonian units described

above and magmatic rocks (Borrego, 2009; Araujo *et al*., 2013). Geochemical studies of the Terena Formation greywackes and sandstones suggest a probable volcanic arc and a recycled orogen sediment sources (Borrego *et al*., 2006; Borrego, 2009), in contrast with the Colorada Formation (siliciclastic unit of Ordovician to Early Silurian age; Borrego *et al*., 2006) which indicates continental platform sedimentation in stable conditions. Detrital zircons studies on the Terena Formation (Pereira *et al*., 2014) show that the youngest population was Ordovician in age, thus inconclusive as respect to the age of sediment source areas, specifically to the age of the volcanic arc magmatism.

It is important to emphasize that in Spain, an Upper Member was described (Fig. 2), with (Famennian?) Tournaisian-Visean age (Boogaard and Vázquez, 1982; Geise *et al*., 1994; Gutiérrez-Marco and Robardet, 2004), in the Terena Formation. According to Azor *et al* (2004), the Carboniferous Member is, probably, deposited discordantly on top of the Devonian member.

The above mentioned Devonian formations are deposited in the Terena Basin (Araujo *et al*., 2013 and references therein), with a spatial and temporal arrangement that seems to shows lateral facies variation (Fig. 3 and 4). Indeed, the Terena flysch outcrops in the western domains of the basin, showing coarse-grained rocks (greywacke and conglomerates) at the bottom of sequence, while the Monte das Russianas Formation only crops out in Eastern domains, with Xistos Raiados Formation as a transitional unit. The Terena and Xistos Raiados Formations have evidences of syn-sedimentary deformation and also erosion followed by reworking of Silurian rocks within these Early Devonian siliciclastic Formations (Fig. 4C; Borrego *et al*., 2005; Araújo *et al*, 2013).

V.2.3.2. Devonian Carbonate Sedimentation

Devonian carbonate sedimentation is poorly developed in OMZ. In the south-western branch of this zone, several Early to Late Devonian limestone occurrences are known (Fig. 1B; Boogaard, 1972; 1983; Conde and Andrade, 1974; Piçarra and Sarmiento, 2006; Machado *et al*., 2009; 2010; Machado and Hladil 2010; Oliveira *et al*., 2013b). Late Silurian-Devonian limestones are also described in the Estremoz-Ferrarias-Barrancos alignment (Fig. 4; Piçarra and Le Menn, 1994; Sarmiento *et al*., 2000; Piçarra and Sarmiento, 2006; Araújo *et al*., 2013; Piçarra *et al*., 2014) and in some synclines in Spain. Upper Devonian-Carboniferous limestones are also described (see below; Robardet and Gutiérrez-Marco 1990; 2004; Lenz *et al*., 1996). The description, regional framework and significance of these limestones are the subject of the next section.

V.2.3.2.1. Southwestern OMZ Limestones

In Southwestern OMZ a set of limestone scattered occurrences is observed. Initial paleontological work carried out by Boogaard (1972; 1983) and Conde and Andrade (1974) reveals the Devonian age of these occurrences. Most of the known localities are aligned NNW-SSE close to the trend of the OMZ-SPZ boundary. These localities are restricted to loose boulders, small quarries and natural outcrops spanning in areas usually less than $1km^2$. The limestones are found scattered around the Odivelas reservoir area (Ferreira do Alentejo), named as Odivelas Limestone, in the South, and near the Cabrela village in the North (near Montemor-o-Novo; Fig. 4). They are usually associated to volumetrically reduced cherts, tuffites and marly limestones (Fig. 5A).

The Devonian limestones are found interbedded or spatially associated with the Rebolado basalts (Fig. 2 and 5B; Odivelas Limestone; Andrade *et al*. 1976; Santos *et al*. 1990; Moreira *et al*., 2010) or with the Toca da Moura-Cabrela Complex (Fig. 2; Pena, Caerinha, Cabrela, Pedreira da Engenharia and Estação de Cabrela Limestones; Pereira and Oliveira, 2003; Pereira *et al*., 2006a; Machado and Hladil 2010; Oliveira *et al*., 2013b).

Most of the limestone occurrences are composed of crinoidal wackestones (with subordinate proportions of other bioclasts such as forams, tentaculites, corals and stromatoporoids; Fig. 5C) and fine-grained calcimudstones. These have occasional mixing of coarser grains such as crinoidal fragments, tentaculites and radiolarians. These two lithofacies are interbedded and generally interpreted as calciturbidites, in more distal (calcimudstones) or more proximal (wackestones) settings, with evidences of slumping and convolute bedding (Fig. 5D; Machado *et al*. 2010).

The origin of the carbonate material is most likely a reef system, although the only locality with bioherm/biostromal facies is Cortes (Machado *et al*., 2009). Here, the authors describe very coarse grained packstone-grainstones (locally rudstones and boundstones) with abundant crinoids (Fig. 5C), rugose and tabulate corals, brachiopods and stromatoporoids occur in the central part of the outcrop area, surrounded by calciturbidite facies. The age of Odivelas Limestone is constrained by paleontological data (e.g. conodonts, crinoids), being Middle Devonian in age, with the exception to Covas Ruivas succession that also includes the latest Emsian (Early Devonian) conodont biozone (Machado *et al*., 2009; 2010).

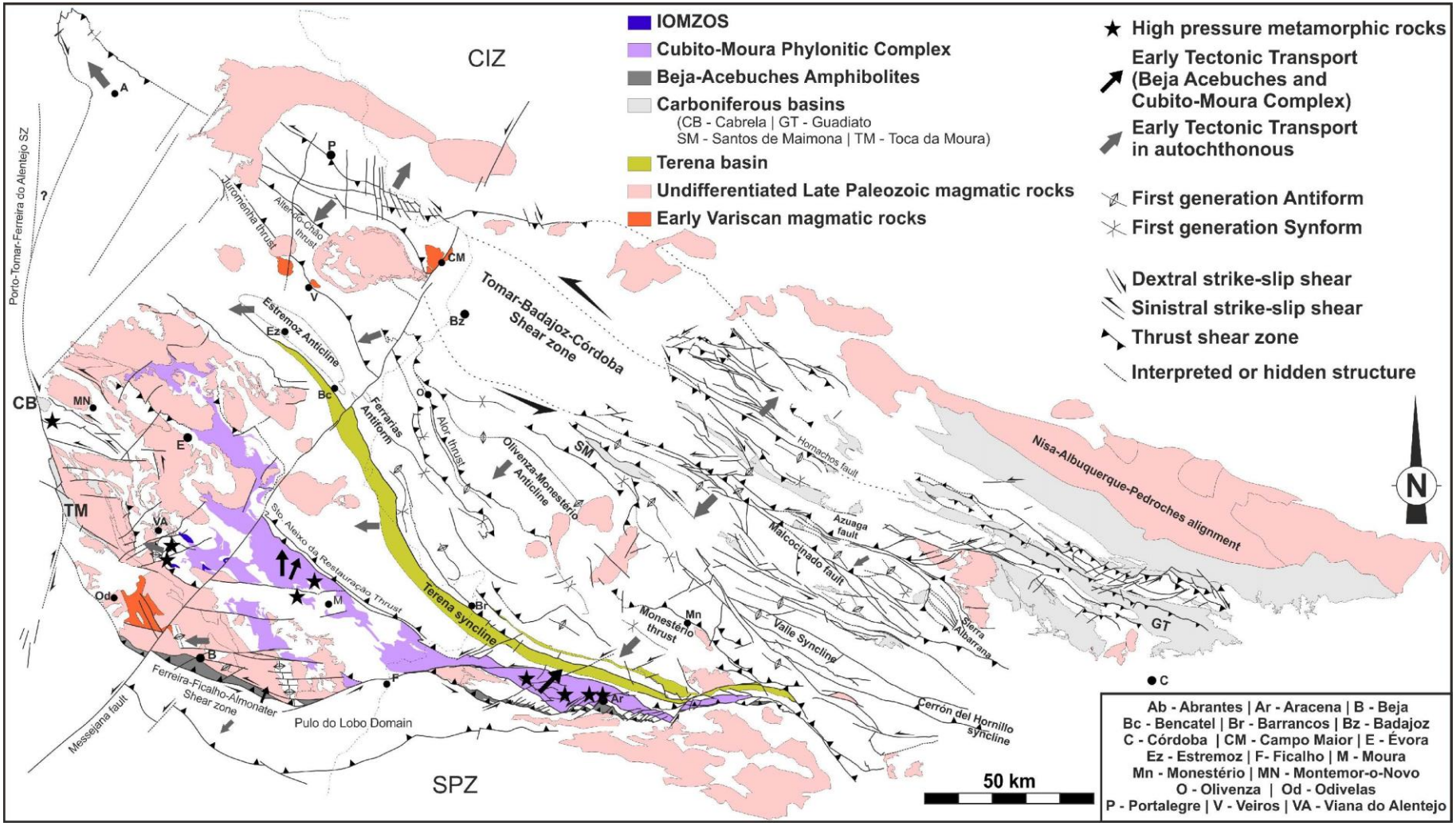
IOMZOS
Cubito-Moura Phylonitic Complex
Beja-Acebuches Amphibolites
Carboniferous basins
(CB - Cabrela | GT - Guadiato
SM - Santos de Maimona | TM - Toca da Moura)
Terena basin
Undifferentiated Late Paleozoic magmatic rocks
Early Variscan magmatic rocks
High pressure metamorphic rocks
Early Tectonic Transport (Beja Acebuches and Cubito-Moura Complex)
Early Tectonic Transport in autochthonous
First generation Antiform
First generation Synform
Dextral strike-slip shear
Sinistral strike-slip shear
Thrust shear zone
Interpreted or hidden structure
CIZ
SPZ
Porto-Tomar-Ferreira do Alentejo SZ
Juromenha thrust
Alentejo-Chão thrust
Tomar-Badajoz-Córdoba Shear zone
Estremoz Anticline
Ferrarias Antiform
Alor thrust
Olivenza-Monesterio Anticline
Terena syncline
Sto Aleixo da Restauração Thrust
Ferreira-Ficalho-Almonater Shear zone
Messejana fault
Pulo do Lobo Domain
Hornachos fault
Azuaga fault
Malcocinado fault
Monesterio thrust
Valle Syncline
Sierra Albarrana
Cerrón del Hornillo syncline
Nisa-Albuquerque-Pedroches alignment
CB
TM
SM
GT
50 km
N
Ab - Abrantes | Ar - Aracena | B - Beja
Bc - Bencatel | Br - Barrancos | Bz - Badajoz
C - Córdoba | CM - Campo Maior | E - Évora
Ez - Estremoz | F- Ficalho | M - Moura
Mn - Monestério | MN - Montemor-o-Novo
O - Olivenza | Od - Odivelas
P - Portalegre | V - Veiros | VA - Viana do Alentejo

Figure 4 – Simplified geological map of OMZ, putting on evidence the location Devonian magmatic rocks, the Moura-Cubito Phyllonitic Complex and Terena Basin, as well the general structural pattern emphasizing the Early Variscan deformation episode structures (cartographic sources: Magna 50 – 2nd series – of IGME; Geological map of Portugal at the scale 1:50 000 of LNEG; Geological map of Portugal at the scale 1:500 000 of LNEG; Geological map of Iberia at the scale 1:2 000 000 of IGME).

In some of the localities (Pena, Caerinha, Cabrela) these lithofacies are partially overprinted by intense dolomitization and/or silicification (Machado and Hladil 2010; Moreira *et al*., 2016). Nevertheless, crinoid columnal sections and remnants of the original facies are partially preserved. In Pena and Caeira localities, Machado and Hladil (2010), describe crinoidal fragments, indicating a Middle Devonian age.

Frequently, these calciturbidites are interbedded with tuffites (Fig. 5A), always volumetrically less relevant than the carbonates. They are interpreted as hemipelagic sediments, frequently cherty or with millimetric carbonate lenses, which in some levels have radiolarians, tentaculites and ostracod shells (Machado *et al*., 2010; Moreira and Machado, in press).

Within the Mississippian Cabrela Complex, mainly composed of shales and greywackes, Middle Devonian (Eifelian) limestone occurrences were described (Fig. 2; Pedreira da Engenharia Limestone; Boogaard 1972), but also limestone boulders of Frasnian age embedded in the Mississippian shales (Fig. 2; Estação de Cabrela Limestones; Boogaard, 1983). Fransnian limestones are not described in SW OMZ and thus its source area is unknown, being interpreted as olistoliths (Pereira and Oliveira, 2003). Therefore, the carbonate sedimentation continued from the Early-Middle Devonian, possibly extending into the Frasnian.

$^{87}Sr/^{86}Sr$ isotopic data (Moreira *et al*., 2016) show clear similarities between the strontium ratio signature presented in Pena, Cortes and Covas Ruivas limestones which are in agreement with the global values defined for Early-Middle Devonian times (Veizer *et al*. 1999; McArthur *et al*. 2012). In turn, the Pedreira da Engenharia Middle-Devonian dolomitized limestones presents significant higher $^{87}Sr/^{86}Sr$ values, which could be the result of post-depositional secondary dolomitization (Moreira *et al*., 2016).

The Odivelas Limestone, clearly in situ, is associated to Rebolado volcanics (see below), although the other limestone occurrences along the Western border of the OMZ may be tectonically displaced or remobilized into the Toca da Moura and Cabrela Complexes (Fig. 2).

Finally a mention to the Ficalho region, where unclassifiable fragments of conodonts in black limestones have been described (Piçarra and Sarmiento, 2006), which suggest Upper Silurian or Devonian ages, based on denticulation type and shape of the basal cavity (Fig. 2).

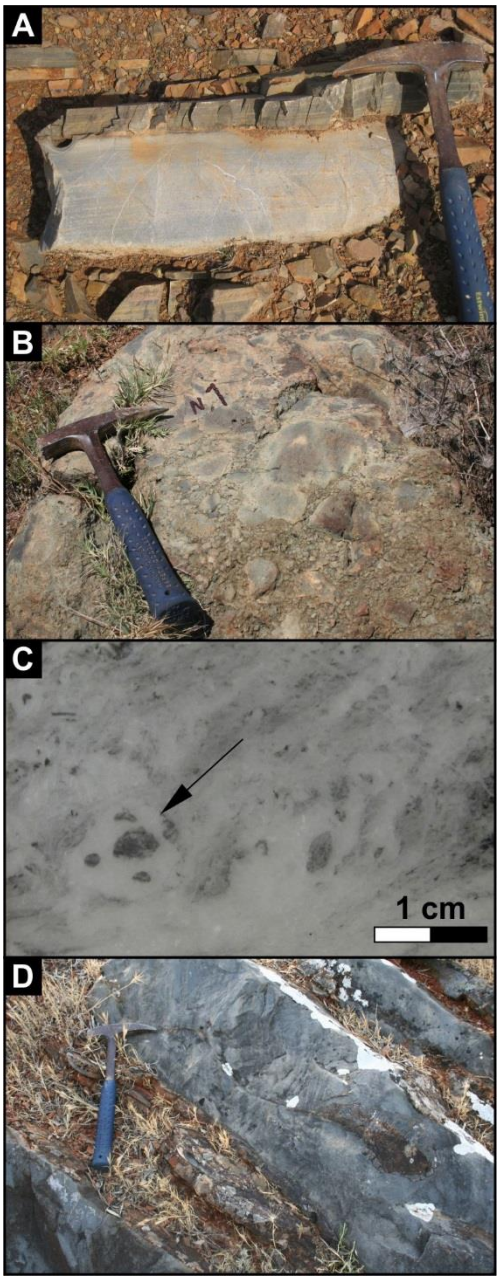

Figure 5 – General features of Odivelas Limestones:
A – Intercalation between calciturbidite limestone and hemipelagic tuffites;
B – Pyroclastic rocks from Rebolado Basalts, clearly showing primary textural features;
C – Transverse or slightly oblique sections of (?) *cupressocrinitids columnals* from Odivelas Limestones;
D – Syn-sedimentary deformation of limestones showing slump structures.

V.2.3.2.2. Estremoz-Ferrarias-Barrancos Limestones

These limestones occur in the Central Domain of the OMZ (Fig. 1B and 2), in a NW-SE alignment, spreading through Bencatel (SE termination of SW Estremoz Anticline limb), Ferrarias Anticline and Barrancos (Fig. 6A). These limestones are spatially associated with bimodal magmatic rocks, with unknown age, and occasionally breccias (Fig. 6A$_1$; Piçarra, 2000; Araújo *et al*., 2013).

The marbles from Estremoz Volcano-Sedimentary Complex, considered by some authors (e.g. Piçarra, 2000; Sarmiento *et al*., 2000) equivalent to the Ferrarias Limestones, have been considered to be Early Cambrian to Late Ordovician-Silurian (see Oliveira *et al*., 1991 and Araujo *et al*., 2013 for a discussion).

However, the discovery of crinoid fragments (Fig. 6A$_2$) and conodont faunas in the Ferrarias Limestone seems to show a Late Silurian or Devonian age for some of these limestones (Piçarra and Le Menn, 1994; Piçarra, 2000; Sarmiento *et al*., 2000). The conodont fauna is fragmentary and inconclusive, notably with *Oulodus* sp. and *Ozarkodina* sp. (Fig. 6A$_3$). The limestones with conodont faunas are found in layers that contain clasts of quartzites and black shales, suggesting reworking of Palaeozoic units (Sarmiento *et al*., 2000). Also in Bencatel-Alandroal and Barrancos, fragments of crinoids are found (Piçarra and Le Meen, 1994; Piçarra and Sarmiento, 2006) in black impure limestones. The fragmentary fossiliferous content brackets the age as younger than Ordovician, possibly Early Devonian, based on free-living tentaculitoids found near Bencatel-Alandroal (Piçarra *et al*., 2014).

Recently, a radiometric age of 499.4 ± 3.3 Ma (U-Pb in zircons) have been obtained for a rhyolite from Estremoz (Fig. 6B; Pereira *et al*., 2012a). According to these authors this Middle-Late Cambrian age should also be the age of the Estremoz Marbles in which the rhyolite is intercalated. However, the regional geological maps clearly show that the rhyolite sample (ETZ-1) is not interbedded in the marble sequence, outcropping along the boundary between this unit and the overlying Silurian / Devonian ones (Fig. 6B). Moreover, this boundary has been considered a mechanical contact (Coelho and Gonçalves, 1970), which made the stratigraphic relation between the rhyolite and the Estremoz marbles debatable (Fig. 6C; Coelho and Gonçalves, 1970; Gonçalves, 1972; Piçarra *et al*., 2014). Thus the previous rhyolite age could not be considered equivalent of the marbles.

The correlation between Estremoz Marbles and Ferrarias Limestones, with Upper Silurian-Devonian age, is not totally accepted. Alternatively, some authors (Lopes, 2003; Pereira *et al*., 2012a) argue that the Upper Silurian-Devonian ages are not the carbonated depositional age, but the result of remobilization of younger Devonian faunal material during sub-aerial exposure, which is not excluded by Piçarra and Sarmiento (2006). Despite the discussion, the presence of Late Silurian-Devonian carbonated sedimentation in this area is clear.

Besides the $^{87}Sr/^{86}Sr$ isotopic signature is not conclusive in this case and the Estremoz, Ferrarias and Barrancos carbonates do not present a similar signature with the previously described Early-Middle Devonian limestones of SW OMZ (Moreira *et al*., 2016), showing values most similar to Cambrian marbles and limestones.

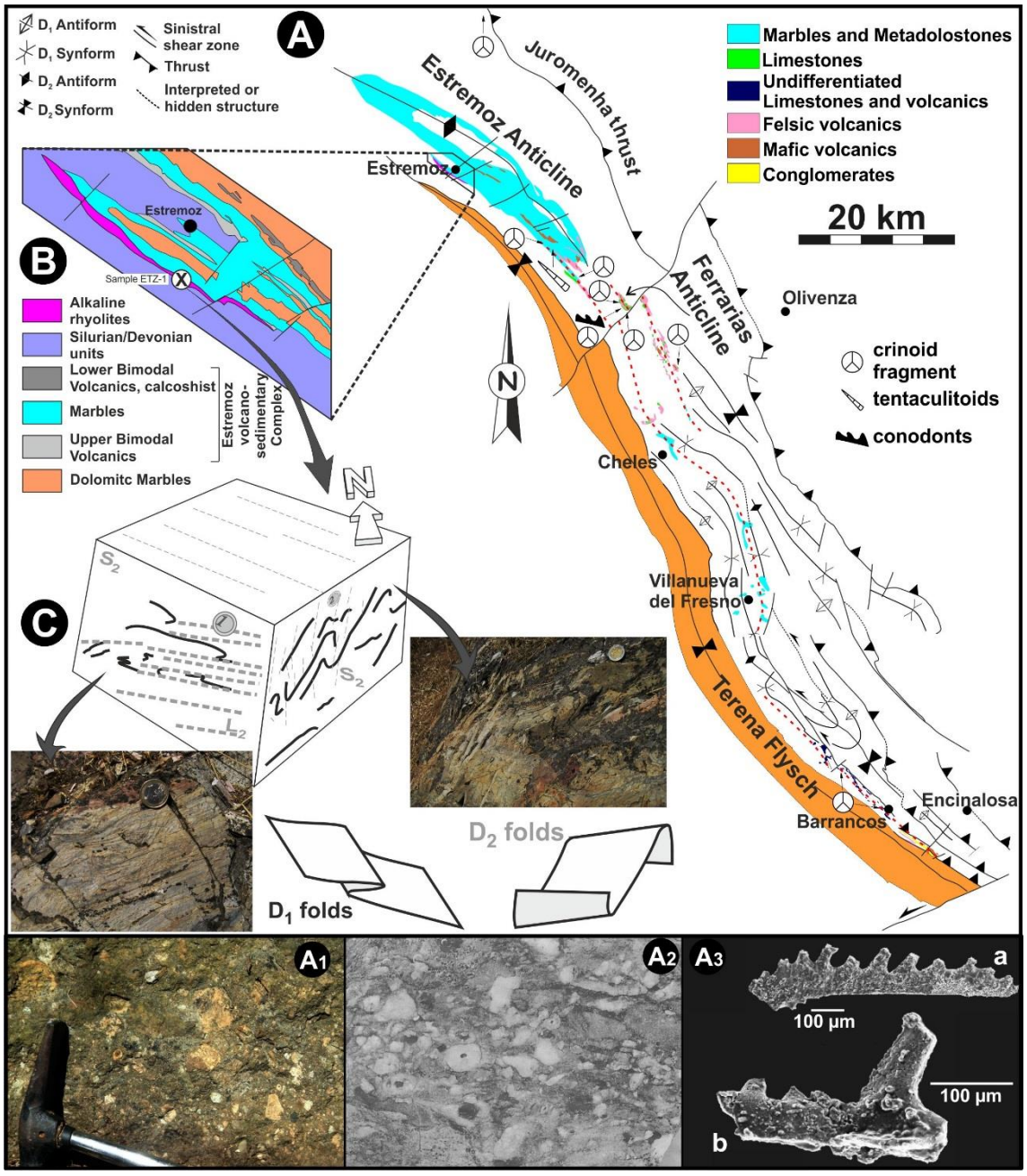

Figure 6 – General framework of Estremoz-Ferrarias-Barrancos Limestones alignment:

A – Simplified geological mapping (adapted from LNEG, 2010) and characterization of lithologic and paleontological features of limestones: (A1) Breccia from Barrancos locality, showing siliciclastic and magmatic remobilized clasts; (A2) Crinoid fragments from Ferrarias Limestones; (A3) conodonts from Ferrarias Limestones (a - Ozarkodina ? sp. ; b - Oulodus ?; adapted from Piçarrra and Sarmiento, 2006);

B – Geological context of the Estremoz volcanics (sample ETZ-1) dated by Pereira *et al* (2012) (Coelho and Gonçalves, 1970; Gonçalves, 1972; LNEG, 2010);

C – Interference between main variscan folding events in the ETZ-1 sample locality.

V.2.3.2.3. Valle and Cerrón del Hornillo Synclines Limestones

The Devonian sequence in Spain is clearly developed in 2nd order synclines (e.g. Valle and Cerrón del Hornillo; Fig. 1B) located in limbs of the Olivenza-Monestério Antiform (Gutiérrez-Marco and Robardet, 2004; Robardet and Gutiérrez-Marco, 2004). The Early Devonian (Pragian-Emsian; Robardet *et al*., 1991) sequence is siliciclastic, mainly composed of siltstones and shales (e.g. Tamajoso Formation and Lower part of El Pintado Group; Fig. 2) in stratigraphic continuity with Late Silurian ones (Lenz *et al*, 1996; Robardet and Gutiérrez-Marco, 2004). Over this siliciclastic series, a Middle Devonian hiatus is present (Fig. 2; Robardet and Gutiérrez-Marco 1990; 2004).

In these synclines, Late Devonian to Early Carboniferous limestones are described (Robardet and Gutiérrez-Marco, 2004). In the Valle Syncline, in the uppermost part of El Pintado Group, limestones, sandy limestones and shales with limestones nodules are described and attributed to the Late Devonian (Famennian), based on conodont and brachiopod faunas (Robardet *et al*., 1991; García-Alcalde *et al*., 2002; Gutiérrez-Marco and Robardet, 2004). The uppermost part overlies concordantly the Early Devonian part of the El Pintado Group (Robardet and Gutiérrez-Marco, 2004). Similar Early Devonian successions are described in Cerrón del Hornillo syncline, however this succession is unconformably overlain by Early Carboniferous conglomerates and limestones (Robardet *et al*., 1991; Gutiérrez-Marco and Robardet, 2004; Robardet and Gutiérrez-Marco, 2004).

V.2.4. Odivelas and Veiros-Vale Maceira Magmatism; the Devonian Volcanic-Arc

Devonian magmatism is poorly known in the Iberian Massif. However, some relics of this magmatism seem to be present in OMZ. Indeed, in southwestern domains of the OMZ, occurs a suite of magmatic rocks, generally included in the Beja Igneous Complex (BIC; e.g. Andrade 1983; Oliveira *et al*. 1991; Jesus *et al*. 2007; 2016). The BIC is Carboniferous in age (Jesus *et al*. 2007; Pin *et al*., 2008) and obliterate the previous structure and magmatism.

However, in the Peroguarda Complex, mainly composed of mafic to intermediate volcanic rocks, Andrade *et al*. (1976) individualize three distinct units, among which the Rebolado Basalts (Fig. 4; OD-6 for Santos *et al*., 1990). This volcanic unit presents mafic to intermediate nature with abundant effusive lithotypes and tephra rocks (Fig. 5B; Santos *et al*. 1990; Silva *et al*. 2011). The Early-Middle Devonian Odivelas Limestones are spatially associated to this unit, being its sedimentation substrate (Conde and Andrade 1974; Andrade *et al*., 1976; Machado *et al*., 2010; Moreira *et al*., 2010). These basalts exhibit low grade hydrothermal metamorphism (Andrade *et al*. 1976; Santos *et al*. 1990; Silva *et al*. 2011), which does not obliterate the original volcanic textures.

Geochemical data suggests that the mafic-intermediate sub-alkaline volcanic rocks contained in the Rebolado Basalts present significant similarities with the typical orogenic volcanic arc magmatism, exhibiting a low-K tholeiitic to calc-alkaline signature (Santos *et al*. 1990; Silva *et al*. 2011). However, Santos *et al*. (1990) remark a slight difference between two sectors: the North sector (Odivelas-Penique) where the calc-alkaline signature is more pronounced and the South sector (Alfundão-Peroguarda) where a predominant tholeiitic nature is found. Recently, Santos *et al*. (2013) supported this distinction based in isotopic data (Sm-Nd and Rb-Sr isotope pairs). The data provide evidences of common mantle (or very similar) sources for the mafic magmas in both sectors, although the North sector shows some evidences of crustal assimilation.

Also with (Late) Devonian age, in Central Domains of OMZ, shoshonitic to calc-alkaline magmatic bodies (Fig. 4; Vale Maceira, Veiros and Campo Maior; Costa *et al*., 1990; Moita *et al*. 2005a; Carrilho Lopes *et al*., 2005) are described. These massifs provide radiometric ages of 362±12Ma for Gabbro-Dioritic body of Veiros-Vale Maceira cooling age (Rb/Sr whole rock-felspar pair and K/Ar in amphibole; Moita *et al*., 2005a) and 376±22Ma for the emplacement age Campo Maior Massif (Sm-Nd Carrilho Lopes *et al*., 2005).

Indirect evidences of Devonian magmatism are also present in Carboniferous syn-orogenic metasedimentary rocks of the Cabrela Complex (OMZ), as well as in the Mértola, Mira and Santa Iria Formations of the SPZ, where significant populations of inherited zircons (with no overgrowths or inherited cores, implying a magmatic origin; Pereira *et al*., 2012b) are found, ranging from Early to Late Devonian (Braid *et al*., 2011; Pereira *et al*., 2012b; 2013; Rodrigues *et al*., 2015; Pérez-Cáceres *et al*., 2016b). Indeed, the Mississippian Cabrela Complex siliciclastics provide two Devonian inherited zircons clusters, with Eifelian-Givetian and Famennian ages (Pereira *et al*. 2012b). Similar clusters are also obtained in the SPZ Mississippian siliciclastic lithotypes of Mértola and Mira Formations (Pereira *et al*. 2012b; 2013; Rodrigues *et al*. 2015). In turn, the Santa Iria Formation presents a Late Devonian cluster of inherited zircons (Braid *et al*. 2011; Pérez-Cáceres *et al*. 2016b), while in Ribeira de Limas and Ronquillo Formations Early Devonian (Emsian) inherited zircons are present, representing the youngest Devonian cluster of these units (Pérez-Cáceres *et al*. 2016b).

V.2.5. Early Metamorphism and Structure of OMZ

The spatial distribution of early metamorphism and structure is heterogeneous in the OMZ (Fig. 4). In the SW border of the OMZ, an early HP-LT metamorphic event is described by several authors (e.g. Fonseca *et al*., 1999; Araújo *et al*., 2005; Moita *et al*., 2005b; Booth-Rea *et al*., 2006; Pedro *et al*, 2013; Rubio Pascual *et al*., 2013). This metamorphic prograde high-pressure event

was produced blueschists and eclogites (P=8-18 kbar in Viana do Alentejo-Alvito region, Fonseca *et al*., 1999 and Rosas *et al*., 2008; 16-18 kbar in Safira (Montemor-o-Novo), Moita *et al*., 2005b; 7-12 kbar in Moura-Cubito Phyllonitic Complex, Moita *et al*., 2005b and Rubio Pascual *et al*., 2013). Geochronological data indicate a Late Devonian age to HP metamorphism peak (371 ± 17 Ma; Sm/Nd isochronous whole rock-garnet; Moita *et al*, 2005b; Pedro *et al*., 2013). The effects of HP-LT metamorphism were also recognised by the occurrence of aragonite remnants in calcite-rich marbles of Viana-Alvito region associated with pelitic rocks comprising kyanite + garnet + onfacite + glaucophane (Fonseca *et al*, 2004).

The HP rocks are spatially associated to the Moura-Cubito Phyllonitic Complex and to parautochthonous units from OMZ (Fig. 4; Fonseca *et al*., 1999; Araújo *et al*., 2005; Moita *et al*., 2005b; Booth-Rea *et al*., 2006; Pedro *et al*, 2013; Rubio Pascual *et al*., 2013).

The Moura-Cubito Phyllonitic Complex is interpreted as an allochthonous imbricate complex, emplaced over the OMZ southernmost autochthonous domains (Araújo *et al*., 2005; 2013; Booth-Rea *et al*., 2006; Ponce *et al*., 2012). The complex is mostly formed by monotonous and strongly deformed phyllites, including dismembered fragments of internal ophiolite complexes (IOMZOS; Pedro *et al*., 2010), as well slivers of autochthonous units (Cambrian marbles, Silurian flints and anorogenic volcanic rocks), in addition to the above mentioned HP metamorphic rocks (Araújo *et al*., 2005; 2013).

This complex displays a fold and thrust pattern characterized by a mylonite foliation, showing tangential transport with top to N-NNE in the Western sectors (Fig. 7A; Araújo *et al*., 2005) and to ENE in the Eastern ones (Ponce *et al*., 2012). This deformation episode is only preserved in this complex and in the Beja-Acebuches Amphibolites (Fig. 2; Fonseca *et al*., 1999; Araújo *et al*., 2005), being considered a local deformation episode possibly related to the emplacement of this allochthonous unit (Ribeiro *et al*., 2010; Moreira *et al*., 2014a). The Moura-Cubito Phyllonitic Complex develops a sinistral sigmoidal cartographic pattern, quite wide in the Western sectors of the OMZ, but considerably condensed in the East ones (Fig. 4).

The emplacement of this unit is interpreted as Middle to Late Devonian in age (Araújo *et al*, 2005; Ribeiro *et al*., 2010). The structural pattern related to the emplacement of this allochthonous imbricate complex produces an interference pattern with the autochthonous deformation, characterized by recumbent folding, facing to SW-W quadrant (Fig. 4). The interference shows a northern propagation of the deformation related to the emplacement of the Moura-Cubito Phyllonitic complex, with synchronous deformation of autochthon with a distinct geometric pattern (Ribeiro *et al*., 2010).

The age of early deformation episodes is constrained by the deposition of Toca da Moura and Cabrela Volcano-Sedimentary Complexes. These complexes are characterized by syn-

sedimentary deposits constituted by shales, siltstones and greywackes, sometimes with carbonated levels (e.g. Pedreira da Engenharia Limestone) and bimodal volcanics (Oliveira *et al*., 1991, 2013b). The palynomorph associations in the siliciclastic sequence indicate a Late Tournasian to Late Viséan age (Pereira *et al*., 2006a). The Cabrela Complex stratigraphic succession presents a basal conglomerate, emphasising an angular unconformity with the deformed Pre-Carboniferous basement (Ribeiro, 1983; Pereira *et al*., 2006a; Oliveira *et al*., 2013b and references therein).

In the Central domains of the OMZ, during early Variscan evolving stage (D_1), a prograde metamorphic event under low grade metamorphic conditions, not exceeding greenschist facies (Expósito *et al*. 2002; Araújo *et al*., 2013; Moreira *et al*, 2014b), is described. This metamorphic event is associated to a progressive deformation regime, with intense strain partition, characterized by N-S to NW-SE recumbent folds and low dipping shear zones with transport with top to W-SW quadrant (Fig. 4 and 7B; e.g. Expósito *et al*, 2002; Simancas *et al*., 2004; Araújo *et al*., 2013; Moreira *et al*, 2014b). The seismic profile shows a basement control (thick skinned tectonics) associated with kilometre scale recumbent folds, rooting in the northern sectors of the OMZ (Simancas *et al*., 2004).

The genesis of the Terena Basin is attributed to D_1 (Araújo *et al*., 2013), which could explain the N-S anomalous orientation of Terena Syncline, in its central domains, with respect to NW-SE regional trend (Fig. 4). Indeed, the anomalous trend is interpreted as conditioned by the development of the N-S D_1 structures, which are contemporaneous of basin genesis during the Devonian (Rocha *et al*., 2009; Araújo *et al*., 2013).

The Terena Formation (Pragian-Emsian in age; Araújo *et al*., 2013) is deposited in this syn-tectonic trench. This Formation does not present evidences of the first deformation episode, although presenting evidences of syn-sedimentary deformation (Borrego *et al*., 2005; Rocha *et al*., 2009; Araújo *et al*., 2013), showing flyschoid nature and containing clasts of Silurian flints (Borrego *et al*., 2005). The deposition of Terena flysch is considered contemporaneous of the D_1, showing a lateral facies variation, with the presence of coarse-grained lithotypes in SW, which seems to shows proximal sources from the SW (Fig. 3; Borrego *et al*., 2005; Araújo *et al*., 2013). The Terena Formation only has one foliation related to NW-SE subvertical folds, attributed to the third regional tectonic event (D_3; Rocha *et al*., 2009; Moreira *et al*., 2014a).

As mentioned, an upper member with Late Carboniferous age is described in the Terena Formation, which was probably deposited discordantly on top of the Devonian member (Azor *et al*., 2004). This Carboniferous member is also deformed by the regional D_3 event (e.g. Apalategui *et al*., 1987), showing similar structural behaviour to the Cabrela Complex.

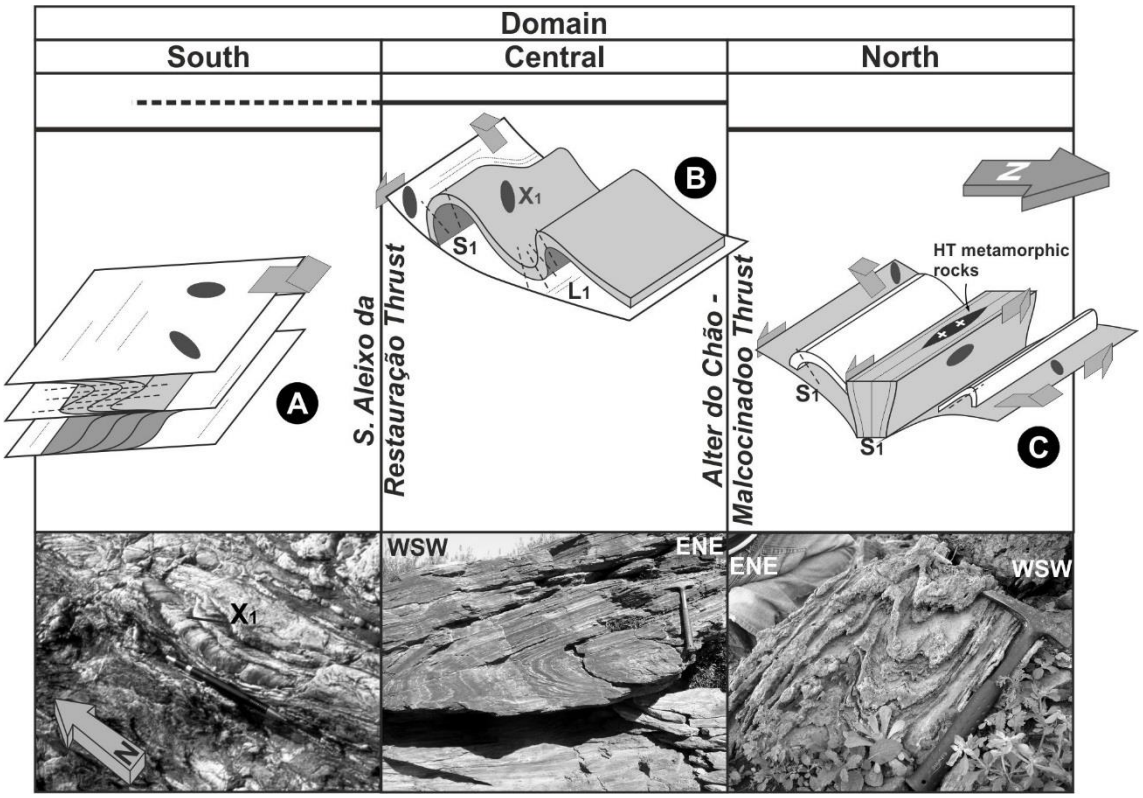

Figure 7 – Devonian structural features of the OMZ:

A – Imbricated complex with top-to-north transport of Moura-Cubito Phyllonitic Complex;

B – Recumbent folds and thrusts facing to southwest from Central Domain;

C – Flower structure of North Domain, rotting in TBCSZ.

In the northernmost domain of the OMZ, a Devonian HT metamorphic event was described, associated to central units of the Tomar-Badajoz-Córdoba Shear Zone (TBCSZ; Fig. 4 and 7C). Geochronological data from mylonite, paragneisses and migmatites (Las Grullas, Sierra Albarrana and Campo Maior Migmatite) show a Middle-Late Devonian age for an early metamorphic event related to this lithospheric scale structure (390-360Ma; Rb/Sr whole rock-muscovite pair García Casquero *et al*., 1988; Ar-Ar in amphiboles Quesada and Dallmeyer, 1994; U/Pb in zircons Pereira *et al*., 2012c). During the D_1, this structure acts as a sinistral transpressive intra-continental shear zone (Burg *et al*., 1981; Abalos and Cusí, 1995; Ribeiro *et al*., 2009), generating the mentioned high-grade metamorphic rocks. The transpressive regime of the TBCSZ presents evidences of strain partition, with generation of a composite flower structure, with a facing to SW in most developed SW branch and a short NE branch facing to NE (Fig. 4; e.g. Ribeiro *et al*., 2009; Romão *et al*., 2010). This thick-skinned structure could be responsible for the Central Domain early deformation episode, with recumbent folds facing to W-SW (Fig. 7B and 7C). The western propagation of this structure is blocked by the Porto-Tomar-Ferreira do

Alentejo Shear Zone, generating in Abrantes region during the D_1 a kilometric scale sheath fold (Fig. 4; Ribeiro *et al*, 2009; Moreira *et al*., 2011).

V.2.6. Proposal for OMZ Geodynamic Evolution during Devonian Times

The first stratigraphic evidence of uplift in the Central and Southern domains of the OMZ is preserved in the Devonian sedimentary record, reflecting most probably the tectonic instability triggered by the subduction beginning, being the Ludlow succession characterized by stable environment sedimentation (Fig. 8A).

The Odivelas Limestone (SW area of the OMZ), with Early-Middle Devonian ages are spatially associated with orogenic volcanism with tholeiitic to calc-alkaline geochemistry (Rebolado Basalts), indicating that basalts were generated in a supra-subduction setting (Fig. 8B; Santos *et al*., 1990; 2013; Silva *et al*., 2011). Indeed, during the Early-Middle Devonian, volcanic processes become active, showing geochemical features that are compatible with proximal volcanic-arc magmatism. This magmatism is developed near the suture zone between South Portuguese Terrane (Ribeiro *et al*, 2007) and the Iberian Autochthonous Terrane (which includes the OMZ, included in North Gondwana Margin), being interpreted as the suture of the SW Iberian Variscan Ocean (Fig. 8B). Preserved Ordovician magmatic rocks with MORB geochemical features are obducted over the OMZ during Devonian times (see below), being interpreted as ophiolite fragments (Pedro *et al*., 2010).

Associated to the volcanism, a reef shallow carbonate sedimentation is developed. The association between tuffites and peri-reef limestones with Emsian-Givetian age (Machado *et al*., 2009; 2010; Moreira *et al*., 2010) clearly shows the association between magmatism and sedimentation. Indeed, Machado *et al*., (2009, 2010) and Moreira and Machado (in press) interpret the Odivelas Limestone as a reef system developed around the top of volcanoes like atolls, in shallow environments. On the volcanic edifices flanks, coeval peri-reef sedimentation occurred related to dismantled reef structures, represented by calciturbite facies.

At the same time, in the Central Domains of the OMZ, the Silurian euxinic sedimentation gives rise to Early Devonian flyschoid, deposited in the Terena syn-tectonic basin (Fig. 8B). The genesis of this basin is probably conditioned by N-S to NNW-SSE recumbent folds, developed during the earlier episodes of Variscan chain edification (Exposito *et al*., 2002; Borrego *et al*., 2005; Araújo *et al*., 2013; Moreira *et al*, 2014a; 2014b). This fact could also explain the anomalous geometry of this trench, with N-S trend in its central segment, and that should have conditioned the shape of the Terena Syncline (Rocha *et al*., 2009; Araújo *et al*., 2013).

The turbiditic nature of Terena Formation with basal facies variation (coarse-grained in the South and fine-grained in the North), the absence of strain accommodation during the first

deformation phase and the presence of syn-tectonic sedimentation (with remobilized volcanics and Silurian sedimentary rocks) show that the deposition of this Formation was conditioned by the presence of an active orogenic environment in the SW of the OMZ (Fig. 8B; Borrego *et al*., 2005; 2006; Borrego, 2009; Araújo *et al*., 2013 and references therein). Also the geochemical data in greywackes from the Terena Formation (Borrego *et al*., 2006; Borrego, 2009) indicates a probable volcanic arc and a recycling orogen provenance for these siliciclastic lithotypes. The proximal Devonian subduction related volcanic-arc magmatism was partially obliterated by BIC, Carboniferous in age (e.g. Jesus *et al*., 2007). The Rebolado Basalts can be considered as relics of OMZ proximal early volcanic arc preserved within BIC.

The significance of Late Silurian-Devonian limestones in the Estremoz-Ferrarias-Barrancos axis are unknown and its spatial association with bimodal magmatic rocks and intense fracturing and fluid circulation its clear, being deformed during D_2 episode. Several hypotheses must be considered:

- they represent (Early?) Devonian discontinuous reef structures developed in the North of the Terena basin, being associated to volcanism. Although the fossiliferous record is fragmentary, preventing its age and stratigraphic precise control, the isotope fingertprint of these limestones are clearly distinct from Odivelas Limestone (Moreira *et al*., 2016), which seems to show that they are not similar in age;
- they represent the Late Silurian-Early Devonian Limestones, similar to *Scyphocrinites* Limestones, Pridoli-Lochkovian in age, described in Valle and Cerrón del Hornillo synclines (Lenz *et al*., 1996; Gutiérrez-Marco and Robardet, 2004). The spatial disposition is not totally concordant with this hypothesis, because in Barrancos, they are spatially associated to Monte das Russianas Formation and the described stratigraphic sequence from Early Silurian until Emsian are continuous and well controlled based on paleontological content (Piçarra, 2000);
- they are olistholiths, remobilized during early deformation episodes, which includes Late Silurian-Devonian limestones and bimodal magmatic rocks, being associated to breccias. In this case, two possibilities arise: (a) they represent an intraformational breccia within the Terena Basin, as described by Bard (1965) in Alamo Breccia (Robardet and Gutiérrez-Marco, 2004) or (b) they are included in a non-described unit, which could be discordant over the Cambrian to Devonian Formations, or;
- they represent Late Devonian to Early Carboniferous limestones, which are described in some Carboniferous basins in North and Central Domains of the OMZ, as in Santos de Maimona or Guadiato (Azor *et al*., 2004; Armendáriz *et al*., 2008) basins and in Valle and Cerron del Hornillo synclines.

Although, all these possibilities could be tested, none of them could be excluded at this time. However, the most probable hypotheses are (a) the presence of Early Devonian discontinuous reef structures developed at north of Terena Basin, which is also compatible to the existence of carbonated cement of Monte das Russianas Formation sandstones (North of Terena Basin), and (b) the remobilized nature of these limestones, being contained in a non-mature syn-tectonic unit. It is important to emphasize, that the Bencatel-Ferrarias-Barrancos alignement (Fig. 6A), in Spain, intersects the Villanueva del Fresno and Cheles limestones, interpreted as Cambrian klippes related to D_1 fold and thrust episodes (Vegas and Moreno, 1973; Moreno and Vegas, 1976). This seems to indicate that these limestones could also be remobilized (possibly sedimentary). In both hypothesis, the presence of these limestones seems to constrain temporally the beginning of deformation episodes as Early Devonian.

A Middle Devonian gap is described in the OMZ (Oliveira *et al*., 1991; Robardet and Gutiérrez-Marco, 1990; 2004), with the exception of the Eifelian-Givetian Odivelas and Pedreira de Engenharia Limestone (Boogaard, 1972; Machado *et al*., 2009; 2010; Moreira and Machado, in press). This could be interpreted as related to a generalized uplift of OMZ during this period, possibly related to the subduction process, creating a regional scale hiatus, in some cases marcated by an angular unconformity or a paraconformity.

The metamorphic and structural pattern during Devonian times is clearly controlled by the SW Iberian Oceanic Suture and the 1st order TBCSZ. Indeed, in the South Domain, near the suture, a HP-LT path is recorded, reaching eclogite facies conditions (e.g. Fonseca *et al*., 1999; Booth-Rea *et al*., 2006; Pedro *et al*., 2013; Rubio Pascual *et al*., 2013). Geochronological data limits the baric peak of this HP-LT metamorphism at 370 Ma (Moita *et al*., 2005b), materializing an active subduction process (Fig. 8B and 8C).

The majority of HP metamorphic rocks are spatially associated to the Moura-Cubito Phyllonitic Complex, interpreted as an imbricated complex resulting from the emplacement of this pile of slivers as a consequence of the progression of subduction / obduction process that generates the SW Iberian ophiolite complexes (Araújo *et al*., 2005; 2013; Ribeiro *et al*., 2010).

The age of the HP metamorphic rocks contained in Moura-Cubito Phyllonitic complex is poorly constrained. As a Late Devonian age was obtained in Alvito and Safira HP metamorphic rocks (Moita *et al*., 2005b) and the Odivelas Limestones (Early-Middle Devonian in age) are also affected by top-to-north thrusts (Moreira *et al*., 2010), the emplacement of ophiolite complexes and, consequently, the Moura-Cubito Phyllonitic Complex, must also be Middle-Late Devonian (Fig. 8C). On top of Moura-Cubito Phyllonitic Complex, the Mississippian Toca da Moura-Cabrela Complexes are deposited (Araújo *et al*., 2005; 2013). This constrain the maximum age for the installation of the Phyllonitic Complex as pre-Carboniferous, which is compatible with the

absence of early deformation episodes in Toca da Moura and Cabrela Carboniferous Complexes (Ribeiro, 1983; Oliveira *et al*., 2013b). The emplacement of the Moura-Cubito Phyllonitic Complex could be related with the last subduction pulses of the SW Iberia Variscan Ocean and, consequently, the beginning of the collision process during Mississippian (e.g. Moreira *et al*., 2014a).

In the North Domain of the OMZ, the TBCSZ is responsible by the strain accommodation of early Variscan deformation. Geochronological data show that during Devonian times this lithospheric scale shear zone was active (at least since 390-380 Ma; García Casquero *et al*., 1988; Quesada and Dallmeyer, 1994; Pereira *et al*., 2012c), as a sinistral transpressive intra-continental shear zone (Fig. 8B and 8C; Ribeiro *et al*., 2009). The recumbent folds and thrusts with transport to SW-W quadrant of the Central Domain roots in this lithospheric scale shear zone.

During Late Devonian times (Fig. 8D), in the Central Domain of the OMZ, a calc-alkaline to shoshonitic magmatism was established, preserved in the Veiros-Vale Maceira and Campo Maior Massifs (Costa *et al*., 1990; Moita *et al*, 2005a; Carrilho Lopes *et al*., 2005). This suggests that volcanic-arc magmatism related to subduction activity should have migrated to the North and extends until Upper Devonian (ca. 365 Ma), as suggested by the age of the shoshonitic magmatism (Moita *et al*., 2005a; Carrilho Lopes *et al*., 2005; Araújo *et al*., 2013).

Indeed, the subduction of the SW Iberia Variscan Ocean beneath the Iberian Autochthonous Terrane (North Gondwana Margin) should have polarity to the North (current coordinates), with proximal tholeiitic to calc-alkaline volcanic-arc represented by the Rebolado Basalts and the distal shoshonitic volcanism represented by Veiros-Vale Maceira and Campo Maior Massifs.

Thus, the Rebolado basalts, the Veiros-Vale Maceira and the Campo Maior Massifs represent relics of early volcanic arc magmatism in the OMZ. Part of this earlier Variscan magmatism, associated to the first episodes of the Variscan Orogeny, was obliterated (eroded or melted?) during Carboniferous times. Some indirect evidences of Devonian magmatic episode are also preserved through Early to Late Devonian detrital zircons present in Early Carboniferous syn-orogenic basins in OMZ and in SPZ (Braid *et al*., 2011; Pereira *et al*., 2012b; 2013; Rodrigues *et al*., 2015; Pérez-Cáceres *et al*., 2016b).

While in OMZ the generation of HP-LT metamorphic rocks and the volcanic-arc are a consequence of subduction progression, to the South of suture zone (now marked by Ferreira-Ficalho-Almonaster Shear zone) begins the deposition of siliciclastic sediments, generating an accretionary prism. The Middle-Late Devonian uplift of the orogenic chain induces the erosional processes that will feed these basin. These sediments could be represented in Pulo do Lobo Domain by the Early Frasnian Ribeira de Limas and Atalaia Formations and by Pulo do Lobo

Formation, older than previous ones, but with unconstrained age (Oliveira *et al*., 1991; 2013; Pereira *et al*., 2006b). However, some authors attribute an exotic nature to the Pulo do Lobo Domain, being still a matter of debate (e.g. Braid *et al*., 2011).

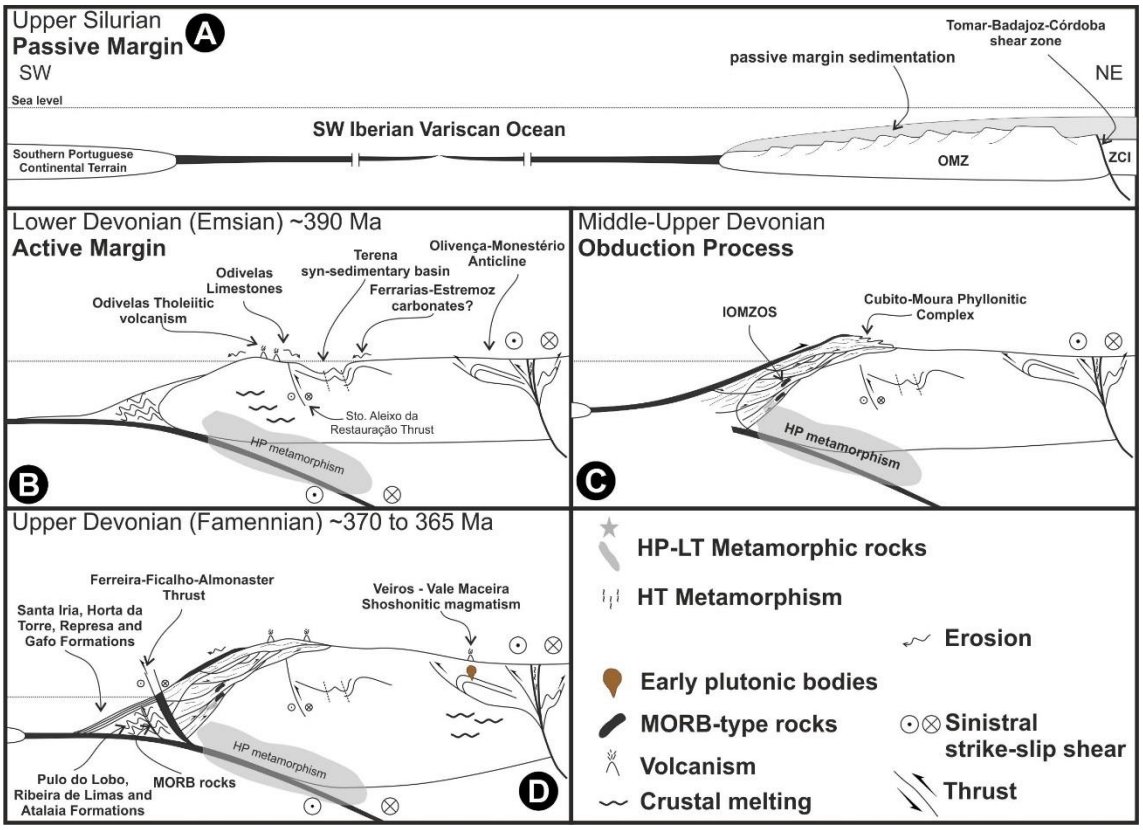

Figure 8 – Geodynamic evolution of OMZ during last episodes of passive margin setting (A) and early convergent phases of the Variscan Cycle (B to D).

With the evolution of the subduction, these sedimentary units were buried, deformed and metamorphosed. These lowermost formations attained higher metamorphic grade conditions, presenting multiphase deformation episodes in comparison with the top ones, as expected in an accretionary prism (Fig. 8D; Eden, 1991; Ribeiro *et al*., 2007, 2010). The early deformation phases preserved in all these metasedimentary flysch-like sequences took place before Middle-Late Famennian (Oliveira *et al*., 1991; 2013a). The Santa Iria, Horta da Torre, Represa and Gafo Formations, with Famennian age, cover unconformably the previous ones, constraining the early deformation episode (Oliveira *et al*, 2013a and references therein). These data are compatible with a subduction beginning at Early Devonian times.

V.2.7. Final Remarks

The review of data shows the presence of early deformation processes during Devonian times, being interpreted as related to subduction of the SW Iberia Variscan Ocean. This subduction probably initiated during Early Devonian times, more precisely during early Pragian times (ca. 410 Ma). The subduction related processes was active until the Late Devonian (latest Famennian). During Famennian-Tournaisian times (ca. 360-355 Ma) a change of sedimentation, magmatism and type of metamorphism took place (Quesada *et al*., 1990; Quesada, 1990; Oliveira *et al*., 1991), which could be interpreted as the result of a transitional step between subduction and the beginning of collisional processes.

During Devonian a North forward migration of volcanic-arc magmatism is expressed, being in agreement with spatial disposition of metamorphic rocks, with HP rocks near the suture, in South Domain of OMZ. The almost absence of Middle Devonian sedimentary rocks is in agreement with general uplift of OMZ, having started yet in Early Devonian times, as reported by stratigraphic record.

The Devonian oblique subduction generates a general sinistral transpressive regime (Oliveira *et al*., 1991; Dias *et al*., 2016; Pérez-Cáceres *et al*., 2016a), which is responsible by the reactivation of TBCSZ as a sinistral transpressive structure with intense strain partition in a thick-skin regime (Ribeiro *et al*., 2009). The SW thrusting and early recumbent folds developed during early deformation episodes in Central Domains could be related with the previous mentioned general framework.

References

Abalos, B., Cusí, J. D. (1995). Correlation between seismic anisotropy and major geological structures in SW Iberia: a case study on continental lithosphere deformation. Tectonics, 14, 1021-1040. DOI: 10.1029/95TC01204

Andrade, A., Pinto, A., Conde, L. (1976). Sur la géologie du Massif de beja: Observations sur la transversale d`Odivelas. Comun. Serv. Geol. Portugal, 60, 171-202.

Andrade, A.A.S. (1983). Contribution à l'analyse de la suture hercynienne de Beja (Portugal): perspectives métallogéniques. Laboratoire de Métallogénie I Nancy, Institut National Polytechnique de Lorraine. PhD thesis, 137 p.

Apalategui, O., Quesada, C. (1987). Transversal geologica Zona Ossa-Morena. Field trip Guidebook, 90p.

Apalategui, O., Contreras Vázquez, F., Eguiluz, L., (1987). Mapa Geologico de España escala 1: 50.000. Hoja N° 918 (Sant Olalla del Cala) and memoria descritiva (1990). IGME.

Araújo, A., Fonseca, P., Munhá, J., Moita, P., Pedro, J., Ribeiro, A. (2005). The Moura Phyllonitic complex: An accretionary complex related with obduction in the Southern Iberia Variscan Suture. Geodin Acta, 18(5), 375-388. DOI: 10.3166/ga.18.375-388

Araújo, A., Piçarra, J., Borrego, J., Pedro, J., Oliveira, J.T. (2013). As regiões central e sul da Zona de Ossa-Morena. In: Dias, R., Araújo, A., Terrinha, P., Kullberg, J.C. (Ed.) Geologia de Portugal (Vol. I), Escolar Editora, Lisboa, 509-549

Armendáriz, M., López Guijarro, R., Quesada, C., Pin, C., Bellido, F. (2008). Genesis and evolution of a syn-orogenic basin in transpression: Insights from petrography, geochemistry and Sm–Nd systematics in the Variscan Pedroches basin (Mississippian, SW Iberia). Tectonophysics, 461, 395–413. DOI: 10.1016/j.tecto.2008.02.007

Azor, A., Expósito, F., González Lodeiro, F., Simancas, J.F., Martinez Poyatos, D. (2004). Sucesión sinorogénica. In: Vera, J.A. (Ed.) Geología de España, Sociedad Geologica de España, 172-173.

Bard, J.P. (1965). Introduction à la geologie de la chaine hercinienne dans la Sierra Morena occidentale (Espagne). Rev Geogr Phys Geol Dynam, 7 (4), 323-337.

Boogaard, M. (1972). Conodont faunas from Portugal and Southwestern Spain. Part 1: A Middle Devonian fauna from near Montemor-o-Novo. Scripta Geologica, 13, 1-11.

Boogaard, M. (1983). Conodont faunas from Portugal and southwestern Spain. Part 7. A Frasnian conodont fauna near the Estação de Cabrela (Portugal). Scripta Geologica, 69, 1-17.

Boogaard, M., Vazquez, F. (1981). Conodont faunas from Portugal and southwestern Spain. Part 5: Lower Carboniferous conodonts at Santa Olalla de Cala (Spain). Scripta Geologica, 61, 1-8.

Booth-Rea, G., Simancas, J.F., Azor, A., Azañón, J. M., González Lodeiro, F., Fonseca, P. (2006). HP–LT Variscan metamorphism in the Cubito-Moura schists (Ossa-Morena Zone, southern Iberia). C. R. Geosci., 338, 1260– DOI: 10.1016/j.crte.2006.08.001

Borrego, J., Araújo, A., Fonseca, P., Ribeiro, M. A. (2006). Estudos de Proveniência em litologias detríticas do Sinclinal de Terena (ZOM): tectónica e evolução geodinâmica durante o Silúrico e o Devónico inferior. VII Congresso Nacional de Geologia, Estremoz (Portugal), abstract book, 53-56.

Borrego, J., Araújo, A., Fonseca, P.E. (2005). A geotraverse through the south and central sectors of the Ossa-Morena Zone in Portugal (Iberian Massif). In: Carosi, R., Dias, R., Iacopini, D., Rosenbaum, G. (Ed.) The southern Variscan belt, J. Virtual Explorer, 19, 10. DOI: 10.3809/jvirtex.2005.00117

Borrego, J. (2009). Cartografia Geológico-Estrutural de um sector da Zona de Ossa-Morena (Subsector de Estremoz – Barrancos-Ficalho) e sua interpretação Tectónica. PhD Thesis (unpublished), Évora University, Portugal, 479 p.

Braid, J.A., Murphy, J.B., Quesada, C., Mortensen, J. (2011). Tectonic escape of a crustal fragment during the closure of the Rheic Ocean: U–Pb detrital zircon data from the Late Palaeozoic Pulo do Lobo and South Portuguese zones, southern Iberia. J Geol Soc London 168:383-392. DOI: 10.1144/0016-76492010-104

Burg, J. P., Iglesias, M., Laurent, P., Matte, P., Ribeiro, A. (1981). Variscan intracontinental deformation: the Coimbra-Córdoba Shear zone (SW Iberian Peninsula). Tectonophysics, 78, 161-177. DOI: 10.1016/0040-1951(81)90012-3

Carrilho Lopes, J., Munhá, J., Tassinari, C., Pin C. (2005). Petrologia e Geocronologia (Sm-Nd) do Maciço de Campo Maior (Alentejo, Portugal Central). Comunicações Geológicas, 92, 05-30.

Coelho, A., Gonçalves, F. (1970). Rocha hiperalcalina de Estremoz. Bol. Soc. Geol. Portugal, XVII, 181-185.

Conde, L.N., Andrade, A.A.S. (1974). Sur la faune meso et/ou néodévonienne des calcaires du Monte das Cortes, Odivelas (Massif de Beja). Memórias e Notícias, Univ. Coimbra, 78, 141-146.

Costa, D., Viana, A., Munhá, J. (1990). Petrologia e geoquímica dos maciços de Veiros e Vale Maceira. In: Abstrats of the VIII Semana de Geoquímica, Lisboa.

Dias, R., Ribeiro, A., Romão, J., Coke, C., Moreira, N. (2016). A review of the Arcuate Structures in the Iberian Variscides; Constraints and Genetic Models. Tectonophysics, 681C, 170-194. DOI: 10.1016/j.tecto.2016.04.011

Eden, C. (1991). Tectonostratigraphic analysis of the northern extent of the oceanic exotic terrane, northwestern Huelva province, Spain. PhD Thesis, University of Southampton, 223 p.

Expósito, I., Simancas, J. F., González Lodeiro, F., Azor, A., Martínez Poyatos D. J. (2002). Estructura de la mitad septentrional de la zona de Ossa-Morena: Deformación en el bloque inferior de un cabalgamiento cortical de evolución compleja. Rev. Soc. Geol. Esp., 15, 3–14.

Fonseca, P., Fonseca, M., Munhá, J. (2004). Ocorrência de Aragonite em Mármores da Região de Alvito-Viana do Alentejo (Zona de Ossa Morena): Significado geodinâmico. Cad. Lab. Xeo. Laxe, 29, 79-96.

Fonseca, P., Munhá, J., Pedro, J., Rosas, F., Moita, P., Araújo, A., Leal, N. (1999). Variscan Ophiolites and High-Pressure Metamorphism in Southern Ibéria. Ophioliti, 24(2), 259-268. DOI: 10.4454/ofioliti.v24i2.106

García Casquero, J.L., Priem, H.N.A.I., Boelrijk, N.A.I.M., Chacón, J. (1988). Isotopic dating of the mylonitization of the Azuaga Group in the Badajoz-Córdoba belt, SW Spain. Geol. Rundsch. 77(2), 483-489. DOI: 10.1007/BF01832393

García-Alcalde J. L., Carls P., Pardo Alonso M. V., Sanz López J., Soto F., Truyols-Massoni M., Valenzuela-Ríos J. (2002). Devonian. In: Gibbons W., Moreno T. (eds) The Geology of Spain. Geological Society, London, 67–91.

Giese, U., Hoegen, R. von, Hollmann, G., Walter, R. (1994). Geology of the southwestern Iberian Meseta I. The Palaeozoic of the Ossa-Morena Zone north and south of the Olivenza-Monesterio Anticline (Huelva province, SW Spain). Neues Jahrbuch für Geologie und Paläontologie, Abhandlungen, 192, 293-331.

Gonçalves, F. (1972). Geological Map of Portugal, scale 1:50 000, 36-B (Estremoz), Serviços Geológicos de Portugal, Lisboa.

Gutiérrez-Marco, J.C., and Robardet, M. (2004). Ordovícico-Silúrico-Devónico inferior. In: Vera, J.A. (Eds.) Geología de España, Sociedad Geologica de España, 170-172.

Jesus, A.P., Munhá, J., Mateus, A., Tassinari, C., Nutman, A.P. (2007). The Beja layered gabbroic sequence (Ossa-Morena Zone, Southern Portugal): geochronology and geodynamic implications. Geodin Acta, 20, 139-157. DOI: 10.3166/ga.20.139-157

Jesus, A.P., Mateus, A., Munhá, J.M., Tassinari, C.G.C., Bento dos Santos, T.M., Benoit, M. (2016). Evidence for underplating in the genesis of the Variscan synorogenic Beja Layered Gabbroic Sequence (Portugal) and related mesocratic rocks. Tectonophysics, 683(30), 148-171. DOI: 10.1016/j.tecto.2016.06.001

Lenz, A.C., Robardet, M., Gutierrez-Marco, J.C., Picarra, J.M. (1996). Devonian graptolites from southwestern Europe: a review with new data. Geological Journal, 31, 349-358. DOI: 10.1002/(SICI)1099-1034(199612)31:4<349::AID-GJ714>3.0.CO;2-K

Linnemann, U., Pereira, M.F., Jeffries, T., Drost, K., Gerdes, A. (2008). Cadomian Orogeny and the opening of the Rheic Ocean: new insights in the diacrony of geotectonic processes constrained by LA–ICP–MS U–Pb zircon dating (Ossa-Morena and Saxo-Thuringian Zones, Iberian and Bohemian Massifs). Tectonophysics, 461, 21–43. DOI: 10.1016/j.tecto.2008.05.002

LNEG (2010). Geological map of Portugal at 1:1.000.000, 3rd edition, Laboratório Nacional de Energia e Geologia, Lisboa.

Lopes, J.L. (2003). Contribuição para o conhecimento Tectono-Estratigráfico do Nordeste Alentejano, transversal Terena-Elvas. Implicações económicas no aproveitamento de rochas ornamentais existentes na região (Mármores e Granitos). PhD Thesis (unpublished), Évora University, Portugal 568 p.

Machado, G., Hladil, J. (2010). On the age and significance of the limestone localities included in the Toca da Moura volcano-sedimentary Complex: preliminary results. In: Santos A, Mayoral E, Melendez G, Silva CMD, Cachão M (Ed), III Congresso Iberico de Paleontologia / XXVI Jornadas de la Sociedad Espanola de Paleontologia, Lisbon, Portugal. Publicaciones del Seminario de Paleontologia de Zaragoza, 9, 153-156.

Machado, G., Hladil, J., Koptikova, L., Fonseca, P.E., Rocha, F.T., Galle, A. (2009). The Odivelas Limestone: Evidence for a Middle Devonian reef system in western Ossa-Morena Zone. Geol Carpath, 60(2), 121-137.

Machado, G., Hladil, J., Koptikova, L., Slavik, L., Moreira, N., Fonseca, M., Fonseca, P.E. (2010). An Emsian-Eifelian Carbonate-Volcaniclastic Sequence and the possible Record of the basal choteč event in western Ossa-Morena Zone, Portugal (Odivelas Limestone). Geol Belg,, 13, 431-446.

Matte, P. (2001). The Variscan collage and orogeny (480-290 Ma) and the tectonic definition of the Armorica microplate: a review. Terra Nova, 13, 122-128. DOI: 10.1046/j.1365-3121.2001.00327.x

McArthur, J.M., Howarth, R.J., Shields, G.A. (2012). Strontium Isotope Stratigraphy. In: Gradstein FM, Ogg JG, Schmotz MD, Ogg GM (Ed), A Geologic Time Scale 2012 (Chapter 7), Elsevier, 127-144.

Moita, P., Munhá, J., Fonseca, P.E., Tassinari, C., Araújo, A., Palácios, T. (2005a). Dating orogenic events in Ossa-Morena Zone. In: Abstract of the XIV Semana de Gequimica/VIII Congresso de geoquimica dos Paises de Lingua Portuguesa, Aveiro, 2, 459-461.

Moita, P., Munhá, J., Fonseca, P., Pedro, J., Tassinari, C., Araújo, A., Palacios, T. (2005b). Phase equilibria and geochronology of ossa morena eclogites. In: Abstracts of the XIV Semana de Gequimica/VIII Congresso de geoquimica dos Paises de Lingua Portuguesa, Aveiro, 2, 471-474.

Moreira, N., Machado, G. (in press). Devonian sedimentation in Western Ossa-Morena Zone and its geodynamic significance. In Quesada. C., Oliveira, J.T. (Eds.), The Geology of Iberia: a geodynamic approach. Springer (Berlin), Regional Geology Review series.

Moreira, N., Machado, G., Fonseca, P.E., Silva, J.C., Jorge, R.C.G.S., Mata, J. (2010). The Odivelas Palaeozoic volcano-sedimentary sequence: Implications for the geology of the Ossa-Morena Southwestern border. Comunicações Geológicas, 97, 129-146.

Moreira, N., Pedro, J., Dias, R., Ribeiro, A., Romão, J. (2011). Tomar-Badajoz-Córdoba shear zone in Abrantes sector; the presence of a kilometric sheath fold?. Deformation mechanisms, Rheology and Tectonics, DRT 2011 Meeting, Oviedo, Espanha, 90.

Moreira, N., Araújo, A., Pedro, J., Dias, R. (2014a). Evolução geodinâmica da Zona de Ossa-Morena no contexto do SW Ibérico durante o Ciclo Varisco. Comunicações Geológicas, 101 (I), 275–278.

Moreira, N., Dias, R., Pedro, J.C., Araújo, A. (2014b). Interferência de fases de deformação Varisca na estrutura de Torre de Cabedal; sector de Alter-do-Chão – Elvas na Zona de Ossa-Morena. Comunicações Geológicas, 101 (I), 279-282.

Moreira, N., Pedro, J., Santos, J.F., Araújo, A., Romão, J., Dias, R., Ribeiro, A., Ribeiro, S., Mirão, J. (2016). 87Sr/86Sr ratios discrimination applied to the main Palaeozoic carbonate sedimentation in Ossa-Morena Zone. In: IX Congreso Geológico de España (special volume). Geo-Temas, 16(1), 161-164. ISSN 1576-5172.

Moreno, F., Vegas, R. (1976). Tectónica de las séries ordovícias y siluricas en la región de Villanueva del Fresno. Estudios geológicos, 32, 47-52.

Nance, R.D., Gutierrez-Alonso, G., Keppie, J.D., Linneman, U., Murphy, J.B., Quesada, C., Skrachan, R; Woodcock, V., (2012). A brief history of the Rheic Ocean. Geoscience Frontiers, 3(2), 125- 135. DOI: 10.1016/j.gsf.2011.11.008

Oliveira, J.T., Oliveira, V., Piçarra, J. (1991). Traços gerais da evolução tectono-estratigráfica da Zona de Ossa-Morena, em Portugal. Comun. Serv. Geol. Portugal, 77, 3-26.

Oliveira, J. T., Relvas, J., Pereira, Z. Matos, J., Rosa, C. Rosa, D. Munhá, J. Fernandes, P. Jorge, R., Pinto, A. (2013a). Geologia da Zona Sul Portuguesa, com ênfase na estratigrafia, vulcanologia física, geoquímica e mineralizações da Faixa Piritosa. In: Dias, R., Araújo, A., Terrinha, P., Kullberg, J.C. (Ed.), Geologia de Portugal (Vol. I), Escolar Editora, Lisboa, 673-765.

Oliveira, J.T., Relvas, J., Pereira, Z., Munhá, J., Matos, J., Barriga, F., Rosa, C. (2013b). O Complexo Vulcano-Sedimentar de Toca da Moura-Cabrela (Zona de Ossa Morena): evolução tectono-estratigráfica e mineralizações associadas. In: Dias, R., Araújo, A., Terrinha, P., Kullberg, J.C. (Ed.), Geologia de Portugal (Vol. I), Escolar Editora, Lisboa, 621-645.

Palacios González, M.J., Palacios, T., Gómez Valenzuela, J.M. (1990). Trilobites y goniatited de la cuenca carbonífera de los Santos de Maimona: deducciones bioestratigráficas. Geogaceta, 8, 66-67.

Pedro, J.C., Araújo, A., Tassinari, C., Fonseca, P.E., Ribeiro, A. (2010). Geochemistry and U-Pb zircon age of the Internal Ossa-Morena Zone Ophiolite Sequences: a remnant of Rheic Ocean in SW Iberia. Ofioliti, 35(2), 117-130. DOI: 10.4454/ofioliti.v35i2.390

Pedro, J., Araújo, A., Fonseca, P., Munhá, J., Ribeiro, A., Mateus, A. (2013). Cinturas Ofiolíticas e Metamorfismo de Alta Pressão no Bordo SW da Zona de Ossa-Morena. In: Dias, R., Araújo, A., Terrinha, P., Kullberg, J.C. (Ed.), Geologia de Portugal (Vol. I), Escolar Editora, Lisboa, 647-671.

Perdigão, J.C., Oliveira, J.T., Ribeiro, A. (1982). Notícia explicativa da folha 44-B (Barrancos) da Carta Geológica de Portugal à escala 1:50 000, Serviços Geológicos de Portugal, Lisboa.

Pereira, M.F., Solá, A.R., Chichorro, M., Lopes, L., Gerdes, A., Silva, J.B. (2012a). North-Gondwana assembly, break up and paleogeography: U–Pb isotope evidence from detrital and igneous zircons of Ediacaran and Cambrian rocks of SW Iberia. Gondwana Res, 22(3–4), 866-881. DOI: 10.1016/j.gr.2012.02.010

Pereira, M.F., Chichorro, M., Johnston, S.T., Gutiérrez-Alonso, G., Silva, J.B., Linnemann, U., Drost, K. (2012b). The missing Rheic Ocean magmatic arcs: Provenance analysis of Late Palaeozoic sedimentary clastic rocks of SW Iberia. Gondwana Res, 22(3-4), 882-891. DOI: 10.1016/j.gr.2012.03.010

Pereira, M.F., Silva, J.B., Chichorro, M., Ordóñez-Casado, B., Lee, J.K.W., Williams, I.S. (2012c). Early Carboniferous wrenching, exhumation of high-grade metamorphic rocks and basin instability in SW Iberia: constraints derived from structural geology and U-Pb and 40Ar-39Ar geochronology. Tectonophysics, 558-559, 28-44. DOI: 10.1016/j.tecto.2012.06.020

Pereira, M.F., Ribeiro, C., Vilallonga, F., Chichorro, M., Drost, K., Silva, J.B., Albardeiro, L., Hofmann, M., Linnemann, U. (2013). Variability over time in the sources of South-Portuguese Zone turbidites: evidence of denudation of different crustal blocks during the assembly of Pangaea. International Journal of Earth Sciences, 103 (5), 1453-1470. DOI: 10.1007/s00531-013-0902-8

Pereira, M.F., Chichorro, M., Lopes, C., Solá, A.R., Silva, J.B., Hofmann, M., Linnemann, U. (2014). Provenance analysis of Lower Palaeozoic siliciclastic rocks of SW Iberia (Ossa-Morena Zone): distal shelf deposition in the North Gondwanan passive margin. In: Rocha, P., Pais, J., Kullberg, J.C., Finney, S. (Eds.), First International Congress on Stratigraphy – At the cutting edge of Stratigraphy. STRATI2013, Elsevier, 747-751. DOI: 10.1007/978-3-319-04364-7_141

Pereira, Z., Oliveira, J.T. (2003). Estudo palinostratigráfico do sinclinal da Estação de Cabrela. Implicações tectonostratigráficas. Cienc. Terra UNL Lisboa, 5, 118–119.

Pereira, Z., Piçarra, J.M., Oliveira, J.T. (1999). Lower Devonian palynomorphs from the Barrancos region, Ossa Morena Zone, Portugal. Bolletino della società paleontologica italiana, 38 (2-3), 239-245.

Pereira, Z., Oliveira, V., Oliveira, J.T. (2006a). Palynostratigraphy of the Toca da Moura and Cabrela Complexes, Ossa Morena Zone, Portugal. Geodynamic implications. Rev Palaeobot Palyno, 139, 227-240. DOI: 10.1016/j.revpalbo.2005.07.008

Pereira, Z., Oliveira, V., Oliveira, J.T. (2006b). Palynostratigraphy of the Toca da Moura and Cabrela Complexes, Ossa Morena Zone, Portugal. Geodynamic implications. Review of Palaeobotany and Palynology, 139, 227-240. DOI: 10.1016/j.revpalbo.2005.07.008

Pérez-Cáceres, I., Simancas, J.F., Martínez Poyatos, D., Azor, A., Lodeiro, F.G. (2016a). Oblique collision and deformation partitioning in the SW Iberian Variscides. Solid Earth, 7, 857–872. DOI: 10.5194/se-7-857-2016

Pérez-Cáceres, I., Poyatos, D.M., Simancas, J.F., Azor, A. (2016b). Testing the Avalonian affinity of the South Portuguese Zone and the Neoproterozoic evolution of SW Iberia through detrital zircon populations, Gondwana Research. DOI:10.1016/j.gr.2016.10.010

Piçarra, J.M., Le Meen, J. (1994). Ocorrência de crinóides em mármores do Complexo Vulcano-Sedimentar Carbonatado de Estremoz: implicações estratigráficas. Comunicações do Instituto Geológico e Mineiro, 80, 15-25

Piçarra, J.M., Gutiérrez-Marco, J. C., Sarmiento, G. N., Rábano, I. (2009). Silurian of the Barrancos-Hinojales domain of SW Iberia: a contribution to the geological heritage of the Barrancos area (Portugal) and the Sierra de Aracena-Picos de Aroche Natural Park (Spain), in: Corriga, M.G., Piras, S. (Eds.), Time and Life in the Silurian: a multidisciplinary approach. Rendiconti della Società Paleontologica Italiana, 3 (3), 321-322.

Piçarra, J.M., Sarmiento, G.N., Gutiérrez-Marco, J.C. (2014). Geochronological vs. Paleontolgical dating of the Estremoz Marbles (OMZ)-new data and reappraisal. Gondwana 15 conference, Madrid. Abstract book. 140.

Piçarra, J.M. (2000). Stratigraphical study of the Estremoz-Barrancos sector, Ossa-Morena Zone, Portugal. Middle Cambrian?-Lower Devonian Lithostratigraphy and Biostratigraphy. PhD Thesis (unpublished), Évora University, vol.1, 268p.

Piçarra, J.M., Sarmiento, G. (2006). Problemas de posicionamento estratigráfico dos Calcários Paleozóicos da Zona de Ossa Morena (Portugal). In: Abstract book of the VII Congresso Nacional de Geologia, vol. II, 657-660.

Pin, C., Fonseca, P.E., Paquette, J.L., Castro, P., Matte, Ph. (2008). The ca. 350 Ma Beja Igneous Complex: a record of transcurrent slab break-off in the Southern Iberia Variscan Belt? Tectonophysics, 461, 356–377. DOI: 10.1016/j.tecto.2008.06.001

Ponce, C., Simancas, J.F., Azor, A., Martínez Poyatos, D., Booth-Rea, G., Expósito, I. (2012). Metamorphism and kinematics of the early deformation in the Variscan suture of SW Iberia, J. Metamorph. Geol., 30, 625–638. DOI: 10.1111/j.1525-1314.2012.00988.x

Quesada, C. (1990). Introduction of the Ossa-Morena Zone (part V). In: Dallmeyer, R.D., Martínez García, E. (Ed.), Pre-Mesozoic geology of Iberia, Springer-Verlag, Berlin, 249-251.

Quesada, C. (1991). Geological constraints on the Paleozoic tectonic evolution of tectonostratigraphic terranes in the Iberian Massif. Tectonophysics, 185, 225-245. DOI: 10.1016/0040-1951(91)90446-Y

Quesada, C., Dallmeyer, R.D. (1994). Tectonothermal evolution of the Badajoz-Cordóba shear zone (SW Iberia): characteristics and 40Ar/ 39Ar mineral age constraints. Tectonophysics, 231, 195-213. DOI: 10.1016/0040-1951(94)90130-9

Quesada, C., Robardet, M., Gabaldón, V. (1990). Synorogenic phase (Upper Devonian-Carboniferous- Lower Permian). In: Dallmeyer, R.D., Martínez, García E. (Ed.), Pre-Mesozoic geology of Iberia, Springer-Verlag, Berlin, 249-251.

Ribeiro, A. (1983). Relações entre formações do Devónico superior e o Maciço de Évora na região de Cabrela (Vendas Novas). Comun. Serv. Geol. Portugal, 69(2), 267-269.

Ribeiro, A., Munhá, J., Fonseca, P.E., Araújo, A., Pedro, J., Mateus, A., Tassinari, C., Machado, G., Jesus, A., (2010). Variscan Ophiolite Belts in the Ossa-Morena Zone (Southwest Iberia): geological characterization and geodynamic significance. Gondwana Res, 17, 408-421. DOI: 10.1016/j.gr.2009.09.005

Ribeiro, A., Munhá, J., Dias, R., Mateus, A., Pereira, E., Ribeiro, L., Fonseca, P., Araújo, A., Oliveira, T., Romão, J., Chaminé, H., Coke, C., Pedro, J. (2007). Geodynamic evolution of the SW Europe Variscides. Tectonics, 26(6). DOI: 10.1029/2006TC002058

Ribeiro, A., Munhá, J., Mateus, A., Fonseca, P., Pereira, E., Noronha, F., Romão, J., Rodrigues, J.F., Castro, P., Meireles, C., Ferreira, N. (2009). Mechanics of thick-skinned Variscan overprinting of Cadomian basement (Iberian Variscides). Comptes Rendus Geoscience, 341(2-3), 127-139. DOI: 10.1016/j.crte.2008.12.003

Robardet, M., Groos-Uffenorde, H. Gandl, J., Racheboeuf, P.R. (1991). Trilobites et Ostracodes du Dévonien Inferieur dela Zone D'Ossa-Morena (Espagne). Geobios, 24(3), 333-348.

Robardet, M., Gutiérrez-Marco, J.C. (1990). Passive margin phase (Ordovician-Silurian-Devonian). In: Dallmeyer RD, Martínez García E (Ed), Pre-Mesozoic geology of Iberia, Springer-Verlag, Berlin, 249-251.

Robardet, M., Gutiérrez-Marco, J.C. (2004). The Ordovician, Silurian and Devonian sedimentary rocks of the Ossa-Morena Zone (SW Iberian Peninsula, Spain). J Iber Geol, 30, 73-92.

Rocha, R., Araújo, A., Borrego, J., Fonseca, P. (2009). Transected folds with opposite patterns in Terena Formation (Ossa Morena Zone, Portugal): anomalous structures resulting from sedimentary basin anisotropies. Geodinamica Acta, 22(4), 157-163. DOI: 10.3166/ga.22.157-163

Rodrigues, B., Chew, D.M., Jorge, R.C.G.S., Fernandes, P., Veiga-Pires, C., Oliveira, J.T. (2015). Detrital zircon geochronology of the Carboniferous Baixo Alentejo Flysch Group (South Portugal); Constraints on the provenance and geodynamic evolution of the South Portuguese Zone, J. Geol. Soc. London. DOI: 10.1144/jgs2013-084.

Romão, J., Ribeiro, A., Pereira, E., Fonseca, P., Rodrigues, J., Mateus, A., Noronha, F., Dias R. (2010). Interplate versus intraplate strike-slip deformed belts: examples from SW Iberia Variscides. Trabajos de Geologia, Universidad Oviedo, 29, 671-677. DOI: 10.17811/tdg.30.2010.%25p

Rosas, F.M., Marques, F.O., Ballèvre, M., Tassinari, C. (2008). Geodynamic evolution of the SW Variscides: orogenic collapse shown by new tectonometamorphic and isotopic data from western Ossa-Morena Zone, SW Iberia, Tectonics 27, TC6008. DOI: 10.1029/2008TC002333

Rubio Pascual, F., Matas, J., Martín-Parra, L. (2013). High-pressure metamorphism in the Early Variscan subduction complex of the SW Iberian Massif. Tectonophysics 592, 187-199. DOI: 10.1016/j.tecto.2013.02.022

San-José, M.A., Herranz, P., Pieren, A. P. (2004). A review of the Ossa-Morena Zone and its limits. Implications for the definition of the Lusitan-Marianic Zone. J. Iber. Geol., 30, 7-22.

Sánchez-García, T., Bellido, F., Pereira, M.F., Chichorro, M., Quesada, C., Pin, C., Silva, J.B. (2010). Rift-related volcanism predating the birth of the Rheic Ocean (Ossa-Morena zone, SW Iberia). Gondwana Res., 17, 392–407. DOI: 10.1016/j.gr.2009.10.005

Santos, J.F., Andrade, A., Munhá, J. (1990). Magmatismo orogénico varisco no limite meridional da Zona de Ossa-Morena. Comun. Serv. Geol. Portugal, 76, 91-124.

Santos, J.F., Mata, J., Ribeiro, S., Fernandes, J., Silva, J. (2013). Sr and Nd isotope data for arc-related (meta) volcanics (SW Iberia), Goldschmidt Conference Abstracts, 2132.

Sarmiento, G.N., Piçarra, J.M., Oliveira, J.T. (2000). Conodontes do Silúrico (Superior?)-Devónico nos "Mármores de Estremoz", Sector de Estremoz-Barrancos (Zona de Ossa Morena, Portugal). Implicações estratigráficas e estruturais a nível regional. I Congresso Ibérico de Paleontologia/VIII International Meeting of IGCP 421 (abstract book), Évora, 284-285.

Silva, J.C., Mata, J., Moreira, N., Fonseca, P.E., Jorge, R.C.G.S., Machado, G. (2011). Evidence for a Lower Devonian subduction zone in the southeastern boundary of the Ossa-Morena-Zone. In: Absctracts of the VIII Congresso Ibérico de Geoquímica, Castelo Branco, 295-299.

Simancas, J.F, Carbonell, R., González Lodeiro, F., Pérez Estaún, A., Juhlin, C., Ayarza, P., Azor, A., Martínez Poyatos, D., Almodóvar, G.R., Pascual, E., Sáez, R., Kashubin, A., Alonso, F., Álvarez Marrón, J., Bohoyo, F., Castillo, S., Donaire, T., Expósito, I., Flecha, I., Galadí, E., Galindo Zaldívar, J., González, F., González Cuadra, P., Macías, I., Martí, D., Martín, A., Martín Parra, L.M., Nieto, J. M., Palm, H., Ruano, P., Ruiz, M., Toscano, M. (2004). The seismic crustal structure of the Ossa Morena Zone and its geological interpretation. Journal of Iberian Geology, 30, 133-142.

Vegas, R., Moreno, R. (1973). Sobre la tectónica del flanco meridional de la Antiforma de Burgillos (sur de la provincia de Badajoz). Estudios Geologicos, 29, 513-517.

Veizer, J., Ala, D., Azmy, K., Bruckschen, P., Buhl, D., Bruhn, F., Carden, G.A.F., Diener, A., Ebneth, S., Godderis, Y., Jasper, T., Korte, C., Pawellek, F., Podlaha, O.G., Strauss, H. (1999). 87Sr/86Sr, δ13C and δ18O evolution of Phanerozoic seawater. Chem Geol, 161, 59-88. DOI: 10.1016/S0009-2541(99)00081-9

VI

Proposta de Evolução da Zona de Ossa-Morena durante o Ciclo Varisco

A Zona de Ossa-Morena é uma zona heterogénea, não só no que respeita à distribuição espacial do magmatismo e do metamorfismo, mas também a nível das sucessões estratigráficas e das suas características estruturais. Vários estudos têm sido realizados nesta zona tectonoestratigráfica, contudo, os trabalhos publicados muitas vezes não enquadram de forma integrada, espacial e temporalmente, a totalidade dos dados existentes. Esta é uma limitação importante, pois só assim é possível a compreensão ajustada da evolução geodinâmica desta zona paleogeográfica.

Como mencionado, toda a evolução geodinâmica desta zona paleogeográfica não pode ser vista de forma desintegrada da evolução do bordo Norte da Gondwana, onde para além do Ciclo Varisco, surgem também evidências de um Ciclo Orogénico anterior, o Ciclo Cadomiano (vide capítulo II.2). A presença de um forte *imprint* Cadomiano diferencia esta zona paleogeográfica das restantes zonas incluídas no Maciço Ibérico. Contudo, neste capítulo, focam-se essencialmente os dados referentes à evolução geodinâmica desta zona durante o Ciclo Varisco, que apresentam também elas características próprias que diferenciam esta zona das restantes zonas do Maciço Ibérico.

Deste modo, o trabalho em causa pretende enquadrar sumariamente os dados previamente publicados, incorporando os dados existentes, desde as etapas iniciais (Paleozóico inferior) até às finais (Paleozóico superior) do Ciclo Orogénico Varisco, integrando-os numa síntese multidisciplinar crítica, incluindo ainda os dados inéditos obtidos. A (re)interpretação dos dados existentes para esta zona permitiu colocar em evidência a presença de vários impulsos de extensão crustal durante as fases iniciais do Ciclo de Wilson Varisco (Câmbrico-Ordovícico) que se iniciaram durante o Câmbrico inferior e que culminam com a abertura do oceano Rheic durante a transição Câmbrico superior-Ordovícico inferior. O processo de *rift* e *drift* permanecem activos até ao Silúrico terminal – Devónico inferior. No que respeitas às fases colisionais Variscas, enfatiza-se a presença de quatro episódios tectono-metamórficos e magmáticos de carácter regional, os quais se correlacionam com os processos de subducção e colisão continental, actuantes entre o Devónico e o Pérmico, os quais originam a Cadeia

Orogénica Varisca. Para além destes, episódios de carácter local, uma das quais confinada ao bordo sul desta zona, onde se localiza a sutura do SW Ibérico, e a outra aos seus domínios ocidentais, onde se desenvolve uma importante estrutura transcorrente Varisca, de cinemática direita (*i.e.* a Zona de Cisalhamento de Porto-Tomar-Ferreira do Alentejo).

O texto apresentado neste capítulo segue na íntegra o artigo publicado na revista Comunicações Geológicas em 2014 (vide referência abaixo), no volume especial relativo ao IX Congresso Nacional de Geologia, realizado no Porto no mesmo ano. Contudo, apresentar-se-á, para além da figura publicada no referido artigo, uma figura adicional que permite a melhor compreensão do capítulo em causa.

- *Capítulo VI.1*

MOREIRA, N., ARAÚJO, A., PEDRO, J.C., DIAS, R. (2014). Evolução geodinâmica da Zona de Ossa-Morena no contexto do SW Ibérico durante o Ciclo Varisco. Comunicações geológicas, 101 (Vol. Especial I), 275-278.

De referir ainda que, sendo a publicação um artigo curto publicado num volume especial no âmbito do congresso, como previamente referido, esta publicação acarreta limitações de espaço que impossibilitaram a citação de todos os trabalhos pertinentes para o efeito. Desta forma, e seguindo na íntegra o trabalho publicado, alguns trabalhos com indubitável pertinência não foram citados.

VI.1

Evolução geodinâmica da Zona de Ossa-Morena no contexto do SW Ibérico durante o Ciclo Varisco

Índice

VI.1.1. Introdução

O Maciço Ibérico (MI) surge como local privilegiado no estudo da Cadeia Orogénica Varisca. Neste maciço, afloram materiais de idades compreendidas entre o Proterozóico e o Paleozóico superior, que testemunham a evolução geodinâmica do orógeno Varisco, contendo também testemunhos do Ciclo Cadomiano desenvolvido no Neoproterozóico (*e.g.* Ribeiro *et al.*, 2007).

A Zona de Ossa-Morena (ZOM) representa o bordo Sul (em coordenadas actuais) do Terreno Autóctone Ibérico (TAI). É uma zona muito heterogénea e complexa do ponto de vista estratigráfico, magmático, metamórfico e estrutural, a que não é alheio o facto de algumas das litologias presentes terem sido afectadas pela actuação de dois ciclos de Wilson sobrepostos (*e.g.* Ribeiro *et al.*, 2007; 2009).

O trabalho em causa pretende ser uma síntese pluridisciplinar crítica dos dados existentes, tentando correlacionar os diversos episódios tectono-metamórficos e magmáticos da ZOM com a sua evolução geodinâmica durante o Ciclo de Wilson.

VI.1.2. Do *rifting* continental à Abertura do Oceano Rheic

Após a colisão entre a ZOM e o TAI e consequente edificação da Cadeia Cadomiana durante o Neoproterozóico, na transição Neoproterozóico-Câmbrico, iniciam-se os processos de distensão da margem norte da Gondwana, que culminarão na Abertura do Oceano Rheic (*e.g.* Ribeiro *et al.*, 2009; Sánchez-García *et al.*, 2010). Esta passagem é marcada estratigraficamente pela presença de unidades conglomeráticas discordantes sobre as unidades do Ediacariano (Série Negra), às quais se associa um vulcanismo félsico de assinatura calco-alcalina (*e.g.* Oliveira *et al.*, 1991; Sanchez-Gárcia *et al.*, 2010).

Sobre esta unidade conglomerática basal, instala-se em toda a ZOM uma extensa plataforma detrítico-carbonatada (Câmbrico inferior – Ovetiano-Marianiano) onde se intercala um vulcanismo bimodal resultante do processo de *rifting* (Mata & Munhá, 1990; Sánchez-García *et al.*, 2010). Este processo de extensão crustal é acompanhado pela instalação de um conjunto de corpos plutónicos de idade compreendida entre os 535-520 Ma (*e.g.* Barquete, Alcáçovas, Táliga). No final do Câmbrico inferior, o estiramento da margem continental mantém-se activo, criando um conjunto de bacias individuais com diferentes depocentros, sendo a estratigrafia da região influenciada pela profundidade destas bacias; nas mais profundas a sedimentação é detrítica (*e.g.* Vila Boim-Cumbres), enquanto nas mais superficiais poderá ocorrer sedimentação carbonatada (Complexos vulcano-sedimentares carbonatados de Estremoz e Ficalho-Moura); esta sedimentação é contemporânea de vulcanismo bimodal, com assinatura toleítica anorogénica (Mata & Munhá, 1990).

O Câmbrico médio é marcado por um importante episódio de estiramento crustal. A sedimentação siliciclástica faz-se acompanhar de um intenso vulcanismo bimodal (*e.g.* Basaltos de Umbria-Pipeta, Complexo Vulcano-Sedimentar de Terrugem; *e.g.* Sánchez-García *et al.*, 2010), que se torna menos abundante na transição entre o Câmbrico médio-superior (*e.g.* Formação Fatuquedo). Este vulcanismo apresenta uma assinatura alcalina-transicional compatível com vulcanismo intraplaca (Mata & Munhá, 1990).

A transição Câmbrico-Ordovícico é marcada pela presença de uma discordância (ou paraconformidade) em toda a ZOM. Esta ausência de sedimentação e/ou episódio erosivo encontra-se temporalmente concordante com a intrusão de um segundo conjunto de corpos intrusivos (*e.g.* Portalegre, Alter Pedroso, Barcarrota; *ca.* 510-485 Ma). Este período poderá resultar de um episódio de instabilidade tectónica em todo o MI, ao qual se associa o levantamento relativo da ZOM (*e.g.* Oliveira *et al*., 1991; Ribeiro *et al.*, 2009). Também desta idade (*ca.* 480-485 Ma) surgem rochas básicas e ultrabásicas com características anorogénicas, de assinatura N/T-MORB (Pedro *et al.*, 2010), intercaladas no Complexo Filonítico de Moura,

apontando para que o processo de oceanização já estivesse concluído no Ordovícico, podendo o episódio anteriormente referido estar directamente relacionado com a abertura do oceano Rheic (*e.g.* Ribeiro *et al.*, 2007).

No Ordovícico inferior existem ainda evidências de instabilidade tectónica, com algum magmatismo associado à sedimentação. Contudo, a partir do Ordovícico médio, o magmatismo extingue-se. A partir daqui as variações estratigráficas poderão resultar apenas de variações eustáticas. Referência ainda para a sedimentação do Silúrico inferior, constituída por uma sequência de xistos negros carbonosos, típica de meios euxínicos com alguma profundidade (Araújo *et al*., 2013). Esta homogeneidade em toda a ZOM parece mostrar estabilidade tectónica durante o Silúrico inferior.

VI.1.3. Do processo de subducção à edificação da Cadeia Varisca

Neste ponto, tenta-se interpretar uma sequência de acontecimentos associados aos estádios finais do Ciclo Varisco na ZOM, vigentes durante o Paleozóico superior. Para efeitos práticos, a sequência de acontecimentos foi subdividida em diversos episódios tectono-metamórficos e magmáticos (TM), alguns de carácter localizado (TM_L); os mesmos encontram-se sintetizados na Figura 1.

VI.1.3.1. TM_1 – Processo de subducção activo (Emsiano-Fameniano inferior)

Este episódio encontra-se relacionado com o processo de subducção para Norte do Terreno Sul Português sobre o TAI. Este ter-se-á iniciado provavelmente antes do Emsiano (Devónico inferior). A polaridade é evidenciada pela migração do quimismo do magmatismo, toleítico a calco-alcalino no bordo Sul, proximal à sutura, e shoshonítico nos sectores mais distais. A idade do magmatismo shoshonítico, presente no domínio de Alter-do-Chão-Elvas, prolonga-se até aos cerca de 365 Ma (Fig. 1; Araújo *et al*., 2013). O magmatismo toleítico-calcoalcalino proximal foi identificado na região de Odivelas, onde se intercala com carbonatos da transição Devónico inferior a médio (Machado *et al.*, 2010). A existência de magmatismo Devónico é apoiada pela presença de zircões detríticos nas bacias de Cabrela e Mértola (com idades no intervalo 390-360 Ma; Pereira *et al.*, 2012). Estas idades são corroborantes com as obtidas para o evento metamórfico de alta pressão (≈370 Ma para pico bárico – fácies eclogítica; Araújo *et al*., 2013) existente no bordo sul da ZOM (Fig. 1 e 2A).

Do ponto de vista estratigráfico surgem evidências da sobrelevação da ZOM no Devónico. A sedimentação do Silúrico inferior vai gradualmente evoluindo, sendo que no Devónico inferior, surgem evidências de sedimentação carbonatada pouco profunda com formação de

estruturas recifais (Machado *et al.*, 2010). Também a sedimentação do Devónico inferior no Sinclinal de Terena (Fig. 2; Araújo *et al.*, 2013), mostra características de sedimentação sin-tectónica.

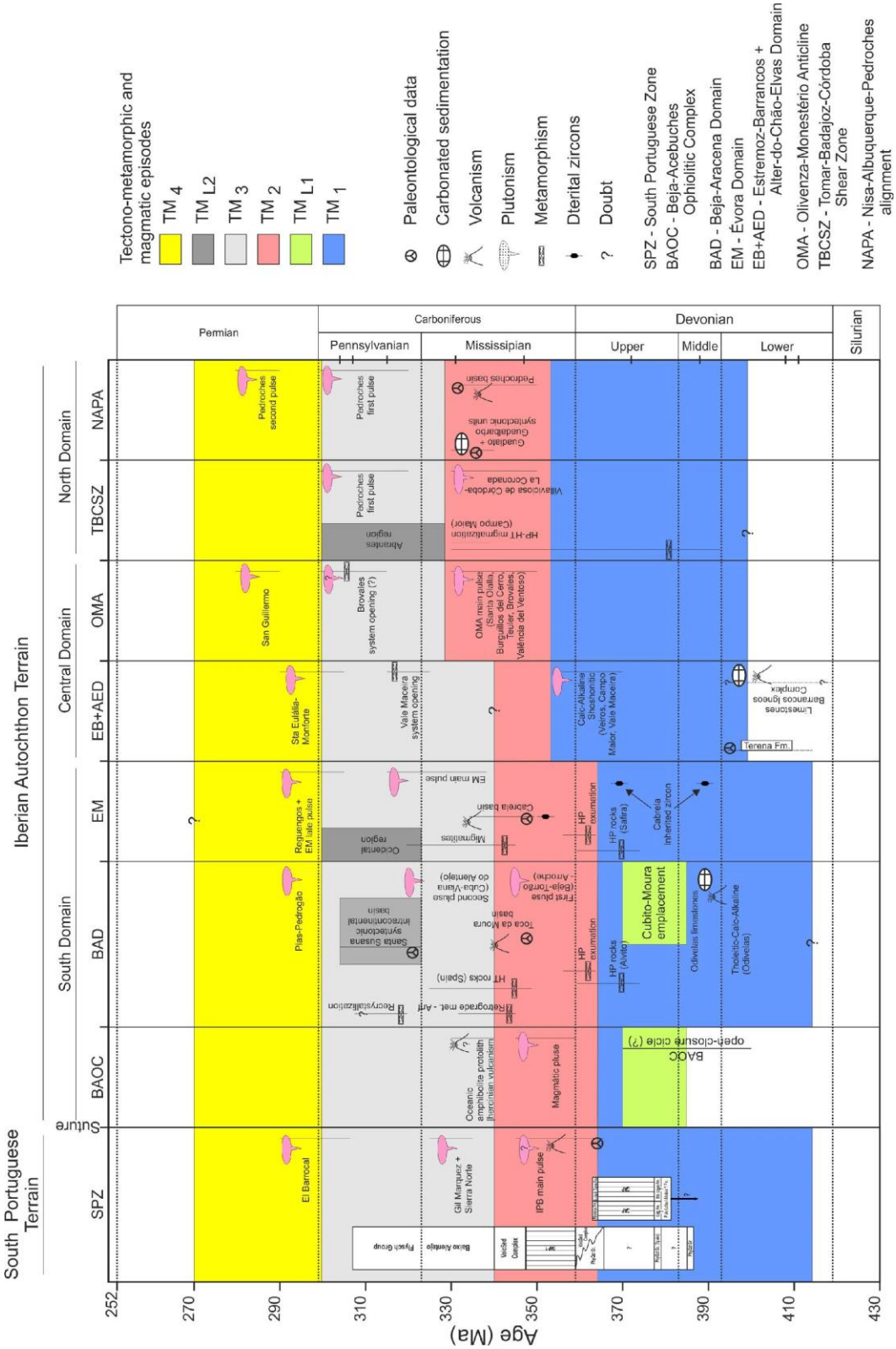

Figura 1 – Síntese dos principais eventos tectono-metamórficos e magmáticos na Zona de Ossa-Morena, durante as fases finais do Ciclo Varisco.

No que respeita à estrutura, este episódio caracteriza-se pela presença de dobras deitadas vergentes para o quadrante W associadas a zonas de cisalhamento com transporte com topo para SW, compatível com um regime transpressivo esquerdo com uma intensa partição da deformação (Fig. 2B; *e.g.* Vera, 2004*;* Araújo *et al.*, 2013).

VI.1.3.2. TM_{L1} (Bordo Sul da ZOM) – A instalação do Complexo Filonítico de Moura

Contemporaneamente ao episódio TM_1, na margem sul da Zona de Ossa-Morena, instala-se sobre os complexos vulcano-sedimentares autóctones, deformados pelo TM_1, um complexo imbricado alóctone (Araújo *et al.*, 2005). A instalação para Norte deste prisma de acreção associa-se ao processo de obducção dos complexos ofiolíticos, gerando-se uma estrutura do tipo *flake tectonics* (Araújo *et al.*, 2005). Neste complexo intercalam-se fragmentos da sequência autóctone bem como de sequências ofiolíticas (Fig. 2A; Pedro *et al.,* 2010). A instalação deste complexo ocorreu posteriormente ao Silúrico/Devónico inferior (Devónico médio a superior?; Araújo *et al.*, 2005).

VI.1.3.3. TM_2 – Tectónica extensiva – o *slab roll-back* e/ou o *slab breakoff* (Fameniano inferior a Carbónico inferior – Tournasiano-Viseano?)

A este episódio é atribuída a rápida exumação dos eclogitos em torno dos 360 Ma, assim como o início do magmatismo associado aos processos de colisão continental (Jesus *et al.*, 2007). Este episódio pode ser interpretado como resultado do processo de *slab roll-back* e/ou de *slab breakoff*. O processo de *slab roll-back,* bem como o *slab breakoff,* poderiam induzir extensão nas unidades localizadas na placa superior e nas unidades previamente acrecionadas. Evidências de extensão encontram-se localizadas no domínio de Évora-Beja-Aracena (onde se localizam rochas de alta pressão exumadas; Fig. 1) e no bordo norte da Zona Sul Portuguesa (e.g. Vera, 2004). Associado ao processo de *slab breakoff,* encontra-se descrito e modelado a existência de um *upwelling* astenosférico que induz sobreaquecimento da litosfera e, consequentemente, fusão crustal.

Atribui-se assim a este episódio, os primeiros impulsos do Complexo Ígneo de Beja (Fig. 1 e 2) e o vulcanismo na Faixa Piritosa Ibérica, com idades entre os 360-345 Ma (Jesus *et al.,* 2007), o magmatismo de Villaviciosa-La Coronada e Anticlinal de Olivenza-Monestério (bordo centro-norte da ZOM; 350-330 Ma), bem como a génese das Bacias de Cabrela e Toca da Moura e das Bacias Carbónicas do bordo Norte da ZOM.

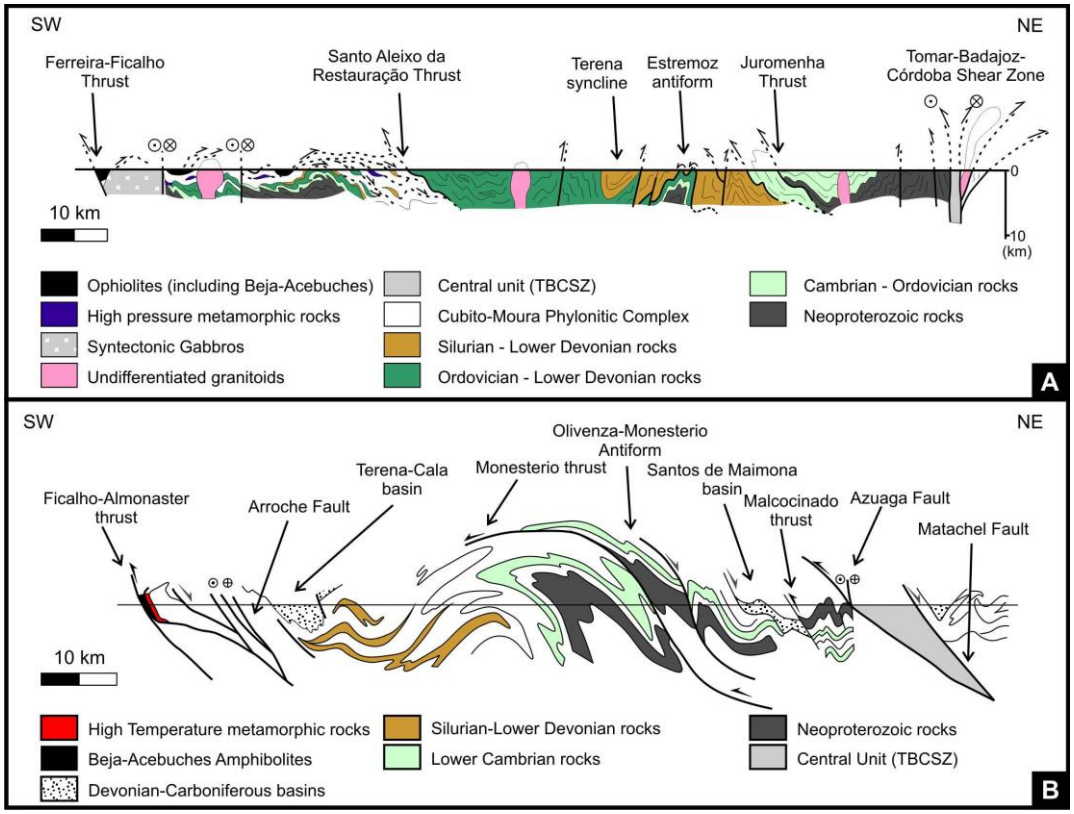

Figura 2 – Cortes geológicos simplicados da ZOM (A – Araújo *et al*., 2013; B – Simancas *et al*., 2004).

VI.1.3.4. TM_3 – A colisão continental (Mississipiano superior - Pensilvaniano)

Este episódio é resultante do processo de colisão continental. Do ponto de vista estrutural este caracteriza-se pela presença de dobras sub-verticais, raramente com vergência (Vera, 2004). Atribui-se a este episódio a génese de dobras à escala regional como sejam o Anticlinal de Estremoz e o Sinclinal de Terena (Fig. 2A). No que respeita ao metamorfismo, este é geralmente de baixo grau, com excepção para o Domínio Évora-Beja-Aracena, onde o metamorfismo pode atingir a fácies granulítica, e na Zona de Cisalhamento Tomar-Badajoz-Córdoba. Este facto poderá indiciar um elevado fluxo térmico a Sul, associado ao *upwelling* astenosférico, e que está na origem dos processos de fusão crustal que se mantêm durante este episódio. Atribui-se a este episódio um impulso magmático em todo o Maciço de Évora-Beja-Aracena, com idade compreendida entre os 340-320 Ma (Fig. 1; Jesus *et al.,* 2007). No Maciço de Évora, os magmas apresentam origem na fusão crustal, com assinatura calco-alcalina herdada, apresentando também contaminação de líquidos magmáticos de origem mantélica.

VI.1.3.5. TM_{L2} (Bordo Ocidental da ZOM) – Porto-Tomar-Ferreira do Alentejo (Pensilvaniano)

Junto ao bordo ocidental da ZOM, surgem evidências de um regime de deformação não-coaxial dextrógira, associada a cisalhamentos de orientação N-S a NNW-SSE, associada à actuação da zona de cisalhamento Porto-Tomar-Ferreira do Alentejo. Esta fase é responsável pela génese da Bacia sin-tectónica de Santa Susana, bem como pela segunda fase de deformação actuante na região de Abrantes.

VI.1.3.6. TM_4 – Deformação e magmatismo pós-colisional (Pérmico)

Após os processos de colisão continental, o sobre-espessamento crustal leva a que o regime de deformação intraplaca se altere. Nas fases mais tardias o regime de deformação intraplaca deixa de ser do tipo cavalgamento, passando a um regime transcorrente dominante. Todo o SW ibérico é então afectado por desligamentos esquerdos de orientação NNE-SSW a NE-SW. As características desta fase de deformação têm sido interpretadas por diversos autores como resultado da existência de anisotropias litosféricas de 1ª ordem com uma orientação E-W (*e.g.* Ribeiro *et al.*, 2007), que por sua vez induzem a formação de estruturas de 2ª ordem com orientação NNE-SSW a NE-SW.

O magmatismo, de idade compreendida entre os 300-270 Ma, é essencialmente granítico, apresentando menor expressão geográfica (*e.g.* Pedrógão, Sta Eulália, Nisa-Albuquerque-Pedroches). Este possui uma assinatura calco-alcalina, interpretada como resultado da fusão da crusta continental com essa assinatura.

Referências

Araújo, A., Fonseca, P. Munhá, J., Moita, P., Pedro, J., Ribeiro, A. (2005). The Moura Phyllonitic Complex: An Accretionary Complex related with obduction in the Southern Iberia Variscan Suture. *Geodinamica Acta,* 18(5), 375-388.

Araújo, A., Piçarra de Almeida, J., Borrego, J., Pedro, J., Oliveira, J. T. (2013). As regiões central e sul da Zona de Ossa-Morena. In: R. Dias, A. Araújo, P. Terrinha, J.C. Kullberg (Ed.), Geologia de Portugal (vol. I), Escolar Editora, 509-549.

Dias, R., Araújo, A., Terrinha, P., Kullberg, J.C. (Ed.) (2013). Geologia de Portugal (vol. I), Escolar Editora, 807p.

Jesus, A., Munhá, J., Mateus, A., Tassinari, C., Nutman, A.P. (2007). The Beja Layered Gabbroic Sequence (Ossa-Morena Zone, Southern Portugal): geochronology and geodynamic implications. *Geodinamica Acta*, 20(3), 139-157.

Machado, G., Hladil, J., Koptikova, L., Slavik, L., Moreira, N., Fonseca, M., Fonseca, P. (2010). An Emsian-Eifelian Carbonate-Volcaniclastic Sequence and the possible Record of the basal chote? event in western Ossa-Morena Zone, Portugal (Odivelas Limestone), *Geologica Belgica* 13(4), 431-446. DOI: 10.2478/v10096-009-0008-1.

Mata, J., Munhá, J. (1990). Magmatogénese de metavulcanitos câmbricos do nordeste alentejano: os estádios iniciais de "rifting" continental. *Comun. Serv. Geol. Portugal,* 76, 61-89.

Oliveira, J. T., Oliveira, V., Piçarra, J.M. (1991). Traços gerais da evolução tectono-estratigráfica da Zona de Ossa morena, em Portugal: síntese critica do estado actual dos conhecimentos. *Comun. Serv. Geol. Portugal,* 77, 3-26.

Pedro, J. C., Araújo, A., Tassinari, C., Fonseca, P. E., Ribeiro, A. (2010). Geochemistry and U-Pb zircon age of the Internal Ossa-Morena Zone Ophiolite Sequences: a remnant of Rheic Ocean in SW Iberia, *Ofioliti,* 35(2), 117-130.

Pereira, M.F., Chichorro, M., Johnston, S.T., Gutiérrez-Alonso, G., Silva, J.B., Linnemann, U., Hofmann, M., Drost, K., (2012). The missing Rheic Ocean magmatic arcs: Provenance analysis of Late Paleozoic sedimentary clastic rocks of SW Iberia, *Gondwana Research*, 22(3–4), 882–891. DOI: 10.1016/j.gr.2012.03.010

Ribeiro, A., Munhá, J., Dias, R., Mateus, A., Pereira, E., Ribeiro, M.L., Fonseca, P., Araújo, A., Oliveira, T., Romão, J., Chaminé, H., Coke, C., Pedro J. (2007). Geodynamic evolution of SW Europe Variscides, *Tectonics,* 26 DOI: 10.1029/2006/TC002058.

Ribeiro, A., Munhá, J., Mateus, A., Fonseca, P., Pereira, E., Noronha, F., Romão, J., Rodrigues, J.F., Castro, P., Meireles, C., Ferreira, N. (2009). Mechanics of thick-skinned Variscan overprinting of Cadomian basement (Iberian Variscides). *C. R. Geoscience*, 341(2–3), 127–139. DOI: 10.1016/j.crte.2008.12.003

Sánchez-García, T., Bellido, F., Pereira, M.F., Chichorro, M., Quesada, C., Pin, C., Silva, J.B. (2010). Rift related volcanism predating the birth of the Rheic Ocean (Ossa-Morena Zone, SW Iberia). *Gondwana Research*, 17 (2–4), 392–407. DOI: 10.1016/j.gr.2009.10.005

Simancas, J.F, Carbonell, R., González Lodeiro, F., Pérez Estaún, A., Juhlin, C., Ayarza, P., Azor, A., Martínez Poyatos, D., Almodóvar, G.R., Pascual, E., Sáez, R., Kashubin, A., Alonso, F., Álvarez Marrón, J., Bohoyo, F., Castillo, S., Donaire, T., Expósito, I., Flecha, I., Galadí, E., Galindo Zaldívar, J., González, F., González Cuadra, P., Macías, I., Martí, D., Martín, A., Martín Parra, L.M., Nieto, J. M., Palm, H., Ruano, P., Ruiz, M., Toscano, M. (2004). The seismic crustal structure of the Ossa Morena Zone and its geological interpretation. Journal of Iberian Geology 30, 133-142.

Vera, J. A. (Ed.) (2004). Geología de España. Sociedad Geológica de España e Instituto Geológico y Minero de España, 884 p.

VII

O Terreno Finisterra

Os trabalhos de cartografia geológica, iniciados com a dissertação de Mestrado, na região de Abrantes identificaram a presença de uma unidade tectonoestratigráfica (então denominada de Micaxistos Granatíferos do Tramagal; Moreira, 2012), que ostentava um carácter "exótico" relativamente à restante sequência que apresenta claras afinidades com as sucessões típicas do Neoproterozóico-Câmbrico inferior da Zona de Ossa-Morena, como descrito nos capítulos anteriores (capítulos II.1, II.2 e III.1). Os Micaxistos Granatíferos do Tramagal apresentavam um grau metamórfico mais elevado que a restante sucessão e uma deformação muito intensa e complexa, associando-se espacialmente a um granito sin-tectónico (Granito do Tramagal) com evidências de deformação contemporânea da sua instalação.

A progressão dos trabalhos de Cartografia Geológica para Oeste, domínios estes inseridos quer na folha 27-D (Abrantes) quer na 27-B (Tomar) da Carta Geológica de Portugal à escala 1/50.000, revelaram a presença de uma outra unidade de carácter "exótico" relativamente à restante sucessão definida na região de Abrantes: um complexo intensamente deformado e com litótipos típicos de metamorfismo de alta temperatura como sejam Gnaisses e Migmatitos.

Estas duas unidades tectonoestratigráficas apenas afloram a Oeste de uma importante zona de cisalhamento com componente transcorrente direita, a Zona de Cisalhamento Porto-Tomar-Ferreira do Alentejo. As unidades são alongadas segundo uma direcção geral próxima de N-S, acompanhando a orientação geral desta zona de cisalhamento, a qual condiciona/controla a evolução destas unidades. Embora esta zona de cisalhamento apresente importância cartográfica à escala do Orógeno, a sua interpretação/significado não é de todo consensual. Contudo, na região de Abrantes-Tomar, esta zona de cisalhamento de caracter polifásico marca claramente o limite entre as sucessões com similaridades à Zona de Ossa-Morena e as unidades tectonoestratigráficas previamente referidas.

A comparação e revisão crítica dos dados previamente publicados para sectores homólogos, como sejam os sectores de Coimbra, Albergaria-a-Velha-Porto e Berlengas (todas elas localizadas a Oeste desta zona de cisalhamento), com os dados agora obtidos mostra claras afinidades entre as unidades tectonoestratigráficas definidas nestes sectores. Em todos os

casos, os dados publicados mostram a presença de características geológicas dispares relativamente ao restante Terreno Ibérico, como a presença de eventos tectono-metamórficos e magmáticos precoces relativamente ao restante Autóctone Ibérico. Quer no sector de Coimbra quer no sector de Albergaria-a-Velha-Porto, estas unidades também contactam com o Terreno Ibérico através da Zona de Cisalhamento Porto-Tomar-Ferreira do Alentejo, mas em ambas as situações, o contacto é feito com uma outra zona paleogeográfica: a Zona Centro Ibérica. A região localizada a Oeste desta Zona de Cisalhamento parece apresentar uma evolução geodinâmica díspar relativamente ao restante Terreno Ibérico, individualizando-se assim um novo Terreno Tectonoestratigráfico na Ibéria, denominado de Terreno Finisterra. Este Terreno havia sido previamente proposto por outros autores (e.g. Ribeiro *et al*., 2007; 2010; 2013), embora a sua caracterização exaustiva e a sua correlação com os restantes domínios da Cadeia Varisca Europeia não havia sido realizada. A fronteira Oeste deste Terreno é desconhecida, enquanto a fronteira Este, como previamente referido, é demarcada pela Zona de Cisalhamento Porto-Tomar-Ferreira do Alentejo. O significado desta zona de cisalhamento continua em discussão (vide Ribeiro *et al*., 2007 e Pereira *et al*., 2010), contudo parece claro que a mesma representa uma fronteira de placas importante no contexto da evolução do Orógeno Varisco, em particular da relação entre os Terrenos Finisterra e Ibérico.

A comparação das características tectonoestratigráficas do Terreno Finisterra com os restantes domínios e zonas da Cadeia Varisca Europeia mostra claras similaridades com um outro bloco "exótico" localizado nos domínios a Norte do Maciço Armoricano (Bloco de Léon), bem como um outro domínio complexo definido na Europa Central (Mid-German Crystalline Rise; MGCR). Estas similaridades levaram a propor a individualização de um novo Terreno Tectonoestratigráfico, com características próprias e que se diferenciam das demais, estendendo-se desde a Europa central até ao Maciço Ibérico; o Terreno Finisterra-Léon-MGCR.

Os dados aqui apresentados não foram ainda alvo de publicação em nenhuma revista internacional da especialidade. Parte dos dados obtidos, e seguidamente apresentados no capítulo VII.1, foram já apresentados em congressos geológicos diversos, quer nacionais quer internacionais. Contudo, prevê-se a submissão de um artigo, que terá como base o capítulo em causa, a uma revista internacional com elevado factor de impacto, uma vez que a existência deste novo terreno, que agora se caracteriza, tem um impacto inegável nos modelos paleogeográficos para o Varisco Ibérico e consequentemente para o Varisco Europeu.

- *Capítulo VII.1*

MOREIRA, N. *et al*. (em preparação). Tectonostratigraphy of western block of Porto-Tomar Shear zone; the Finisterra Terrane.

Referências

Moreira, N. (2012). Caracterização estrutural da zona de cisalhamento Tomar-Badajoz-Córdova no sector de Abrantes. Tese de Mestrado (não publicada), Universidade de Évora, 225 p.

Pereira, M.F., Silva, J.B., Drost, K., Chichorro, M. y Apraiz, A. (2010). Relative timing of the transcurrent displacements in northern Gondwana: U-Pb laser ablation ICP-MS zircon and monazite geochronology of gneisses and sheared granites from the western Iberian Massif (Portugal). Gondwana Research, 17(2-3), 461-481. DOI: 10.1016/j.gr.2009.08.006

Ribeiro, A., Munhá, J., Dias, R., Mateus, A., Pereira, E., Ribeiro, L., Fonseca, P., Araújo, A., Oliveira, T., Romão, J., Chaminé, H., Coke, C., Pedro, J. (2007). Geodynamic evolution of the SW Europe Variscides. Tectonics, 26(6).

Ribeiro, A., Munhá, J., Fonseca, P.E., Araújo, A., Pedro, J.C., Mateus, A., Tassinari, C., Machado, G., Jesus, A. (2010). Variscan ophiolite belts in the Ossa-Morena Zone (Southwest Iberia): geological characterization and geodynamic significance. Gondwana Res, 17, 408–421.

Ribeiro, A., Romão, J., Munhá, J., Rodrigues, J., Pereira, E., Mateus, A., Araújo, A. (2013). Relações tectonostratigráficas e fronteiras entre a Zona Centro-Ibérica e a Zona Ossa-Morena do Terreno Ibérico e do Terreno Finisterra. In: R. Dias, A. Araújo, P. Terrinha, J.C. Kullberg (Eds), Geologia de Portugal, vol. 1, Escolar Editora, 439-481.

VII.1

Tectonostratigraphy of western block of Porto-Tomar Shear zone; the Finisterra Terrane

Index

VII.1.1. Introduction and General Framework

The Iberian Massif has a well-developed arcuate pattern, induced by the genesis of the Variscan Ibero-Armorican Arc (Fig. 1A; Dias *et al*., 2016). Its internal domains with a WNW-ESE to NW-SE general trend (e.g. Dias *et al*., 2013; Moreira *et al*., 2014) are interrupted to the west by one of the most important Iberian Variscan structures, the Porto-Tomar-Ferreira do Alentejo shear zone (Fig. 1B; PTFSZ). The geodynamic evolution of this shear zone is controversial, presenting a polyphasic evolution not only during the Variscan orogeny, but also during Meso-

Cenozoic times (Ribeiro *et al*., 2013). The superposition of different tectonic events difficult its geodynamical interpretation.

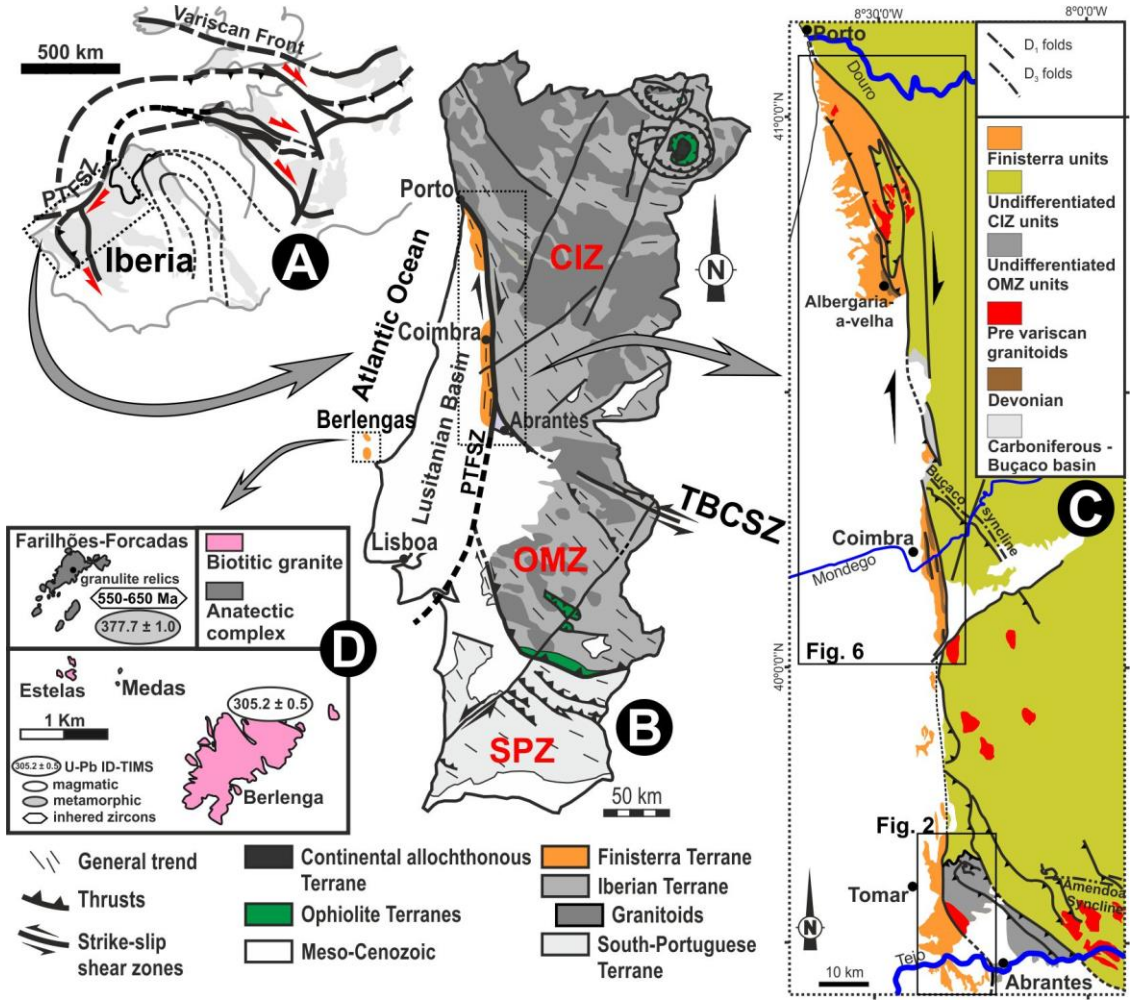

Figure 1 –The Finisterra Terrane in the context of the Iberian Variscides Massif:

A – The Ibero-Armorican Arc general pattern (adapted from Dias *et al*., 2016);

B – General overview of Finisterra Terrane (adapted from LNEG, 2010; Ribeiro *et al*., 2013);

C – The Finisterra outcrops in the PTFSZ vicinity (adapted from Chaminé *et al*., 2003a; LNEG, 2010; Romão *et al*, 2014);

D – The Berlengas islands main geological features (adapted from Bento dos Santos *et al*., in press).

In fat, the complexity of its evolution led to strongly different interpretations. Some authors consider the PTFSZ as the eastern boundary of Finisterra Terrane, a new tectonostratigraphic zone in Iberia (Ribeiro *et al*., 2007; 2009; 2013; Romão *et al*., 2013; 2014; Moreira *et al*., 2016a; 2016b). In such approach the PTFSZ is interpreted as a lithospheric transform fault (Ribeiro *et al*., 2007; 2013) active since, at least, the early Devonian stages of the Variscan Cycle (Dias and Ribeiro, 1993), but possibly reactivating an Early Variscan (or even Cadomian) structure. A

different interpretation is sometimes considered and the PTFSZ is considered a major high-strain Carboniferous dextral shear zone that dismembered the western edge of Tomar-Badajoz-Córdoba Shear Zone (TBCSZ; Pereira *et al*., 2010). Similar chronological interpretation is taken by Gutiérrez-Alonso *et al*. (2015), which relate this first order structure to the Iberian Orocline genesis.

Recent geological mapping in Abrantes-Tomar sector (Fig. 1C) emphasize a N-S High Temperature (HT) tectonostratigraphic succession without similarities with well-known units of the Iberian Massif (Romão *et al*., 2013; 2014; Moreira *et al*., 2016a; 2016b). The strong disparities with the adjacent Central Iberian (CIZ) and Ossa-Morena (OMZ) Zones successions, indicates a distinct geodynamical evolution, at least, during the Palaeozoic times.

Along the western block of the PTFSZ, similar HT tectono-metamorphic units were also described in Porto-Espinho-Albergaria-a-Velha and Berlengas Islands sectors (Fig. 1C and 1D) (Chaminé, 2000; Chaminé *et al*., 2003a; Pereira *et al*., 2007; Ribeiro *et al*., 2009; 2013; Bento dos Santos *et al*., 2010; in press). In Porto-Espinho-Albergaria-a-Velha as well as in Coimbra sectors, low-grade tectono-metamorphic units are also found, which were correlated with Proterozoic units of OMZ ("Série Negra" (Black Series); Chaminé *et al*., 2003a; 2003b; Ferreira Soares *et al*., 2005). Nevertheless some authors considerer a distinct geodynamic significance, origin and age to this unit (Chaminé *et al*., 2003b; Machado *et al*., 2008; 2011).

This paper presents a general overview of the tectonostratigraphic organization for the westernmost sectors of PTFSZ, describing and discussing the distinctive features that lead to individualize the Finisterra as a new tectonostratigraphic Terrane in the Iberian Massif.

VII.1.2. The Abrantes-Tomar Finisterra Sector

VII.1.2.1. Tectonostratigraphy

Near the PTFSZ, in the westernmost sectors of Abrantes-Tomar region, a N-S to NNW-SSE elongate HT tectonostratigraphic succession was defined (Fig. 2). These metamorphic units, with a probable Neoproterozoic-Lower Cambrian age, displays a complex polyphasic deformation and cannot be correlated with neighbouring variscan zones (i.e. OMZ and CIZ). Recent geological mapping (Fig. 2) enhanced the knowledge of these units.

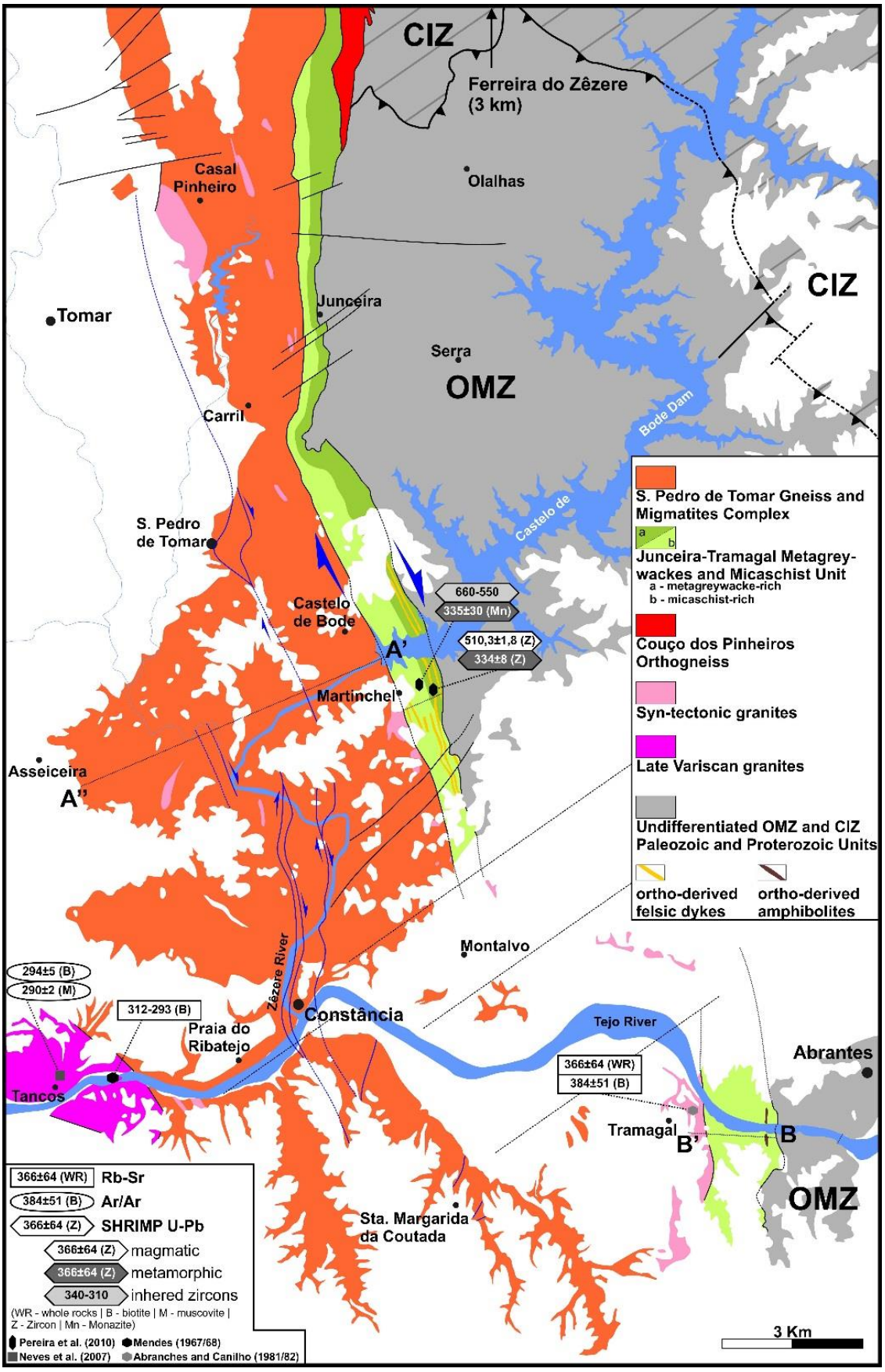

Figure 2 – Simplified geological map of the Abrantes-Tomar sector (marked cross section on figure 4B).

VII.1.2.1.1. S. Pedro de Tomar Complex

The western limit of this basal tectonostratigraphic unit is covered by the Meso-Cenozoic formations, while to the East it contacts with the Junceira-Tramagal Metagreywackes and Micaschists Unit, through a shear zone. This complex is characterized by medium to fine-grained strongly deformed gneisses, interlayered with micaschists and migmatites (Fig. 3A and 3B).

Two distinct macroscopic facies could be recognized in gneiss lithotypes. The most common are the para-derived gneisses dominated by a mineral paragenesis of plagioclase + quartz + biotite + sillimanite + muscovite + opaque minerals ± garnet ± cordierite. The other facies consists of orto-gneiss bodies, some of them less deformed and clearly related to the anatexis and melting of para-derived rocks (Fig. 3B). Its mineral paragenesis includes plagioclase + quartz + K-feldspar + biotite + sillimanite + muscovite ± cordierite. Plagioclase porphyroblasts are sometimes developed in the orthogneisses. In thin-section, the feldspar *s.l.* crystals has undulose extinction and some recrystallization, which coupled with the presence of sillimanite suggests temperatures around 500º-600ºC (Passchier and Trouw, 2005; Bucher and Graper, 2011; Singh and Gururajan, 2011). In both gneisses, the presence of chlorite intergrowth with silimanite crystals is common, being related to retrograde metamorphism.

The migmatites, abundant at south of S. Pedro de Tomar village, present a banded structure with alternations of melanosomes and thinner leucosome layers. The leucosomes are mostly composed of quartz + feldspar *s.l.* + muscovite, while the melanosome presents similar paragenesis with para-derived gneisses. Indeed, some gneisses are in fact migmatite lithotypes strongly deformation by the high-strain dextral shearing which develops a gneissic foliation (Fig. 3A). This suggest that the HT metamorphism and related migmatization are previous to the dextral shearing. Sometimes, quartz-mylonites are present in the vicinity of the Junceira-Tramagal Metagreywackes and Micaschists contact. These mylonitic bands are parallel to the main foliation produced by the regional dextral shearing.

There are no available geochronological data that constrain the photolith and metamorphic ages of these gneisses and migmatites. However, the para-derived lithotypes are considered Neoproterozoic to Lower Palaeozoic in age (see discussion below).

VII.1.2.1.2. Junceira-Tramagal Metagreywackes and Micaschist Unit

This unit crops out along a narrow and elongated 40 km N-S to NNW-SSE band, from Ferreira do Zêzere, at north, to Tramagal, at south.

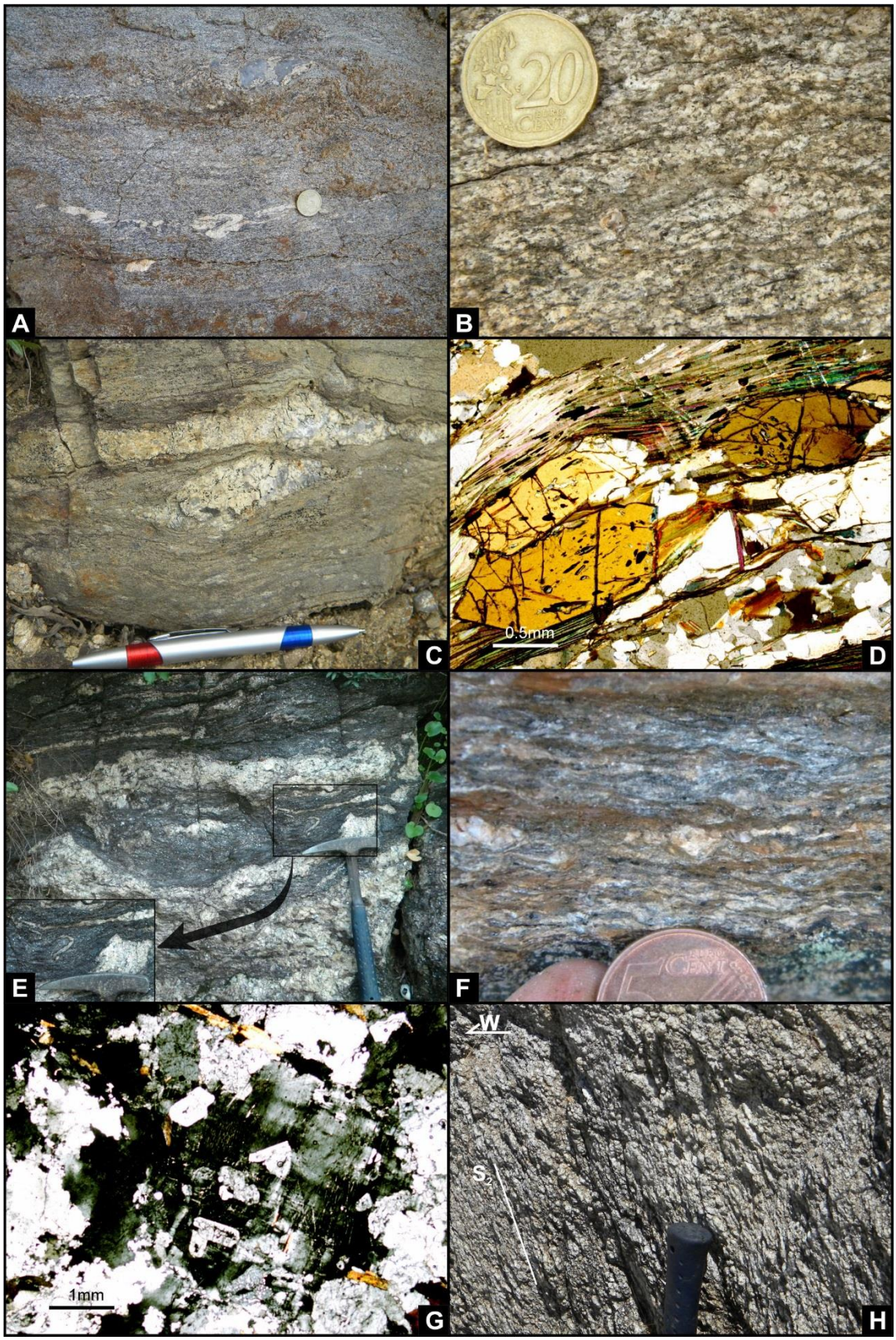
A
B
20
C
D
0.5mm
E
F
G
1mm
W
S_2
H

Figure 3 – Main features of the lithotypes of the Abrantes-Tomar tectono-stratigraphic units:

A – Deformed migmatites from S. Pedro de Tomar Complex;

B – (Ortho-)Gneisse from S. Pedro de Tomar Complex;

C – Felsic coarse-grained deformed ortho-derived dyke (pegmatite) intruded in the Junceira-Tramagal Unit;

D – Prismatic staurollite + biotite + muscovite + quartz + opaque minerals paragenesis contained in micaschiscts of the Junceira-Tramagal Unit;

E – Evidences of migmatization in the Junceira-Tramagal Unit, showing syn-migmatization folds;

F – Couço dos Pinheiros Orthogneiss, showing the highly deformed fabric, with feldspar sigmoidal crystal;

G – Deformed plagioclase crystal contained in the Tramagal Granite;

H – Foliated structure emphasized by biotite alignment in the Casal Pinheiro Granite.

In the Martinchel-Ferreira do Zêzere section, the succession displays an apparent thickness of circa 100 m and seems to correspond to a "coarsening upward" sequence expressed by the increase in the thick and number of metagreywackes beds towards the top of the unit. In this section, two different members could be individualized in this unit. The Lower Member is mainly composed of micaschists, sometimes interlayered with garnet-micaschists and subordinate thin metagreywacke beds, cropping out in the western domains and becomes thinner to northwards. The Upper Member is mainly composed of medium to fine-grained centimetric to metric metagreywackes and metaquartzwackes layers, interbedded with thin layers of micaschists and, sometimes, garnet-micaschists. In the Martinchel region quartz-feldspatic orthogneisses are sometimes recognized and could be considered the result of deformation and metamorphism in felsic-rich rocks (pegmatitic dykes?; Fig. 3C). Some of these bodies present mylonitic textures with quartz ribbons due to intense dynamic recrystallization of quartz. Some late less deformed granitic dykes are also described.

In Tramagal section, this unit appears to be thicker, being mostly composed of micaschists, with subordinate metaquartzwackes, metagreywackes and black schists. The coarse-grained lithotypes predominate in the westernmost domains of this section, where the centimetric metaquartzwackes beds could reach decimetric thickness. The micaschists paragenesis is dominated by biotite + muscovite + quartz + plagioclase + opaque minerals ± K-feldspar. A distinctive feature is the presence of millimetric to centimetric garnet and staurolite porphyroblasts, which could represents the metamorphic peak conditions (Fig. 3D). Such paragenesis are ascribable to amphibolite facies conditions in staurolite zone. The edges of the staurolite porphyroblasts are sometimes corroded, being associated to biotite, possibly related with the retrograde metamorphic episode. Also in Tramagal section, evidences of local migmatization is found to western domains (Fig. 3E), near the contact with Tramagal Granite. Contained in Junceira-Tramagal Metagreywackes and Micaschist Unit, some ortho-derived dykes with a monotonous paragenesis of green amphibole + plagioclase + opaque minerals ± quartz, typical of amphibolite facies conditions, are described.

Several ages have been recently established for the Junceira-Tramagal unit in Martinchel sector (Fig. 2; Pereira *et al*., 2010). The para-derived lithotypes are considered Neoproterozoic, based on the Ediacarian age (550-660 Ma) of the most recent group of inhered zircons population. The quartz-feldspatic orthogneiss cutting previous metasedimentary lithotypes shows a Lower Cambrian age (510.3±2.0 Ma; LA-ICP-MS, U-Pb in zircons). Monazites from the para-derived lithotypes displays Carboniferous metamorphic age (ca. 335 Ma), which is similar to the ones obtained in the quartz-feldspar gneiss (334.1±8.0 Ma for the discordia age anchored at intrusion age). A late granitic dyke intruded in pelitic lithotypes provide a 318.7±1.2 Ma for

the emplacement age, which could be interpret as related to the last pulses of HT metamorphic episode.

The inhered zircon populations show the presence of Neoproterozoic (690-780, 820-840 and 920 Ma), Mesoproterozoic (1050-1150 and ca. 1300 Ma), Paleoproterozoic (ca. 1650 and 1880-2200 Ma) and Paleoproterozoic-Archean (2350-2800 and ca. 2900 Ma) populations (Pereira *et al*., 2010). Some of the Mesoproterozoic zircons are slightly discordant (Fig. 4A; Pereira *et al*., 2010).

However, Silurian (ca. 440 Ma) and some Devonian-Carboniferous (350-400 Ma) zircons are also obtained in the Carboniferous granitic dyke intruded in the Junceira-Tramagal Unit (Fig. 4A; Pereira *et al*., 2010). Their origin and significance are poorly constrained: the Devonian-Carboniferous ages could represent relics of a metamorphic zircon overgrowth event (Devonian metamorphism?) and the Silurian age could represent an inhered zircon. However, this Silurian age have a high error (ca. ±40 Ma) and thus a Devonian age could not be excluded.

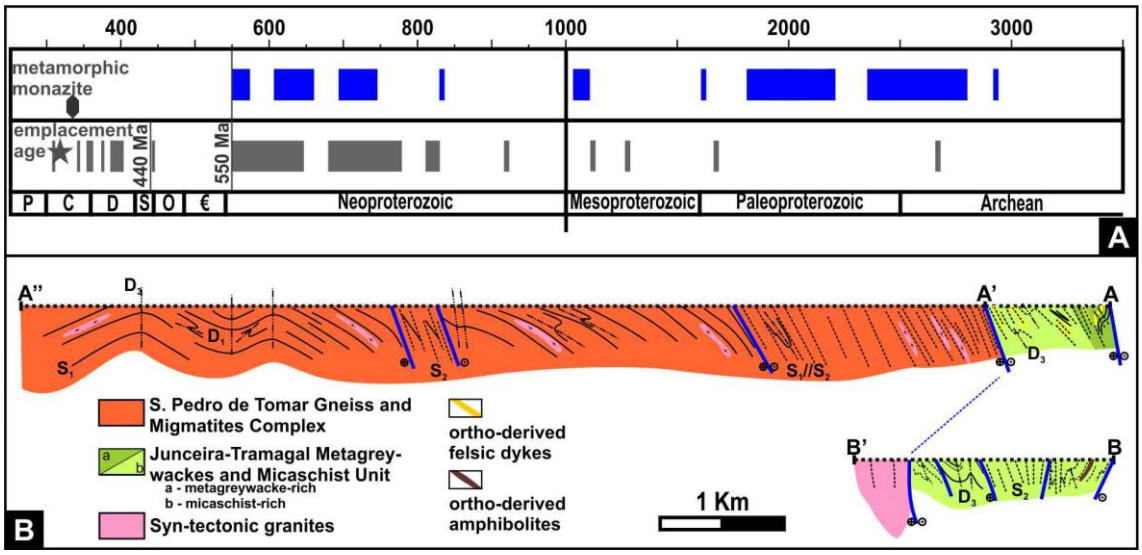

Figure 4 – Finisterra Terrane features in Tomar-Abrantes sector:

A – Zircon patterns of samples collected in Junceira-Tramagal Unit ($^{207}Pb/^{206}Pb$ ages obtained by Pereira *et al*., 2010);

B – Simplified geological cross sections.

VII.1.2.1.3. Couço dos Pinheiros Orthogneiss

This unit corresponds to a strongly stretched N-S sigmoidal ortogneiss body, with typical gneissic texture composed of millimetric felsic-rich layers (quartz and feldspars *s.l.*) and iron-magnesium silicates rich ones. The presence of sigma shaped K-feldspar porphyroblasts and strongly stretched quartz ribbons have been interpreted as the result of intense ductile non-

coaxial deformation (Fig. 3F). These gneisses are intruded by less deformed felsic coarse-grained layers.

The origin and age of the Couço dos Pinheiros orthogneisses are unknown. However, its petrographic and structural similarities with those observed in HT tectono-metamorphic units, mainly the S.Pedro de Tomar Complex, suggest it is a (early- or) pre- orogenic magmatic body, with possible Neoproterozoic-Lower Cambrian age. However, an Ordovician to Devonian age for emplacement of this orthogneiss could not be excluded.

VII.1.2.1.4. Syn-orogenic Variscan Granites

Some N-S elongated granitic bodies intrude the Abrantes-Tomar HT tectonostratigraphic units. The most representatives are the Tramagal and Casal Pinheiro two mica granites, being mainly composed of quartz + K-feldspar + plagioclase (with abundant perthites) + muscovite + biotite ± tourmaline, sometimes with K-feldspar phenocryst. The presence of in the Tramagal Granite indicate an anatectic origin, probably related with the HT metamorphism.

Both granites show evidences of deformation coeval of their crystallization, developing preferential elongation of mica crystals, sometimes leading to the development of a weak foliation. This plastic deformation is also visible in micro-anisotropies like undulose extinction and kinking in feldspar crystals and quartz sub-grains recrystallization (Fig. 3G). In the Casal dos Pinheiros Granite, the deformation also give rise to biotite alignment (Fig. 3H) and sigmoidal shape of feldspar crystals, compatible with dextral shearing along foliation planes.

There is no geochronological data allowing a detailed constraining of the emplacement of these granites. However, using structural data (see 2.2 section), a Carboniferous age could be assumed to the emplacement of these felsic bodies. This assumption is compatible with the geochronological data obtained for the Tramagal Granite, although its error margin is too high to confirm (Fig. 2; Rb/Sr method in whole rock 366±64 Ma and in biotite 384±51 Ma; Abranches and Canilho, 1981/82).

VII.1.2.2. General Structure

The Abrantes-Tomar tectonostratigraphic units, as well the ortho-derived bodies, are elongated in N-S to NNW-SSE direction, following the general trend of PTFSZ (Fig. 2). The N-S trend predominate from Ferreira do Zêzere to Martinchel, while in southward section, between Martinchel and Tramagal, the general trend present a SE deflection becoming NNW-SSE. This inflection seems to be a local effect, related to the interaction between PTFSZ and TBCSZ. The presence in the Abrantes-Tomar region of a kilometric sheath fold related to the WNW termination of TBCSZ (Ribeiro, *et al*., 2009; Moreira *et al*., 2011; 2013; Moreira, 2012) could

generate the inflection of PTFSZ, which is compatible with the early activity of the PTFSZ, at least since the beginning of compressional stages of Variscan orogeny, as previously proposed (Dias and Ribeiro, 1993; Ribeiro *et al*., 2007; 2013). The structural data of Junceira-Tramagal Unit and S. Pedro de Tomar Complex show, at least, the presence of three deformation episodes.

The gneissic foliation in S. Pedro de Tomar Complex is the most common structure related to the first deformation episode (D_1), being often associated with quartz-veins. The geometry and kinematics of the D_1 is poorly constrained, mainly due to the overprinting of younger deformations. As the intensity of the main D_2 deformation episode increase eastwards towards the PTFSZ, the D_1 structures are usually transposed near this main shear zone (Fig. 4B). However, in the west domains of S. Pedro de Tomar Complex, far from PTFSZ where the D_2 is less pervasive, a low dipping S_1 gneissic foliation is developed (Fig. 4B). The S_1 foliation is sometimes associated to asymmetric ptygmatic recumbent folds with sub-horizontal to low dipping hinges and, although highly dispersed, a NNW-SSE trend (Fig. 5A). The sense of transport is debatable, nevertheless the relation between D_1 structures seems to show transport with top-to-West.

Also in the Junceira-Tramagal Unit, some D_1 recumbent folds, with a westward geometric vergence are found (Fig. 5B). These folds, which are refolded by D_2-D_3 event, are associated to a S_1 HT foliation, which is compatible with the evidences of migmatization during the D_1 tectonic event (Fig. 3E). The leucosome and melanosomes are clearly deformed by D_2 dextral shearing episode being synchronous with the D_1 event. Although, the D_1 geometry is poorly constrained, being only preserved where the D_2 event is not pervasive.

The D_2 event develops a pervasive ductile S_2, parallel to the general N-S to NNW-SSE PTFSZ trend. Usually S_2 strongly dips to East (Fig. 4B), being associated to sub-horizontal to low SE plunging D_2 stretching mineral lineation. In the vicinity of PTFSZ, the S_2 foliation transposes previous structures (S_1//S_2), becoming less penetrative towards West. This foliation is associated to a non-coaxial dextral regime induced by PTFSZ. In the more deformed sectors, S_2 behave as C planes (Fig. 5C) with coeval development of several structures emphasizing the dextral kinematics: C-S and C-C' structures (Fig. 5D) or asymmetric folds with steeply plunged hinges and sigmoidal shape structures. Sometimes, the S_2 foliation is associated with an intense mylonitization, also showing dextral kinematics. The C' structures displays NNE-SSW to NE-SW strike, dipping to E and contain a down-dip to SE plunging oblique stretching lineation, showing top-to-SE criteria (Fig. 5E). This general dextral kinematic with a slightly oblique transport with top to East is compatible with the presence of the high temperature unit in the westernmost domain. It should be stressed that, not only the boundaries between all the Abrantes-Tomar tectonostratigraphic units but also the contact between the Finisterra and the Iberian Autochthon Terrane (*i.e.* the PTFSZ), are always D_2 1st order dextral shear zones.

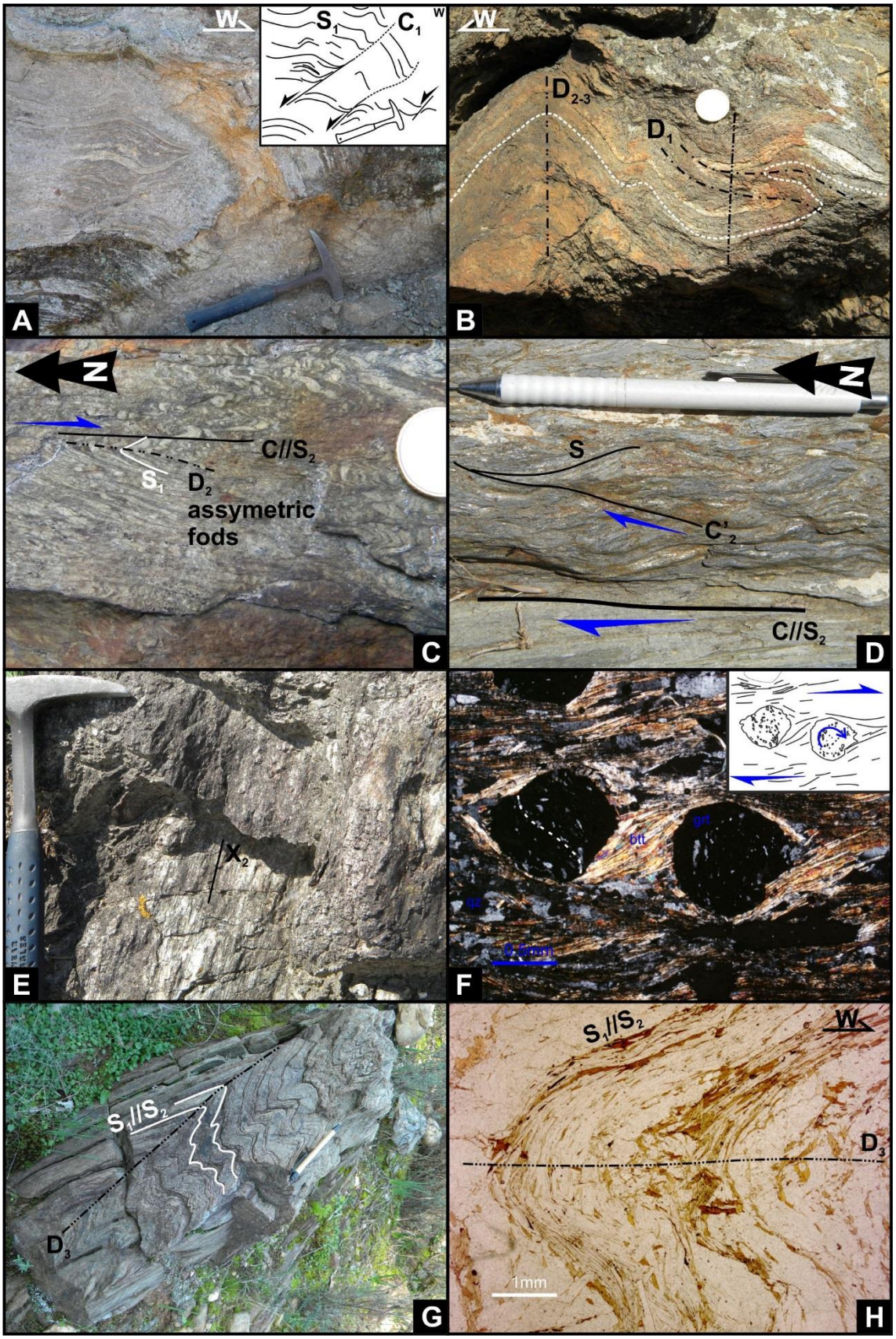
W
S1
C1
W
A
W
D2-3
D1
B
Z
C//S2
S1
D2
assymetric
fods
C
Z
S
C'2
C//S2
D
X2
E
grt
btt
qz
0.5mm
F
S1//S2
D3
G
S1//S2
W
D3
1mm
H

Figure 5 – Main structural features of Abrantes-Tomar sector:

A – Syn-metamorphic D_1 recumbent folds and shear-bands in the S. Pedro de Tomar Complex;

B – Refolded D_1 recumbent folds in Junceira-Tramagal Unit;

C – D_2 shear bands affecting the previous D_1 HT foliation generated;

D – C-C' fabric related to dextral shearing during D_2 affecting the Junceira-Tramagal Unit;

E – Macroscale C' band showing down-dip stretching lineation associated to mylonitic S_2;

F – Poikilitic garnet, showing dextral synthetic spinning;

G – D_3 low grade overturned tight folds in the Junceira-Tamagal Unit;

H – Biotite foliation in a quartz-rich lithotype folded by low-grade D_3 folds.

The D_2 deformation episode is associated to a HT and high strain fabric. In Junceira-Tramagal Unit, the garnet grow and have a synthetic rotation during the D_2 dextral shearing, presenting generally poikilitic structures overlapping a previous foliation (S_1; Fig. 5F).

The Tramagal and Casal Pinheiro granites have also been deformed by D_2. They present a poorly developed N-S to NNW-SSE S_2 cleavage demarked by biotite alignment, generally dipping to E, which often bound sigmoidal shape structures compatible with dextral shear (Fig. 3H). This geometry and kinematics of S_2 shows similarities with D_2 features previously described in both HT tectonostratigraphic units. Evidences of hot-plastic deformation of feldspar crystal seems to show that the deformation is active during granite emplacement. Thus, it is considered that the emplacement of these granite bodies are contemporaneous from D_2 deformation episode.

The S_2 foliation is folded by the third deformation phase (D_3). Near the main Eastern D_2 shear zones, the D_3 folds are tight with a West facing related to moderately to steeply inclined axial surfaces (Fig. 5G and 5H). Towards the West domains, they progressively open, while the axial surfaces become subvertical (Fig. 4B). Whatever their geometry, the D_3 folds are always characterized by low dipping hinges with a N to NNW plunges, associated to poorly developed low-grade axial planar cleavage, sometimes crenulation cleavage. The influence of the D_2 main shear zones in the D_3 folds pattern, show that they also control the D_3 folding.

Concerning the deformation age, all these episodes are interpreted as Variscan. The D_1 event, related to the HT gneissic foliation, could be Late Silurian to Devonian in age (ca. 420?-350 Ma), being associated to the zircon growth emphasized in the Junceira-Tramagal Unit. This early deformation was followed by two Carboniferous episodes: the HT and high-strain D_2 event could be Mississippian in age (ca. 340-320 Ma), being associated to dextral shearing of PTFSZ, which almost completely transposes the D_1 structures, and the D_3 event Pennsylvanian-Early Permian in age (ca. 310-295 Ma), showing low-grade conditions which could be related to the exhumation and cooling related to the retrogressed metamorphism.

The proposal chronological relation was based in Pereira *et al*. (2010) ages that show the presence of metamorphic ages around 335 Ma associated with high strain deformation. The D_2 high strain deformation do not affect prevasively the granitic dyke intruded in pelitic rocks (318.7±1.2 Ma), constraining the maximum age of high strain deformation. Finally, the Tancos granite (Fig. 2), a post-tectonic porphyritic two-mica granite not affected by any of the previous deformation events, constrain the maximum ages of D_3 event; Ar/Ar geochronological data in micas (Neves *et al*., 2007) shows an Early Permian age to its emplacement (Biotite - 294±5Ma and Muscovite – 290±2 Ma). This data which is compatible with ages obtained by Mendes (1967/68) with Rb/Sr method in biotites (ca. 312-293 Ma).

Finally, it should be noted that all the study area is affected by intense subvertical fracturing with two main trends: N35ºE and N70-80ºE. The fracture pattern could be related either to the Late Variscan event (Dias *et al*., 2017), or with the Meso-Cenozoic processes associated to the opening of Lusitanian Basin and consequently the Atlantic Ocean.

VII.1.3. The North and Central Finisterra Domains

The northern continuity of the Abrantes-Tomar Finisterra domain is disrupted due to the complex interaction with the Meso-Cenozoic formations strongly deformed by the PTFSA fracture system. Two main independent domains are found in the vicinity of this first order shear zone: the Porto-Espinho-Albergaria-a-Velha and the Coimbra sectors (Fig. 6). Both are characterized by high-temperature metamorphism and/or low-grade tectonostratigraphic units not possible to correlate either to the CIZ or to the OMZ.

VII.1.3.1. Porto-Espinho-Albergaria-a-Velha Sector

West of the PTFSZ four pre-Mesozoic tectonostratigraphic units have been defined between Espinho and Albergaria-a-Velha (Fig. 6; Chaminé, 2000, Chaminé *et al*., 2003a, Pereira *et al*., 2007; Ribeiro *et al*., 2013). From the bottom to the top:

- Lourosa Unit – Composed of gneisses, migmatites, micaschists and garnet-micaschists, this unit could be divided in two members: the lower member is mostly composed of migmatites, ortho- and paragneisses while the upper member is dominated by the biotite-micaschists, sometimes with garnet. Both members present amphibolites and amphibolic schists, withgeochemical affinities similar to within-plate basalts to MORB, being derived from mafic (and ultra-mafic – Engenho Novo Olivine amphibolites) rocks (Montenegro Andrade, 1977; Aires and Noronha, 2010; Silva, 2007). This Unit has been correlated with the Pindelo Unit previously defined in the same sector (Chaminé, 2000; Chaminé *et al*., 2003a).

- Espinho Unit – West of the previous unit outcrops a narrow band of staurolite-garnet-biotite micaschists, sometimes with mylonitic garnet-quartzites and, occasionally, impure quartzites. The metamorphic paragenesis shows the presence of two distinct HT metamorphic events: the first one reaches the sillimanite zone and second one the staurolite zone (Chaminé, 2000; Fernandez *et al*., 2003).

- Arada Unit – A low-grade metamorphic unit composed of a monotonous sequence of black to green phyllites, derived mafic rocks with tholeiitic geochemical features (Silva, 2007) and black quartzites. The similarities and correlation between this succession and

the Ediacarian "Série Negra" of OMZ was initially proposed (Chaminé, 2000; Pereira *et al.*, 2007).

- Albergaria Unit – Within Arada Unit, imbricate very low-grade rocks, mainly composed of black shales, with Frasnian-Serpukhovian age were described (Chaminé *et al.*, 2003b; Machado *et al.*, 2011).

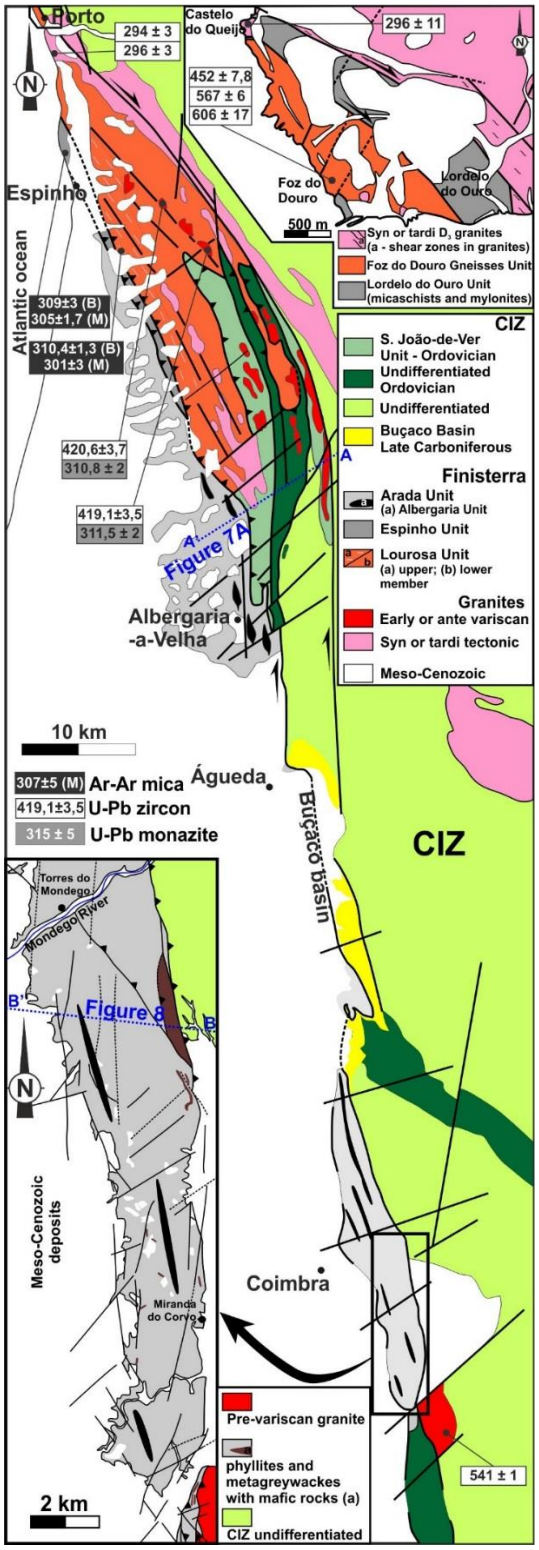

Figure 6 – Simplified geological map and geochronological data for the Porto-Coimbra Finisterra sectors (references in the text; adapted from Chaminé *et al.*, 2003a; Ferreira Soares *et al.*, 2005; Pereira *et al.*, 2007; LNEG, 2010; Machado *et al.*, 2011; Dinis *et al.*, 2012).

Although the Arada, Espinho and Lourosa units have been usually considered as Neoproterozoic (Beetsma, 1995; Chaminé, 2000; Chaminé *et al*., 2003a; Ribeiro *et al*., 2009; 2013), such assumption has been debated in recent studies. The Upper Devonian-Carboniferous imbrications within the Arada Unit show, that at least in part, this unit is more recent (Albergaria Unit; Chaminé *et al*., 2003b; Machado *et al*., 2011). Moreover, the presence of acritarch assemblages in Albergaria Unit with affinities with the Late Devonian Laurassia marine acritarchs, contrasts with the Late Devonian assemblages from South Portuguese Zone which show clear affinities with North Gondwana margin (Machado *et al*., 2008).

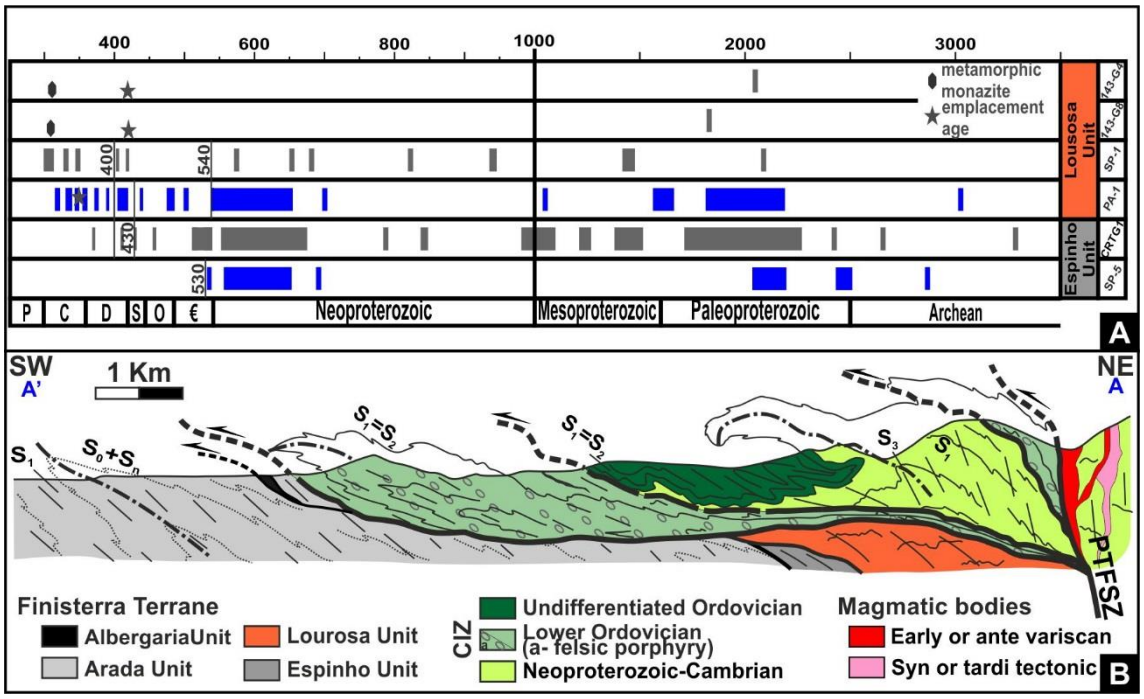

Figure 7 – Finisterra Terrane features in Porto-Espinho-Albergaria sector:

A – Zircon patterns of samples collected in Lourosa and Espinho Units (geochronological data from Chaminé *et al*., 1998; Almeida, 2013; Almeida *et al*., 2014);

B – Simplified geological cross section (adapted from Pereira *et al*., 2007).

Concerning the age of the Espinho and Lourosa Units, although the most representative detrital zircon population are Lower Cambrian to Neoproterozoic (510-680 Ma in the Espinho Unit and 540-650 Ma in the Lourosa Unit; Almeida, 2013; Almeida *et al*., 2014), they also present Upper Cambrian-Ordovician to Silurian zircons (Fig. 7A; Almeida, 2013; Almeida *et al*., 2014). Thus, at least part of these tectonostratigraphic units are Palaeozoic (Silurian?), once some of these zircons presents detrital morphology (Almeida *et al*., 2014). As expected, older inhered zircon populations are found in both units (Fig. 7A; Almeida, 2013):

- Neoproterozoic (ca. 690, ca. 790 and ca 840 Ma), Mesoproterozoic (980-1250 and 1400-1500 Ma), Paleoproterozoic (1700-2250 and 2400-2500 Ma) and Archean (ca. 2650, ca. 2850 and ca. 3280 Ma) in the Espinho Unit;
- Neoproterozoic (ca. 680, ca. 700, ca. 820 and ca. 940 Ma), Mesoproterozoic (ca. 1050 and 1400-1500 Ma), Paleoproterozoic (1550-1650 and 1800-2200 Ma) and Archean (ca. 3050 Ma) in the Lourosa Unit.

The zircon patterns from Lourosa and Espinho Units are not equal for all samples (Almeida, 2013; Almeida *et al*., 2014). Some samples do not present Mesoproterozoic populations, while in other samples the Mesoproterozoic population is representative (Fig. 7A).

Upper Silurian-Devonian overgrowths in inhered zircon are found in both units (370-410 Ma in the Espinho Unit and 350-420 Ma in the Lourosa Unit; Almeida, 2013; Almeida *et al*., 2014). This suggests the presence of a metamorphic and/or magmatic event with Silurian-Devonian age. The presence of Silurian felsic magmatism in Lourosa Unit (Lourosela and Souto Redondo Orthogneisses; ca. 420 Ma; Chaminé *et al*., 1998), is compatible with such interpretation. Also in this unit, a Lower Devonian age was obtained for the protolith of a mafic amphibolite (392±2 Ma; LA-ICP-MS in zircon; Almeida, 2013; Almeida *et al*., 2014). However, older concordant ages are Silurian (ca. 420-430 Ma) and which could represent the protolith age, being the Devonian ages obtained in some zircons (ca. 390-350 Ma) resulted from the metamorphic and/or magmatic events previously referred.

However, the amphibolites age is not consensual. Indeed, a Mesoproterozoic Sm-Nd model age (TDM; ca. 1050 Ma; Noronha and Leterrier, 2000) was obtained to the mantle protolith of similar amphibolites in the Porto region. This Precambrian age were considered similar to the emplacement of mafic magmatism with tholeiitic MORB affinities in the Foz do Douro gneiss unit (Noronha and Leterrier, 1995; 2000).

These amphibolites are contained in the Foz do Douro Gneissic Unit which is equivalent of the Lourosa unit (Fig. 6; Noronha and Leterrier, 1995; 2000; Chaminé *et al*. 2003a; Ribeiro *et al*., 2009). This unit is mainly composed of orthogneisses, sometimes with mylonitic bands, paragneisses and amphibolites. The orthogneisses have tonalitic to granitic composition, being subdivided in four distinct lithotypes (Noronha and Leterrier, 2000): (i) biotite gneisses, (ii) felsic gneisses, (iii) augen-gneisses and (iv) highly deformed felsic gneisses. The eastern boundary of the Foz do Douro Gneissic Unit is a major dextral shear zone, considered the contact between the CIZ and the Finisterra Terrane (Ribeiro *et al*., 2009). However, this contact is done with is a narrow band of micaschists and quartz-tectonites (Lordelo do Ouro Unit; Chaminé *et al*., 2003a). The strong similarities of this unit with the micaschists interlayered in Foz do Douro Gneisses Unit, seems to indicate that the Lordelo do Ouro Unit could also be part of Finisterra Terrane.

The age of Foz do Douro Gneisses Unit is debatable (Fig. 6). Ediacarian ages are sometimes assumed (Ribeiro *et al*., 2009) based in geochronological data from the biotitic orthogneisses (567± 6 Ma) and the augen felsic gneisses (606 ± 17 Ma; U/Pb – isotope dilution in zircon; Noronha and Leterrier, 2000). However, an Ordovician age have been recently obtained to the protolith of biotitic orthogneisses from this unit (452±8 Ma; SHRIMP U-Pb in zircon; Sousa *et al*., 2014). Similar Ordovician age was also obtained in a granite orthogneiss emplaced in Lourosa Unit (459±7 Ma, U/Pb LA-ICP-MS in zircon; Almeida, 2013).

Regarding the metamorphism in Porto-Espinho-Albergaria-a-Velha Sector two distinct Carboniferous clusters were identified:

- ca. 340-325 Ma, evidenced by zircon overgrowths (Almeida *et al*., 2014);
- ca. 310-300 Ma, obtained by Ar-Ar in micas and amphibole (Acciaioli *et al*., 2003; Munhá *et al*., 2008; Gutiérrez-Alonso *et al*., 2015), but also U-Pb in monazites (Chaminé *et al*., 1998; Munhá *et al*., 2008) and Rb-Sr using whole rock-feldspar-biotite-muscovite isochron (Santos *et al*., 2012).

Concerning the structure, all units have a polyphased deformation (Chaminé, 2000; Ribeiro *et al*., 2013) giving rise to a N-S general trend, deflecting to NNW-SSE in the northernmost domains (Fig. 6). Not only the boundaries between all the units are major thrusts, but also both Lourosa and Arada Units are thrusted by CIZ Neoproterozoic-Ordovician successions always with top to SW transport (Chaminé, 2000; Pereira *et al*., 1880; 2007; Ribeiro *et al*., 1880; 2013; Fig. 7B).

This sector is characterized by two ductile deformation episodes (D_1 and D_2), followed by a third brittle one (D_3). During D_1 major recumbent folds with low dipping N-S hinges, subparallel to a X_1 stretching mineral lineation, and a western vergence were developed (Pereira *et al*., 1980; Ribeiro *et al*. 1980; 1995; 2013). These folds are coeval of a penetrative axial planar penetrative foliation (S_1) cleavage generally transposed by the second foliation (S_2). The D_1 event is probably related to an early HT fabric with flattened garnet and sillimanite observed in the Espinho Unit (P = 4-5 kbar; T=700±50ºC; Fernandez *et al*., 2003).

The D_2 deformation event develops a penetrative NW-SE to N-S axial planar S_2 cleavage associated to subvertical folds with low dipping SE-plunge hinges (Ribeiro *et al*., 1980; Chaminé, 2000). The N-S trends are pervasive near the PTFSZ, deflecting to NW-SE in the western domains far from this 1st order shear zone (Ribeiro *et al*., 1980) The Espinho and Lourosa Units have been strongly deformed during D_2, giving rise to the pervasive development of S_2. This foliation, often with mylonitic and gneissic features, is associated to subhorizontal to low plunging to SE stretching mineral lineation, subparallel to fold hinges. The D_2 deformation was the result of a non-coaxial dextral shear regime, often completely transposing D_1 structures. In the Arada Unit,

the S_2 foliation presents low-grade features, although also usually to a high strain deformation pattern.

The non-coaxial dextral D_2 movement along the N-S sector of PTFSZ induces space problems when approaching its NNW-SSE segment between Albergaria-a-Velha and Porto (Fig. 6), that behaved has a restraining bend (Ribeiro *et al*., 2013). Such geometrical constrain give rise to an imbricated thrust complex with a SW facing, giving rise to the superposition of the Arada and Lourosa units by the CIZ sequences (Fig. 6 and 7B; Pereira *et al*., 2007; Ribeiro *et al*., 2013). This tangential deformation roots in the lithospheric subvertical or steeply dipping to East PTFSZ, which bound two distinct basement blocks (Ribeiro *et al*., 1995; 2013).

In the Espinho Unit the D_2 event generates a second HT metamorphic paragenesis with garnet overgrowth and staurolite porphyroblasts (P=3-6 kbar; T=600±30ºC), which partially reset the first HT paragenesis in sillimanite zone (P=4-5 kbar; T=685-750ºC Fernandez *et al*., 2003). Migmatites from the Lourosa Unit also show a HT metamorphic event during D_2 (P = 8 ± 0,7 kbar; T=730±25ºC), being characterized by garnet + sillimanite + K-feldspar + biotite ± muscovite (+ melt) assemblage (Munhá *et al*., 2008).

Although D_1 and D_2 are usually consider two distinct deformation events westwards of the PTFSA, they could also be considered the result of a progressive deformation (Ribeiro *et al*., 1995; Chaminé, 2000).

The third and last deformation event (D_3) is characterized by brittle structures with cataclasites related, not only to N-S shear zones, but also to the reactivation of top-to-SW thrusts often underlined by fault-gouge (Chaminé, 2000; Ribeiro *et al*., 2013).

The D_1 is considered previous to the sedimentation of Frasnian-Serpukhovian black shales while the D_2 must to be younger (Ribeiro *et al*., 2013). Therefore, previous mentioned geochronological data led to postulate a Late Silurian-Devonian age to the HT D_1 event (ca. 420-350 Ma). Concerning the D_2 HT metamorphism, it could be related to the zircon overgrowth during Mississippian (ca. 340-325 Ma). The Ar-Ar geochronological data (Acciaioli *et al*., 2003; Munhá *et al*., 2008; Gutiérrez-Alonso *et al*., 2015) could indicate that the exhumation of the HT metamorphic rocks extending up until Pennsylvanian times (310-300 Ma). The younger age is constrained by the emplacement of Castelo do Queijo and Madalena-Lavadores post-tectonic Granites (ca. 295-290 Ma; Martins *et al*., 2011; 2014). As N-S D_3 brittle structures are observed in the Madalena-Lavadores granite (Ribeiro *et al*., 2015). This younger deformation event could be considered as contemporaneous of the emplacement of post orogenic magmatism (ca. 300-290 Ma).

VII.1.3.2. Coimbra Sector

The western block of PTFSZ in Coimbra sector is characterized by one low-grade unit strongly similar to previously described to Porto-Espinho-Albergaria-a-Velha sector (Arada Unit; Chaminé *et al*., 2003a; Machado *et al*., 2008; 2011). It is a siliciclastic sequence mainly composed of black phyllites and metagreywackes, with black quartzites and ortho-derived mafic rocks (Ferreira Soares *et al*., 2005). The lithological resemblances led to consider this unit equivalent of the OMZ "Série Negra" (Ferreira Soares *et al*., 2005), with a Neoproterozoic age (Ribeiro *et al*., 2013). However, also here are described the presence of very low-grade imbricate metasedimentary rocks (black shales, with less abundant siltstones and sandstones; Fig. 6 and 8) with Frasnian-Serpukhovian age (Chaminé *et al*., 2003b; Machado *et al*., 2011), which led to consider that, at least part of the sequence could be equivalent of the Albergaria Unit.

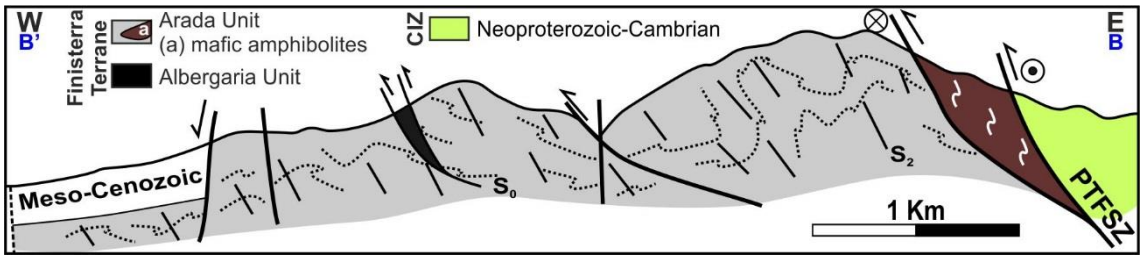

Figure 8 – Simplified geological cross section of Coimbra sectors (adapted from Ferreira Soares *et al*., 2005; Machado *et al*., 2011).

This low-grade unit has polyphased deformation, being trusted by the CIZ successions (Fig. 8; Ferreira Soares *et al*., 2005). The most important deformation are characterized by N-S dextral ductile-brittle to brittle shear zones related to the PTFSZ. These structures are subparallel to sub-vertical axial plane folds, where an axial planar cleavage is found (Ribeiro *et al*., 2013). The parallelism between both structures indicate an intense shear component related to the PTFSZ (Ribeiro *et al*., 2013). These intense deformation is superposed on an early deformation episode, poorly geometrically constrained, with recumbent folds (early Variscan or Cadomian?).

VII.1.4. The Berlengas Archipelago Finisterra Domain

The Berlengas Archipelago was considered a "suspect" terrane due the presence of deformed two mica granites, gneisses and micaschists West of Meso-Cenozoic Lusitanian Basin (Ribeiro *et al*., 1991). The similarities with the lithotypes of Tomar-Abrantes sector, which is the nearest Variscan basement, led to consider the Berlengas Islands part of the Western block of PTFSZ.

In the Farilhões and Forcadas islands outcrop an anatectic complex, mainly composed of gneisses, migmatites and micaschists, while the Berlengas, Estelas and Medas are mainly composed of a coarse-grained biotite pink granite (Fig. 1D; Valverde Vaquero *et al*., 2010a; 2010b; Bento dos Santos *et al*., in press).

The Berlenga granite is mainly composed of quartz + K-feldspar + plagioclase + biotite with no evidences of ductile deformation (Valverde Vaquero *et al*., 2010b). Initially considered as a Permian granite (280±15 Ma; $^{87}Rb/^{86}Sr$ de whole rock; Priem *et al*., 1965), recent data led to consider its emplacement as Upper Carboniferous (307,4±0,8 Ma; U/Pb concordant age in monazite and zircon, ID-TIMS; Valverde Vaquero *et al*., 2010a; 2010b). This granite was deformed by brittle-ductile N-S thrusts with low dips and an E vergence (Ribeiro, 2013).

The Farilhões metatexites are composed of quartz + plagioclase + k-feldspar + biotite ± sillimanite ± garnet ± muscovite, sometimes with granulite relics with plagioclase + quartz + biotite + amphibole ± garnet ± clinopyroxene ± ilmenite ± titanite paragenesis (Bento dos Santos *et al*., in press). Geothermobarometric studies show a prograde metamorphism reaching granulite facies conditions (P=8.6±1 kbar; T=915±50ºC; Bento dos Santos *et al*., 2010; in press), followed by retrograde metamorphism. The same authors consider these metatexistes genetically related to the diatexites composed of K-feldspar + plagioclase + sillimanite + biotite ± muscovite.

Monazites fractions from the diatexites provide Upper Devonian (377±1 Ma; U/Pb, ID-TIMS), which has been considered the age of the HT metamorphism in sillimanite zone that follows the granulite facies conditions (Valverde Vaquero *et al*., 2010a; 2010b; Bento dos Santos *et al*., in press). Some inhered zircons with Neoproterozoic ages (550-650 Ma; LA-ICP-MS, U-Pb in zircons; Bento dos Santos *et al*., in press) seems to indicate a siliciclastic Neoproterozoic protolith for the para-derived series.

VII.1.5. Distinctive Features of Finisterra Terrane

The individualization of the Finisterra Terrane from the adjacent Iberian one, must be supported by stratigraphic, tectonic, metamorphic and magmatic features, emphasizing a distinct geodynamical evolution (Coney *et al*., 1980). These terranes must to be representative at lithospheric scale, presenting distinct geodynamical evolution until its collage/accretion.

The presence of Ediacarian magmatism in Foz do Douro Gneiss Unit (Fig. 9; ca. 600-550 Ma; Noronha and Leterrier, 2000) and Ediacarian-Lower Cambrian inhered zircon populations in the Finisterra units (Pereira *et al*, 2010; Almeida, 2013; Almeida *et al*, 2014; Bento dos Santos, in press) are compatible with the Cadomian Orogeny, developed in North Gondwana margin (Linnemann *et al*., 2008). Thus, this could not be considered a distinctive feature, because in the

OMZ of the Iberian Terrane, an intense magmatism related to Cadomian event is also found (e.g. Salman, 2004; Simancas *et al*., 2004; Linnemann *et al*., 2008; Sánchez-Lorda *et al*., 2016). This should indicate a similar evolution of Finisterra and Iberian Terranes during Neoproterozoic times.

However, from Lower Cambrian until Lower Carboniferous times, several features indicate that the Finisterra was a terrane distinct from the Iberian one, being its contact outlined by the lithospheric scale PTFSZ.

The tectonostratigraphic units are clearly distinct from the Iberian Terrane successions. The Finisterra Terrane is characterized by the widespread occurrence of two HT tectonostratigraphic units: a basal gneiss and migmatite complex and an upper staurolite-garnet-micaschists unit. Between Espinho and Coimbra, there is also the development of a low-grade metamorphic unit (Arada Unit). Although the age of these HT tectonostratigraphic units are generally attributed to Proterozoic (e.g. Chaminé, 2000; Ribeiro *et al*., 2009), some Ordovician-Silurian ages are obtained in detrital zircons contained in these units (Fig. 9; Pereira *et al*., 2010; Almeida, 2013; Almeida *et al*., 2014), indicating that these units, or part of them, are possibly Silurian in age, also constraining the lower age of metamorphic event.

These HT tectonostratigraphic successions seem to be spatially (and generically?) associated to PTFSZ, presenting Silurian-Devonian zircon overgrowths (ca. 420-350 Ma; Fig. 9). The observed pre-Carboniferous HT foliation (Fernandez *et al*., 2003), could probably be related with such Silurian-Devonian event. This conclusions are compatible with the Berlengas data, where the HT early metamorphic event was attributed to Upper Devonian (ca. 380 Ma; Valverde Vaquero *et al*., 2010a; 2010b; Bento dos Santos *et al*., in press). In the Porto-Espinho-Albergaria-a-Velha sector this HT metamorphism is associated to Silurian felsic magmatism (Fig. 9; ca. 420 Ma; Chaminé *et al*., 1998). In the Iberian Terrane there are no evidences of a similar metamorphic and magmatic event, with exception to local HP metamorphic ages obtained in the southernmost domains of OMZ (ca. 370 Ma; Moita *et al*., 2005).

The low grade Arada Unit, is also considered as Neoproterozoic (Beetsma, 1995; Chaminé, 2000), but without recent geochronological constrains. In this unit occurs imbrications of very low-grade Frasnian-Serpukhovian black shales (Fig. 9; Chaminé *et al*., 2003b; Machado *et al*., 2011). Assuming the Arada Unit as Neoproterozoic, it requires the presence of an angular unconformity of a very low-grade Lower Devonian-Carboniferous cover over a Neoproterozoic low-grade metamorphic unit. Both Palaeozoic and Neoproterozoic units were tectonically imbricate by the Variscan deformation, possibly during the Mississippian event. Furthermore, the acritarchs assemblages of the very low-grade Palaeozoic unit show affinities with Laurussian

Late Devonian faunas (Machado *et al*., 2008) and not to Gondwana one as expected if an Iberian Terrane correlation exist.

Other particular feature, is the presence of a Silurian (or Proterozoic?) mafic and ultramafic magmatism with tholeiitic nature and within plate to MORB signature interlayered in all Finisterra units (Noronha and Leterrier, 2000; Silva, Almeida *et al*., 2014). This contrast with the Iberian Terrane because, although in OMZ some rocks with this nature are described, they have a Cambrian to Ordovician age (Mata and Munhá, 1990; Sánchez-García *et al*., 2008; Pedro *et al*., 2010).

The inhered zircons older than 500 Ma contained in the Finisterra units (Pereira *et al*., 2010; Almeida, 2013; Almeida *et al*., 2014) also have a distinct pattern from the observed in Neoproterozoic and Cambrian units of the Iberian Terrane from, either OMZ (e.g. Fernandez-Suárez *et al*., 2002; Linnemann *et al*., 2008; Pereira *et al*., 2008; 2011; 2012b), or CIZ (e.g. Pereira *et al*., 2012c; Talavera *et al*., 2012; Orejana *et al*., 2015).

The general patterns of OMZ and CIZ and Finisterra Terrane present similar representative populations in 500-750 Ma and 1800-2000 Ma (Fig. 10 and 11). One of distinctive feature of OMZ and CIZ patterns is the almost absence of Mesoproterozoic inhered zircons (ca. 1000-1600 Ma; Fig. 10). In some samples collected in Finisterra Terrane the absence of Mesoproterozoic ages are also denoted, although some samples presents significant populations of Mesoproterozoic ages, representing 9% of all Neoproterozoic-Archean obtained ages for all samples, suggesting dissimilar sources of clastic sediments (Fig. 10 and 11).

The peculiar features of Finisterra Terrane in the context of the Iberian Geology, is also expressed by its structural pattern which strongly contrast with the general trend of the Iberian Terrane. Indeed the oldest observed deformation episode (D_1), although highly disturbed by the Carboniferous tectono-metamorphic events, shows the presence of N-S recumbent folds with top-to-W transport and a possible root zone in the PTFSZ. Such geometry has no equivalent in the Iberian Terrane, where a NW-SE general trend prevails (Dias *et al*., 2013; Moreira *et al*., 2014). We consider this deformation episode contemporaneous of the Silurian-Devonian metamorphic event, which has no equivalent in the Iberian Terrane.

During Carboniferous, both Terranes seem to have been a similar geodynamical evolution. Indeed, similar Mississippian HT metamorphic ages (ca. 340-310 Ma) are also described in the Iberian Terrane, not only in the CIZ (e.g. Bea *et al*., 2006; Castiñeiras *et al*. 2008) but also in OMZ (e.g. Pereira *et al*., 2012a). The same happens with the Ar-Ar Pennsylvanian metamorphic ages of the NW Iberian shear zones (Gutiérrez-Alonso *et al*., 2015). Also the late magmatism have Permian age, denoting similar evolution during the Carboniferous and Permian times.

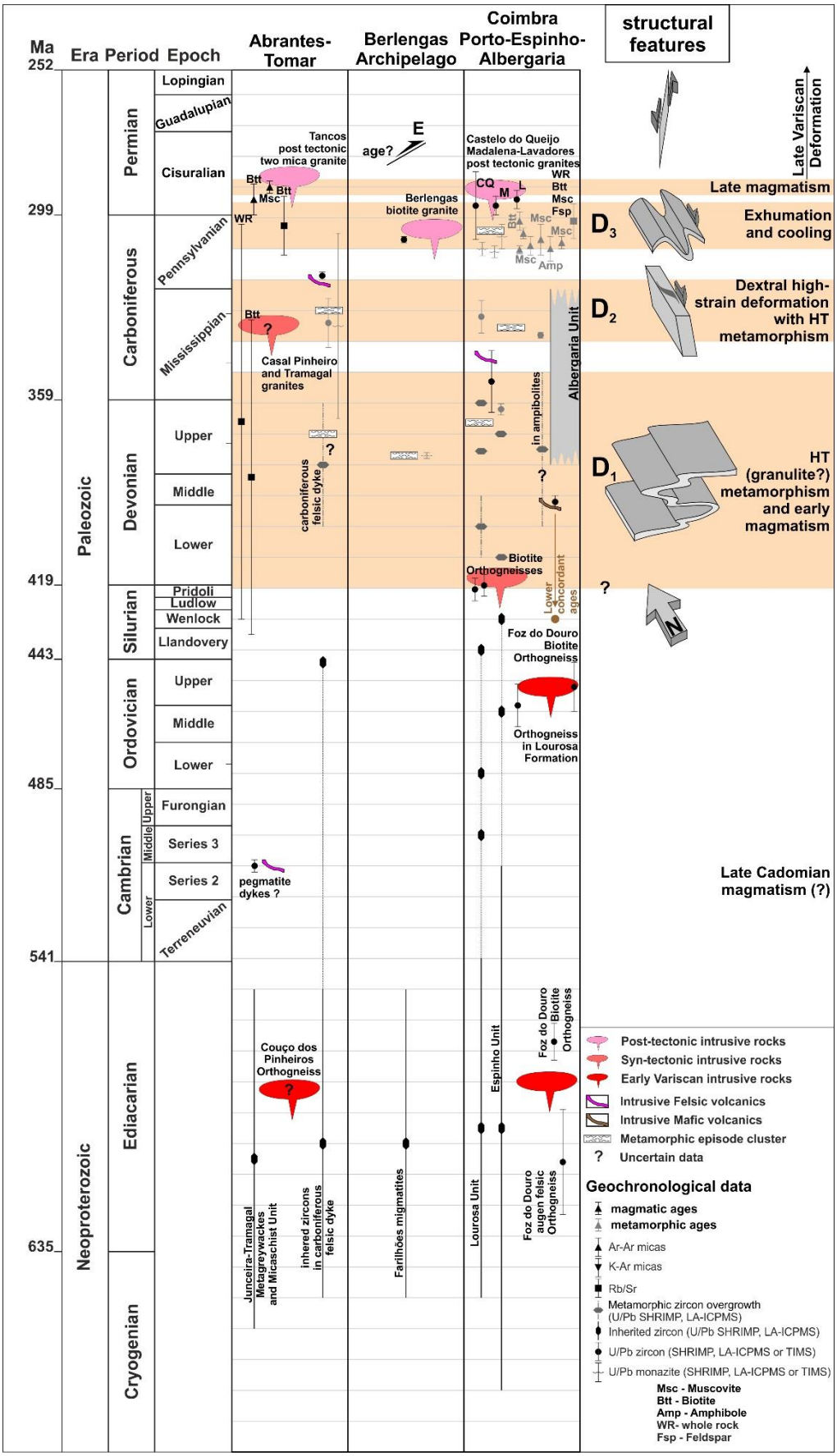

Figure 9 –Geological and geochronological features of Finisterra Terrane (data references on text).

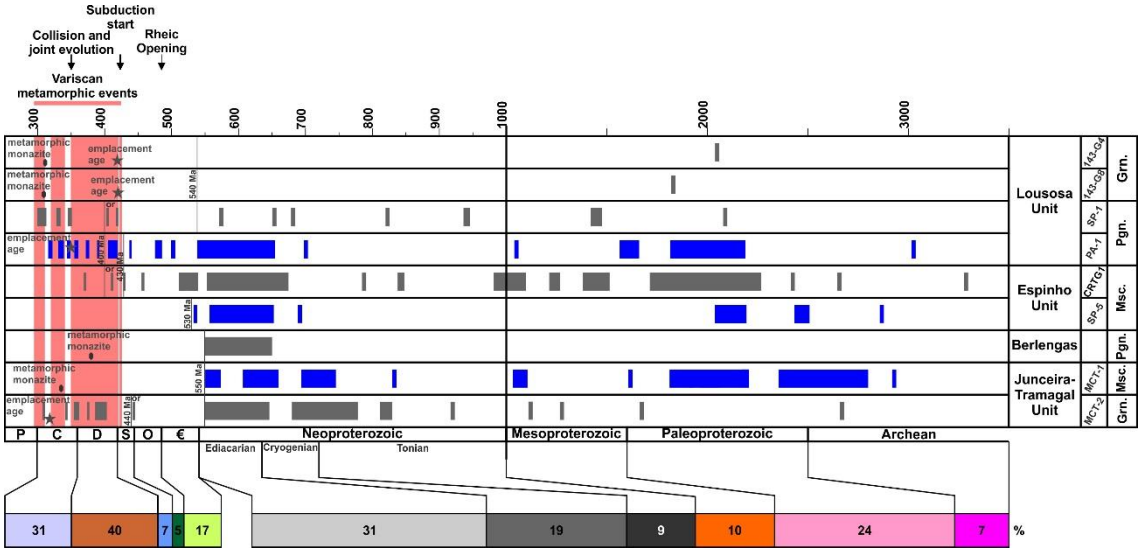

Figure 10 –Distribution of zircon and monazite ages from Finisterra Terrane units ($^{207}Pb/^{206}Pb$ ages from Pereira *et al*., 2010; Almeida, 2013; Almeida *et al*., 2014).

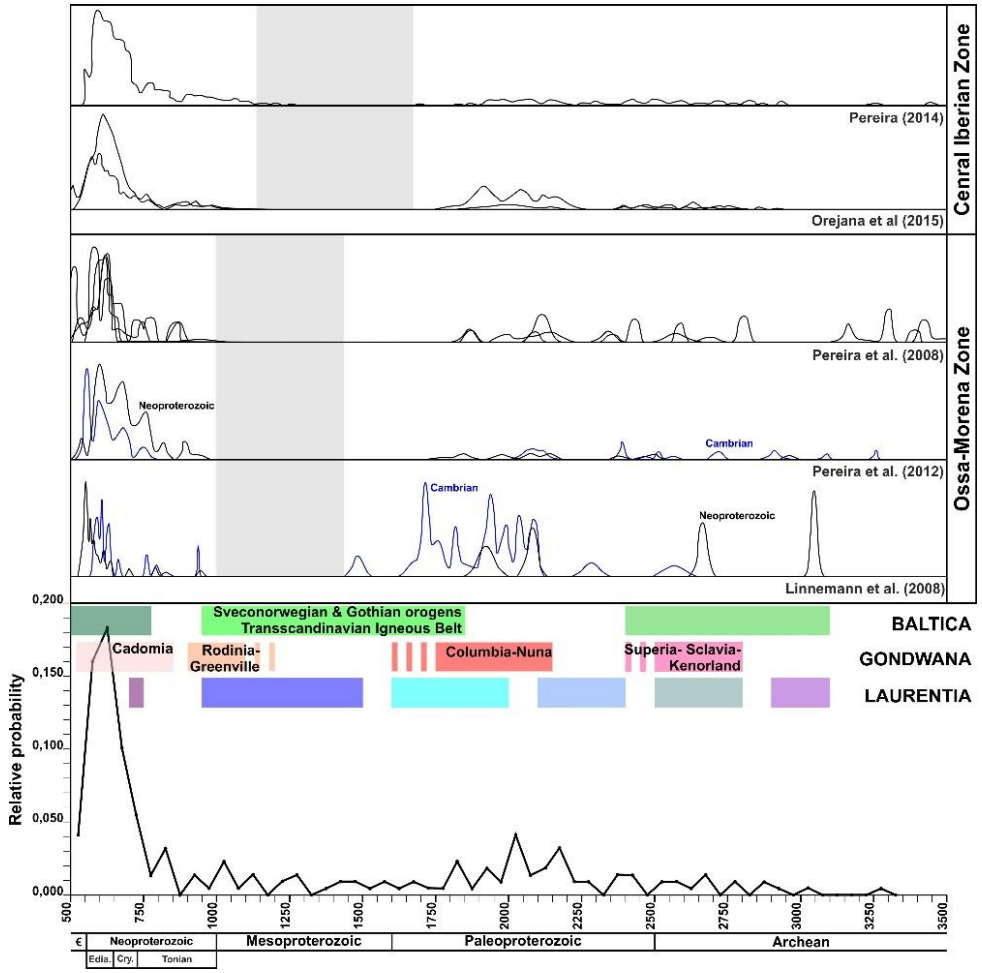

Figure 11 – Synthesis of Lower Cambrian-Neoproterozoic published zircon ages from Finisterra Terrane as probability plots, comparing with OMZ and CZI patterns and with possible zircon sources (adapted from Murphy *et al*., 2004; Pollock *et al*., 2007; Kuznetsov *et al*. 2014; Petterson *et al*., 2015).

Inhered zircons studies are performed in the Late Pennsylvanian Buçaco Basin (LA-ICP-MS; U-Pb in zircon; Dinis *et al*., 2012), located in the western border of CIZ near the Finisterra Terrane (Fig. 6), being identified some Silurian-Devonian (ca. 440-360 Ma) and also Mesoproterozoic (ca. 1350-1600 Ma) populations. This fact also emphasize the joint evolution of Iberian and Finisterra Terrane during Carboniferous times, being the Buçaco molasses Basin feed by both Terranes.

VII.1.6. Final Remarks and Paleogeographic Considerations

The geodynamics of the Finisterra Terrane cannot be dissociated from the European Variscides evolution. The nature of its eastern boundary (PTFSZ), its geological features and its relation with surrounding domains is crutial to understand its relation either with the northern branch of the Ibero-Armorican Arc (Dias *et al*., 2016), or with the northern Africa and the eastern America. This is not an easy task, due to Atlantic opening and the complexity of the Azores-Gibraltar plate boundary. The continuity of the narrow Finisterra Terrane is not obvious because it is isolated from the Iberian Terrane by a lithospheric shear zone and from the Central European Variscides due the Ibero-Armorican Arc. Nevertheless, its geological similarities with the Léon Domain and the Mid-German Crystalline Rise (MGCR), allow the establishment of some correlations among them.

VII.1.6.1. The Léon Domain

The Léon Domain is the small and northernmost domain of the Armorican Massif (Ballèvre *et al*., 2009; Faure *et al*., 2010; Fig. 12A). Its “exotic” features were extensively described since classical works (Bale and Brun, 1986; Le Corre *et al*., 1989). This block is composed of strongly deformed metamorphic rocks with Palaeozoic and Proterozoic age (Schulz *et al*., 2007; Ballèvre *et al*., 2009). It is interpreted as a complex stack of nappes, composed of several tectono-stratigraphic units (Faure *et al*., 2005; 2010; Ballèvre *et al*., 2009). The contact between the Léon Domain and the North and Central-Armorican Domains is debatable. While some considers the boundary in the Elorn fault, a (back)thrust with southward transport during Carboniferous times (Ballèvre *et al*., 2009), others put this limit in the Le Conquet-Penzé Shear Zone, a shear zone with tangential top-to-north transport, reactivated as a dextral strike slip fault during Carboniferous times (Faure *et al*., 2010).

VII.1.6.1.1. Main Tectonostratigraphic Units

In Léon Domain, a pile of nappes generated during the early Variscan deformation episode was emphasized (Faure *et al*., 2010), which will be summary described below.

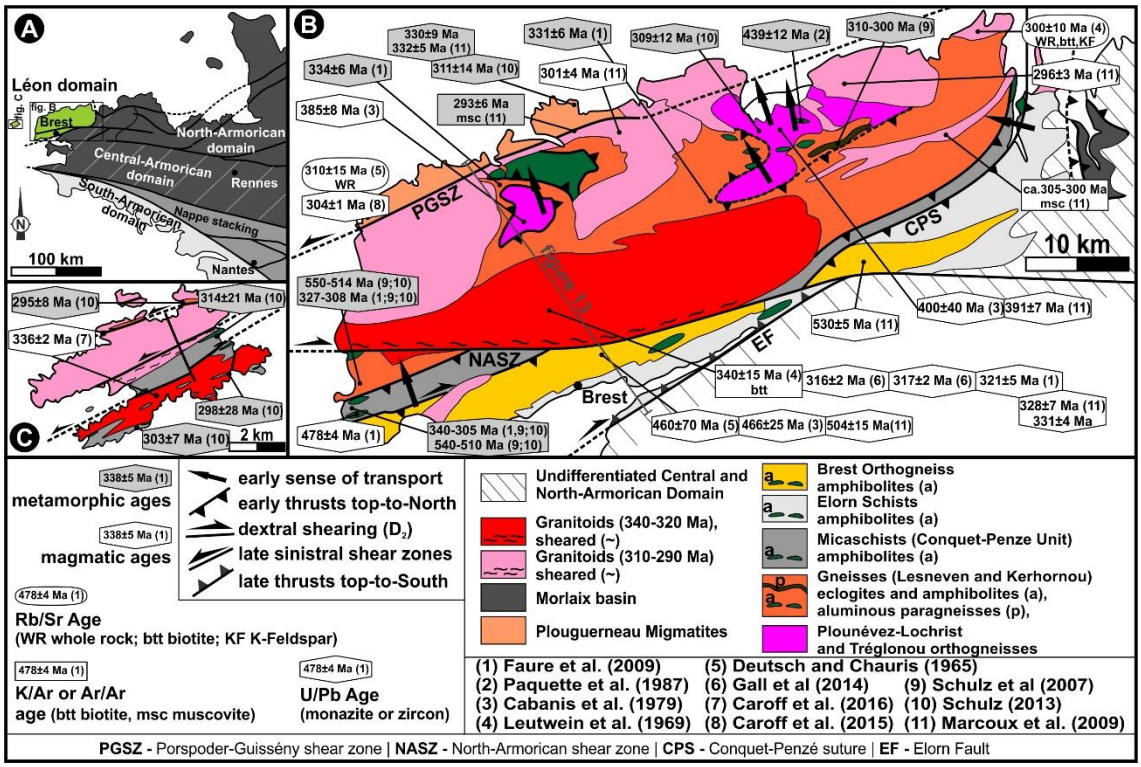

Figure 12 – The Léon Domain general framework:

A – Geographical relation wbetween the Léon Block and the Armorican Domains (adapted from Ballévre *et al*., 2009);

B – Simplified geological map of Léon Domain (adapted from Faure *et al*., 2010; Schulz, 2013);

C – Simplified geological map of Ouessant Island, the westernmost Léon outcrop (adapted from Schulz, 2013; Caroff *et al*., 2016).

- Parautochthonous unit

The lower unit (i.e. the Plounevez-Lochrist and Tréglonou Augen gneisses) is considered a parautochthonous unit composed of paragneisses intruded by K-feldspar Augen orthogneiss with biotite, garnet and sillimanite, both with intense migmatization. The emplacement age of the magmatic bodies is Lower-Middle Devonian (400±40 and 385±8 Ma, Ma, U-Pb in zircon, Cabanis *et al*., 1979; 391±7 Ma, U-Pb in zircon TIMS, Marcoux *et al*., 2009). Geochronological data on monazites, shows a HT metamorphic event during Late Carboniferous (ca. 320-310 Ma; Schulz, 2013) affecting the orthogneisses. Marcoux *et al*. (2009) notice a Lower Cambrian (ca. 530 Ma) inhered zircons in this ortho-derived body. The contact with the overlying lower nappe unit is marked a shear zone with blastomylonite rocks (Bale and Brun, 1986).

- Lower nappe

The lower nappe is a paragneiss unit (Lesneven and Kerhornou gneisses), mainly composed of biotite-garnet-sillimanite gneisses and micaschists bearing. Occasionally, they present

evidences of migmatization, sometimes with generation of quartz-feldspar-biotite leucossomes related to an incipient crustal melting and anatetic granitoid dykes, as well deformed quartz-mylonites (Bale and Brun, 1986; Ballèvre *et al*., 2009; Faure *et al*., 2010). The transition from high-grade gneiss to sillimanite metatexites and diatexites is progressive (Faure *et al*., 2010).

This unit includes ortho-derived mafic tholeiites, with amphibolites, pyroxenites, serpentinites and eclogites (Bale and Brun, 1986; Faure *et al*., 2010). The eclogites presents garnet+clinopyroxene+plagioclase paragenesis, with amphiboles resulting from retrograde metamorphism. The age of the HP metamorphism is Silurian (439±12 Ma, U-Pb in zircon; Paquette *et al*., 1987), while the age of migmatization in the para-derived gneiss has been considered either Upper Mississippian (ca. 335-330 Ma; Faure *et al*., 2010), or Pennsylvanian (ca. 310-300 Ma; Schulz *et al*., 2007). The presence of Neoproterozoic-Cambrian metamorphic monazites in these gneisses (ca. 550-514 Ma) shows that the siliciclastic protolith is probably Neoproterozoic (Schulz *et al*., 2007; Schulz, 2013). Indeed, the uniform monazite chemical composition and the narrow range of Cadomian ages, exclude the detrital origin of these monazites (Schulz *et al*., 2007).

- Intermediate nappe

This nappe is mainly composed of biotite-garnet-staurolite to biotite-muscovite-oligoclase micaschists (Conquet-Penze Micaschists) with metacherts, quartzites and conglomeratic lenses (Faure *et al*., 2010). Some ortho-derived amphibolites and Early Ordovician meta-gabbros (478±4 Ma; U-Pb in zircon, LA-ICP-MS, Faure *et al*., 2010) are also present.

The staurolite zone metamorphism present a Carboniferous age (ca. 340-305 Ma; U-Ph in monazites; Schulz *et al*., 2007; Faure *et al*., 2010; Schulz, 2013). This unit also presents Neoproterozoic-Cambrian monazites, showing a Proterozoic age for its protolith (ca. 540-510 Ma; Schulz *et al*., 2007; Schulz, 2013). Also in this case the detrital origin of these monazites is excluded by Schulz *et al*. (2007).

- Upper nappe

The upper nappe consists of micaschists (Elorn Schists) intruded by ortho-gneiss (Brest orthogneiss), being considered the Armorican Massif basement (Faure *et al*., 2010).

The Elorn Schists, considered Late Proterozoic (Ballèvre at al., 2009; Faure at al., 2010), is a low-grade metamorphic unit (greenschists facies; Ballèvre *et al*., 2009), mainly composed of quartz phyllites, metagreywackes and metasandstones. Nevertheless, sometimes the metamorphic grade is slightly higher, generating low-grade micaschists (Faure *et al*., 2010).

The Brest gneiss is considered an ortho-derived gneiss with granodiorite composition (Bradshaw *et al*., 1967), showing hornfels metamorphism in Elorn metasediments (Bradshaw *et al*., 1967). The emplacement of this granodiorite is considered Cambrian-Early Ordovician in age (460±70 Ma, U-Pb in zircon – Deutsch and Chauris, 1965; 466 ± 25 Ma, U-Pb dissolution in zircon – Cabanis *et al*. 1979; 504±15 Ma and 530±5 Ma, U-Pb in zircons LA-ICP-MS and TIMS respectively – Macoux *et al*., 2009). Some inhered zircon populations are identified in Brest gneiss, being Neoproterozoic (600-700 Ma), Mesoproterozoic (ca. 1350 Ma) and Paleoproterozoic (ca. 1600, 1850 and 1900-2100 Ma) in age (Macoux *et al*., 2009).

- Migmatites of Plouguerneau

North of the Porspoder-Guissény shear zone outcrop the Migmatites of Plouguerneau, whose relation with the southern nappe pile units is not clear (Fig. 12B; Faure *et al*., 2010). These migmatites are strongly deformed, presenting monazites that indicate a Carboniferous age for the metamorphism (ca. 330-300 Ma; Ballèvre *et al*., 2009; Marcoux *et al*., 2009; Schulz, 2013), and inhered cores of Cadomian monazites (ca. 580 Ma; Ballèvre *et al*., 2009; Marcoux *et al*., 2009). Similar lithotypes and metamorphic ages were also obtained in the Ouessant Island (Fig. 12C; Caroff *et al*., 2015).

- Carboniferous magmatism

The Léon Domain was affected by an extensive Variscan magmatism comprising two main events (Fig. 12B):

- The oldest one, composed of granites and granodiorites with calco-alcaline signature (Bale and Brun, 1986), were intruded between 340 and 320 Ma (Cabanis *et al*., 1979; Faure *et al*., 2010; Marcoux *et al*., 2009; Le Gall *et al*., 2014). Some enclaves of Lesneven gneiss were identified in the Saint Renan-Kersaint massif (Bale and Brun, 1986). Inhered zircon populations with Neoproterozoic age were reported (540-650 and ca. 900 Ma; Marcoux *et al*., 2009).
- The younger assemblage, located in the northern sectors of Léon Domain, is composed of sub-alkaline granites and monzogranites (Bale and Brun, 1986), with ages ranging between 310-290 Ma (Cabanis *et al*., 1979; Marcoux *et al*., 2009; Caroff *et al*., 2015).

VII.1.6.1.2. Structural pattern

The high to medium-grade tectono-metamorphic units of the Léon Domain present a general ENE-WSW to NE-SW trend, affected by three main tectonic events.

The early deformation episode (D_1) is related to the nappe stacking of the tectonostratigraphic units. The contact between the tectono-metamorphic units are always D_1 tangential shears with transport top-to-the-N or NNW (Fig. 13; Faure *et al*., 2010; Bale and Brun, 1986), sometimes outlined by blastomylonite rocks (Bale and Brun, 1986). As mentioned, Lesneven and Kerhornou gneisses include eclogitic rocks (mostly retrogressed into amphibolites) with Silurian metamorphic ages (Paquette *et al*., 1987). Faure *et al*. (2010) considers the HP-metamorphism previous to nappe stacking episode (D_1), that constrain the timing of the episode as Late Silurian(?)-Devonian. In the Upper Unit, there is progressive increase of the deformation towards north, in direction of the contact with the Penzé-Le Conquet Micaschists unit (Le Conquet-Penzé Shear Zone; Bradshaw *et al*., 1967; Faure *et al*. 2010). These major shear zone presents poly-phasic deformation (Fig. 13; Faure *et al*., 2010), being reactivated during the second deformation episode (D_2) as a dextral strike-slip shear zone (Balé and Brun, 1986).

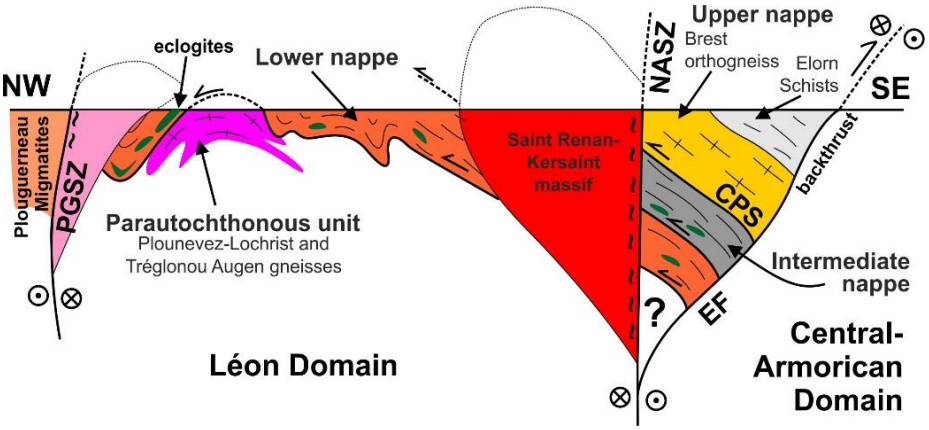

Figure 13 – Simplified cross-section from Léon Domain (adapted from Ballévre *et al*., 2009; Faure *et al*., 2010; Schulz, 2013).

All these units were deformed by a HT D_2 event (Bale and Brun, 1986) that often deeply reworked previous D_1 fabrics (Le Corre *et al*., 1989; Faure *et al*., 2005; 2010). In the Lesneven and Kerhornou gneisses, where D_2 is weaker, it is possible to show that the D_2 migmatization and crustal melting postdate the HP metamorphism (Faure *et al*., 2010). The metamorphic ages for D_2 are consistent with the Mississippian metamorphic event age (Schulz *et al*., 2007; Faure *et al*., 2010, Schulz, 2013). Thus, the HT metamorphism is temporally related with the emplacement of the previously mentioned first plutonic episode (ca. 340-320 Ma), represented by the Saint Renan-Kersaint massif, considered syn-tectonic with the D_2 E-W dextral kinematics of North-Armorican shear zone (NASZ; Bale and Brun, 1986; Schulz *et al*. 2007; Faure *et al*.,

2010). Similar dextral wrench kinematics is described in Elorn Fault, which could be interpreted as a branch of the NASZ (Faure *et al*., 2005).

A late episode of deformation (D_3) is described, not only in the northern sectors of Léon Domain (Fig. 12B and 13; Le Corre *et al*., 1989; Marcoux *et al*., 2009), but also in the Ouessant Island (Fig. 12C; Caroff *et al*., 2016). This D_3 event in contemporaneous of the Plouguerneau migmatites and related to the NE-SW Porspoder-Guissény sinistral shear zone (Le Coure *et al*., 1989). The metamorphic ages obtained in the migmatites (311±14Ma, Th-U-Pb in Monazites; Schulz, 2013) and in the moscovites contained in myllonites of the Porspoder-Guissény shear zone (293±3 Ma, Ar-Ar; Marcoux *et al*., 2009), constrain this deformation episode between 310 and 290 Ma. However, some older metamorphic ages were also obtained in this migmatites (ca. 330 Ma; Marcoux *et al*., 2009), which seem to indicate that the migmatization could have begun during D_2 episode. The age for D_3 is compatible with field observations. Indeed, the NE-SW lineaments seem to have controlled the emplacement of the Late Carboniferous-Permian magmatic bodies (Fig. 12B; Ballèvre *et al*., 2009; Caroff *et al*., 2015) and the D_3 Porspoder-Guissény shear zone generates mylonites and ultramylonites that affects those granitoids (Marcoux *et al*., 2009; Le Gall *et al*., 2014; Caroff *et al*., 2016). These granites are considered posterior to D_2 dextral deformation episodes (Bale and Brun, 1986).

VII.1.6.2. The Mid-German Crystalline Rise

The Mid-German Crystalline Rise (MGCR), with a SW-NE trend, is mainly composed of medium- to high-grade gneisses, migmatites and plutonic rocks, partially covered by Permian to Quaternary deposits (Zeh and Will, 2010). This domain is located in northern sectors of the Saxo-Thuringian Domain, south of the low-grade metasediments and volcanic rocks of the Northern Phyllite Belt and the Rhenohercynian domain (Zeh and Will, 2010). It appears in small basement outcrops, generally called crystalline complexes, such as the Spessart, Kyffhäuser, Ruhla or Odenwald (e.g. Nasir *et al*., 1991; Dombrowski *et al*., 1995; Will and Schmädicke, 2003; Zeh and Will, 2010), being subdivided in several tectonostratigraphic units.

The crystalline complexes are mainly composed of gneisses and migmatites, containing amphibolite and, occasionally, marbles, calcisilicate rocks and quartzites. The gneisses, usually with para-derived nature, are interlayered with migmatites, micaschists and some ortho-derived gneisses (Dombrowski *et al*., 1995; Altherr *et al*., 1999). The metamorphism reaches high-temperature conditions, equivalent to amphibolite(-granulite) facies, with generation of cordierite+sillimanite+garnet+staurolite paragenesis (Will and Schmädicke, 2003). In the Odenwald Crystalline Complex, it was described retrogressed eclogites, now garnet amphibolites presenting tholeiitic nature and MORB to within-plate basalts geochemical

signature (Scherer *et al*., 2002, Will and Schmädicke, 2001; 2003). This indicates the presence of a HP metamorphism previous to the HT one. The minimum age of this eclogites was considered to be Upper Devonian (357±6 Ma; Lu-Hf, garnet-whole rock; Scherer *et al*., 2002); according to authors, some resetting during the retrograde metamorphism may happen. Similar metamorphic ages have been also obtained in the Odenwald (375± 5 Ma; U-Pb in zircon, Todt *et al*., 1995) and Ruhla Crystalline Complexes (356.7±4.7 – zircon – and 352±8 Ma – monazite; U-Pb SHRIMP, Zeh *et al*., 2003), although in these cases the association with the HP event is not clear (Zeh and Will, 2010). The existence of an Upper Devonian metamorphic event is also supported by the presence of zircon grown in para-derived lithotypes (ca. 380-360 Ma; Reischmann and Anthes, 1996; Anthes and Reischmann, 2001). This metamorphic event is temporally associated to the emplacement of felsic (e.g. Albersweiler granitic gneiss; Reischmann and Anthes, 1996) and mafic-intermediate (e.g. Frankenstein gabbro; Kirsch *et al*., 1988; Zeh *et al*., 2005) bodies.

Concerning to the HT metamorphic event, its Mississippian age (340-320 Ma) is constrained by several geochronological studies (Nasir *et al*., 1991; Todt *et al*., 1995; Zeh *et al*., 2003; 2005), although some older ages are obtained in Odenwald (349±14 and 430±43 Ma, Th–U–Pb in Monazites; Will *et al*., 2016), emphasizing an early HT episode. The Mississippian metamorphic event is coeval with the emplacement of plutonic bodies, with granitic and granodiorite composition, such as Spessart diorite-granodiorite, Pretzsch-Prettin granite (Anthes and Reischmann, 2001), Edenkoben granite, Windstein granodiorite (Reischmann and Anthes, 1996) or Borntal intrusive complex (Anthes and Reischmann, 2001; Zeh *et al*., 2005).

However, in MGCR the plutonism is not restricted to previous events having a wide temporal range: Late Cambrian-Early Ordovician (e.g. Volkach Syenite; Anthes and Reischmann, 2001), Silurian-Devonian (ca. 420-410 Ma; e.g. Thal, Erbstrom and Silbergrund granite gneisses; Dombrowski *et al*., 1995; Brätz, 2000; Zeh *et al*., 2003) and Pennsylvanian-Early Permian bodies (310-290 Ma; e.g. Delitzsch granite; Anthes and Reischmann, 2001).

Geochronological studies in para-derived gneisses and migmatites (e.g. Zeh *et al*., 2001; 2003; 2005; Gerdes and Zeh, 2006; Zeh and Gerdes, 2010) and some ortho-derived gneisses (Anthes and Reischmann, 2001) show the presence of several populations of detrital zircons, although the general pattern of inhered zircons presents great dispersion within MGCR (Zeh and Gerdes, 2010). Indeed, the authors emphasize distinct patterns of inhered zircons, showing the presence of distinct clusters in Brotterode and Ruhla Groups (Fig. 14; both in Ruhla Crystalline Complex):

- Brotterode Group (Zeh *et al*., 2001; 2003; Gerdes and Zeh, 2006) – Lower Palaeozoic to Neoproterozoic representative populations (460-489, 500-590, 640-670 and 720-740 Ma)

and clusters of Mesoproterozoic (ca. 1000 Ma), Paleoproterozoic (ca. 1800, 1950-2150 and ca. 2500 Ma) and Archean (ca. 2650 and 2830-2900 Ma) populations.

- Ruhla Group (Zeh and Gerdes, 2010) – Lower Palaeozoic to Ediacatian (435-485, 550-650Ma) and Meso- to Paleoproterozoic (900-1800 Ma with peaks at 1100, 1250, 1450, 1600 and 1800 Ma) representative populations and clusters of Paleoproterozoic (1850-1900 and ca. 2000 Ma) and Archean (ca. 2550, 2650 and 2800 Ma) populations.

The Meso- to Paleoproterozoic population, highly represented in Ruhla Group, is absence in Brotterode Group (Zeh and Gerdes, 2010). Similar Lower Paleozoic-Neoproterozoic and Mesoproterozoic populations were also described in Spessart and Kyffhäuser Crystalline Complexes (Anthes and Reischmann, 2001; Zeh *et al*., 2005).

Towards the southern boundary of the MGCR there are three (very) low-grade metamorphic units (Fig. 15), which contact with the Moldanubian Zone by the Lalaye-Lubine dextral shear zone (LLSZ; Franke, 2000; Zeh and Will, 2010). From south to north are:

- Villé unit: It is composed of late Cambrian to early Ordovician metapelitic to metapsammitic schists and quartzites;
- Steige unit: It is a monotonous metapelitic sucession deposited in a shallow marine environment during Ordovician to Silurian times. This unit thrusts the Villé unit;
- Bruche unit: It is a sedimentary and tectonic mélange comprising Frasnian black shales and Fammenian to early Carboniferous shelf and slope sediments, greywackes and conglomerates with calc-alkaline volcanic rocks.

The Steige and Villé Units are more deformed than the Bruche Unit (Skrzypek *et al*., 2014). Indeed, the Bruche unit is only affected by a Carboniferous tectono-metamorphic event (ca. 340-330) while the other units have a previous deformation episode (Skrzypek *et al*., 2014). All these very volcano-sedimentary sequences were intruded by diorites and granites during Carboniferous times.

6.3. Finisterra-Léon-MGCR Terrane; an essay of correlation

The Finisterra Terrane geological features shows clear similarities with the Léon Domain and MGCR. The correlation between the Léon Domain and the MGCR had already been established by several authors (e.g. Schulz *et al*., 2007; Faure *et al*., 2010; Ballévre *et al*., 2009; Franke, 2014; Franke and Dulce, 2016; Will *et al*., 2016). The strong similarities of these units with the geological features observed in the Finisterra Domain, led us to propose that the Léon-MGCR Domain extends up until Finisterra Terrane, defining the Finisterra-Léon-MGCR Terrane (Fig. 16).

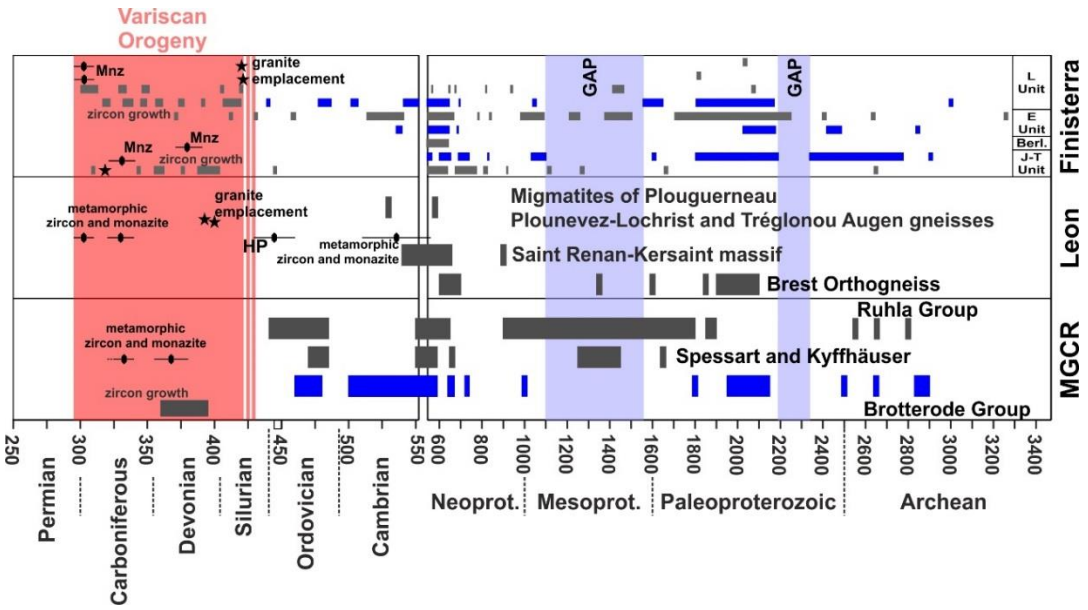

Figure 14 – Zircon patterns of Finisterra-Léon-MGCR Terrane (see references on text).

As previously described all these domains present an early magmatic event ca. (420-370 Ma), with the emplacement of several early granites (Fig. 15; Cabanis *et al*., 1979; Chaminé *et al*. 1998; Dombrowski *et al*., 1995; Brätz, 2000; Marcoux *et al*., 2009). The early magmatic event is accompanied by an early Variscan HT metamorphism (granulite facies conditions) during Devonian times (ca. 390-360 Ma; Fig. 15), however in the Léon Domain the geochronological data of such event seems to be absent (Schulz, 2013). Similar Late Silurian-Devonian metamorphic and felsic magmatic ages are rare in European Variscides. Although similar metamorphic ages are known, not only in the South and Central Armorican Domains (Balévre *et al*., 2009; Schulz, 2013), but also at OMZ (Moita *et al*., 2005), being generally associated to HP metamorphic rocks.

Also concerning the structural features, the three domains of the Finisterra-Léon-MGCR share a complex and polyphased deformation. The early tectono-metamorphic episodes are characterized by fold and thrust structures facing to N-NW in Léon and MGCR Domains (Faure *et al*., 2010; Zeh and Will, 2010) and to W in the Finisterra, probably rooting in its south (Le Conquet-Penzé Suture) and Eastern (PTFSZ) boundaries respectively.

Devonian HP metamorphic episode with eclogites is present both in Léon and MGCR Domains. These eclogites, which have been retrograded during Carboniferous events, have distinct ages (ca. 420 Ma in Léon Domain and ca. 360 Ma in MGCR; Paquette *et al*., 1987; Scherer *et al*., 2002). This seems to indicate a diachronic Variscan subduction during Devonian times that controls the early tectono-metamorphic stages of the Finisterra-Léon-MGCR Terrane, being developed at North of the proposed Terrane (Rheic Ocean subduction?). Although, until now,

the eclogitic rocks are not described in the Finisterra Domain, this can be the result of the absence of detailed metamorphic studies in these area.

Abundant mafic and ultramafic magmatism associated to HT metamorphic units is described in all domains, but also to low-grade ones in Finisterra Terrane. The geochemical signature of this magmatism is compatible with within-plate to MORB basalts. Nevertheless, the meaning of this magmatism is not well constrained, it could be the result of the Cambrian-Ordovician times (or even during Silurian?) extensional processes related to the Variscan Ocean opening. More geochronological and isotopic studies should help to constrain the age and melting sources of such mafic magmatism.

Also the zircon patterns of MGCR and Finisterra Terrane show clear similarities. In both domains, two distinct patterns are present (Pereira *et al*., 2010; Zeh and Gerdes, 2010; Almeida *et al*., 2014; Fig. 14): samples with abundant Mesoproterozoic zircons and samples without Mesoproterozoic zircons. In both groups, Ordovician and Silurian zircons are sometimes found, showing that, at least, some of the metasedimentary protoliths of these rocks are Palaeozoic (Fig. 14). The existence of two distinct patterns of inhered zircons shows contrasting sources during sedimentation. As the Mesoproterozoic gap is one of the most distinctive feature of Gondwana-derived metasediments (e.g. Zeh and Gerdes, 2010; Pereira, 2014), the presence of significant populations of Mesoproterozoic zircons in some samples seems to preclude a Gondwana source for some samples. This shows that the Finisterra-Léon-MGCR represents a composite terrane, containing affinities with Peri-Gondwana terranes, but also with Laurussia-Baltica (?) continents (Zeh and Gerdes, 2010), where significant Mesoproterozoic ages are described (e.g. Murphy *et al*., 2004; Pollock *et al*., 2007; Kuznetsov *et al*. 2014; Petterson *et al*., 2015).

The low-grade metamorphic units described in Finisterra Terrane, namely as the black shales of Albergaria Unit, contains acritarchs with Laurussian affinities, imbricated in the previously deformed Arada Unit. The acritarchs assemblage is quite similar to those described in Rhenish massif (northern of MGCR; Fig. 16; Machado *et al*., 2008), which also includes Devonian clastic sediments derived from Caledonian Laurussia sources (Franke, 2000). Such data reinforce the zircon pattern previously described. The Albergaria Unit could also be a lateral equivalent of the Bruche unit (MGCR), presenting similar ages and lithotypes during the Upper Devonian, although the Carboniferous succession is slightly distinct. In both cases, the Devonian-Carboniferous units are spatially associated to older and mostly deformed low-grade units. The proximity of the Finisterra-Léon-MGCR Terrane to Laurussia in the Upper Devonian, contrasts to the Iberia and Armorica paleogeography that were still close to Gondwana.

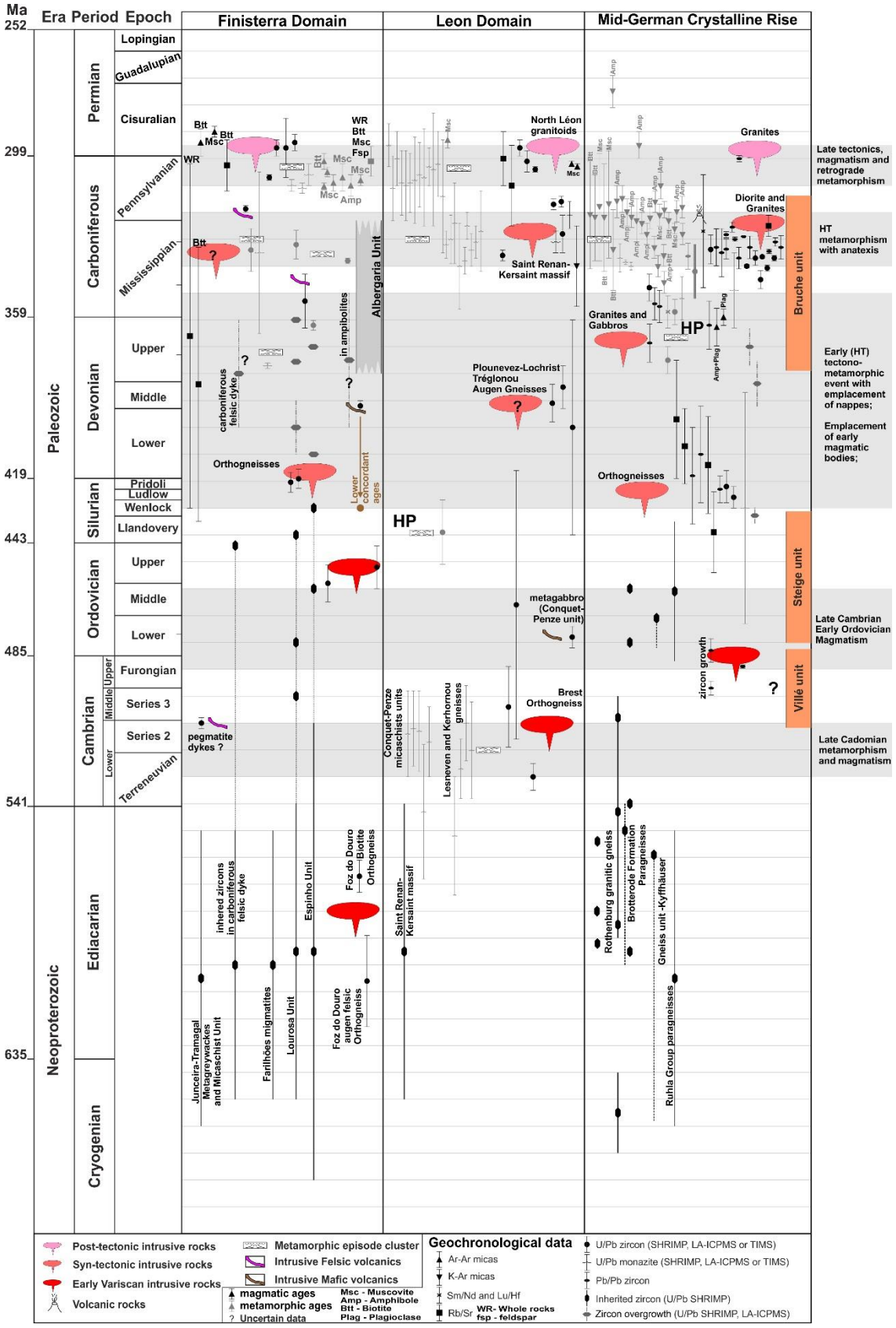

Figure 15 – Main tectono-metamorphic and magmatic features of Finisterra-Léon-MGCR Terrane (based on references presented on text).

The similarity of the MGCR zircon pattern with those exhibited in Pulo do Lobo Domain (*i.e*. Alájar Melange, Ribeira de Limas – Braid *et al*., 2011 – and Horta da Torre Formations – Perez-Cáceres *et al*., 2016) led to consider their possible correlation (Franke and Dulce, 2016; Fig. 16). Nevertheless, although the inhered zircon patterns are similar, the early magmatic event is absent in the Pulo do Lobo Domain and such correlation must to be strengthen.

Concerning the geodynamical meaning of the Finisterra-Léon-MGCR boundaries, distinct interpretation are possible for these lithospheric-scale shear zones:

- The Eastern Boundary of the Finisterra Terrane (PTFSZ) was considered a Paleo-transform fault with polyphasic deformation, at least, since early Variscan Cycle (Ribeiro *et al*., 2007). The western Finisterra boundary is unknown;

- The southern boundary of Léon (Le Conquet-Penzé Shear Zone) was be interpreted as an oceanic suture, separating this domain from the Armorican Massif (Faure *et al*., 2010). Nevertheless, the same authors do not exclude that this suture could represent only the closure of a thinned continental crust basin. Its northern boundary is presently hidden below the sea, being interpreted as the Rheic suture zone (Faure *et al*., 2010).

- The MGCR boundaries are generally covered by Permian to Quaternary sediments (Zeh and Will, 2010). Nevertheless, the contact with the southern Moldanubian Zone, is sometimes exposed, where it corresponds to the dextral LLSZ. The dextral shearing is Carboniferous, being superimposed on previous deformation (Skrzypek *et al*., 2014). However, the geodynamical significance of this major shear zone is not consensual, being interpreted either as a suture or an early Variscan detachment reactivated during Carboniferous (Skrzypek *et al*., 2014 to a discussion). The non-exposed northern limit of MGCR is considered a Variscan Suture (e.g. Skrzypek *et al*., 2014; Franke and Dulce, 2016).

According to previous data and interpretations the northernmost boundary of Finisterra-León-MGCR Terrane appears be consensual, representing a Variscan Oceanic suture (Rheic and/or Rheno-Hercynian Oceanic Suture?; Franke, 2000; Faure *et al*., 2010; Franke and Dulce, 2016). However, its southernmost boundary with Gondwana derived Terranes (Armorica and Iberia) is debatable and two distinct interpretations are possible:

- An active transform margin expressed by the PTFSZ, which connects the SW Iberian suture with the northern European suture(s), mainly the Le Conquet-Penzé Suture (and/or Paleotethys suture);

- All this boundary represents the suture zone of a secondary Palaeozoic Ocean (or a stretched continental crust basin) opened during Palaeozoic times.

The second hypothesis could explain the abundant Ordocivian to Silurian mafic and ultramafic rocks (Faure *et al*., 2010; Almeida *et al*., 2014), interspersed in the clastic rocks, which

subsequently undergo HP metamorphism during Upper Silurian to Devonian times (Paquette *et al*., 1987; Scherer *et al*., 2002). The obtained Mesoproterozoic Sm-Nd model age for the amphibolites in Finisterra Terrane (Noronha and Leterrier, 2000) seems to be incongruent with the remaining data. Indeed, the mafic and ultramafic rock could represent, either mafic dykes intruded in Lower Palaeozoic siliciclastic sequences related to the Palaeozoic continental stretching or even oceanic floor rocks obducted during collisional processes.

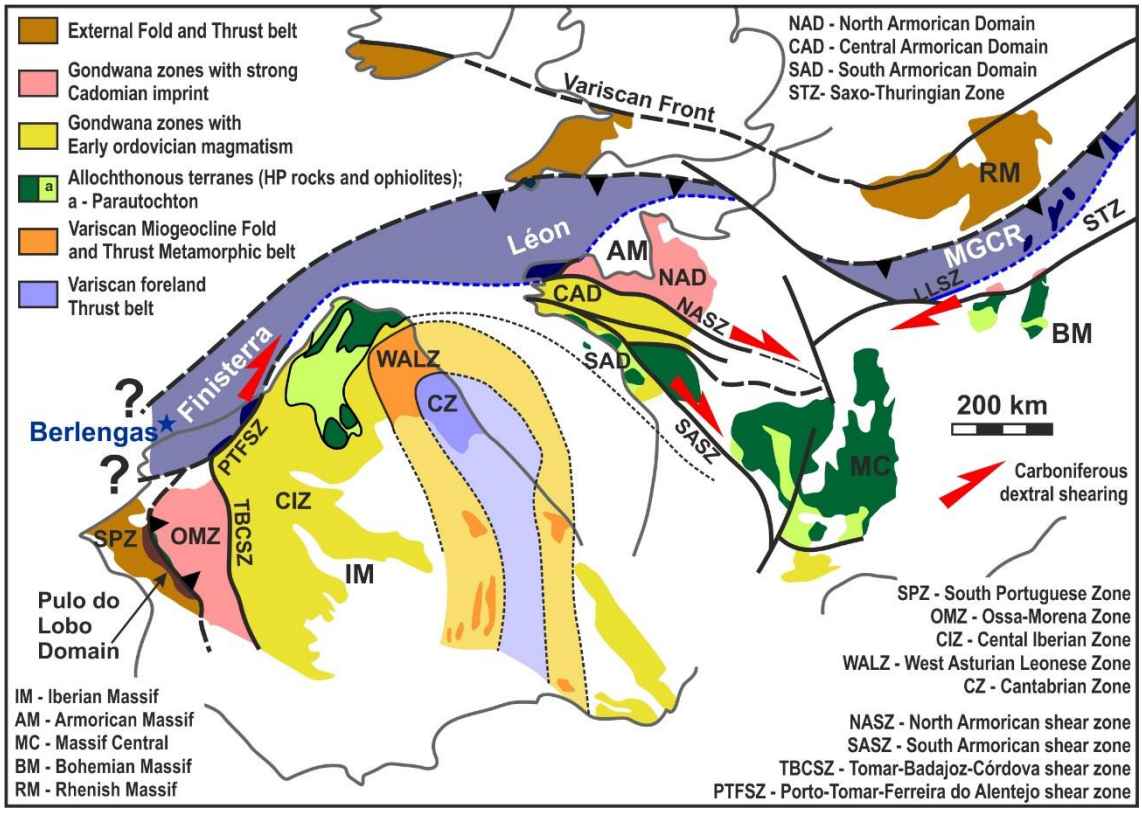

Figure 16 – The Finisterra-Leon-MGCR Terrane in the context of the European Variscides (adapted from Dias *et al*., 2016; Franke and Dulce, 2016).

Since Mississippian (ca. 340-330 Ma), the described Terrane and the other Peri-Gondwana Terranes shows similar metamorphic and magmatic ages (Fig. 15), which suggest they began to evolve together. Thus, such could represent the beginning of collision between Gondwana and Laurentia as often considered (Ribeiro *et al*., 2007; Moreira *et al*. 2014; Dias *et al*., 2016). In Mississippian, not only the Finisterra-León-MGCR Terrane but also the Iberian and Armorican Terranes, where affected by a pervasive dextral kinematics (e.g. PTFSZ, NASZ and LLSZ). The strong HT metamorphism related to the collisional process with melting generation was superimposed on previous events (Fig. 15), almost obliterating the early Variscan events in the Finisterra-Léon-MGCR Terrane.

The Neoproterozoic magmatism and metamorphism of Finisterra and Léon Domains (ascribable to the Cadomian event) and the presence of Late Cambrian-Early Ordovician magmatism (Fig. 15), also seems to indicate their North Gondwana affinities. Thus, the Finisterra-Léon-MGCR Terrane have a distict evolution of North Peri-Gondwana realm during Early Palaeozoic times, sharing, not only a common origin and evolution during Cadomian Cycle, but also a similar evolution after the Variscan collision during Carboniferous times (ca. 340-330 Ma).

References

Abranches, M.C.B, Canilho, M.H. (1981/82). Determinação de idade pelo método Rb-Sr de granitos portuguese. Men. Acad. Cienc. Lisboa, 24, 17-31.

Acciaioli, M.H., Santos, J.F., Munhá, J.M., Cordani, G.G., Couto, A., Sousa, P. (2003). Idades Ar-Ar em micas de metapelitos da zona de Espinho: Datação do Metamorfismo relacionado com a F3 Varisca. IV Congresso Ibérico de Geoquímica (Coimbra), abstract book, 161-163.

Aires, S. Noronha, F. (2010). O anfibolito olivínico do Engenho Novo (Norte de Portugal) revisitado. X Congresso de Geoquímica dos Países de Língua Portuguesa and XVI Semana de Geoquímica abstract book. 69-77.

Almeida, N. (2013). Novos dados geocronológicos do Terreno Finisterra no Sector entre Espinho e Albergaria-a-Velha, Portugal. MsC Thesis (unpublished). University of São Paulo, 98 p.

Almeida, N., Egydio Silva, M., Fonseca, P. E., Bezerra, M. H., Basei, M., Chaminé, H. I., Tassinari, C. (2014). Novos dados geocronológicos do Finisterra. Comunicações Geológicas, 101 (I), 31-34.

Altherr, R., Henes-Klaiber, U., Hegner, E., Satir, M., Langer, C. (1999). Plutonism in the Variscan Odenwald (germany): from subduction to collision. Int J Earth Sci, 88, 422–443. DOI: 10.1007/s005310050276

Anthes, G., Reischmann, T. (2001). Timing of granitoid magmatism in the eastern Mid-German Crystalline Rise. J Geodyn, 31, 119-143. DOI: 10.1016/S0264-3707(00)00024-7

Balé, P., Brun, J.P. (1986). Les complexes métamorphiques du Léon (NW Bretagne): un segment du domaine éo-hercynien sud armoricain translaté au Dévonien Bull. Soc Geol Fr, 2, 471-477.

Ballèvre, M., Bosse, V., Ducassou, D., Pitra, P. (2009). Palaeozoic history of the Armorican Massif: models for the tectonic evolution of the suture zones. C R Geosci, 341, 174–201. DOI: 10.1016/j.crte.2008.11.009

Bea, F., Montero, P.G., Gonzalez-Lodeiro, F., Talavera, C., Molina, J.F., Scarrow, J.H., Whitehouse, M.J., Zinger, T. (2006). Zircon thermometry and U–Pb ion-microprobe dating of the gabbros and associated migmatites of the Variscan Toledo Anatectic Complex, Central Iberia. Journal of the Geological Society, 163, 847-855. DOI: 10.1144/0016-76492005-143.

Beetsma, J. J. (1995). The late Proterozoic/Paleozoic and Hercynian crustal evolution of the Iberian Massif, N Portugal, as traced by geochemistry and Sr-Nd-Pb isotope systematics of pre-Hercynian terrigenous sediments and Hercynian granitoids. PhD Thesis (unpublished), Vrije Universiteit, Amsterdam.

Bento dos Santos, T., Ribeiro, M.L., González Clavijo, E., Díez Montes, A, Solá, A.R., (2010). Geothermobarometric estimates and P-T paths for migmatites from Farilhões Islands, Berlengas Archipelago, W Portugal. VIII Congresso Nacional de Geologia, Braga. e-Terra, 16(11). Available online: http://e-terra.geopor.pt.

Bento dos Santos, T., Valverde Vaquero, P., Ribeiro, M. L., Solá, A. R., Clavijo, E. G., Díez Montes, A. Dias da Silva, I. (in press). The Farilhões Anatectic Complex (Berlengas Archipelago). In Quesada, C., Oliveira, J.T. (Eds.), The Geology of Iberia: a geodynamic approach. Springer (Berlin), Regional Geology Review series.

Bradshaw, J. D., Renouf, J.T., Taylor, R. T. (1967). The development of Brioverian structures and BrioverianlPalaeozoic relationships in west Finistere (France). Geologische Rundschau, 56, 567-96. DOI: 10.1007/BF01848744

Braid, J.A., Murphy, J.B., Quesada, C., Mortensen, J. (2011). Tectonic escape of a crustal fragment during the closure of the Rheic Ocean: U–Pb detrital zircon data from the Late Palaeozoic Pulo do Lobo and South Portuguese zones, southern Iberia. J Geol Soc London, 168, 383-392. DOI: 10.1144/0016-76492010-104

Brätz, H. (2000). Radiometrische Altersdatierungen und geochemische Untersuchungen von Orthogneisen, Granite und Granitporphyren aus dem Ruhlaer Kristallin, Mitteldeutsche Kristallinzone. Thesis Dr. rer. nat. University Würzburg, Germany, pp. 151.

Bucher, K., Grapes, M. (2011). Petrogenesis of Metamorphic Rocks. Springer-Verlag, 8th Ed., 428 p.

Cabanis, B., Peucat, J., Michot, J., Deutsch, S. (1979). Remise en cause de l'existence d'un socle orthogneissique antécambrien dans le pays de Léon (domaine Nord-armoricain); étude géochronologique par les méthodes Rb/Sr et U/Pb des orthogneiss de Tréglonou et de Plouvenez-Lochrist. Bull BRGM 4, 357–364.

Caroff, M., Labry, C., Le Gall, B., Authemayou, C., Bussin Grosjean, D., Guillong, M. (2015). Petrogenesis of late-Variscan high-K alkali-calcic granitoids and calc-alkalic lamprophyres: the Aber-Ildut/North-Ouessant complex, Armorican massif, France. Lithos, 238, 140-155. DOI: 10.1016/j.lithos.2015.09.025

Caroff, M., Le GalL, B., Authemayou, C., Grosjean, D.B., Labry, C., Guillong, M. (2016). Relations between basalts and adakitic/felsic intrusive bodies in a soft substrate environment: The South Ouessant Visean basin in the Variscan belt, Armorican Massif, France. Canadian Journal of Earth Science, 53(4), 441-456. DOI: 10.1139/cjes-2015-0230

Castiñeiras, P., Villaseca, C., Barbero, L., Martín Romera, C. (2008). SHRIMP U-Pb zircon dating of anatexis in high-grade migmatite complexes of Central Spain: implications in the Hercynian evolution of Central Iberia. Int J Earth Sci, 97, 35-50. DOI: 10.1007/s00531-006-0167-6

Chaminé, H. (2000). Estratigrafia e estrutura da Faixa Metamórfica de Espinho – Albergaria-a-Velha (Zona de Ossa Morena: Implicações geodinâmicas). Tese de Doutoramento, Universidade do Porto, 497 p.

Chaminé, H. I., Leterrier, J., Fonseca, P. E., Ribeiro, A., Lemos de Sousa, M. J., (1998). Geocronologia U/Pb em zircoes e monazites de rochas ortoderivadas do sector Espinho–Albergaria--a-Velha (Zona de Ossa Morena, NW de Portugal). In: Azeredo, A. (Eds.). Actas V Congresso Nacional de Geologia. Comun. Inst. Geol. Min., 84 (1), B115-B118

Chaminé, H. I., Gama Pereira, L. C., Fonseca, P. E., Noronha, F., Lemos de Sousa, M. J., (2003a). Tectonoestratigrafia da faixa de cisalhamento de Porto–Albergaria-a-Velha–Coimbra–Tomar, entre as Zonas Centro-Ibérica e de Ossa-Morena (Maciço Ibérico, W de Portugal). Cad. Lab. Xeol. Laxe, A Coruña, 28, 37-78.

Chaminé, H., Pereira, G., Fonseca, P., Pinto de Jesus, A., Rocha, F., Moco, L., Fernandes, J., Flores, D., Gomes, C., Araujo, A., Soares de Andrade, A. (2003b). Tectonostratigraphy of middle and upper Palaeozoic black-shales from the Porto-Tomar-Ferreira do Alentejo shear zone (W Portugal): new perspectives on the Iberian Massif, Geobios, 36, 649–663. DOI: 10.1016/j.geobios.2003.03.002

Coney, P., Jones, D. L., Monger, J. W. H. (1980). Cordilleran suspect terranes. Nature, 288, 329-333. DOI:10.1038/288329a0

Deutsch, S., Chauris, L. (1965). Age de quelques formations cristallophylliennes et granitiques du Pays de Léon (Finistère). C R Acad Sci Paris, 260, 615-617.

Dias, R., Ribeiro, A. (1993). Porto-Tomar shear zone, a major structure since the begining of the Variscan orogeny. Comun. Inst. Geol. Mineiro, 79, 29-38.

Dias, R., Ribeiro, A., Coke, C., Pereira, E., Rodrigues, J., Castro, P., Moreira, N., Rebelo, J. (2013). Evolução estrutural dos sectores setentrionais do autóctone da Zona Centro-Ibérica. In: Dias, R., Araújo, A., Terrinha, P., Kullberg, J.C. (Eds.) Geologia de Portugal, vol 1. Escolar Editora, Lisbon, pp 73–147

Dias, R., Ribeiro, A., Romão, J., Coke, C., Moreira, N. (2016). A review of the arcuate structures in the Iberian Variscides; constraints and genetical models. Tectonophysics, 681, 170–194. DOI: 10.1016/j.tecto.2016.04.011

Dias, R., Moreira, N., Ribeiro, A., Basile, C. (2017). Late Variscan Deformation in the Iberian Peninsula; A late feature in the Laurasia-Gondwana Dextral Collision. Int J Earth Sci (Geol Rundsch), 106(2), 549-567. DOI: 10.1007/s00531-016-1409-x

Dinis, P., Andersen, T., Machado, G., Guimarães, F. (2012). Detrital zircon U-Pb ages of a late-Variscan Carboniferous succession associated with the Porto-Tomar shear zone (West Portugal): Provenance implications. Sedimentary Geology, 273–274, 19–29. DOI: 10.1016/j.sedgeo.2012.06.007

Dombrowski, A., Henjes-Kunst, F., Höhndorf, A., Kröner, A., Okrusch, M., Richter, P. (1995). Orthogneisses in the Spessart Crystalline Complex, Northwest Bavaria: witnesses of Silurian granitoid magmatism at an active continental margin. Geol Rundsch, 84, 399-411. DOI: 10.1007/BF00260449

Faure, M., Bé Mézème, E., Duguet, M., Cartier, C., Talbot, J. (2005). Paleozoic tectonic evolution of Medio-europa from the example of the French Massif Central and Massif Armoricain. In: Carosi, R., Dias, R., Iacopini, D., Rosenbaum, G. (Eds.) The southern Variscan belt. J Virt Explor, 19, 5 DOI: 10.3809/jvirtex.2005.00120

Faure, M., Sommers, C., Melleton, J., Cocherie, A., Lautout, O. (2010). The Léon domain (French Massif armoricain): a westward extension of the Mid-German Crystalline Rise? Structural and geochronological insights. Int J Earth Sci, 99, 65-81. DOI: 10.1007/s00531-008-0360-x

Fernández, F. J.; Chaminé, H. I.; Fonseca, P. E.; Munhá, J. M.; Ribeiro, A.; Aller, J.; Fuertes-Fuentes, M., Borges, F. S. (2003). HT-fabrics in a garnet-bearing quartzite from Western Portugal: geodynamic implications for the Iberian Variscan Belt. Terra Nova, 15 (2), 96-103. DOI: 10.1046/j.1365-3121.2003.00472.x

Fernández-Suarez, J., Gutierrez-Alonso, G., Jeffries, T. E. (2002). The importance of along-margin terrane transport in northern Gondwana: Insights from detrital zircon parentage in Neoproterozoic rocks from Iberia and Brittany. Earth and Planetary Science Letters, 204, 75-88. DOI: 10.1016/S0012-821X(02)00963-9

Ferreira Soares, A.F., Marques, J., Rocha, R., Cunha, P.P., Duarte, L.V., Sequeira, A., Sousa M.B., Pereira, E., Gama Pereira, L.C., Gomes, E., Santos, J.R. (2005). Carta Geológica de Portugal à escala 1:50.000, Folha 19-D Coimbra-Lousã. LNEG.

Franke, W. (2000). The Mid-European segment of the Variscides: tectonostratigraphic units, terrane boundaries and plate tectonic evolution. In: Franke, W., Haak, V., Oncken, O., Tanner, D. (Eds.) Quantification and modelling in the Variscan Belt (Geological Society of London special publication 179). Geological Society, London, 21-34. DOI: 10.1144/GSL.SP.2000.179.01.05

Franke, W. (2014). Topography of the Variscan orogen in Europe: failed—not collapsed. Int J Earth Sci (Geol Rundsch), 103, 1471-1499. DOI: 10.1007/s00531-014-1014-9

Franke, W., Dulce, J-C. (2016). Back to sender: tectonic accretion and recycling of Baltica‐derived Devonian clastic sediments in the Rheno‐Hercynian Variscides. Int J Earth Sci (Geol Rundsch). DOI: 10.1007/s00531-016-1408-y

Gama Pereira, L. (1987). Tipologia e evolução da sutura entre a Zona Centro-Ibérica e a Zona de Ossa Morena no sector entre Alvaiázere e Figueiró dos Vinhos (Portugal Central). Tese de Doutoramento, Universidade de Coimbra, 331 p.

Gerdes, A., Zeh, A. (2006). Combined U–Pb and Hf isotope LA–(MC)– ICP–MS analyses of detrital zircons: comparison with SHRIMP and new constraints for the provenance and age of an Armorican metasediment in Central Germany. Earth Planet Sci Lett. 249. 47–61. DOI: 10.1016/j.epsl.2006.06.039

Gutiérrez-Alonso, G., Collins, A.S., Fernández-Suárez, J., Pastor-Galán, D., González-Clavijo, E., Jourdan, F., Weil, A.B., Johnston, S.T. (2015). Dating of lithospheric buckling: $^{40}Ar/^{39}Ar$ ages of syn-orocline strike–slip shear zones in northwestern Iberia. Tectonophysics, 643, 44–54. DOI: 10.1016/j.tecto.2014.12.009

Kirsch, H., Kober, B., Lippolt, H.J. (1988). Age of intrusion and rapid cooling of the Frankenstein gabbro (Odenwald, SW Germany) evidenced by $^{40}Ar/^{39}Ar$ and single zircon $^{207}Pb/^{206}Pb$ measurements. Geol Rundsch, 77, 693–711. DOI: 10.1007/BF01830178

Kuznetsov, N.B., Meert, J.G., Romanyukc, T.V. (2014). Ages of detrital zircons (U/Pb, LA-ICP-MS) from the LatestNeoproterozoic–Middle Cambrian(?) Asha Group and Early Devonian Takaty Formation, the Southwestern Urals: A test of an Australia-Baltica connection within Rodinia. Precambrian Research, 244, 288–305. DOI: 10.1016/j.precamres.2013.09.011

Le Corre, C., Balé, P., Geoget, Y. (1989). Le Léon: un domaine exotique au Nord-Ouest de la chaîne varisque armoricaine. Geodin Acta, 3, 57–71. DOI: 10.1080/09853111.1990.11105200

Le Gall, B., Authemayou, C., Ehrhold, A., Paquette, J-L., Bussien, D., Chazot, G., Aouizerat, A., Pastol, Y. (2014). LiDAR offshore structural mapping and U/Pb zircon/monazite dating of Variscan strain in the Léon metamorphic domain, NW Brittany. Tectonophysics, 630, 236-250. DOI: 10.1016/j.tecto.2014.05.026

Leutwein, F., Chauris, L., Sonet, J., Zimmermann, J.L. (1969). Etudes géochronologiques et géotectoniques dans le Nord-Finistère (Massif Armoricain). Sci Terre, 14, 331–358.

Linnemann, U., Pereira, M.F., Jeffries, T., Drost, K., Gerdes, A. (2008). Cadomian Orogeny and the opening of the Rheic Ocean: new insights in the diacrony of geotectonic processes constrained by LA–ICP–MS U–Pb zircon dating (Ossa-Morena and Saxo-Thuringian Zones, Iberian and Bohemian Massifs). Tectonophysics, 461, 21–43. DOI: 10.1016/j.tecto.2008.05.002

LNEG (2010). Geological map of Portugal at 1:1.000.000, 3rd Ed., Laboratório Nacional de Energia e Geologia, Lisboa.

Machado, G., Vavrdová, M., Fonseca, P.E., Chaminé, H., Rocha, F. (2008). Overview of the Stratigraphy and initial quantittive Biogeocgraphical results from the Devoniano f the Albergaria-a-Velha Unit (Ossa-Morena zone, W Portugal). Acta Musei Nationalis Pragae, 64(2-4), 109-113.

Machado, G., Francu, E., Vavrdová, M., Flores, D., Fonseca, P.E., Rocha, F., Gama Pereira, L.C., Gomes, A., Fonseca, M., Chaminé, H.I. (2011). Stratigraphy, palynology and organic geochemistry of the Devonian-Mississippian metasedimentary Albergaria-a-Velha Unit (Porto-Tomar Shear Zone, W Portugal). Geological Quarterly, 55(2), 139-164.

Marcoux, E., Cocherie, A., Ruffet, G., Darboux, J.R., and Guerrot, C. (2009). Géochronologie revisitée du dôme du Léon (Massif armoricain, France). Géologie de la France, (2009)1, 19-40.

Martins, H.C.B., Sant'Ovaia, H., Abreu, J., Oliveira, M., Noronha, F. (2011). Emplacement of the Lavadores granite (NW Portugal): U/Pb and AMS results. Comptes Rendus Geoscience, 343(6), 387-396.

Martins, H. C. B., Ribeiro, M. A., Sant'Ovaia, H., Abreu, J., Garcia de Madinabeitia, S. (2014). SHRIMP and LA-ICPMS U–Pb zircon geochronology of post-tectonic granitoid intrusions in NW of Central Iberian Zone. Comunicações Geológicas, 101, I, 147-150.

Mata, J., Munhá, J. (1990). Magmatogénese de metavulcanitos câmbricos do nordeste alentejano: os estádios iniciais de "rifting" continental. Com. Serv. Geol. Portugal 76, 61-89.

Mendes, F. (1967/1968). Contribution à l'étude géochronologique, par la méthode au strontium, des formations cristallines du Portugal. Bol. Mus. Labor. miner. Geol. Fac. Ciênc., 11(1), 3-155.

Moita, P., Munha, J., Fonseca, P., Pedro, J., Tassinari, C., Araújo, A., Palacios, T. (2005). Phase equilibria and geochronology of Ossa Morena eclogites. XIV Semana de Gequimica/VIII Congresso de geoquimica dos Paises de Lingua Portuguesa (abstract book) 2, 471-474.

Montenegro de Andrade, M. (1977). O Anfibolito olivínico do Engenho Novo (Vila da Feira). Comunicações dos Serviços Geológicos de Portugal. 61, 43-61.

Moreira, N. (2012). Caracterização estrutural da zona de cisalhamento Tomar-Badajoz-Córdova no sector de Abrantes. MsC Thesis (unpublished), University of Évora, 225 p.

Moreira, N., Pedro, J., Dias, R., Ribeiro, A., Romão, J. (2011). Tomar-Badajoz-Córdoba shear zone in Abrantes sector; the presence of a kilometric sheath fold?. Deformation mechanisms, Rheology and Tectonics abstract book, Oviedo, Spain, 90.

Moreira, N., Dias, R., Romão, J., Pedro, J.C., Ribeiro, A. (2013). Influência da Zona de Cisalhamento Porto-Tomar-Ferreira do Alentejo na região de Abrantes; uma estrutura de primeira ordem à escala do Orógeno Varisco na Ibéria, In: Moreira, N., Pereira, I., Couto, F., Silva, H. (Eds.), III CJIG, LEG 2013 and 6th PGUE abstract book, Estremoz, Portugal 161-165.

Moreira, N., Araújo, A., Pedro, J.C., Dias, R. (2014). Geodynamic evolution of Ossa-Morena Zone in SW Iberian context during the Variscan Cycle. Comunicações Geológicas, 101(I), 275–278.

Moreira, N., Pedro, J., Romão, J., Dias, R., Araújo, A., Ribeiro A. (2015). The Neoproterozoic-Cambrian transition in Abrantes Region (Central Portugal); Litostratigraphic correlation with Cambrian Series of Ossa-Morena Zone. The Variscan belt: correlations and plate dinamics. Géologie de la France (Variscan 2015 special issue, Rennes), 2015(1), 101-102.

Moreira, N., Romão, J., Pedro, J., Dias, R., Ribeiro, A. (2016a). The Porto-Tomar-Ferreira do Alentejo Shear Zone tectonostratigraphy in Tomar-Abrantes sector (Portugal). In: IX Congreso Geológico de España (special volume). Geo-Temas, 16(1), 85-88. ISSN 1576-5172.

Moreira, N., Romão, J., Dias, R., Pedro, J.C., Riberiro, A. (2016b). Tectonostratigraphy proposal for western block of Porto-Tomar Shear zone; the Finisterra Terrane. Abstract book of Workshop on Earth Sciences 2016, Évora (Portugal), p. 44.

Munhá, J., Mendes, M.H., Santos, J.F., Tassinari, C., Cordani, U., Nutman, A.P. (2008). Timing and duration of migmatization recorded in Ovar-Espinho metamorphic belt (northern sector of Ossa-Morena Zone, Porto-Tomar Shear Zone). XI congress de geoquimica dos PLP, abstract book, p. 111.

Murphy, J.B., Fernández-Suárez, J., Keppie, J.D., Jeffries, T.E. (2004). Contiguous rather than discrete Paleozoic histories for the Avalon and Meguma terranes based on detrital zircon data. Geology, 32, 585-588. DOI: 10.1130/G20351.1

Nasir, S., Okrusch, M., Kreuzer, H., Lenz, H., Höhndorf, A. (1991). Geochronology of the Spessart crystalline complex, Mid-German Crystalline Rise. Mineral Petrol, 44, 39-55. DOI: 10.1007/BF01167099

Neves, L., Pereira, A., Macedo, C. (2007). Alguns dados geoquímicos e geocronológicos (K-Ar) sobre o plutonito granítico de Tancos (Portugal Central). XV Semana – VI Congresso Ibérico de Geoquímica abstract book, 137-140.

Noronha, F., Leterrier, J. (1995). Complexo metamórfico da Foz do Douro. Geoquímica e geocronologia. Resultados preliminares. Abstract book of IV Congresso Nacional de Geologia. Mem. Mus. Lab. Min. Geol. Fac. Ciênc. Univ. Porto, 4, 769-774.

Noronha, F., Leterrier, J. (2000). Complexo Metamórfico da Foz do Douro (Porto). Geoquímica e Geocronologia. Revista Real Academia Galega de Ciências, XIV, 21-42.

Orejana, D., Martínez, E.M., Villaseca, C., Andersen T., (2015). Ediacaran–Cambrian paleogeography and geodynamic setting of the Central Iberian Zone: Constraints from coupled U–Pb–Hf isotopes of detrital zircons. Precambrian Research, 261, 234-251. DOI: 10.1016/j.precamres.2015.02.009

Paquette, J.L., Balé, P., Ballèvre, M., Georget, Y. (1987). Géochronologie et géochimie des éclogites du Léon: nouvelles contraintes sur l'évolution géodynamique du Nord-Ouest du Massif armoricain. Bulletin de Minéralogie, 110, 683-696.

Passchier, C.W., Trouw, R.A.J. (2005). Microtectonics. 2nd Ed., Springer, 382p.

Pedro, J.C., Araújo, A., Tassinari, C., Fonseca, P.E., Ribeiro, A. (2010). Geochemistry and U-Pb zircon age of the Internal Ossa-Morena Zone Ophiolite Sequences: a remnant of Rheic Ocean in SW Iberia. Ofioliti, 35(2), 117-130. DOI: 10.4454/ofioliti.v35i2.390

Pereira, E., Gonçalves, L.S., Moreira, A. (1880). Carta Geológica de Portugal à Escala de 1:50.000 – Folha 13-D Oliveira de Azemeis and Explanatory Note. Serviços Geológicos de Portugal. Lisboa.

Pereira, E., Rodrigues, J.F., Gonçalves, S., Moreira, A., Silva, A. (2007). Carta Geológica de Portugal à escala 1:50.000, Folha 13-D Oliveira de Azemeis. LNEG.

Pereira, M.F. (2014). Potential sources of Ediacaran strata of Iberia: a review. Geodinamica Acta, 1 (1), 1-14, DOI: 10.1080/09853111.2014.957505.

Pereira, M.F., Chichorro, M., Williams, I.S., Silva, J. B. (2008). Zircon U-Pb geochronology of paragneisses and biotite granites from the SW Iberian Massif (Portugal): Evidence for a paleogeographic link between the Ossa-Morena Ediacaran basins and the West African craton. In: Liégeois, J. P., Nasser, E. (Eds.), The boundaries of the West African Craton. Geological Society of London Special Publication, 297, 385-408. DOI: 10.1144/SP297.18

Pereira, M.F., Silva, J.B., Drost, K., Chichorro, M. y Apraiz, A. (2010). Relative timing of the transcurrent displacements in northern Gondwana: U-Pb laser ablation ICP-MS zircon and monazite geochronology of gneisses and sheared granites from the western Iberian Massif (Portugal). Gondwana Research, 17(2-3), 461-481. DOI: 10.1016/j.gr.2009.08.006

Pereira, M.F., Chichorro, M., Sola, A.R., Silva, J.B., Sanchez-Garcia, T., Bellido, F. (2011). Tracing the Cadomian magmatism with detrital/inherited zircon ages by in-situ U-Pb SHRIMP geochronology (Ossa-Morena Zone, SW Iberian Massif). Lithos, 123(1-4), 204-217. DOI: 10.1016/j.lithos.2010.11.008

Pereira, M.F., Silva, J.B., Chichorro, M., Ordóñez-Casado, B., Lee, J.K.W., Williams, I.S. (2012a). Early Carboniferous wrenching, exhumation of high-grade metamorphic rocks and basin instability in SW Iberia: constraints derived from structural geology and U-Pb and ^{40}Ar-^{39}Ar geochronology. Tectonophysics, 558-559, 28-44. DOI: 10.1016/j.tecto.2012.06.020

Pereira, M.F., Solá, A.R., Chichorro, M., Lopes, L., Gerdes, A., Silva, J.B. (2012b). North-Gondwana assembly, break up and paleogeography: U–Pb isotope evidence from detrital and igneous zircons of Ediacaran and Cambrian rocks of SW Iberia. Gondwana Research, 22(3–4), 866-881. DOI: 10.1016/j.gr.2012.02.010

Pereira, M. F., Linnemann, U., Hofmann, M., Chichorro, M., Sola, A. R., Medina, J., Silva, J. B. (2012c). The provenance of Late Ediacaran and Early Ordovician siliciclastic rocks in the Southwest Central Iberian Zone: Constraints

from detrital zircon data on northern Gondwana margin evolution during the late Neoproterozoic. Precambrian Research, 192–195, 166–189. DOI: 10.1016/j.precamres.2011.10.019

Pérez-Cáceres, I., Poyatos, D.M., Simancas, J.F., Azor, A. (2016). Testing the Avalonian affinity of the South Portuguese Zone and the Neoproterozoic evolution of SW Iberia through detrital zircon populations, Gondwana Research. DOI: 10.1016/j.gr.2016.10.010

Petersson, A., Scherstén, A., Andersson, J., Möller, C. (2015). Zircon U-Pb and Hf - isotopes from the eastern part of the Sveconorwegian Orogen, SW Sweden: implications for the growth of Fennoscandia. Geological Society, London, Special Publications 289, 281-303. DOI: 10.1144/SP389.2

Pollock, J.C., Wilton, D.H.C., van Staal, C.R., Morrissey, K.D. (2007). U-Pb detrital zircon geochronological constraints on the Early Silurian collision of Ganderia and Laurentia along the Dog Bay Line: The terminal Iapetan suture in the Newfoundland Appalachians. American Journal of Science, 307(2), 399-433. DOI: 10.2475/02.2007.04

Priem, H.N.A., Boelrijk, N.A.I.M., Verschure, R.H., Hebeda, E.H. (1965). Isotopic ages of two granites on the Iberian continental margin: The Traba Granite (Spain) and the Berlenga Granite (Portugal). Geologie en Mijnbow, 44e, 353-354.

Reischmann, T., Anthes, G. (1996). Geochronology of the Mid-German Crystalline Rise west of the River Rhine. Geol Rundsch, 85, 761-774. DOI: 10.1007/BF02440109

Ribeiro, A. (2013). Evolução geodinâmica de Portugal; os Ciclos ante-mesozóicos. In: Dias, R., Araújo, A., Terrinha, P., Kullberg, J.C. (Eds.), Geologia de Portugal, vol. 1, Escolar Editora, 15-57.

Ribeiro, A., Pereira, E., Severo, L. (1980). Análise da deformação da zona de cisalhamento Porto-Tomar na transversal de Oliveira de Azemeis. Comum. Serv. Geol. Portugal, 66, 3-9.

Ribeiro, A., Silva, J.B., Dia, R., Romão, J. (1991). The Berlenga Suspect Terrabe abd the spatial and Temporal end of the Variscan Orogene. Abstract book of III Congresso Nacional de Geologia, Coimbra, p.70.

Ribeiro, A. Pereira, E., Chaminé, H.I., Rodrigues, J., (1995). Tectónica do megadomínio de cisalhamento entre a Zona de Ossa-Morena e a Zona Centro-Ibérica na região de Porto-Lousã. In Sodré Borges, F., Marques, M. (coord.) IV Congresso Nacional de Geologia, Porto. Men. Mus. Labor. Miner. Geol. FCUPorto, 299-303-

Ribeiro, A., Munhá, J., Dias, R., Mateus, A., Pereira, E., Ribeiro, L., Fonseca, P., Araújo, A., Oliveira, T., Romão, J., Chaminé, H., Coke, C., Pedro, J. (2007). Geodynamic evolution of the SW Europe Variscides. Tectonics, 26(6), TC6009. DOI: 10.1029/2006TC002058

Ribeiro, A., Pereira, E., Fonseca, P., Mateus, A., Araújo, A., Munhá, J., Romão, J., Rodrigues, J.F. (2009). Mechanics of thick-skinned Variscan overprinting of Cadomian basement (Iberian Variscides). C. R. Geosciences, 341(2-3), 127-139. DOI: 10.1016/j.crte.2008.12.003

Ribeiro, A., Romão, J., Munhá, J., Rodrigues, J., Pereira, E., Mateus, A., Araújo, A. (2013). Relações tectonostratigráficas e fronteiras entre a Zona Centro-Ibérica e a Zona Ossa-Morena do Terreno Ibérico e do Terreno Finisterra. In: Dias, R., Araújo, A., Terrinha, P., Kullberg, J.C. (Eds.), Geologia de Portugal, vol. 1, Escolar Editora, 439-481.

Romão, J., Moreira, N., Pedro, J. C., Mateus, A., Dias, R., Ribeiro, A. (2013). Contribuição para o conhecimento das unidades tectono-estratigráficas do Terreno Finisterra na região de Tomar. In: Moreira, N., Dias, R., Araújo, A. (Eds.), Geodinâmica e Tectónica Global; a Importância da cartografia geológica, Livro de actas da 9ª Conferência Anual do GGET-SGP, Estremoz, 87-91.

Romão, J., Moreira, N., Dias, R., Pedro, J., Mateus, A., Ribeiro, A. (2014). Tectonoestratigrafia do Terreno Ibérico no sector Tomar-Sardoal-Ferreira do Zêzere e relações com o Terreno Finisterra. Comunicações geológicas, 101(I), 559-562.

Salman, K. (2004). The timing of the Cadomian and Variscan cycles in the Ossa-Morena zone, SW Iberia: Granitic magmatism from subduction to extension. Journal of Iberian Geology, 30, 119–132.

Sánchez-García, T., Quesada, C., Bellido, F., Dunning, G.R., González de Tánago, J. (2008). Two-step magma flooding of the upper crust during rifting: the Early Palaeozoic of the Ossa Morena Zone (SW Iberia). Tectonophysics, 461, 72–90. DOI: 10.1016/j.tecto.2008.03.006

Sánchez-Lorda, M.E., Ábalos, B., García de Madinabeitia, S., Eguíluz, L., Gil Ibarguchi, J.I., Paquette, J.L. (2016). Radiometric discrimination of pre-Variscan amphibolites in the Ediacaran Serie Negra (Ossa-Morena Zone, SW Iberia). Tectonophysics, 681(20), 31–45. DOI: 10.1016/j.tecto.2015.09.020

Santos, J.F., Mendes, M.H., Gonçalves, A.C., Moita, P. (2012). New geochemical and isotopic constraints on the genesis of the Oliveira Azeméis granitoid melts (Porto-Tomar Shear Zone, Iberian Variscan Chain, Central-Western Portugal). Geophysical Research Abstracts, 14, EGU2012-3430-1.

Scherer, E.E., Mezger, K., Münker, C. (2002). Lu-Hf ages of high pressure metamorphism in the Variscan fold belt of southern Germany. Goldschmidt Conference Abstract 2002. Geochimica et Cosmochimica Acta Suppl., 66, A677.

Schulz, B. (2013). Monazite EMP-Th-U-Pb age pattern in Variscan metamorphic units in the Armorican Massif (Brittany, France). German Journal of Geosciences, 164, 313-335. DOI: 10.1127/1860-1804/2013/0008

Schulz, B., Krenn, E., Finger, F., Bratz, H., Klemd, R. (2007). Cadomian and Variscan metamorphic events in the Léon Domain (Armorican massif, France): P-T data and EMP monazite dating. In The evolution of the Rheic ocean from Avalonian-Cadomian active margin to Alleghenian-Variscan collision. Geological Society of America Special Papers, 423, 267-285. DOI: 10.1130/2007.2423(12).

Silva, S. (2007). Estudo geoquímico de metabasitos da ZOM e da ZCI aflorantes na região Centro-Norte de Portugal. MsC Thesis (unpublished), University of Aveiro, 180 p.

Simancas, J.F., Expósito, I., Azor, A., Martínez Poyatos, D.J., González Lodeiro, F., (2004). From the Cadomian orogenesis to the Early Palaeozoic Variscan rifting in southwest Iberia. Journal of Iberian Geology, 30, 53-71.

Singh, R.K.B., Gururajan, N.S (2011). Microstructures in quartz and feldspars of the Bomdila Gneiss from western Arunachal Himalaya, Northeast India: Implications for the geotectonic evolution of the Bomdila mylonitic zone. Journal of Asian Earth Sciences, 42, 1163-1178.

Skrzypek, E., Schulmann, K., Tabaud A-S, Edel, J-B. (2014). Palaeozoic evolution of the Variscan Vosges Mountains. In: Schulmann, K., Martínez Catalán, J. R., Lardeaux, J. M., Janousek, V., Oggiano, G. (Eds.) The Variscan Orogeny: Extent, Timescale and the Formation of the European Crust. Geological Society, London, Special Publications, 405, 45-75. DOI: 10.1144/SP405.8

Sousa, M., Sant'Ovaia, H., Tassinari, C., Noronha F. (2014). Geocronologia U-Pb (SHRIMP) e Sm-Nd do ortognaisse biotítico do Complexo Metamórfico da Foz do Douro (NW de Portugal). Comunicações Geológicas, 101(I), 225-228.

Talavera, C., Montero, P., Martínez Poyatos, D., Williams, I. S. (2012). Ediacaran to Lower Ordovician age for rocks ascribed to the Schist–Graywacke Complex (Iberian Massif, Spain): Evidence from detrital zircon SHRIMP U-Pb geochronology. Gondwana Research, 22, 928–942. DOI: 10.1016/j.gr.2012.03.008

Todt, W.A., Altenberger, U., von Raumer, J.F. (1995). U–Pb data on zircons for the thermal peak of metamorphism in the Variscan Odenwald, Germany. Geol Rundsch, 84, 466-472. DOI: 10.1007/BF00284514

Valverde Vaquero, P., Bento dos Santos, T., González Clavijo, E., Díez Montes, A., Ribeiro, M.L., Solá, R. (2010a). Geochronology and P-T-t paths of the Berlengas Archipelago rocks, W Portugal. 2010 Goldschmidt Conference, Knoxville (E.U.A.), Geochimica et Cosmochimica Acta, 74, 12, 1, A1070.

Valverde Vaquero, P., Ribeiro, M. L., González Clavijo, E., Díez Montes, A., Bento Dos Santos, T. (2010b). Idades preliminares U-Pb (ID-TIMS) das Ilhas Berlengas (Portugal). VIII Congresso Nacional de Geologia, Braga. e - Terra, 13 (8). Available online: http://e-terra.geopor.pt.

Will, T.M., Schmädicke, E. (2001). A first report of retrogressed eclogites in the Odenwald Crystalline Complex: evidence for high-pressure metamorphism in the Mid-German Crystalline Rise, Germany. Lithos, 59, 109–125. DOI: 10.1016/S0024-4937(01)00059-7

Will, T.M., Schmädicke, E. (2003). Isobaric cooling and anti-clockwise P–T paths in the Variscan Odenwald Crystalline Complex. J Metamorph Geol, 21, 469–480. DOI: 10.1046/j.1525-1314.2003.00453.x

Will, T.M., B. Schulz, B., Schmädicke, E. (2016). The timing of metamorphism in the Odenwald–Spessart basement, Mid‑German Crystalline Zone. Int J Earth Sci (Geol Rundsch). DOI 10.1007/s00531-016-1375-3

Zeh, A., Gerdes, A. (2010). Baltica- and Gondwana-derived sediments in the Mid-German Crystalline Rise (Central Europe): implications for the closure of the Rheic ocean. Gondwana Res, 17, 254–263. DOI: 10.1016/j.gr.2009.08.004

Zeh, A., Will, T.M. (2010). The Mid-German Crystalline Rise. In: Linnemann, U., Romer, R.L. (Eds.) Pre-Mesozoic geology of Saxo-Thuringia–From the Cadomian active margin to the Variscan orogen. Schweizerbart, Stuttgart, 195–220.

Zeh, A., Brätz, H., Millar I. L., Williams I. S. (2001). A combined zircon SHRIMP and Sm-Nd isotope study on high-grade paragneisses from the Mid-German Crystalline Rise: Evidence for northern Gondwanan and Grenvillian provenance. Journal of the Geological Society, London, 158, 983-994. DOI: 10.1144/0016-764900-186

Zeh, A., Williams, I.S., Brätz, H., Millar, I.L. (2003). Different age response of zircon and monazite during the tectonometamorphic evolution of a high grade paragneiss from the Ruhla Crystalline Complex, Central Germany. Contrib. Mineral. Petrol., 145, 691-706. DOI: 10.1007/s00410-003-0462-1

Zeh, A., Gerdes, A., Will, T. M., Millar, I.L. (2005). Provenance and Magmatic-Metamorphic Evolution of a Variscan Islandarc Complex: Constraints from U-Pb dating, Petrology, and Geospeedometry of the Kyffhäuser Crystalline Complex, Central Germany, Journal of Petrology, 46, 1393-1420. DOI: 10.1093/petrology/egi020

VIII

Estruturas em Dominós; um modelo genético

Como referido anteriormente, a Zona de Cisalhamento Porto-Tomar-Ferreira do Alentejo apresenta uma deformação polifásica que se estende desde as fases mais precoces do Orógeno Varisco até às suas fases mais tardias. Contrariamente ao que acontece nas fases precoces, onde esta zona de cisalhamento actua num regime de deformação dúctil (vide capítulo VII.1), gerando um padrão de deformação intensa, nas fases mais tardias o regime apresenta características mais frágeis com a génese de estruturas mais discretas e de desenvolvimento localizado. Estas estruturas tardias apresentam cinemática direita, tal como nas suas fases mais precoces.

As fases mais tardias desta zona de cisalhamentos, de carácter dúctil-frágil associado a intensa cataclase, gera na região de Abrantes um padrão de fracturação local, em níveis de natureza siliciosa constituintes da Unidade dos Felsitos do Castelo de Abrantes. Este padrão de fracturação é resultante da cinemática não-coaxial direita, resultando daí um *fabric* planar complexo.

O *fabric* planar desenvolvido é heterogéneo, composto por um conjunto de estruturas planares que apresentam características geométricas e cinemáticas que permitem distinguir três famílias distintas. A família dominante de estruturas planares é caracterizada por delimitar um conjunto de estruturas, de dimensões centimétricas a milimétricas, que delimitam blocos com deformação interna não visível a olho nu. Estes blocos apresentam uma rotação sintética em relação à cinemática direita geral zona de cisalhamento, gerando um padrão típico de estruturas em dominó. Estes dominós apresentam um desenvolvimento local, resultando da vorticidade interna da zona de cisalhamento. Estas estruturas encontram-se restritas aos domínios onde a cinemática direita dos cisalhamentos principais se conjuga com uma segunda família de 2ª ordem com elevada continuidade e de cinemática esquerda.

A análise da geometria e cinemática dos cisalhamentos que bordejam as estruturas em dominós permitiu a reconstituição da sua geometria inicial. A sua geometria mostra que estes cisalhamentos se geraram como cisalhamentos do tipo R' durante as fases precoces da actuação do cisalhamento direito principal, sendo a rotação resultado do regime não-coaxial direito. As características gerais do padrão de fracturação heterogéneo é compatível com um regime de

deformação típico de regimes transpressivos dominados por uma componente de cisalhamento simples.

O trabalho que se apresenta no capítulo VIII.1 resulta de uma análise exaustiva destas estruturas em dominó, apresentando uma proposta de modelo evolutivo temporal para a sua génese. O trabalho em causa apresenta um carácter específico, tendo sido submetido a um jornal de especialidade de elevado factor de impacto, nomeadamente o *Journal of Structural Geology*. Esta revista está inserida no quartil Q1 no SJR, contendo um factor de impacto de 2.084 de acordo com a Thomson Reuters (2015/2016). O trabalho, após análise pelos revisores propostos pelo editor da revista, foi recentemente aceite para publicação, embora seja necessário a revisão do manuscrito submetido para posterior re-submissão, algo que ainda não foi efectuado.

- *Capítulo VIII.1*

MOREIRA, N., DIAS, R. (*submetido*), Domino Structures as a local accommodation process in shear zones. Journal of Structural Geology.

XIII.1

Domino Structures as a local accommodation process in shear zones

Index

XIII.1.1. Introduction

Domino (sometimes called bookshelf) structures have been described from low to high-grade metamorphic rocks, although they are commonly developed in brittle to ductile-brittle deformation regimes (Mandl, 2000; Ribeiro, 2002; Goscombe and Passchier, 2003; Figueiredo *et al*., 2004), obeying to Coulomb criterion for failure (Jaeger and Cook, 1981). These structure are characterized by block rotation, which are delimited by one dominant shear/fracture orientation (e.g. Mandl 2000; Nixon et al., 2011; Fossen, 2010).

Dominos can be used as a shear sense criteria (Passchier *et al.*, 1990; Mandl, 2000; Goscombe and Passchier, 2003; Goscombe et al., 2004; Passchier and Trouw, 2005; Fossen, 2010), helping the knowledge of the shear zones dynamics. These structures are described in all geodynamic settings (e.g. Wernicke and Burchfiel, 1982; Mandl, 1984; 1987; Cowan, 1986; Axen, 1988; La Femina et al., 2002) and from the microscale to orogenic scale (e.g. Ribeiro, 2002; La Femina et al., 2002; Goscombe et al., 2004; Nixon et al., 2011; Dias et al, 2016a). The careful analysis of its geometry and kinematics, as well its genesis mechanism, becomes essential to a correct dynamic interpretation of shear zones.

The dominos could have either antithetic or synthetic rotation relative to the main shear (e.g. Goscombe and Passchier, 2003; Scholz *et al.*, 2010; Dabrowski and Grasemann, 2014). This is a major constrain for their use as kinematic criteria, unless they are coupled with other structures. If this is not a major problem in extensional regimes, because rotation of dominos generally occurs antithetically to the main shear planes, in this cases a low angle ductile decollement (e.g. Wernicke and Burchfiel, 1982; Mandl, 1987; Axen, 1988; Fossen and Hesthammer, 1998; Bahroudi et al., 2003; Karlstrom et al, 2010), it strongly limits their use as kinematical criteria in strike-slip environments where both types of block rotations are described (e.g. Cowan et al., 1986; Mandl, 2000; Goscombe and Passchier, 2003; Goscombe *et al.*, 2004; Nixon *et al*., 2011; Dabrowski and Grasemann, 2014). In such cases, the block rotation (synthetic or antithetic) seems to be constrained by several factors such as flow type, rheological contrast, initial angle of the previous foliation to the main shear zone, existence of previous anisotropies bounding blocks or the shape of the block (e.g. Mandal *et al.*, 2000; Goscombe and Passchier, 2003; Dabrowski and Grasemann, 2014). However, analogue experiments (Karmakar and Mandal, 1989; Mandal and Khan, 1991; Mandal *et al.*, 2007) indicate that the orientation and the spacing of fractures in the brittle layers are the main factors that control the kinematics of domino structures. Mandl (2000) refers that in brittle domino structures, the sense of rotation depends on the nature of the planar structures that limits the blocks: when the blocks are bounded by R 'or P' shears, the synthetic rotations tend to prevail.

This work shows as a detailed geometrical and kinematical analysis of a domino domains could help to constrain some of the mechanisms to domino formation. Such approach is based on simple and easily measurable linear and angular geometric parameters. The use of this methodology in a small and well outcropping sector in relation to one of the most important Iberian Variscan Structure, the Porto-Tomar-Ferreira do Alentejo dextral shear zone (PTFASZ; *e.g.* Ribeiro *et al.*, 2007), prove to be useful in highlighting its geodynamical evolution.

XIII.1.2. Geological Setting

The Variscan chain is part of a major orogenic belt, with 1000 km wide and 8000 km of extension long from Caucasus to Appalaches and Ouachita mountains (Matte, 2001; Nance *et al.*, 2010; 2012). This orogenic belt was formed between 480-250 Ma, due to a complex collision process between three major plates: Gondwana, Laurentia and Baltica (Matte, 2001; Ribeiro *et al.*, 2007; Nance *et al.,* 2010; 2012; Dias *et al.*, 2016b). The Variscides, with rocks ranging from Neoproterozoic to upper Palaeozoic, are well exposed in the Iberian Peninsula in the so called Iberian Massif (Fig. 1A). In the older rocks of this Massif the Variscan deformation overprints previous tectonic events (*e.g.* Ribeiro *et al.,* 2007; 2009).

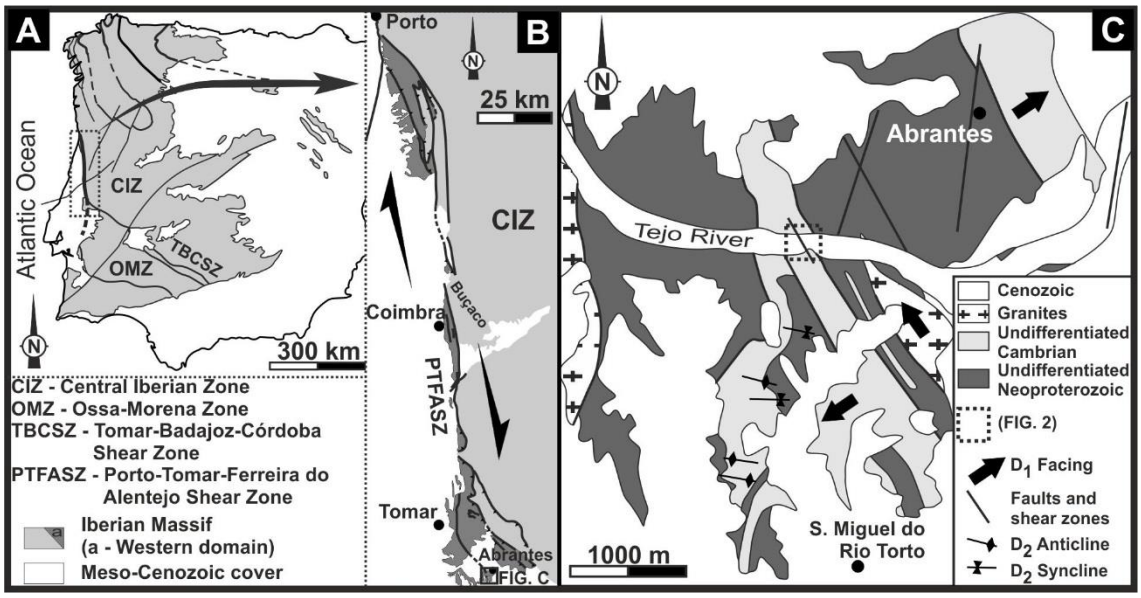

Figure 1 – The Abrantes sector in the context of the Iberian Variscides:

A – Major features of the pre-Mesozoic domains (in grey; adapted from Ribeiro et al., 1979; 2007; 2013; Dias et al, 2016b);

B – General pattern of Porto-Tomar-Ferreira do Alentejo Shear Zone (PTFASZ);

C – Geological sketch of Abrantes region.

The Iberian Massif was initially subdivided in several zones by Lotze (1945) based on stratigraphic, paleogeographic, tectonic, magmatic and metamorphic features. Subsequently, several authors (*e.g.* Julivert *et al.*, 1974; Ribeiro *et al.*, 1979) reinterpreted such zones and their boundaries, although preserving the general pattern. Since then, the Central Iberian Zone (CIZ) has been considered the internal domain of the Iberian Variscides. The boundary of this zone is marked by two first-order structures (Ribeiro *et al.*, 2007; Romão et al., 2014): the sinistral NW-SE Tomar-Badajoz-Cordova Shear Zone (TBCSZ; Fig. 1A) at South and Southwest, and the dextral NNW-SSE to N-S Porto-Tomar-Ferreira do Alentejo Shear Zone (PTFASZ; Fig. 1B) in its Western domain.

XIII.1.2.1. The Porto-Tomar-Ferreira do Alentejo Shear Zone

The PTFASZ is a lithospheric scale structure (Iglesias and Ribeiro, 1981; Shelley and Bossière, 2000; Chaminé *et al.*, 2003; Ribeiro *et al.*, 2007; Dias et al., 2016b), with a total length of, at least, 400 km. Most of the observed structures are compatible with a progressive dextral strike-slip deformation under a ductile to brittle-ductile regimes (Lefort and Ribeiro, 1980; Iglesias and Ribeiro, 1981; Ribeiro *et al.*, 2007; 2009; Pereira *et al.*, 2010; Romão *et al.*, 2014; Moreira et al., 2016). Nevertheless, despite the general agreement concerning its kinematics, the geodynamic interpretation of this structure is still a debatable subject.

The PTFASZ, sometimes considered a major dextral transform fault (Ribeiro *et al.*, 2007; 2009), put the CIZ in contact with a western domain, either considered as the Ossa-Morena paleogeographic zone (Chaminé et al., 2003; Pereira et al., 2010) or a small terrain called Finisterra (Ribeiro et al., 2007; 2013; Romão et al., 2014; Moreira et al., 2016). However, the age of this major shear zone is debatable. Although an important dextral shearing during Upper Carboniferous is accepted in all models (e.g. Ribeiro et al., 2007; Pereira et al., 2010; Moreira et al 2014; 2016), some authors (Ribeiro *et al.*, 2007; 2009; Romão *et al.*, 2013; 2014; Dias *et al.*, 2016b) considered that it was already active, with a similar kinematics, at least since Lower Devonian during the D_1 Variscan tectonic event. This conclusion is also supported by the pattern of finite strain ellipsoids in the Ordovician Quartzites of the Buçaco region (Fig. 1B; Dias and Ribeiro, 1993; 1994) and by recent geological mapping (Moreira, 2012; Romão *et al.,* 2013; 2014; Moreira et al., 2016), which shows that the interaction between PTFASZ and TBCSZ prevails during most of the Variscan deformation in Iberia.

The evidences for a strong Upper Cambrian compressive deformation in the Southwest domains of CIZ, coupled with its geometry and kinematics, indicate that PTFASZ could have been a dextral intraplate transform before the Variscan cycle (Lefort and Ribeiro, 1980; Romão *et al.*, 2005; 2013).

Nevertheless, Pereira *et al.* (2010) sustain that there is no evidence to consider PTFASZ as major structure active during the Early Palaeozoic evolution, being active only after Serpukhovian-Kasimovian (*c.a.* 318-308 Ma). According to these authors, the dextral ductile-brittle strike-slip kinematics that predominates at that time displaced older structures, like such as the TBCSZ and OMZ units, carrying his fragments towards the vicinity of Porto.

XIII.1.2.2. Variscan Deformation in Abrantes; Geometry and Kinematics

Some previous works consider the influence of the PTFASZ deformation in the Abrantes region negligible (Pereira *et al.*, 2010). However, recent studies (Moreira, 2012; Romão et al., 2014; Moreira et al., 2016; Fig. 1C) emphasize an important deformation related with this first order shear zone. Indeed, two major Variscan deformation phases have been reported for this region. The first one (D_1) generates NNW-SSE folds with a pervasive S_1 foliation developed at medium grade metamorphism, which often transpose bedding planes. Although there is a homogeneous orientation of the D_1 folds, their geometry is highly heterogeneous (Fig. 1C). In fact, an inner NNW-SSE sector with tangential transport towards NW (*i.e.* parallel to the orogenic trend) is bounded by two external domains with opposite vergences that are orthogonal to the strike of the main structures: at northeast the folds face NE while at southwest they face SW (Fig. 1C).

The D_1 structures are usually strongly deformed by a second deformation Variscan event (D_2) under a ductile to brittle-ductile regime. Such deformation is associated with an important dextral righ-lateral kinematics subparallel to previous main structures that often have been reworked during D_2. The geometry and kinematics of the D_2 structures are highly heterogeneous in the Abrantes region, due to the strong influence of previous fabrics. Nevertheless, the dextral D_2 NNW-SSE strike-slip component is always present as shown by a diversity of structures, like the frequent asymmetric boudins with subvertical necks affecting D_1 quartz veins. Associated to dextral pervasive kinematics two different styles of D_2 folding are found, often developed in adjacent domains:

- Tight to isoclinal orthorombic folds of previous planar fabrics, with subvertical axial planes and sub-horizontal to low dipping hinges (<10º). Locally, a slightly penetrative axial planar S_2 cleavage is found;
- Monoclinic folds with E-W subvertical axial planes and strongly plunging hinges (Fig. 1C). Such folds have usually en-echelon geometry in relation to the main shear enhancing the dextral kinematics. The interference with the major NW-SE D_1 folds gives rise to a macroscopic type 3 fold interference patterns (Ramsay, 1967).

XIII.1.2.3. D_2 Variscan Deformation in Abrantes; Geodynamical Evolution

The juxtaposition of domains with very different D_2 fold styles (Moreira, 2012), which are always coupled with the pervasive coeval dextral kinematics, indicates a strong strain partitioning in a general D_2 dextral transpression regime. The domains where the E-W to NW-SE D_2 monoclinic asymmetric folds with plunged hinges are dominant enhance a simple shear dominated transpression (according to Fossen *et al.*, 1994 nomenclature), where the NNW-SSE orthorhombic folds with low dipping hinges have been produced in a pure shear dominated transpressive regime. The boundaries between such domains are major D_2 dextral shear zones. Similar behaviour, with domains exhibiting pure-shear and simple shear dominated regimes, is well known and described by several authors at transpressive regimes with highly strain partitioning (e.g. Tikoff and Teyssier, 1994; Dias and Ribeiro, 1994; 2008; Fossen and Tikoff, 1998; Dias et al., 2003; Weinberger, 2014).

The existence of dextral kinematical markers ranging from ductile to brittle regimes seems to indicate that the dextral shearing along the NNW-SSE trend was a long lasting D_2 process. In the Abrantes region, the intensity of the D_2 deformation increases westwards in the direction of the PTFASZ (Moreira et al., 2016), which shows that D_2 Variscan deformation was induced by the activity of this dextral first order transcurrent shear.

XIII.1.3. The Abrantes Local Strike-Slip Domino

One of the major D_2 Abrantes NNW-SSE dextral shear zones makes the boundary between a limestone and a felsic volcano-sedimentary unit (Figs. 2A; Moreira, 2012). The felsic volcano-sedimentary unit has been strongly deformed by D_1, generating a penetrative subvertical NNW-SSE foliation (S_1) that often transpose bedding (N27ºW, 84ºNE; Fig. $2C_1$). In the S_1 plane is observed a stretching lineation (X_1) with very low plunges towards NNW, being subparallel to the regional L_1 intersection lineation (Fig. $2C_2$ and $2C_3$). Monoclinic and orthorhombic D_2 mesoscopic folds are common, sometimes with the local development of a slightly penetrative S_2 cleavage (N43ºW, 75ºE), mainly in the more pelitic layers (Fig. $2C_4$ and 3). The D_2 axial planes are subvertical and their trends range from E-W in the lower deformed domains, to NW-SE in the more deformed ones. The orientation of the fold hinges shows a strong dispersion induced by the interference with the D_1 structures (Fig. $2C_5$).

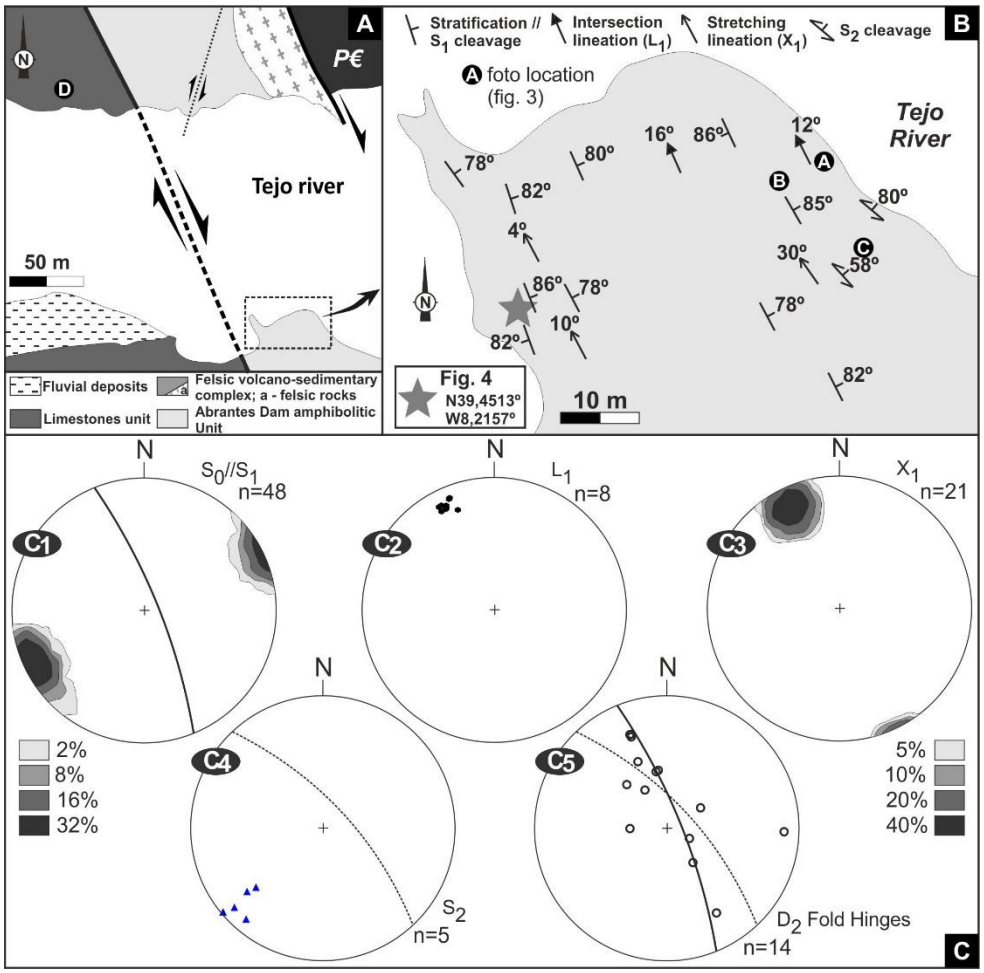

Figure 2 – Structural framework of Abrantes Domino region:

A – General Variscan structural map;

B – Structural detail in the vicinity of the domino outcrop;

C – Equal area lower hemisphere stereographic projections of main structures.

The angular relation between the E-W to NW-SE axial planes and the NW-SE S_2 cleavage with the NNW-SSE D_2 shear zones (N20ºW a N30ºW), indicates the *en-echelon* pattern expected in a D_2 regional dextral wrenching regime (Figs. 3A an 3B). Such non-coaxial dextral shearing is supported by a great diversity of D_2 structures, including folds asymmetry induced by the D_2 dextral centimetric to decametric 2nd order shear zones, associated to *en-echelon* behaviour of the D_2 minor folds (Figs. 3A an 3B), angular relation between the S_2 cleavage and the adjacent shear zones (Figs. 3C), sigmoidal bodies and shear bands (Fig. 3D).

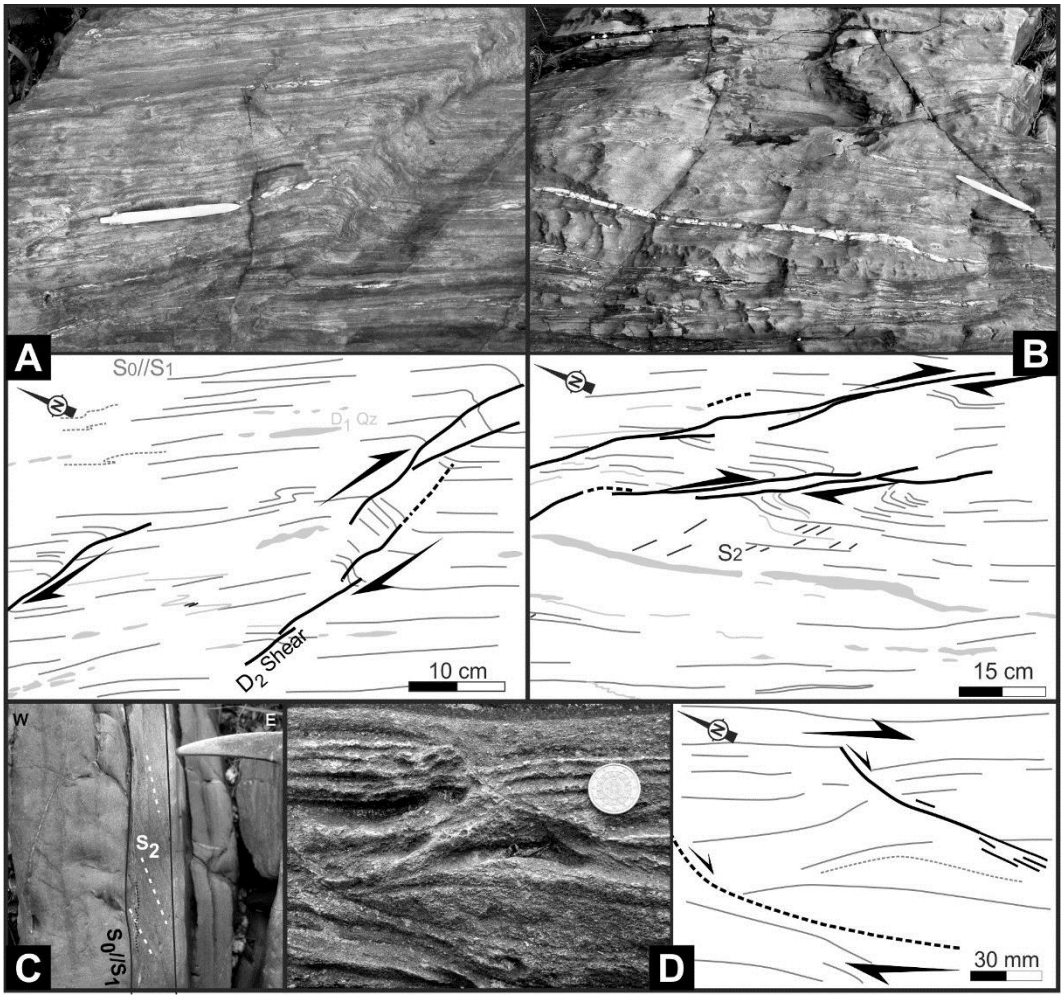

Figure 3 – Kinematical markers of D_2 dextral shearing:

A and B – Asymmetry of en-echelon D_2 minor folds associated to dextral shear bands;

C – Angular relation between S_2 and shear zones subparallel to $S_0//S_1$ layering;

D – Dextral Shear bands developed in the Limestone Unit, near the main shear zone.

In the felsic volcano-sedimentary unit, the dextral D_2 shearing give rise to a localized complex fracture pattern (Fig. 4A), strongly controlled by the decimetric silicate-rich layer, with millimetric to centimetric lamination. Such layering results from the transposition of the

stratification (S_0) by a S_1 cleavage (S_0 // S_1). The understanding of the evolution of this complex structure, where different shear zone families could be individualize (Fig. 4B), is the main aim of this work.

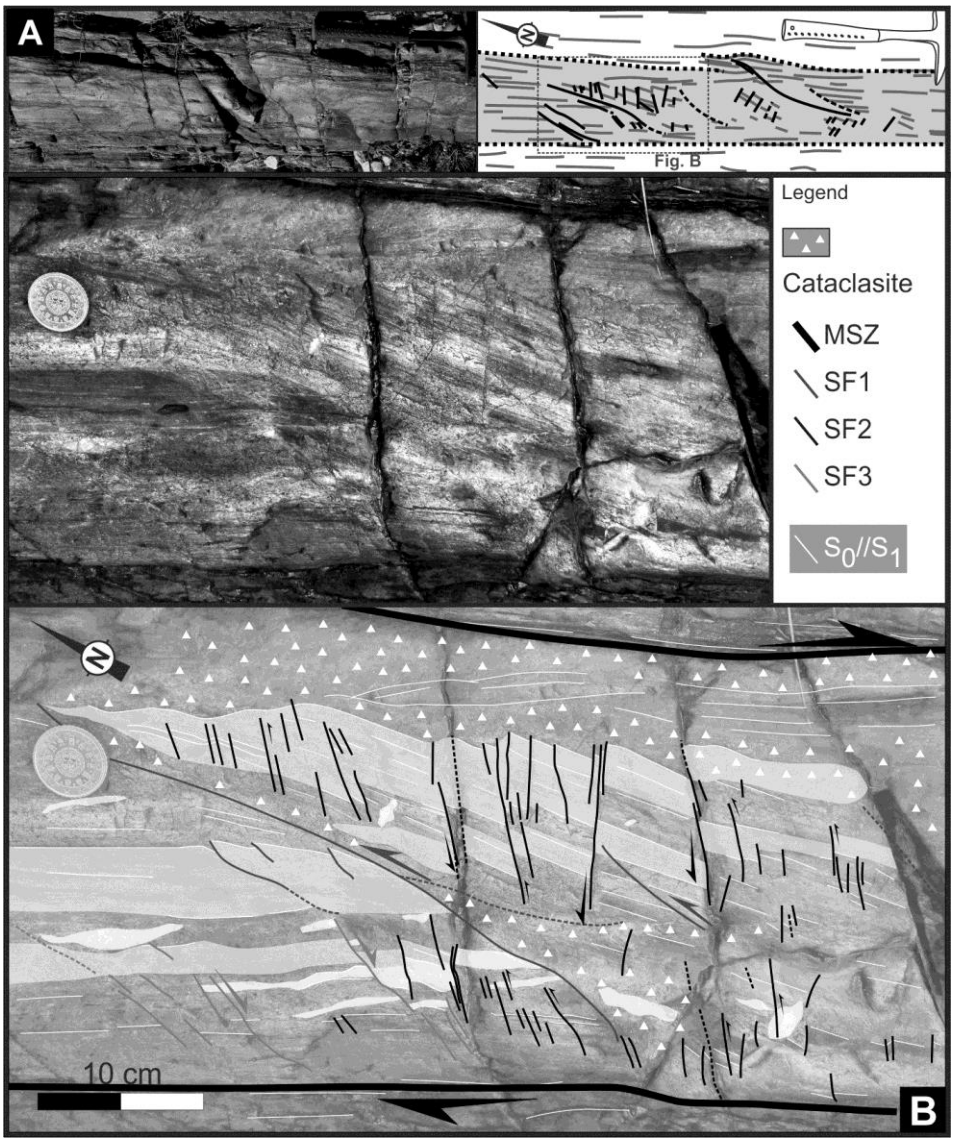

Figure 4 – Studied fracture pattern of Abrantes:

A – General pattern, showing the development of a heterogeneous fracture pattern;

B – Detail of figure A, enhancing the main structural pattern with discrimination of several shear families.

XIII.1.3.1. Geometrical and Kinematical Characterization

The complexity of the fracture pattern of Abrantes is due to the coexistence of several planar structures that accommodates the local stress within the shear zone (Fig. 4). As the layering is subvertical and the outcrop developed in a subhorizontal plane, the observed displacements along the individual shear zones are representative of horizontal offsets. This

does not preclude the existence of any subvertical component of movement, although it should be very small, because there is no evidence of such displacement has been found.

The fracture pattern has a localized development, being restricted to a decimetric domain bounded by NNW-SSE subvertical shear zones (MSZ). Such shears result from the reactivation of previous layering (S_0 // S_1) and act as a rigid barrier to the other shear zone families' propagation (Fig. 4), which were formed in its dependence.

The dextral movement along the MSZ during the D_2 regional event gives rise to a complex deformation of the inner domain, where the distortion, rotation and translation of several small blocks are common. These blocks are individualized by a numerous array of centimetric to decimetric shear zones. The exhibit fracture pattern could be considered divided in three main families according to their geometric and kinematics behaviour (Table 1; Fig. 5A).

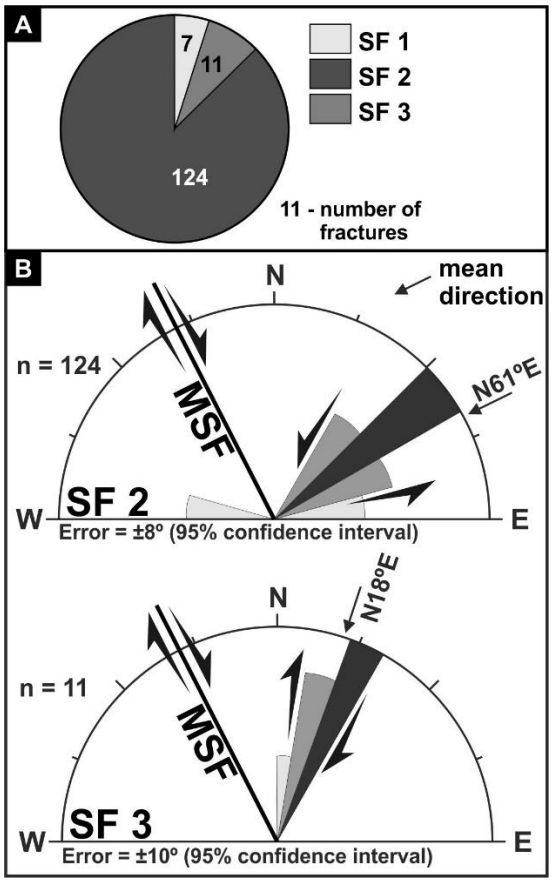

Figure 5 – Statistical analysis of the orientation of the shear zones orientations:

A – Relative distribution of shear zones family by number;

B – Variability of SF2 and SF3 orientations.

Table 1 – Geometric and kinematic features of Abrantes fracture pattern.

	Actual shear family main direction	Kinematics	Rotation of blocks	Cataclasis associated
MSZ	N27ºW	Dextral	No	Yes
SF1	N14ºE	Sinistral	No	Yes
SF2	N15ºE to S75ºE	Sinistral	Yes	No
SF3	N18ºE	Dextral	No	No

Shear Family 1 (SF1)

They are subvertical with a trend ranging from NNE-SSW to N-S direction (average orientation N14ºE, subvertical). They show a 45º mean angle to the MSZ, which tend to decrease when approaching the shear zone boundaries (FIG. 4B), that blocks its propagation. Although these discontinuities are not common when compared to other shear zone families (Fig. 5A, 6A and B), they have a large lateral continuity (Fig. 4), making them inescapable in any model that tries to explain the general pattern. The displacement induced by them in the regional $S_0//S_1$ layering enhance a sinistral kinematics (Fig. 6C), although in most continuous shears the kinematics is more dubious due to an intense cataclasis.

Shear Family 2 (SF2)

The SF2 shear zones are the most abundant family (Fig. 5A), individualizing several millimetric to centimetric blocks (Fig. 4B and 6A). These blocks exhibit a clear clockwise rotation, expressed by the angle between the $S_0//S_1$ layering inside the blocks and the regional layering, which is subparallel to MSZ (Fig. 4B). This rigid spinning always exhibits a clockwise sense, inducing a sinistral kinematics in the SF2 shears (Fig. 6A). However, the rotation angle between the blocks is not constant (see below), giving rise to a large dispersion in the trend of the planar structures belonging to this family (ranging between N15ºE and S75ºE, with a predominance of N60ºE direction; Fig. 5B). Nevertheless, the SF2 always exhibit a high angle to the MSZ general trend.

It is important to emphasize that this family has not a uniform distribution in the studied domain, being spatially restricted to SF1 and MSZ surrounding sectors (Fig. 4B and 6A). Therefore, these structures should have been dynamically related to the MSZ and SF1 activity.

Shear Family 3 (SF3)

The SF3 has an occasional development, appearing only in the marginal sectors of the area bordered by MSZ and SF1 (Fig. 4A and 6B), where the complex planar fabric is well marked and the SF1 and SF2 structures are predominant (Figs. 4B). It is characterized by dextral N-S to NNE-SSW shears (average direction N18ºE; Fig. 5C) and does not induce any rotation of blocks. This family appears to play a minor role in the observed pattern and in its dynamics.

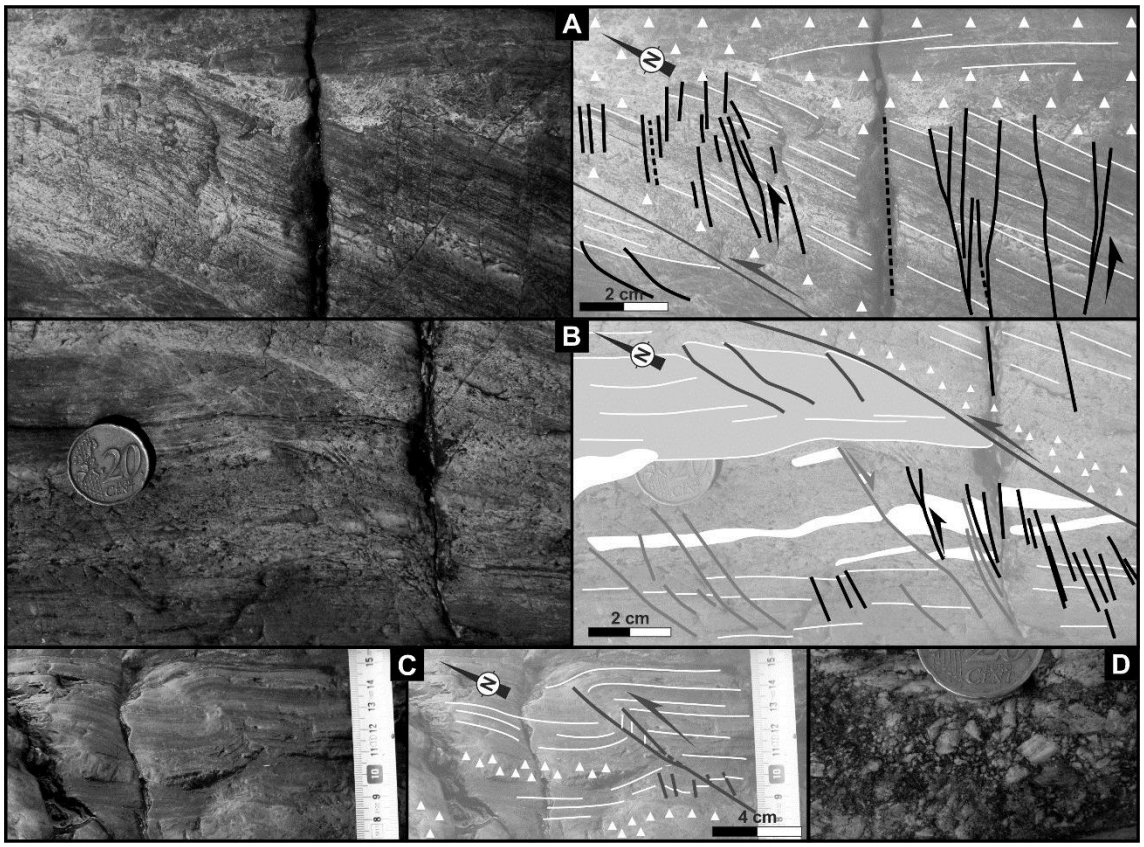

Figure 6 – Detailed geometric and kinematic features of the studied outcrop:

A – MSZ, SF1 and SF2 pattern, showing the presence of cataclasis associated to MSZ and SF1 shears and the rotated blocks bounded by SF2;

B – SF1 main shear ant its geometrical relation with the dominoes development domain, also showing the relation with dextral SF3;

C – Sinistral kinematics of SF1 structure;

D – Cataclasite associated to MSZ.

XIII.1.3.2. Rotational and Translational Characterization

Assuming fixed boundaries for the studied Abrantes shear zone, in a simple (or quasi-simple) shear mechanism, the rigid rotation of the domino blocks bounded by SF2 generates overlaps and gaps (Fig. 7). Such process could induce the formation of cataclasites, either in brittle, or in brittle-plastic transition (Engelder, 1974; Sibson, 1977; Ismat, 2006). In Abrantes shear zone the cataclasites are characterized by angular centimetric to millimetric lithoclasts, making difficult the distinction by simple mesoscopic observation between thin-crashed matrix and the larger centimetric fragments that compose the cataclasite (Fig. 6D).

Cataclastic flow, which accommodates ductile deformation in elastico-frictional regime (Sibson, 1977; Ismat, 2006), is located near the MSZ and SF1 shear zones (Figs. 4B, 6A and 6B), defining crushed zones. Such zones are characterized by distributed fracture and grain size

reduction throughout these families. Therefore, the blocks bounded by SF2 have a heterogeneous flux, with rigid (or quasi rigid) rotation, in a plastic matrix (constituted by cataclasite), which accommodates the overlaps and gaps created due the shear zones activity. The rigid block rotation, with no internal deformation, bounded by static boundaries generated in a simple shear regime are commonly named rigid-domino model (see Walsh and Watterson, 1991, Fossen and Hesthammer, 1998 and Fossen, 2010 references therein). However, in this model the planar structures that bound the blocks must exhibit constant rotation, strain rate, offsets and orientation, being parallel to each other, which was not observed in the study case (see discussion below).

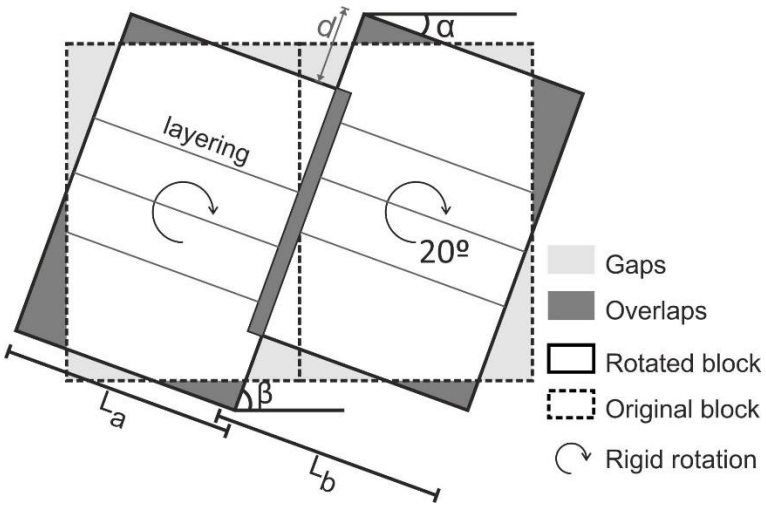

Figure 7 – Space problems induced by rigid block rotation and main geometrical parameters used in this study.

XIII.1.3.2.1. The Initial Angles; a Geostatistical Approach

A detailed analysis of the geometrical parameters related with block rotation in the Abrantes shear zone allowed the calculation of the initial angles between MSZ and SF2. These values are essential to establish the genetic relationships between the different shear zone families. Two angular parameters have been used: α (angle between the MSZ and S_0 // S_1 layering within blocks) and β (angle between the MSZ and SF2; Fig. 7). If the block rotation is totally rigid, these parameters should correlate; if the value of α increases, the β angle should decrease proportionately, in equal value. Therefore, the sum of the two angular parameters can provide an insight into the initial angle (β_0) of SF2 structures and its dispersion:

$$\beta_0 = \beta + \alpha$$

For the initial statistical analysis of β_0 population (n=121), it was used a box-plot graphic. The calculation of several statistical parameters of the β_0 population (*e.g.* median, quartiles,

maximum and minimum non-outliers) shows the presence of two outliers that deviate significantly from the general set (Fig, 8A$_1$). This analysis also shows that 50% of the data range between 107º and 120º values, with a median value of 115º. To minimize the errors, the two β_0 outliers (which could result either from sample variability, errors in the data collection or complex dynamic evolution) were not considered in the remaining statistical analysis.

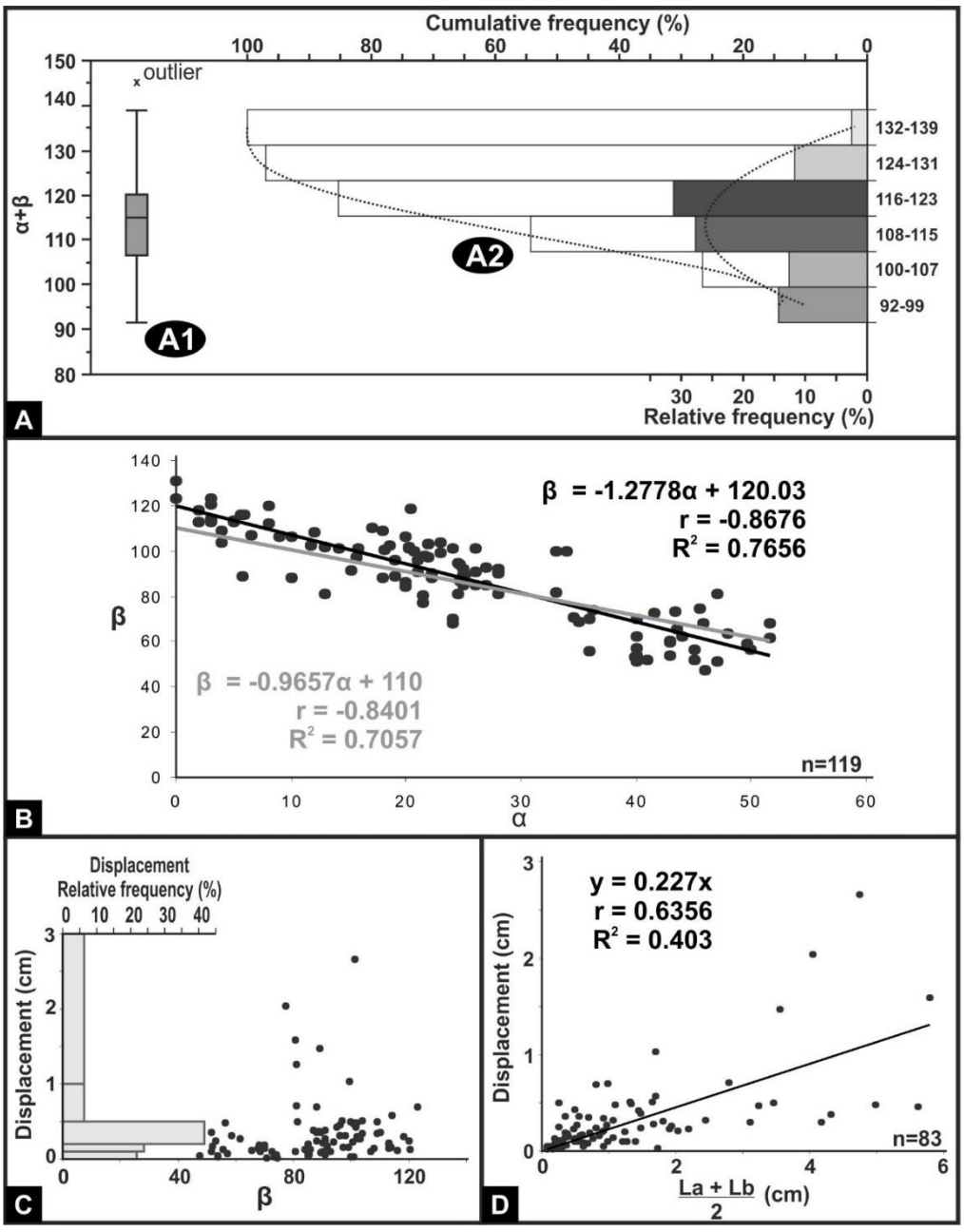

Figure 8 – Statistical analysis of the geometrical parameters of dominoes rotation shown in figure 7:

A – Variability of the β_0 data;

B – Correlation between α and β parameters;

C – Relation between the β parameter and the induced offset of adjacent blocks;

D – Relation between the offset between adjacent blocks and their wide.

The dataset, without outliers (n = 119), was projected in a histogram with six classes of seven degrees interval (Fig. 8A_2). To create representative statistical classes, it was used the Sturges' formula (valid for n <200). The histogram shows a data distribution close to a normal distribution, which was validated using the Kolmogorov-Smirnov test (*p-value*=0,36 to a 95% significance), with 59% of the data shared between the two central classes (106-115º and 116-123º). This indicates that the initial orientation of SF2 shears was not uniform, although there is a clear predominance (more than 50%) of β_0 values between 106º and 123º, which was also emphasized by the box-plot diagram.

In order to estimate the applicability of the theoretical model (Fig. 7) to the Abrantes dominoes, the correlation between α and β angular parameters was investigated (Fig. 8B). The obtained data show a strong negative linear correlation (Pearson's correlation coefficient r = -0.8676):

$$\beta = -1.2778\alpha + 120.03$$

The coefficient of determination (R^2) shows that 77% of β data (dependent variable) can be explained by a corresponding α (independent variable) variation of rigid blocks, as anticipated in initial assumption. This enables to estimate a mean angle of 60º between the shear zones that limit the blocks (SF2) and the main trend of the dextral shear (MSZ). Indeed, when the $S_0//S_1$ layering is parallel to the MSZ (*i.e.* when α =0º) the coeval β is 120º.

Nevertheless, the slope value obtained for this linear correlation (1.2778) slightly deviates from the value of 1.0 expected for a rigid rotation without internal deformation. Instead, if an initial value of 110º for SF2 is assumed, the coefficient of determination is slightly lower (R^2=0.7057), but the correlation between angular variables remains strong (Fig. 8B). In this case, the value of the slope strongly approaches the unit (0.9657). This seems to indicate that the initial acute angle between MSZ and SF2 families ranges between 60 and 70º.

The correlation between the angular parameters and the offsets of adjacent blocks (d parameter in Fig. 7) shows a random dispersion of data with no simple correlation (see Fig. 8C for a β parameter example). This seems to indicate the existence of other criteria controlling the offsets. Clearly the width of the blocks bounded by SF2 is one of the main factors which influence the offset between blocks. As the width of the left block (L_a) and he right one (L_b) equally affects the shear displacement (Fig. 7), any study of the offsets induced by domino rotation should use a mean block width:

$$\frac{L_a + L_b}{2}$$

The correlation between this parameter and the corresponding offsets should have a linear trend crossing the plot origin, because if the block width tends to zero, so does the offset. When

such approach is applied to Abrantes data (Fig. 8D) a moderate positive correlation is obtained (Pearson's correlation coefficient r = 0.6356), indicating that wider blocks induce bigger offsets. Nevertheless, the low value of the coefficient of determination (R^2 = 0,403) indicates that the width of the blocks could not be the only parameter affecting the offsets between adjacent blocks, because only 40% of the data could be explained by such correlation. This is not unexpected, because as α and β angular parameters also influence the offsets. Blocks with different spins must have different offsets.

The figure 8D diagram also shows the presence of some offsets well above the obtained correlation. Such anomalous values could have been influenced by a later reworking of SF2 shear zones. Moreover, the heterogeneous internal flow in the main shear zone could give rise to differential offsets along the SF2 shear planes, which will be independent of the offsets directly related to the domino rigid rotation. This additional movement could also explain the observed anomalous values.

XIII.1.3.2.2. Rotation and Translation of Dominos Blocks

As most of the deformation in the Abrantes studied shear zone (Fig. 9A) was the result of a rigid clockwise rotation between blocks, it is possible to restore the pre-deformation initial stage by the connection of homologous points of $S_0//S_1$ layering (Fig. 9B). This process allows estiating, not only the trajectories of the deformation, but also the shortening associated with heterogeneous deformation (next section). This restoration could confirm the previous statistical analysis.

The spatial analysis of isolated block rotation through pairs of homologous particles indicate a slightly differential spinning component between blocks (ranging from 13-14º to 20-23º; Fig. 9C). This variation is not random because the blocks in the vicinity of the SF1 shear zones have been less rotated. This shows the strong influence of this family in the deformation process.

Finite deformation pattern was obtained by two different methods. In the first one, the initial (Fig. 9B) and the final (Fig. 9A) stages are overlap using a point (P) which is considered fixed, defined in the central region of the deformed area. Then, each pair of homologous points is joint by arrowed linear segments (Fig. 9D).

The obtained pattern is an efficient way to study the flow pattern related to the shear activity (Passchier and Trouw, 2005). The strong symmetry of the Abrantes pattern around *P* point, emphasize a clockwise rotational component of deformation, compatible with synthetic spinning induced by the regional dextral simple shear dominated component. When approaching the MSZ that bounds the studied sector, the flow trajectories become almost

parallel to them (Fig. 10). The differential spinning between blocks inside the shear zone is also evident, contrasting with the absence of rotation outside the domino domain.

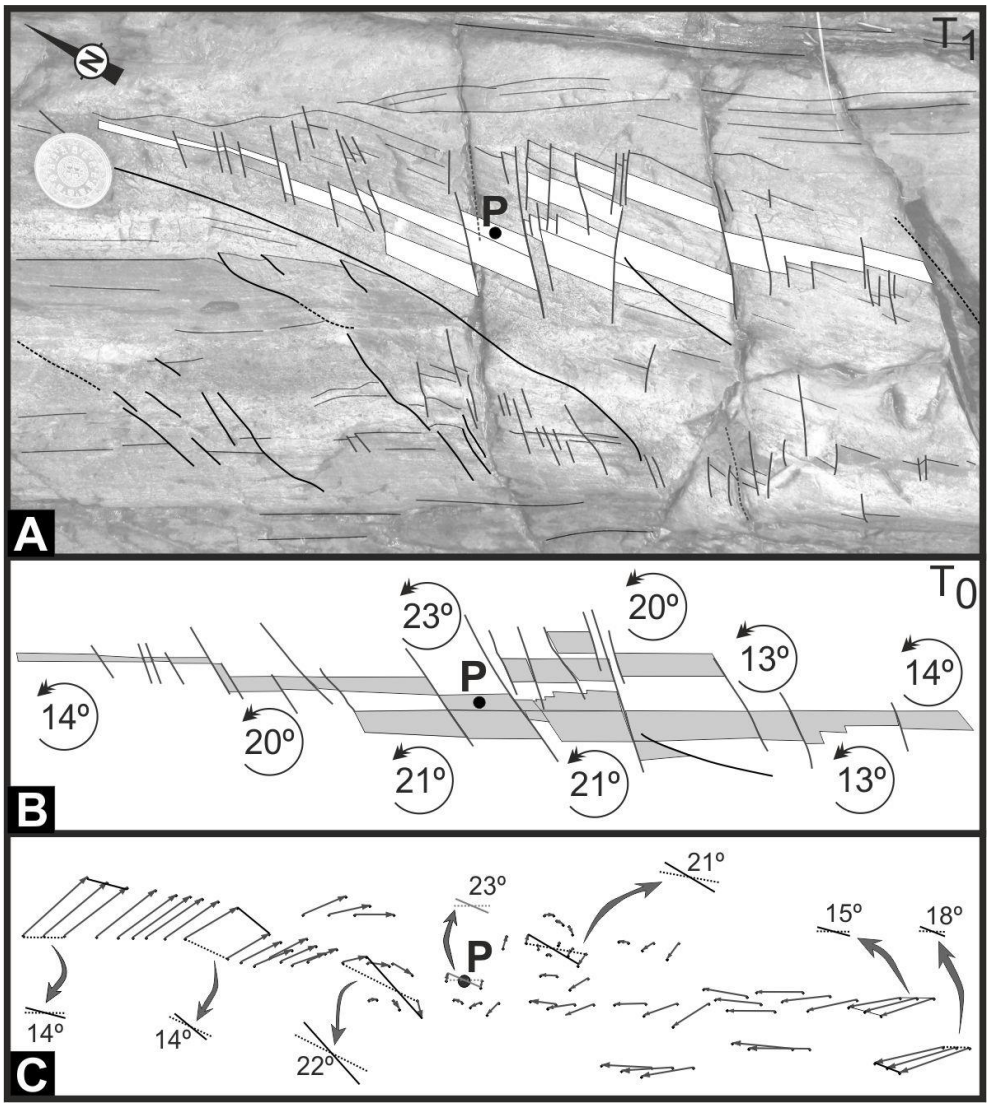

Figure 9 – Establishment of the deformation trajectories, using a central fixed point (P):

A – Final deformed stage;

B – Rigid block rotation restoration of the pre-deformation stage, with rigid rotation value used to restore the block early position;

C – Flow pattern induced by deformation, showing the individual particle rotation.

The second method (Fig. 10) intends to obtain the total displacement particle vectors during deformation. This pattern is generated by overlapping the final stage (Fig. 10A) and the pre-deformation one (Fig. 10B) using as a fixed point (P) located outside the domino domain. The obtained pattern (Fig. 9C) shows an important translational component induced by the overall activity of all shear zone families. The clockwise rotational component remains present,

although it is masked by the translational component related to SF1. This pattern is usually considered less useful (Passchier and Trouw, 2005), because some of the observed translation and rotation components have no geodynamical significance, masking the relative particle motion. Nevertheless, the strong parallelism between the general trajectories and the SF1 trend seems to confirm the important role of this family during deformation.

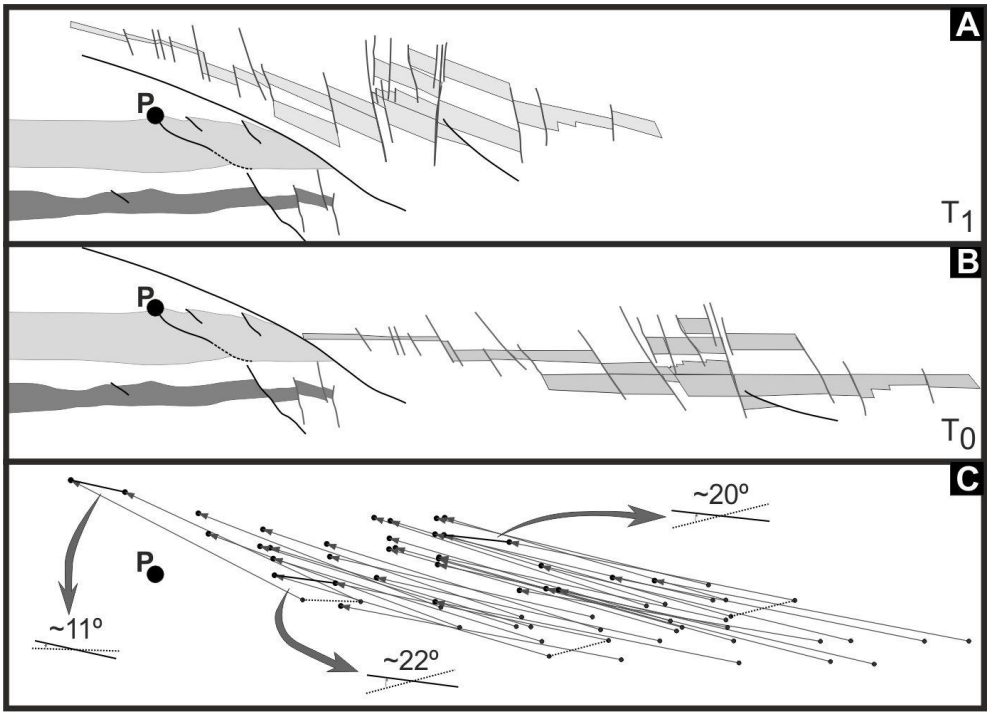

Figure 10 – Establishment of the deformation trajectories, using an outside fixed point (P):

A – Final deformed stage;

B – Restoration of the pre-deformation stage;

C – Flow pattern induced by deformation.

XIII.1.3.2.3. Quantitative approach to Deformation

Although the particle flow within the Abrantes domino has not been homogeneous due to the interaction between the several shear zones, two different geometrical approaches have been used to estimate the finite strain induced by the dextral shear deformation. In both cases, the final geometry (T_1 moment: Fig. 11A) is compared to the restore initial pattern (T_0 moment; Fig. 11B) which enables to quantify the stretch in homologous linear segments.

In the first method the stretch in three linear segments (lines A, B and C; Fig. 11) making high angles between them was obtained comparing their length in the deformed (L_1) and undeformed (L_0) states (Figs. 11A and 11B). When the stretches are known for any three different directions, the strain ellipse can be estimated (De Paor, 1988). The geometrical data

that have been used to estimate the finite strain using this approach, as well as the strain ellipse parameters, is resumed in table 2 and figure 11C. They show a moderate distortion (Rs=1,6) while the orientation of the ellipse is compatible with the dextral shearing along the MSZ.

As the three segments were chosen in order to enclose most of the domino domain, the obtained finite strain is representative of the deformation of the overall zone.

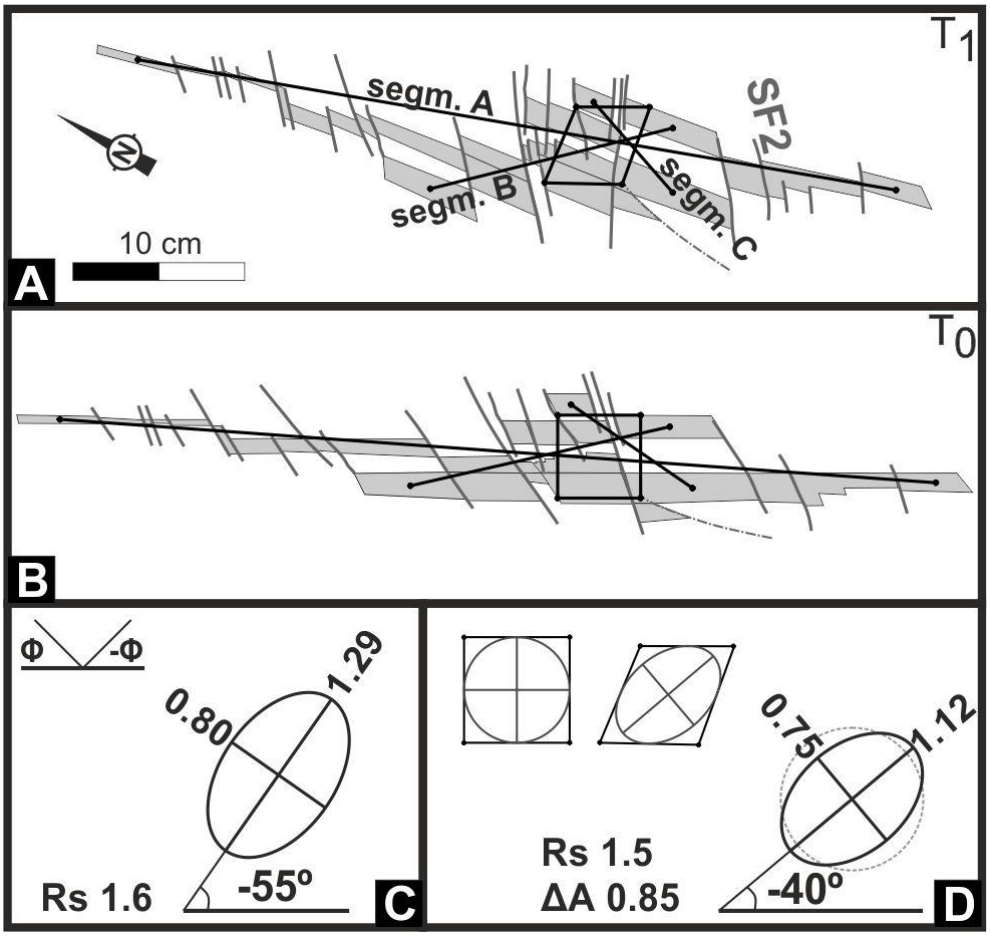

Figure 11 – Geometrical approach to estimate the finite strain in Abrantes shear zone:

A – Geometrical data in the final deformed stage that have been used;

B – Previous data restored to the pre-deformation stage;

C – Strain ellipse for the "three segments" approach;

D – Strain ellipse for the "square" approach.

The second method focus on the strain analysis in the inner zone of the Abrantes domino, where the block rotation has been greater (Fig. 9B and 9C). In this approach four points have been selected within the shear zone in the undeformed pattern, whose arrangement defines a square at T_0 moment (Fig. 11B). The same 4 corners of this square were identified in the deformed T_1 state, allowing to define a "rhombohedra" homologous of the previous square (Fig.

11A). A circumference was incircle in the undeformed square, while an ellipse was inscribed in the deformed rhombus (Fig. 11D). As the undeformed circle could be considered unitary, the ellipse represents the finite strain related to the distortion of the fabric. Table 3 and figure 11D synthesize the obtained strain parameters, which also show a moderate intensity (Rs=1,5) and also an orientation compatible with the dextral regional shear.

Table 2 – Strain data for the three studied segments.

		segment A	**segment B**	**segment C**
General trend		N20ºW	N44ºW	N29ºE
Angle to MSZ (φ)		6.7º	-17.1º	45.9º
Rotation		5.6º	1.4º	14.4º
L_0 (cm)		51.2	21.1	8.6
L_1 (cm)		44.9	22.4	7.0
Stretch ratio (L_1/L_0)		0.88	1.06	0.81
% shortening		12	-6	19
Strain ellipse	Major axis (s ; φ)	1.29 ; -55.1º		
	Minor axis (s ; φ)	0.80 ; 34.9º		
	Rs	1.6		

Table 3 – Strain data for "*square*" method.

	major axis	**minor axis**
General trend	N70ºW	N20ºE
Angle to MSZ (φ)	-40º	50º
L_0 (cm)	4.83	4.83
L_1 (cm)	5.43	3.64
Stretch ratio (L_1/L_0)	1.12	0.75
Shortening (%)	-12	25
Rs	1.5	
Δ area ($A_{ellipse}/A_{circle}$)	0.85	

As the strain ellipse was designed independently of the unitary circle, with this method it is also possible to estimate the area change induced by the deformation. The comparison between both areas indicates an area decrease of 15%. This decrease should be related with the space problems induced by the overlaps during block rotation. These problems led to material migration by cataclastic flow from the overlaps giving rise to the important concentration of cataclasites in the vicinity of the Abrantes shear zone boundaries (Fig. 4 and 6). Another possible explanation could be internal block deformation at the microscopic scale. Nonetheless**,** as previously mentioned, there is no mesoscopic evidence of internal deformation within blocks.

When comparing the finite strains estimated by both methods, although the approaches are strongly different, the results are rather similar. Indeed, not only the intensity of strain is comparable (1.5 and 1.6 strain ratios), but also both strain ellipses have major axes almost

parallel (-55º and -40º). This seems to indicate that even if the deformation inside the Abrantes shear zone could not be considered homogeneous, the heterogeneities are restricted.

XIII.1.4. Dynamic Processes and Genesis of Domino Structures; Discussion

The previous geometric and kinematic analysis of all shear zone families of Abrantes Domino, with special emphasis on SF2, allowed the perception of the genetic relations between them. The MSZ and SF1 clearly have a main role in the observed pattern, because they bound the domain where the rigid block rotation, circumscribed by SF2, is found, generating a domino structure.

The MSZ presents a right-lateral kinematics, while SF1 has an antithetic movement. The 45º acute angle between both families tends to decrease in the vicinity of the main shear zone boundary (Fig. 4B), where it can attain 25º. The reorientation of SF1 structures in the vicinity of MSZ could be the result of the reorientation of the local stress field induced by the movement along the previous $S_0//S_1$ anisotropy (Dyer, 1988), the drag of SF1 during MSZ activity or even of the internal material vorticity within the shear zone. In such context, important space problems should arise due to the interaction between these shear zone families, since the SF1 left-lateral displacements are blocked by the shear zone boundary (MSZ).

The sinistral kinematics of the SF2 family, which is antithetic to the general dextral shear (MSZ), indicates that they could be the result of a strike-slip domino mechanism. Similar behaviour has been proposed in Iberia for the Late Variscan deformation (Ribeiro, 2002; Dias et al., 2016a). The statistical analysis of the general orientation of SF2 (see section 3.1) seems to indicate it has genetic relation with SF1 family. As the initial acute angle between SF2 and MSZ (β0) usually ranges between 60 and 70º, the SF2 could be interpreted either as the sinistral conjugate of MSZ or R' shears (Logan *et al.*, 1992; Mandl, 2000; Brosch and Kurz, 2008). Thus, although the final geometry and kinematic of SF1 and SF2 are different, not only they could have been formed at the same time but, in the early stages, they were also sub-parallel.

It is now possible to present a model that explains the complex fracture pattern studied in the Abrantes shear zone (Fig 12).

In the early stages of D_2 deformation (T_0) the regional stress field induced the local reactivation of some previous major $S_0//S_1$ anisotropy as dextral shears (Fig. 12A). This reactivation was generated by a simple or quasi simple shear, which induces a non-coaxial internal deformation in the more competent layers of the Abrantes shear zone. The interference between closely spaced MSZ brittle-ductile shear zones could generate a dense fracture pattern of 2nd order shear zones oriented at 60º-70º to them (SF1 and SF2), with distinct spacing and size. Due to the highly non-coaxial deformation of Abrantes dextral shear zone and the

dispersion of the final trend observed in each family (see section 3.2.1), it is not easy to decide between a conjugated shear mechanism and the R´ one for such new shear zones. Whatever their initial origin, during the progression of deformation these new fractures could had different behaviours (Fig. 12B). The most continuous (SF1) interfere with the MSZ, bounding an inner high-strain domain, where the vorticity is stronger. Concerning the shorter shear zones (SF2) they rotated synthetically with the MSZ due to the overall vorticity, giving rise to an important rigid block spinning in a domino model. The space problems inside the Abrantes shear zone induced by this rigid rotation (Fig. 7) were partially solved by cataclasis, which removed material from the overlaps towards the local gaps, generating a cataclastic flow. This cataclastic flow also helps the rigid domino rotation, acting as a plastic matrix where the blocks could spin. A similar rigid block rotation in a plastic matrix has been described in asymmetric domino-like structures developed in high grade conditions (Goscombe and Passchier, 2003). Nevertheless, the quantitative approach using the "square" method shows a slightly area decrease (i.e. circa 15%) in the domino domain (Fig. 11D and table 3), which indicates that such flow could not be the only mechanism responsible to account for this geometrical problems.

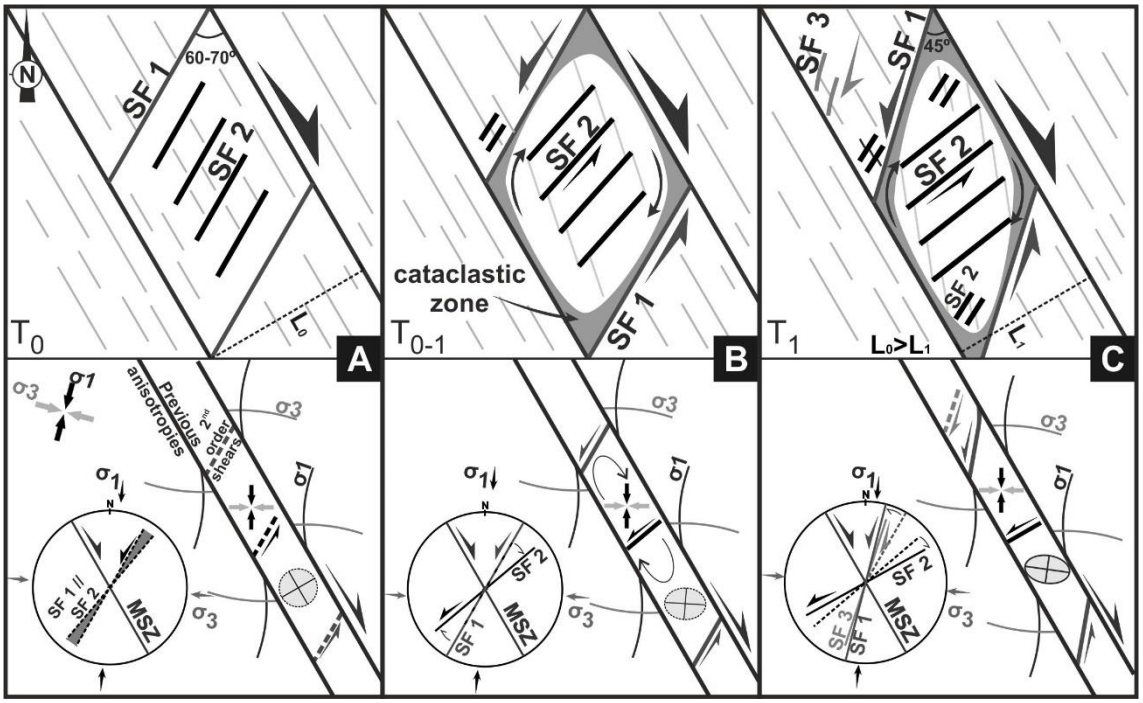

Figure 12 – Evolutionary proposal for the D_2 Abrantes shear zone.

A – Early stage of regional dextral shearing;

B – Major block rotation and coeval cataclastic formation;

C – Final rotation and shortening.

The rotation of R' structures during the progression of deformation is not uncommon (Mandl, 2000; Brosch and Kurz, 2008). Thus, although SF1 and SF2 have been subparallel in the early stages of D_2, their trend will diverge during the non-coaxial deformation. The continuity of D_2 dextral shearing (Fig. 12C), not only amplifies previous processes but also could induces the formation of new shear zones. This may explain the presence of small rotated narrow blocks inside the high strain zone, as well as the observed higher outlier's values. If it is considered a 2^{nd} generation of R' shears affecting a previously rotated layering, the α+β value does not represent the initial angle between MSZ and the SF2 (β_0), because α parameter is not equal to 0 when the new shear is created.

The geometry and kinematics of SF3 indicates they could be considered c' bands or Riedel shears of the D_2 MSZ dextral shear. Nevertheless, the angle between both families is slightly larger than what is expected for these structures (Mandl, 2000; Xypolias, 2010 and references therein). Such discrepancy could result from some orthogonal flattening during the late stages of D_2 deformation (Fig. 12C).

The proposed evolution has some discrepancies with the theoretical rigid-domino model (see Walsh and Watterson, 1991; Fossen and Hesthammer, 1998 for a discussion). Indeed, although the blocks have a rigid behaviour, there are some data which could not be explained:

- The SF2 are not perfectly linear, presents distinct sizes and present a range of general trends with an almost normal distribution around a mean value (Fig. 8A_2);
- The blocks present differential rotations, distinct sizes and consequently the shear zones present distinct offsets (Figs. 8D and 9);
- Although there is no evidence of internal mesoscopic deformation in the blocks, the finite strain analysis shows an area variation during the deformation process, suggesting an internal block deformation.

Previous data are more compatible with the so called soft-domino model (Walsh and Watterson, 1991; Fossen and Hesthammer, 1998). Yet, in the Abrantes domino, the blocks are more rigid than it was assumed by such model, which was possible due to the intense heterogeneous cataclastic flow, which acts as a matrix to the rigid block spinning that can generate the dissimilar rotations and offsets of SF2.

The strong non-coaxial deformation in the Abrantes shear zone, alongside the sin-kinematic synthetic rotation of earlier shear zones, give rise to a highly complex final pattern where the rigid block rotation is a crucial process in the fabric evolution.

XIII.1.5. Final Remarks

The studied Abrantes domino highlights:

- A close connection between the main dextral shearing and the clockwise synthetic rotation of domino structures, associated to a simple shear dominated transpression;

- A heterogeneous deformation, generating a complex pattern of shear structures;

- The presence of 2nd order shear zones, with antithetic kinematics (SF1), which together with the MSZ generates a clockwise internal flow within shear zone, is responsible by the rigid block spinning;

- The shear family that bounds the domino structures (SF2) could be formed as R' shears in initial stages, forming with an angle of 60-70º relatively to the MSZ;

- Although the deformation is highly heterogeneous, the finite strain data suggest the existence of a simple shear dominated transpression;

- The rigid block rotation was related to an intense cataclastic flow within the shear zone. The blocks have differential rotations and sizes, and consequently SF2 presents a distinct offset, compatible with the soft-domino model.

- Interpretation of domino structures, must be done carefully and its kinematic and dynamic analysis must to be supported by the general framework.

References

Axen, G.J. (1988). The geometry of planar domino-style normal faults above a dipping basal detachment. Journal of Structural Geology, 10, 405-411. DOI: 10.1016/0191-8141(88)90018-1

Bahroudi, A., Koyi, H. A., Talbolt, C. J. (2003). Effect of ductile and frictional décollements on style of extension, Journal of Structural Geology, 25, 1401–1423. DOI: 10.1016/0191-8141(88)90018-1

Brosch, F-J., Kurz, W. (2008). Fault damage zones dominated by high angle fractures within layer-parallel brittle shear zones: examples from the eastern Alps. In: Wibberley, C.A.J., Kurz, W., Imber, J., Holdsworth, R.E., Collettini, C (Eds.) The Internal Structure of Fault Zones: Implications for Mechanical and Fluid-Flow Properties, Geological Society, London, Special Publications, 299, 75–95. DOI: 10.1144/SP299.5

Chaminé, H. I., Gama Pereira, L. C., Fonseca, P. E., Noronha, F., Lemos de Sousa, M. J. (2003). Tectonoestratigrafia da faixa de cisalhamento de Porto–Albergaria-a-Velha–Coimbra–Tomar, entre as Zonas Centro-Ibérica e de Ossa-Morena (Maciço Ibérico, W de Portugal). Cad. Lab. Xeol. Laxe, A Coruña, 28, 37-78.

Cowan, D. S., Botros, M., Johnson, H. P. (1986). Bookshelf tectonics: Rotated crustal blocks within the Sovanco fracture zone, Geophys. Res. Lett., 13, 995-998. DOI: 10.1029/GL013i010p00995

Dabrowski, M., Grasemann, B., (2014). Domino boudinage under layer-parallel simple shear. Journal of Structural Geology, 68, 58–65. DOI: 10.1016/j.jsg.2014.09.006

De Paor, D. (1988). Strain determination from three known stretches. Journal of Structural Geology, 10, 639-642. DOI: 10.1016/0191-8141(88)90029-6

Dias, R., Ribeiro, A. (1993). Porto-Tomar shear zone, a major structure since the beginning of the Variscan orogeny. Comunicações do Instituto Geológico e Mineiro, 79, 29-38.

Dias, R., Ribeiro, A. (1994). Constriction in a transpressive regime: an example in the Ibero-Armoricain Arc. Journal of Structural Geology, (11), 1543–1554. DOI: 10.1016/0191-8141(94)90032-9

Dias, R., Ribeiro, A. (2008). Heterogeneous strain behaviour in competent layers during folding in transpressive regimes. Geodinamica Acta, 21(4), 219-229. DOI: 10.3166/ga.21.219-229

Dias, R., Mateus, A., Ribeiro, A. (2003). Strain partitioning in transpressive shear zones in the southern branch of the Variscan Ibero-Armorican Arc. Geodinamica Acta, 16, 119-129. DOI: 10.1016/j.geoact.2003.04.001

Dias, R., Moreira, N., Ribeiro, A., Basile, C. (2016a). Late Variscan Deformation in the Iberian Peninsula; A late feature in the Laurasia-Gondwana Dextral Collision. International Journal of Earth Sciences. DOI: 10.1007/s00531-016-1409-x

Dias, R., Ribeiro, A., Romão, J., Coke, C., Moreira, N. (2016b). A Review of the Arcuate Structures in the Iberian Variscides; Constraints and Genetical Models. Tectonophysics, 681, 170-194. DOI: 10.1016/j.tecto.2016.04.011

Dyer, R. (1988). Using joint interactions to estimate paleostress ratios. Journal of Structural Geology, 10, 685-699. DOI: 10.1016/0191-8141(88)90076-4

Engelder, J.T. (1974). Cataclasis and the generation of fault gouge. Geological Society of America Bulletin, 85(10), 1515-1522. DOI: 10.1130/0016-7606(1974)85<1515:CATGOF>2.0.CO;2

Figueiredo, R.P., Vargas, E.A., Moraes, A. (2004). Analysis of bookshelf mechanisms using the mechanics of Cosserat generalized continua. Journal of Structural Geology, 26, 1931–1943. DOI: 10.1016/j.jsg.2004.03.002

Fossen, H. (2010). Structural Geology. 1st Ed.. Cambridge University Press, 463 p.

Fossen, H., Hesthammer, J. (1998). Structural geology of the Gullfaks field, northern North Sea. In: Coward, M.P., Johnson, H., Daltaban, T.S. (Eds.), Structural Geology in Reservoir Characterization. Geological Society London Special Publication, 127, 231-261. DOI: 10.1144/GSL.SP.1998.127.01.16

Fossen, H., Tikoff, B. (1998). Extended models of transpression and transtension, and application to tectonic settings. In: Holdsworth, R.E., Strachan, R.A. and Dewey, J.F. (Eds.), Continental transpressional and transtensional tectonics. Geol. Soc. Lond. Spec. Publ., 135, 15-33. DOI: 10.1144/GSL.SP.1998.135.01.02

Fossen, H., Tikoff, B., Teyssier, C. (1994). Strain modeling of transpressional and transtensional deformation, Norsk Geologisk Tidsskrift, 74, 134–145.

Goscombe, B., Passchier, C.W. (2003). Asymmetric boudins as shear sense indicators – an assessment from field data. Journal of Structural Geology, 25(4), 575–589. DOI: 10.1016/S0191-8141(02)00045-7

Goscombe, B. D., Passchier, C. W., Hand, M. (2004). Boudinage classification: end-member boudin types and modified boudin structures. Journal of Structural Geology, 26(4), 739-763. DOI: 10.1016/j.jsg.2003.08.015

Iglésias, M., Ribeiro, A. (1981). Zones de cisaillement ductile dans l'arc ibéro-armoricain. Comunicações do Instituto Geológico e Mineiro, 67, 85-87.

Ismat, Z. (2006). Cataclastic flow: a means for ensuring ductility within the elastico-frictional regime. Geological Society of America Annual Meeting Abstract with Programs, 38 (7), 310.

Jaeger J.C., Cook N.G.W. (1987). Fundamentals of rock mechanics, 3rd ed., Chapman and Hall, London, 593 p.

Julivert, M., Fontbote, J. M., Ribeiro, A., Conde, L.E.N. (1974). Memória Explicativa do Mapa Tectónico da Península Ibérica Y Baleares, Escala 1:1 000 000, Inst. Geol. Min. España, 1-113.

Karlstrom, K.E., Heizler, M., Quigley, M.C. (2010). Structure and $^{40}Ar/^{39}Ar$ K-feldspar thermal history of the Gold Butte block: Reevaluation of the tilted crustal section model. In: Umhoefer, P.J., Beard, L.S., Lamb, M.A. (Eds.), Miocene Tectonics of the Lake Mead Region, Central Basin and Range. Geological Society of America Special Paper, 463(15), 331–352. DOI: 10.1130/2010.2463(15).

Karmakar, S., Mandal, N. (1989). Rotation and offset of shear fracture boudins. Indian Journal of Geology 61, 41-49.

La Femina, P.C., Dixon, T.H., Strauch, W. (2002). Bookshelf faulting in Nicaragua, Geology, 30, 751–754. DOI: 10.1130/0091-7613(2002)030<0751:BFIN>2.0.CO;2

Lefort, J.P., Ribeiro, A. (1980). La faille de Porto-Badajoz-Cordobe a-t-elle contrôlé l'évolution de lócéan paleéozoique sud-Armoricain?. Bull. Soc. Géol. France, 7, XXII (3), 455-462.

Logan J.M., Dengo C.A., Higgs N.G., Wang Z.Z. (1992). Fabrics of experimental fault zones: their development and relationship to mechanical behaviour. In: Evans B., Wong T.F. (Eds.), Fault mechanics and transport properties of rocks. International Geophysics, 51, 33-67. DOI: 10.1016/S0074-6142(08)62814-4

Lotze, F. (1945). Zur Gliderung der Varisziden in der Iberischen Meseta. Geotekt. Forsch., 6, 78- 92.

Mandal, N., Khan, D. (1991). Rotation, offset and separation of oblique-fracture (rhombic) boudins: theory and experiments under layer-normal compression. Journal of Structural Geology, 13, 349-356. DOI: 10.1016/0191-8141(91)90134-5

Mandal, N., Chakraborty, C., Samanta, S.K. (2000). Boudinage in multilayered rocks under layer-normal compression: a theoretical analysis. Journal of Structural Geology, 22(3), 373–382. DOI: 10.1016/S0191-8141(99)00156-X

Mandal, N., Dhar, R., Misra, S., Chakraborty, C. (2007). Use of boudinaged rigid objects as a strain gauge: Insights from analogue and numerical models. Journal of Structural Geology, 29(5), 759-773. DOI: 10.1016/j.jsg.2007.02.007

Mandl, G. (1984). Rotating Parallel Fault – "Book Shelf" Mechanism. American Association of Petroleum Geologists Bulletin, 68, 502-503.

Mandl, G. (1987). Tectonic deformation by rotating parallel faults: the "bookshelf' mechanism. Tectonophysics, 141 (4), 277-316. DOI: 10.1016/0040-1951(87)90205-8

Mandl, G. (2000). Faulting in brittle rocks: an introduction to the mechanics of tectonic faults. Springer-Verlag, Berlin. ISBN: 978-3-662-04262-5

Matte, P. (2001). The Variscan collage and Orogeny (480 – 290 Ma) and the tectonic definition of the Armorica microplate: A review, Terra Nova, 13, 122 – 128. DOI: 10.1046/j.1365-3121.2001.00327.x

Moreira, N. (2012). Caracterização estrutural da zona de cisalhamento Tomar-Badajoz-Córdova no sector de Abrantes. Unpublished MSc thesis, University of Évora, 225 p.

Moreira, N., Romão, J., Pedro, J., Dias, R., Ribeiro, A. (2016). The Porto-Tomar-Ferreira do Alentejo Shear Zone tectonostratigraphy in Tomar-Abrantes sector (Portugal). Geo-Temas, 16(1), 85-88. ISSN 1576-5172.

Moreira, N., Araújo, A., Pedro, J.C., Dias, R. (2014). Evolução geodinâmica da Zona de Ossa-Morena no contexto do SW Ibérico durante o Ciclo Varisco. Comunicações Geológicas, 101 (I), 275-278.

Nance, R.D., Gutierrez-Alonso, G., Keppie, J.D., Linnemann, U., Murphy, J.B., Quesada, C., Strachan, R.A., Woodcock, N.H. (2010). Evolution of the Rheic Ocean. Gondwana Research, 17, 194-222. DOI: 10.1016/j.gr.2009.08.001

Nance, R.D., Gutiérrez-Alonso, G., Keppie, J.D., Linnemann, U., Murphy, J.B., Quesada, C., Strachan, R.A., Woodcock, N.H. (2012). A brief history of the Rheic Ocean. Geoscience Frontiers, 3(2), 125-135. DOI: 10.1016/j.gsf.2011.11.008

Nixon, C. W., Sanderson, D. J., Bull, J. M. (2011). Deformation within a strike-slip fault network at Westward Ho!, Devon U.K.: Domino vs conjugate faulting. Journal of Structural Geology, 33, 833-843. DOI: 10.1016/j.jsg.2011.03.009

Passchier, C.W., Myers, J.S., Kröner, A. (1990). Field Geology of High-Grade Gneiss Terrains. Springer-verlag Berlin Heidelberg New York, 150 p. ISBN: 3-540-53053-3.

Passchier, C.W., Trouw, R.A.J. (2005). Microtectonics. 2nd Ed., Springer, New York, 382 p. ISBN 978-3-540-64003-5

Pereira, M.F., Silva, J.B., Drost, K., Chichorro, M., Apraiz, A. (2010). Relative timing of the transcurrent displacements in northern Gondwana: U-Pb laser ablation ICP-MS zircon and monazite geochronology of gneisses and

sheared granites from the western Iberian Massif (Portugal). Gondwana Research, 17, 461–481. DOI: 10.1016/j.gr.2009.08.00.

Ramsay, J.G. (1967). Folding and Fracturing of rocks. MacGraw Hill, New York, 568 p.

Ribeiro, A. (2002). Soft Plate and Impact Tectonics. Springer Verlag, Berlin, 324 p. ISBN: 978-3540679639

Ribeiro, A., Antunes, M. T., Ferreira, M. P., Rocha, R. B., Soares, A. F., Zbyszewski, G., Moitinho de Almeida, F., Carvalho, D., Monteiro, J. H. (1979). Introduction à la géologie générale du Portugal. Serviços Geológicos de Portugal, 114 p.

Ribeiro, A., Munhá, J., Dias, R., Mateus, A., Pereira, E., Ribeiro, M.L., Fonseca, P., Araújo, A., Oliveira, T., Romão, J., Chaminé, H., Coke, C., Pedro, J. (2007). Geodynamic evolution of SW Europe Variscides, Tectonics, 26(6). DOI: 10.1029/2006TC002058

Ribeiro, A., Munhá, J., Mateus, A., Fonseca, P., Pereira, E., Noronha F., Romão, J., Rodrigues, J. F., Castro, P., Meireles, C., Ferreira, N. (2009). Mechanics of thick-skinned Variscan overprinting of Cadomian basement (Iberian Variscides). Comptes Rendus Geoscience, 341 (2-3), 127-139. DOI: 10.1016/j.crte.2008.12.003

Ribeiro, A., Romão, J., Munhá, J., Rodrigues, J., Pereira, E., Mateus, A., Araújo, A. (2013). Relações tectonostratigráficas e fronteiras entre a Zona Centro-Ibérica e a Zona Ossa-Morena do Terreno Ibérico e do Terreno Finisterra. In: Dias, R., Araújo, A., Terrinha, P., Kullberg, J.C. (Eds.), Geologia de Portugal, vol. 1, Escolar Editora, 439-481. ISBN: 978-972-592-364-1

Romão, J., Coke, C., Dias, R., Ribeiro, A. (2005). Transient inversion during the opening stage of the Wilson Cycle "Sardic phase" in the Iberian Variscides: stratigraphic and tectonic record. Geodin. Acta, 18/2, 15-29.

Romão, J., Metodiev, D., Dias, R., Ribeiro, A. (2013). Evolução geodinâmica dos sectores meridionais da Zona Centro-Ibérica. In: Dias, R., Araújo, A., Terrinha, P., Kullberg, J.C. (Eds.), Geologia de Portugal, vol. 1, Escolar Editora, 206-257. ISBN: 978-972-592-364-1.

Romão, J., Moreira, N., Dias, R., Pedro, J., Mateus, A., Ribeiro, A. (2014). Tectonoestratigrafia do Terreno Ibérico no sector Tomar-Sardoal-Ferreira do Zêzere e relações com o Terreno Finisterra. Comunicações Geológicas, 101 (I), 559-562.

Scholz, C.H., Ando, R. Shaw, B.E. (2010). The mechanics of first order splay faulting: The strike-slip case. Journal of Structural Geology, 32, 118–126, DOI: 10.1016/j.jsg.2009.10.007

Shelley, D., Bossière, G. (2000). A new model for the Hercynian orogen of Gondwanan France and Iberia. Journal of Structural Geology, 22, 757–776. DOI: 10.1016/S0191-8141(00)00007-9.

Sibson, R.H. (1977). Fault rocks and fault mechanism. Journal of the Geological Society, London, 133 (3), 191-213. DOI: 10.1144/gsjgs.133.3.0191

Tikoff, B., Teyssier, C. (1994). Strain modeling of displacement-field partitioning in transpressional orogens. Journal Structural Geology, 16, 1575-1588. DOI: 10.1016/0191-8141(94)90034-5

Walsh, J. J., Watterson, J. (1991). Geometric and kinematic coherence and scale effects in normal fault systems. Geological Society, London, Special Publication, 56, 193-203. DOI: 10.1144/GSL.SP.1991.056.01.13

Weinberger, R. (2014). Pleistocene strain partitioning during transpression along the Dead Sea Transform, Metulla Saddle, northern Israel. In: Garfunkel, G., Ben-Avraham, Z., Kagan, E., (Eds.), Dead Sea Transform Fault System: Reviews, Chapter 6, Springer-Verlag, Heidelberg, 151-182. DOI:10.1007/978-94-017-8872-4_6.

Wernicke, B., Burchfiel, B.C. (1982). Modes of extensional tectonics. Journal of Structural Geology, 4(2), 105-115. DOI: 10.1016/0191-8141(82)90021-9

Xypolias, P. (2010). Vorticity analysis in shear zones: A review of methods and applications. Journal of Structural Geology, 32, 2072-2092. DOI: 10.1016/j.jsg.2010.08.009

IX

As estruturas arqueadas Ibéricas; o Arco Ibero-Armoricano

A existência de uma estrutura arqueada no Maciço Ibérico foi identificada desde muito cedo, ainda no século XIX por Schulz em 1858. Ainda no mesmo século, reconheceu-se que esta estrutura arqueada centrada na Cantábria (norte de Espanha) fazia parte de uma estrutura maior (Bertrand, 1887; Suess, 1888), ligando o Maciço Ibérico ao Maciço Armoricano (França), o que levou à definição do denominado Arco Ibero-Armoricano. Cerca de um século e meio depois, esta temática contínua actual e dezenas de trabalhos têm sido publicados nas últimas duas décadas sobre as estruturas arqueadas Variscas Europeias. Para além do Arco Ibero-Armoricano, outros dois arcos foram propostos na Ibéria, nomeadamente o Arco Cantábrico e o Arco Centro-Ibérico. O primeiro "sobrepõe-se" espacialmente ao Arco Ibero-Armoricano, sendo definido de forma clara nas regiões setentrionais do Maciço Ibérico, nomeadamente na Zona Cantábrica, onde apresenta um raio de curvatura maior que o Arco-Ibero-Armoricano. Embora a sua existência seja consensual, a sua relação com o Arco Ibero-Armoricano não é totalmente clara. Por sua vez, o Arco Centro-Ibérico, com eixo de curvatura no interior da Zona Centro Ibérica, não é uma estrutura que gere consenso na comunidade científica e essa discussão será integrada em ambos os subcapítulos aqui contidos. Este capítulo apresentará uma caracterização geral de todo o Maciço Ibérico, embora com enfase na Zona Centro Ibérica, integrando dados das diversas zonas paleogeográficas do Orógeno, razão pela qual precede os capítulos referentes aos dados obtidos durante os estudos conducentes à obtenção do grau de Doutor.

Embora a maioria dos dados aqui integrados neste capítulo não sejam originais, tendo sido previamente publicados por outros autores, este capítulo discute, reinterpreta e rebate cientificamente algumas das propostas recentes sobre as estruturas arqueadas Ibéricas, apresentando-se como um trabalho de revisão crítica aprofundada dos dados existentes.

Este capítulo integra assim dois subcapítulos, ambos publicados em revistas indexadas com *peer-review*, um dos quais na revista *Tectonophysics*, uma revista de elevado impacto científico na área das geociências, inserida no quartil Q1 no SJR e apresentando um factor de impacto de

2.65 de acordo com a *Thomson Reuters* (2015/2016). Abaixo seguem as referências dos trabalhos em causa:

- *Capítulo IX.1*

DIAS, R., RIBEIRO, A., COKE, C., MOREIRA, N., ROMÃO, J. (2014), Arco Ibero-Armoricano; indentação versus auto-subducção. Comunicações geológicas, 101 (Vol. Especial I), 261-264.

- *Capítulo IX.2*

DIAS, R., RIBEIRO, A., ROMÃO, J., COKE, C., MOREIRA, N. (2016), A review of the Arcuate Structures in the Iberian Variscides; Constraints and Genetic Models. In: Murphy, J.B., Nance, R.D., Johnston, S.T. (Eds.), Tectonic evolution of the Iberian margin of Gondwana and of correlative regions: A celebration of the career of Cecilio Quesada, Tectonophysics, 681C, 170-194. DOI: 10.1016/j.tecto.2016.04.011

Ambos os capítulos seguirão na íntegra os trabalhos publicados. O primeiro subcapítulo abordará/discutirá um pouco a existência ou não dos Arcos Ibéricos, bem como os modelos para a sua génese. O segundo é um artigo de revisão sobre as estruturas arqueadas da Ibéria, discutindo profundamente a sua génese e natureza e interligando-a com a evolução geodinâmica do Varisco Ibérico. Em ambos os trabalhos defende-se, por um lado, que não existem dados que permitam suportar a existência do Arco Centro-Ibérico e, por outro, argumentando e defendendo o modelo de indentação em detrimentos dos restantes modelos para a génese do Arco Ibero-Armoricano.

Importa contudo reportar que dados obtidos posteriormente à publicação dos trabalhos em causa vêm trazer novos conhecimentos que, embora não refutem os modelos propostos, trazem novas luzes sobre as estruturas arqueadas Ibéricas, nomeadamente a definição do Terreno Finisterra (vide capítulo XII.1), não incorporado nos modelos aqui propostos. Desta forma, embora na presente dissertação dois modelos "distintos" de reconstituições paleogeográficas sejam apresentados, estes apresentam inúmeros aspectos comuns, não contradizendo o modelo geral de indentação proposto. A grande diferença nos dois modelos prende-se à inclusão do novo Terreno Tectono-estratigráfico, no modelo previamente proposto. Esta actualização reflecte a evolução de pensamentos, conceitos e ideias, algo que é um processo comum em ciência.

De referir ainda que o Capítulo IX.1, sendo a publicação um artigo curto publicado num volume especial no âmbito do congresso, como previamente referido, esta publicação acarreta

limitações de espaço que impossibilitaram a citação de todos os trabalhos pertinentes para o efeito. Desta forma, e seguindo na íntegra o trabalho publicado, alguns trabalhos com indubitável pertinência não foram citados.

Referências

Bertrand, M. (1887). La Chaîne des Alpes et la formation du continent européen. Bull. Soc. Geol. Fr., 15 (3), 423–447.

Schulz, G. (1858). Atlas geológico y topográfico de Asturias. Lit. de G. Pfeiffer (2 Maps +1 Plate).

Suess, E. (1888). Das Antlitz der Erde, Vol. II. Vol. IV. F. Tempsky, Prag and Wien, and G.Freytag, Leipzig (704 p).

IX.1

Arco Ibero-Armoricano: indentação versus auto-subducção

Índice

IX.1.1. Introdução

A existência de um arco à escala orogénica, definido por estruturas variscas orientadas predominantemente NW-SE na Ibéria e aproximadamente E-W na Bretanha, é bem conhecida pelo menos desde os trabalhos de Carey (1955) que o descreveu sob o nome de Arco Ibero-Bretão; posteriormente passou a ser denominado como Arco Ibero-Armoricano (AIA; Fig. 1). No Norte de Espanha, esta estrutura arqueada é possível de identificar na sua totalidade, registando-se uma rotação praticamente contínua das estruturas variscas de cerca de 180º (definindo o por vezes denominado Arco Cantábrico - AC). Se a existência do AIA é aceite pela generalidade dos geocientistas que trabalham nesta região, os modelos que têm vindo a ser propostos para a sua génese não o são, o que seria expectável tendo em consideração a sua complexidade.

Mais recentemente, começou a ser defendida uma outra estrutura arqueada (*e.g.* Weil *et al.*, 2013; Martínez Catalán *et al.*, 2014; Shaw *et al.*, 2014 e referências incluídas), em continuidade com a anteriormente referida, designada de Arco Centro-Ibérico (ACI).

Neste trabalho elabora-se uma revisão crítica de alguns dos aspectos relacionados com a individualização e génese destas estruturas de primeira ordem à escala da Ibéria.

IX.1.2. Estruturas arqueadas à escala do Terreno Ibérico

Um dos problemas associados à compreensão da génese das estruturas variscas arqueadas de primeira ordem no Terreno Ibérico tem a ver com a sua individualização e relações genéticas.

Com efeito, não só a falta de continuidade dos afloramentos, mas também o facto da deformação observada resultar geralmente de um processo polifásico e/ou policíclico, torna difícil a caracterização das grandes estruturas.

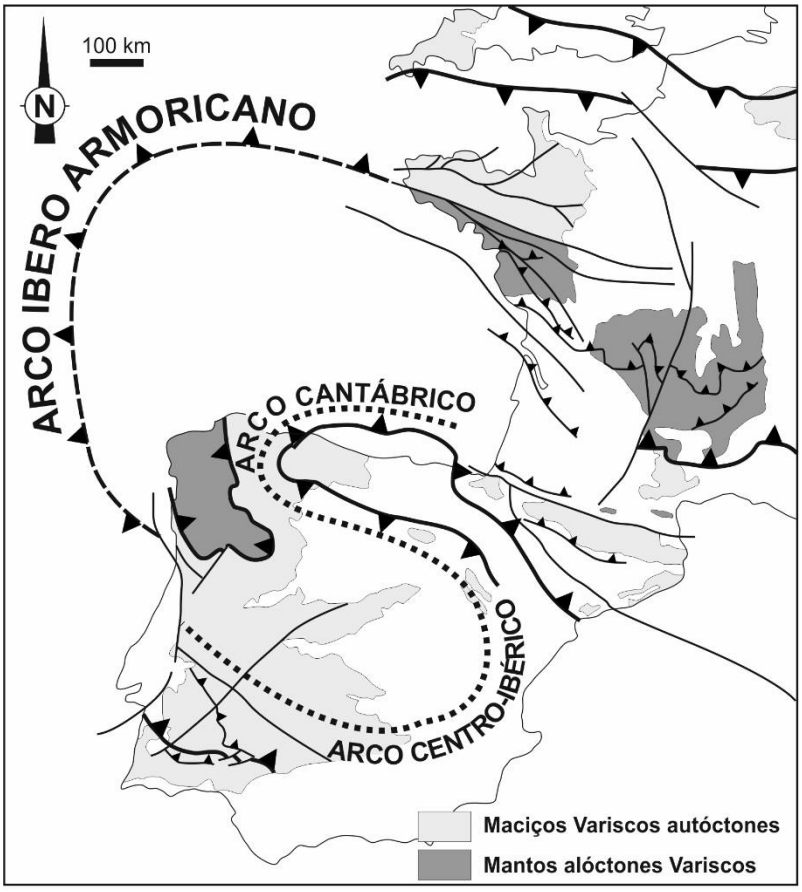

Figura 1 – Principais estruturas arqueadas variscas propostas para a Ibéria.

IX.1.2.1. Arco Ibero-Armoricano

Corresponde à estrutura arqueada principal e, pela sua dimensão e complexidade, aquela sobre a qual persistem diversas dúvidas. Apesar da continuidade entre os ramos Ibérico e Armoricano não ser possível de seguir, devido aos processos associados à abertura do Atlântico/ golfo da Biscaia, a sua existência não é actualmente posta em causa.

Porém, a sua estruturação no ramo ibérico é questionável, principalmente no que se refere à presença de apenas um arco, gerado essencialmente num único evento tectónico, ou se na realidade o processo é mais complexo; segundo esta última opção existirá uma estrutura mais recente (AC) que se sobrepõe de uma forma simétrica, a uma megaestrutura varisca arqueada, mais antiga, definida pelas estruturas na Bretanha e nas Zonas Centro-Ibérica e Ossa-Morena (*e.g.* Dias & Ribeiro, 1995; Braid *et al.*, 2011). Qualquer que seja o modelo proposto para a formação do AIA, ele tem que explicar a existência de um regime transpressivo esquerdo no

ramo Ibérico e direito no ramo Armoricano (*e.g.* Dias & Ribeiro 1994, 1995), bem como uma idade de deformação que se escalona entre o Devónico (*e.g.* Braid *et al.*, 2011), nas zonas mais externas do arco, e o Carbónico superior, nos sectores mais internos da Cantábria (*e.g.* Weil *et al.*, 2013).

IX.1.2.2. Arco Cantábrico

Esta é sem dúvida a estrutura arqueada que, do ponto de vista geométrico, levanta menos dúvidas, visto ser a única cuja continuidade lateral é possível de evidenciar com base nos afloramentos. Mais recentemente têm surgido uma série de argumentos (*e.g.* paleomagnetismo, evolução temporal do padrão de diaclases, paleocorrentes da base do Ordovícico e maclas da calcite) que indicam o carácter essencialmente secundário desta estrutura (ver Weil *et al.*, 2013 para uma síntese). Esta situação torna desnecessário, num trabalho com esta índole, uma descrição mais pormenorizada do AC.

IX.1.2.3. Arco Centro-Ibérico

Embora o ACI tenha sido inicialmente proposto por Staub em 1926, todos os trabalhos realizados nas décadas seguintes, tanto a nível da ZCI como do Varisco Ibérico (*e.g.* Lotze, 1945; Carey, 1955; Dias *et al.*, 2013a; Vera, 2004 e referências incluídas) ignoram a sua existência. Contudo, desde 2010 têm surgido uma série de trabalhos (*e.g.* Martínez Catalán *et al.*, 2014; Shaw *et al.*, 2014 e referências incluídas) que retomam a proposta de Staub.

Os argumentos utilizados para apoiar a existência do ACI são:

- O padrão de anomalias magnéticas;
- A geometria dos dobramentos variscos (orientação e vergência);
- Os sentidos de paleocorrentes na Formação do Quartzito Armoricano que são consideradas centrífugas em relação aos oróclinos.

No entanto, a análise cuidada dos dados apresentados em trabalhos que defendem a existência do ACI, bem como dos dados existentes noutros trabalhos de índole estrutural e litoestratigráfica sobre a região, que são completamente ignorados pelos autores que defendem o ACI, não permitem defender a existência desta estrutura arqueada dentro da ZCI. Com efeito:

- No que diz respeito aos dados de índole geofísica (Martínez Catalán *et al.*, 2014 e referências incluídas) a sua interpretação não é simples, pois as anomalias observadas, principalmente as que ocorrem sob a cobertura meso-cenozóica, podem ser resultado de uma evolução policíclica e não de uma interpretação monocíclica, que tem sido privilegiada na interpretação que favorece a existência do oróclino.

- Quanto à geometria dos dobramentos a estrutura arqueada só se torna defensável porque os autores ignoram a generalidade dos trabalhos existentes na ZCI, essencialmente no sector português e, sem apresentarem qualquer justificação, consideram que as macrodobras bem definidas pelos quartzitos ordovícicos não são D_1, como têm normalmente sido interpretadas (*e.g.* Romão *et al.*, 2013 e referências incluídas) mas sim D_3. A situação é ainda mais estranha, quando a única dobra que consideram como D_1 nos domínios meridionais da ZCI (em Portugal), o sinclinal da Amêndoa-Carvoeiro, é na realidade uma dobra D_3 que redobra estruturas anteriores (Romão *et al.*, 2013 e referências inclusas). Em relação à vergência das dobras D_1, mais uma vez são postos de lado muitos dos dados existentes, tendo sido apresentado um modelo que considera apenas três situações em todo o sector a S da zona da Galiza – Trás-os-Montes, o que torna possível a defesa de um padrão centrífugo simples em torno do AIA. Contudo as vergências apresentadas (N de Viana do Castelo, Valongo e Caramulo) constituem a excepção e não a regra, não se percebendo sequer porque é que estas três estruturas são consideradas pelos autores como sendo da D_1, quando consideraram todas as outras como sendo D_3. Na realidade o padrão da vergência das dobras D_1 no sector português da ZCI apresenta-se muito mais heterogéneo (*e.g.* Dias & Ribeiro, 2013 e referências incluídas) caracterizando-se por uma *flower structure* assimétrica de primeira ordem, nos domínios setentrionais, e por dobras sem vergência, nos domínios meridionais.

- Em relação às paleocorrentes que são consideradas como centrífugas em relação quer ao AC quer ao ACI (*e.g.* Shaw *et al.*, 2014), situação que foi utilizada para defender que os oróclinos afectaram uma bacia linear pré-existente com 2300 km de extensão, a reinterpretação dos mesmos dados mostra que elas tendem a ser centrífugas no AC, mostrando contudo um padrão muito mais irregular no suposto ACI (Fig. 2), o que está em completo desacordo com o previsto pelos modelos.

Finalmente, são ainda de destacar dois aspectos que nunca são focados nos artigos que defendem o ACI:

- No que diz respeito à cinemática das estruturas (aspecto que é muito pouco explorado nos referidos artigos), não existe qualquer simetria entre os dois ramos do ACI (*e.g.* Ribeiro *et al.*, 1990; Dias & Ribeiro, 2013). O estiramento vertical em S_1 que é referido como predominante (*e.g.* Martínez Catalán *et al.*, 2014) não existe nos sectores setentrionais da ZCI em Portugal onde predomina um regime transpressivo esquerdo com estiramento segundo o eixo cinemático *b* (*e.g.* Ribeiro *et al.*, 1990; Dias *et al.*, 2013b).

- Do ponto de vista litoestratigráfico, a distribuição cartográfica das unidades mais antigas que afloram no núcleo do suposto ACI (*i.e.* o Supergrupo Dúrico-Beirão), não mostram continuidade entre os sectores S e N, como seria de esperar com o padrão de dobramento isoclinal proposto no modelo do oróclino.

Sintetizando, consideramos que os dados existentes não permitem defender a existência do ACI.

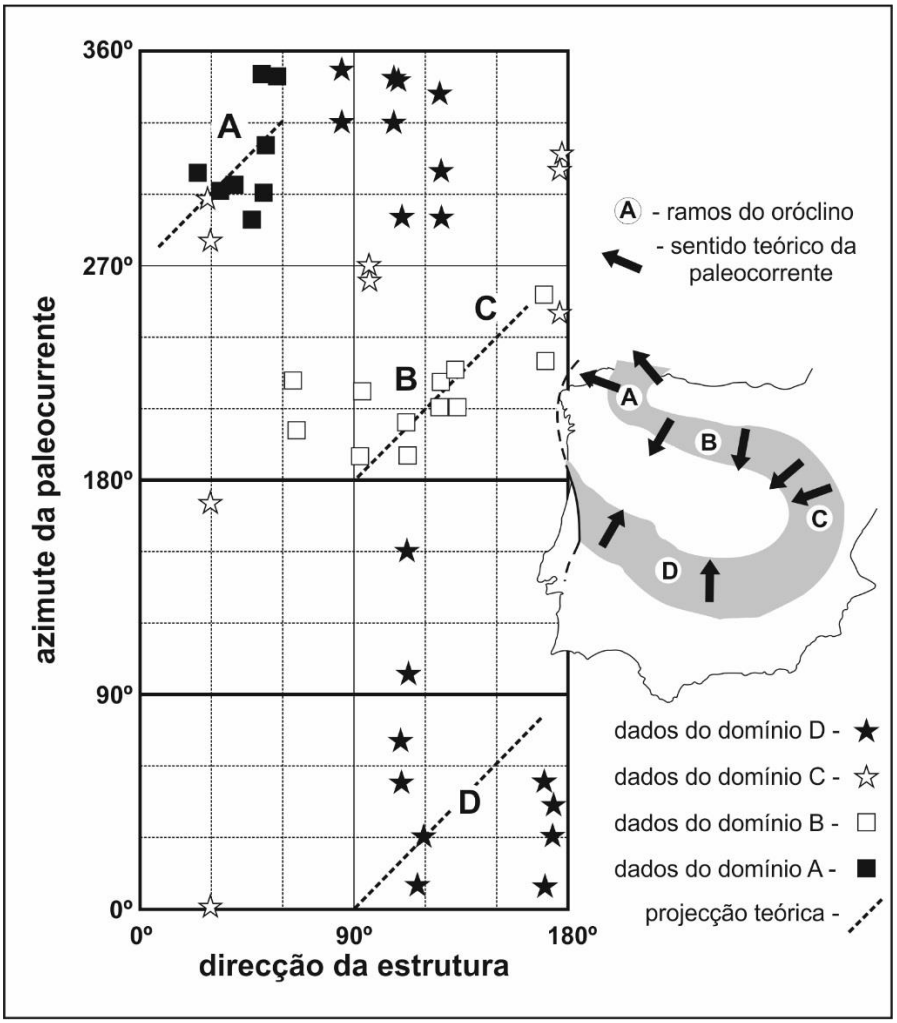

Figura 2 – Relação angular entre o sentido das paleocorrentes da base do Ordovícico e a orientação das estruturas (reinterpretação dos dados de Shaw *et al*., 2014).

IX.1.3. Os modelos

Como seria de esperar para estruturas com a complexidade dos grandes arqueamentos variscos evidenciáveis na Ibéria/Bretanha, existe uma grande diversidade de modelos propostos para a sua génese cuja discussão detalhada não é possível num trabalho desta índole. Em virtude de considerarmos que, com os dados existentes, não é possível defender a existência do ACI iremos centrar-nos na análise crítica dos modelos relacionados com a génese do AIA. Neste

sentido, iremos abordar os trabalhos que defendem a auto-subducção (*self subduction*) da litosfera oceânica da Pangeia (*e.g.* Johnston *et al.*, 2013; Weil *et al.*, 2013; Shaw *et al.*, 2014) *versus* os que privilegiam uma génese por indentação de um promontório da Gondwana (*e.g.* Dias & Ribeiro, 1995; Braid *et al.*, 2011).

IX.1.3.1. Auto-subducção

No final do Carbónico, o processo denominado pelos autores de auto-subducção da litosfera oceânica terá induzido *buckling* de toda a litosfera em torno de um eixo vertical que, nos níveis estruturais mais altos, se traduziu pela formação do AC, segundo um mecanismo de dobramento semelhante ao tangencial longitudinal; neste modelo, o arqueamento seria secundário e muito rápido (cerca de 10 milhões de anos) afectando uma cadeia inicialmente linear.

Se este modelo pode ser defensável em termos do AC, a extrapolação que os mesmos autores têm efectuado para os restantes sectores da Ibéria coloca enormes problemas. Com efeito, como foi referido anteriormente (*vide* secção IX.1.2.3), o predomínio dos regimes transpressivos (esquerdos na Ibéria e direitos na Armorica) nos ramos do AIA e a idade devónica para esta deformação na Ibéria, mostram que o modelo de formação do AC não pode ser considerado como válido para todo o AIA.

IX.1.3.2. Indentação

Quando se admite uma génese polifásica para a formação do AIA, torna-se possível conciliar as diversas situações observadas. No que diz respeito aos regimes transpressivos e à cinemática observada na Ibéria e na Armorica, com predomínio da componente transcorrente (predominantemente esquerda e direita respectivamente) em largos sectores do Terreno Ibérico, ela sugere a existência de um importante processo de indentação. Com efeito, as cinemáticas observadas, não só nunca são abordadas nos modelos anteriores, como também estão em completo desacordo com o processo de *buckling*. O diacronismo previsível num processo de indentação torna compatível um começo mais precoce para a formação do AIA com uma génese mais tardia do CA, como sugerido pelos dados (*vide* secção IX.1.2.2).

Referências

Braid, J., Murphy, J., Quesada, C., Mortensen, J. (2011). Tectonic escape of a crustal fragment during the closure of the Rheic Ocean: U–Pb detrital zircon data from the Late Palaeozoic Pulo do Lobo and South Portuguese zones, southern Iberia. Journal of the Geological Society (London), 168, 383–392.

Carey, S. (1955). The Orocline concept in Geotectonics. Proceedings of the Royal Society of Tasmania, 89, 255-288.

Dias, R., Ribeiro, A. (1994). Constriction in a transpressive regime: an example in the Ibero-Armoricain Arc. Journal of Structural Geology, 16(11), 1543-1554.

Dias, R., Ribeiro, A. (1995). The Ibero-Armorican arc: a collisional effect against an irregular continent? Tectonophysics, 246(1-3), 113-128.

Dias, R., Ribeiro, A. (2013). O Varisco do sector norte de Portugal. In: Dias, R., Araújo, A., Terrinha, P., Kullberg, J., (Eds.). Geologia de Portugal, vol. 1, Escolar Editora, 59-71.

Dias, R., Araújo, A., Terrinha, P., Kullberg, J., (Eds.) (2013a). Geologia de Portugal. 2 volumes, Escolar Editora, 1605 p.

Dias, R., Ribeiro, A., Coke, C., Pereira, E., Rodrigues, J., Castro, P., Moreira, N., Rebelo, J. (2013b). Evolução estrutural dos sectores setentrionais do autóctone da Zona Centro-Ibérica. In: R. Dias, A. Araújo, P. Terrinha, J.C. Kullberg, (Eds.), Geologia de Portugal, vol. 1, Escolar Editora, 73-147.

Johnston, S., Weil, A., Gutiérrez-Alonso, G. (2013). Oroclines: thick and thin. Geological Society of America Bulletin, 125(5-6), 643-663.

Lotze, F. (1945). Zur Gliederung der Varisziden der Iberischen Meseta. Geotektonische Forschungen, 6, 78-92.

Martínez Catalán, J., Rubio Pascual, J., Díez Montes, A., Díez Fernández, R., Gómez Barreiro, J., Dias da Silva, I., González Clavijo, E., Ayarza, P., Alcock, J. (2014). The late Variscan HT-LP metamorphic event in NW and Central Iberia: relationships to crustal thickening, extension, orocline development and crustal evolution. In: Schulmann, K., Martínez Catalán, J.R., Lardeaux, J.M., Janousek, V., Oggiano, G. (Eds.). The Variscan Orogeny: Extent, Timescale and the Formation of the European Crust. Geological Society, London, Special Publications, 405, 225-247.

Ribeiro, A., Pereira, E., Dias, R. (1990). Structure of the Northwest of the Iberian Peninsula. In: Dallmeyer, R.D., Martinez Garcia, E. (Eds.). Pre-Mesozoic Geology of Iberia, Springer-Verlag, 220-236.

Romão, J., Metodiev, D., Dias, R., Ribeiro, A. (2013). Evolução geodinâmica dos sectores meridionais da Zona Centro-Ibérica. In: Dias, R., Araújo, A., Terrinha, P., Kullberg, J., (Eds.), Geologia de Portugal, vol. 1, Escolar Editora, 206-257.

Shaw, J., Gutiérrez-Alonso, G., Johnston, S.T., Pastor Galán, D. (2014). Provenance variability along the Early Ordovician north Gondwana margin: Paleogeographic and tectonic implications of U-Pb detrital zircon ages from the Armorican Quartzite of the Iberian Variscan belt. Geological Society of America Bulletin, 126(5-6), 702-719.

Staub, R. (1926). Gedanken zur Tektonik Spaniens. Vierteljahrsschrift der Naturforschenden Gesellschaft, 71, 196-260.

Vera, J. (Ed.) (2004). Geologia de España. SGE-IGME, Madrid, 890 p.

Weil, A., Gutiérrez-Alonso, G., Johnston, S., Pastor-Galán, D. (2013). Kinematic constraints on buckling in a lithospheric-scale orocline along the northern margin of Gondwana: a geologic synthesis. Tectonophysics, 582, 25-49.

IX.2

Reviewing the Arcuate Structures in the Iberian Variscides; Constraints and Genetical Models

Index

IX.2.1. Introduction

First order arcuate structures are a common feature in orogenic belts (Argand, 1924; Carey, 1955). Their understanding is an important issue in Plate Tectonics, because similar shapes could result from different processes. Primary arcs are induced by the formation of the fold belt, as happens when moulding the orogen around a promontory. When the curved shape is not a pre-orogenic feature but the result of an impressed strain on a previous linear

belt, it is known as an orocline (Carey, 1955). Curved arcuations could also be considered as thick skinned or thin skinned: in the formers ones the strain pattern was developed both in the cover and the basement of the orogen, while the strain pattern in thin skinned arcs is restricted to the cover.

The understanding of orogenic arcs is usually easier in active orogens because the continuity of major structures between both branches is often visible. In such young tectonic environments, major arcuations are common in convergent settings, either related to ocean-ocean (*e.g.* Scotia Arc, Dalziel, 1971; De Wit, 1977), ocean-continent (*e.g.* the Central Andean orocline, Eichelberger and McQuarrie, 2014 or the Banda Arc, Vroon *et al.*, 1995; Harris, 2011) or continent-continent (*e.g.* western and eastern syntaxis of Himalayas; Tapponier and Molnar, 1976; Matte, 1986) collisions.

In old orogens major arcs are more difficult to emphasize because the original continuity is often:

- disrupted by the superposition of younger structures or magmatic batholiths;
- hidden below younger sediments;
- dismembered by the opening of new oceans.

Nevertheless, since the early works several major arcs have been described in the Variscan Belt, not only at the orogen scale but also in Iberia (*e.g.* Du Toit, 1937; Carey, 1955). However, at this moment there is still a lack of understanding concerning the formation of the first order Variscan arcs in Iberia, which is the main purpose of this work. A four step approach will be used:

- A historical review of the major arcuate structures;
- A critical review of the existing data (*e.g.* structural, deformation age, lithostratigraphic, and paleomagnetic);
- A discussion of the previous models;
- A unifying approach trying to conciliate the previous data.

The discussion of the Iberian Variscan arcs is crucial, mostly because since 2010 several papers strongly emphasize the so-called Central-Iberian Arc (*e.g.* Martínez Catalán, 2011a; 2011b; Johnston *et al.*, 2013). In spite of the weakness of the data supporting this Arc, several models were proposed for its formation, considering an Upper Carboniferous-Permian age for all the Iberian Arcs (*e.g.* Martínez Catalán, 2011c; Johnston *et al.*, 2013; Weil *et al.*, 2013; Martínez Catalán *et al.*, 2014), which is difficult to conciliate with most of the data.

This paper is also a contribution to the subject concerning the primary or secondary origin of curved orogenic belts, emphasizing the complexity of these structures and the care which should be taken when using simple models.

IX.2.2. Arcuate Variscan Patterns in Iberia; a Historical Approach

Any discussion concerning the geodynamical evolution related to the major Variscan arcs in Iberia should address the major zoning of this sector of the fold belt.

IX.2.2.1. Zones in Iberian Variscides

Since Lotze (1945) the Iberian Variscides has been divided in several zones based on stratigraphic, structural, metamorphic and magmatic features. Later works have led to some minor modifications in their number and boundaries (Fig. 1; Julivert *et al.*, 1972; Julivert and Martínez, 1983; Farias *et al.*, 1987; Arenas *et al.*, 1988; Martínez Catalán, 1990). This zoning reflects the complex evolution due to the superposition mainly of the Neoproterozoic Cadomian collision, the Lower Palaeozoic extensional tectonic activity and the Upper Palaeozoic Variscan Orogen.

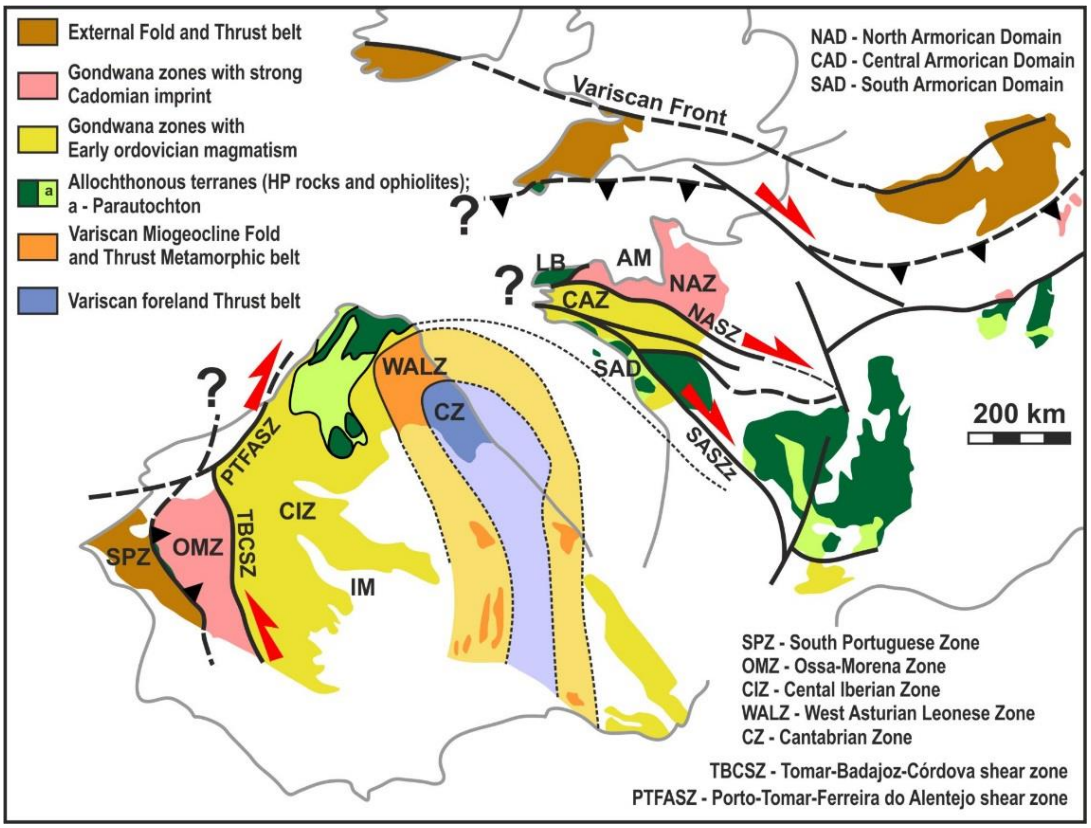

Figure 1 – Main Variscan tectonostratigraphic units in Iberia in the framework of the European Variscides (adapted from Lotze, 1945; Julivert *et al.*, 1972; Julivert and Martínez, 1983; Farias *et al.*, 1987; Arenas *et al.*, 1988; Martínez Catalán, 1990; 2011; Ribeiro *et al.*, 2007; Ballèvre *et al.*, 2014).

The Cantabrian Zone (CZ), considered the thin skinned foreland fold and thrust belt in the NW part of the Iberian Variscides (Pérez-Estaún, 1990), is characterized by a decollement level

within the Palaeozoic cover above a non-exposed Precambrian basement overlaid by its fixed cover. The Lower Palaeozoic is composed of a passive margin sequence of shallow-marine to shoreface facies (Julivert and Marcos, 1973), which becomes progressively thinner towards the East (Pérez-Estaún *et al.*, 1991). This Cambro-Devonian sequence (Pérez-Estaún, 1990) was deformed in the Pennsylvanian, giving rise to a thin-skinned fold-and-thrust belt verging towards Gondwana craton (Pérez-Estaún *et al.*, 1988). The progressive emplacement of this imbricate complex structure, which is rooted below the West Asturian Leonese Zone (Pérez-Estaún *et al.*, 1991), controls the deposition of syn-kinematic marine to terrestrial foreland basin successions (Marcos and Pulgar, 1982; Pérez-Estaún *et al.*, 1988; 1991). The metamorphism related to this Variscan shortening is almost absent, although it could locally attain a low grade (Pérez-Estaún, 1990).

The boundary between the CZ and the West Asturian Leonese Zone, is considered the Neoproterozoic rocks outcropping in the complex Narcea Antiform (Julivert *et al.*, 1972).

The West Asturian Leonese Zone (WALZ) is often considered the transition between the foreland CZ and the more internal zones of the Variscan hinterland core (Pérez-Estaún *et al.*, 1991). It consists of a thick Upper Proterozoic flyschoid series unconformably overlain by a thick cover (Marcos *et al.*, 2004) of shallow-water Lower Cambrian to Lower Devonian deposits, where thick siliciclastic units are dominant (Pérez-Estaún *et al.*, 1990; 1991; Fernández-Suárez *et al.*, 2000). Such unconformity, has also been found in the Cantabrian Zone (Lotze, 1956; De Sitter, 1961), being a major characteristic of these two domains. The previous WALZ sequence presents a pervasive Variscan deformation due to the interference of at least three major tectonic events, that have originated a general structure (sometimes with large recumbent folds, like the Mondoñedo anticline and the Courel syncline) facing the external part of the orogenic belt (Bastida *et al.*, 1986; Martínez Catalán *el al.*, 1990; Pérez-Estaún *et al.*, 1991; Fernández *et al.*, 2007; Bastida *et al.*, 2010). The Variscan metamorphic grade increases towards the West, from greenschist to amphibolite facies (Suárez *et al.*, 1990). The granitoid plutonism exhibits a similar trend, becoming abundant in the western sectors of WALZ (Corretgé *et al.*, 1990; Pérez-Estaún *et al.*, 1991).

The western limit of the WALZ is still controversial. While some authors (*e.g.* Ábalos *et al.*, 2002) follow the initial proposal of Ollo de Sapo anticlinorium (Julivert *et al.*, 1972), others (*e.g.* Marcos, 2004) consider the more complex boundary proposed by Martínez Catalán (1985) formed by the main Vivero normal fault and its southern continuation in the Peñalba and Courel synclines (Martínez Catalán *et al.*, 1992; Fernández *et al.*, 2007).

The rather heterogeneous Central Iberian Zone (CIZ) is the axial domain of the Iberian Variscan Fold Belt with abundant granitic plutonism and metamorphism ranging from very

low-grade to high-grade. Three main stratigraphic features have been fundamental for its individualization (Julivert *et al.*, 1972), because its Palaeozoic succession from Arenig to Middle Devonian is similar to the one found in adjacent zones (Ribeiro, 1990):

- The predominance of Pre-Ordovician sequences;
- The transgressive character of the Lower Ordovician quartzites;
- The presence of a pervasive unconformity which places the Lower Ordovician over Precambrian to Cambrian rocks (Douro-Beiras Super Group).

The presence of high-grade metamorphic allochthonous complexes and the abundant Silurian volcanism, led some authors to individualize in the NW of CIZ a Galicia - Trás-os-Montes domain, which has been considered either as a sub-Zone (Julivert *et al.*, 1972) or a Zone (Tex and Floor, 1971; Farias *et al.*, 1987). Whatever the option, its allochthonous behaviour over the CIZ autochthon is recognized (*e.g.* recent compilations of the Iberian Geology of Gibbons and Moreno, 2002; Vera, 2004; Dias *et al.*, 2013a). This Galicia - Trás-os-Montes Zone comprises two domains, bounded by a major thrust, with distinct paleogeographic and tectonometamorphic histories (*e.g.* Martínez Catalán *et al.*, 2004; Dias and Ribeiro, 2013):

- The parautochthonous "schistose" domain with clear lithostratigraphic affinities with the CIZ autochthon, mainly with its upper part;
- The domain of the allochthonous complexes with high-grade massifs.

Concerning the southern boundary of CIZ, Lotze (1945) proposed the elongated Los Pedroches granitic batholith. The Tectonic Map of the Iberia (Julivert *et al.*, 1972) still uses this batholith for the Spanish limit, while in Portugal it is marked by the Ferreira do Zêzere and Portalegre thrusts. However, some authors (*e.g.* Díez Balda *et al.*, 1990; Azor *et al.*, 1994; Martínez Catalán *et al.*, 2004) considered that the main stratigraphic and structural changes are marked by the main Tomar - Badajoz - Cordoba intra-continental shear zone (TBCSZ).

The Ossa-Morena Zone (OMZ), considered the southernmost zone of the hinterland orogenic domain of Iberian Massif, presents a magmatic, metamorphic and sedimentary complex evolution. One of its most distinctive features is the presence of two orogenic cycles (Cadomian and Variscan; Quesada, 1990; Ribeiro *et al.*, 2007; 2009; 2010), giving rise to three general stratigraphic successions (*e.g.* Quesada, 1990; Nance *et al.*, 2012; Araújo *et al.*, 2013; Moreira *et al.*, 2014):

- A Neoproterozoic sequence related to the Cadomian Cycle;
- A Lower Paleozoic anorogenic sequence related to the Rheic Ocean rifting and drifting;
- Syn-orogenic series of Lower-Middle Devonian to Carboniferous age linked to the Variscan convergence.

The magmatism also emphasizes three main different pulses: Neoproteroic, Cambrian-Ordovician and Devonian-Carboniferous (*e.g.* Quesada, 1990; Moreira *et al.*, 2014). The geochemical signature and the temporal span of these rocks match the episodes recorded in the stratigraphic successions. The structure and metamorphism are complex, due to the superimposed of main Neoproterozoic and Paleozoic tectonometamorphic episodes with a heterogeneous distribution.

The classic southern limit of OMZ is emphasized by oceanic like rocks, which compose the Beja-Acebuches Amphibolites and, in their absence by the Ferreira-Ficalho-Almonaster thrust. These mafic rocks are interpreted either as an ophiolite complex (Quesada *et al.*, 1994; Fonseca *et al.*, 1999; Ribeiro *et al.*, 2010), or a narrow and very ephemeral realm of oceanic-like crust generated by mantle upwelling (*e.g.* Azor *et al.*, 2008).

The South Portuguese Zone (SPZ) is considered the SW foreland fold-and-thrust belt of Iberian Variscides, characterized by a thin-skinned SW facing structure, also emphasized by geophysical data (Ribeiro and Silva, 1983; Silva *et al.*, 1990; Simancas *et al.*, 2003; Ribeiro *et al.*, 2007). This zone comprises a stratigraphic sequence mainly composed of detrital rocks, occasionally with abundant magmatic rocks, with Devonian to Upper Carboniferous ages (Oliveira *et al.*, 2013). The deformation as a progressive behavior, which is older and more intense near the NE suture, and younger and less deformed towards SW (Ribeiro and Silva, 1983; Silva *et al.*, 1990; Dias and Basile, 2013). The metamorphism also presents a NE-SW progression, from greenschist facies at north and very low to absente in SW sectors (Oliveira *et al*., 2013).

IX.2.2.2. The Variscan Arcs in Iberia

Since the early regional studies it has become evident that the trend of the major geological structures have a strongly wavy pattern in Iberia. The remarkable pioneering geological map of Asturias by Schulz (1858), clearly shows a tight fold at northern Iberia scale (Fig. 2A). Such arc was detailed by the work of Barrois (1882) and used by Suess (1888), who was the first to recognize it as a mountain range bend. Soon it has become evident that this arcuate structure is not restricted to Iberia being part of a larger structure, the so-called Ibero-Armorican Arc (IAA) that continues in Brittany (Bertrand, 1887; Suess, 1888; Stille, 1924; Fig. 2B). Indeed, the NW-SE trend that predominates in most Iberia and rotates to a N-S orientation in NW Iberia, was assumed to continue in the E-W structures in Brittany (Choubert, 1935; Carey, 1955; 1958; Lotze, 1963; Cogné, 1967; 1971; Bard *et al.*, 1971; Lefort, 1979; Perroud and Bonhommet, 1981; Burg *et al.*, 1987). Although the continuity between the southern Iberian branch and the northern Armorican one is not possible to follow due to the

opening of the oceanic rift of Biscay essentially during Upper Cretaceous (Ries, 1978), the arcuate structural pattern not only in the CZ, but also in the WALZ / CZ seems to confirm this interpretation (Staub, 1927, Fig. 2C; Carey, 1955, Fig. 2D). Indeed, here the continuity of the Variscan structures, completely underline an orocline known as the Asturian Knee (Staub, 1927; Julivert and Marcos, 1973; Julivert *et al.*, 1977), the Asturian Arc (Pérez-Estaún and Bastida, 1990; Aramburu and Garcia-Ramos, 1993; Ábalos *et al.*, 2002), the Cantabrian Arc (Parés and Van der Pluijm, 2004; Weil and Sussman, 2004), the Cantabrian - Asturian Arc (Parés *et al.*, 1994; Weil *et al.*, 2013) or, more recently, the Cantabrian orocline (Gutiérrez-Alonso *et al.*, 2008: 2011; Johnston *et al.*, 2013; Sengör, 2013; Weil *et al.*, 2013).

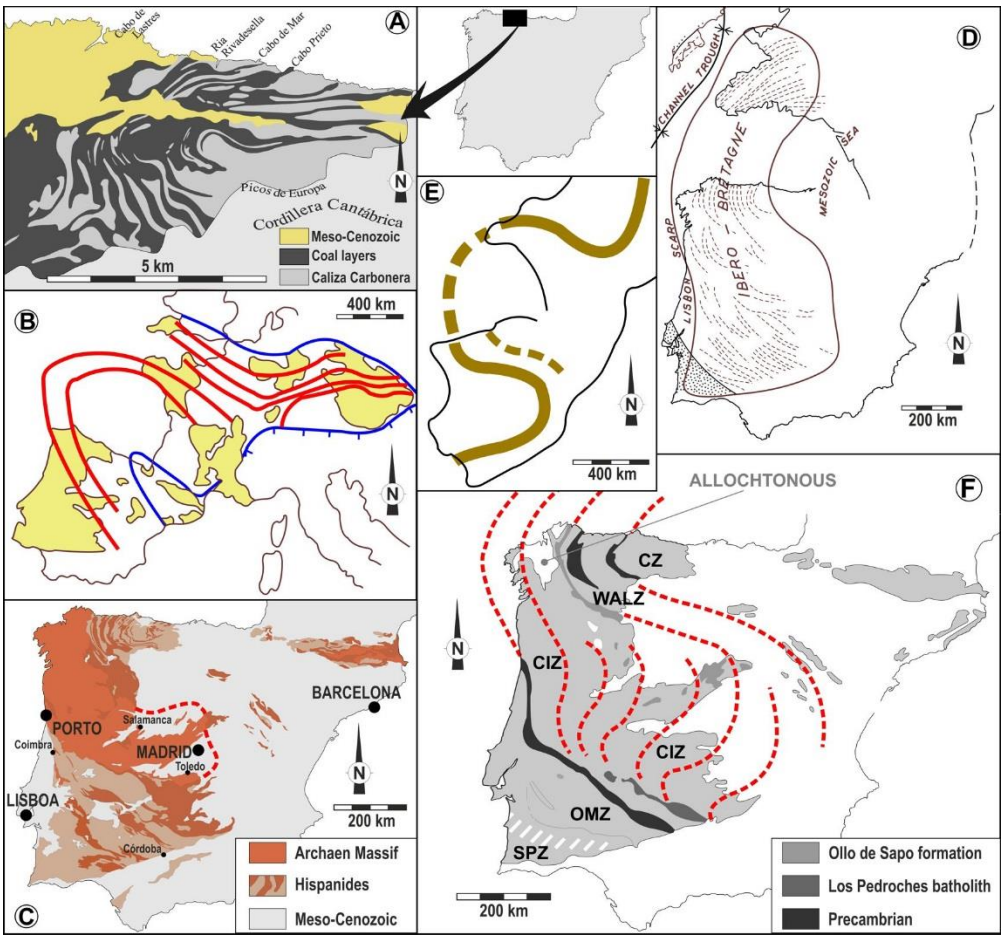

Figure 2 – Historical evolution of major Variscan Arcs proposed to Iberia:

A – Simplified version of the geological map of Eastern Asturias (redrawn from Schulz, 1858);

B – The structural continuity between Iberia and Brittany (Stile, 1924)

C – Asturian and Castilian major Iberian Arcs (Staub, 1927);

D – Matching geological structures across the Biscay Sea (redrawn from Carey, 1955);

E – Major structural arcuations in the Ibero - Brittany region (adapted from Du Toit, 1937);

F – Speculative sigmoidal pattern of the main Variscan structures in Iberia (adapted from Aerden, 2004).

As the Cantabrian Arc (CA) is located in the core of the IAA (Parés and Van der Pluijm, 2004) they are often considered the same structure, with a curvature increasing from external domains to its centre (Sengör, 2013). Such geometry led some authors to propose a common origin (Johnston *et al.*, 2013; Gutierrez-Alonso *et al.*, 2010; Sengör, 2013; Weil *et al.*, 2013; Martínez Catalán *et al.*, 2014).

Early works also emphasize another orocline in the Iberian Variscides, the Central-Iberian Arc (CIA). According to Staub (1927), the Caledonian and Hercynian folds have developed in lower metamorphic formations wraps around an Archaen core composed of schists and old granites, enhancing a Castilian Arc (Fig. 2C). This arc was also considered in the classical work of Du Toit concerning the world Palaeozoic fold systems (1937; Fig. 2E). Subsequent studies concerning the paleogeographic zoning of the Iberian Palaeozoic (*e.g.* Lotze, 1945; Julivert *et al.*, 1972) show that the original assumptions of Staub are no longer valid and the idea of a Castilian Arc was abandoned. More recently this major arcuate structure was again considered (Aerden, 2004). Indeed, extrapolating to SE the interpretation of a porphyroblasts study in NW Iberia he considered, in a "*still very speculative*" model (*op cit.* p. 194), that the observed structural relationships are apparently consistent with a late-Variscan sinistral transpression, delineating a sigmoidal shape (Fig. 2F) that partly follow the Staub proposal.

Since 2010 several papers consider the existence of the CIA or Central Iberian Orocline in the Iberian Variscides, but with two slightly different shapes:

- A short version where most of the southern branch is cut by the Tomar-Badajoz-Cordoba Shear Zone (Martínez Catalán 2011a; 2011b; 2011c; Simancas *et al.*, 2013; Martínez Catalán *et al.*, 2014; Fig. 3A)
- A long version, with the orocline assuming a major isoclinal shape and where the southern domain of the CIZ is considered a lateral equivalent of the WALZ (Johnston *et al.*, 2013; Weil *et al.*, 2013; Shaw *et al.*, 2012*a*; 2012*b*; 2014; Fig. 3B). The palinspatic restoration of both the Cantabrian-Central Iberian orocline pair, yields an initial linear ribbon of over 1500 km long (Shaw *et al.*, 2012*a*; 2012*b*) or even more than 2300 km (Shaw *et al.*, 2014; 2012b).

Although the coupled geometry of previous oroclines are sometimes considered the result of a coeval formation (Johnston *et al.*, 2013), some authors (*e.g.* Martínez Catalán *et al.*, 2014 and Simancas *et al.*, 2013) proposed that they could be slightly diachronic with the CIA older than the CA/IAA.

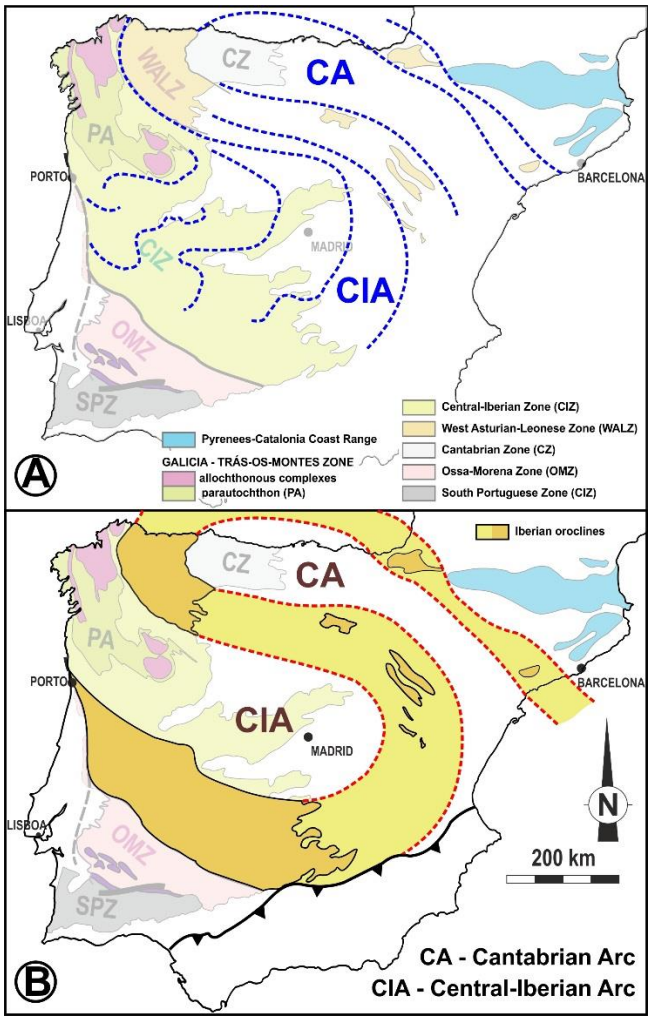

Figure 3 – The pattern of the Central-Iberian oroclines according to the:

A – short version (adapted from Martínez Catalán *et al.*, 2014);

B – long version (adapted from Johnston *et al.*, 2013).

IX.2.3. Reviewing the Data

In the last 40 years a huge amount of data concerning the Variscan geology of Iberia have been produced. A critical review of these data is fundamental to the main subject of this work.

IX.2.3.1. Variscan Folds and coeval Shear Zones

The strong shortening related to the Variscan orogeny gives rise to pervasive folding at all scales, well expressed in the lithostratigraphic units with higher competence (*e.g.* the Lower Ordovician quartzites).

Interference among folds in Iberia is often referred (*e.g.* Pérez-Estaún and Bea, 2004) and could be locally important. Nevertheless the general pattern at the Iberian scale is usually considered the result of the first and main Variscan tectonic event (D_1). However, this does not mean that all the folds are coeval because, not only there is a strong diachronism transversally to the orogen (Noronha *et al.*, 1981; Dallmeyer *et al.*, 1997), but also their development could

be slightly heterogeneous being older close to some major anisotropies either on the basement or on the cover.

Although the main trend of the regional D_1 folds have a simple arcuate pattern, geometrical and kinematical details emphasize a more complex behaviour, allowing the individualization of several sectors. We focus our analysis mostly on the CIZ, because this is a key sector to discuss the problem of the Iberian oroclines. It is not easy to make the Portuguese and Spanish data compatible mainly in the central and southern sectors of ZIC. This could partly reflect a change in the behaviour of the folds parallel to the trend of the orogen, related to the distance to the hinge zone of the IAA. Whatever the causes, six main distinct behaviours for the D_1 deformation in the CIZ could be emphasized (Fig. 4):

- Domain A (Ribeiro *et al.*, 1990; Dias, 1998; Moreira *et al.*, 2010a; Dias *et al.*, 2013b). It is a central segment where the D_1 Variscan deformation is very weak. The bedding is usually subhorizontal or presents open folds with subhorizontal hinges and subvertical axial planes. When present, the coeval cleavage is subvertical and spaced. The transition to the adjacent domains is sharp, usually marked by high dip sinistral shear zones sometimes with a thrusting component.

- Domain B (Ribeiro, 1974; Ribeiro *et al.*, 1990; Dias and Ribeiro, 1991; 1994; Pereira and Ribeiro, 1992; Pereira *et al.*, 1993; Dias, 1998; Moreira *et al.*, 2010a; Dias *et al.*, 2003; 2013b; Pamplona *et al.*, 2013). NE and N of this central segment the Variscan deformation strongly increases, becoming pervasive. The facing of the folds is towards NE and N and there is a continuous transition to the next domain. The pervasive S_1 cleavage is axial planar and has often developed a stretching lineation subparallel to the subhorizontal fold axes (*b* kinematical axes of Ramsay, 1967). Coeval of the D_1 folding, sinistral shear zones subparallel to the axial planes of the folds and a regional development have been developed. The finite strain ellipsoids estimated for the Armorican Quartzites are prolate.

- Domain C (Ribeiro, 1974; Díez Balda, 1986; Díez Balda *et al.*, 1990; Dias *et al.*, 2013b). Towards the NE foreland, despite preserving subhorizontal axes, the D_1 folds become recumbent with a NE to E facing. This geometry is similar to the WALZ Variscan general structure.

- Domain D (Ribeiro *et al.*, 1990; Dias and Ribeiro, 1994; 1995a; 1998; Dias, 1998; Dias *et al.*, 2013b). W and SW of the weakly deformed domain A, is found a narrow domain where the folds, still with a subhorizontal axes, have a monoclinic symmetry with a W to SW vergence. The deformation is intense and the axial plane S_1 cleavage is pervasive, mainly in the short and usually overturned limbs. As in domain B, there are frequent

sinistral shear zones with a trend parallel to the orientation of the D_1 folds, and the prolate finite strain ellipsoids are also dominant.

- Domain E (Ribeiro *et al.*, 1990; Dias, 1998; Metodiev *et al.*, 2009; Romão *et al.*, 2013). In most of the Portuguese southern sector of ZCI, the pervasive D_1 folds have subvertical axial planes and no clear vergence. The cleavage is usually present and a stretching lineation subperpendicular to the subhorizontal fold axes (*a* kinematical axes of Ramsay, 1967) predominates in deeply stepping axial plane cleavage. There is no evidence of the D_1 sinistral shear zones which are common farther north, and the finite strain ellipsoids are plane strain to slightly oblate.

- Domain F (Burg *et al.*, 1981; Azor *et al.*, 1994; Dias, 1998; Martínez Poyatos, 2002; Martínez Poyatos *et al.*, 2004; Pereira *et al.*, 2010). Adjacent to the boundary with the OMZ there is a narrow sector with an intense deformation and NE facing folds, which could attain recumbent shapes in the Spanish sector (the Puebla de la Reiña anticline and the Hornachos syncline). There is a penetrative S_1 axial plane foliation (often mylonitic), with a low dipping NW-SE stretching lineation subparallel to fold axes. In the Portuguese sector, the kinematical criteria indicate a predominant sinistral shear sense.

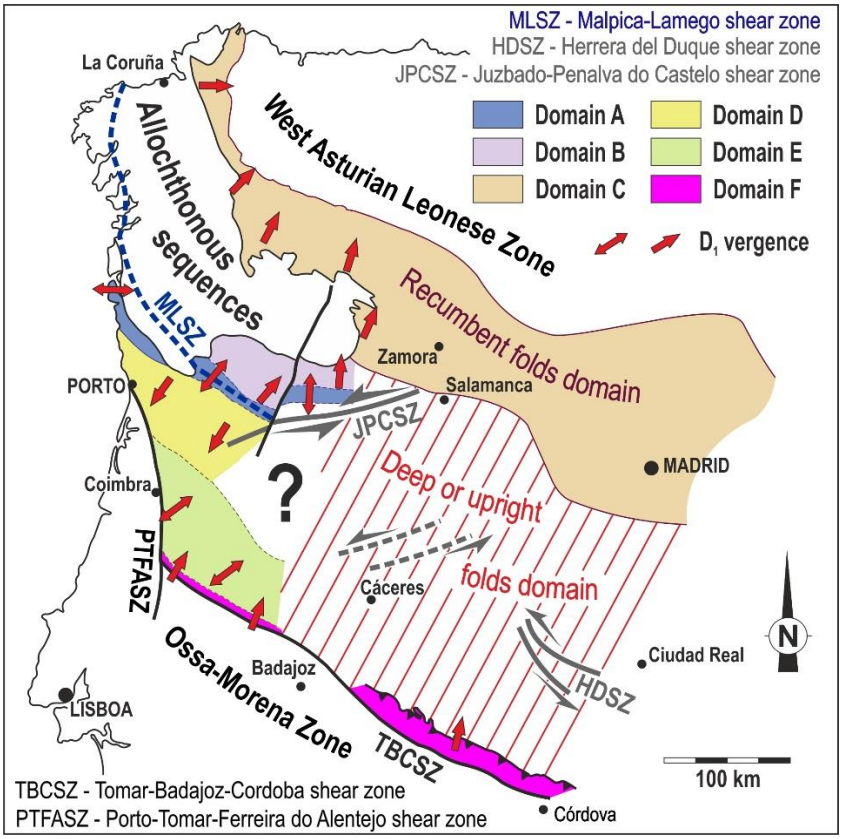

Figure 4 – Main fold pattern in the CIZ of NW Iberia (adapted from Azor *et al.*, 1994; Díez Balda *et al.*, 1990; Ribeiro *et al.*, 1990; Dias and Ribeiro, 1994; Dias, 1998; Dias *et al.*, 2013b; Romão *et al.*, 2013).

Despite the geometrical diversity of the regional D_1 folds of CIZ, their axes are always subhorizontal or low dipping. Such behaviour indicates either the lack of a pervasive superposition between Variscan deformation events, or a strong coaxiality of these events.

The predominance in northern Portugal of sinistral strike-slip shear zones subparallel to the axial planes of the D_1 folds, and the centripetal vergences around a less deformed sector has been interpreted as an asymmetrical positive flower structure (with a longer NE branch) centred in domain A (Dias, 1998; Moreira *et al.*, 2010a; Dias *et al.* 2013b) and developed in a transpressive regime (Dias and Ribeiro, 1994). This first order structure, which can be followed for more than 80 km (Moreira *et al.*, 2010a), was controlled by a Precambrian basement anisotropy (the Porto-Viseu-Guarda lineament; Dias, 1998) depicted by gravimetric (Mendes Victor *et al.*, 1993) and magnetic anomalies (Miranda, 1990; Miranda and Mendes Victor, 1990). Analogue modelling supports this interpretation (Richard and Cobbold, 1990). Towards NW this structure is in continuity with the Malpica-Tui unit, which seems to indicate the existence of an Early Variscan first order shear zone (the Malpica-Lamego shear zone - MLSZ in Fig. 4; Llana-Fúnez and Marcos, 2001; Pamplona *et al.*, 2016) controlling, not only the exhumation and emplacement of the high-pressure –low to intermediate temperature rocks of this unit (Llana-Fúnez and Marcos, 2002) but also the Variscan deformation in NW Iberia autochthon.

This CIZ flower structure is not observed SW of the first order Juzbado - Penalva do Castelo shear zone (JPCSZ; Fig. 4), showing that this structure has already been active since the beginning of the main folding event of the CIZ, as previously proposed (Iglésias and Ribeiro, 1981).

Previous geometrical and kinematical CIZ zoning must be expanded to the Iberian scale in order to understand its Variscan arcs. Indeed, the combination of the finite strain pattern of folded layers and the coeval kinematics is a powerful tool to discriminate among folding mechanisms (Dias and Ribeiro, 2008). Such approach has been used since the early models for the IAA (Matte and Ribeiro, 1975; Ries and Shackleton, 1976).

Using the relation of the finite strain axes with the coeval folds / thrusts, Matte and Ribeiro (1975) emphasize a major distinction between inner and external domains of the IAA, separated by a narrow transition zone less than 10 km wide (Ries and Shackleton, 1976). The inner domain (*i.e.* the Cantabrian, West Asturian-Leonese and previous domain C) is characterized by thrusts and folds with a well-developed vergence towards the core of the arc. The coeval maximum stretching lineation is subparallel to the *a* kinematical axes. In spite of this regional behaviour (well expressed in the Mondoñedo nappe unit), the complexity of the folding evolution could generate local anomalies as in Courel recumbent fold; here the

stretching lineation coincides with the fold axes due to the superposition of an homogeneous strain after the active folding process (Bastida *et al.*, 2010). Concerning the external domain, the stretching lineation has been considered to be always subparallel to the pervasive subhorizontal fold axes. Such relation (stretching subparallel to the *b* kinematic axis), has been described not only for the Iberian branch of the IAA but also for the Armorican one. Nevertheless, Matte and Ribeiro (1975) emphasise a major contrast in both branches: while in the southern branch the folds are coeval of pervasive sinistral shears with the same trend of the folds, in Brittany the dominant regional shear is dextral. However, Audren *et al.* (1976) show that the regional shears in both branches are not synchronous: while in Iberia the sinistral shears are older than the Carboniferous granitic intrusions, the dextral shearing in Brittany is essentially coeval of this major magmatic event. Moreover as previously described, the external domain of Matte and Ribeiro (1975) presents a much more complex behaviour.

IX.2.3.2. Folding Events and Ages

The age of the main Variscan folds in Iberia is a key issue for the genesis of the Iberian Variscan arcs. This is not easy being necessary to distinguish between local and regional tectonic events, a problem enhanced by the heterogeneity of deformation. At a more regional scale, the orogeny migrates both transversally and longitudinally to structures. The transverse migration operates from the suture zones to the relative foreland and, in the autochthon, from the axis of positive flower structures to their branches. The longitudinal migration operates from the hinge of the IAA towards its flanks.

In spite of these limitations and some minor discrepancies, three main compressive tectonic events are usually recognized in the autochthon of NW Iberia Variscides (Gibbons and Moreno, 2000; Vera, 2004; Dias *et al.*, 2013a):

- D_1, the only that is pervasive, usually induces the formation of upright to slightly overturned structures in the more internal domains (*i.e.* most of the CIZ) and recumbent folds and thrusts facing towards the core of the CA in the most external ones (*i.e.* domain C of CIZ, as well as the WALZ end CZ). As expected, D_1 intensity usually increases from the foreland towards the hinterland, where a well-developed cleavage is pervasive.
- D_2 has a very heterogeneous development being restricted to the vicinity of the NW Iberian allochthonous and parautochthonous units. It corresponds to a second folding phase associated to shallow dipping shear zones, developing an S_2 axial planar cleavage to schistosity which can completely transpose S_1. This behaviour, as well as the similarities between the kinematics of the structures found in the nappes and in the

autochthon, show that this tectonic event has been induced by the emplacement of the napes.

- D_3 is also non penetrative, being expressed by upright folds often linked to subvertical strike-slip shear zones, like the major ENE-WSW Juzbado-Penalva do Castelo with a left lateral kinematics. The widespread granitic plutonism is also related to the D_3 tectonic event.

Since the recognition of sin-D_2 subhorizontal shear zones with displacements parallel to the orogenic trend in the Tormes gneiss dome (Escuder Viruete *et al.*, 1994; Escuder Viruete, 1998) and in Martinamor antiform (Díez Balda *et al.*, 1995), both in the vicinity of Salamanca, widespread similar low dipping fabrics has been described. They are generally more frequent in the vicinity of the parautochthonous /allochthonous units of the NW Iberia, being usually related with large antiforms and domes where outcrop high grade rocks (Escuder Viruete *et al*., 2004). A recent review (Martínez Catalán *et al.*, 2014), emphasizes two major extensional events, the first one coeval with the end of D_2, and the other sin to post-D_3. Although most authors considered such events related to the extensional collapse of the orogen (Escuder Viruete *et al*., 2004 Martínez Catalán *et al.*, 2014; Ballèvre *et al.*, 2014) for others (*e.g.* Ribeiro *et al.*, 2007; Dias *et al.*, 2013b), they could result from local compressions related to the allochthonous / autochthonous units

The Variscan orogeny in Iberia has recently been consider the result of a major Late Carboniferous collision followed by a Permian wrenching (Schulmann *et al.*, 2014). This is different from previous models where the deformation began in Lower/Middle to Upper Devonian times (*e.g.* Burg *et al.*, 1981; Noronha *et al.*, 1981; Matte 1986; Pérez-Estaún *et al.*, 1991; Azor *et al.*, 1994; Ábalos *et al.*, 2002; Franke *et al.*, 2005). The D_1 age (Fig. 5) is crucial to understand the Iberian arcs.

The 359 Ma age is often considered the beginning of the D_1 deformation in the CIZ autochthon (Martínez Catalán *et al.*, 2014; Ballèvre *et al.*, 2014). This age (Fig. 5B) was obtained (Dallmeyer *et al.*, 1997) by $^{40}Ar/^{39}Ar$ in white micas on S_1 cleavage NE of Morais Massif, in the normal limb of the Ollo de Sapo anticline (Fig. 5A). It is similar to the ages obtained in Somosierra also in the CIZ autochthon (354 and 353 Ma; Rubio Pascual *et al.*, 2013; Fig. 5B). Using the ages obtained farther E in the WALZ (336 and 322 Ma; Dallmeyer *et al.*, 1997) they estimate the diachronism related to the migration of the D_1 deformation towards the foreland (*circa* 23 Ma difference per 125 km of present distance). This value is similar to the range they found in D_2 mylonites. Thus, an average convergence rate of *circa* 1-2 cm/year was then proposed.

Such evolution is consistent with the estimations for the West Asturian-Leonese and Cantabrian zones based on stratigraphical evidences in synorogenic deposits (Pérez-Estaún *et al.*, 1988; Fig. 5B). While in the WALZ the deformation began in Lower Carboniferous (Pérez-Estaún, 1974) in the rearmost units of CZ it could be Westephalian B (*i.e.* Lower Moscovian; Arboleya, 1981) or even Namurian (*i.e.* Serpukhovian; Alonso *et al.*, 2009). The emplacement of nappes in the more external sectors of CZ persists until Stephanian (*i.e.* Kasimovian: Maas, 1974; Marquínez, 1978; Alonso *et al.*, 2009). Nevertheless, there is still some controversy with some works proposing that the foreland basin system had already developed during the Late Devonian (Keller *et al.*, 2008). This eastwards progression of NW Iberia autochthon deformation is consistent with the emplacement of the allochthonous nappes in the same sense (Fig. 5B): beginning of the accretion at 400-390 Ma with the old continental arc preserved in the Upper Allochthon (Arenas *et al.*, 2014), followed at 390-380 Ma by the Middle Allochthon unit with ophiolitic affinities (Ballèvre *et al.*, 2014) and the Lower Allochthon emplacement at 370-365 Ma (Ballèvre *et al.*, 2014).

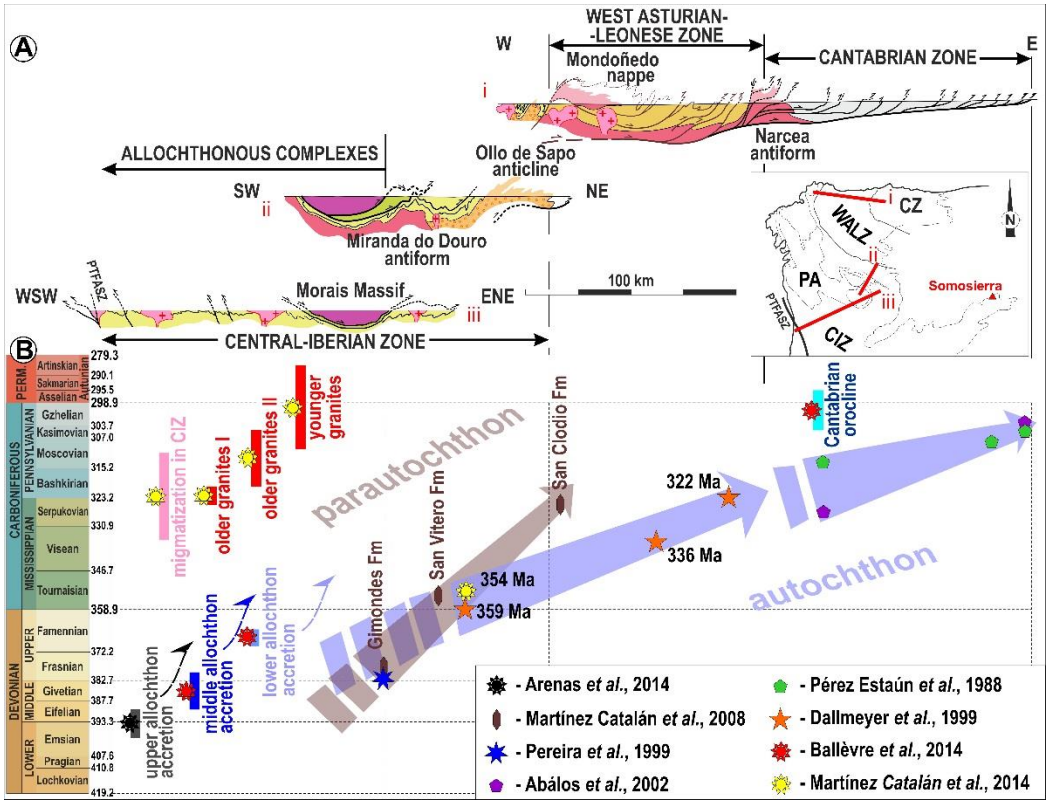

Figure 5 – Age distribution of main Variscan tectonic events in NW Iberia since Lower Devonian:

A – Simplified cross-sections emphasizing the main structural features of NW Iberia (adapted from Pérez Estaún *et al.*, 1991; Ribeiro *et al.*, 2005; Ballèvre *et al.*, 2014; Martínez Catalán *et al.*, 2014);

B – Main tectonic events evolution in the NW Iberia.

Such diachronism shows that it is not plausible to assume 359 Ma as the lower limit to the D_1 deformation in the CIZ autochthon, because such age has been obtained, at least 200 km away from any suture. Thus, the deformation must be older in the more far-travelling nappes rooted there and in the inner domains of the autochthon. This older age for the D_1 deformation in the autochthon is supported by further evidence:

(1) The Gimondes, San Vitero and San Clodio formations are considered flyschoid deposits related to the frontal thrusts of the allochthonous / parautochthonous unit of NW Iberia (Martínez Catalán *et al.*, 2008). NE of the Bragança Massif, the paleontological contend of the Gimondes formation (Ribeiro, 1974) indicates an age close to the Givetian - Frasnian boundary (Fig. 6B; Teixeira and Pais, 1973; Pereira *et al.*, 1999). This unit presents pebbles from the allochthonous complexes showing that they were already exhumed (Ribeiro and Ribeiro, 1974). Based on the youngest zircon contend of these three synorogenic deposits, it was emphasized a diachronism of the parautochthon deformation (Martínez Catalán *et al.*, 2008) with the younger ages towards the more external domains of the orogen (Fig 6B; 378 ± 6 Ma for Gimondes; 355 ± 8 Ma for San Vitero and 324 ± 7 Ma for San Clodio). Such behaviour is compatible with the observed in the autochthon.

(2) In the inner domains of CIZ, D_1 regional folds are cut by the imbricated basal thrusts of parautochthon (*e.g.* N of Marão; Pereira, 1987; 1989).

(3) The emplacement of the parautochthon in northern Portugal is subparallel to the trend of major D_1 folds and coeval sinistral strike slip shear zones (Pereira, 1987; 1989; Ribeiro *et al.*, 1990; Rodrigues *et al.*, 2005; Rodrigues, 2008; Rodrigues *et al.*, 2013). This indicates an already well structured autochthon where major anisotropies were reactivated has lateral ramps of the nappes. Such model is common in other orogenic domains, as in the Appalaches (Pohn, 2000) or the Greenville of Canada (Dufréchou, *et al.*, 2014).

(4) The stable platform environment that predominate in the CIZ since the Early Cambrian change by the end of Lower Devonian (Martínez Catalán *et al.*, 2008; Ballèvre *et al.*, 2014; Martínez Catalán *et al.*, 2014). The absence of Middle Devonian in northern Portugal is probably related to the beginning of the Variscan deformation in the CIZ autochthon (Pereira, 1988).

The beginning of a pervasive and intense deformation in the innermost sectors of CIZ, at least since the Middle / Upper Devonian, is also coherent with Iberian geodynamics. In the OMZ, the stratigraphic, metamorphic and magmatic data shows that the beginning of subduction, and consequently the first deformation episode, had Lower Devonian age. Indeed

in Odivelas (southernmost domains of OMZ) the Emsian-Eifelian limestones, which are spatially associated with volcanic rocks with tholeiitic orogenic signature, show evidences of syn-sedimentary deformation (Machado *et al.*, 2009; 2010; Moreira *et al.*, 2010b; Silva *et al.*, 2011). Also in the OMZ the Lower Devonian Terena formation, in which the D_1 is absent, shows evidences of syn-sedimentary deformation (*e.g.* Oliveira *et al.*, 1991; Araújo *et al.*, 2013). Geochronological data (Pereira *et al.*, 2012; Braid *et al.*, 2011; Rodrigues *et al.*, 2014) also show clusters of inherited zircons around Lower-Middle Devonian, which seems to indicate that the orogenic magmatic processes was active during lower Devonian (*e.g.* Moreira *et al.*, 2014). The first deformation events in northern and central domains of OMZ are associated with a sinistral kinematic component (*e.g.* Expósito *et al.*, 2002; Araújo *et al.*, 2013). In the TBCSZ, where a pervasive sinistral kinematics is described (*e.g.* Ábalos, 1992; Quesada and Dallmeyer, 1994), Upper Devonian metamorphic ages were obtained in Neoproterozoic volcanic rocks (370 and 360 Ma by $^{40}Ar/^{39}Ar$ in amphibole; Quesada and Dallmeyer, 1994).

Thus, the Iberian Variscides is the result of a Lower Devonian - Upper Carboniferous complex evolution like its northeast extension and not an essentially Late Carboniferous collision as recently proposed (*e.g.* Schulmann *et al.*, 2014).

IX.2.3.3. The Regional CIZ Folding

Most of the regional folds of the CIZ autochthon have been traditionally attributed to the main D_1 Variscan shortening (Fig. 6A). However, recently a drastically different proposal was presented (Martínez Catalán, 2011a; 2011b; 2011c; Martínez Catalán *et al.*, 2014), where most of these folds are now considered to related to the D_3 event (Fig. 6B). This new definition of the folding events in CIZ is one of the main arguments favouring the existence of the CIA. The age of these CIZ folds is thus a key issue.

All the recent syntheses of the Iberian Geology, either from the Spanish groups (Ábalos *et al.*, 2002; Martínez Poyatos *et al.*, 2004) or from the Portuguese ones (Dias *et al.*, 2013b; Romão *et al.*, 2013) consider that these regional folds were formed during the early D_1 Variscan phase. A similar conclusion is obtained comparing the great number of works supporting their formation during D_1, with the scarcity of papers considering they are D_3 (Table I).

In order to discriminate between both models (*i.e.* Fig. 6A versus Fig. 6B) three situations will be discussed (see location in Fig. 6B): the Marão complex folded structure in the vicinity of the allochthon / parautochthon of northern Portugal, the Amêndoa - Carvoeiro syncline close to the intersection between the first order PTFA and TBC shear zones and the Mora - Madridejos region south of Toledo.

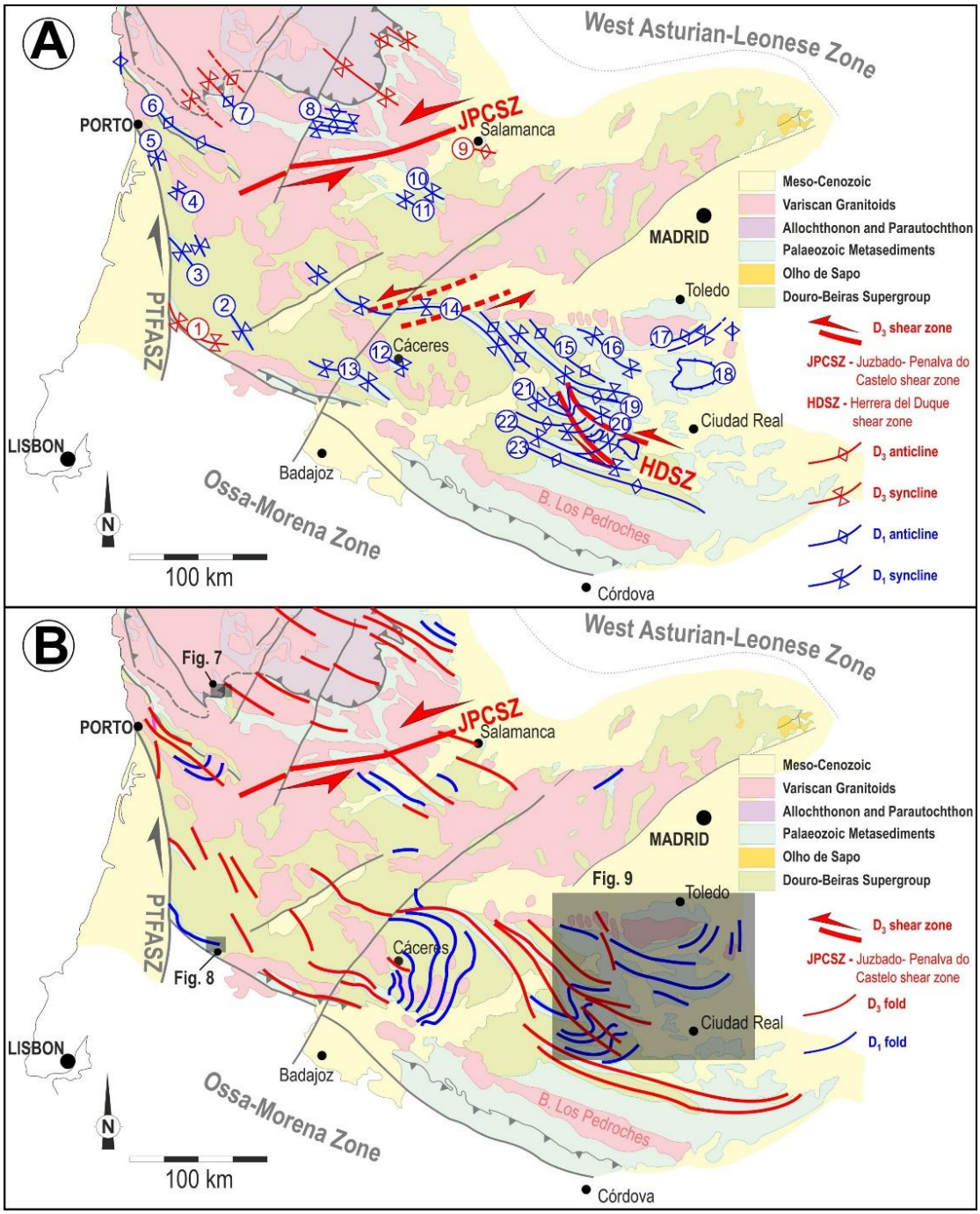

Figure 6 – Central-Iberian Zone major folds according to their Variscan tectonic event:

A – Classical interpretation (based in Díez Balda *et al.*, 1990; Ribeiro *et al.*, 1990; Ábalos *et al.*, 2002; Martínez Poyatos *et al.*, 2004; Dias *et al.*, 2013b; Romão *et al.*, 2013). See table I for the association between the numbers inside the circles and the structures;

B – Recent interpretation emphasizing the Central-Iberian Arc (based in Martínez Catalán 2011a; 2011b; Martínez Catalán *et al.*, 2014), with locations of figures 7, 8 and 9.

Table I – Relation between main CIZ Variscan folds and regional tectonic events according to different authors.

Ref.	structure	D_1	D_3
1	Amêndoa-Carvoeiro syncline	Martínez Catalán, 2011a; 2011b; 2011c; Martínez Catalán *et al.*, 2014	Romão, 2000; Romão *et al.*, 2013
2	Vila Velha de Ródão syncline	Ribeiro *et al.*, 1990; Dias, 1994; Metodiev *et al.*, 2009; Romão *et al.*, 2013	Martínez Catalán, 2011a; 2011b; 2011c; Martínez Catalán *et al.*, 2014
3	Buçaco syncline	Ribeiro *et al.*, 1990; Dias and Ribeiro, 1993; Dias, 1994; Dias *et al.*, 2013b; Romão *et al.*, 2013	Martínez Catalán, 2011a; 2011b; 2011c, Martínez Catalán *et al.*, 2014
4	Caramulo syncline	Ribeiro *et al.*, 1990; Dias, 1994; Dias and Ribeiro, 1995a; Dias *et al.*, 2013b; Romão *et al.*, 2013	Martínez Catalán, 2011a; 2011b; 2011c; Martínez Catalán *et al.*, 2014
5	Oliveira de Azeméis syncline	Ribeiro *et al.*, 1990; Dias *et al.*, 2013b	Martínez Catalán, 2011a; 2011b; 2011c; Martínez Catalán *et al.*, 2014
6	Valongo anticline	Ribeiro *et al.*, 1990; Pereira and Ribeiro, 1992; Dias, 1994; Dias and Ribeiro, 1998; Dias *et al.*, 2013b; Pamplona and Ribeiro, 2013	Martínez Catalán, 2011a; 2011b; 2011c; Martínez Catalán *et al.*, 2014; Valle Aguado, 1992
7	Marão anticline	Ribeiro *et al.*, 1990; Dias, 1994; Coke, 2000; Coke *et al.*, 2003; Rodrigues *et al.*, 2005; Moreira *et al.*, 2010a; Dias *et al.*, 2013b	Martínez Catalán, 2011a; 2011b; 2011c; Martínez Catalán *et al.*, 2014
8	Moncorvo and Poiares synclines	Díez Balda *et al.*, 1990; Ribeiro *et al.*, 1990; Dias and Ribeiro, 1991; Dias, 1994; Dias *et al.*, 2003; 2013b; Rodrigues *et al.*, 2005; Moreira *et al.*, 2010a	Martínez Catalán, 2011a; 2011b; 2011c; Martínez Catalán *et al.*, 2014; Dias da Silva, 2013
9	Martinamor anticline		Díez Balda, 1986; Díez Balda *et al.*, 1990; Martínez Poyatos *et al.*, 2004
			Martínez Catalán, 2011a; 2011b; 2011c; Martínez Catalán *et al.*, 2014
10	Tamames and Salamanca synclines	Díez Balda, 1986; Rölz, 1975; Díez Balda *et al.*, 1990; Ábalos *et al.*, 2002; Martínez Poyatos *et al.*, 2004	
		Martínez Catalán, 2011a; 2011b; 2011c; Martínez Catalán *et al.*, 2014	
11	Peña de Francia syncline	Rölz, 1975; Macaya, 1981; Díez Balda *et al.*, 1990; Ábalos *et al.*, 2002; Martínez Poyatos *et al.*, 2004	Martínez Catalán, 2011a; 2011b; 2011c; Martínez Catalán *et al.*, 2014
12	Cáceres syncline	Tena, 1980; Díez Balda *et al.*, 1990; Ábalos *et al.*, 2002; Martínez Poyatos *et al.*, 2004	Martínez Catalán, 2011a; 2011b; 2011c; Martínez Catalán *et al.*, 2014
13	Sierra de S. Pedro syncline	Bascones *et al.*, 1980; Díez Balda *et al.*, 1990; Ábalos *et al.*, 2002; Martínez Poyatos *et al.*, 2004	
14	Cañaveral syncline	Díez Balda *et al.*, 1990; Gil Toja and Pardo Alonso, 1991; Ábalos *et al.*, 2002; Martínez Poyatos *et al.*, 2004	Martínez Catalán, 2011a; 2011b; 2011c; Martínez Catalán *et al.*, 2014
15	Valdelacasa anticline	Díez Balda *et al.*, 1990; Ábalos *et al.*, 2002; Martínez Poyatos *et al.*, 2004	Martínez Catalán, 2011a; 2011b; 2011c; Martínez Catalán *et al.*, 2014
16	Navalucillos syncline	Martínez Poyatos *et al.*, 2004	Martínez Catalán, 2011a; 2011b; 2011c; Martínez Catalán *et al.*, 2014
17	Mora anticline	Días Balda *et al.*, 1992; Martínez Catalán, 2011a; 2011b; 2011c; Martínez Catalán *et al.*, 2014	
18	Urda dome	Díez Balda *et al.*, 1990	
19	Navalpiño anticline	Díez Balda *et al.*, 1990; Ábalos *et al.*, 2002; Martínez Poyatos *et al.*, 2004	Martínez Catalán, 2011a; 2011b; 2011c; Martínez Catalán *et al.*, 2014
20	Puebla de D. Rodrigo syncline	Martínez Poyatos *et al.*, 2004	Martínez Catalán, 2011a; 2011b; 2011c; Martínez Catalán *et al.*, 2014
21	Herrera del Duque syncline	Díez Balda *et al.*, 1990; Ábalos *et al.*, 2002; Martínez Poyatos *et al.*, 2004; Martínez Catalán, 2011a; 2011b; 2011c; Martínez Catalán *et al.*, 2014	
22	Almadén syncline	Díez Balda *et al.*, 1990; Ábalos *et al.*, 2002; Martínez Poyatos *et al.*, 2004	Martínez Catalán, 2011a; 2011b; 2011c; Martínez Catalán *et al.*, 2014
23	Alcudia anticline	Díez Balda *et al.*, 1990; Ábalos *et al.*, 2002; Martínez Poyatos *et al.*, 2004	Martínez Catalán, 2011a; 2011b; 2011c; Martínez Catalán *et al.*, 2014

(1) In the region around Marão the regional Variscan fold pattern in the autochthon is well expressed in the Armorican quartzites formation. These folds have always been considered as D_1 (Pereira and Ribeiro, 1983; Ribeiro *et al.*, 1990; Pereira *et al.*, 1993; Coke *et al.*, 2000; 2003; Rodrigues *et al.*, 2005). Such conclusion is well supported because some of the folds are truncated by the basal thrusts of the NW Iberia parautochthon (Fig. 7; Pereira 1987; 1989), related with the nappe emplaced during the regional Variscan D_2 (Pereira 1987; Ribeiro *et al.*, 1990; 2007). These D_2 thrusts were locally folded during the D_3 shortening, a less intense and not pervasive deformation event (Pereira 1987; 1989). Nevertheless this clear cartographic interference pattern, the major D_1 Marão folds have been recently considered (Martínez Catalán, 2011a; 2011b; 2011c; Martínez Catalán *et al.*, 2014) due to the regional D_3 Variscan event (Fig. 7B), although they did not present any arguments to support this new interpretation.

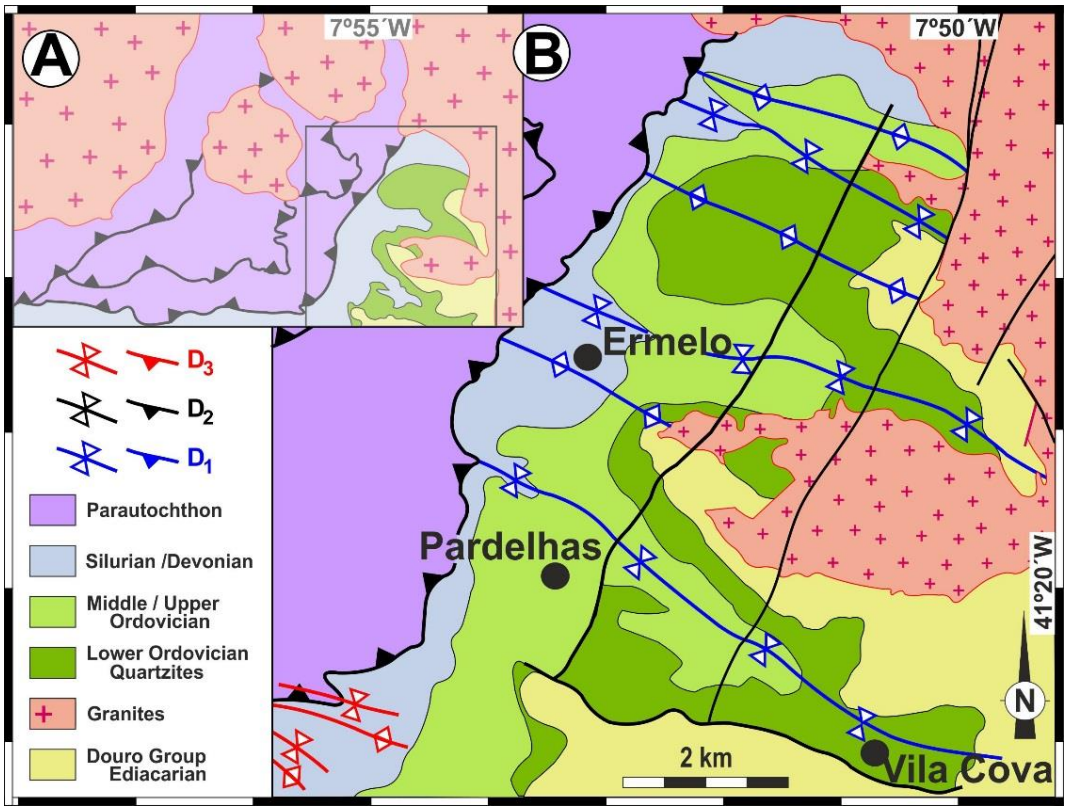

Figure 7 – General structural map northern of Marão Mountain showing the interference between D_1 and D_3 folds with D_2 thrusts (adapted from Pereira, 1989).

(2) In the models supporting the CIA, the E-W Amêndoa-Carvoeiro syncline (Fig. 8) has been considered (Martínez Catalán 2011a; 2011b; Martínez Catalán *et al.*, 2014) a D_1 structure deformed during D_3 by regional folds and the movement of the PTFASZ (Fig. 7B). Nevertheless, these authors never present any justification for such assumption.

Moreover, previous studies (Romão, 2000; Romão *et al.*, 2013; Fig. 8A), show a complex cartographic pattern due to the overprint of, at least three major tectonic events:

1º. NW-SE D_1 folds and thrusts with a NE facing (Fig. 8A);

2º. NNW-SSE D_2 folds and thrusts with a ENE facing (Fig. 8A) and clear interference patterns with D_1 structures (Fig. 8B);

3º. E-W D_3 folds and coeval thrusts, facing towards N (Fig. 8A). The interference with previous D_1 and D_2 structures (Fig. 8C) shows that the major Amêndoa syncline must be considered a D_3 structure and not D_1.

It should be emphasized that this local D_3 tectonic event expressed in the Amêndoa - Carvoeiro syncline, could be related to the Late Variscan deformation.

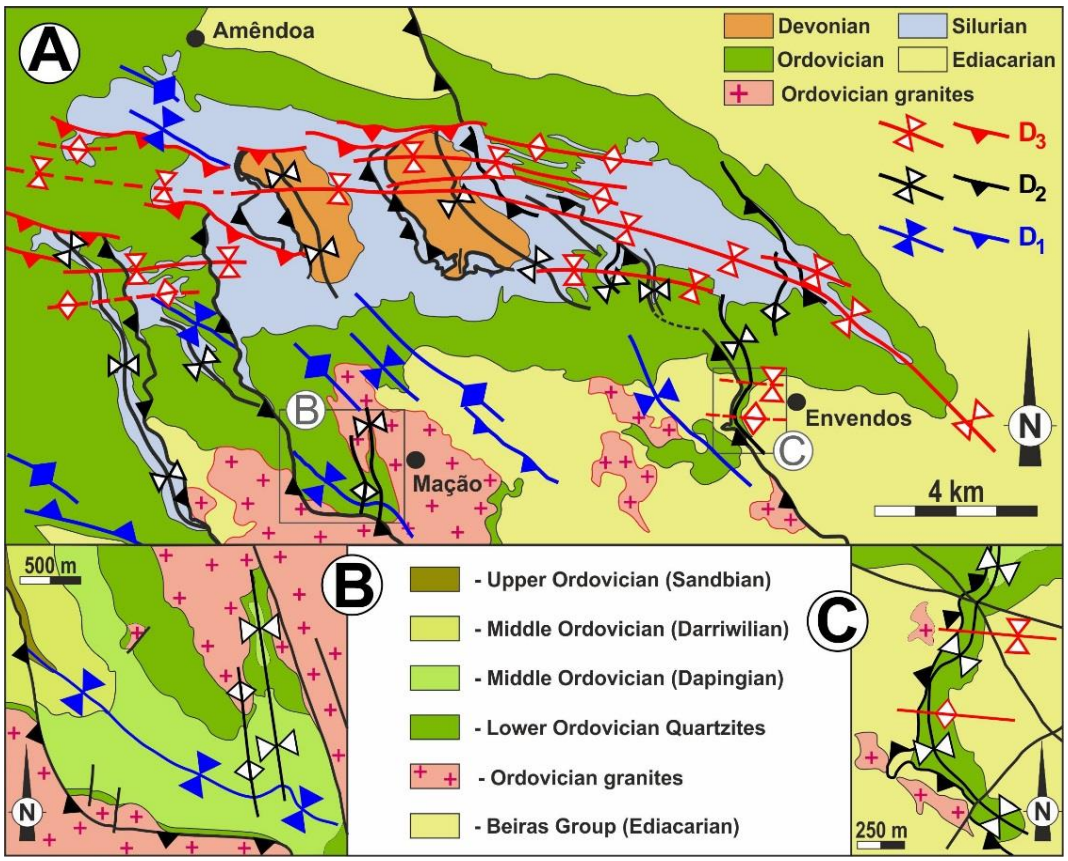

Figure 8 – The Amêndoa - Carvoeiro syncline structure:

A – General structural map (adapted from Romão, 2000);

B – D_1 syncline folded by D_2 structures at Monte de João Dias, W of Mação city (adapted from Romão, 2000);

C – D_2 structures folded by younger E-W D_3 folds at Sanguinheira sector, W of Envendos village (adapted from Romão, 2000).

(3) The Mora - Madridejos region is very important because it is close to the hinge zone of the supposed CIA. Detailed mapping has recently been presented trying to emphasize the regional development of D_3 folds in this sector (Fig. 9A; Martínez Catalán, 2011c). Nevertheless, the observed rotation of the D_1 folds from the regional NW-SE trend to the local N-S was already known (Díez Balda *et al.*, 1990; Díez Balda and Vegas, 1992; Julivert and Martínez, 1983; Julivert *et al.*, 1983) and its meaning is debatable. According to Martínez Catalán (2011c) it is the result of the intense D_3 folding related to the CIA (Figs. 6B, 9C). However, when considering the proximity to the D_3 Herrera del Duque shear zone (Fig. 9C; Martínez Poyatos *et al.*, 2004) such rotation could reflect the presence of another WNW-ESE D_3 sinistral shear zone (Fig. 9D).

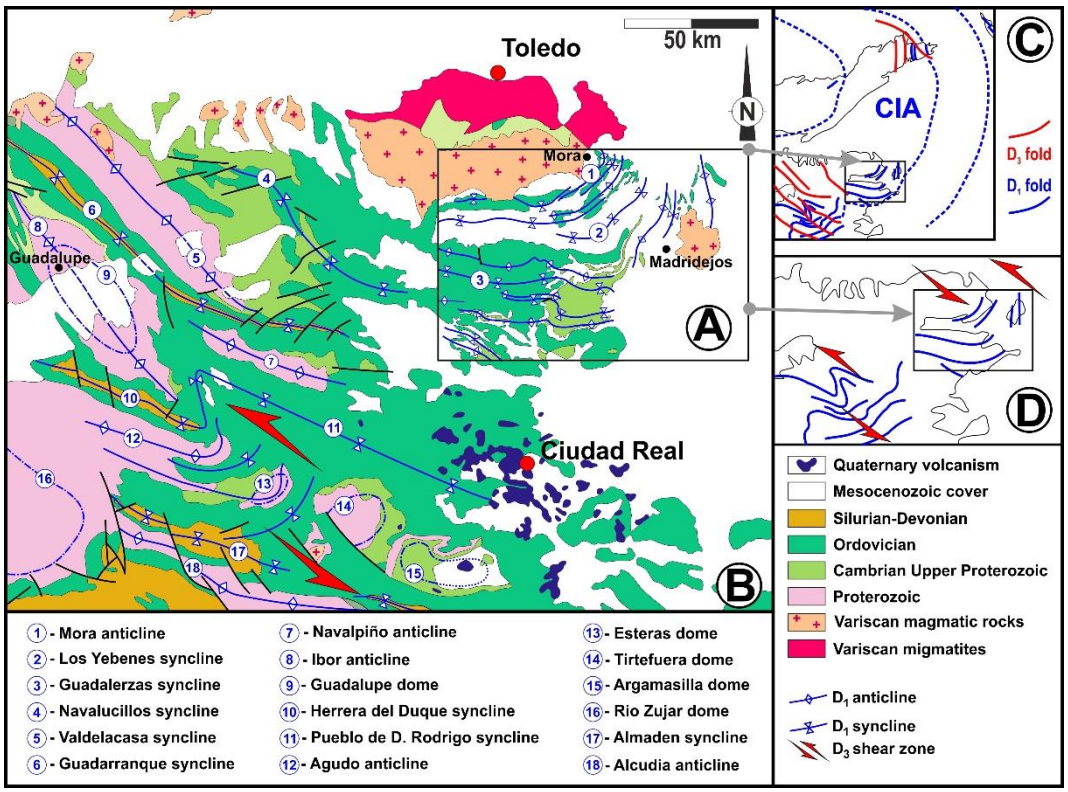

Figure 9 – Variscan structural map of Toledo - Ciudad Real region:

A – Rotation of main D_1 structures at Mora - Madridejos sector (simplified from Martínez Catalán, 2011c);

B – Geological map, emphasizing the general pattern of D_1 major folds (based on Julivert *et al.*, 1983; Días Balda *et al.*, 1992; Rodríguez-Fernández, 2004);

C – Mora - Madridejos D_1 structures in the framework of the CIA (redrawn from Martínez Catalán, 2011c);

D – Deflection of D_1 folds in Herrera del Duque and Mora sectors induced by D_3 WNW-ESE sinistral shear zones.

It is not easy to choose between both models because the deformation occurred at a low structural level without a pervasive cleavage and thus, the interference structures are rare. Moreover, whatever the proposals, the Cenozoic sediments of the Tagus basin hide the northern continuation of the N-S Mora structures (Fig. 9A). Thus, the deflection of the Variscan structures in the Mora - Madridejos region could not be used to support the existence of a pervasive regional D_3 folding (Fig 6B). Nevertheless, we favour the existence of a discrete D_3 sinistral shear zone, not only due to the vicinity of the Herrera de Duque one, but also due to the proximity to the major TBCSZ (Fig. 1).

As a major conclusion, we consider that the structural data show that the only pervasive Variscan tectonic event at the CIZ is D_1. D_2 and D_3 have an heterogeneous spatial distribution and are mostly important in the northern sectors (Julivert *et al.*, 1972: Díez Balda *et al.*, 1990; Ribeiro *et al.*, 1990; 2007; Ábalos *et al.*, 2002; Martínez Poyatos *et al.*, 2004; Rodrigues *et al., 2005; 2013;* Ribeiro *et al.*, 2013).

IX.2.3.4. Lithostratigraphic constraints in Pre-Orogenic Sequences

The lithostratigraphic Palaeozoic data are fundamental when trying to reconstruct the original shape of the proposed CIA where the continuity of the outcrops is often hidden by the overlap of younger sediments. This is particularly important in the "long-version" of the arc (Fig. 3B) where the southern domain of the CIZ (*i.e.* the Luso-Alcudian Zone of Lotze, 1945) is considered the lateral equivalent of the WALZ (Shaw *et al.*, 2012*a*; 2012*b*; 2014; Johnston *et al.*, 2013; Weil *et al.*, 2013). Thus, 2 critical review of the lithostratigraphy around the Iberian oroclines is thus fundamental to check the strength of previous proposals:

- To explain the different transition between the Lower Ordovician and older sequences in the WALZ (where there is stratigraphic continuity) and in CIZ (where a clear unconformity is pervasive), a possible "topographic high that was more proximal to the southern portion of the Gondwana margin" was suggested (Shaw *et al.*, 2012*a*), but no evidence of it has been presented.
- The correlation between (Shaw *et al.*, 2012*a*) the Lower Ordovician Ollo the Sapo volcanism (close to the boundary between CIZ and WALZ) and the Urra formation (in the vicinity between CIZ and OMZ) cannot be sustained. Indeed, in the proposed pattern of the CIA, the lateral equivalent of Ollo de Sapo must be in the central domains of CIZ (Fig. 3B).
- The S-pattern of paired CA and CIA oroclines is not compatible with the presence of the larger IAA. Indeed the continuity of the southern CIZ and OMZ in the French Armorican massif should imply a refolding of the Iberian oroclines (Shaw *et al.*, 2012*a*). Any model

constraining the continuity between the Iberian and Armorican branches of the IAA is difficult to accept due, not only to the strong correlation not only between the autochthonous formations of CIZ (*e.g.* the Lower Ordovician from Crozon in West Brittany and Buçaco in central Portugal; Robardet, 2002), but also between the allochthonous units exposed in the NW Iberian Massif and the southern Armorican Massif (Ballèvre *et al.*, 2014).

Previous correlations of paired CA and CIA oroclines are unable to propose any southward lateral correlation to the CZ, because OMZ or SPZ could not be considered its lateral equivalents (Shaw *et al.*, 2012*a; Fig. 3*). Several possibilities have been proposed to explain this major constraint: the vanishing of CZ along the strike (Shaw *et al.*, 2015), the possibility of OMZ and SPZ representing cryptic nappes not preserved in the core of the CA (Shaw *et al.*, 2012*a*) or an important offs*et al*ong the TBCSZ (Shaw *et al.*, 2012*a*). However, these proposals are never supported by observed data.

As a major conclusion, the existence of the CIA puts major lithostratigraphic constrains, which are difficult to solve.

IX.2.3.5. Lower Ordovician Paleocurrents

The Lower Ordovician paleocurrents in the CZ were considered as a western deposition in a N-S linear basin subsequently folded during the formation of the CA (Aramburu and Garcia-Ramos, 1993). Paleocurrent studies in Lower Ordovician rocks have recently extended to most of the NW Iberian autochthon. Although several papers have been published (Johnston *et al.*, 2013; Shaw *et al.*, 2012a; 2012b; 2014; Weil *et al.*, 2013) they all use the same data set concerning 50 localities from CZ, WALZ and CIZ. All these works considered the data compatible with a model of a long N-S linear basin (> 1500 km or even > 2300 km) filled from E. This basin was folded by a Carboniferous-Permian N-S shortening giving rise to two major oroclines (*e.g.* Johnston *et al.*, 2013; Weil *et al.*, 2013): the CA, preserving a centrifugal pattern of the Lower Ordovician paleocurrents, and the CIA with a centripetal pattern (Fig. 10A). However, the visual inspection of the published Rose diagrams of the paleocurrents, shows a great dispersion of the data in both branches of the CIA (sectors C and D in Fig. 10A). This led us to rework the same data (available at Shaw *et al.*, 2012a, *doi:10.1016/j.epsl.2012.02.014*), using a slightly different approach. When the trend of the arc limbs (sectors A, B, C and D of Fig. 11A) is projected against the expected paleocurrents (*i.e.* orthogonal to the trend), several linear segments are expected, one for each limb (dashed lines in Fig. 10B). When in this graphic the principal paleocurrents for each locality are projected, their dispersion around the theoretical dashed linear segments is a measure of the strength of the proposed model.

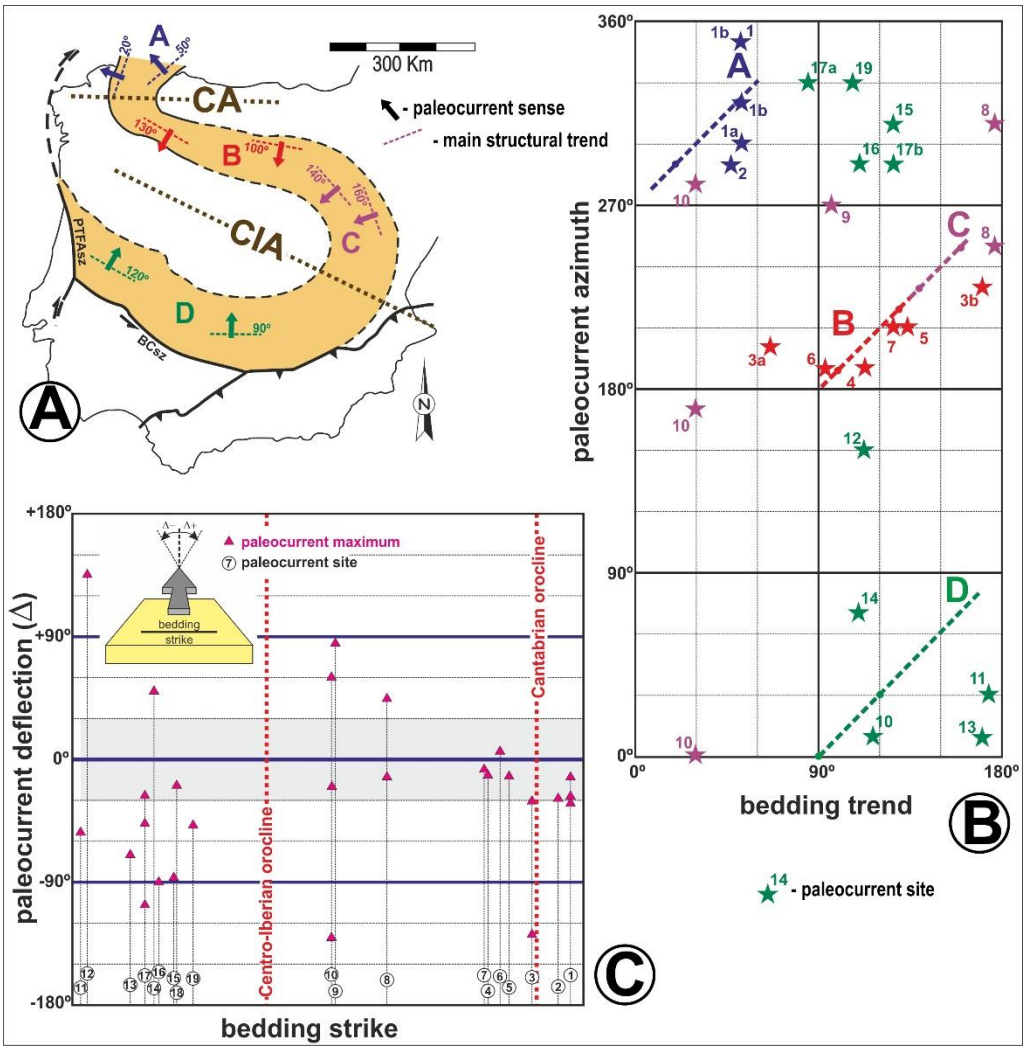

Figure 10 – The Lower Ordovician paleocurrents pattern around the Iberian oroclines:

A – Theoretical relation between paleocurrents and Variscan trend assuming an early N-S basin filled from E;

B – Predicted paleocurrent azimuths versus observed values (the numbers refer to sample localities as in Shaw *et al.*, 2012);

C – Divergence between the predicted and observed paleocurrents (the numbers refer to sample localities as in Shaw *et al.*, 2012).

The results (Fig. 10B and C) show that the paleocurrents around the Cantabrian orocline are compatible with a secondary origin for the arc. Indeed, there is a good linear correlation between the data and the theoretical predictions, either for the northern limb (sector A in fig. 10B) or the southern limb (sector B in fig. 10B). However, such behaviour is not found in the CIA data. Indeed, the great dispersion of the paleocurrents (sectors C and D in fig. 10B) seems to indicate that they could not be the result of uniform sedimentation in a N-S basin filled from East. The same conclusion was obtained when the regional structural trend is projected against the angular deflection (□) away from the perpendicularity to the strike of the bedding

where the paleocurrent has been measured (Fig. 10C). While in both limbs of the CA the deflection is lower than 30º, in the CIA the deflection is much higher.

Some early paleocurrent studies in Lower Ordovician Quartzites of the Portuguese southern sectors of CIZ (Conde, 1966) are also not compatible with the CIA. Indeed, although located in the southern limb (sector D of Fig. 10A) they emphasize paleocurrents towards NW instead of NE.

In conclusion, although the Lower Ordovician paleocurrents support the existence of the Cantabrian orocline, they cannot be used to sustain the Central Iberian one as previously considered by several authors (Johnston *et al.*, 2013; Shaw *et al.*, 2012; 2013; 2014; Weil *et al.*, 2013).

IX.2.3.6. Variscan Paleomagnetism in Iberia

Paleomagnetism has always been considered fundamental to understand the Iberian Variscan arcs (Ries *et al.*, 1980; Bonhommet *et al.*, 1981; Perroud and Bonhommet, 1981; Hirt *et al.*, 1992). These early data demonstrate that, at least some of the CA curvature is secondary due to the Variscan deformation. Recent works show the weakness of this conclusion, not only because it was based on very few data, but mostly due to the inability of the used methodology to differentiate between secondary syn-tectonic and post-tectonic remagnetizations (Weil *et al.*, 2013). Such limitations have been overcome in more recent studies, mostly concentrated on the CA (see Weil *et al.*, 2013 for a detailed resume), which show:

- The oroclinal occurred after the regional orogenic folding / thrusting has been nearly completed;
- Undoing the orocline leads to a nearly straight original belt with a N-S trend;
- The bending occurred primarily about near-vertical axes, without much further tilting of the already folded thrust sheets;
- The orocline formed between the Late Carboniferous and the Early Permian (Moscovian to Asselian, *i.e.* around 310–297 Ma; Weil, 2006).

Although there is some consensus in previous statements, it is still debatable how far the orocline rotation perpetuates downward (Van der Voo, 2004). Moreover, several models assume that it seems dynamically impossible for the Cantabrian orocline to be a thin-skinned crustal structure, due to space problems related to a 180º bent of a previous linear belt (Weil *et al.*, 2013). However, it is even harder to understand how this difficulty is solved by the bending of all the lithosphere as proposed by these models.

The CIA paleomagnetic data are much scarcer. However, recent data from the supposed southern limb of this orocline (Pastor-Gálan *et al.*, 2015), show that the rotation during the Late Carboniferous - Early Permian is comparable to the one estimated in the southern limb of the CA. This indicates that, either this arc did not exist, or it must be older than the CA, being an inherited major structure (Pastor Gálan *et al.*, 2015).

IX.2.4. Iberian Arcs; reviewing the Models

The complexity of the first order arcuate Variscan structures in Iberia, gave rise to a wide range of interpretative models.. A brief critical review of the geodynamical mechanisms that have been used to explain the Iberian arc(s), helps to narrow the range of possibilities.

IX.2.4.1. How many Arcs?

When discussing the mechanisms that have induced the formation of the first order arcuate structures in Iberia, it is fundamental to identify how many Variscan Arcs could be recognized in Iberia.

IX.2.4.1.1. Cantabrian Arc

The CA, sometimes called Asturian Arc (Pérez-Estaún and Bastida, 1990; Aramburu and Garcia-Ramos, 1993; Ábalos *et al.*, 2002), is the only unquestionable Variscan Arc in Iberia. Indeed, due to the almost continuous outcrops of CZ, it is possible to follow an almost 180º trend rotation of the Variscan structures. Moreover, the existence of this arc is well supported by several other data, (discuss in detail in Alonso *et al.*, 2007; Weil *et al.*, 2013) like the centripetal trend of Lower Palaeozoic sediments (Aramburu and Garcia-Ramos, 1993) and coeval paleocurrents (Shaw *et al.*, 2012; Fig. 10), the spatial and temporal pattern of tensile joints in rock units with different ages (Pastor-Galán *et al.*, 2011) or paleomagnetic studies (Weil, 2006; Weil *et al.*, 2013). The CA mostly overlaps the region where the Variscan structures are related to a stretching lineation subparallel to the *a* kinematical axis (Matte & Ribeiro, 1975; Ries and Shackleton, 1976).

IX.2.4.1.2. Central-Iberian Arc

Although since 2010 this orocline became very popular (Johnston, *et al.*, 2013; Martínez Catalán, 2011a; 2001b; 2011c; Martínez Catalán *et al.*, 2014; Shaw *et al.*, 2012a; 2012b; 2014; 2015) its existence is highly doubtful:

- There is no continuity of the main structures from one branch to the other, because the supposed hinge zone is hidden below Cenozoic basins (Fig. 3).

- The supposed arcuate pattern of the geophysical anomalies is not clear. It often differs from study to study (*e.g.* Ardizone, 1989 versus Álvarez García, 2002). It is are almost impossible to ascribe such anomalies to an unquestionable Variscan age and, in some cases, they are clearly related, either to Alpine events (like in the vicinity of Béticas Chain), or inherited Cadomian basement structures.

- The new pattern of the D_1 and D_3 Variscan folding events (Fig. 6B; *e.g.* Martínez Catalán, 2011a) are in clearly contradicts most of the published structural studies and the new interpretation is not supported by new structural studies.

- The supposed centripetal trend of the Lower Ordovician paleocurrents around the orocline (*e.g.* Shaw *et al.*, 2012) results from a very crude interpretation of the data set (Fig. 10).

- The proposed correlation between the WALZ and the southern domains of the CIZ (Shaw *et al.*, 2012) is not supported by lithostratigraphic data (see compilations concerning WALZ in Pérez-Estaún *et al.*, 1990; Marcos *et al.*, 2004 and for the CIZ in Gutiérrez Marco *et al.*, 1990; San José*et al.*, 1990; Díez Montes *et al.*, 2004; Rodríguez Alonso *et al.*, 2004; Romão *et al.*, 2013 and Fig. 1). Thus, this correlation implies (Shaw *et al.*, 2012) along strike variation (not observed because it is hidden below the Cenozoic Douro and Tejo basins) in order to accomplish the differences between the supposed northern limb of the Arc (in the WALZ) and the southern limb (in the southern domains of the CIZ). Moreover, the lithostratigraphy of the CIZ southern domains (*e.g.* Romão *et al.*, 2013) is very similar to the one found in the northern ones (*e.g.* Dias *et al.*, 2013b), mainly concerning the post-Cambrian metasediments, which suggests a common basin.

- Recent paleomagnetic data (Pastor-Galán *et al.*, 2015) discard a major bend at the CIA.

Thus, the geological arguments supporting the CIA are highly questionable and this proposal should be abandoned.

IX.2.4.1.3. Ibero-Armorican Arc

The continuity between the northern Armorican and the southern Iberian branches of the IAA cannot be followed due to the Atlantic and Biscay Mesozoic oceanic rifting. Nevertheless, there is a strong similarity between the geological formations found in both sectors, not only of the autochthon but also of the allochthonous units (Ballèvre *et al.*, 2013). This led to a strong consensus concerning the IAA.

IX.2.4.2. Previews Models

The complexity of the Variscan arcs in Iberia, gave rise to a wide range of models. A major constraint results because some models explain such arcs using a plate tectonic framework with only one ocean (the Rheic), while others also considered a second minor ocean related to the southern Brittany suture (the Paleotethys of Stampfli and Borel, 2002, also called Galicia-Massif Central Ocean by Matte, 2002; Ballèvre *et al.*, 2009). A brief critical review of these models helps to narrow the range of possible mechanisms. In this approach, previous models have been grouped using a simplification of Macedo and Marshak classification (1999).

IX.2.4.2.1. Arcs due to Margin Irregularities

Even before the establishment of plate tectonics, Dana (1886) proposed that the arcuate shape of some mountain belts was due to their wrapping around nonlinear margins of a pre-existing craton. Since then, several works recognize that the heterogeneous compressive stress induced by the collision with an irregular continental margin should produce wavy fold-thrust belts (Marshak, 1988). Such arcuations could be either margin-controlled curves or indenter-controlled curves (Macedo and Marshak, 1999). In the first situation, the thrusting is related to an originally nonlinear continental margin, while in the second case the arc forms because at the lateral edge of the indentor the deforming rock layer is subject to a shear couple, whereas at the front of the indentor the deforming rock layer is subject to a normal stress in plan (Marshak, 1988). Both solutions have been used since the early attempts to explain the IAA formation (Fig. 11).

Using mostly paleomagnetic, paleontological, sedimentary and magmatic data Lorenz (1976) and Lorenz and Nichols (1984) consider a paleogeographic realm for Lower Carboniferous times (Fig. 11A_1) with a small and very elongated Southern Europe continental plate between two large ones: the northern North America - Europe and the southern Africa. The minor plate was limited by two oceans: the northern Mid - European (Buret, 1972) or Rheic Ocean (Mckerrow and Ziegler, 1972) and the southern Paleotethys (Stampfli, 1996). The metamorphic and magmatic processes induced by the two centripetal subduction in the overriding Southern Europe Plate (Fig. 11A_2) have weakened this continental plate due to widespread partial melting in the lower and middle crust (Lorenz and Nichols, 1984). Thus, when in the Visean to Westephalian times, Southern Europe collided with both large neighbouring North America-Europe and Africa plates the irregular continental margins of the larger and thicker major continental plates induced oroclinal bending of Variscan Europe (Fig. 11A_3). Such process gave rise to the IAA induced by the northern Brabant-Newfoundland embayment, due to clockwise rotation of the Armorican sub-plate (western France) and

anticlockwise rotation of Iberian sub-plate, explaining the sinistral shears in Iberia and the dextral ones in Brittany. However, a major objection to such model, emphasizes the diachronism behaviour of the shear zones in both limbs of the IAA (Audren *et al.*, 1976), which are Devonian in Iberia and Carboniferous in Brittany (Dias and Ribeiro, 1995b). Another main problem concerns the proposed location of Iberia in Southern Europe minor plate (Fig. 11A$_3$), when most recent reconstructions show its close affinity to the major Gondwana (*e.g.* Ribeiro *et al.*, 2007).

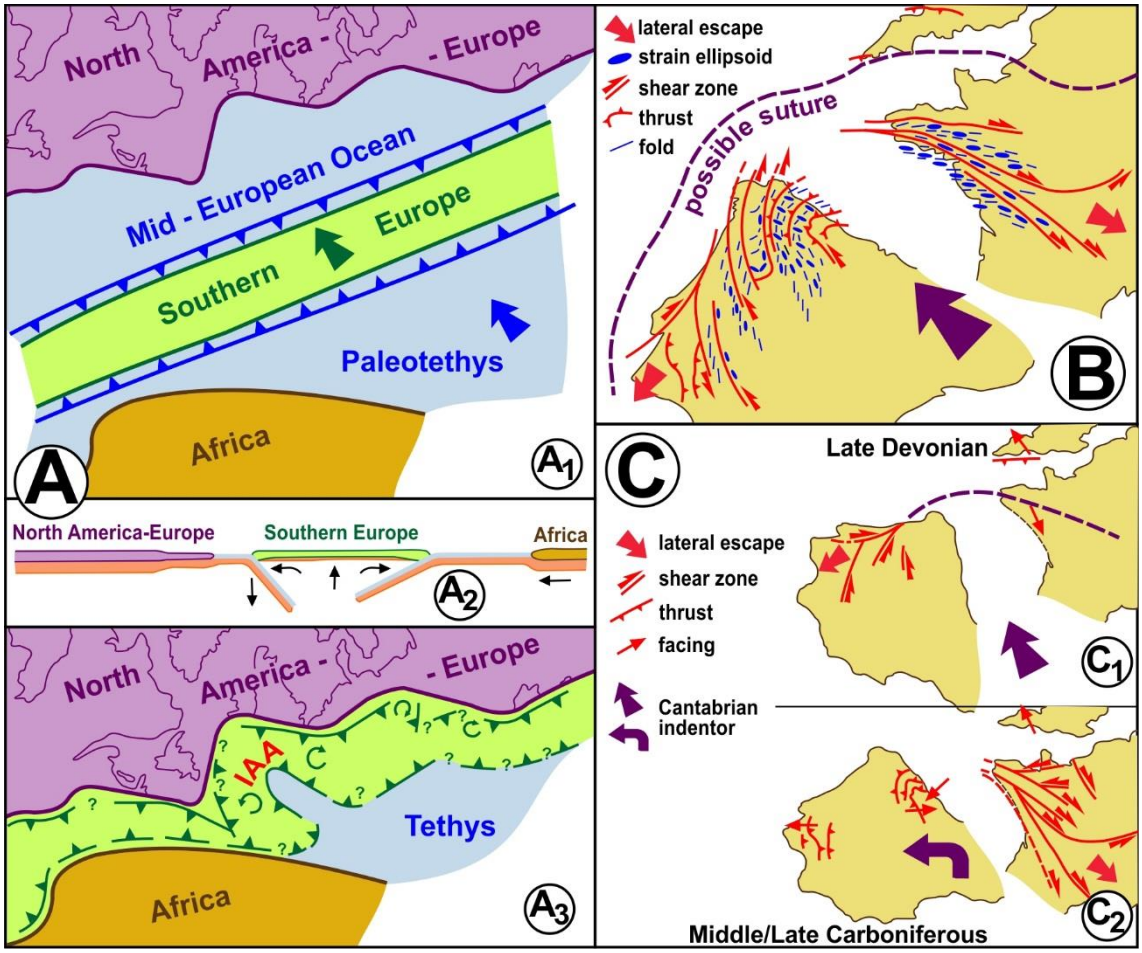

Figure 11 – Proposed models for the IAA formation in relation to major irregularities of continental margins:

A – Internal plastic distortion of the Southern Europe plate by the adjustment to irregular continental margins of large neighbouring plates (adapted from Lorenz and Nicholls, 1984);

B – Indentation related to one tectonic event (adapted from Matte and Ribeiro, 1982; Matte, 1991);

C – Indentation during two tectonic events (adapted from Dias and Ribeiro, 1995a).

An alternative approach considers the IAA the result of a wrapped Southern Europe microplate around a rigid indentor of northern margin of a major Africa plate. Using the opposed kinematics of the NW-SE sinistral shear zones in Iberia and the E-W dextral ones in Brittany, coupled with the Variscan finite strain pattern (orthogonal to the main structures in the core of the arc, and longitudinal in the more external domains) the IAA was explained (Matte and Ribeiro, 1975) as the result of an indentation process giving rise to a thin skinned arc with centripetal vergences (Fig. 11B). Although in this model the arc is essentially the result of a tectonic process, it was suggested that the deformed Palaeozoic basins and their boundary basement faults could have some initial curvature. This early indentation model also did not take into account the diachronism between shearing events in northern and southern branches of the arc (Audren *et al.*, 1976). Nevertheless, similar models were often used in later works where the arcuation was due, either to the impingement of a promontory of the African continent (Matte and Burg, 1981; Matte, 1991) or to the more rigid behaviour of the West African Precambrian craton (Lefort, 1989; Lefort and Van der Voo, 1981).

In order to account for the age disparity between the Iberia and Armorican shears, a two stage indentation model was presented (Dias and Ribeiro, 1995b; Ribeiro *et al.*, 1995). During Upper Devonian (Fig. 11C_1) the northward displacement of the Gondwana indentor produced NW-SE sinistral transpression in Iberia and almost orthogonal collision farther north, either towards NNW (Lizard obduction in southwest Britain) or SE (Bretonic phase in the Armorican Massif). The collision of Iberia with the irregular southern margin of Laurentia/Baltica induced an anticlockwise rotation of Iberia during Late Carboniferous tightening the arc. This led to a change in the deformation regime in the IAA; in the northern branch dextral strike-slip shear zones were predominant, while in Iberia thrusts overprinted previous structures (Fig. 11C_2). This model not only explains the differences in the structural behaviour between both branches during Devonian / Carboniferous times, but also the younger origin of the CA. Moreover, it is still consistent with the recent data concerning the southern Pulo do Lobo domain (located in the boundary between Ossa-Morena and South Portuguese Zones), which indicates it was a Southern Uplands terrane displaced along a major sinistral shear zone in Early to Middle Devonian times due to the indentation of the Iberian promontory in the British Caledonides (Braid *et al.*, 2011).

It has recently been it was proposed that the Cantabrian orocline was due to the westward drift of the Pyrenees between a major dextral E-W northern fault and the left-lateral shear system of inner Iberia during Late Carboniferous (Sengör, 2013). As in the early indentation models (Matte and Ribeiro, 1975) this also presents the major problem of diachronism between the NW-SE sinistral shears and the dextral E-W ones.

IX.2.4.2.2. Arcs controlled by Major Strike-Slip Shear Zones

Several models consider the formation of Iberian Variscan arcs mostly the result of the movement along major strike-slip shear zones. Slip on wrench faults could induce pronounced curvature of fold-thrust belt (Marshak, 1988; Macedo and Marshak, 1999), as the Cenozoic South Island orocline in New Zealand (Sutherland, 1999; Hall *et al.*, 2004). Such process could result, either from a younger fault overprinting a previous belt, or from the fact that the movement on the fault and the growing belt are contemporaneous (Marshak, 2004).

One of the first proposals (Ries and Shackleton, 1976) considered the IAA a secondary arc due to a counter-clockwise rotation of Iberia relative to Brittany, with the amount of rotation around the arc increasing southwards in direction to a supposed transform fault (Fig. 12A). Such simple mechanism, in spite of explaining the arcuate shape and the finite strain contrast between the inner and the external domains of the arc (Fig. 5A), is unable to explain the main regional sinistral shear of northern CIZ (Fig. 5B). Moreover, it only considered one tectonic event, which is incapable of explaining the variability of deformation observed in both branches of the IAA.

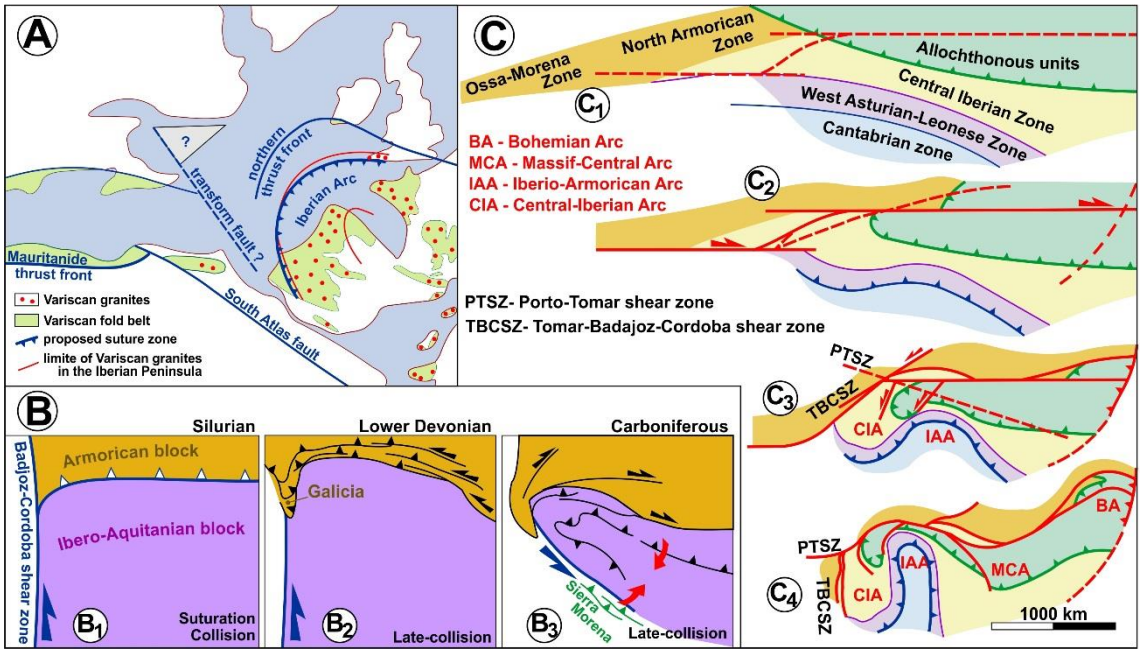

Figure 12 – Proposed models for the IAA formation in relation to major strike-slip shear zones:

A – Iberian rotation in relation with a major E-W transform fault (adapted from Ries and Shackleton, 1976);

B – The predominance of the Badajoz-Cordoba shear zone (adapted from Brun and Burg, 1982; Burg *et al.*, 1987);

C – The major role of E-W major shears (adapted from Martínez Catalán, 2011c).

Later models mostly explore the role of major TBCSZ and PTFASZ Iberian shear zones (Fig. 1). One of the early approaches (Brun and Burg, 1982; Burg *et al.*, 1987) considers a long-lasting interaction between the TBCSZ and an E-W southwards dipping intra-oceanic subduction zone, related to the emplacement of the Limousin ophiolites. During oceanic subduction the TBCSZ behaves has a sinistral transform fault (Fig. 12B_1). With the collision of the two continents In Lower Devonian, the deformation becomes intra-continental increasing the interaction transform fault / continental subduction. As the subduction of the continental crust is limited, a so-called "corner effect" was produced at the intersection of the transcurrent shear zone and the thrust zone (Fig. 12B_2). During Carboniferous collision, the intra-continental deformation increases the previous incipient curvature (Fig. 12B_3). This tightening of the arc is coeval of the foreland thrusting on its core and of the important dextral and sinistral shearing on the outer Armorican and Iberian domains. This model has the main advantage of considering two main stages with different kinematics for the Devonian and Carboniferous deformation. Nevertheless, the correlation between the different tectonostratigraphic zones of the southern and northern limbs of the arcs is difficult to explain.

A different proposal relates the formation of the IAA with a 4000-5000 km dextral displacement of Laurentia around northern Gondwana during closure of the Rheic and the formation of Pangaea (Shelley and Bossière, 2000; 2002). The arc was formed, either by wrapping the mobile dextral transpressive shear belt around a rigid Iberian basement block (Shelley and Bossière, 2000), or counter clockwise rotation of the south-western part of Iberia around a possible extensional bend of the major dextral shears (Shelley and Bossière, 2002). Whatever the options, they do not exclude some indentation of an Iberian promontory synchronous of the major dextral transpressive shearing. Such idea is questionable, because oblique indentation originates asymmetric arcs (Marshak, 2004), which is not the case. Even if one does not question the existence of the proposed huge shear for the Variscan Fold Belt origin (a highly debatable topic; *e.g.* Stampfli and Borel, 2002), some assumptions are difficult to accept. One is the proposal that the sinistral faults of Iberia (*e.g.* the TBCSZ) are bookshelf-type related to the dextral shearing along the PTFASZ, considered the most important shear zone of Iberian Variscides, because it does not explain the pervasive D_1 sinistral kinematics in northern sectors of the CIZ. As they assume some part of the arcuation is primary, the degree of bending of the arc should be much less than the estimated using recent paleomagnetic data (section 3.4; Weil *et al.*, 2013).

A recent model (Martínez Catalán, 2011c; Martínez Catalán *et al.*, 2014) also relates the formation of the Iberian arcs with major E-W dextral shearing but only during Middle to Upper Carboniferous (Fig. 12C). This approach does not only explain the formation of the arcuate

geometry and the correlation between the different variscan domains, but also the paleomagnetic behaviour established in the CA (Weil *et al.*, 2013). The deformation starts with the emplacement of the allochthonous nappes oblique to the zones in the autochthon (Fig. $12C_1$) giving rise to the thickening of the northern Gondwana continental margin. The tectonic setting changes with the onset of two major E-W right-lateral strike-slip faults with a stair-case geometry (Fig. $12C_2$). The evolution of the previous pattern gave rise to the bending of the wrench system in the sector where the major shears overlap, creating a restraining bend forming the CIA as a fault-bend or a fault-propagation fold. Subsequent movement along dextral major shears induced domino-style antithetic structures (Fig. $12C_3$), explaining the last motion along the TBCSZ. Such event was superposed on the pre-existing CIA and is older than the PTFASZ. Finally, the tightening of the IAA (Fig. $12C_4$), occurred due to the counter clockwise ductile rotation of the bounding shear zones to the west (TBCSZ) and to the east (Moldanubian thrusts), perhaps because their orientation was no longer able to allow the gliding of the blocks. The formation of the Bohemian and Massif Central arcs was produced during this last intra-continental deformation. The major problems with the previous model is, not only the existence of the highly dubious CIA, but also the assumption that all the Variscan deformation in Iberia has a Middle to Upper Carboniferous age.

IX.2.4.2.3. Arcs Related to Lithospheric Delamination

A different approach was recently proposed mostly based on the location of the CA in the core of Pangaea supercontinent precisely, on the western tip of Paleotethys (Fig. $13A_1$). If the first proposals only considered the CA (Gutiérrez-Alonso *et al.*, 2004; 2008; Fig. $13A_2$), soon these models evolved to include also the CIA with a "S" general pattern for the paired oroclines (Gutiérrez-Alonso *et al.*, 2011; 2012; Johnston *et al.*, 2013; Weil *et al.*, 2013; Fig. $13A_3$).

In spite of some variations, these models have always considered two tectonic events (Fig. 13B). During Carboniferous the closure of Rheic Ocean between Gondwana and Laurussia, due to an E-W shortening (in present-day coordinates), produces a N-S linear orogen facing East (Fig. $13B_1$). Close to the Permian-Carboniferous boundary (from 315 to 299 Ma) the shortening becomes N-S inducing orocline buckling around a vertical axis (Fig. $13B_2$). From the early works concerning the IAA (Matte and Ribeiro, 1975; Ries and Shackleton, 1976), the resultant strain field was considered to be close to tangential longitudinal strain leading to strong space problems in the inner arc (Fig. 13C). The extensive magmatism coeval of the CA formation was considered to reflect a thick-skinned process with the involvement of all the lithosphere (Gutiérrez-Alonso *et al.*, 2004; 2008; 2011; Fig. $13D_1$). The outer arc extension and the inner

arc compression gave rise to a strong lithospheric thinning in the outer arc coupled with a strong thickening in the CA core. The continuity of the process induced delamination of the mantle lithosphere under the core of the CA, solving some space problems (Fig. 13D$_2$).

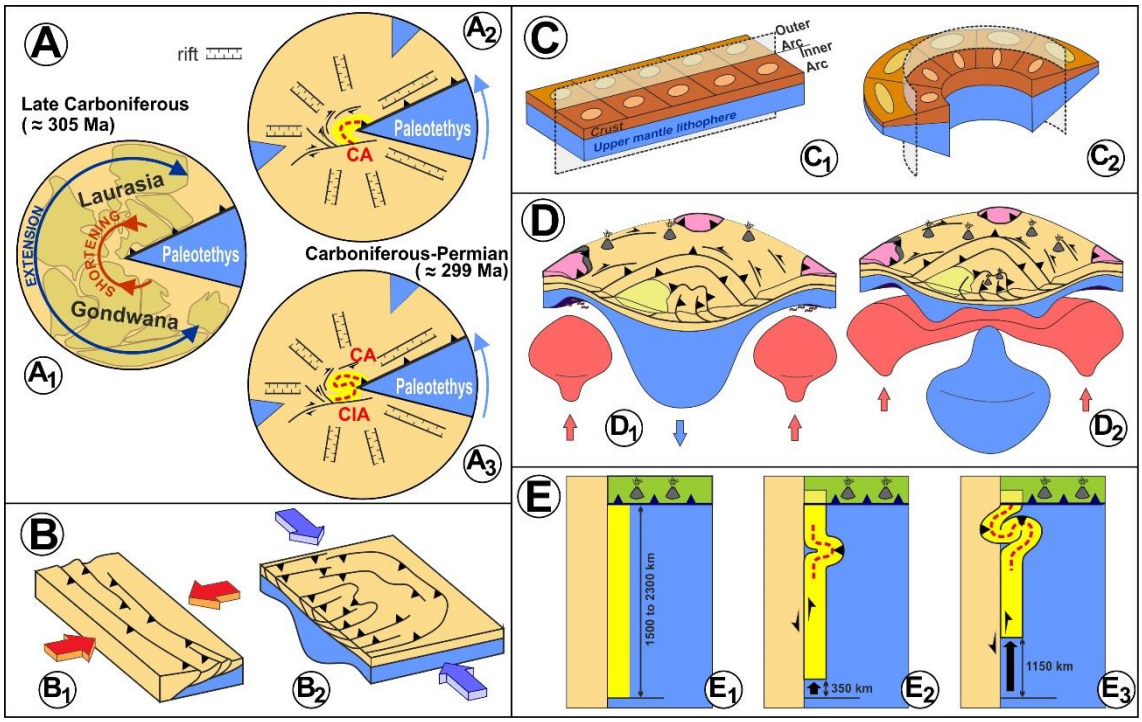

Figure 13 – Proposed models for the IAA formation by lithospheric delamination:

A – Schematic diagrams showing simplified Pangaea reconstructions (adapted from Gutiérrez-Alonso *et al.*, 2012; Johnston *et al.*, 2013);

B – Stress rotation inducing secondary Cantabrian orocline formation by buckling (adapted from Johnston *et al.*, 2013; Weil *et al.*, 2013);

C – Neutral surface model (adapted from Gutiérrez-Alonso *et al.*, 2012; Weil *et al.*, 2013);

D – Schematic block diagram illustrating Cantabrian orocline development (adapted from Gutiérrez-Alonso *et al.*, 2012; Weil *et al.*, 2013);

E – Geometric tectonic model for secondary development of coupled orocline (adapted from Johnston *et al.*, 2013).

Despite always coupling the CA and CIA, these models never discuss how to solve the space problems in the southern CIA. Another major problem concerns the mechanism that has induced a 90º rotation of the major compression from normal to subparallel to the orogenic belt. This is not an easy task and several mechanisms have been proposed:

- The so-called self subduction of Pangaea (Gutiérrez-Alonso *et al.*, 2004; 2008 Fig. 13A$_2$) where the Upper Carboniferous compressive stress field inside the plate was induced by

the oceanic margin of a continent being subducted beneath the continental edge at the other end of the same plate.

- The buckling of a ribbon continent between Laurussia and Gondwana during the final amalgamation of Pangaea (Johnston and Gutierrez-Alonso, 2010; Weil *et al.*, 2010; Fig. 13E).

If in the first case a possible explanation for the strong reorientation of the stress field was advanced, in the second, the rotation of the very long (at least 1500 km) Cantabrian - Central Iberian ribbon continent from the Early Palaeozoic E-W trend to its N-S pre-orocline position during the Late Carboniferous is unclear (Shaw *et al.*, 2014).

However the rotation mechanism isn't the only problematic situation (Sengör, 2013):

- There are frequent Late Carboniferous - Permian E-W dykes, showing that σ_1 (maximum compression) is oriented E-W and not N-S, as predicted by the models.

- Lithostratigraphic arguments show that the core of the CA was never very high as it should be expected in a region above a delaminated lithospheric mantle.

- The Early Permian volcanics which have been considered in NW Iberia induced by the lithospheric detachment are not exclusive of this region, being characteristic of the entire Late Variscan magmatism of Europe.

- It is difficult to explain the preservation of the highest supracrustal sedimentary rocks in the core of the Cantabrian orocline, if a lower lithospheric detachment has occurred.

IX.2.5. A Unifying Approach

Any discussion of Iberian arcs models must take into account some major constraints:

- There is no evidence concerning the existence of the CIA and so, only the IAA and the CA should be considered.

- The age of the first and main Variscan tectonic event is at least middle Devonian in the inner domains of the Iberian Variscides and it propagates towards its external domains where it has an Upper Carboniferous age (Fig. 5).

- Although the data show that the CA was formed during Carboniferous / Permian (*e.g.* Weil *et al.*, 2013), this does not mean that the IAA has a coeval formation, representing an earlier stage of arc generation.

- The E-W trend of the axial planes of IAA and CA was used to deduce a N-S major compressive stress, inducing orocline buckling around a vertical axis (Fig. $13B_2$). However, the same geometry could be obtained by bending (Hobbs *et al.*, 1976; Twiss and Moores, 1992). So, a westwards indentation is also compatible with the CA data, and it is going to be used here because it is more able to explain the observed features.

- Although recent models concerning the Variscan evolution mostly focus on Rheic Ocean without considering an Armorica plate, the existence of a Paleotethys / Galicia - Massif Central Ocean is well established in Brittany and is going to be used (Fig. 14).

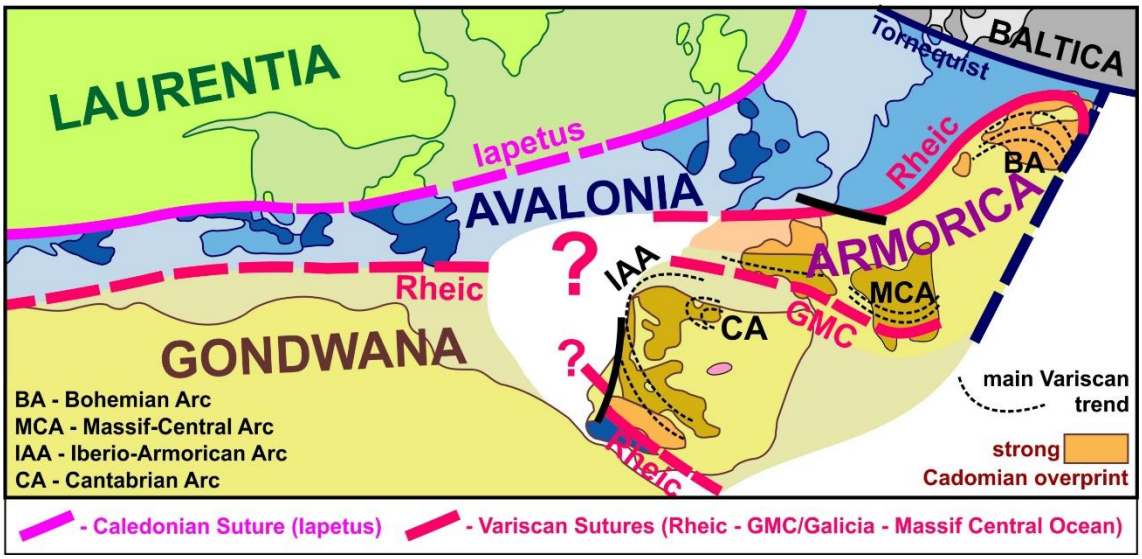

Figure 14 – Major plates and Palaeozoic sutures in the vicinity of the IAA on an Early Mesozoic reconstruction of the North Atlantic (adapted from Matte, 2001; Ribeiro *et al.*, 2007; Ballèvre *et al.*, 2009; Nance *et al.*, 2012).

The previous assumptions have been integrated in a general model. In Upper Ediacarian, oblique subduction below the northern margin of Gondwana gives rise to the Cadomian arc-continent collision (Fig. 15A). The sectors closer to the trench were strongly deformed, being included in the so-called Cadomia microplate (Linnemann *et al.*, 2008; Nance *et al.*, 2012). During Lower Palaeozoic stretching predominates in this continental margin, inducing a widespread thinning. In Lower / Middle Cambrian, Avalonia began to drift (Linnemann *et al.*, 2008) due to the opening of Rheic Ocean (Fig. 15B), mostly following an old Neoproterozoic suture (Murphy *et. al.*, 2006). Farther north, the subduction of Iapetus below Laurentia compensate the widening of Rheic and the continuous stretching in northern margin of Gondwana (Fig. 15C), giving rise to the Iberia and Armorica paleogeographic domains (Fig. 1). The position of these domains is difficult to establish due to the intense Variscan deformation of Peri-Gondwana Terranes during Pangaea assemblage.

Another ribbon continent, Armorica, began to be isolated from Gondwana due to the opening of Galicia-Massif Central Ocean (Fig. 15D; Matte, 2001; Ballèvre, 2013). Such opening could be related to the subduction of the Rheic below the northern margin of Armorica (Ribeiro *et al.,* 2007). Due to the obliquity between previous paleogeographic zones and the

major trend of this new ocean, some of the zones appear in both margins, while others are restricted to the Iberian side (*i.e.* CZ and WALZ).

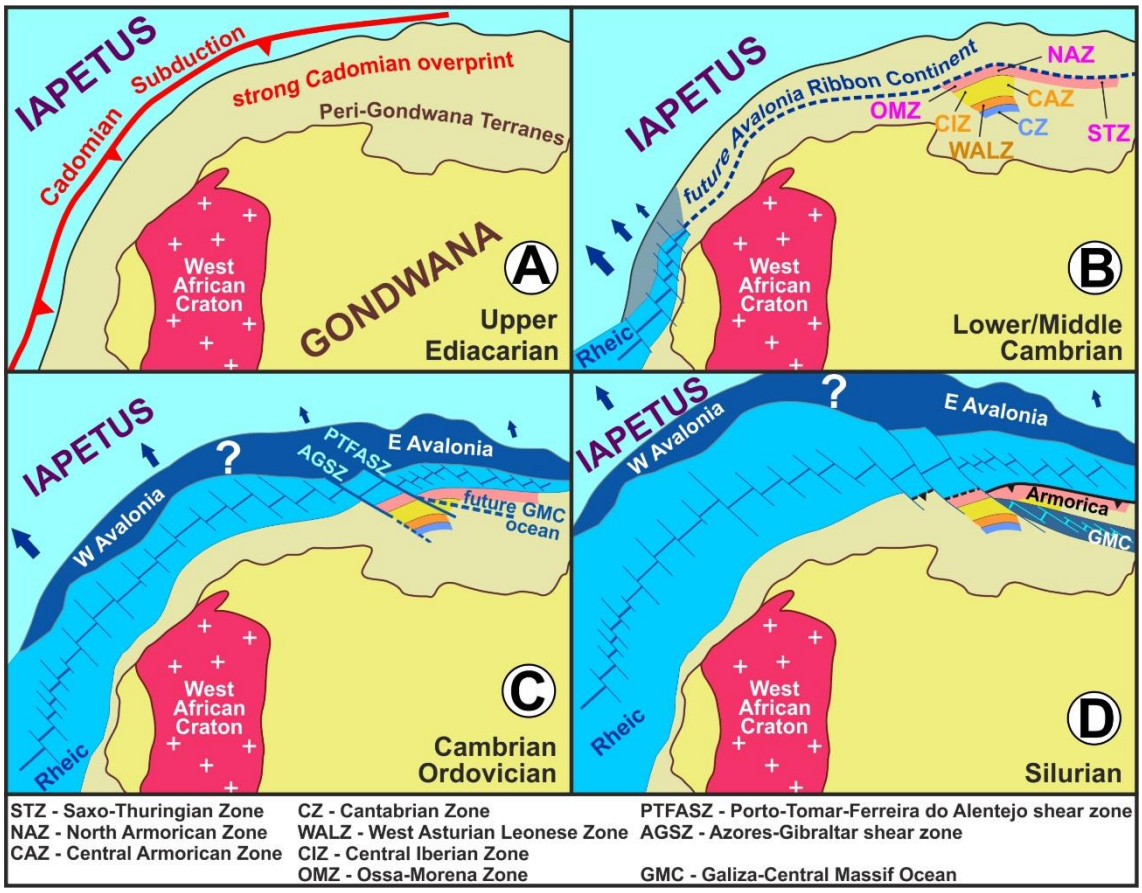

Figure 15 – Schematic Lower Palaeozoic evolution of northern margin of Gondwana (adapted from Matte, 2001; Linnemann, *et al.,* 2008; Nance *et al.*, 2012).

A – The Cadomian Arc during Upper Ediacarian;

B – Individualization of Avalonia by the opening of Rheic Ocean;

C – The northward drift of Avalonia due to widening of Rheic;

D – The drift of Armorica due to the Galicia-Massif Central Ocean.

During Devonian / Carboniferous the convergence of the continents to form Pangaea led to a strong inversion of initial basins. In the Devonian, the subduction of Variscan oceans produce (Fig. 16A) an almost orthogonal thrust tectonics in the Brittany branch (Burg *et al.*, 1987; Dias and Ribeiro, 1995b), with sense of movement either towards the NNW (Lizard obduction in southwest Britain) or SE (Bretonic phase in the Armorican Massif). At the same time in Iberia due to the interaction between the subduction of the Rheic and the wavy northern Gondwana margin an oblique collision occurs, inducing the predominance of a sinistral transpressive regime. Due to the location of the Iberian suture in the external boundary of OMZ, the deformation propagates from there towards the CZ (Fig. 5). However,

due to a strong strain partitioning, the Devonian deformation in Iberia was very heterogeneous, with regions where sinistral transpression was predominant, adjacent to regions deformed by almost pure compression (Dias and Ribeiro, 1994; 1995b; Dias *et al.*, 2013b). This explains the coexistence of regions dominated by almost a pure thrusting tectonics, like happens in ZOM (e.g. Simancas *et al.*, 2003 and references therein).

In Early Carboniferous the tectonic setting is similar, but previous plate convergence has evolved to continental collision (Fig. 16B). The allochthonous units were then emplaced with the movement above the CIZ subparallel to the main D_1 structures, which were often reworked as lateral ramps (Rodrigues *et al.* 2005; 2013; Dias *et al.*, 2013b).

In the Upper Carboniferous / Lower Permian a drastic change occurs (Weil *et al.*, 2013). The irregular shape of the southern margin of Laurentia/Baltica block has probably induced an anticlockwise rotation of Iberia during the intra-continental deformation (Dias and Ribeiro, 1995b). Thus, in the northern branch of the IAA major dextral strike-slip shear zones occur, while in Iberia thrusts overprinted previous structures. Such process is not unusual and has already been proposed not only for the Variscan orogen (Lorenz and Nicholls, 1984), but also for the Alpine Himalayan Fold Belt (Treloar *et al.*, 1992) and the Oligocene collision between Africa and Euro-Asian plates (Carvalho *et al.*, 1983-85). The Cantabrian basement was displaced westwards producing indentation on the WALZ and CZ metasediments above the indenter, giving rise to a tight first order arcuate shape, the CA (Fig. 16C). A thin-skinned arc was produced with the major thrusts displaced towards E above a decollement located within the limestones and dolomites of the Lancara Formation of Lower-Middle Cambrian age (Pérez-Estaún and Bastida, 1990; Alonzo *et al.*, 2009). This indentation also affects the NW Iberian units, not only the allochthonous nappes but also the autochthon ones. The more open shape of this western thick-skinned IAA, reflects not only the higher metamorphic grade of the rocks of the inner domains of the Iberian Variscides, but also the greater distance to the indentor. Moreover, it should be stressed that the arcuate shape of this arc, between the NW-SE structures in Iberia, and the E-W ones in Brittany, did not represent a strong rotation of a previous liner belt, but two major trends of mostly independent structures that have been at a high angle in the early stages, and were slightly bent at a latter phase.

We are well aware that this model didn't take into account the interpretation of the axial zone of Tomar-Badajoz-Córdoba as an Eo-Variscan suture (Simancas *et al.*, 2001; Gomez Pugnaire *et al.*, 2003). However, we disagree with such interpretation, because we consider this structure is a Cadomian suture reactivated as a transpressive intraplate flower structure, for reasons exposed in detail elsewhere (Ribeiro *et al.*, 2007) and confirmed by recent geochronological data (Henriques *et al.*, 2015).

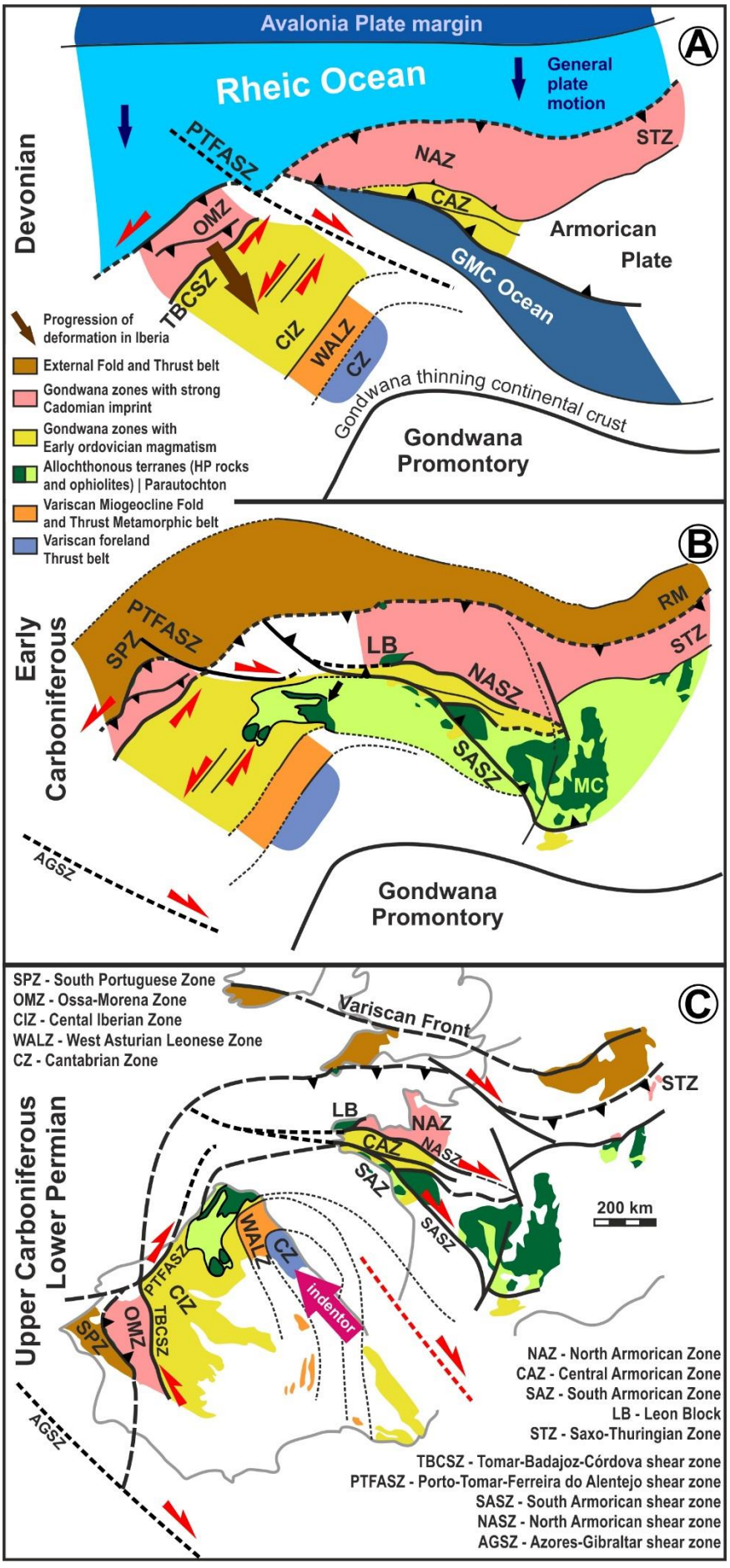
A
Avalonia Plate margin
Rheic Ocean
General plate motion
Devonian
PTFASZ
NAZ
STZ
CAZ
OMZ
Armorican Plate
GMC Ocean
TBCSZ
CIZ
WALZ
CZ
Gondwana thinning continental crust
Gondwana Promontory
Progression of deformation in Iberia
External Fold and Thrust belt
Gondwana zones with strong Cadomian imprint
Gondwana zones with Early ordovician magmatism
Allochthonous terranes (HP rocks and ophiolites) | Parautochton
Variscan Miogeocline Fold and Thrust Metamorphic belt
Variscan foreland Thrust belt
B
Early Carboniferous
PTFASZ
SPZ
RM
STZ
LB
NASZ
SASZ
MC
AGSZ
Gondwana Promontory
SPZ - South Portuguese Zone
OMZ - Ossa-Morena Zone
CIZ - Cental Iberian Zone
WALZ - West Asturian Leonese Zone
CZ - Cantabrian Zone
C
Variscan Front
Upper Carboniferous Lower Permian
STZ
LB
NAZ
CAZ
NASZ
SAZ
SASZ
200 km
WALZ
CZ
PTFASZ
CIZ
TBCSZ
OMZ
SPZ
indentor
AGSZ
NAZ - North Armorican Zone
CAZ - Central Armorican Zone
SAZ - South Armorican Zone
LB - Leon Block
STZ - Saxo-Thuringian Zone
TBCSZ - Tomar-Badajoz-Córdova shear zone
PTFASZ - Porto-Tomar-Ferreira do Alentejo shear zone
SASZ - South Armorican shear zone
NASZ - North Armorican shear zone
AGSZ - Azores-Gibraltar shear zone

Figure 16 – Schematic interaction between Avalonia / Armorica and northern Gondwana during Upper Palaeozoic (colours and abbreviations like in figure 1).

A –Convergence between Iberia and Armorica during Middle Devonian;

B –The collision stage with all the plates assembled;

C –The westward indentation of the Cantabrian basement and the formation of major Iberian Arcs.

References

Ábalos, B. (1992). Variscan shear-zone deformation of late Precambrian basement in SW Iberia: implications for circum-Atlantic pre-Mesozoic tectonics. J. Struct. Geol., 14(7), 807-823.

Ábalos, B., Carreras, J., Druguet, E., Viruete, J., Pugnaire, M., Alvarez, S., Quesada, C., Fernández, L., Gil-Ibarguchi J. (2002). Variscan and Pre-Variscan Tectonics. In: Gibbons, W., Moreno, M.T. (Eds.), The Geology of Spain. Geol. Soc. London, 155-183.

Aerden, D. (2004). Correlating deformation in Variscan NW-Iberia using porphyroblasts; implications for the Ibero-Armorican Arc. J. Struct. Geol., 26, 177-196.

Álvarez García, J. (2002). Análisis gravimétrico e isostético en el Macizo Hespérico. Diploma de Estudios Avanzados, Univ. Complutense de Madrid. 72 p.

Aramburu, C., Garcia-Ramos, J. (1993). La sedimentación Cambro-Ordovícica en la Zona Cantábrica (NO de España). Trab. Geol., 45-73.

Araújo, A., Piçarra de Almeida, J., Borrego, J., Pedro, J., Oliveira, J. T. (2013). As regiões central e sul da Zona de Ossa-Morena. In: Dias, R., Araújo, A., Terrinha, P., Kullberg, J.C. (Eds.), Geologia de Portugal (vol. 1). Escolar Editora, 509-549.

Arboleya, M. (1981). La estructura del manto del Esla (Cordillera Cantábrica, León). Bol. Inst. Geol. Min. Esp., XCII/I, 19-40.

Ardizone, J., Mezcua, J., Socías, I. (1989). Mapa Aeromagnético de España Peninsular 1:1.000.000. Instituto Geográfico Nacional, Madrid.

Arenas, R., Farias, P., Gallastegui, G., Gil Ibarguchi, J., González Lodeiro, F., Klein, E., Marquinez, J., Martin Parra, L., Martinez Catalán, J., Ortega, E., Pablo Macia, J., Peinado, M., Rodriguez Fernández, L. (1988). Características geológicas y significado de los dominios que componen la Zona de Galicia-Trás-os-Montes. Simposio sobre Cinturones Orogénicos, II Congresso de Geologia de España, Granada, 75-84.

Arenas, R., Díez Fernández, R., Sánchez Martínez, S., Gerdes, A., Fernández-Suárez, J., Albert, R. (2014). Two-stage collision: Exploring the birth of Pangea in the Variscan terranes. Gondwana Research, 25, 756–763.

Argand, E, 1924. La Tectonique de l'Asie. In: Proc. XIII Int. Geol. Congr., Brussels, 171-173.

Audren, C., Brun, J. Cobbold, P., Cogné, J., Iglésias, M., Jegouzo, P., Le Correm C., Le Metour, J., Le Théoff, N., Rabu, D. (1976). Données complémentaires sur la géométrie du plissement et sur les variations de forme et orientation de l'ellipsoïde de déformation dans l'arc Hercynien Ibéro-Armorican, Bol. Soc. Géol. Fr., XVIII, 757-762.

Azor, A., González Lodeiro, F., Simancas, J. (1994). Tectonic evolution of the boundary between the Central Iberian and Ossa-Morena zones (Variscan belt, southwest Spain), Tectonics, 13, 45–61.

Azor, A., Rubatto, D., Simancas, J.F., González Lodeiro, F., Martínez Poyatos, D., Martín Parra, L.M., Matas, J. (2008). Rheic Ocean ophiolitic remnants in southern Iberia questioned by SHRIMP U-Pb zircon ages on the Beja-Acebuches amphibolites. Tectonics 27, TC5006.

Ballèvre, M., Bosse, V., Ducassou, C., Pitra, P. (2009). Palaeozoic history of the Armorican Massif: Models for the tectonic evolution of the suture zones. C. R. Geoscience, 341, 174–201.

Ballèvre, M., Bosse, V., Dabard, M., Ducassou, C., Fourcade, S. (2013). Histoire Géologique du massif Armoricain : Actualité de la recherche. Bull. Soc. Géol. Min. Bretagne, D/10-11, 5-96.

Ballèvre, M., Martínez Catalán, J., López-Carmona, A., Pitra, P., Abati, J., Díez Fernández, R., Ducassou, C., Arenas, R., Bosse, V., Castiñeiras, P., Fernández-Suárez, J., Gómez Barreiro, J., Paquette, J., Peucat, J., Poujol, M., Ruffet, G., Sánchez Martínez, S. (2014). Correlation of the nappe stack in the Ibero-Armorican arc across the Bay of Biscay: a joint French–Spanish project. In: Schulmann, K., Martínez Catalán, J., Lardeaux, J., Janousek, V., Oggiano, G. (Eds.), The Variscan Orogeny: Extent, Timescale and the Formation of the European Crust. Geological Society, London, Special Publications, 405, 77–113.

Bard, J., Matte, P., Capdevila, R. (1971). Le structure de la Chaîne Hercynienne de la Meseta Ibérique: comparaison avec les segments voisins. Publ. Inst. Fr. Pétrole, Collections Coll. et Sémin., 22 (Histoire Structurale du Golfe de Gascogne, 1, 1-68.

Barrois, C. (1882). Recherches sur les Terrains Anciens des Asturies et de la Galice, Mémoires de la Société Géologique du Nord, 2, 630 p.

Bastida, F., Martínez Catalán, J., Pulgar, J. (1986). Structural, metamorphic and magmatic history of the Mondoñedo nappe (Hercynian belt, NW Spain). J. Struct. Geol., 8, 415–430.

Bastida, F., Aller, J., Pulgar, J., Toimil, N., Fernández, F., Bobillo-Ares, N., Menéndez, C. (2010). Folding in orogens: a case study in the northern Iberian Variscan Belt. Geol. J., 45, 597–622.

Bertrand, M. (1887). La Chaîne des Alpes et la formation du continent européen. Bull. Soc. Géol. France, 15(3), 423-447.

Bonhommet, N., Cobbold, P., Perroud, H., Richardson, A. (1981). Paleomagnetism and cross-folding in a key area of the Asturian Arc (Spain). Journal of Geophysical Research, 86, 1873–1887.

Braid, J., Murphy, J., Quesada, C., Mortensen, J. (2011). Tectonic escape of a crustal fragment during the closure of the Rheic: U-Pb detrital zircon data from the Late Palaeozoic Pulo do Lobo and South Portuguese zonas, southern Iberia. J. Geol. Soc. London, 168, 383-392.

Brun, J., Burg, J. (1982). Combined thrusting and wrenching in the Ibero-armorican arc — a corner effect during continental collision. Earth and Planetary Science Letters, 61, 319–332.

.Burg, J., Iglesias, M., Laurent, P., Matte. P., Ribeiro, A. (1981). Variscan intracontinental deformation: the Coimbra-Córdoba shear zone (SW Iberian Peninsula). In: Lister, G. S., Behr, H. J., Weber, K., Zwart, H. J. (Eds.), The effect of deformation on rocks. Tectonophysics, 78, 161-177.

Burg, J., Bale, P., Brun, J., Girardeau, J. (1987). Streching lineations and transport direction in the Ibero-Armorican Arc during the Siluro-Devonian collision. Geodinamica Acta, 1, 71-81.

Carey, S. (1955). The orocline concept in geotectonics. Proceedings of the Royal Society of Tasmania, 89, 255–288.

Carey, S. (1958). The tectonic approach to continental drift. In: S.W. Carey (Ed.), Continental Drift, a Symposium, Univ. Tasmania, 177-356.

Carvalho, A., Ribeiro, A., Cabral, J. (1983-85). Evolução paleogeográfica da bacia Cenozóica do Tejo-Sado. Bol. Soc. Geol. Portugal 24, 209-212.

Choubert, B. (1935). Recherche sur la genèse des chaînes paléozoïque et antécambriennes. Rev, Géogr. Phys. Géol. Dynam. 8(1), 1-50.

Cogné, J. (1967). L'Arc hercynien ibéro-armoricain. Publ. Inst. Fr. Pétrole, Collections Coll. et Sémin., 22 (Histoire Structurale du Golfe de Gascogne), 1, 1-23.

Cogné, J. (1971). Le massif Armoricain et sa place dans la structure des socles ouest européens: l'arc hercynien ibéro-armoricain. In Histoire structurale du Golfe de Gascogne. Editions Technip, Paris (ed. Debyser), I, 1-24.

Coke, C., Dias, R., Ribeiro, A. (2000). Evolução Geodinâmica da bacia do Douro durante o Câmbrico e o Ordovícico; um exemplo de sedimentação controlada pela tectónica. Comum. Inst. Geol. Min., 87, 5-12.

Coke, C., Dias, R., Ribeiro, A. (2003). Rheologically induced structural anomalies in transpressive regimes, J. Struct. Geol., 25/3, 409-420.

Conde, L. (1966). Direcções de correntes na base do Ordovícico do afloramento de Amêndia-Mação e sua importância paleogeográfica. Mem. Not., Publ. Mus. Lab. Geol. Univ. Coimbra. 61, 44-55.

Corretgé, L., Suarez, O., Galan, G. (1990). West Asturian-Leonese Zone; igneous rocks. In: Dallmeyer, R.D., Martínez García, E. (Eds.), Pre-Mesozoic Geology of Iberia. Springer-Verlag, Berlin, 115–128.

Dallmeyer, D., Martínez Catalán, J., Arenas, R., Gil Ibarguchi, J., Gutiérrez Alonzo, G., Farias, P., Bastida, F., Aller, J. (1997). Diachronous Variscan tectonothermal activity in the NW Iberian Massif: Evidence from $^{40}Ar/^{39}Ar$ dating of regional fabrics. Tectonophysics, 277, 307-337.

Dalziel, I. (1971). Evolution of the Scotia Arc. Nature, 233/5317, 246-252.

Dana, J. D. (1866). A texbook of geology. Philadelphia, Theodore Bliss, 354 p.

De Sitter, L. (1961). Le Précambrien dans le Chaîne Cantabrique. C. Rend. Soc. Géol. France, 9, 253 p.

De Wit, M. (1977). The evolution of the Scotia Arc as a Key to the reconstruction of southwestern Gondwanaland, Tectonophysics, 37(1-3), 53-81.

Dias da Silva, I. (2013). Geología de las Zonas Centro Ibérica y Galicia – Trás-os-Montes en la parte oriental del Complejo de Morais, Portugal/España. Ph. D. Thesis. Salamanca University, 389 p.

Dias R. (1998). Estrutura Varisca do autóctone do Terreno Ibérico, uma herança Precâmbrica?, Comun. Serv. Geol. Portugal, 85, 29-38.

Dias, R., Basile, C. (2013). Estrutura dos sectores externos da Zona Sul Portuguesa; implicações geodinâmicas. In: Dias, R., Araújo, A., Terrinha, P., Kullberg, J.C. (Eds.), Geologia de Portugal (vol. 1) Escolar Editora, 787-807.

Dias, R., Ribeiro, A. (1991). Finite-strain analysis in a transpressive regime (Variscan autochthon, NE Portugal). Tectonophysics, 191, 389-397.

Dias, R., Ribeiro, A. (1993). Porto-Tomar shear zone, a major structure since the begining of the Variscan orogeny. Comun. Serv. Geol. Portugal, 79, 29-38.

Dias, R., Ribeiro, A. (1994). Constriction in a transpressive regime: an example in the Ibero-Armoricain Arc. J. Struct. Geol., 16/11, 1543-1554.

Dias, R., Ribeiro, A. (1995ª). Caramulo region: a transition domain between trasnpressive constriction and plane strain in the Centro-Iberian zone. Gaia, Museu Nacional de História Natural, 11, 35-42.

Dias, R., Ribeiro, A. (1995b). The Ibero-Armorican arc: a collisional effect against an irregular continent? Tectonophysics, 246(1-3), 113-128.

Dias, R., Ribeiro, A. (1998). Interaction between major sinistral wrench faults and coeval folds in a variscan transpressive regime (NE Portugal), Comun. Serv. Geol. Portugal, 85, 19-27.

Dias, R., Ribeiro, A. (2008). Heterogeneous strain behaviour in competent layers during folding in transpressive regimes. Geodinamica Acta, 21(4), 219-229.

Dias, R., Ribeiro, A. (2013). O Varisco do sector norte de Portugal. In: Dias, R., Araújo, A., Terrinha, P., Kullberg, J.C. (Eds.), Geologia de Portugal (vol. 1), Escolar Editora, 59-71.

Dias, R., Mateus, A., Ribeiro, A. (2003). Strain partitioning in transpressive shear zones in the southern branch of the Variscan Ibero-Armorican Arc. Geodinamica Acta, 16, 119-129.

Dias, R., Araújo, A., Terrinha, P., Kullberg J. (Eds.) (2013a). Geologia de Portugal, Escolar Editora, vol. 1, Geologia Pré-Mesozóica de Portugal, 807 p.

Dias, R., Ribeiro, A., Coke, C., Pereira, E., Rodrigues, J., Castro, P., Moreira, N., Rebelo, J. (2013b). Evolução estrutural dos sectores setentrionais do autóctone da Zona Centro-Ibérica. In: Dias, R., Araújo, A., Terrinha, P., Kullberg, J.C. (Eds.), Geologia de Portugal (vol. 1), Escolar Editora, 73-147.

Díez Balda, M. (1986). El Complejo Esquisto-Grauváquico, las series paleozóicas y la estructura hercínica al Sur de Salamanca. Acta Salmanticensia, Sección Ciencias, Ediciones Universidad de Salamanca, Spain, 52, 162 p.

Díez Balda, M., Vegas, R. (1992). La estructura del Dominio de los pliegues verticales de la Zona Centro-Ibérica. In: Gutiérrez-Marco, J.C., Saavedra, J., Rábano, I. (Eds.), Paleozoico Inferior de Ibero-América, Universidad de Extremadura, 523-534.

Díez Balda, M., Vegas, R., González Lodeiro, F. (1990). Structure of the autochthonous sequences of Central Iberian-Zone. In: Dallmeyer, R. D., Martínez García, E. (Eds.), Pre-Mesozoic Geology of Iberia, Springer-Verlag, New York, 172–188.

Díez Balda, M., Martinez Catalán, J., Ayarza Arribas, P. (1995). Syn-collisional extensional collapse parallel to the orogenic trend in a domain of steep tectonics: the Salamanca Detachment Zone (Central Iberian Zone, Spain). J. Struct. Geol., 17, 163-182.

Díez Montes, A., Navidad, M., González Lodeiro, F., Martínez Catalán, J. (2004). Estratigrafia do Dominio del Ollo de Sapo. in: Vera, J. (Ed.), Geologia de España. SGE-IGME, Madrid, 69-75.

Dufréchoua, G, Harris, L., Corriveau, L. (2014). Tectonic reactivation of transverse basement structures in the Grenville orogen of SW Quebec, Canada: Insights from gravity and aeromagnetic data. Precambrian Research, 241, 61-84.

Du Toit, A. (1937). Our wandering continents: an hypothesis of continental drifting. Oliver and Boyd, Edinburgh, 366 p.

Eichelberger, N., McQuarrie, N. (2014). Three-dimensional (3-D) finite strain at the central Andean orocline and implications for grain-scale shortening in orogens, Geological Society of America Bulletin, 127(1-2), 87-112.

Escuder Viruete, J. (1998). Relationships between structural units in the Tormes gneiss dome (NW Iberian massif, Spain): geometry, structure and kinematics of contractional and extensional Variscan deformation. Geol. Rundschau, 87, 165-170.

Escuder Viruete, J., Arenas, R., Martinez Catalán, J. (1994). Tectonothermal evolution associated with Variscan crustal extension in the Tormes Gneiss Dome (NW Salamanca, Iberian Massif, Spain). Tectonophysics, 238, 117-138.

Escuder Viruete, J., Diez Balda, M., Rubio Pascual, F., González Casado, J., Barbero, L., Martínez Poyatos, D., Villar, P., Martínez Catalán, J. (2004). La extensión varisca tardiorogénica y las deformaciones tardías. In: Vera, J. (Ed.), Geología de España. SGE-IGME, Madrid, 87-92.

Expósito, I., Simancas, J., González Lodeiro, F., Azor, A., Martínez Poyatos D. (2002). Estructura de la mitad septentrional de la zona de Ossa-Morena: Deformación en el bloque inferior de un cabalgamiento cortical de evolución compleja, Rev. Soc. Geol. Esp., 15, 3–14.

Farias, P., Gallastegui, G., Lodeiro, F., Marquinez, J., Parra, L., Martínez Catalán, J., Macia, J., Fernandez, L. (1987). Aportaciones al conocimiento de la litoestratigrafia y estructura de Galicia Central. Mem. Mus. Labor. Miner. Geol. Fac. Ciênc. Univ. Porto, 1, 411-431.

Franke, W., Matte, P., Tait, J. (2005). Europe: Variscan orogeny. Encyclopedia of Geology (vol. 2). Elsevier, Oxford, 75–85.

Fernández, F., Aller, J., Bastida, F. (2007). Kinematics of a kilometric recumbent fold: The Courel syncline (Iberian massif, NW Spain). J. Struct. Geol., 29, 1650–1664.

Fernández-Suárez, J., Dunning, G., Jenner, G., Gutiérrez-Alonso, G. (2000). Variscan collisional magmatism and deformation in NW Iberia: constraints from U-Pb geochronology of granitoids. Journal of the Geological Society, London, 157, 565-576.

Fonseca, P., Munhá, J., Pedro, J., Rosas, F., Moita, P., Araújo, A., Leal, N. (1999). Variscan Ophiolites and High-Pressure Metamorphism in Southern Ibéria. Ophioliti, 24(2), 259-268.

Gibbons, W., Moreno, T. (Eds.), 2002. The Geology of Spain. Geological Society, London, 649 p.

Gómez Pugnaire, M., Azor, A., Fernández Soler, J., López Sánchez-Vizcaíno, V. (2003). The amphibolites from the Ossa-Morena/Central Iberian Variscan Suture (Southwestern Iberian Massif): geochemistry and tectonic interpretation. Lithos, 68, 23-42.

Gutiérrez-Alonso, G., Fernández-Suárez, J., Weil, A. (2004). Orocline triggered lithospheric delamination. Geological Society of America Special Paper, 383, 121–131.

Gutiérrez-Alonso, G., Fernandez-Suarez, J., Weil, A., Murphy, J.B., Nance, R.D., Corfu, F., Johnston, S. (2008). Self-subduction of the Pangaean global plate. Nature Geoscience, 1, 549–553.

Gutiérrez-Alonso, G., Murphy, B., Fernández-Suárez, J., Weil, A., Franco, M., Gonzalo, J. (2011). Lithospheric delamination in the core of Pangea: Sm–Nd insights from the Iberian mantle. Geology, 39(2), 155–158.

Gutiérrez-Alonso, G., Johnston, S., Weil, A., Pastor-Galán, D., Fernández-Suárez, J. (2012). Buckling an orogen: the Cantabrian orocline. GSA Today, 22, 4–9.

Gutiérrez Marco, J., San Jose, M., Pieren, A. (1990). Post-Cambrian Palaeozoic Stratigraphy of Autochthonous sequence, Central-Iberian Zone. In: Dallmeyer, R. D., Martínez Garcia, E. (Eds.), Pre- Mesozoic Geology of Iberia, Springer-Verlag, New York, 160 – 171.

Hall, L., Lamb, S., Mac Niocail, C. (2004). Cenozoic distributed rotational deformation, South Island, New Zealand. Tectonics, 23, TC2002, 1–16.

Harris, R. (2011). The Nature of the Banda Arc-Continent collision in the Timor region. In: Brown, D., Ryan, p. (Eds.), Arc-Continent Collision, Frontiers in Earth Sciences, Springer-Verlag, Berlin, 163-211.

Hirt, A., Lowrie, W., Julivert, M., Arboleya, M. (1992). Paleomagnetic results in support of a model for the origin of the Asturian arc. Tectonophysics, 213, 321-339.

Hobbs, B., Means, W., Williams, P. (1976). An outline of structural geology. John Wiley & Sons, Inc., New York. 571 p.

Iglésias, M., Ribeiro, A. (1981). La zone de cisaillement ductile de Juzbado (Salamanca) - Penalva do Castelo (Viseu); un linéament ancien réactivé pendant l'orogénèse hercynienne?. Comum. Serv. Geol. Portugal, 67(1), 89-93.

Johnston, S., Gutiérrez-Alonso, G. (2010). The North American Cordillera and West European Variscides: Contrasting interpretations of similar mountain systems. Gondwana Research, 17(2–3), 516–525.

Johnston, S., Weil, A., Gutiérrez-Alonso, G. (2013). Oroclines: thick and thin. Geol. Soc. Am. Bull. ,125(5-6), 643-663.

Julivert, M., Marcos, A. (1973). Superimposed folding and flexural conditions in the Cantabrian Zone (Hercynian Cordillera, NW Spain). American Journal of Science, 273, 353–375.

Julivert, M., Arboleya, M.L. (1984). Curvature increase and structural evolution of the core (Cantabrian Zone) of the Ibero-Armorican Arc. Sci. Géol. Bull., 37, 5-11.

Julivert, M., Martínez, F. (1983). Estructura de conjunto e visión global de la Cordillera Herciniana. In: Comba, J. A. (Coord.), Geologia de España, Libro Jubilar de J.M. Rios, IGME, 612-630.

Julivert, M., Fonteboté, J., Ribeiro, A., Conde, L. (1972). Mapa Tectónico de la Península Ibérica Y Baleares. 1:1 000 000. Instituto Geológico Y Minero de España. 113 p.

Julivert, M., Marcos, A., Pérez-Estaún, A. (1977). La structure de la Chaîne Hercynienne dans le secteur Ibérique de l'Arc Ibéro-Armoricain. La chaîne varisque d'Europe moyenne et occidentale, Colloque Int. CNRS, Rennes, 243, 429-440.

Julivert, M., Vegas, R., Rotz, J. Martínez Rius, A. (1983). La estructura de la extension SE de la Zona Centroiberica com metamorfismo de Bajo Grado. In: Comba, J. A. (Coord.), Geologia de España, Libro Jubilar de J.M. Rios, IGME, 477-490.

Keller, M., Bahlburg, H., Reuther, C. (2008). The transition from passive to active margin sedimentation in the Cantabrian Mountains, Northern Spain: Devonian or Carboniferous? Tectonophysics, 461, 414–427.

Lefort, J. (1979). Iberian–Armorican arc and Hercynian orogeny in western Europe. Geology, 7, 384–388.

Lefort, J. (1989). Basement correlation across the north Atlantic, Springer-Verlag, Berlin, 148 p.

Lefort, J., Van der Voo, R. (1981). A Kinematic Model for the Collision and Complete Suturing between Gondwanaland and Laurussia in the Carboniferous. The Journal of Geology, 89(5), 537-550.

Linnemann, U., Pereira, F., Jeffries, E., Drost, K., Gerdes, A. (2008). The Cadomian Orogeny and the opening of the Rheic Ocean: the diacrony of geotectonic processes constrained by LA-ICP-MS U/Pb zircon dating (Ossa Morena and Saxo-Thuringian Zones, Iberian and Bohemian Massifs). Tectonophysics, 461, 21-43.

Llana-Fúnez, S., Marcos, A. (2001). The Malpica-Lamego line: A major crustal-scale shear zone in the Variscan Belt of Iberia. J. Struct. Geol., 23, 1299-1312.

Llana-Fúnez, S., Marcos, A. (2002). Structural record during exhumation and emplacement of high-pressure-low to intermediate-temperature rocks in the Malpica-Tui (Variscan Belt of Iberia). In: Martínez Catalán, J.R., Hatcher. R., Arenas. D.R., Díaz Garcia, F. (Eds.) Variscan-Appalachian dynamics: the building of the late Palaeozoic basement. Geol. Soc. Am., Boulder, Colorado, Special Paper, 364, 125-142.

Lorenz, V. (1976). Formation of Hercynian subplates. Possible cause and consequences. Nature, 262, 374–377.

Lorenz, V., Nicholls, I. (1984). Plate and intraplate processes of Hercynian Europe during the Late Paleozoic. Tectonophysics, 107, 25-26.

Lotze, F. (1945). Zur Gliederung der Varisziden der Iberischen Meseta. Geotektonische Forschungen, 6, 78-92.

Lotze, F. (1956). Das Präkambrium Spaniens. Neues Jahrb Geol Paläontol Monatsh, 8, 599-612.

Lotze, F. (1963). Vie Varischischen Gebirgszusammenhägne im Westlichen Europe. Giornale di Geol., sér. 2, 31, 393-412.

Maas, K. (1974). The geology of Liebana, Cantabrian Mountains, Spain: deposition and deformation in a flysch area. Leidse Geol. Meded., 49, 379-465.

Macaya, J. (1981). Estudio geológico estructural de la Sierra de Francia (Provincia de Salamanca y Cáceres). Cuadernos Geología Ibérica, 7, 567-576.

Macedo, J., Marshak, S. (1999). Controls on the geometry of fold-thrust belt salients. Geological Society of America Bulletin, 111, 1808–1822.

Machado, G., Hladil, J., Koptíková, L., Fonseca, P., Rocha, F., Galle, A. (2009). The Odivelas Limestone: Evidence for a Middle Devonian reef system in western Ossa-Morena Zone. Geologica Carpathica, 60(2), 121-137.

Machado, G., Hladil, J., Koptikova, L., Slavik, L., Moreira, N., Fonseca, M., Fonseca, P. (2010). An Emsian-Eifelian Carbonate-Volcaniclastic Sequence and the possible Record of the basal choteč event in western Ossa-Morena Zone, Portugal (Odivelas Limestone), Geologica Belgica, 13(4), 431-446.

Marcos, A. (2004). Zona Asturoccidental -Leonesa. In: Vera, J. (Ed.), Geologia de España. SGE-IGME, Madrid, 49.

Marcos, A., Pulgar, J. (1982). An Approach to the tectonostratigraphic evolution of the Cantabrian foreland thrust and fold belt, Hercynian Cordillera of NW Spain. Neues Jahrb. Geol. Palaeontol., Abh., 163(2), 256-260.

Marcos, A., Martínez Catalán, J., Gutiérrez-Marco, J., Pérez-Estaún, A. (2004). Estratigrafia y paleogeografia da Zona Asturoccidental-Leonesa. In: Vera, J. (Ed.). Geologia de España. SGE-IGME, Madrid, 49-52.

Marshak, S. (1988). Kinematics of orocline and arc formation in thin-skinned orogens. Tectonics, 7, 73–86.

Marshak, S. (2004). Salients, recesses, arcs, oroclines, and syntaxes - A review of ideas concerning the formation of map-view curves in fold-thrust belts. In K. R. McClay (Ed.), Thrust tectonics and hydrocarbon systems, AAPG Memoir, 82, 131 – 156.

Marquínez, J. (1978). Estudio geológico del sector SE de los Picos de Europa (Cordillera Cantábrica, NW de España). Trab. Geol. Univ. Oviedo, 10, 295-315.

Martínez Catalán, J. (1985). Estratigrafía y estructura del Domo de Lugo (sector W da zona Asturoccidental-Leonesa). Corpus Geol. Gallaeceae (2ª serie), 2, 1-291.

Martínez Catalán, J. (1990). West Asturian-Leonese Zone: Introduction. In: Dallmeyer, D., Martinez Garcia, E. (Eds.), Pre-Mesozoic Geology of Iberia. Springer-Verlag, 91.

Martínez Catalán, J. (2011a). The Central Iberian arc: implications for the Iberian Massif. Geogaceta, 50/1, 7-10.

Martínez Catalán, J. (2011b). The Central Iberian arc, an orocline centered in the Iberian Massif and some implications for the Variscan belt. Int. J. Earth Sc., 101, 1299–1314.

Martínez Catalán, J. (2011c). Are the oroclines of the Variscan belt related to late Variscan strike-slip tectonics? Terra Nova, 23, 241–247.

Martínez Catalán, J., Pérez Estaún, A., Bastida, F., Pulgar, J., Marcos, A. (1990). West Asturian-Leonese Zone; structure. In: Dallmeyer, R.D., Martínez García, E. (Eds.), Pre-Mesozoic Geology of Iberia, Springer-Verlag, Berlin, 103–114.

Martínez Catalán, J., Hacar Rodrguez, M., Villar Alonzo, P., Pérez Estaún, A., González Lodeiro, F. (1992). Lower Paleozoic extensional tectonics in the limit between the West Asturian-Leonese and Central-Iberian Zones of the Variscan Fold Belt in NW Spain. Geol. Rundschau, 85, 545-560.

Martínez Catalán, J., Martínez Poyatos, D., Bea, F. (2004). Introducción to Zona Centroibérica. in: Vera, J., (Ed.), Geología de España. SGE-IGME, Madrid, 68-69.

Martínez Catalán, J., Fernández-Suárez, J., Meireles, C., González Clavijo, E., Belousova, E., Saeed, A. (2008). U-Pb detrital zircon ages in synorogenic deposits of the NW Iberian Massif: interplay of syntectonic sedimentation and thrust tectonics. Journal of the Geological Society of London, 165, 687-698.

Martínez Catalán, J., Rubio Pascual, F., Díez Montes, A., Díez Fernández, R., Barreiro, J., Dias da Silva, I., Clavijo, E., Ayarza., P., Alcock, J. (2014). The late Variscan HT-LP metamorphic event in NW and Central Iberia: relationships to crustal thickening, extension, orocline development and crustal evolution. In: Schulmann, K., Martínez Catalán, J., Lardeaux, J., Janousek, V., Oggiano, G. (Eds.), The Variscan Orogeny: Extent, Timescale and the Formation of the European Crust. Geol. Soc. London, Sp. Publ., 405, 225-247.

Martínez Poyatos, D. (2002). Estructura del borde meridional de la Zona Centroibérica y su relación con el contacto entre las zonas Centroibérica y de Ossa-Morena. Laboratorio Xeologico de Laxe, Serie Nova Terra, 18, 295 p.

Martínez Poyatos, D., Díez Balda, M., Macaya, J., González Lodeiro, F., Martínez Catalán, J., Vegas, R. (2004). El acortamiento varisco inicial del Dominio del Complejo Esquisto-grauváquico. In: Vera, J. (Ed.), Geologia de España. SGE-IGME, Madrid, 84-87.

Matte, Ph. (1968). La structure de la virgation hercynienne de Galice (Espagne). Revue de Géologie Alpine, 44, 155-280.

Matte, Ph. (1986). Tectonics and Plate Tectonics Model for the Variscan Belt of Europe. Tectonophysics, 126, 329-374.

Matte, Ph. (1991). Accretionary history and crustal evolution of the Variscan belt in Western Europe. Tectonophysics, 196, 309-337.

Matte, Ph. (2001). The Variscan collage and orogeny (480-290 Ma) and the tectonic definition of the Armorica microplate: a review. Terra Nova, 13, 122-128.

Matte, Ph. (2002). Variscides between the Appalachians and the Urals: similarities and differences between Palaeozoic subduction and collision belts. In: Martínez Catalán, J., Hatcher, R., Arenas R., Díaz Garcia, F. (Eds.) Variscan-Appalachian dynamics: the building of the late Paleozoic basement. Geol. Soc. Am., 364, 239-251.

Matte, Ph., Burg, J. (1981). Sutures, thrusts and nappes in the Variscan arc of western Europe: Plate tectonics interpretation. In: McClay, K. R., Price, N. J. (Eds.), Thrust and Nappe Tectonics, Geol. Soc. London, Spec. Publication, 8, 353-358.

Matte, Ph., Ribeiro, A. (1975). Forme et orientation de l´ellipsoïde de déformation dans la virgation hercynienne de Galice. Relations avec le plissement et hypothèses sur la genèse de l´arc ibéro-armoricain. C. R. Académie Sciences Paris, D/280, 2825-2828.

Mendes Victor, L., Miranda, M., Matias, L. (1993). Crustal structure of western Iberia from geophysical studies. Publ. Inst. Geog. Nac. España, Série monográfica, 10, 179-196.

Metodiev, D., Romão, J., Dias, R., Ribeiro, A. (2009). Sinclinal de Vila Velha de Ródão (Zona Centro-Ibérica, Portugal): litostratigrafia, estrutura e modelo de evolução da tectónica Varisca. Comunicações Geológicas, 96, 5-18.

Miranda, M. (1990). O levantamento aeromagnético de Portugal - contribuição para o conhecimento da estrutura geológica do continente português. Ph. D. Thesis, Lisbon University, 146 p.

Miranda, M., Mendes Victor, L. (1990). Aeromagnetic Map of Portugal, 1/1 000 000. Serv. Geol. Portugal.

McKerrow, W., Ziegler, A. (1972). Paleozoic oceans. Nature (London), Phys. Sci., 240, 92-94.

Moreira, N., Búrcio, M., Dias, R., Coke, C. (2010a). Partição da deformação Varisca nos sectores de Peso da Régua e Vila Nova de Foz Côa (Autóctone da Zona Centro Ibérica). Comunicações Geológicas, 97, 147-162.

Moreira, N., Machado, G., Fonseca, P., Silva, J., Jorge, R.., Mata, J. (2010b). The Odivelas Palaeozoic volcanosedimentary sequence: Implications for the geology of the Ossa-Morena Southwestern border. Comunicações Geológicas, 97, 129-146.

Moreira, N., Araújo, A., Pedro, J., Dias, R. (2014). Evolução geodinâmica da Zona de Ossa-Morena no contexto do SW Ibérico durante o Ciclo Varisco. Comunicações geológicas, 101(I) 275-278.

Murphy, J., Gutierrez-Alonso, G., Nance, R., Keppie, J., Quesada, C., Strachan, R., Dostal, J. (2006). Origin of the Rheic Ocean: Rifting along a Neoproterozoic suture? Geology, 34, 325–328.

Nance, R., Gutierrez-Alonso, G., Keppie, J., Linnemann, U., Murphy, J., Quesada, C., Strachan, R., Woodcock, N., (2012). A brief history of the Rheic Ocean. Geoscience Frontiers, 3/2, 125-135.

Noronha, F., Ramos, J., Rebelo, J., Ribeiro, A., Ribeiro, M. L. (1981). Essai de corrélation des phases de déformation hercynienne dans le Nord-Ouest Péninsulaire. Leidse Geologische Mededelingen, 52(1), 87-91.

Oliveira, J., Oliveira, V., Piçarra, J. (1991). Traços gerais da evolução tectono-estratigráfica da Zona de Ossa Morena, em Portugal: síntese crítica do estado actual dos conhecimentos. Comun. Serv. Geol. Port., 77, 3-26.

Oliveira, J.T., Relvas, J., Pereira, Z., Matos, J., Rosa, C. Rosa, D., Munhá, J. Fernandes, P., Jorge, R., Pinto, A. (2013). Geologia Sul portuguesa, com ênfase na estratigrafia, vulcanologia física, geoquímica e mineralizações da faixa piritosa. In: Dias, R., Araújo, A., Terrinha, P., Kullberg, J.C. (Eds.), Geologia de Portugal (vol. 1), Escolar Editora, 673-767.

Pamplona, J., Ribeiro, A. (2013). Evolução geodinâmica da região de Viana do Castelo (Zona Centro-Ibérica, NW de Portugal). In: Dias, R., Araújo, A., Terrinha, P., Kullberg, J.C. (Eds.), Geologia de Portugal (vol. 1), Escolar Editora, 149-203.

Pamplona, J., Rodrigues, B., Llana-Fúnez, S., Simões, P., Ferreira, N., Coke, C., Pereira, E., Castro, P., Rodrigues, J.. (2016). Structure and Variscan evolution of Malpica–Lamego ductile shear zone (NW of Iberian Peninsula). In: Mukherjee, S., Mulchrone, K. F. (Eds.), Ductile Shear Zones: From Micro- to Macro-scales, John Wiley & Sons, 206-223.

Parés J., Van der Pluijm, B. (2004). Correlating magnetic fabrics with finite strain: Comparing results from mudrocks in the Variscan and Appalachian Orogens. Geologica Acta, 2 /3, 213-220.

Parés, J., Van der Voo, R., Stamatakos, J., Pérez-Estaún, A. (1994). Remagnetization and postfoldingd oroclinal rotations in the Cantabrian/Asturian arc, northern Spain. Tectonics, 13(6), 1461-1471.

Pastor-Galán, D., Gutiérrez-Alonso, G., Weil, A. (2011). Orocline timing through joint analysis: Insights from the Ibero-Armorican Arc. Tectonophysics, 507, 31–46.

Pastor-Galán, D., Groenewegen, T., Brouwer, D., Krijgsman, W., Dekkers, M. (2015). One or two Oroclines in the Variscan orogen of Iberia? Implications for Pangea amalgamation. Geology, 43(6), 527-530.

Pereira, E. (1987). Estudo geológico-estrutural da área de Celorico de Basto e sua interpretação geodinâmica. Ph. D. Thesis, Lisbon University, 274 p.

Pereira, E. (1988). Soco Hercínico da Zona Centro-Ibérica – Evolução Geodinâmica. Geonovas, 10, 13-35.

Pereira, E. (1989). Carta Geológica de Portugal na Escala 1:50.000 e notícia explicativa da Folha 10-A (Celorico de Basto), Serv. Geol. Portugal, 53 p.

Pereira, E., Ribeiro, A. (1983). Tectónica do sector noroeste da Serra do Marão. Com. Serv. Geol. Port., 69(2), 283-290.

Pereira, E., Ribeiro, A. (1992). Paleozóico. In: Pereira, E. (Ed.), Carta Geológica de Portugal na Escala 1:200.000 e notícia explicativa da Folha 1. Serviços Geológicos de Portugal, 9-26.

Pereira, E., Ribeiro, A., Meireles, C. (1993). Cisalhamentos hercínicos e controlo das mineralizações de Sn-W, Au e U na Zona Centro-Ibérica em Portugal. Cuaderno Lab. Xeolóxico de Laxe, La Coruña, 18, 89-119.

Pereira, M., Silva, J., Ribeiro, C. (2010). The role of bedding in the formation of fault–fold structures, Portalegre - Esperanca transpressional shear zone, SW Iberia. Geol. J., 45, 521–535.

Pereira, M., Chichorro, M., Johnston, S., Gutiérrez-Alonso, G., Silva, J., Linnemann, U., Hofmann, M., Drost, K. (2012). The missing Rheic Ocean magmatics arcs: Provenance analysis of Late Paleozoic sedimentary clastic rocks of SW Iberia. Gondwana Research, 22, 882-891.

Pereira, Z., Meireles, C., Pereira, E. (1999). Upper Devonian Palinomorphs of the NE sector of Trás-os-Montes (Central Ibéria Zone). XV Reunião do Oeste Peninsular – International Meeting on Cadomian orogens, Badajoz, 201-206.

Pérez Estaún, A. (1974). Aportaciones al conocimiento del Carbonífero de San Clodio (Prov. de Lugo). Breviora Geologica Asturica, 18, 23-25.

Pérez Estaún, A. (1990). Introduction to the Cantabrian. In: Dallmeyer, R. D., Martínez-Garcia, E. (Eds.), Pre-Mesozoic Geology of Iberia, Springer-Verlag, Berlin, 7-8.

Pérez Estaún, A., Bastida, F. (1990). Structure of the Cantabrian. In: Dallmeyer, R. D., Martínez-Garcia, E. (Eds.), Pre-Mesozoic Geology of Iberia, Springer-Verlag, Berlin, 55-69.

Pérez-Estaun, A., Bea F. (2004). Macizo Iberico. in: Vera, J.A. (Ed.). Geologia de España. Sociedad Geológica de España, Geologia de España. SGE-IGME, Madrid, 19–230.

Pérez Estaún, A., Bastida, F., Alonso, J., Marquinez, J., Aller, J., Alvarez, M., Marcos, A., Pulgar, J. (1988). A thin-skinned tectonics model for an arcuate fold and thrust belt, the Cantabrian Zone (Variscan Ibero-Armorican Arc), Tectonics, 7, 517-537.

Pérez Estaún, A., Bastida, F., Martínez Catalán, J., Gutierrez Marco, J., Marcos, A., Pulgar, J. (1990). Stratigraphy of the West Asturian-Leonese Zone. In: Dallmeyer, R. D., Martínez-Garcia, E. (Eds.), Pre-Mesozoic Geology of Iberia, Springer-Verlag, Berlin, 92-102.

Pérez Estaún, A., Martínez Catalán, J., Bastida, F. (1991). Crustal thickening and deformation sequence in the footwall to the suture of the Variscan belt of northwest Spain, Tectonophysics, 191, 243-253.

Perroud, H., Bonhommet, N. (1981). Palaeomagnetism of the Ibero-Armorican arc and the Hercynian orogeny in Western Europe. Nature, 292, 445–448.

Pohn, H. (2000). Lateral Ramps in the Folded Appalachians and in Overthrust Belts Worldwide—A Fundamental Element of Thrust-Belt Architecture. USGS Bullletin, 2163, 63 p.

Quesada, C. (1990). Ossa Morena Zone, Introdution, In: Dallmeyer, R. D., Martínez-Garcia, E. (Eds.), Pre-Mesozoic Geology of Iberia, Springer-Verlag, Berlin, 249-251.

Quesada, C., Dallmeyer, R. (1994). Tectonothermal evolution of the Badajoz-Cordóba shear zone (SW Iberia): characteristics and $^{40}Ar/^{39}Ar$ mineral age constraints. Tectonophysics, 231, 195-213.

Quesada, C., Fonseca, P., Munhá, J., Oliveira, J., Ribeiro, A. (1994). The Beja-Acebuches Ophiolite (Southern Iberia Variscan fold belt): geological characterization and geodynamic significance. Bol. Geol. Y Min., 105/1, 3-49.

Ramsay, J. (1967). Folding and Fracturing of Rocks. McGraw-Hill, New York, 568 p.

Ribeiro, A. (1974). Contribution à l'étude tectonique de Trás-os-Montes Oriental. Mem. Serv. Geol. Portugal, 24, 168 p.

Ribeiro, A. (1990). Central-Iberian Zone: Introduction. In: Dallmeyer, R. D., Martínez-Garcia, E. (Eds.), Pre-Mesozoic Geology of Iberia, Springer-Verlag, Berlin, 143-144.

Ribeiro, A., Silva, J. (1983). Structure of the South Portuguese Zone. In: Lemos de Sousa, M.J., Oliveira, J.T. (Eds.), The Carboniferous of Portugal, Serv. Geol. Portugal, 29, 83-89.

Ribeiro, A., Pereira, E., Dias, R. (1990). Allochthonous Sequences: Structure in the Northwest of the Iberian Peninsula. In: Dallmeyer, R. D., Martínez-Garcia, E. (Eds.), Pre-Mesozoic Geology of Iberia, Springer-Verlag, Berlin, 220-236.

Ribeiro, A., Dias, R., Silva, J. B. (1995). Genesis of the Ibero-Armorican Arc. Geodinamica Acta, 8(2), 173-184.

Ribeiro, A., Munhá, J., Dias, R., Mateus, A., Pereira, E., Ribeiro, L., Fonseca, P., Araújo, A., Oliveira, T., Romão, J., Chaminé, H., Coke, C., Pedro, J. (2007). Geodynamic evolution of SW Europe Variscides. Tectonics, 26, 1-24.

Ribeiro, A., Munhá, J., Mateus, A., Fonseca, P., Pereira, E., Noronha, F., Romão, J., Rodrigues, J.F., Castro, P., Meireles, C., Ferreira, N. (2009). Mechanics of thick-skinned Variscan overprinting of Cadomian basement (Iberian Variscides). Comptes Rendus Geoscience, 341(2-3), 127-139.

Ribeiro, A., Munhá, J., Fonseca, P.E., Araújo, A., Pedro, J.C., Mateus, A., Tassinari, C., Machado, G., Jesus, A. (2010). Variscan ophiolite belts in the Ossa-Morena Zone (Southwest Iberia): geological characterization and geodynamic significance. Gondwana Res, 17, 408–421.

Ribeiro, A., Romão, J., Munhá, J., Rodrigues, J., Pereira, E., Mateus, A., Araújo, A. (2013). Relações tectonostratigráficas e fronteiras entre a Zona Centro-Ibérica e a Zona Ossa-Morena do Terreno Ibérico e do Terreno Finisterra. In: Dias, R., Araújo, A., Terrinha P., Kullberg, J.C. (Eds.), Geologia de Portugal (vol. 1), Escolar Editora, 439-481.

Ribeiro, M. L., Ribeiro, A. (1974). Signification paleogéographique et tectonique de la présence de galets de roches métamorphiques dans un flysch d'âge dévonien supérieur du Trás-os-Montes Oriental (Nord-Est du Portugal). C. R. Acad. Sc. Paris, série D, 278, 1361- 1363.

Richard, P., Cobbold, P. (1990). Experimental insights into partitioning of fault motions in continental convergent wrench zones. Annales Tectonicae, IV/2, 35-44.

Ries, A. (1978). The opening of the Bay of Biscay - a review. Earth-Science Reviews, 14, 35-63.

Ries, A., Shackleton, R. (1976). Patterns of strain variation in arcuate fold belts. Phil. Trans. R. Soc. Lond. A283, 281-288.

Ries, A., Richardson, A., Shackleton, R. (1980). Rotation of the Iberian arc: paleomagnetic results from north Spain. Earth and Planetary Science Letters, 50, 301–310.

Robardet, M. (2002). Alternative approach to the Variscan Belt in southwestern Europe. Variscan–Appalachian Dynamics. Geol. Soc. Am., 364, 1–15.

Rodrigues, B., Chew, D., Jorge, R., Fernandes, P., Veiga-Pires, C., Oliveira, J. (2014). Idades U-Pb de zircões detríticos do Grupo do Flysch do Baixo Alentejo, Zona Sul Portuguesa, Comunicações geológicas 101/I, 301-305.

Rodrigues, J. (2008). Estrutura da Arco da Serra de Santa Comba – Serra da Garraia; Parautóctone de Trás-os-Montes. Ph.D. Thesis, Lisbon Univ., 308 p.

Rodrigues, J., Coke, C., Dias, R., Pereira, E., Ribeiro, A. (2005). Transition from autochthonous to parautochtonous deformation regimes in Murça-Marão sector (Central-Iberian Zone, northern Portugal). In: Carosi, R., Dias, R., Iacopini D., Rosebaum, G. (Eds.) The southern Variscan belt, Journal of the Virtual Explorer, Electronic Edition, ISSN 1441-8142, 19, paper 8.

Rodrigues, J., Pereira, E., Ribeiro, A. (2013). Complexo de mantos parautóctones do NE de Portugal: estrutura interna e tectonoestratigrafia. In: Dias, R., Araújo, A., Terrinha P., Kullberg, J.C. (Eds.), Geologia de Portugal (vol. 1), Escolar Editora, 275-331.

Rodríguez Alonso, M., Balda, D., Perejón, A., Pieren, A., Liñan, E., López Díaz, F., Moreno, F., Gámez Vintaned, J., González Lodeiro, F., Martínez Poyatos, D., Vegas, R. (2004). Estratigrafía do Dominio del Complejo Esquisto-Grauváquico. in: Vera, J. (Ed.). Geología de España. SGE-IGME, Madrid, 78-83.

Rölz, P. (1975). Beiträge zum Aufbau des junpräkambrischen und attpalaozoischen Grundgebirges in den Provinzen Salamanca und Cáceres (Sierra de Tamames, Sierra de Francia und östliche Sierra de Gata) Spanish (Auszug). Münster Forsch, Geol. Paläont. Heft, 36, 1-68.

Romão, J. (2000). Carta Geológica de Portugal na Escala 1:50.000 e notícia explicativa da Folha 28-A (Mação), Inst. Geol. Min., Lisboa, 85 p.

Romão, J., Metodiev, D., Dias, R., Ribeiro, A. (2013). Evolução geodinâmica dos sectores meridionais da Zona Centro-Ibérica. In: Dias, R., Araújo, A., Terrinha P., Kullberg, J.C. (Eds.), Geologia de Portugal (vol. 1), Escolar Editora, 206-257.

Rubio Pascual, F., Arenas, R., Martínez Catalán, J., Rodríguez Fernández, L., Wijbrans, J. (2013). Thickening and exhumation of the Variscan roots in the Iberian Central System: tectonothermal processes and $^{40}Ar/^{39}Ar$ ages. Tectonophysics, 587, 207–221.

San José, M., Pieren, P., Garcia Hidalgo, F., Vilas, L., Herranz, P., Pelaez, J., Perejon, A. (1990). Ante-Ordovician stratigraphy of Autochthonous sequence, Central-Iberian Zone. In: Dallmeyer, D., Martinez Garcia, E. (Eds.), Pre-Mesozoic Geology of Iberia. Springer-Verlag, 147-159.

Schulmann, K., Martínez Catalán, J., Lardeaux, J., Janousek, V., Oggiano. G. (Eds.) (2014). The Variscan Orogeny: extend, timescale and the formation of the European Crust. Geological Society of London, 405, 406 p.

Schultz, G. (1858). Atlas geológico y topográfico de Asturias. Lit. de G. Pfeiffer (2 maps +1 plate).

Sengör, A. (2013). The Pyrenean Hercynian Keirogen and the Cantabrian Orocline as genetically coupled structures. Journal of Geodynamics, 65, 3– 21.

Shaw, J., Johnston, S., Gutierrez-Alonso, G., Weil, A. (2012a). Oroclines of the Variscan orogen of Iberia: Paleocurrent analysis and paleogeographic implications. Earth and Planetary Science Letters, 329/330, 60–70.

Shaw, J., Johnston, S., Gutierrez-Alonso, G., Weil, A. (2012b). Oroclines of the Variscan orogen of Iberia: Paleocurrent analysis, U-Pb detrital zircon age dating, and paleogeographic implications. Geotemas, 13, 116.

Shaw, J., Gutierrez-Alonso, G., Johnston, S., Pastor Galán, D. (2014). Provenance variability along the Early Ordovician north Gondwana margin: Paleogeographic ant tectonic implications of U-Pb detrital zircon ages from the Armorican Quartzite of the Iberian belt. Geol. Soc. Am. Bull., 126, 702–719.

Shaw, J., Johnston, S., Gutierrez-Alonso, G. (2015). Orocline formation at the core of Pangea: A structural study of the Cantabrian orocline, NW Iberian Massif. Lithosphere, 7-6; 653–661. doi: 10.1130/L461.1.

Shelley, D., Bossière, G. (2000). A new model for the Hercynian orogen of Gondwanan France and Iberia. J. Struct. Geol., 22, 757-776.

Shelley, D., Bossière, G. (2002). Megadisplacements and the Hercynian orogen of Gondwanan France and Iberia. In: Martínez Catalán, J., Hatcher Jr., R., Arenas, R., Díaz García, F. (Eds.), Variscan-Appalachian dynamics: The building of the late Paleozoic basement: Boulder, Colorado. Geological Society of America, Special Paper, 364, 209–222.

Silva J., Oliveira J., Ribeiro A. (1990). South Portuguese Zone. Structural outline. In: Dallmeyer, D., Martinez Garcia, E. (Eds.), Pre-Mesozoic Geology of Iberia. Springer-Verlag, 348-362.

Silva, J., Mata, J., Moreira, N., Fonseca, P., Jorge, R., Machado, G. (2011). Evidência para o funcionamento, desde o Devónico inferior, de subducção no bordo meridional da zona de Ossa-Morena, VIII Congresso Ibérico de Geoquímica - XVII Semana de Geoquímica, Instituto Politécnico de Castelo Branco.

Simancas, J., Martínez Poyatos, D., Expósito, I., Azor, A., González Lodeiro, F. (2001). The structure of a major suture in the SW Iberian Massif: the Ossa-Morena/Central Iberian contact. Tectonophysics, 332, 295–308.

Simancas, J. F., *et al*. (2003). Crustal structure of the transpressional Variscan orogen of SW Iberia: SW Iberia deep seismic reflection profile (IBERSEIS), Tectonics, 22(6), 1062.

Simancas, J., Ayarza, P., Azor, A., Carbonell, R., Martínez Poyatos, D., Pérez-Estaún, A., González Lodeiro, F. (2013). A seismic geotraverse across the Iberian Variscides: orogenic shortening, collisional magmatism, and orocline development. Tectonics, 32, 417–432.

Stampfli, G. (1996). The intra-alpine terrain: a paleotethyan remnant in the Alpine Variscides. Eclogae Geologicae Helvetiae, 89, 13–42.

Stampfli, G., Borel, G. (2002). A plate tectonic model for the Paleozoic and Mesozoic constrained by dynamic plate boundaries and restored synthetic oceanic isochrones, Earth Planet. Sci. Lett., 196, 17-33.

Staub, R. (1927). Ideas sobre la tectónica de España. Spanish version and prologue: Carbonell, T. Real Academia de Ciencias, Bellas Letras y Nobles Artes de Córdoba, 1–83.

Stille, H. (1924). Grundfragen der vergleichenden tektonic. Brontraeger, 443 p.

Suárez, O., Corretge, L., Martínez, F. (1990). West Asturian-Leonese Zone; distibution an characteristics of Hercynian metamorphism. In: Dallmeyer, R.D., Martínez García, E. (Eds.), Pre-Mesozoic Geology of Iberia, Springer-Verlag, Berlin, 129-133.

Sutherland, R. (1999). Cenozoic bending of New Zealand basement terranes and Alpine Fault displacement: a brief review. New Zealand Journal of Geology and Geophysics, 42, 295-301.

Suess, E. (1888). Das Antlitz der Erde, vol. II. F. Tempsky, Prag and Wien, and G. Freytag, Leipzig, IV, 704 p.

Tapponier, P., Molnar, P. (1976). Slip-line field theory and large scale continental tectonics. Nature, 264, 319-324.

Teixeira, C., Pais, J. (1973). Sobre a presença do Devónico na região de Bragança (Guadramil e Mofreita) e de Alcañices (Zamora). Bol. Soc. Geol. Portugal, 18(2-3), 199-202.

Tena, M. (1980=. Mapa Geológico Nacional, E. 1/50 000, 704/11-28, Cáceres, Inst. Geol. Min. España, Madrid.

Tex, E., Floor, P. (1971). A synopsis of the geology of the western Galicia. Histoire structurale du Golfe de Gascogne. Technip., 1, 3-13.

Treloar, P., Coward, M., Chambers, A., Izatt, C., Jackson, K. (1992). Thrust geometries, interferences and rotations in the northwest Himalaya. In: McClay, K. (Ed.), Thrust Tectonics. Chapman and Hall, London, 25-342.

Twiss, R., Moores, E. (1992). Structural Geology. W. H. Freeman and Company, 532 p.

Valle Aguado, B. (1992). Geología estructural de la Zona de Cisalla de Porto-Tomar en la región de Oliveira de Azeméis-Serra de Arada (Norte de Portugal). Ph. D. Thesis, Salamanca Univ., 254 p.

Van der Voo, R. (2004). Paleomagnetism, oroclines, and growth of the continental crust. GSA Today, 14, 4–9.

Vera, J. (Ed.) (2004). Geología de España. SGE-IGME, Madrid, 890 p.

Vroon, P., van Bergen, M., Klaver, G., White, W. (1995). Strontium, neodymium, and lead isotopic and trace-element signatures of the East Indonesian sediments: provenance and implications for Banda arc magma genesis. Geochimica et Cosmochimica Acta, 59/12, 2573-2598.

Weil, A. (2006). Kinematics of orocline tightening in the core of an arc: paleomagnetic analysis of the Ponga Unit, Cantabrian Arc, northern Spain. Tectonics, 25, 1–23, TC3012.

Weil, A., Sussman, A. (2004). Classifying curved orogens based on timing relationships between structural development and vertical-axis rotations. In: Sussman, A., Weil, A. (Eds.), Orogenic curvature: Integrating paleomagnetic and structural analyses. Geological Society of America Special Paper, 383, 1–15.

Weil, A., Gutiérrez-Alonso, G., Conan, J. (2010). New time constraints on lithospheric scale oroclinal buckling of the Ibero-Armorican arc: a palaeomagnetic study of earliest Permian rocks from Iberia. Journal of the Geological Society of London, 167, 127-143.

Weil, A., Gutiérrez-Alonso, G., Johnston, S., Pastor-Galán, D. (2013). Kinematic constraints on buckling in a lithospheric-scale orocline along the northern margin of Gondwana: a geologic synthesis. Tectonophysics, 582, 25-49.

X

O Tardi-Varisco Ibérico

O estudo das estruturas Tardi-Variscas Ibéricas é essencial para a compreensão dos estádios finais da evolução geodinâmica do Orógeno Varisco e, consequentemente, para a génese do Supercontinente Pangeia. Após o fecho dos Oceano(s) Varisco(s), com a consequente colisão entre os diversos blocos continentais e a génese do Arco Ibero-Armoricano previamente discutidos (ver capítulo IX), o sobreespessamento crustal associado à orogénese associado às alterações do comportamento reológico dos mareriais induzida pelo processo metamórfico gera uma alteração do campo de tensões do orógeno; esta alteração resulta do câmbio entre os tensores de compressão intermédio e mínimo (σ_2 e σ_3 respectivamente) por incremento da pressão litostática (Fig. 1). Em consequência disto, o regime de deformação com geração de dobramentos às mais diversas escalas acompanhados de acidentes tangenciais de cinemática cavalgante dominante é abandonado, dando origem a um regime de transcorrência dominante.

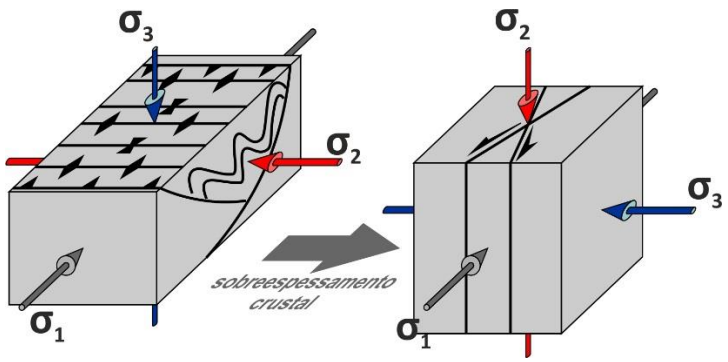

Figura 1 – Modelo teórico da inversão do campo de tensões, com inversão dos tensores de compressão intermédio e mínimo, por aumento da pressão litostática.

Na Ibéria estas estruturas transcorrentes encontram-se bem evidenciadas com a génese de um padrão generalizado de fracturação geralmente incluído no denominado Sistema Messejana-Vilariça. Este padrão de fracturação, de direcção predominante NNE-SSW a NE-SW, é desenvolvido em regime de deformação frágil a dúctil-frágil durante o Ciclo Varisco, sendo que algumas destas estruturas são posteriormente reactivadas durante o Ciclo Alpino. A

compreensão da sua geometria e cinemática é sem margem para dúvidas essencial para qualquer modelo geodinâmico da colisão entre a Laurentia e a Gondwana durante os Carbónico-Pérmico. Com efeito, a existência de interpretações díspares destas estruturas condicionam os modelos propostos para a evolução da Ibéria durante o Tardi-Varisco.

Importa referir que os trabalhos efectuados caracterizam as estruturas Tardi-Variscas, constrangendo a idade desta fase de deformação (Carbónico terminal a Pérmico). Estas estruturas (falhas e bandas *kink*) apresentam uma cinemática Varisca esquerda ao longo da direcção NNE-SSW a NE-SW, como evidenciado pelos dados que apresentados neste capítulo. Embora o enfoque dos trabalhos realizados na dissertação sejam os domínios setentrionais da Zona de Ossa-Morena, a existência de estruturas com paridade genética desenvolvidas na Zona Sul Portuguesa, localizada no *foreland* orogénico e como tal menos afectada pelos processos tectono-metamórficos Variscos, levaram à sua caracterização cuidada neste domínio, tanto mais que a existência de Formações de idade Triásica permite constranger a idade da cinemática observada. Consequentemente, os dados estruturais obtidos nesta zona são comparados com os dados existentes para as regiões setentrionais da Zona de Ossa-Morena permitindo uma caracterização dos mecanismos de deformação actuantes nas bandas *kink* esquerdas desta Idade.

Embora aparentemente contraditório, estas estruturas NNE-SSW de cinemática esquerda são interpretadas como sendo cogenéticas do regime geral de colisão transcorrente direita entre os dois blocos continentais principais, leia-se Gondwana e Laurentia, durante o Carbónico terminal-Pérmico. Com efeito, estas estruturas são interpretadas como estruturas de segunda ordem à escala do Varisco Ibérico, sendo resultado da componente de transcorrência direita com a mesma idade enfatizada nos domínios a Norte da Ibéria, concretamente na Zona Pirenáica. O modelo geodinâmico proposto para o Tardi-Varisco considera que a Ibéria é bordejada por dois grandes cisalhamentos direitos (Zonas de Cisalhamento Açores-Gibraltar e Cantábrica-Pirenéus), os quais geram uma estrutura em dominó de segunda ordem à escala Ibérica com direcção NNE-SSW. O modelo em causa, e que os dados apresentados corroboram, foi inicialmente proposto por António Ribeiro em 2002 no seu livro *Soft Plate Tectonics*.

Os trabalhos realizados resultaram na publicação de um artigo numa revista internacional com elevado factor de impacto (capítulo X.1), inserida no quartil Q1 no SJR e contendo um factor de impacto de 2.133 de acordo com a *Thomson Reuters* (2015), bem como a preparação de um segundo trabalho, ainda não submetido, com especificidades para o *Journal of Structural Geology*.

Seguidamente, apresentam-se os dois capítulos elaborados com base nos dados obtidos, onde se abordarão as seguintes temáticas:

- O capítulo X.1 descreve a deformação Tardi-Varisca na região de Almograve e Ponta Ruiva (ambos na Zona Sul Portuguesa), propondo o modelo geodinâmico geral para a evolução desta fase de deformação tardia do Orógeno Varisco no Maciço Ibérico;
- O segundo capítulo (X.2) aborda os mecanismos de deformação associado à génese das bandas *kink* esquerdas de idade Tardi-Varisca. Este capítulo compara duas bandas *kink* Tardi-Variscas com excelentes condições de afloramento, uma desenvolvida na região de Almograve e uma outra na região de Abrantes, analisando os mecanismos de deformação associados a estas estruturas e propondo uma nova metodologia simples para estimar os encurtamentos teóricos no interior das bandas *kink* contracionais, com base em parâmetros geométricos simples de obter.

- *Capítulo X.1*

DIAS, R., MOREIRA, N., RIBEIRO, A., BASILE, C. (2017), Late Variscan Deformation in the Iberian Peninsula; A late feature in the Laurasia-Gondwana Dextral Collision. International Journal of Earth Sciences (Geol Rundsch), 106(2), 549-567. DOI: 10.1007/s00531-016-1409-x

- *Capítulo X.2*

MOREIRA, N., DIAS, R. (em preparação), Area change during kink band evolution; examples from the Late Variscan of Portugal.

Referências

Ribeiro, A. (2002). Soft Plate Tectonics. Springer-Verlag, Berlin, 324 p.

X.1

Late Variscan Deformation in the Iberian Peninsula; a Late Feature in the Laurentia-Gondwana Dextral Collision

Index

X.1.1. Introduction

A complex network of major shear zones was developed during the last stages of intracontinental deformation of the Variscan orogeny. This Late Variscan deformation episode was considered the result of internal deformation along first order E-W dextral shear zones (Arthaud and Matte, 1975; 1977). Such kinematics is often considered a pervasive feature of most of the Variscan orogenic evolution (Ribeiro *et al.*, 1995; Shelley and Bossière, 2000; 2002;

Ribeiro, 2002; Ribeiro *et al.*, 2007; Martínez Catalán, 2011; Nance *et al.*, 2012; Dias *et al.*, 2016). In the Iberian Massif this Late Variscan deformation gave rise to some of the most important observed basement faults (Ribeiro, 1974; Iglesias and Ribeiro, 1981), like the NNE-SSW Vilariça and Régua-Chaves-Verin faults in NW Iberia (Ribeiro *et al.*, 1990; Marques *et al.*, 2002; Dias *et al.*, 2013). Although several works focus on this major event there are still some doubts concerning the kinematics and the timing of the deformation. Such controversy mainly results from the strong reworking of the Late Variscan structures by the Meso-Cenozoic deformation episodes. The scarcity of Lower Mesozoic outcrops in the vicinity of these major structures strongly limits the temporal constrain of observed deformations to the Palaeozoic. The transition between the Late Variscan wrench faulting and the early Alpine extensional regime is essential to the understanding of the Late Palaeozoic dynamics of Western Europe. In such a debate, the Variscan kinematics of the NNE-SSW main faults is crucial because they have been considered, either sinistral (Ribeiro, 1974; Ribeiro *et al.*, 2007; Moreira *et al.*, 2010; 2014; Dias and Basile, 2013), or dextral with a sinistral kinematics alpine reworking (Marques *et al.*, 2002). Obviously such opposite interpretations give rise to strongly different geodynamical models for the transition between the late stages of the collision that formed the Pangaea, and the beginning of its dispersion leading to the opening of the Atlantic Ocean.

The SW Portuguese coast, where the outcrops are remarkably well exposed, is a key sector to discriminate between the previous models. Indeed, in this region it is possible to highlight:

- A continuity between the sedimentation of the Upper Carboniferous turbiditic sediments (Moscovian; Pereira *et al.*, 2007) and the late stages of the Variscan deformation (Dias and Basile, 2013);
- The influence of the brittle-ductile Late Variscan structures in the opening of the intracontinental Triassic rift basins (Dias and Ribeiro, 2002; Dias and Basile, 2013).

In this paper, new detailed structural mapping in two key sectors of SW Portugal enables the understanding of the kinematical, chronological and geodynamical behaviour of the Late Variscan deformation in Iberia.

X.1.2. Geological Setting of Southwest Iberian Variscides

The main Variscan structure in the South Portuguese Zone is a typical fold and thrust belt (Ribeiro *et al.*, 1979, 1983; Ribeiro and Silva, 1983; Silva *et al.*, 1990) with a slightly arcuate pattern ranging from NW-SE to a NNW-SSE trend towards W (Fig. 1A; *e.g.* Ribeiro *et al.*, 1979; Dias and Basile, 2013). This deformation was the result of the basin inversion induced by the

SW Iberia Variscan subduction zone (Ribeiro *et al.*, 2007). Such process generated a SW facing imbricated complex (Fig. 1B), related to a thin skinned tectonic regime (Ribeiro and Silva, 1983; Ribeiro *et al.*, 1983).

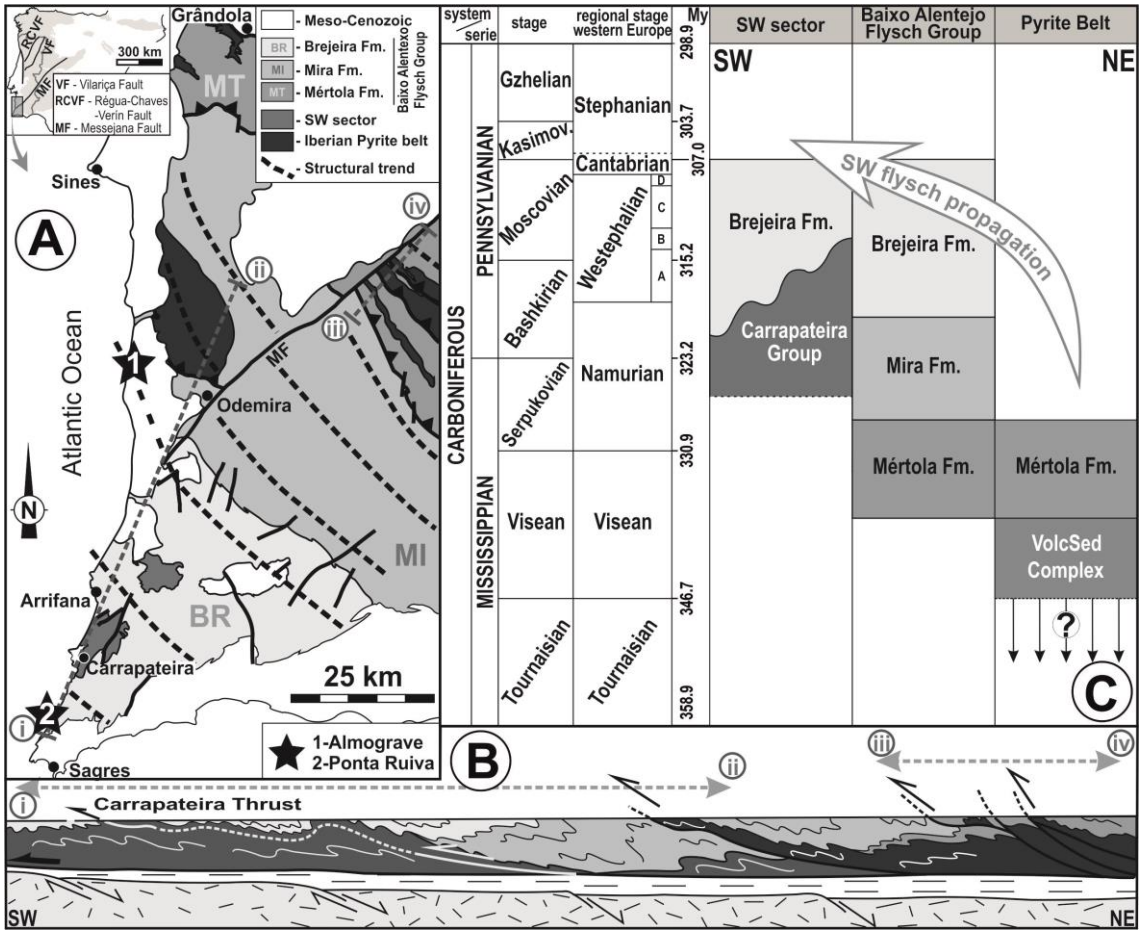

Figure 1 – Main geological features of the southern Portuguese Variscides.

A – Spatial distribution of the main geological domains (adapted from Oliveira, 1984; Ribeiro *et al.*, 1979).

B – Geological profile along the South-Portuguese zone (adapted from Ribeiro *et al.*, 2007; location is shown in figure 1A).

C – Main lithostratigraphic units emphasizing the Carboniferous turbidites (adapted from Oliveira, 1990; Silva *et al.*, 1990; 2113; Oliveira *et al.*, 2013).

The lithostratigraphy of the South Portuguese Zone allows the individualization of three domains in SW Portugal (see Oliveira *et al.*, 2013 for a review); from NE to SW, the Pyrite Belt, Baixo Alentejo Flysch Group and Southwest Sector (Fig. 1C). In the framework of this work the Baixo Alentejo Flysch Group, a deep water turbidite sequence with more than 5 km thickness (Oliveira *et al.*, 2013) must be highlighted. Sedimentological and paleontological data allow the

establishment of three main lithostratigraphic units in this group (Oliveira, 1990): Mértola, Mira and Brejeira formations. The spatial relation of these units shows a southward propagating of the basin, from Upper Visean to Upper Moscovian (Oliveira *et al.*, 2013; Jorge *et al.*, 2013).

The continuous interaction between deformation and sedimentation (Ribeiro and Silva, 1983) highlights a diachronous propagation of the deformation from NE to SW in a piggy back regime (Carvalho *et al.*, 1971; Silva, 1989; Silva *et al.*, 1990). The deeper structural levels with a pervasive cleavage are thus present in the NE, while southwards a shallower deformation is found (Ribeiro *et al.*, 1983; Marques *et al.*, 2010; Dias and Basile, 2013). The Variscan metamorphic grade reflects the structural pattern, ranging from the greenschist facies in the NE to top diagenesis / anchizone toward the SW (Schermerhorn, 1971; Munhá, 1983; Abad *et al.*, 2004).

Although strongly deformed, the general pattern of the SW Variscan imbricated complex is the result of a very homogeneous stress field. This lead to consider an unique and continuous diachronous tectonic phase (Ribeiro *et al.*, 1979; Ribeiro and Silva, 1983; Caroça and Dias, 2001; Marques *et al.*, 2010; Reber *et al.*, 2010; Zulauf *et al*, 2011; Dias and Basile, 2013). As it is the first and main tectonic phase found in this sector, it is usually considered a local D_1 event (Ribeiro, 1983; Ribeiro and Silva, 1983; Silva *et al.*, 1990; Dias and Caroça, 2001; Marques *et al.*, 2010; Dias and Basile, 2013).

The understanding of the D_1 structures in the external sectors of SW Iberia is essential to the study of the more discrete and heterogeneous Late Variscan deformation (D_2) which developed in a different geodynamical context (Dias and Basile, 2013).

X.1.3. The First Variscan Deformation Phase (D_1) in SW of South Portuguese Zone

The D_1 structures overlap syn-sedimentary normal faults with local expression. Although they have been considered the result of an extensional regional environment leading to the deepening of the sedimentary basins (Marques *et al.*, 2010), they could also result from flexural extension, due to bending of lithospheric plate, in the foredeep-foreland transition zones during collisional processes (*e.g.* Bradley and Kidd, 1991; Scisciani *et al.*, 2001).

The continuity of the shortening related to the D_1 tectonic event gives rise to a frequent superposition of mesoscopic structures with complex interference patterns. As these structures share a common stress field, they must be ascribed to the same deformation phase. Nevertheless, their well defined geometry and kinematics made possible the subdivision of several stages.

The oldest D_1 structures (D_{1a}) were developed by layer parallel shortening (Fig. 2A), when the layers were still sub-horizontal. In the more competent quartzwacke layers conjugated shear zones underlined by en-echelon quartz veins were developed (Marques *et al*., 2010; Dias and Basile, 2013). The trends of the conjugate dextral NNE-SSW and the sinistral ENE-WSW to E-W shear zones indicate a stress field with a sub-horizontal NE-SW σ_1, a NW-SE σ_3 also sub-horizontal and a sub-vertical σ_2. Quartzwacke boudins and extensional fractures orthogonal to σ_3 are common structures. In the pelitic layers this early tectonic shortening was accommodated essentially by thickening.

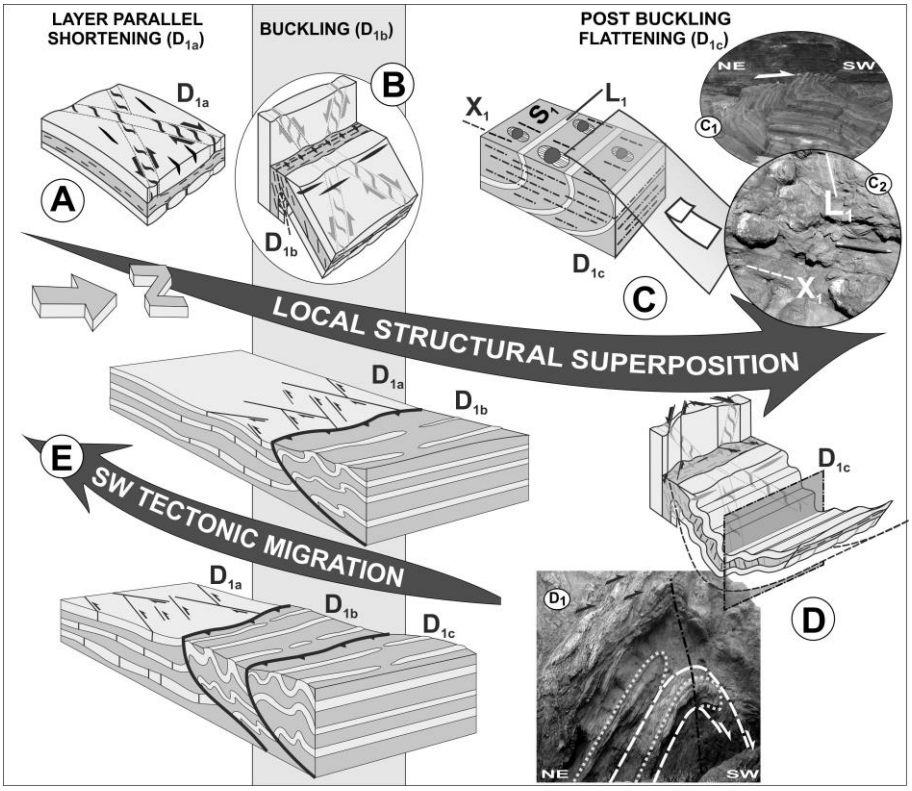

Figure 2 – Main structural features of the D_1 deformation evolution in SW Portugal (adapted from Dias and Basile, 2013).

A – Conjugated shear zones and extensional fractures developed during D_{1a} layer parallel shortening stage;

B – D_{1b} folds with outer arc extensional veins (in black) cutting D_{1a} en echelon quartz veins (in gray);

C – D_{1c} thrusts cutting previous folds (C_1- Mouranitos thrust north of Sagres) emphasizing the X_1 stretching lineation orthogonal to fold axes (C_2- quartz pressure shadows parallel to stretching lineation in Carrapateira nappe);

D – D_{1c} deformation superposed on previous D_1 folds and thrusts (D_1 in the Sagres sector);

E – Diachronous D_1 SW migration.

The continuity of the compressive deformation induced general folding (D_{1b}), not only of the layers, but also of the D_{1a} structures (Fig. 2B). As expected in a SW propagating fold and thrust belt (Carvalho *et al.*, 1971), the vergence of these folds is towards the SW foreland. As the folds have been developed in a relatively upper structural level (Marques *et al.*, 2010; Zulauf *et al.,* 2011) the axial planar S_1 cleavage is only predominant in the hinge zones and reverse limbs of the D_{1b} folds, affecting preferentially the more pelitic lithologies.

Probably related with the post buckling flattening (Marques *et al.*, 2010), low dipping thrusts where formed (Fig. 2C; Ribeiro, 1983; Ribeiro *et al.*, 1983; Caroça and Dias, 2001; Dias and Basile, 2013). Due to the out of sequence propagation of these thrusts (Ribeiro, 1983; Ribeiro and Silva, 1983), which are considered D_{1c} structures, they often cut previous D_{1b} folds (Fig. $2C_1$). In the vicinity of major thrusts (*e.g.* the Carrapateira nappe; Ribeiro, 1983; Fig. 1B), a stretching lineation (X_{1c}) is found parallel to the top-to-SW Variscan transport. This lineation is parallel to quartz fibres in pressure shadows adjacent to pyrite crystals (Fig. $2C_2$).

The effect of this post buckling D_{1c} shortening on previous folds is mostly controlled by the D_{1b} geometry (Fig. 2D). In the steeply dipping short limbs, the late regional D_1 shortening produced conjugated brittle to brittle-ductile subvertical D_{1c} shear zones: N-S to NNE-SSW dextral and ENE-WSW to E-W sinistral (Caroça and Dias, 2001; Marques *et al.*, 2010). In the low dipping D_{1b} normal limbs and early D_{1c} thrusts, the late shortening mostly induced the formation of open to tight folds with sub-vertical axial planes and sub-horizontal fold hinges, which refolded the older structures (Fig. $2D_1$; Caroça and Dias, 2001).

Although the use of previous D_1 deformation stages is useful at local scale, care should be taken at the regional level due to the diachronous propagation of the deformation (Fig. 2E).

X.1.4. Variscan Geometry and Kinematics at external domains of the South Portuguese Zone

In order to improve the knowledge of the Late Variscan deformation in SW Iberia two sectors have been chosen: Almograve and Ponta Ruiva (Fig. 1A). While in Almograve it is possible to detail the superposition of different stages related to the Variscan deformation, in Ponta Ruiva their relation with the extensional Triassic events, due to the opening of the Atlantic Ocean, can also be studied.

X.1.4.1. The Almograve Sector

The most evident structures in Almograve are the sudden regional D_1 strike changes by decametric to hectometric NNE-SSW brittle to brittle-ductile kink-bands (Fig. 3). Although well

exposed, its genesis is debatable (Caroça and Dias, 2002; Marques *et al.*, 2010; Dias and Basile, 2013).

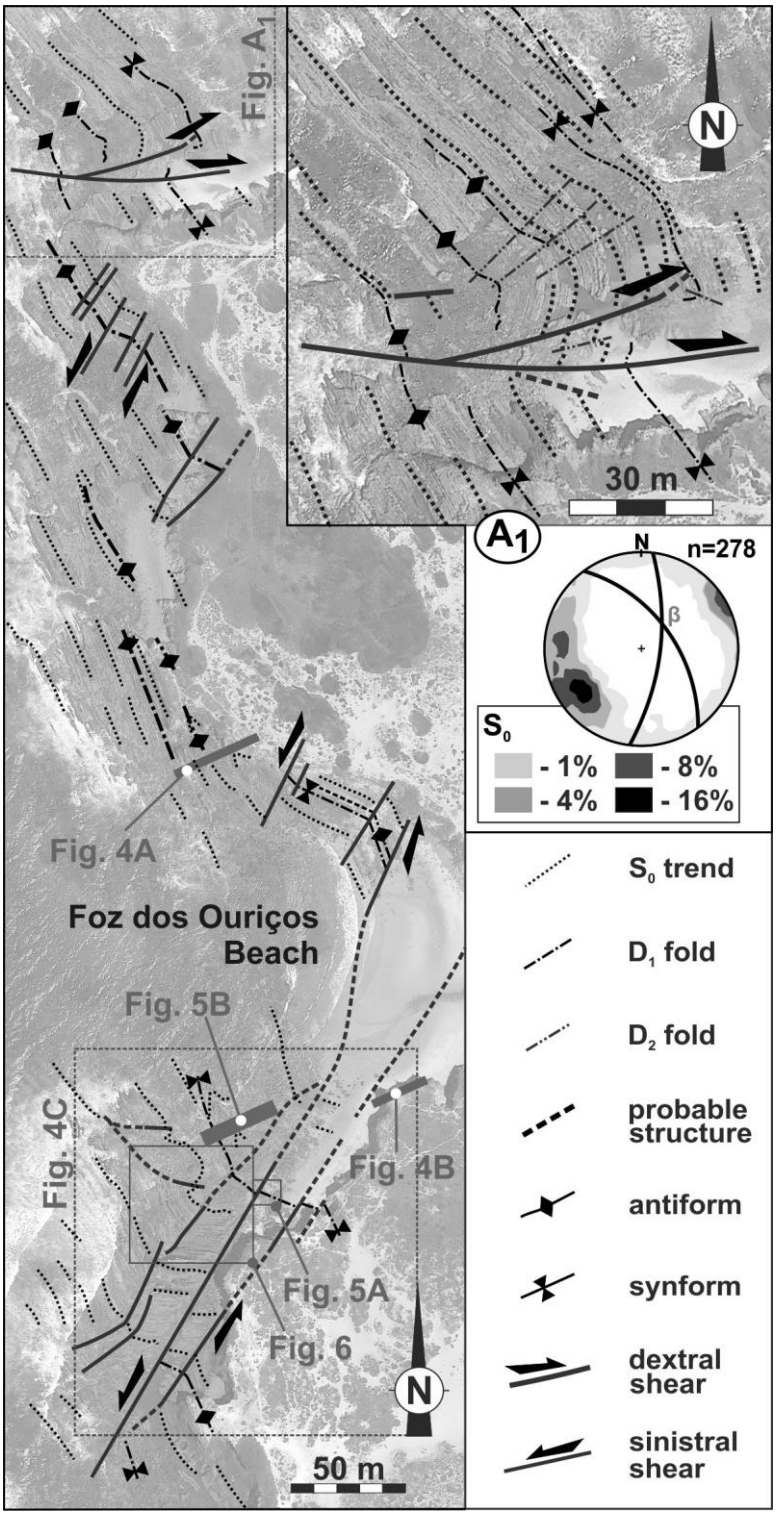

Figure 3 – General Variscan structural map for the Almograve-Foz dos Ouriços area. The inset (A_1) shows structural details of northern sector.

X.1.4.1.1. Structural Pattern of Almograve Sector

Concerning the Variscan major structure of Almograve, there is a strong contrast between the NNW-SSE bedding trend domains and the WNW-ESE to E-W ones (Fig. 4A$_2$).

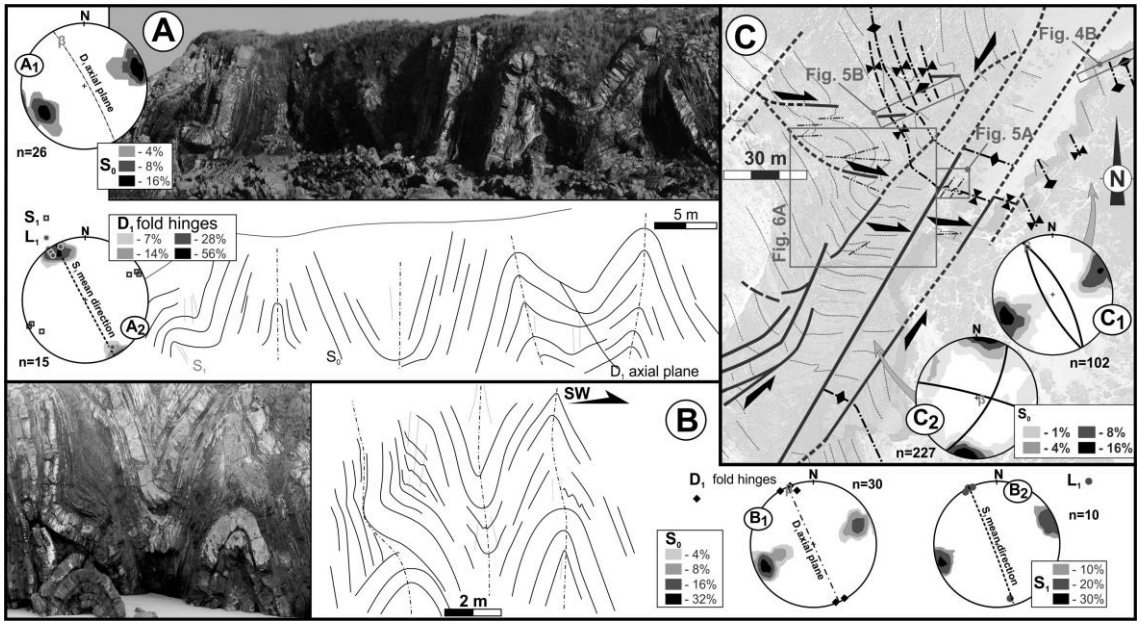

Figure 4 – Main geometry features of Variscan folds for the Almograve-Foz dos Ouriços beach NNW-SSE sectors (equal area lower hemisphere stereographic projections).

A – Fold array and geometrical data (A_1-bedding; A_2-D_1 fold hinges) in northern Foz dos Ouriços;

B – Fold array and geometrical data (B_1- D_1 fold hinges; B_2- L_1 intersection lineation) in southern Foz dos Ouriços;

C – Structural map of southern Foz dos Ouriços sectors with bedding stereographic analysis (symbols as in figure 3).

X.1.4.1.1.1. Variscan Folds

In the NNW-SSE segments (Figs. 4A; 4B), although the D_1 folds have sometimes complex shape profiles due to rheological contrasts of the turbiditic multilayer (Fig. 4B) and intense fluid migration (Marques *et al.*, 2010), they have a very regular, N20ºW - N30ºW trend (Figs. 4A$_1$, 4B$_1$ and 4C$_1$), which is also the direction of the locally developed axial planar S_1 cleavage (Fig. 4A$_2$ and 4B$_2$). When present, the L_1 intersection lineation (S_0^S_1) is subhorizontal or very low dipping to NNW (usually <10º), being subparallel to the fold hinges (Figs. 4A$_2$ and 4B$_2$). As the axial planes are subvertical, the folds in Foz dos Ouriços/Almograve have no clear vergence, although immediately SW of the studied domain the SW vergence is well expressed (Dias and Basile, 2013).

The Variscan folds in the WNW-ESE to E-W sectors have a much more complex geometry due to the pervasive superposition of a different folding event. The pattern of these post-D_1 folds are highly heterogeneous due to the coexistence of two completely different set of D_2 folds, which are easily distinguish by their symmetry in an orthorhombic (Fig. 5) and a monoclinic set (Fig. 6).

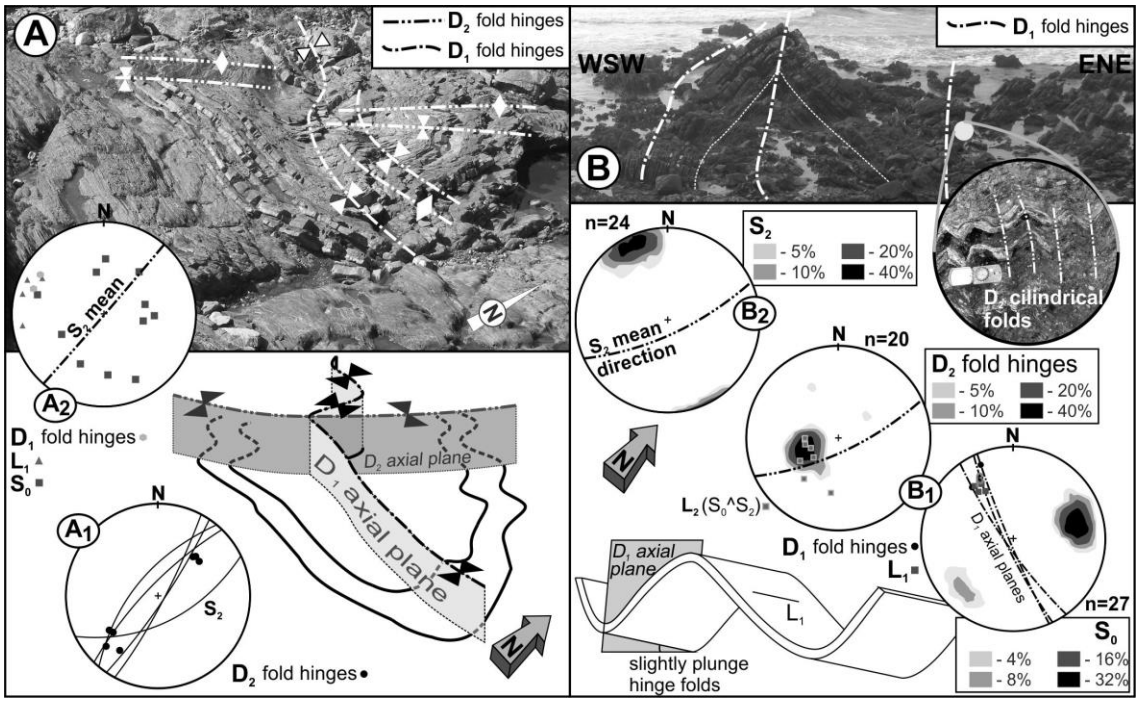

Figure 5 – NNE-SSW orthorhombic D_2 structures in the E-W Almograve sector (equal area lower hemisphere stereographic projections).

A – Wavy D_2 hinges in a D_1 syncline refolded by D_2 folds;

B – Moderate NNW dipping of D_1 folds overprinted by D_2 folding.

The orthorhombic D_2 folds (Fig. 5) have a NNE-SSW to NE-SW trend and variable axes, which were mostly controlled by the dip of the D_1 fold limbs (Figs. $5A_1$ and $5B_1$). The weak flattening related to these D_2 folding led to the development of an incipient S_2 crenulation cleavage, which is usually restricted to the more pelitic layers. When present, the S_2 cleavage (Figs. $5A_1$ and $5B_2$) is axial planar giving rise to a L_2 (S_0^S_2) intersection lineation parallel to D_2 hinges (Fig. $5A_2$ and $5B_2$).

As both the D_1 and the D_2 orthorhombic folds have subvertical axial planes and subperpendicular trends, a type 1 fold interference (Ramsay and Huber, 1987) was produced.

Although the D_2 orthorhombic folds are common in most of the WNW-ESE kinked domains, they are more frequent in the vicinity of the NNE-SSW faults that bound them. This

shows that such folds were developed due to the movement along these faults. The slight obliquity between the NE-SW folds and the N30ºE fault, is compatible with a sinistral kinematics along the NNE-SSW trend. Such conclusion is also supported by previous works in other sector of SW Portugal (Caroça and Dias, 2002), that described en-echelon NE-SW D_2 folds transected by an ENE-WSW S_2 cleavage, indicating a sinistral kinematics associated with NE-SW shear bands.

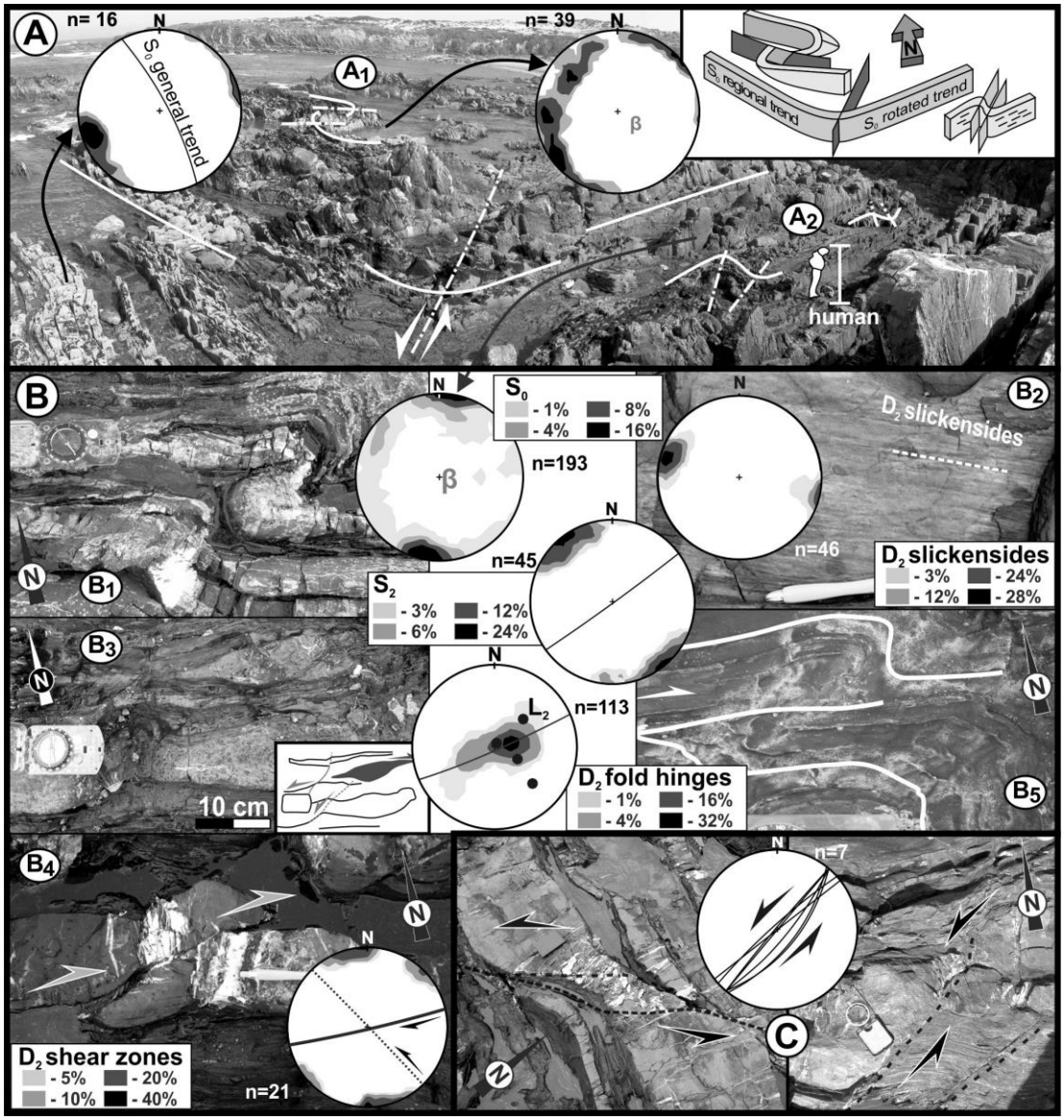

Figure 6 – Geometrical and kinematical features related with D_2 monoclinic structures in the E-W Almograve sector (equal area lower hemisphere stereographic projections).

A – Western boundary of the main Foz dos Ouriços kink-band (see Fig. 4A for location);

B – E-W D_2 dextral shear structures;

C – NNE-SSW D_2 sinistral shears.

Concerning the monoclinic D_2 folds set (Fig. 6) they are only found when the layers have strong dips and a trend close to E-W. They are also typical of places where the turbidites have a predominance of shales interbedded with centimetric to decimetric quartzwackes, often in the vicinity of metric quartzwacke layers not affected by such folding. These D_2 folds have subvertical axial planes slightly oblique to bedding trend, strongly plunging hinges and an eastern facing (Fig. $6B_1$). This geometry is compatible with a dextral shearing along the bedding. This is kinematically consistent with the subhorizontal slickensides in the bedding planes (Fig. $6B_2$), coupled with other sense of movement indicators, like sigma shape competent bodies (Fig. $6B_3$) or dextral faults (Fig. $6B_4$) often nucleating in the short limbs of these D_2 folds (Fig. $6B_5$).

Although both sets of D_2 folds are found in the WNW-ESE domain of the Almograve-Foz dos Ouriços kink-band, due to the different genetic mechanisms they were never observed in the same place. The absence of interference structures between both kinds of fold makes it difficult to determine their relative ages

X.1.4.1.1.2. Variscan Shear Zones

One of the most remarkable structures of Almograve are conjugated en echelon quartz veins related to the Variscan shear zones affecting quartz (Caroça and Dias, 2002; Marques *et al.*, 2010; Reber *et al.*, 2010; Zulauf *et al*, 2011; Dias and Basile, 2013). According to their temporal relation with the folds, they could be classified in two different sets: the early D_{1a} veins deformed by the regional folding (Fig. 7A), and the younger ones which have been superposed on the folds (Fig. 8A). Both families could also be distinguished by their geometries. While the acute angle between the older pre-folding conjugated shear zones is very small (23º to 31º; Fig. 7B), in the younger post folding veins such angle is always close to 60º (Fig. 8B). The unusual small angle between the pre-folding conjugated shear zones is not restricted to the Almograve sector and is the rule in the SW Iberia Variscides (Figs. 7C and 7D).

The temporal relation between the younger shear zones and both Variscan folding events (D_1 and D_2) is easy to establish. Indeed, the pattern of the stress field deduced by the conjugated shear zones in Almograve is consistently deflected by the D_2 major kink-folds (Fig. 8B): *i.e.* anticlockwise rotation in the E-W to WNW-ESE segments and clockwise in the NE-SW ones (Fig. 8C). The conclusion that these shear zones are pre-D_2 structures, is also consistent with the fact that, in each place where the stress field has been determined, the maximum principal compression (σ_1) stress is always orthogonal to the local fold trend (Fig. 8B). Thus the younger shear zones should be considered D_{1c} according to previous nomenclature (Fig. 2).

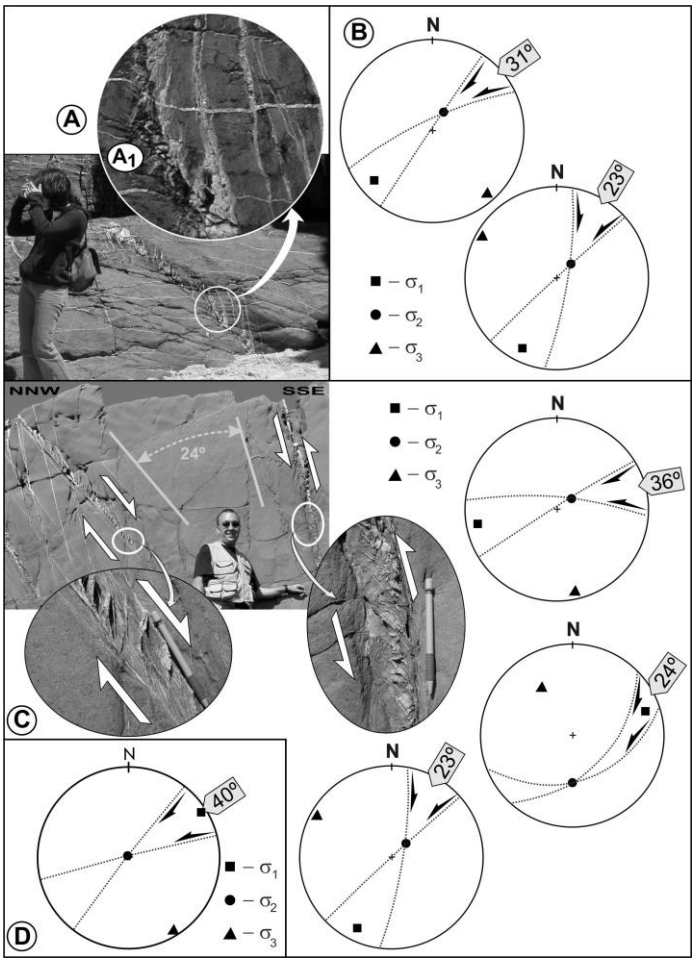

Figure 7 – Geometric and kinematic features of older conjugated Variscan shear zones in SW Iberia coast (equal area lower hemisphere stereographic projections):

A – En echelon quartz veins cut by outer arc fold extensional veins developed in Foz dos Ouriços beach folds (A_1);

B – Conjugated shear zones and related stress field for two situations in the southern domain of Almograve;

C – Conjugated shear zones and related stress field in the Arrifana sector;

D – Conjugated shear zones and related stress field for Cachado sector (north of Sagres).

Table 1 – Conjugated D_1 shear zones in SW Portugal.

sector	tectonic event	shear A		shear B		angle	σ_1	σ_2	σ_3
		attitude	kinem.	attitude	kinem.				
Almograve	**D_{1c}**	N40ºE,90	dextral	N80ºW,90	sinistral	60º	0º,N70ºE	90º	0º,N20ºW
Almograve	**D_{1c}**	N25ºE,80ºW	dextral	EW,70ºN	sinistral	63º	7º.S60ºW	70º,N8ºW	18º,S33ºE
Almograve	**D_{1c}**	N80ºE,75ºN	sinistral	N27ºE,75ºE	Dextral	58º	32º,S52ºW	58º,N54ºE	2º,N37ºW
Almograve	**D_{1a}**	N37ºE,90º	dextral	N68ºE,84ºS	sinistral	31º	20º,S50ºW	70º,N35ºE	5º,S42ºE
Almograve	**D_{1a}**	N56ºE,52ºS	normal	N62ºE,7º4S	reverse	23º	33º,N37ºE	56º,S51W	6º,S48ºE
Arrifana	**D_{1a}**	N68ºE,33ºS	---	N56ºE,68ºS	---	36º	14º,S78ºW	75º,N54ºE	5º,S13ºE
Arrifana	**D_{1a}**	N63ºE,53ºS	normal	N65ºE,77ºS	reverse	24º	20º,N71ºE	47º,S3ºW	37º,N35ºW
Arrifana	**D_{1a}**	N54ºE,83ºN	sinistral	N14ºE,80ºN	dextral	40º	14º,S28ºW	74º,N40ºE	4º,N62ºW
Cachado	**D_{1a}**	N77ºE,78ºN	sinistral	N40ºE,76ºN	dextral	36º	4º,N58ºE	86º,S80ºW	1º,S32ºE

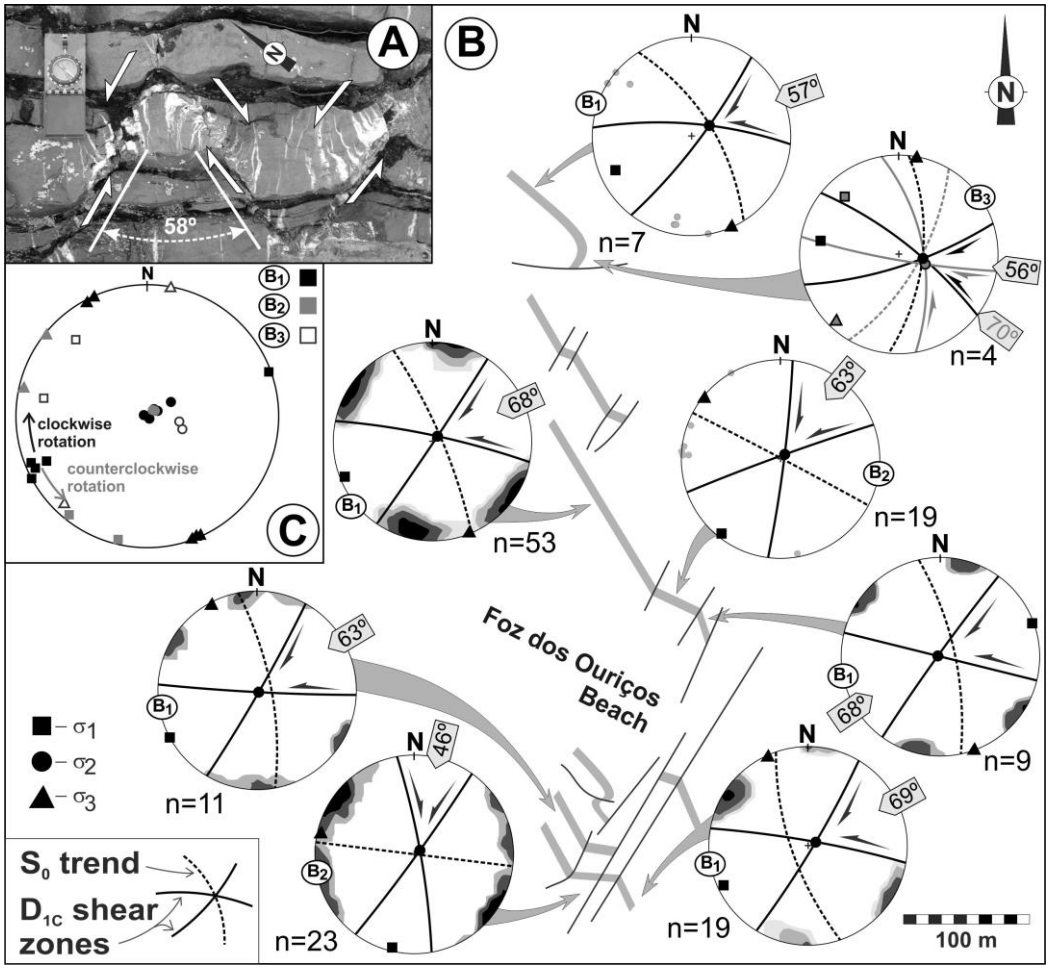

Figure 8 – Geometric and kinematic features of younger conjugated Variscan shear zones in Almograve (same area of figure 3):

A – Conjugated shear zones displacing strongly dipping layers of Almograve sector;

B – Conjugated shear zones and related stress field for several situations in the southern domain of Almograve (equal area lower hemisphere stereographic projections)

C – Compilation of Almograve stress field data.

The preservation of the stress field during the D_1 Variscan structures, shows a progressive and coaxial behaviour. However, if the orientation of the principal axes is preserved, the relative intensities between the main stresses change during the evolution of D_1 deformation (Table I). In the early D_{1a} stages, the acute angle is always below 40º (Fig. 7A), indicating the presence of hybrid fractures (Belayneh and Cosgrove, 2010) formed in a very low D_{1a} differential stress (σ_1-σ_3; Price and Cosgrove, 1990; Cosgrove, 2005). The acute angle is always very constant and close to the normal 60º for the late D_{1c} conjugate shears (Fig. 8B) expressing an higher differential stress (Belayneh and Cosgrove, 2010). Such a difference seems to indicate that during the D_{1c} the deformation occurred at a higher structural level than during

D_{1a}, which could result from the thickening of the turbiditic sequence due to the Variscan deformation. Indeed, the smaller D_{1a} acute angles could not be explained by the superposition of the flattening of younger D_{1b} or D_{1c} Variscan deformation events, because the similar orientation of their stress fields should have increase the initial angle whatever the limb in which they are found.

X.1.4.1.2. Variscan Kinematics of the NNE-SSW Fault Trend

The kinematics and age of the NNE-SSW major Variscan strike-slip faults in SW Portugal has been explained by two different opposite models:

- dextral and contemporaneous of the main D_1 regional folding event (Marques *et al.*, 2010; Fig. 9A);
- sinistral and younger than the main D_1 regional folding event (Caroça and Dias, 2002; Ribeiro *et al.*, 2007; Dias and Basile, 2013; Fig. 9B).

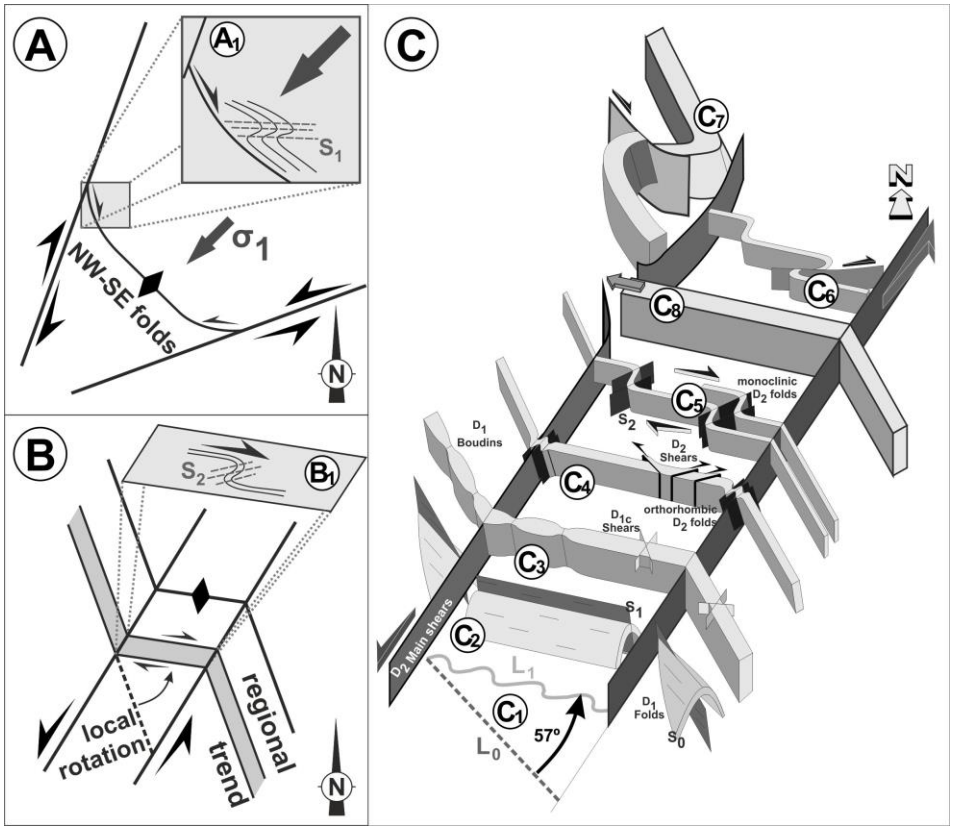

Figure 9 – Geometry and kinematics related to the NNE-SSW structures in SW Portugal.

A – The dextral model (adapted from Marques *et al.*, 2010);

B – The sinistral model (adapted from Caroça and Dias, 2002; Basile and Dias, 2013);

C – Main structural features related with the Foz dos Ouriços kink-band (see text for more details).

In the first model, the NNW-SSE structural trend is the result a local clockwise drag of the regional NW-SE structures due the dextral shearing along the major NNE-SSW wrench faults. This rotation, which was contemporaneous of the main D_1 folding event, gave rise to the E-W monoclinic folds, by a flattening mechanism induced by the interference between the regional compression and the dextral kinematics along the NNW-SSE layers (Fig. $9A_1$). Such dextral shearing was supported either by en-echelon quartz veins, or the deflection of sand dykes (figure 8 of Marques *et al.*, 2010). Concerning the quartz veins, care should be taken because described geometry, is also compatible with both dextral D_{1a} (Fig. 2A) and D_{1c} shears (Fig. 2D). Regarding the sand dykes, although they are usually considered to have initiated as orthogonal fractures to subhorizontal layers during diagenetic compaction (Cosgrove, 1997), field examples show that often they initiate oblique to the layering. This is clearly demonstrated by the coexistence in the same place of sand dykes with opposed deflections (Fig. 10). This strongly argued against the use of sand dykes as kinematic markers.

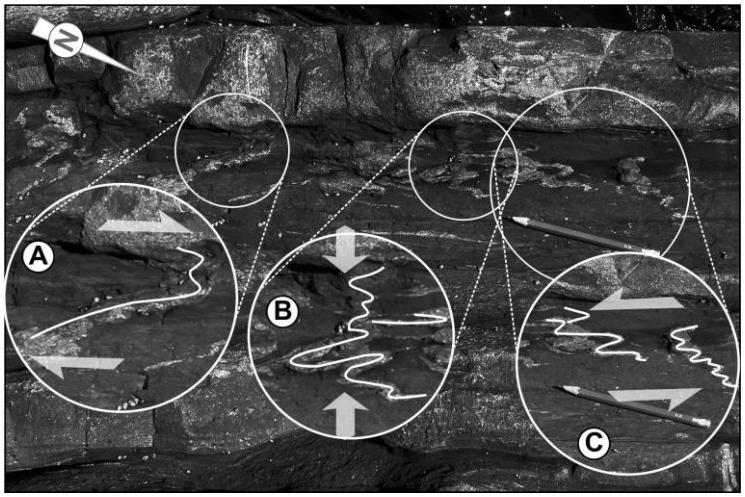

Figure 10 – Geometric complex behaviour of sedimentary dykes induced by diagenetic compaction in Arrifana port region.

A – Apparent dextral kinematics;

B – Orthogonal flattening;

C – Apparent sinistral kinematics.

It should be enhanced that, although the dextral kinematics along NNE-SSW faults could explain the ENE-WSW monoclinic folds (Fig. 6), it is unable to explain the frequent NE-SW orthorhombic folds (Fig. 5).

Moreover, the location of the younger D_2 structures only in the WNW-ESE kinked segment, shows that this orientation has only a local significance. Thus, the NNW-SSE general

trend in Almograve, where only the D_1 structures are found, must be considered the dominant regional trend, which have been anticlockwise deflected to WNW-ESE by the sinistral kink-band mechanism (Fig. 9B). Assuming such sinistral kinematics along the NNE-SSW faults, all the diversity of the structures found in Almograve could be explained (Fig. 9C). Indeed, the strong distortion related to the 57º rotation of the kink-band inner domain in relation with the outer NNW-SSE regional trend, superimposed on a highly anisotropic material, gave rise to the coexistence of different deformation mechanisms. Considering a constant width of the kink band (which is supported by the observation in the sectors near its extremities), and using the trends of the inner and outer domains, a 20% shortening should be expected during the rotation (Fig. $9C_1$). Thus, the simple and rigid rotation of previous D_1 structures (Figs. $9C_2$ and $9C_3$) cannot accommodate all the Late Variscan deformation inside the shear zone. As there is no evidence of considerable volume loss related with the D_2 phase (*e.g.* the intense quartz veining of Almograve is only related with the D_1 deformation), this orthogonal shortening must be compensated by subhorizontal and/or subvertical extension. The deformation induced by this shortening is heterogeneously distributed, being stronger in the vicinity of the kink band subvertical boundaries. The NNE-SSW to NE-SW D_2 folding with orthorhombic symmetry (Fig. 5), as well as conjugated shears displacing layer boundaries are due to such mechanism (Fig. $9C_4$). The lack of vergence of these folds, is explained by the subvertical geometry of the kink band limits which behaves as obstacles to the migration of the D_2 deformation.

The D_2 folds with subvertical hinges and a strong monoclinic symmetry highlight a strong dextral shearing subparallel to layers in the WNW-ESE inner domain (Figs. 6B and $9C_5$), this is an expected behaviour in some sinistral kink band (Ramsay and Huber, 1987; Twiss and Moores, 1992). Indeed, the progression of the sinistral rotation of the kink should be coupled with dextral shear strain on the rotating surfaces (Figs. $9C_5$ and $9C_6$).

The heterogeneities of the turbidite sequence could induce some irregularities in the structural pattern. The anomalous major fold (Figs. $6A_1$ and $9C_7$), although presenting a geometry similar to the D_2 monoclinic folds, is located outside the inner domain of the kink bands is attributed to the indentation of an anomalous metric thick quartzwacke package in adjacent pelitic zones (Fig. $9C_8$). Indeed, the shortening of such a competent package inside the kink band is difficult due to space considerations, which induce its indentation in the sectors adjacent to the kink band where incompetent shales are predominant. Such mechanism will produce, not only the folding/disruption of the boundaries of the kink band, but also anomalous folding in the domains adjacent to the indentor (Coke *et al.*, 2003).

It is worth to notice that in Northern domains of the studied Almograve Sector (Fig. 3), an important E-W dextral shear zone is found in places not related to sinistral kink bands. This shear zone generates a decametric drag fold, with NE-SW subvertical axial plane and steeply plunging hinge (Fig. $3A_1$), which rotate previous structures (Fig. 8B), showing that it is also related with the Late Variscan D_2 episode.

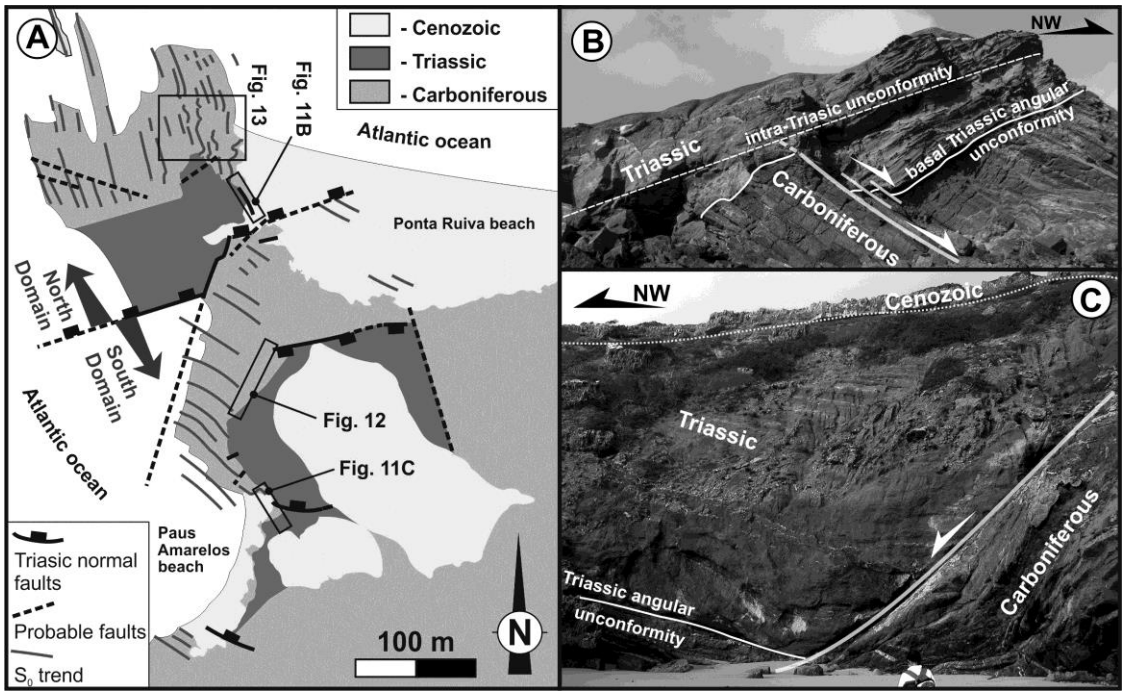

Figure 11 – General structural pattern of Ponte Ruiva area.

A – Structural map emphasizing main features related to D_2 deformation;

B – Triassic unconformity of the northern domain;

C – Triassic unconformity and extensional boundary fault of southern domain.

X.1.4.2. The Ponta Ruiva Sector

In Ponta Ruiva the angular unconformity between the weakly deformed Triassic sediments and the highly folded low metamorphosed Carboniferous units is exceptionally exposed (Fig. 11). As in Almograve, in Ponta Ruiva it is possible to observe adjacent sectors with contrasting Variscan trends (Fig. 11A): NNW-SSE and NW-SE. However, here the transition between both domains is harder to understand, not only due to a strong overprinting by the early episode related to the Atlantic opening, but also to the smaller extent of the outcrops in the wave cut platform. This younger extensional tectonic event gives rise to a complex set of small scale intracontinental basins filled by several syn-rift sedimentary units of Triassic

age (Dias and Ribeiro, 2002). The opening of these basins has been controlled by the reworking of previous Variscan anisotropies (Dias and Basile, 2013) with ENE-WSW to E-W trend.

X.1.4.2.1. Variscan Deformation Geometry in Ponta Ruiva Sector

The geometry of the Variscan deformation in the Carboniferous turbidites led to the individualization of two different domains in Ponta Ruiva (Fig. 11A):

- The southern domain is well expressed along the cliffs and the neighbouring wave cut platform. The main structure (Fig. 12) corresponds to a major NW-SE D_1 recumbent fold facing to SW with subhorizontal axial plane (Fig. 12A). The S_1 cleavage (Fig. 12B), which fans around the fold, is pervasive in the more pelitic layers. It has an axial plane attitude which is also confirmed by the parallelism between the subhorizontal L_1 (S_0^S_1) intersection lineation and the D_1 fold hinges (Fig. 12C). Locally, rare D_2 folds occur with subvertical axes (Fig. 11D), which are more frequent in the vicinity of the major extensional fault of the Paus Amarelos beach (Fig. 11C).

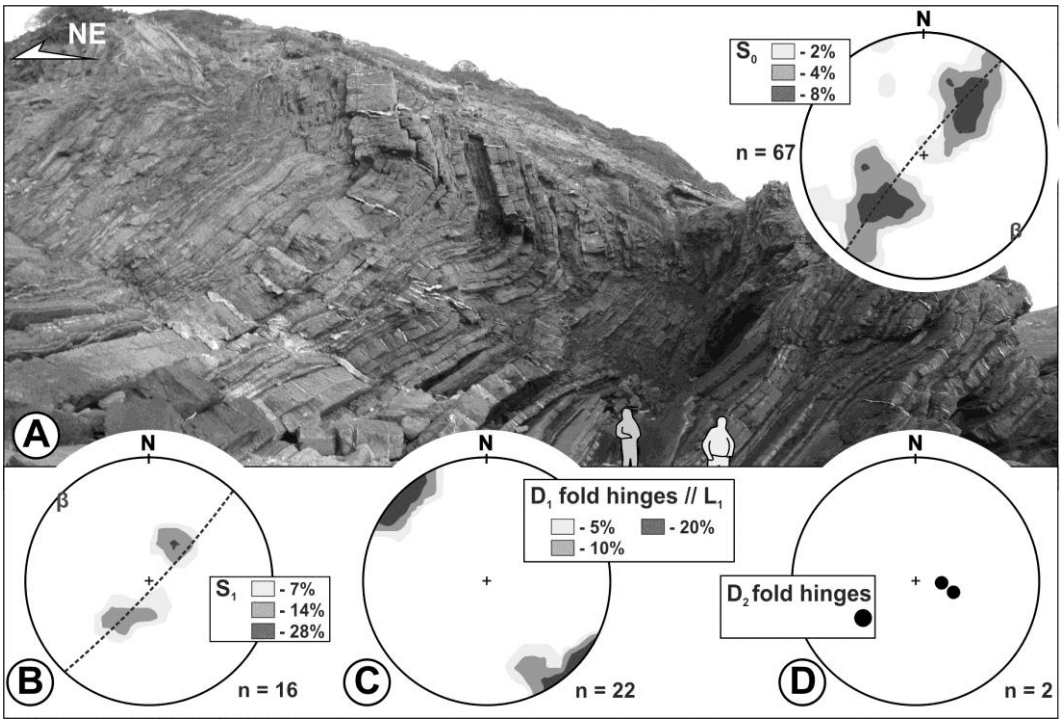

Figure 12 – Structural features in the southern domain of Ponta Ruiva (equal area lower hemisphere stereographic projections):

A – Main D_1 recumbent fold with bedding (S_0) geometry;

B – S_1 cleavage geometry;

C – Geometry of L_1 intersection lineation and D_1 hinges;

D – Geometry of D_2 hinges.

- The northern domain corresponds to the more external sector of the wave-cut platform, where the Variscan structure is a reverse limb of a major D_1 fold. The singularity of this domain in the regional context comes, not only from the NNW-SSE trend (Fig. 13A), but mostly from the dipping hinges of the minor D_1 folds (Fig. 13B and 13C). The present attitude of the fold axes (26º, N44ºW; Fig. 13C) would increase the plunge when the pre-Triassic position is restored by the removal of the Atlantic extensional deformation (37º, N52ºW; Fig. 13D). The plunging hinges of the D_1 mesoscopic folds show that the Variscan geometry of this domain is local and results from the distortion of the regional structure where the folds have always subhorizontal hinges, as observed in the southern domain (Ribeiro and Silva, 1983; Silva *et al.*, 1990; Dias and Basile, 2013).

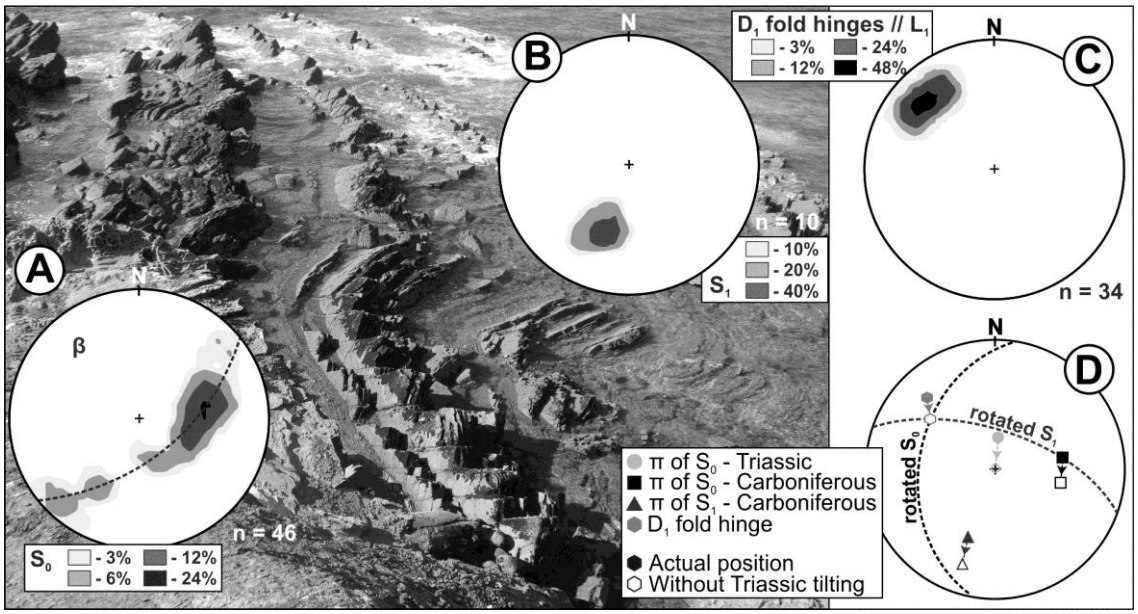

Figure 13 – Structural features in the northern domain of Ponta Ruiva (equal area lower hemisphere stereographic projections):

A – D_1 folds with bedding (S_0) geometry;

B – S_1 cleavage geometry;

C – Geometry of L_1 intersection lineation and D_1 hinges;

D – Rotation of D_1 structures associated with the removal of the Triassic deformation.

X.1.4.2.2. Structural Evolution of Ponta Ruiva Sector

The oldest structures of Ponta Ruiva are the NW-SE D_1 recumbent folds facing SW (Fig. 12A), which is the normal regional trend for the major Variscan folds in SW Portugal (Fig. 1; Ribeiro *et al.*, 1979). The dip of the axial surfaces is controlled by the proximity to major

thrusts (Ribeiro, 1983) and the sub-horizontal geometries observed in Ponta Ruiva results from the vicinity of D_1 major thrusts, which are frequent in SW Portugal (Fig. 1B; Dias and Basile, 2013).

The local rotation of the D_1 Variscan structures observed in the northern Ponta Ruiva domain (Fig. 11A) could not be explained by the Triassic extension and must have been induced by the Late Variscan deformation, which also produced the D_2 folds with subvertical axes (Fig. 12D). The ENE-WSW to E-W trend of the major boundary faults of Ponta Ruiva Triassic basins (Fig. 11A), suggests that such direction must have been dominant during Palaeozoic times. A dextral kinematics along the ENE-WSW boundary fault between the northern and southern domains (Fig. 14), similar to the Almograve Late Variscan behaviour (*i.e.* Fig. $3A_1$), with the expected coeval shortening in the rotated northern sector, explains, not only the more northerly trend but also the plunging hinges of the D_1 structures.

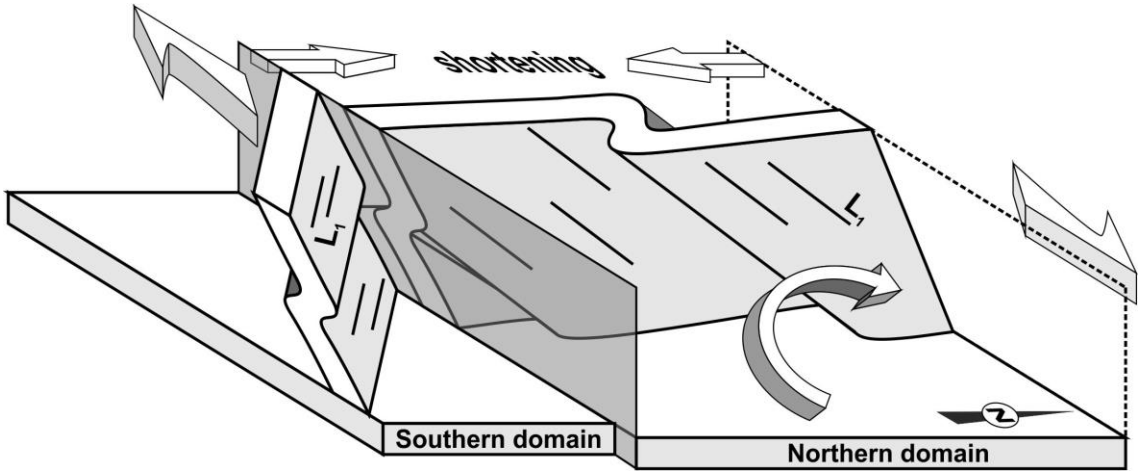

Figure 14 – Distortion of the D_1 structures by the Late Variscan ENE-WSW dextral shear.

The erosive processes, which became predominant after the last increments of the Variscan deformation, gave rise to a subhorizontal surface that is well preserved at the base of the Triassic sediments (Figs. 11B and 11C). The structural mapping of the Triassic-Carboniferous relations shows that the Ponta Ruiva basins opening was mostly controlled by E-W to ENE-WSW normal faults (Dias and Ribeiro, 2002), which locally reworked D_2 dextral strike-slip Late Variscan faults.

X.1.5. Geodynamical Implications

The new data from the SW Iberia help the understanding of Late Variscan geodynamical evolution. Indeed, they can be used to debate the kinematics of NNE-SSW Iberian wrench

faults, described in North of Portugal (*e.g.* Ribeiro, 1974; Ribeiro *et al.*, 1990; Lourenço *et al.*, 2002; Marques *et al.*, 2002; Ribeiro *et al.*, 2007), and also constrain their deformation ages.

X.1.5.1. The deformation ages of SW Iberia Structures

The older formation outcropping in the Almograve (Fig. 4) and Ponta Ruiva (Fig. 10) studied regions belongs to the Baixo Alentejo Flysch Group (Oliveira, 1990). Detailed paleontological studies (Pereira *et al.*, 2007; Jorge *et al.*, 2013; Oliveira *et al.*, 2013) show that this turbiditic formation is diachronous, ranging from Visean in the northern domains to Upper Moscovian in the southern tip. The paleocurrent indicators preserved in the turbidites (*e.g.* groove and flute casts) are often subperpendicular to the D_1 fold axes, which suggests that the sedimentation is coeval with the deformation (Oliveira, 1990; Dias and Basile, 2013). So, the main Variscan deformation of the Carboniferous turbidites (D_1) seems to be also diachronous, being older in the more internal NE domains (Ribeiro and Silva, 1983).

The age of the D_2 dextral shear zones could only be constrained in the Ponta Ruiva sector. The Carboniferous turbidites are here Upper Moscovian (Pereira *et al.*, 2007; Oliveira *et al.*, 2013) and have been strongly folded during D_1 (Figs. 12A and 13A; Caroça and Dias, 2001; Dias and Ribeiro, 2002; Dias and Basile, 2013). The younger sediments on top of the Carboniferous flysch of SW Portugal is at least Middle to Upper Triassic (Palain, 1976), but possibly could attain the Lower Triassic (Rocha, 1976). In Ponta Ruiva, these sediments have been shown to be syn-rift in relation to the early extensional stages of the Atlantic opening (Fig. 11B; Dias and Ribeiro, 2002). As the D_1 age should be close to the local Carboniferous sedimentation (*i.e.* Upper Moscovian) and the D_2 shear zones have been reactivated as normal faults during the Triassic extension, the age of D_2 phase is bracketed by these two events. This means that the D_2 in SW Portuguese coast must be considered a Late Variscan tectonic event, acting during Late Carboniferous and Permian times, as emphasized by Noronha *et al*. (1981) for the Central Iberian Zone in Northern Portugal.

X.1.5.2. The NNE-SSW Late Variscan Kinematics

As the Almograve structural data show (Fig. 9C), the NNE-SSW faults have a sinistral kinematics. This behaviour is pervasive along the SW Portuguese coast, where NNE-SSW to NE-SW hectometric faults and/or kink bands with metric to decametric sinistral displacements are common (Caroça and Dias, 2002; Dias and Basile, 2013). The strongly linear NNE-SSW trend of this coast, seems to indicate that it is controlled by a deep first order Late Variscan sinistral fault, whose superficial expression is the 2nd and 3rd order sinistral fault like structures found in

Almograve type faults (Fig. 15A; Caroça and Dias, 2002; Dias and Basile, 2013). The obliquity between both scales of faults indicates that the minor ones could be interpreted as *p*-type fractures inside a main shear zone (Fig. 15A). A comparison of the trend of the D_2 sinistral fractures of Almograve (NNE-SSW; Fig. 3) with the observed further to SW (NE-SW; Caroça and Dias, 2002) shows a slight rotation (Figs. $15A_1$ and $15A_2$). Such rotation accompanies the linear orientation of the Portuguese coast.

The existence of a probable major NNE-SSW Late Variscan left lateral fault in SW Iberia shows that the dominant trend of Late Variscan faults in northern Portugal (*e.g.* Vilariça and Régua-Chaves-Verin first order faults; Fig. 15B) are also found further south (Fig. 15A). As in SW Portugal the sinistral kinematics is clear (Figs. 4 and 9C), the same kinematics must be expected in the northern Portugal NNE-SSW faults. Nevertheless. although the sinistral kinematics during Late Variscan times is usually considered (Ribeiro, 1974; Ribeiro *et al.*, 1979; Iglesias and Ribeiro, 1981; Choukhroune and Iglésias, 1980; Pereira *et al.*, 1993; Ribeiro *et al.*, 2007; Moreira *et al.*, 2010; 2014; Dias *et al.*, 2013), an alternative proposal is that the sinistral sense was only an alpine reworking of a dextral NNE-SSW Late Variscan kinematics (Marques *et al.*, 2002; Lourenço *et al.*, 2002).

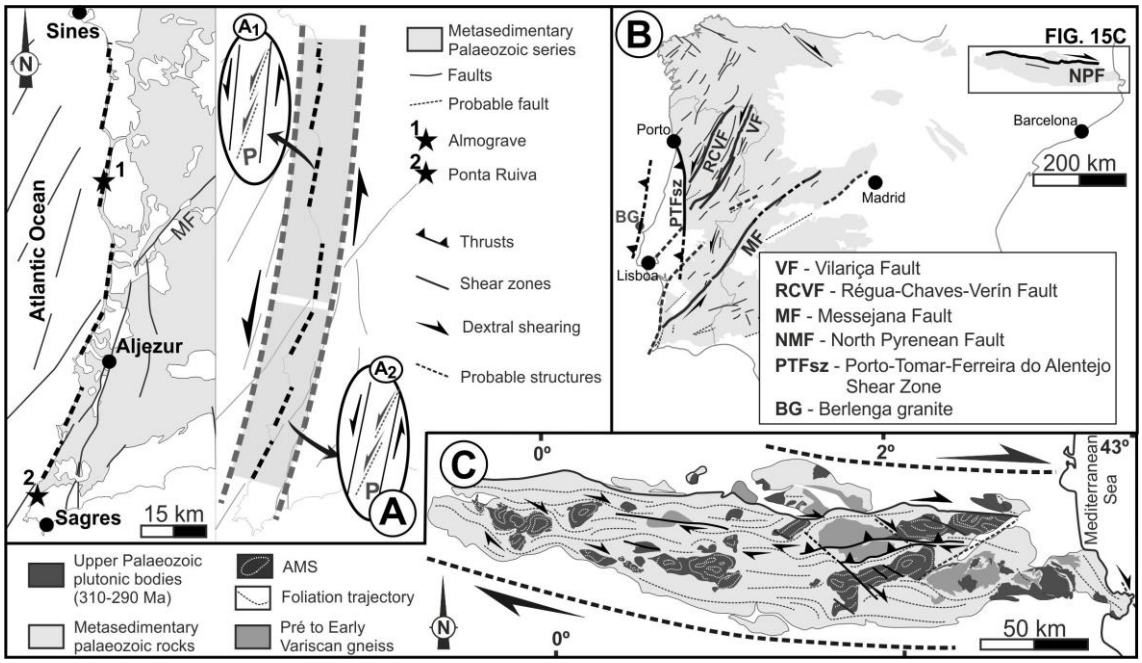

Figure 15 – Late Variscan structural behaviour in Iberia.

A – Interpretative fracture pattern along the SW Portuguese coast;

B – Main fracture pattern in Iberia;

C – Structural sketch of the Variscan Pyrenees (adapted from Zwart, 1986; Carreras, 2001; Denèle *et al.*, 2014).

The dextral interpretation was based essentially in the K-Ar 312 Ma age in muscovites concentrates from aplites and tourmaline-muscovite aggregates related to NE-SW segments in NNE-SSW faults in Northern Portugal (Marques *et al.*, 2002) and the geometrical / kinematical data from quartz veins, which are difficult to ascribe to the different tectonic events. Although these authors considered the obtained age a lower limit for the Late Variscan wrench faulting period, it could also be considered the upper limit for the D_3 Variscan regional event (Dallmeyer *et al.*, 1997). Thus, the proposed dextral movement along the NNE-SSW fault set should be considered as related, not with the Late Variscan kinematics (Marques *et al.*, 2002), but with the regional D_3 Variscan tectonic event as previously reported in several works (Ribeiro, 1974; Ribeiro *et al.*, 1979; Pereira *et al.*, 1993; Dias *et al.*, 2013; Noronha *et al.*, 2013). Therefore, the new data in SW Portuguese coast shows that the predominant movement in the NNE-SSW to NE-SW faults during Late Variscan times (i.e. Post-Moscovian - Pre-Triassic) was left-lateral, as proposed in early works (Ribeiro, 1974; Arthaud and Matte, 1975; 1977; Ribeiro *et al.*, 1979; Choukhroune and Iglésias, 1980; Iglesias and Ribeiro, 1981).

X.1.5.3. The E-W to ENE-WSW Dextral Kinematics

Even if the NNE-SSW fracture pattern has a pervasive development in Iberia (Fig. 15B), the SW Portuguese data show that the Late Variscan deformation cannot be understood without taking into account the E-W to ENE-WSW dextral shear zones. Indeed, although the sinistral NNE-SSW trend is usually more common, the dextral one sometimes becomes predominant.

The E-W to ESE-WNW structural trend is dominant in the axial zone of Pyrenees, in the Neoproterozoic and Palaeozoic rocks (Fig. 15C; *e.g.* Zwart, 1986; Castiñeiras *et al.*, 2008), where a polyphasic tectonotermal evolution with three Variscan deformation events is found (Carreras, 2001; Druguet, 2001). Such trend is usually correlated with the main Variscan tectonometamorphic event (local D_2) characterized by a dextral transpressional regime (Carreras and Druguet, 1994; Leblanc *et al.*, 1996; Druguet and Hutton, 1998; Gleizes *et al.*, 1998; Carreras, 2001; Druguet, 2001; Carreras *et al.*, 2004; Druguet *et al.*, 2014). The D_2 event is related with a progressive high temperature-low pressure metamorphic event (Druguet and Hutton, 1998; Druguet, 2001; Druguet *et al.*, 2014) associated with melt generation and the emplacement of an important set of plutonic bodies. Recent geochronological data constrain the age of emplacement of these syntectonic bodies between 310-290 Ma (*i.e.* Carboniferous-Permian transition; Denèle *et al.*, 2014; Druguet *et al.*, 2014; Pereira *et al.*, 2014), and consequently also constrain the age of the D_2 event. The anisotropy of magnetic susceptibility (AMS) shows clear evidence of dextral kinematics during the emplacement of these D_2

syntectonic plutonic bodies (Fig. 15C; Leblanc *et al.*, 1996; Gleizes *et al.*, 1997; 1998; Antolín-Tomás *et al.*, 2009; Denèle *et al.*, 2014). Gleizes *et al.* (1997; 1998) also remark the presence of continuous deformation from the magmatic state to the high-temperature solid state, which shows that dextral transpression remained active even after the emplacement. The previous data highlight an important Late Variscan WNW-ESE dextral tranpressive shear zone in the basement of the Axial Zone of the Pyrenees, which remained active from the Late Carboniferous until at least the Lower Permian.

Further South in Iberia, the predominance of E-W major right lateral shear zones during Late Variscan times could also be emphasized in the Azores-Gibraltar shear zone (Fig. 16; Ribeiro *et al.*, 2007; Dias *et al.*, 2016). However, these kinematics are poorly constrained due to their reworking as a plate boundary during the Pangaea breakup and the Alpine orogeny.

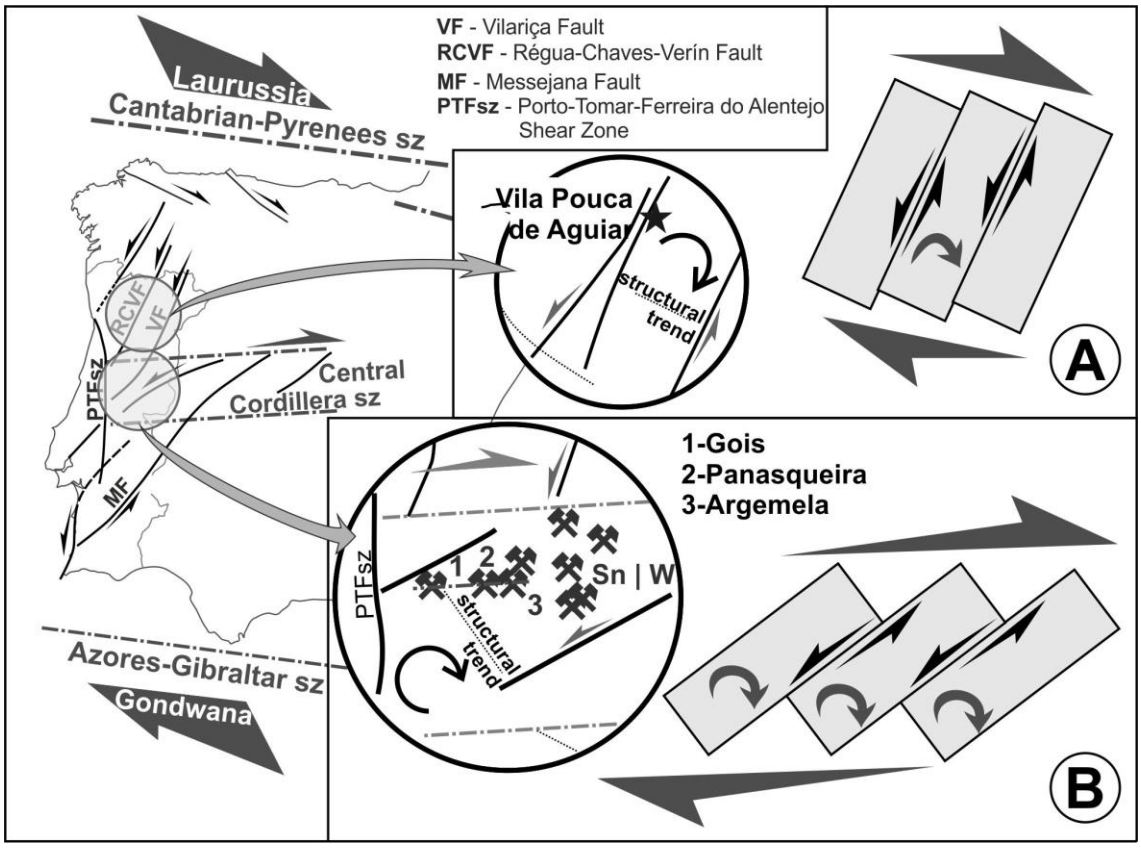

Figure 16 – Interpretative domino model for Iberian geodynamics during Late Variscan times (adapted from Ribeiro, 2002; ore occurrences adapted from Pereira *et al.*, 1993 and Noronha *et al.*, 2013).

A – NNE-SSW faults related to a low block rotation;

B – NE-SW faults related to a moderate/strong block rotation.

The major role that the E-W shear zones play in Iberia could be extended to the neighbouring regions. Indeed, they are also found, not only in southern France (Martínez-García, 1996), but also in the Moroccan Variscides (Piqué *et al.*, 1990; Houari and Hoepffner, 2003; Simancas *et al.*, 2005; Ribeiro, *et al.*, 2007). Although such major shear zones were already active since the main orogenic events, sometimes they are considered to be still active in Late Variscan times (Ribeiro *et al.,* 2007; Dias *et al.*, 2011).

X.1.5.4. An Unifying Approach

The absence of the dextral conjugated set (which in a brittle to brittle-ductile regime should be NNW-SSE; Ribeiro *et al.*, 1979), the relatively moderate offset comparing to the extension of the NNE-SSW major faults and the existence of N-S Late Variscan thrusts with an eastern displacement in the Berlengas archipelago (Fig. 15B), led Ribeiro (2002) to propose a domino model for the Late Variscan deformation (Fig. 16).

In this model, the dextral transpression induced by the Late Variscan oblique collision between Laurentia and Gondwana (Arthaud and Matte, 1975; 1977; Dias and Ribeiro, 1994; 1995; Ribeiro *et al.*, 1995: Shelley and Bossière, 2000; 2002; Ribeiro, 2002; Ribeiro *et al.*, 2007; Dias *et al.*, 2016) was mostly concentrated in the major E-W Iberian shear zones, located in Azores-Gibraltar and North Pyrenean shear zones. The domains between these shear zones where heterogeneously deformed. The important regional D_3 NNE-SSW tensile fractures in Central Iberian Zone (Ribeiro, 1974; Pereira *et al.*, 1993; Mateus, 1995) were rotated clockwise during the Late Variscan times. Such movement gave rise to a dextral domino due to the also clockwise rotation of the blocks bounded by the NNE-SSW faults, which thus will have a coeval sinistral kinematics (Figs. 16A and 16B; Ribeiro, 2002; Ribeiro *et al.*, 2007).

As expected, in a domino model, the amount of block rotation is strongly related with the intensity of distortion induced by the simple shear component. In Iberia, this is supported by the trend of the major sinistral Late Variscan faults (Dias *et al.*, 2013). The rotation from a NNE-SSW trend, either in northern (Fig. 16A; Régua-Chaves-Verin and Vilariça faults), or southern (Fig. 16; Messejana fault) sectors, to a NE-SW on Central Iberia (Fig. 16B), is explained by the lesser or stronger influence of the major ENE-WSW dextral Central Cordillera shear zone (Ribeiro, 2002). The same rotation is also observed using the main regional D_1 Variscan structures, whose general trend of folds have a WNW-ESE direction in northern Portugal (Fig. 16A), and a NW-SE in Central Portugal (Fig. 16B). The Central Cordillera shear zone is also enhanced by discrete E-W Late Variscan lineaments of Late Variscan mineralizations like the tin-tungsten-gold Góis-Panasqueira-Argemela band (Fig. 16B; Ribeiro and Pereira, 1982).

A similar deflection is found in the SW Portuguese coast (Caroça and Dias, 2002), with the main Late Variscan fractures rotating from NNE-SSW (Fig. 15A$_1$) towards NE-SW in the southern sectors (Fig. 15B). Such behaviour should be expected due to a closer proximity of the first order E-W dextral Azores-Gibraltar shear zone.

X.1.6. Conclusions

The principal outcomes of this study are concluded below:

i. The Variscan structures in the SW of South Portuguese Zone are the result of a long lasting diachronic process during the D_1 tectonic event, followed by D_2 deformation ascribed to the Late Variscan times;

ii. The NNE-SSW Late Variscan faults have a predominantly sinistral kinematics;

iii. The Late Variscan fault pattern in Iberia could be explained by a domino model controlled by E-W to ENE-WSW major dextral strike-slip shear zones, inducing the clockwise rotation of the blocks bounded by the NNE-SSW faults;

iv. This model could be considered an improvement of the dextral E-W mega-shear model of Arthaud and Matte (1975; 1977), between what they considered a northern American-European plate and a southern African one.

References

Abad, I., Nieto, F., Vellila, N., Simancas, J. (2004). Metamorfismo de la Zona Sudportuguesa. In: Vera J.A. (ed), Geologia de Espana. SGE-IGME, Madrid, 209-211.

Antolín-Tomás, B., Román-Berdiel, T., Casas-Sainz, A., Gil-Peña, I., Oliva, B., Soto, R. (2009). Structural and magnetic fabric study of the Marimanha granite (Axial Zone of the Pyrenees). Int. J. Earth Sci. (Geol Rundsch), 98, 427–441. DOI 10.1007/s00531-007-0248-1

Arthaud, F., Matte, Ph. (1975). Les decrochements tardi-hercyniens du sud-ouest de l'Europe, geometrie et essai de reconstitution des conditions de la deformation. Tectonophysics, 25, 139-171. doi:10.1016/0040-1951(75)90014-1

Arthaud, F., Matte, Ph. (1977). Late Paleozoic strike-slip faulting in southern Europe and northern Africa: result of a righ-lateral shear zone between the Appalachians and the Urals. Geol. Soc. Am. Bull., 88, 1305-1320. doi: 10.1130/0016-7606(1977)88<1305:LPSFIS>2.0.CO

Belayneh, M., Cosgrove, J. (2010). Hybrid veins from the southern margin of the Bristol Channel Basin, UK. J. Struct. Geology, 32, 192–201. doi:10.1016/j.jsg.2009.11.010

Bradley, D.C., Kidd, W.S.F. (1991). Flexural extension of the upper continental crust in collisional foredeeps, Geological Society of America Bulletin, 103(11), 1416-1438. DOI: 10.1130/0016-7606(1991)103<1416:FEOTUC>2.3.CO;2

Caroça, C., Dias, R. (2001). Estrutura Varisca na região de Sagres; um exemplo de deformação progressiva. Comun. Inst. Geol. Min. Portugal, 88, 1-16.

Caroça, C., Dias, R. (2002). Deformação transcorrente nos sectores externos da zona Sul Portuguesa; os últimos incrementos da tectónica Varisca, Comun. Inst. Geol. Min. Portugal, 89, 115-126.

Carreras, J. (2001). Zooming on Northern Cap the Creus Shear Zones, J. Struct. Geol., 23, 1457-1486. DOI: 10.1016/S0191-8141(01)00011-6

Carreras, J., Druguet, E. (1994). Structural zonation as a result of inhomogeneous non-coaxial deformation and its control on syntectonic intrusions: an example from the Cap de Creus area (eastern-Pyrenees). J. Struct. Geol., 16, 1525–1534. DOI:10.1016/0191-8141(94)90030-2

Carreras, J., Druguet, E., Griera, A., Soldevila, J. (2004). Strain and deformation history in a syntectonic pluton. The case of the Roses granodiorite (Cap de Creus, Eastern Pyrenees). In: Alsop, G.I., Holdsworth, R., McCaffrey, K., Hand, W. (Eds.), Flow Processes in Faults and Shear Zones. Geol. Soc. London, 224, 307–19. DOI:10.1144/GSL.SP.2004.224.01.19

Carvalho, D., Goinhas, J., Oliveira, V., Ribeiro, A. (1971). Observações sobre a geologia do Sul de Portugal e consequências metalogenéticas. Est. Notas e Trab. Serv. Fom. Min., 20, 153-199.

Castiñeiras, P., Navidad, M., Liesa, M., Carreras, J., Casas, J.M. (2008). U–Pb zircon ages (SHRIMP) for Cadomian and Early Ordovician magmatism in the Eastern Pyrenees: new insights into the pre-Variscan evolution of the northern Gondwana margin. Tectonophysics, 461, 228–39. DOI: 10.1016/j.tecto.2008.04.005

Choukhroune, P., Iglésias, M. (1980). Zonas de cisalla dúctil en el NW de la Peninsula Ibérica. Cuad. Lab. Xeol. Laxe, 1, 163-164.

Coke, C., Dias, R., Ribeiro, A. (2003). Rheologically induced structural anomalies in transpressive regimes, J. Struct. Geol., 25(3), 409-420. DOI: 10.1016/S0191-8141(02)00043-3

Cosgrove, J. (1997). Hydraulic fractures and their implications regarding the state of stress in a sedimentary sequence during burial. In: Sengupta, S. (Ed.), Evolution of Geological Structures in Micro- to Macro-scales, Chapman & Hall, 11-25. DOI: 10.1007/978-94-011-5870-1_2

Cosgrove, J. (2005). Tectonics: Fractures (Including joints). In: Selley, R.C., Cocks, L.R.M., Plimer, I.R. (Eds.), Encyclopedia of Geology, Elsevier Academic Press, 352-361.

Dallmeyer, D., Martínez Catalán, J., Arenas, R., Gil Ibarguchi, J., Gutiérrez Alonzo, G., Farias, P., Bastida, F., Aller, J. (1997). Diachronous Variscan tectonothermal activity in the NW Iberian Massif: Evidence from 40Ar/39Ar dating of regional fabrics. Tectonophysics, 277, 307-337. DOI:10.1016/S0040-1951(97)00035-8

Denèle, Y., Laumonier, B., Paquette, J., Olivier, Ph., Gleizes, G., Barbey, P. (2014). Timing of granite emplacement, crustal flow and gneiss dome formation in the Variscan segment of the Pyrenees. In: Schulmann, K., Martínez Catalán, J.R., Lardeaux, J.M., Janousek, V., Oggiano, G. (Eds.) The Variscan Orogeny: Extent, Timescale and the Formation of the European Crust. Geol. Soc. London, 405, 265-287. DOI:10.1144/SP405.5

Dias, R., Ribeiro, A. (1994). Constriction in a transpressive regime: an example in the Ibero-Armoricain Arc. J. Struct. Geol., 16(11), 1543-1554. DOI:10.1016/0191-8141(94)90032-9

Dias, R., Ribeiro, A. (1995). The Ibero-Armorican arc: a collisional effect against an irregular continent? Tectonophysics, 246(1-3), 113-128. DOI:10.1016/0040-1951(94)00253-6

Dias, R., Ribeiro, C. (2002). O Triásico da Ponta Ruiva (Sagres); um fenómeno localizado na Bacia Mesozóica Algarvia. Comun. Inst. Geol. Min Portugal, 89, 39-46.

Dias, R., Basile, C. (2013). Estrutura dos sectores externos da Zona Sul Portuguesa; implicações geodinâmicas. In: Dias, R., Araújo, A., Terrinha, P., Kullberg, J.C. (Eds.), Geologia de Portugal, vol. 1, Escolar Editora, 787-807.

Dias, R., Hadani, M., Leal Machado, I., Adnane, N., Hendaq, Y., Madih, K., Matos, C. (2011). Variscan structural evolution of the western High Atlas and the Haouz plain (Morocco). Journal of African Earth Science, 61, 331-342. DOI:10.1016/j.jafrearsci.2011.07.002

Dias, R., Ribeiro, A., Coke, C., Pereira, E., Rodrigues, J., Castro, P., Moreira, N., Rebelo, J. (2013). Evolução estrutural dos sectores setentrionais do autóctone da Zona Centro-Ibérica. In: Dias, R., Araújo, A., Terrinha, P., Kullberg, J.C. (Eds.), Geologia de Portugal, vol. 1, Escolar Editora, 73-147.

Dias, R., Ribeiro, A., Romão, J., Coke, C., Moreira, N. (2016). A Review of the Arcuate Structures in the Iberian Variscides; Constraints and Genetical Models. Tectonophysics, 681, 170-194. DOI: 10.1016/j.tecto.2016.04.011

Druguet, E. (2001). Development of high thermal gradients by coeval transpression and magmatism during the Variscan orogeny: insights from the Cap de Creus (Eastern Pyrenees). Tectonophysics, 332, 275–293. DOI:10.1016/S0040-1951(00)00261-4

Druguet, E., Hutton, D. (1998). Syntectonic anatexis and magmatism in a mid-crustal transpressional shear zone: an example from the Hercynian rocks of the eastern Pyrenees. J. Struct. Geol., 20, 905–916. DOI: 10.1016/S0191-8141(98)00017-0

Druguet, E., Castro, A., Chichorro, M., Pereira, M., Fernández, C. (2014). Zircon geochronology of intrusive rocks from Cap de Creus, Eastern Pyrenees Geol. Mag., 151(6), 1095–1114. DOI: 10.1017/S0016756814000041

Gleizes, G., Leblanc, D., Bouchez, J. (1997). Variscan granites of the Pyrenees revisited: their role as syntectonic markers of the orogen. Terra Nova, 9, 38–41. DOI: 10.1046/j.1365-3121.1997.d01-9.x

Gleizes, G., Leblanc, D., Santana, V., Olivier, Ph., Bouchez, J. (1998). Sigmoidal structures featuring dextral shear during emplacement of the Hercynian granite complex of Cauterets-Panticosa (Pyrenees). J. Struct. Geol., 20(9-10), 1229-1245. DOI:10.1016/S0191-8141(98)00060-1

Houari, M., Hoepffner, C. (2003). Late Carboniferous dextral wrench-dominated transpression along the North African craton margin (Eastern High-Atlas, Morocco). Journal of African Earth Science, 37, 11-24. DOI:10.1016/S0899-5362(03)00085-X

Iglesias, M., Ribeiro, A. (1981). Zones de cisaillement ductile dans l'arc ibéro-armoricain. Comun. Serv. Geol.Portugal, 67, 85-87.

Jorge, R., Fernandes, P., Rodrigues, B., Pereira, Z., Oliveira, J.T. (2013). Geochemistry and provenance of the Carboniferous Baixo Alentejo Flysch Group, South Portuguese Zone. Sedimentary Geology, 284/285, 133-148. DOI: 10.1016/j.sedgeo.2012.12.005.

Leblanc, D., Gleizes, G., Roux, L., Bouchez, J. (1996). Variscan dextral transpression in the French Pyrenees: new data from the Pic des Trois-Seigneurs granodiorite and its country rocks. Tectonophysics, 261, 331–45. DOI:10.1016/0040-1951(95)00174-3

Lourenço, J., Mateus, A., Coke, C., Ribeiro, A. (2002). A zona de falha Penacova-Régua-Verín na região de Telões (Vila Pouca de Aguiar); alguns elementos determinantes da sua evolução em tempos tardivariscos. Comum. Inst. Geol. Mineiro, 89, 105-122.

Marques, F., Mateus, A., Tassinari, C. (2002). The Late-Variscan fault network in central-northern Portugal (NW Iberia): a re-evaluation. Tectonophysics, 359, 255-270. DOI:10.1016/S0040-1951(02)00514-0

Marques, F., Burg, J., Lechmann, S., Schmalholz, S. (2010). Fluid-assisted particulate flow of turbidites at very low temperature: A key to tight folding in a submarine Variscan foreland basin of SW Europe. Tectonics, 29. DOI:10.1029/2008TC002439

Martínez-García, E. (1996). Correlation of Hercynian units of the Iberin massif and southeartern France. Geogaceta, 20(2), 468-471.

Martínez Catalán, J. (2011). Are the oroclines of the Variscan belt related to late Variscan strike-slip tectonics? Terra Nova, 23, 241–247.

Mateus, A. (1995). Evolução tectono-térmica e potencial metalogenético do troço transmontano da Zona da Falha Manteigas-Vilariça-Bragança, Ph. D. Thesis, Lisbon University, 1189 p.

Moreira, N., Dias, R., Coke, C., Búrcio ,M. (2010). Partição da deformação Varisca nos sectores de Peso da Régua e Vila Nova de Foz Côa (Autóctone da Zona Centro Ibérica); Implicações Geodinâmicas. Comunicações Geológicas, 97, 147-162.

Moreira, N., Araújo, A., Pedro, J.C., Dias, R. (2014). Geodynamic evolution of Ossa-Morena Zone in SW Iberian context during the Variscan Cycle. Comunicações Geológicas, 101(I), 275-278.

Munhá, J. (1983). Hercynian magmatism in the Iberian Pyrite Belt. In: Lemos de Sousa, M., Oliveira, J.T. (Eds.), The Carboniferous of Portugal. Memórias dos Serviços Geológicos de Portugal, 29, 39-81.

Nance, R., Gutiérrez-Alonso, G., Keppie, J., Linnemann, U., Murphy, J., Quesada, C., Strachan, R., Woodcock, N. (2012). A brief history of the Rheic Ocean. Geoscience Frontiers, 3(2), 125-135. DOI:10.1016/j.gsf.2011.11.008

Noronha, F., Ramos, J.M.F., Rebelo, J.A., Ribeiro, A., Ribeiro, M.L. (1981). Essai de corrélation des phases de déformation hercynienne dans le nord-ouest Peninsulaire. *Leidse Geol. Medlingen,* 52 (1), 87-91.

Noronha, F., Ribeiro, M.A., Almeida, A., Dória, A., Guedes, A., Lima A., Martins, H.C., Sant'Óvaia, H., Nogueira, P., Martins, T., Ramos, R., Vieira, R. (2013). Jazigos Filonianos Hidrotermais e Aplitopegmatíticos espacialmente associados a Granitos (Norte de Portugal). In: Dias, R., Araújo, A., Terrinha, P., Kullberg, J.C. (Eds.), Geologia de Portugal, vol. 1, Escolar Editora, 403-438.

Oliveira, J.T. (1984). Carta geológica de Portugal. Escala 1/200.000. Notícia explicativa da Folha 7 (coord), Serviços Geológicos de Portugal.

Oliveira, J.T. (1990). South Portuguese Zone, stratigraphy and synsedimentary tectonism. In: Dallmeyer, R., Martinez Garcia, E. (Eds.), Pre-Mesozoic Geology of Iberia, Springer-Verlag, 334-347.

Oliveira, J.T., Relvas, J., Pereira, Z., Matos, J., Rosa, C., Rosa, D., Munhá, J.., Fernandes, P., Jorge, R.C.G.S., Pinto, A. (2013). Geologia da Zona Sul Portuguesa, com ênfase na estratigrafia, vulcanologia física, geoquímica e mineralizações da Faixa Piritosa. In: Dias, R., Araújo, A., Terrinha, P., Kullberg, J.C. (Eds.), Geologia de Portugal, vol. 1, Escolar Editora, 673-765.

Palain, C. (1976). Une série détritique terrigéne. Les Grés de Silves. Trias et Lias inférieur du Portugal, Mem. 25 (Nova Série) Serviços Geológicos de Portugal.

Pereira, E., Ribeiro, A., Meireles, C. (1993). Cisalhamentos hercínicos e controlo das mineralizações de Sn-W, Au e U na Zona Centro-Ibérica em Portugal. Cuaderno Lab. Xeolóxico de Laxe, 18, 89-119.

Pereira, M.F., Castro, A., Chichorro, M., Fernández, C., Díaz-Alvarado, J., Martí, M., Rodríguez, C., (2014). Chronological link between deep-seated processes in magma chambers and eruptions: Permo-Carboniferous magmatism in the core of Pangaea (Southern Pyrenees). Gondwana Research, 25, 290–308. DOI: 10.1016/j.gr.2013.03.009

Pereira, Z., Matos, J., Fernandes, P., Oliveira, J.T. (2007). Devonian and Carboniferous palynostratigraphy of the South Portuguese Zone, Portugal - An overview. Comunicações Geológicas, 94, 53-79.

Piqué, A., Cornee, J., Muller, J., Roussel, J. (1990). The Moroccan Hercynides. In: Dallmeyer R. D., Lécorché, J. P. (Eds.), "The West African orogens and circum Atlantic correlatives", Springer Verlag, 229-262.

Price, N., Cosgrove, J. (1990). Analysis of geological structures. Cambridge University Press.

Ramsay, J., Huber, M. (1987). The techniques of modern structural geology. Vol.1. Folds and fractures. Academic Press, Inc., London.

Reber, J., Schmalholz, S., Burg, J. (2010). Stress orientation and fracturing during three-dimensional buckling: numerical simulation and application to chocolate-tablet structures in folded turbidites, SW Portugal. Tectonophysics, 493, 187-195. DOI:10.1016/j.tecto.2010.07.016

Ribeiro, A. (1974). Contribuition à l'étude tectonique de Trás-os-Montes. Mem. Serv. Geol. Portugal, 24.

Ribeiro, A. (1983). Structure of the Carrapateira nappe in Bordeira area. south-west Portugal. In: Lemos de Sousa, M. J., Oliveira, J.T. (Eds.), The Carboniferous of Portugal, Mem. Serv. Geol. Portugal, 29, 91-97.

Ribeiro, A. (2002). Soft Plate Tectonics. Springer-Verlag, Berlin, 324 p.

Ribeiro, A., Pereira, E. (1982). Controles paleogeográficos, petrológicos e estruturais na génese dos jazigos portugueses de estanho e volfrámio. Geonovas, 1(3), 23-31.

Ribeiro, A., Silva, J. (1983). Structure of the South Portuguese Zone. In: Lemos de Sousa, M. J., Oliveira, J.T. (Eds.), The Carboniferous of Portugal, Mem. Serv. Geol. Portugal, 29, 83-89.

Ribeiro, A., Antunes, M.T., Ferreira, M.P., Rocha, R.B., Soares, A.F., Zbyszewski, G., Moitinho de Almeida, F., Carvalho, D., Monteiro, J.H. (1979). Introduction à la Géologie Générale du Portugal. Serviços Geológicos de Portugal.

Ribeiro, A., Oliveira, J.T., Silva, J. (1983). La estrutura de la Zona Sur Portuguesa. In: Comba, J.A. (Ed.), Geologia de España, Inst. Geol. Min. Esp. Madrid, 1, 504-511.

Ribeiro A, Pereira E, Dias R (1990) Structure of Centro-Iberian allochthon in northern Portugal. In: Dallmeyer, R., Martinez Garcia, E., (Eds.), Pre-Mesozoic Geology of Iberia, Springer-Verlag, 220-236.

Ribeiro, A., Dias, R., Silva, J. (1995). Genesis of the Ibero-Armorican Arc. Geodinamica Acta, 8(2), 173-184. DOI:10.1080/09853111.1995.11417255

Ribeiro, A., Munhá, J., Dias, R., Mateus, A., Pereira, E., Ribeiro, L., Fonseca, P., Araújo, A., Oliveira, T., Romão, J., Chaminé, H., Coke, C., Pedro, J. (2007). Geodynamic evolution of SW Europe Variscides. Tectonics, 26, 1-24. DOI: 10.1029/2006TC002058

Rocha, R. (1976). Estudo estratigráfico e paleontológico do Jurássico do Algarve ocidental. Ciências Terra, 2.

Schermerhorn, L. (1971). An outline stratigraphy of the Iberian Pyrite Belt. Bol. Geol. Min. España, 82(3-4), 239-268.

Scisciani, V., Calamita, F., Tavarnelli, E., Rusciadelli, G., Ori, G.G., Paltrinieri, W. (2001). Foreland-dipping normal faults in the inner edges of syn-orogenic basins: A case from the Central Apennines, Italy. Tectonophysics, 330, 211-224. DOI: 10.1016/S0040-1951(00)00229-8

Shelley, D., Bossière, G. (2000). A new model for the Hercynian Orogen of Gondwanan France and Iberia. J. Struct. Geol., 22, 757-776. DOI:10.1016/S0191-8141(00)00007-9

Shelley, D., Bossière, G. (2002). Megadisplacements and the Hercynian orogen of Gondwanan France and Iberia. In: Martínez Catalán, J., Hatcher, Jr.R.., Arenas, R., Díaz García, F. (Eds), Variscan-Appalachian dynamics: The building of the late Paleozoic basement: Boulder, Colorado. Geological Society of America, Special Paper, 364, 209–222. DOI: 10.1130/0-8137-2364-7.209

Silva, J. (1989). Estrutura de uma geotransversal da faixa piritosa: zona do vale do Guadiana. PhD Thesis, Lisbon University.

Silva, J., Oliveira, J., Ribeiro, A. (1990). South Portuguese Zone, structural outline. In: Dallmeyer, R., Martinez Garcia, E. (Eds.), Pre-Mesozoic Geology of Iberia, Springer-Verlag, 348-362.

Simancas, J., Tahiri, A., Azor, A., Lodeiro, F., Poyatos, D., Hadi, H. (2005). The tectonic frame of the Variscan-Alleghanian orogen in southern Europe and Northern Africa. Tectonophysics, 398, 181-198. DOI:10.1016/j.tecto.2005.02.006

Twiss, R., Moores, E. (1992). Structural Geology. W. H. Freeman and Company.

Zulauf, G., Gutiérrez-Alonso, G., Krausc, R., Petschick, R., Potel, S. (2011). Formation of chocolate-tablet boudins in a foreland fold and thrust belt: A case study from the external Variscides (Almograve, Portugal). J. Struct. Geol., 33, 1639-1649. DOI:10.1016/j.jsg.2011.08.009

Zwart, H. (1986). The Variscan Geology of Pyrenees, Tectonophyics, 129, 9-27. DOI:10.1016/0040-1951(86)90243-X

X.2

Area change during kink band evolution; examples from the Late Variscan of Portugal

Index

X.2.1. Introduction

Kink bands are a common subject in engineering, earth sciences and physics (Anderson, 1964; Jensen, 1999; Qiao and Winey, 2000; Wadee et al., 2003; Wadee and Edmunds, 2005). They are associated with deformation in solids usually with a strong planar mechanical anisotropy and could occurred at all scales (Anderson 1964; Matte, 1969; Jensen, 1999; Wadee and Edmunds, 2005).

In earth sciences, the kink bands are common in rocks with a strong planar anisotropy (*e.g.* bedding, slaty cleavage or foliation), like shales, slates, phyllites or schists (Anderson 1964; 1974; Dewey, 1965; Matte, 1969; Williams, 1987; Twiss and Moores, 1992) and are found from mineralogical (Starkey, 1968; Tchalenko, 1968; Misra and Burg, 2012; Goswami, 2013) to orogenic scales (Collomb and Donzeau, 1974; Goscombe et al., 1994; Suppe et al., 1997; Pachell et al., 2003). Although anisotropy favours the development of kink bands, occasionally they are also found in isotropic rocks (Borg and Handin, 1966; Hanmer, 1982;

Davies and Pollard, 1986; Williams, 1987; Pachell et al., 2003). The understanding of the genetical processes related to such diversity give rise to several approaches: experimental works (Paterson and Weiss, 1962; Borg and Handin, 1966; Paterson and Weiss, 1966; Donath, 1968; Cobbold *et al.*, 1971; Anderson, 1974; Gay and Weiss, 1974; Stewart and Alvarez, 1991; Hanmer et al., 1996 Wadee *et al.*, 2003), field based studies (Anderson, 1964; Matte, 1969; Babaie and Speed, 1990; Stubley, 1990; Sharma and Bhola, 2005) as well as theoretical studies (Dewey, 1969; Weiss, 1980; Srivastava et al., 1998).

Previous studies led to two main models for the origin of kink bands (*e.g.* Stewart and Alvarez, 1991; Twiss and Moores, 1992): the mobile-hinge and the fixed-hinge models. The first emphasize the gradual growth of kink bands, either by lateral or rotational migration of their boundaries. In the fixed-hinge model, the boundaries are fixed, being the rotation restricted to the internal domain. Although both models enhanced some of the processes related to the genetic mechanisms and geodynamic significance of these structures, the fixed-hinge models did not explain/discuss the inevitable area change within the kink band. Detailed geometrical and kinematical analysis of two mesoscopic late Variscan kink bands in Iberia help, not only to understand the internal distortion related to fixed hinged kink bands, but also to establish a new graphical method to quantify this distortion.

X.2.2. Kink Band structures overview

Kink bands are common in polydeformed areas, being generally generated under low-grade metamorphic conditions; they usually occur in brittle or brittle-ductile regime during late tectonic events (Anderson, 1964; Dewey, 1965; Suppe 1985; Babaie and Speed, 1990; Sharma and Bhola, 2005). These structures mostly result from layer parallel shortening in anisotropic rock induced by a major compression nearly parallel to previous layering (e.g. Anderson 1964; 1974; Hanmer et al., 1996).

The diversity of studies and models concerning kink-bands, led to a strong disparity of the parameters that have been used, turning useful a summary overview of previous works.

X.2.2.1. Kink Band Geometrical and Kinematical features

Kink bands are asymmetric folds with straight limbs and sharp hinges (fig. 1; Ramsay and Huber, 1987; Stewart and Alvarez, 1991; Twiss and Moores, 1992). Kink folds have a short limb (kink band) restrained between two axial surfaces (kink band boundaries) and two undeformed long limbs (Anderson 1964; 1974; Dewey, 1965; Weiss, 1980; Stewart and Alvarez, 1991; Twiss and Moores, 1992). These structures are usually characterized using three angular parameters (fig. 1):

- ϕ is the angle between the planar anisotropy outside the kink band and the kink plane (Paterson and Weiss, 1966; Weiss, 1980; Srivastava et al., 1998; also called α by Anderson, 1964; 1974; Dewey, 1965; Ramsay and Huber, 1987);

- ϕk express the angular parameter between the kink plane and the planar anisotropy inside the kink band (Paterson and Weiss, 1966; Weiss, 1980; Srivastava et al., 1998; also called β by Anderson, 1964; 1974; Dewey, 1965; Ramsay and Huber, 1987);

- ψ is considered the kink angle (Twiss and Moores, 1992) and gives the angular relation between the planar anisotropy outside and inside the kink band.

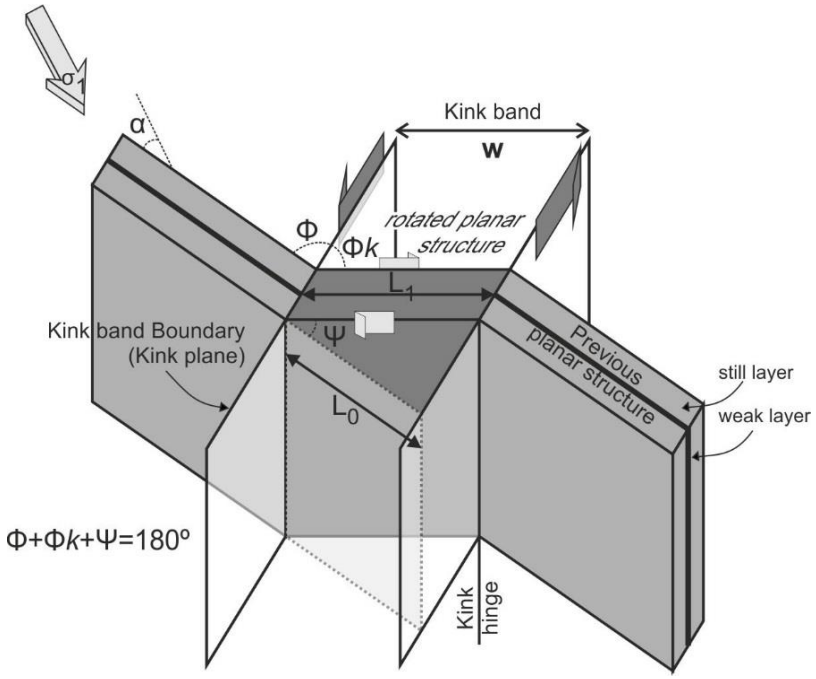

Figure 1 – Geometric and kinematic features of kink bands (adapted from Gay and Weiss, 1974; Srivastava et al., 1998).

Previous angular parameters are not independent (Weiss, 1980; Srivastava et al., 1998):

$$\phi + \phi k + \psi = 180º \text{ (equation 1)}$$

Natural and experimental studies show that kink bands can appeared, either as individual monoclinal sets or two conjugate sets with opposite kinematics (Dewey, 1969; Paterson and Weiss, 1966; Anderson, 1974; Suppe, 1985; Babaie and Speed, 1990).

X.2.2.2. Stress and Strain in Kink Bands

Experimental works on rock mechanics of foliated rocks (Paterson and Weiss, 1962; 1966; Borg and Handin, 1966; Donath, 1968; Gay and Weiss, 1974) and analogical modelling

(Cobbold et al., 1971; Gay and Weiss, 1974; Williams and Price, 1990; Stewart and Alvarez, 1991) show that in kink bands the major principal stress ($\sigma 1$) is parallel or close to the direction of main foliation (Donath, 1961; Anderson, 1964; 1974; Paterson and Weiss, 1962; Gay and Weiss 1974; Williams and Price, 1990). When conjugate kink bands are developed, their geometry and kinematics can be used to determine the three dimensional stress field orientation (Ramsay, 1962; Gay and Weiss, 1974; Tobisch and Fiske, 1976; Suppe, 1985), using the bisectors of the dihedral angles between the conjugate pairs of kink planes (Ramsay, 1962; Tobisch and Fiske, 1976; Stewart and Alvarez, 1991).

Previous relations are valid for pure shear kink bands, but kink-bands could also be developed in a simple shear regime (Stubley, 1990; Williams and Price, 1990). In this case, the 'conjugate bisector' method should be used with caution, because stress could have been variable during folding, modifying in ± 20º the orientation of maximum and minimum strain axis (Ramsay 1967; Stubley, 1990; Williams and Price, 1990).

The formation of one or the two conjugate sets of kink folds depends of the obliquity between the shortening and the main layering (fig. 2; Paterson and Weiss, 1962; 1966; Cobbold et al., 1971; Gay and Weiss, 1974; Williams and Price, 1990; Stubley, 1990). For very low obliquities ($\alpha \leq 5º$; fig. 1) experimental data shows that symmetric conjugate kink bands are developed (fig. 2; Paterson and Weiss, 1962; 1966; Donath, 1968; Cobbold et al., 1971; Anderson, 1974; Gay and Weiss, 1974; Stewart and Alvarez, 1991). With α increase, one set of kink bands starts to prevail and the asymmetry becomes evident. When α attain more than 10º, generally only one set is generated (Paterson and Weiss, 1962; 1966; Cobbold et al., 1971; Gay and Weiss, 1974). However for higher obliquities ($\alpha \geq 30º$) development of kink bands seems to be negligible (Paterson and Weiss, 1966; Donath, 1968; Gay and Weiss, 1974), and sliding along the foliation prevails (fig. 2).

X.2.2.3. Kink Bands Genetic Models

The work done by several authors (Paterson and Weiss, 1966; Anderson, 1974; Gay and Weiss, 1974; Verbeek, 1978; Weiss, 1980; Stewart and Alvarez, 1991) allows to distinguish two main models for kink band development (mobile-hinge and fixed-hinge models), with distinct characteristics summarized in figure 3 and table I.

Mobile-hinge models

In this model kink bands initiates as a small lenticular structure and grow laterally by hinge migration, incorporating more undeformed material (Paterson and Weiss, 1966; Gay and

Weiss, 1974; Weiss, 1980; Stubley, 1990; Stewart and Alvarez, 1991). The growth of the kink bands, with the migration of the hinges could be done either by rotation (type I; fig. 3A) or by lateral migration of kink band boundaries (type II; fig. 3B; table I). Whatever the situation, both types dominates when the confining pressure is high (Gay and Weiss, 1974; Weiss, 1980; Stewart and Alvarez, 1991).

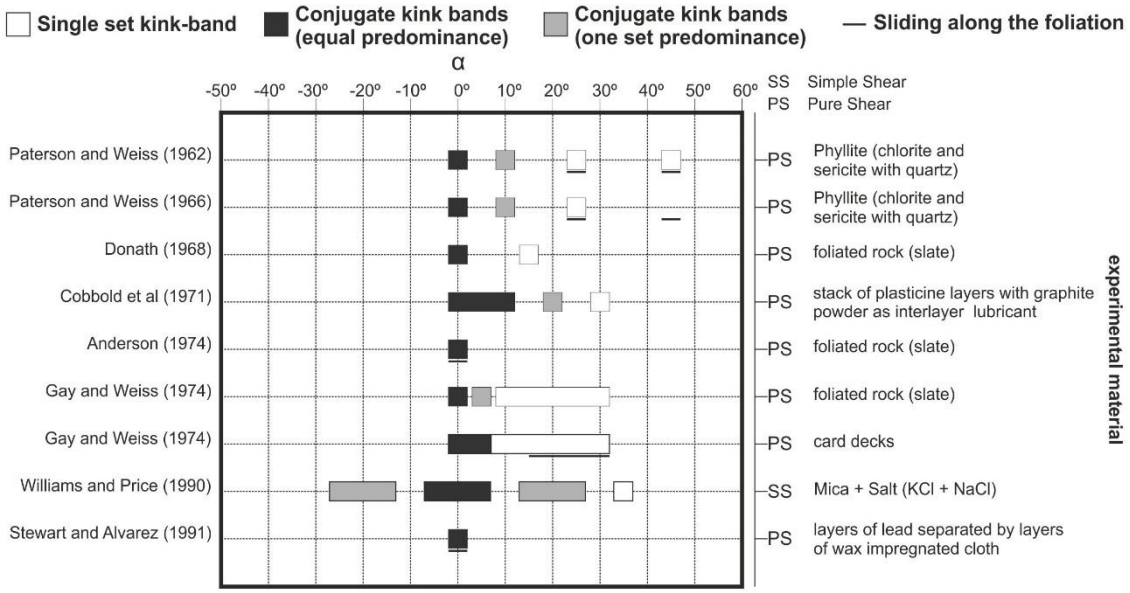

Figure 2 – Experimental relation between the geometry and kinematic of kink bands and the related stress field orientation (α angle).

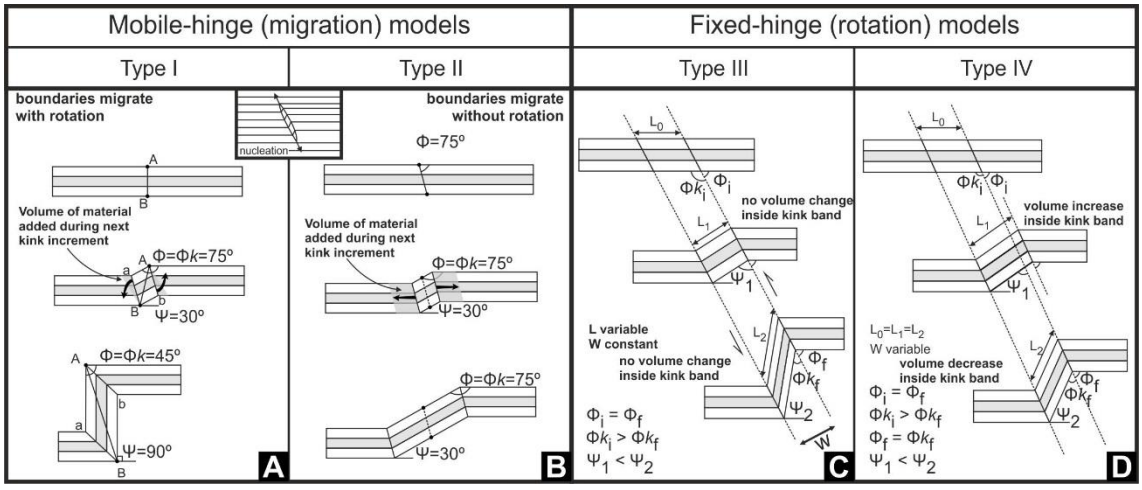

Figure 3 – Main models inducing kink band development (adapted from Twiss and Moores, 1992):

A – Mobile-hinge by boundaries migration with rotation;

B – Mobile-hinge with boundaries migration by lateral propagation

C - Fixed-hinge with simple shear kinking;

D - Fixed-hinge with rigid rotation of internal foliation.

Table I – Main geometric and kinematic characteristics of four types of kink band.

	Mobile-hinge models		**Fixed-hinge models**	
	Type I	Type II	Type III	Type IV
Deformation mechanism	Rotation and migration of hinges	Lateral migration of hinges, without rotation	Simple shear along kink band boundaries	Rigid rotation of internal foliation
ϕk and ϕ	Both decrease progressively but always $\phi k=\phi$	$\phi k=\phi$=constant is satisfied during all process	$\phi k \neq \phi$; ϕ remains constant but ϕk decreases progressively	ϕ remains constant but ϕk decreases progressively until $\phi k=\phi$
ψ	Increases progressively until 90º	Remains constant	Increases progressively	Increases progressively until locking when $\phi k=\phi$
Boundaries	Migrate by rotating about fixed hinges. The amount of rotation for both boundaries is equal but their sense of rotation are opposite	Migrate laterally away from each other by moving parallel to the initial orientation	Remain fixed during the growth	Remain fixed during the growth
Interlayer slip	Yes	Yes(?)	Yes	Yes
Total volume	Remains constant	Remains constant	Remains constant	First increases and then decreases
Width (W)	Increases by incorporation of new material	Increases by incorporation of new material	Remains constant	Variable
Length (L) of internal foliation	Increase during migration, but remains constant during the growth	Increase during migration, but remains constant during the growth	Variable	Remains constant during the growth

Fixed-hinge models

In this model the main layering rotates between two fixed boundaries, while the orientation of the kink plane remain unchanged (Twiss and Moores, 1992). The deformation associated with such kink band growth ceases when ϕ and ϕk angles are equal (Verbeek, 1978; Stewart and Alvarez, 1991). This general deformation pattern could be attained by two different type mechanisms (table I; Twiss and Moores, 1992): in type III (Fig. 3C), kink band produces a deformation equivalent to a homogeneous simple shear parallel to kink band boundaries, while type IV involves a flexural shear mechanism with shearing parallel to the laminations (Fig. 3D).

The relationship between ϕ and ϕk angles have been used to discriminate between mobile-hinge or fixed-hinge models (Anderson, 1974; Gay and Weiss, 1974; Verbeek, 1978; Stewart and Alvarez, 1991). In mobile-hinge kink bands these two angular parameters are equal, whereas fixed-hinge ones should generally have $\phi < \phi k$ (Stewart and Alvarez, 1991). However, small amounts of slip parallel to layering (in or outside of kink band) can produce a fairly large difference in angular values.

The projection of the kink band angular values in a triangular diagram (Srivastava et al., 1998), allows to assign a genetic model to kink bands (Fig. 4). However, in some natural cases, neither the hinge-migration nor the fixed-hinge model can solely explain the geometry of kink bands (Stubley, 1990). It is also possible to consider hybrid models, which involve rotation of the kinked limb and migration of its boundaries (Twiss and Moores, 1992).

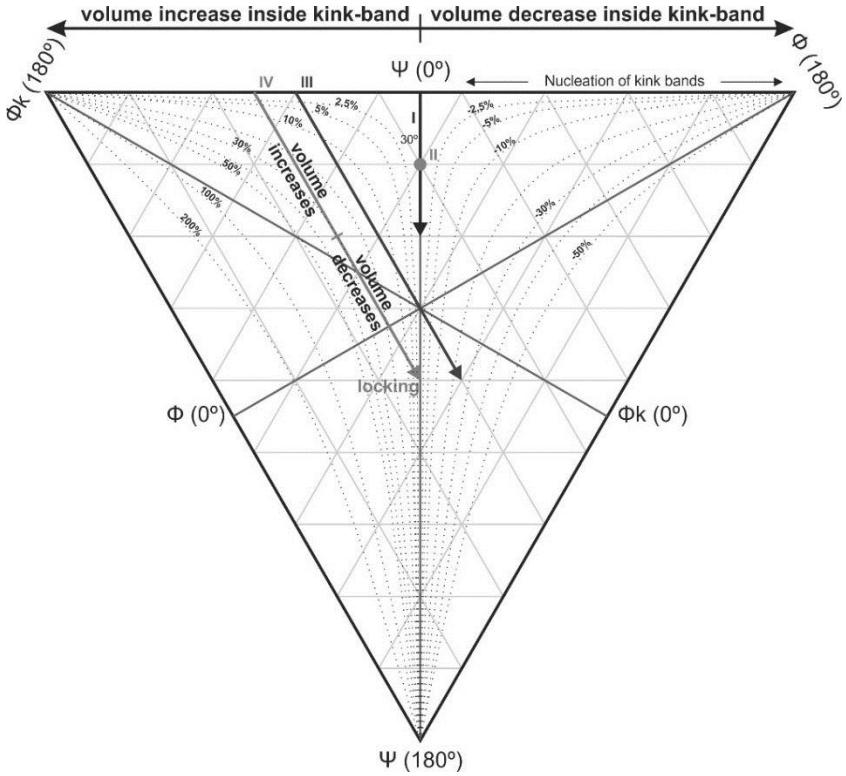

Figure 4 – Triangular diagram for kink band genetical models (adapted from Srivastava et al., 1998).

All the four types of mechanisms could involve a shear component parallel to the main layering inside the kink band, as well as preservation of continuity between planar structures across the kink band boundaries (Stewart and Alvarez, 1991; Twiss and Moores, 1992; Dunham et al., 2011). The internal interlayer slip is always anthithetical in relation to kink band kinematics (e.g. Anderson, 1964; Dewey, 1965; Matte, 1969; Verbeek, 1978; Twiss and Moores, 1992; Dunham et al., 2011). The presence of a synthetical shear component parallel to the layering in the external domains of the kink band is sometimes found (Stubley, 1990; Stewart and Alvarez, 1991).

X.2.3. Late Variscan Deformation in the Iberian Massif

The intracontinental deformation related to the late stages of the Variscan Orogeny, was induced by the dextral oblique collision between Laurentia and Gondwana (Arthaud and

Matte, 1977; Shelley and Boussiére, 2002; Nance et al., 2012; Dias et al., 2016a). Such regime is expressed in Iberia by E-W lithospheric dextral transcurrent shear zones (Fig. 5A; e.g. Ribeiro, 2002; Ribeiro et al., 2007; Denèle et al., 2014; Dias et al., 2015; 2016b), which have been strongly reworked during Meso-Cenozoic times, controlling either the Cantabro-Pyrenean chain at North or the complex the Azores-Gibraltar plate boundary at south (Ribeiro, 2002).

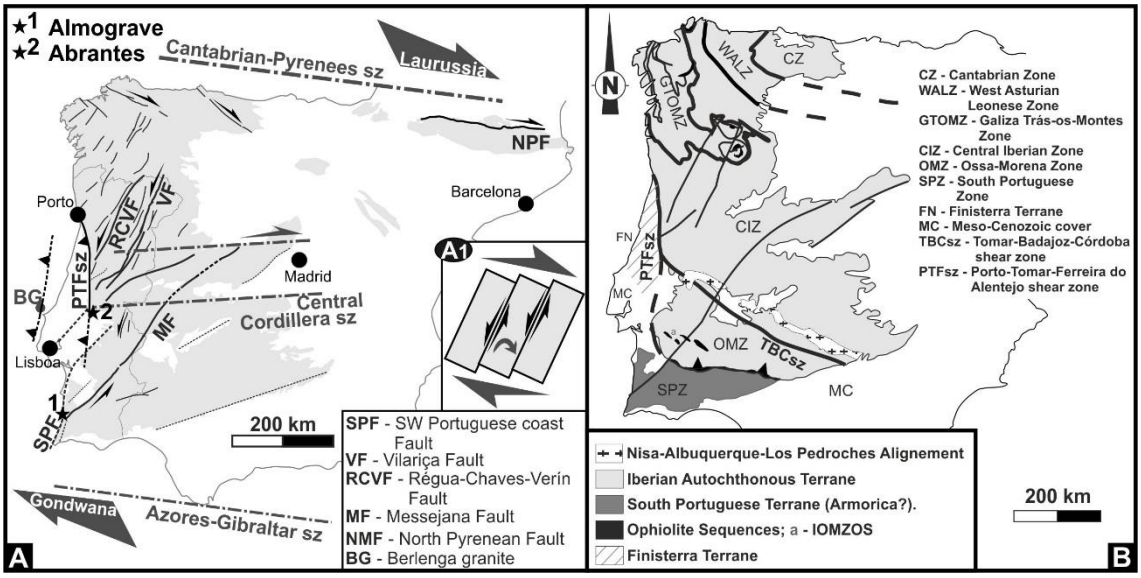

Figure 5 – General features of Iberian Variscides:

A – Late Variscan fracture pattern of Iberia, with localization of studied kink band structures, displaying the interpretative model of clockwise rotation of blocks bounded by NNE–SSW faults in a domino deformation model (a_1; adapted from Dias et al., 2016b);

B – Main Variscan tectonostratigraphic zones and Terranes of Iberia Variscides (adapted from Ribeiro et al., 2007; Romão et al., 2014; Dias et al., 2016a).

Although the main dextral plate collision is accepted, there are some debate concerning the kinematics of the NNE-SSW to NE-SW 2nd order fracture pattern in Iberia (Fig. 5A;-Dias et al., 2016b for a discussion). While most authors consider these late Variscan faults as sinistral (Arthaud and Matte, 1977; Choukhroune and Iglésias, 1980; Iglesias and Ribeiro, 1981; Pereira et al., 1993; Caroça and Dias, 2002; Moreira et al., 2010; 2014; Dias and Basile, 2013; Dias et al., 2013; 2016b), in some works a dextral Variscan kinematics is assumed being the sinistral kinematics ascribed to the Alpine reworking (Marques et al., 2002; 2010; Lourenço et al., 2002).

The dextral kinematics emphasized by Marques et al (2002) in Central Iberian Zone NNE-SSW faults was dated as late Carboniferous (ca. 312 Ma obtained in K–Ar in muscovite concentrates of fault related rocks). Although these authors considered this age a lower limit

for the Late Variscan event, it could also be consider the upper limit for the D_3 Variscan regional event (Dallmeyer et al., 1997; Dias et al., 2016b), where such trends have also a right-lateral kinematic (Pereira et al., 1993; Mateus and Noronha, 2010). The NNE-SSW sinistral kinematics have been confirmed, either by AMS studies in Vila Pouca de Aguiar and Pedras Salgadas D_3 granites (Sant'Ovaia et al., 2000; Sant'Ovaia e Noronha, 2005) of 300 Ma (Martins et al., 2009), or structural detailed data in South Portuguese Zone, where their kinematics were interpreted as the result of a domino mechanism associated with the 1st order E-W transcurrent dextral shear zones (Fig. 5A; Dias et al., 2016b).

X.2.4. Geometric and Kinematic analysis in Late Variscan Kink Bands of Portugal

In the Iberian Variscides the pervasive brittle to brittle-ductile late Variscan fracture pattern is often related to mesoscopic kink band structures. In Almograve region these structures were mostly induced by discrete NNE-SSW sinistral strike-slip faults (Caroça and Dias, 2002; Dias and Basile, 2013; Dias et al., 2016b). The same geometry and kinematics have also been described in Abrantes region (Moreira, 2012). In both cases the good outcrop conditions help to enhance the understanding of their genetic mechanisms.

X.2.4.1. Almograve Kink Bands

The Almograve region (Fig. 6) is located in the South Portuguese Zone (Fig. 5B), a Variscan foreland belt with a SW facing imbricated fold and trusts (Ribeiro et al., 2007; Marques et al., 2010). In Almograve, this complex is a low-grade metamorphic flysch sequence, composed of interlayered greywackes, quartzwackes and shales beds (Marques et al., 2010; Dias and Basile, 2013).

This sequence was deformed by two main Variscan deformation episodes (Dias and Basile, 2013; Dias et al., 2016b). While the first (D_1) is a pervasive deformation giving rise to the NNW-SSE regional structure, the second deformation (D_2) is a discrete event mostly concentrated along NNE-SSW deformation bands (Fig. 6) which is a common situation in the Iberian Variscides (e.g. Dias et al., 2013; 2016b; Moreira et al., 2014).

The D_1 episode in Almograve is the result of a coaxial progressive deformation developed in a low structural level (Marques et al., 2010; Dias and Basile, 2013; Dias et al., 2016b), whose pervasive deformation helps to constrain the D2 geometry and kinematics. The most obvious D_1 structures are general NNW-SSE (N30ºW to N20ºW) orthorhombic upright folds with subvertical axial planes and subhorizontal hinges (less than 10º; Figs. 6 and 7A). Mostly in the hinge zones and in the more fine-grained lithotypes an axial planar S_1 cleavage is found (Fig. 7B), which gives rise to an intersection lineation L_1 (S_0^S_1) parallel to the fold hinges.

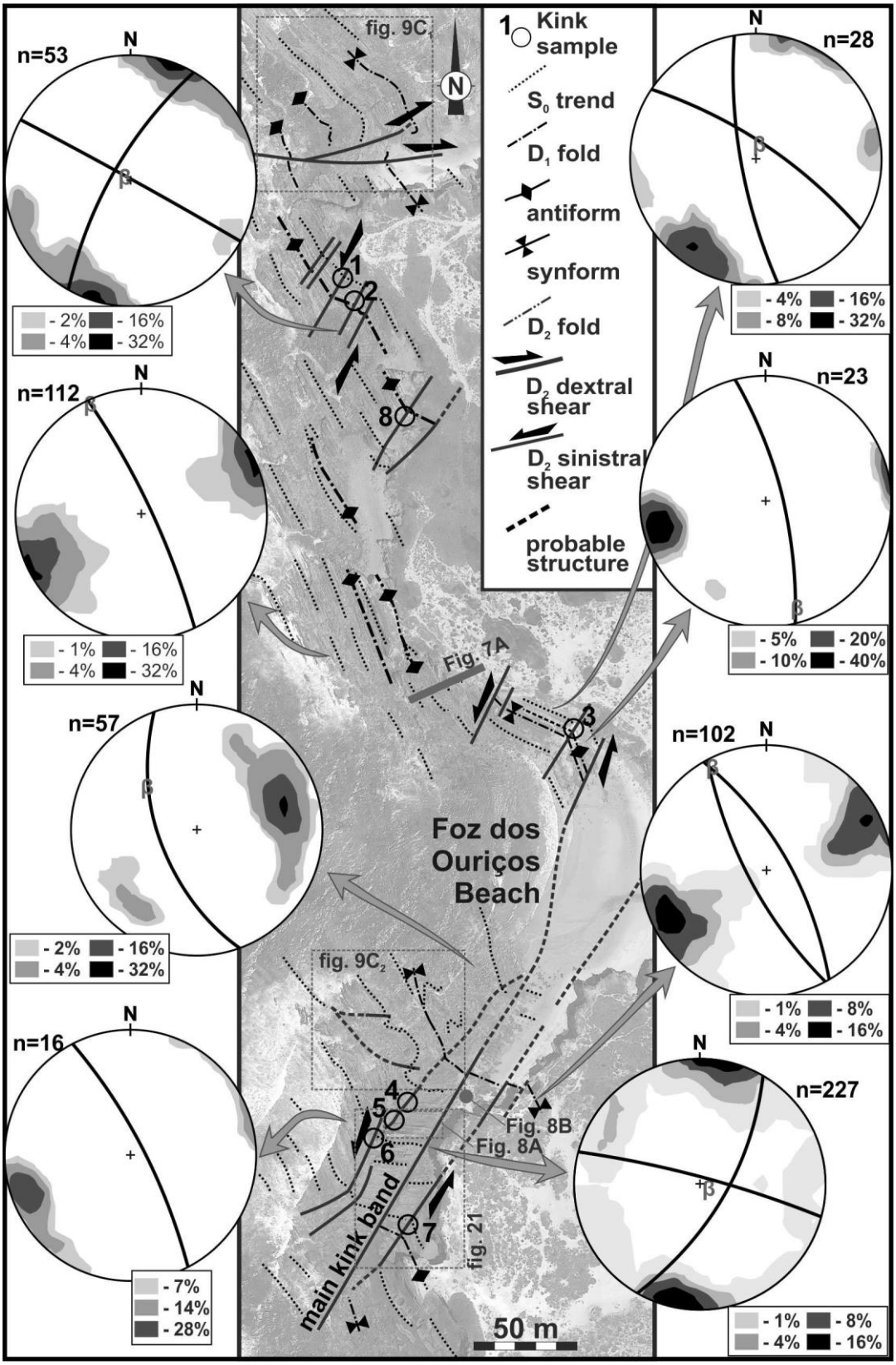

Figure 6 –Structural map of Almograve Kink band emphasizing the heterogeneous geometrical behaviour of bedding due to the interference between both Variscan deformation events (equal area lower hemisphere stereographic projections of S_0).

The late stages of D_1 give rise to sub-vertical brittle to brittle-ductile conjugate shear zones (with an acute angle between them of 60º: Fig, 7C) better expressed in the strongly dipping limbs of D_1 early folds: N-S to NNE-SSW dextral and sinistral ENE-WSW to E-W. This shows a stress field with a NE-SW σ_1 and a NW-SE σ_3 both sub-horizontal and a sub-vertical σ_2. Such stress field is compatible with D_1 folds that are thus considered developed in the same tectonic event (Dias and Basile, 2013; Dias et al., 2016b).

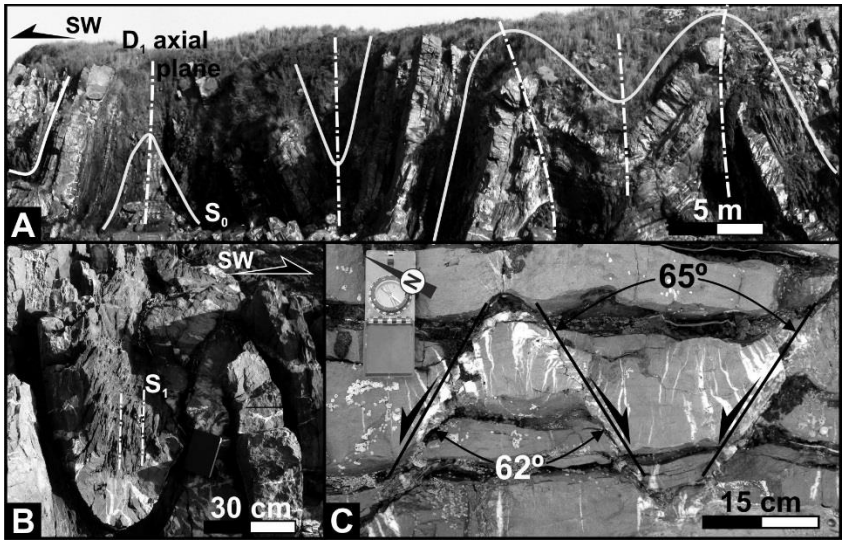

Figure 7 – Geometrical and kinematical features of D_1 structures:

A –D_1 folds general pattern;

B – Axial planar S_1 cleavage in D_1 tight folding;

C – Late D_1 conjugate shear zones.

The D_2 structures have a clear heterogeneous distribution, being mostly concentrated in the vicinity of discontinuous NNE-SSW sub-vertical structures. These planar anisotropies define elongated narrow domains where the regional D_1 NNW-SSE trend were rotated anticlockwise towards WNW-ESE (Fig. 6) defining a mappable D_2 NNE-SSW sinistral kink bands geometry (Fig. $8A_1$ and A_2: Dias *et al.,* 2016b). The transcurrent kinematics is confirmed by several slip evidences like subhorizontal groove lineations (Figs. $8A_3$ and A_4) coupled with the predominance of the minor sinistral kink-bands with high dipping D_2 hinges (Fig. $8A_2$ and A_5).

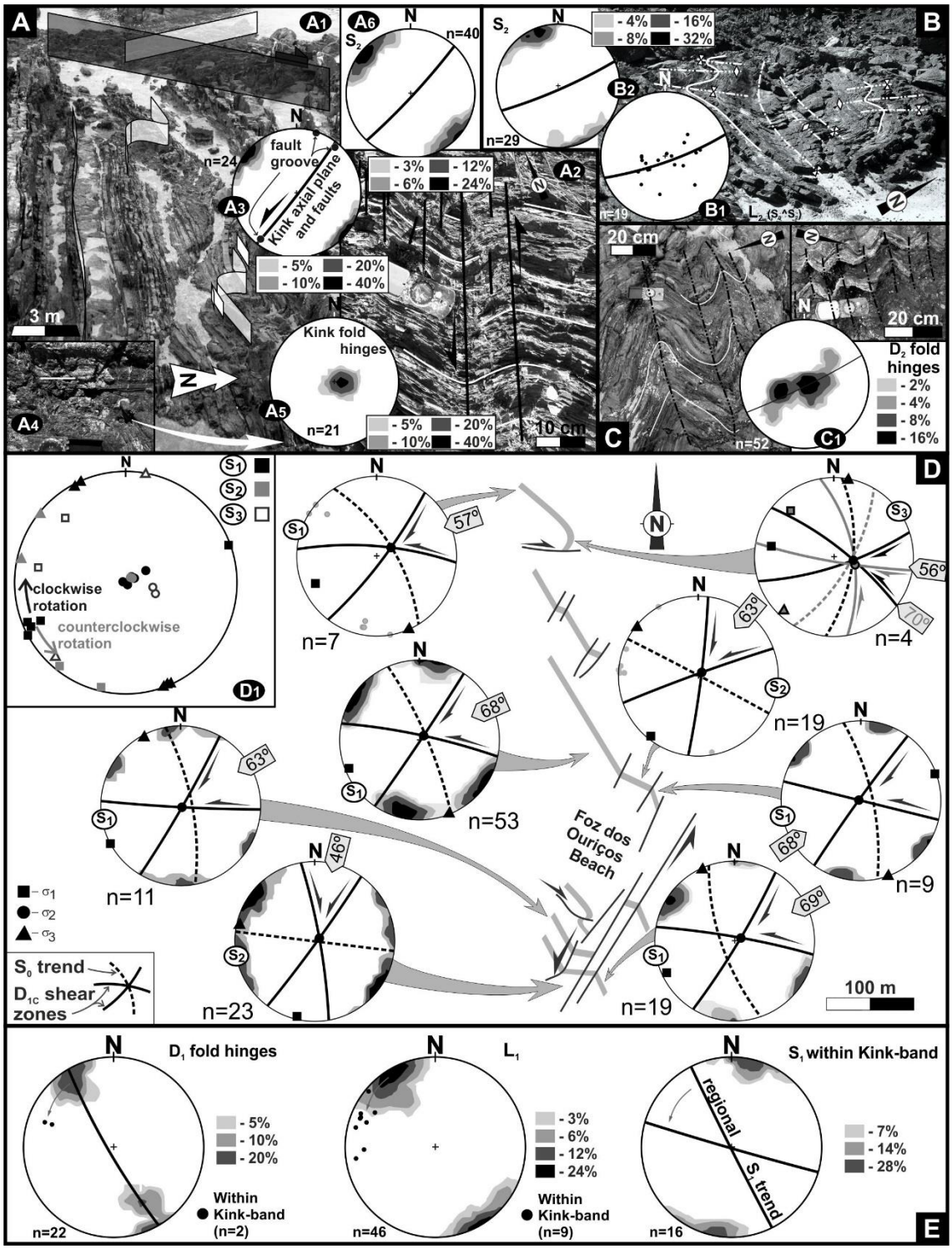
A
A1
A6
S2
N
n=40
n=24
fault groove
Kink axial plane and faults
A3
- 3% - 12%
- 6% - 24%
A2
- 5% - 20%
- 10% - 40%
3 m
Kink fold hinges
A5
n=21
A4
Z
10 cm
B
S2
- 4% - 16%
- 8% - 32%
B2
n=29
n=19
B1
L2 (S1^S2)
20 cm
C
n=52
C1
D2 fold hinges
- 2%
- 4%
- 8%
- 16%
D
S1
S2
S3
clockwise rotation
counterclockwise rotation
D1
57°
n=7
56°
70°
63°
n=4
68°
n=53
n=19
63°
n=11
Foz dos Ouriços Beach
68°
n=9
46°
n=23
69°
n=19
100 m
σ1
σ2
σ3
S0 trend
D1c shear zones
E
D1 fold hinges
- 5%
- 10%
- 20%
Within Kink-band (n=2)
n=22
L1
- 3%
- 6%
- 12%
- 24%
Within Kink-band (n=9)
n=46
S1 within Kink-band
regional S1 trend
- 7%
- 14%
- 28%
n=16

Figure 8 – D_2 sinistral kink bands and its interference with previous D_1 structure (equal area lower hemisphere stereographic projections):

A – Bedding deflection at distinct scales (A_1 and A_2) induced by D_2 sinistral NNE-SSW kink bands (A_3). Sub-horizontal groove lineations (A_3 and A_4), subvertical D_2 fold hinges (A_5) and NE-SW en-echelon cleavage are compatible with sinistral kinematics (A_6)

B – D_1 fold refolded by D_2 with coeval development of L_2 intersection lineation (B_1) and S_2 cleavage (B_2).

C – Orthorhombic D_2 folds with high scatter of fold hinges (C_1) due the interaction with D_1 structure;

D – Rotation of late D_1 conjugate shear zones directions inside the D_2 kink bands;

E – Similar counterclockwise rotation exhibited by D_1 fold hinges, L_1 and S_1 structures within sinistral D_2 NNE-SSW kink bands.

The interference between the progressive coaxial D_1 deformation with the non-coaxial D_2 event produces a complex finite deformation. As the D_1 and D_2 axial planes have sub-perpendicular trends and they are both sub-vertical, a type 1 interference fold pattern was generated (Ramsay e Huber, 1987). Thus, the geometry of the D_2 folds is strongly conditioned by the geometry of previous D_1 folds, with the plunge of the D_2 axes controlled by the geometry of the D1 folds (Fig. 8B). These D_2 folds, are developed near the kink band boundaries, usually presenting an orthorhombic symmetry (Fig. 8C), develop an incipient axial planar S_2 crenulation cleavage (Fig. $8B_2$), generally restricted to fine-grained lithologies. Such geometrical relation give rise to a L_2 intersection lineation (S_0^S_2) subparallel to D_2 hinges (Fig. $8B_1$ and $8C_1$). The axial planes of these orthorhombic D_2 folds are subparallel to slightly oblique (NE-SW) in relation to the NNE-SSW kink planes; this angular discrepancy is compatible with the sinistral kinematics emphasized by the major kink folds (Fig. 6). Such regional left lateral strike-slip component along the NNE-SSW trend has also been emphasized in SW Portugal by en-echelon NE-SW D_2 folds transected by an ENE-WSW S_2 cleavage (Caroça and Dias, 2002).

The conjugate shear zones developed in the late stages the D_1 (Fig. 7C) had also been counter clockwise rotated by the D_2 kink bands (Fig. 8D), showing once more the later development of the kink band structures. The amount of rotation in the inner domains of the kink bands is proportional to the deflection exhibited by the other D_1 structures (S_0, folds in L_1 and S_1; Fig. 8E) ranging from 30 to 60º.

Although the predominant decametric Late Variscan structures in Almograve are the sinistral NNE-SSW kink bands, locally E-W to WNW-ESE kink-like folds are developed (Figs. 6 and 9). They also present a brittle-ductile behavior, underlined by frequent quartz veining and

the common disruption of bedding. Their dextral kinematics is shown by the rotation of previous structures, with the related D_2 folds presenting E-W axial planes and highly plunging hinges (Fig. 9).

The coeval development of these E-W dextral kink-bands with the NNE-SSW sinistral ones is proven by the mutual interferences between structures from both sets (Fig. 6), also rotating the late D_1 conjugate shear zone, in this case with clockwise rotation (Fig. 8D).

Similar dextral E-W kink band, attributed to the Late Variscan stage, have been described along the SW Portuguese coast (Dias and Basile, 2013; Dias et al., 2016b).

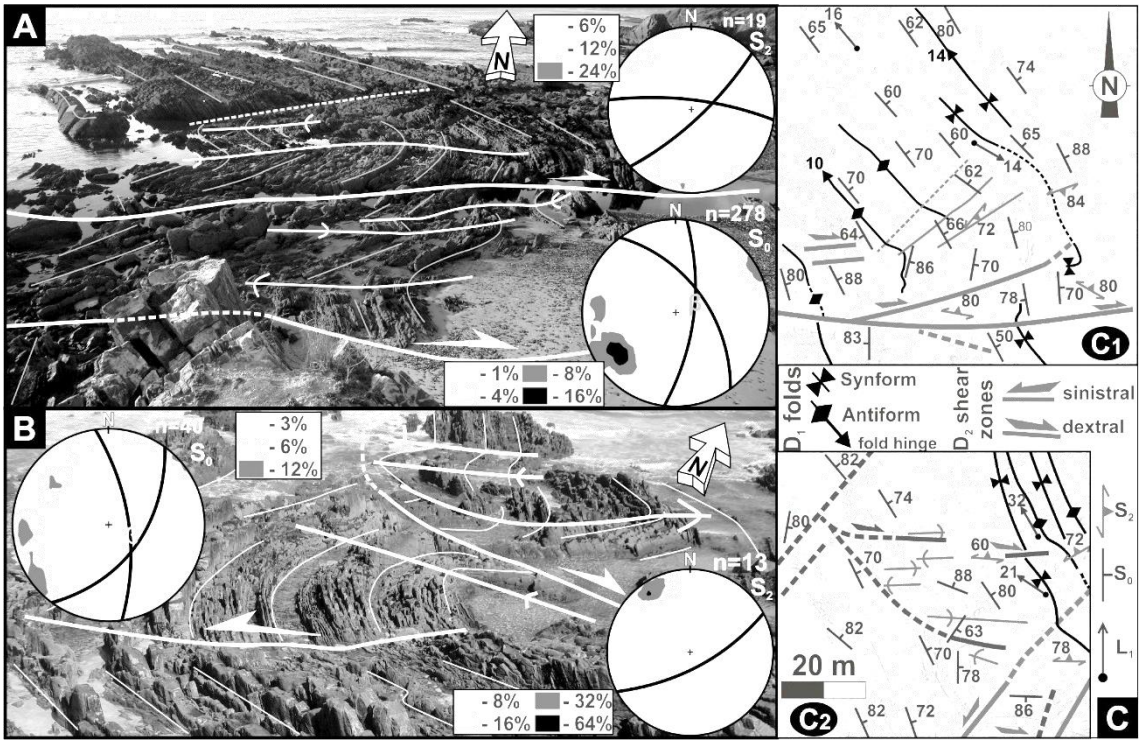

Figure 9 – E-W dextral D2 shear zones (equal area lower hemisphere stereographic projections of S_0 and S_2):

A – Kink-like fold generated by D_2 dextral shear along E-W fault in northern sector;

B – Complex interference between NE-SW kink bands and E-W dextral shears in the southern;

C – Structural map of A (C_1) and B (C_2) domains.

Occasionally closely spaced D_2 conjugate kink bands are developed giving rise to box-folds (Fig. 10), with subvertical to high dipping axial planes and hinges. The shape of the folded layers allows to distinguish two kink band families: the sinistral with a NE-SW trend and the dextral ESE-WNW to E-W one. In the shale rich turbiditic sequences the angle between both families ranges between 55º to 90º (Fig. 10A), while when the greywackes are predominant such angle tends to be smaller (34º; Fig. 10B).

As expected, the space problems related to the quasi-rigid rotation inside the D_2 kink bands, led to the development of accommodation structures. In the NNE-SSW kink bands, the bedding rotation from the regional NNW-SSE to WNW-ESE (Fig. 6), induced in the internal domain a pervasive dextral shearing along the bedding planes giving rise to a diversity of minor structures (Fig. 11; Dias et al., 2016b). The most evident are D_2 asymmetric folds (Fig. 11A) with subvertical to high plunging hinges (Fig. $11A_1$) and subvertical NE-SW axial plane S_2 cleavage (Fig. $11A_2$). In the long limbs of these folds subhorizontal to gently plunging slickensides (> 30º) are often found (Fig. 11B), enhancing the transcurrent kinematics. The dextral shearing is also supported by other structures like sigma shape competent bodies of greywackes inside non-competent shales (Fig. 11C) or dextral shear zones with trends close to ENE-WSW (Fig. 11D). Although less important, also NW-SE sinistral brittle to brittle-ductile shears zones were developed (Fig. $11D_1$), showing a WNW-ESE σ_1 compatible with the dextral shearing pervasive in the kink band. Locally, NW-SE dextral shear zones are developed (Fig. 11E), being geometrically compatible with C' shears bands of the main WNW-ESE dextral layer parallel shearing within kink-band.

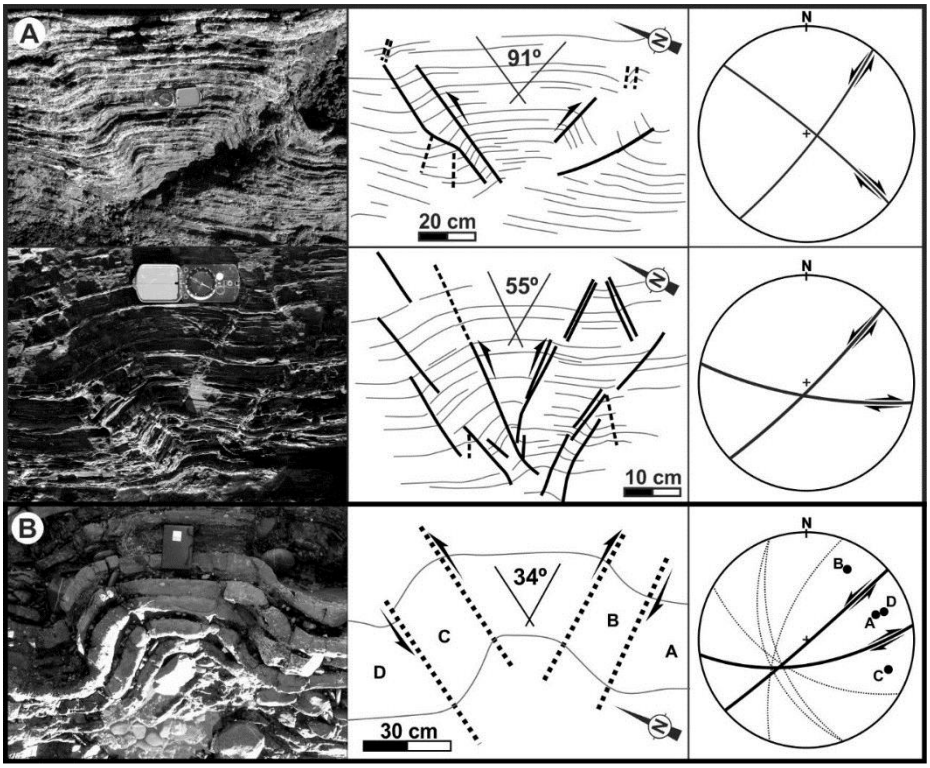

Figure 10 – Geometry and kinematics of D_2 conjugate kink bands inducing box fold geometries in (equal area lower hemisphere stereographic projections of axial planes):

A – Shale rich sequences;

B – Greywacke rich sequences.

Near the kink band boundaries some D_1 subvertical boudins were reworked, generating NE-SW sinistral shear zones (Fig. 11F), which is kinematically compatible with the sinistral shearing of the regional NNE-SSW kink bands.

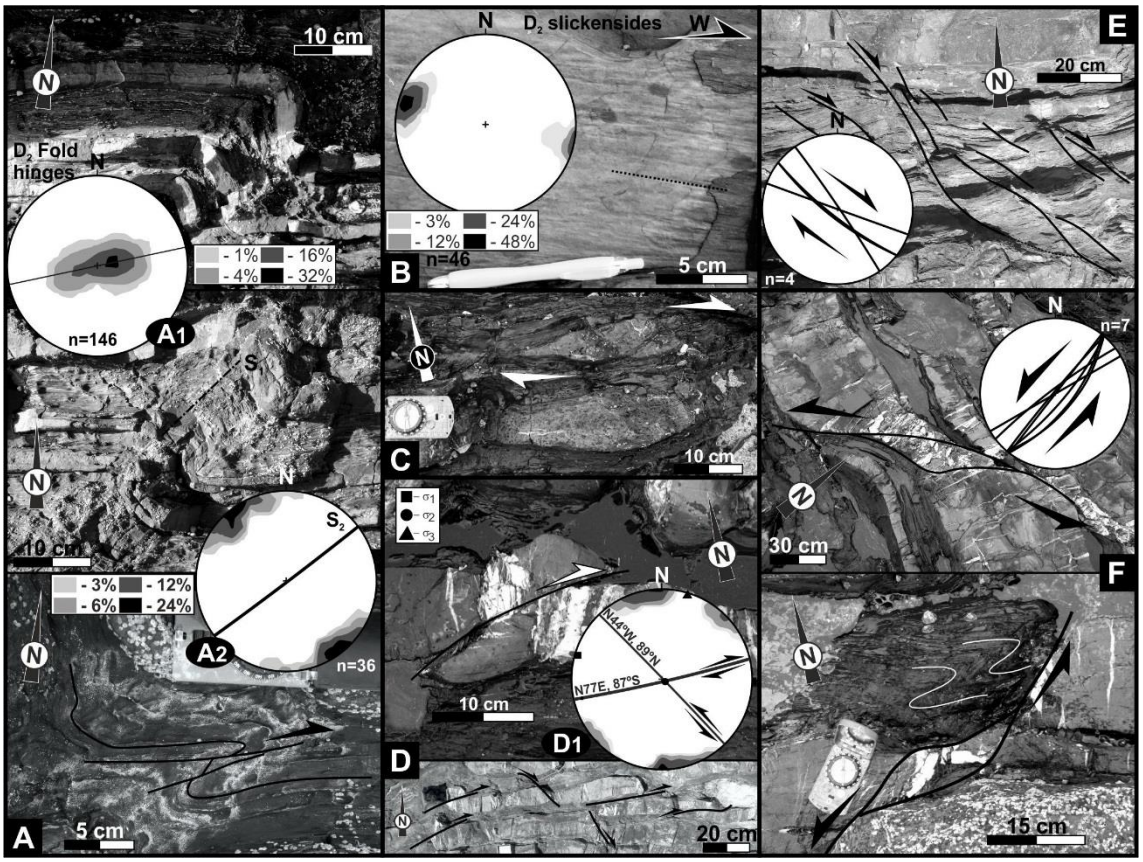

Figure 11 – D_2 structures developed within the NNE-SSW sinistral kink bands (equal area lower hemisphere stereographic projections):

A – Flexural asymmetrical folds with subvertical hinges (A_1) and a NE-SW cleavage (A_2);

B – Sub-horizontal slickensides;

C – Sigmoidal greywacke body developed in a shale-rich turbidite;

D – Dextral shear zones affecting greywacke beds and related stress field obtained using the conjugated sinistral shear (D_1);

E – Dextral NW-SE shears compatible with a C' geometry;

F – Sinistral NE-SW shears developed in a D_1 boudin necks.

X.2.4.2. Abrantes Kink Band

The Abrantes region is located in the northwestern sectors of Ossa-Morena Zone (Fig. 5B) where a Neoproterozoic-Cambrian lithostratigraphic sequence is found (Moreira et al., 2015). These formations were deformed by two ductile Variscan deformation phases (D_1 and D_2) prior to the Late Variscan brittle to brittle-ductile event. As in Almograve the Late Variscan event

induces the formation of mesoscopic kink bands due to the rigid rotation of previous planar anisotropies. However, in Abrantes the deformation of the metasediments, older than the Late Variscan, is stronger than in Almograve, which reflects the position in the orogen: the Ossa-Morena Zone is contained in the highly deformed orogenic hinterland, while the South Portuguese Zone represents the less deformed orogenic foreland (Ribeiro et al., 2007; Moreira et al., 2014).

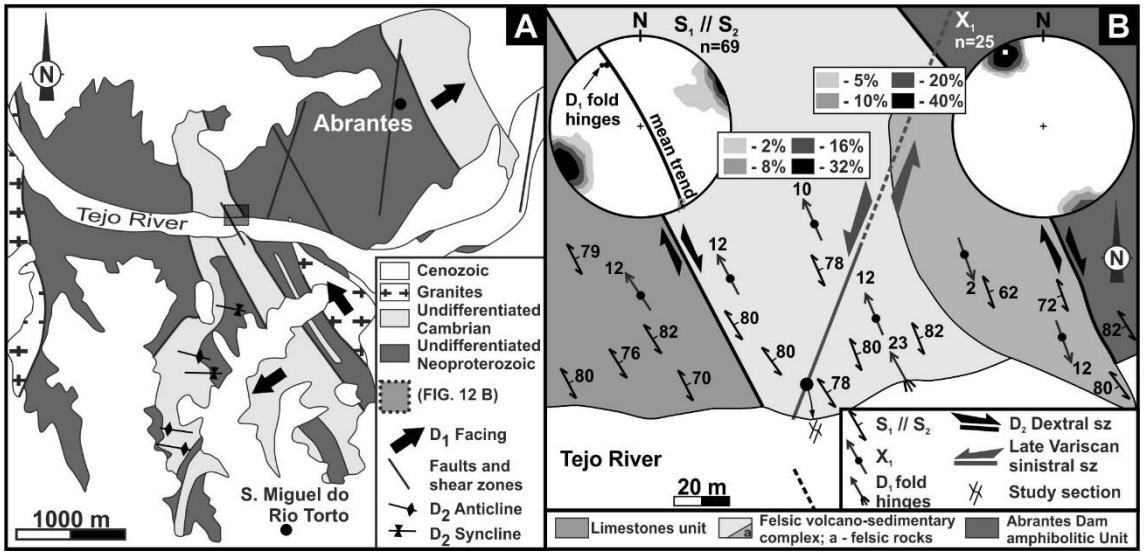

Figure 12 – Geological setting of Abrantes kink band:

A – Simplified geological map of Abrantes region (adapted from Moreira, 2012);

B – Structural map and Schmidt diagrams (equal area lower hemisphere stereographic projections) of early Variscan events, with localization of the studied kink band.

The first deformation episode (D_1), related to a medium grade foliation, generates a complex folded structure with a NNW-SSE trend. Indeed, in an axial zone there is tangential transport to NW, while the facing in the NE sector is towards NE and in SW it is to SW (Fig. 12A). Such pattern has been considered the result of a kilometric D_1 sheath fold associated with the north-west termination of the sinistral Tomar-Badajoz-Cordoba shear zone (Fig. 5B; Ribeiro et al., 2007; Moreira, 2012).

The second deformation phase (D_2) is associated with a right-lateral non-coaxial regime along the NNW-SSE orogenic trend. The D_2 distribution is highly heterogeneous with domains where WNW-ESE folds are predominant (Fig. 12A) juxtapose to others mainly affected by NNE-SSW dextral shear zones. Such pattern was considered due to a strong strain partitioning in a general NNE-SSW dextral transpressive regime (Moreira, 2012). The intensity of D_2 increases westwards towards the dextral Porto-Tomar-Ferreira do Alentejo shear zone (Fig. 5B), which

led to consider that the movement along this first order transcurrent shear zone was responsible by the D_2 episode in this sector (Romão et al., 2014; Moreira et al., 2016).

In the studied area (Fig. 12B), the structure is characterized by a NNW-SSE subvertical to strongly dipping to NE foliation. This foliation, where a sub-horizontal stretching lineation is observed (Fig. 12B), is mostly the result of the D_1 episode, although strongly reworked by the D_2 dextral shearing.

The Late Variscan deformation induces in the Abrantes region a set of subvertical D_3 structures (faults, fracturing, quartz veins, and kink bands; Fig. 13), with NE-SW to NNE-SSW trends (Figs. 13A, 13C and 13D). These structures are often related with quartz veins and cataclasis, which sometimes also affects the quartz veins (Fig. 13B), enhancing their brittle to brittle-ductile behaviour. Either the offsets of previous markers along centimetric faults (Fig.13C), or the geometry of kink bands (Fig. 13D) shows clear left-lateral kinematics along the NE-SW trend.

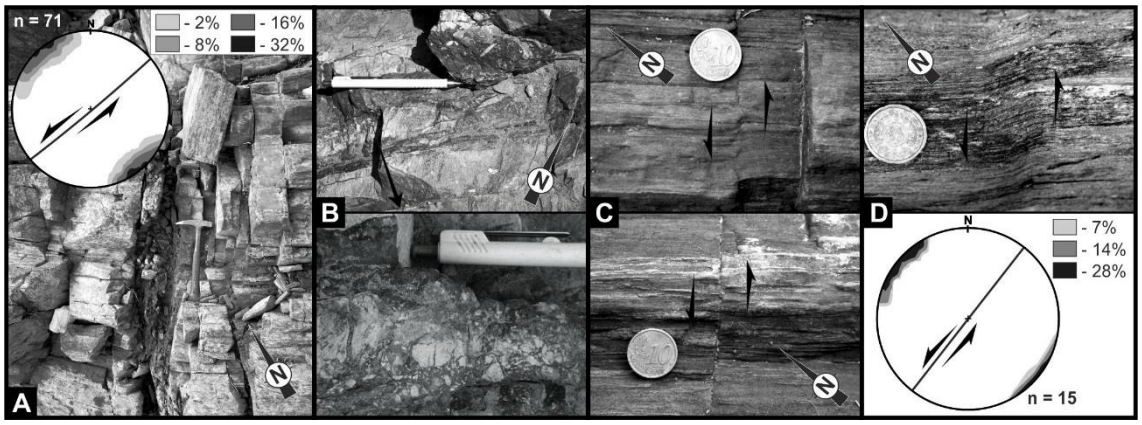

Figure 13 – Late Variscan structures in Abrantes region:

A – Intense fracturing associated to NE-SW mesoscopic fault (equal area lower hemisphere stereographic projection of main fractures);

B – Mesoscopic fault underlined by quartz veining and cataclasis;

C – Centimetric sinistral offsets in NE-SW faults;

D – Centimetric sinistral kink band and geometric behaviour of similar structures (equal area lower hemisphere stereographic projections).

The kink-bands, with a millimetric to a metric scale, are more common in the silica-rich felsic volcano-sedimentary complex where the S_1 foliation is well developed. The study of one of the metric kink band (Fig. 12A and 14) led to a better understanding of the mechanisms related to its formation. This N20ºE to N30ºE subvertical structure deflect previous planar structures (S_1//S_2) from the NNW-SSE regional trend to ENE-WSW.

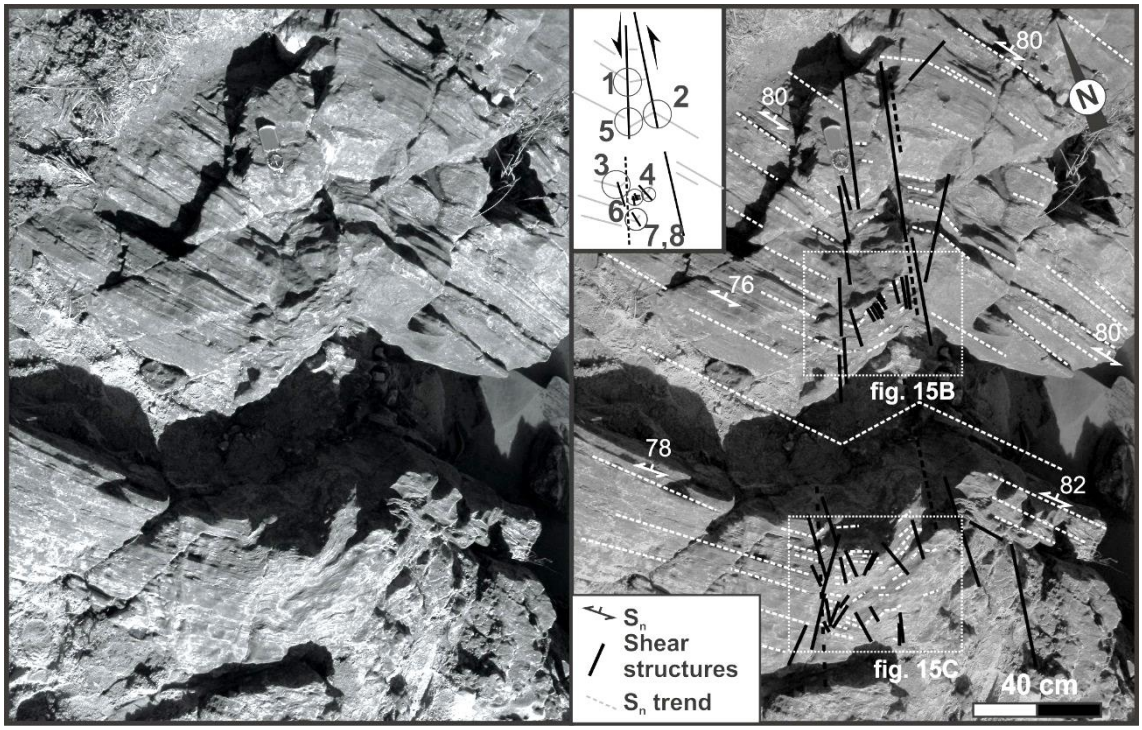

Figure 14 – General pattern of sinistral Abrantes metric kink band.

The boundaries of the Abrantes kink band are complex (Fig. 14), which could indicate it was due to the coalescence of small linear segments separated by steps or relays as proposed by Peacock and Anderson (1995) to strike slip faults. Inside the kink band a pervasive array of subvertical 2nd order fractures, was developed (Fig. 15). The trend of these fractures shows two main sets (Fig. 15A): the main set has a very consistent N-S orientation (±3º, 95% confidence interval), while the second one, is less developed and presents some dispersion around a mean N55ºE average direction (±14º, 95% confidence interval). Nevertheless, the two sets show clear evidences of rigid rotation of the previous anisotropy (S_1//S_2) inside a pair of planar structures (Fig. 15B and 15C). Such rotation generates folds with straight limbs and sharp hinges, acting as 2nd order kink bands. The geometry of both sets shows distinct kinematics: the N55ºE trend shows a pervasive clockwise (dextral) rotation while the N-S orientation generally have a counterclockwise (sinistral) rotation. Thus the N-S set is synthetic in relation to the main NNE-SSW kink band kinematics, while the N55ºE one is antithetic. Nevertheless, when a large amount of N-S structures are developed, a symmetric pattern tends to occur (Fig. 15B1). When both sets are closely spaced box-folds geometries are developed (Fig. 15B2 and 15C).

As usually, often the kink band planes of Abrantes show evidences of some slip leading to the sinistral disruption of previous planar foliation (Fig. 15C1).

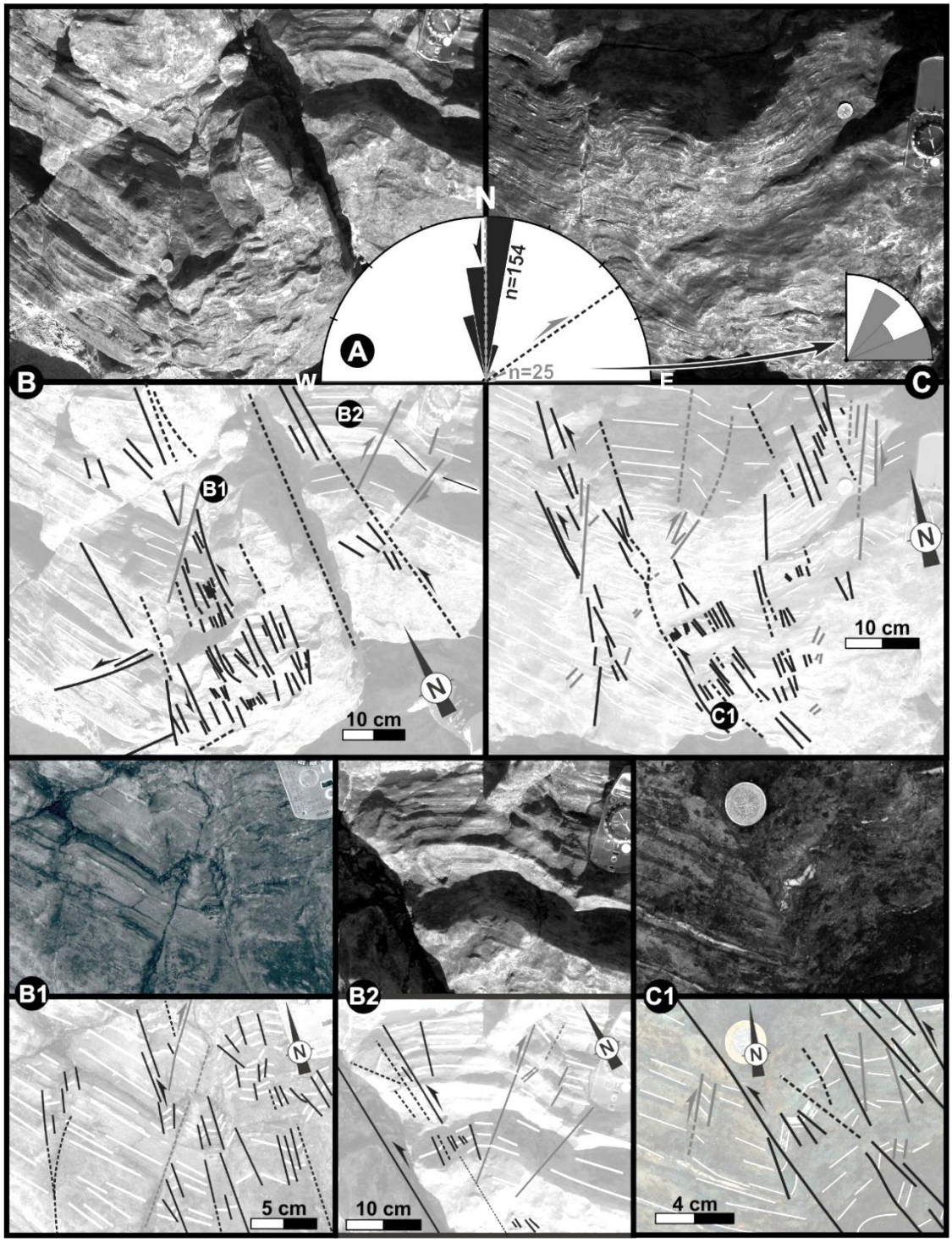

Figure 15 – Main geometric and kinematical features of Late Variscan Abrantes kink band fracture pattern:

A – Rose diagram of 2nd order kink bands;

B – Predominance of sinistral N-S fractures, with symmetrical shape in highly deformed sectors (B1) and local box folds development (B2).

C – Diffuse boundaries of Abrantes kink band, sometimes showing offsets of previous layered structures (C1).

X.2.4.3. Stress Analysis in Almograve and Abrantes Kink Bands

The Almograve and Abrantes kink bands geometry support the sinistral kinematics of the Late Variscan NNE-SSW faults. Nevertheless, they have distinctive features which seems to result mainly from the rheology of the affected formations.

In Almograve, the stress field of the Late Variscan kink bands was estimated using the bisector method (Stewart and Alvarez, 1991) in three sectors where conjugated kink bands are found. All are located outside the major mesoscopic kink band where the D_1 structures have the regional NNW-SSE trend (Fig. 5). Thus the obtained stress fields have a regional meaning because they have not been rotated during the kink band formation. In all cases the intermediate tensor (σ_2) is subvertical, while the maximum (σ_1) and minimum (σ_3) tensors are subhorizontal, with NNW-SSE and ENE-WSW directions respectively (Fig. 16A_3). The angular relation between the σ_1 direction and the primary layering (α), although very small shows positive (i.e. the σ_1 acting in the clockwise side of the primary layering; Fig. 16A_1), or negative (Fig. 16A_2) values. The negative α were obtained near the NNE-SSW sinistral kink bands, showing that they induce a slight counter clockwise rotation of σ_1, synthetic with the rotation of primary layering within the kink band. If is it considered the mean directions of cartographic scale dextral and sinistral kink bands (Fig. 6), similar stress field is obtained: σ_1 and σ_3 contained in horizontal plane, respectively with N30ºW and N60ºE direction and σ_2 subvertical (Fig. 16A_4).

Within Almograve kink bands the shortening of the layers related to their rotation, induced in the more competent layers conjugated shear zones. Their stress field (Fig. 16B) also have subhorizontal σ_1 and σ_3 (respectively 04º, N73ºW and a 01º, N16ºE attitude) and subvertical σ_2 (86º, S57ºE). This internal stress field related to the evolution of the kink band, is counter clockwise rotated in relation to the previous stress fields (Fig. 16A) which are typical of the external domains. Thus, the obtained stress field could be interpreted as related to layer-parallel shortening within kink-band.

In the Abrantes kink band, the internal stress field was obtained using the 2nd order conjugate kink bands developed within kink band. The stress field presents subvertical σ_2 and subhorizontal σ_1 and σ_3 (Fig. 16C), respectively with a WNW-ESE and a NNE-SSW trends. Such stress field is also compatible with the layer parallel shortening during the rotation process.

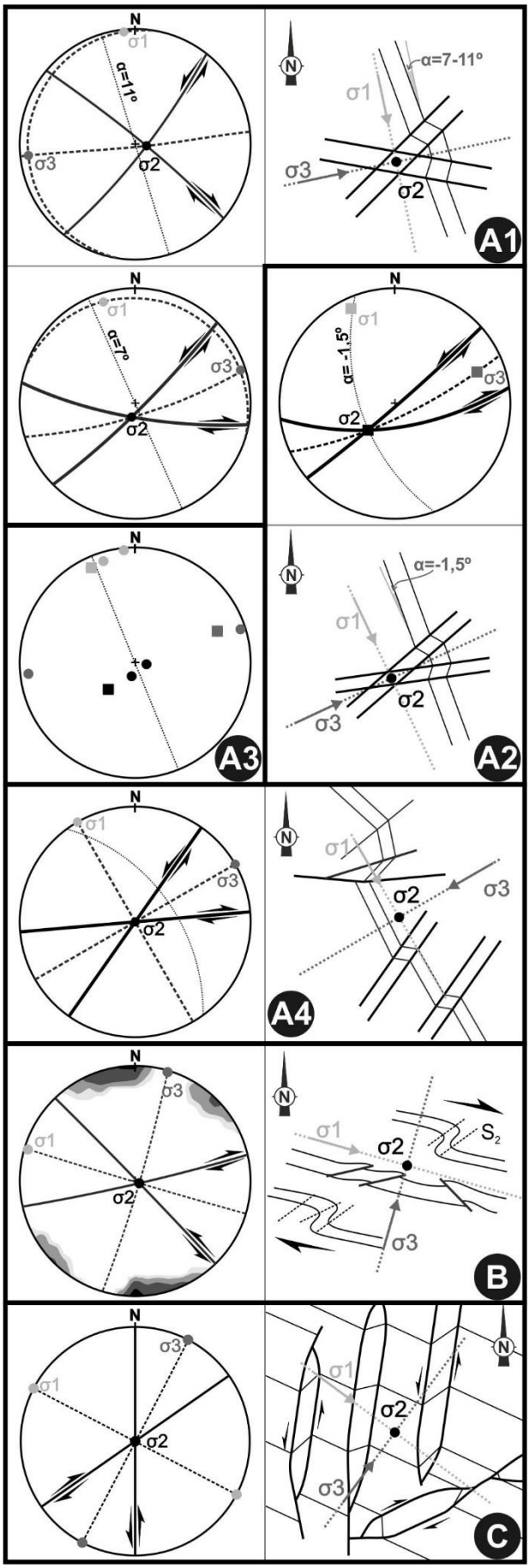

Figure 16 – Stress field analysis based on D_2 structures:

A – External NNW-SSE domains of Almograve kink bands, based on D_2 kink bands. Similar stress field was obtained based on cartographic scale structures (A_4);

B – Internal WNW-ESE domain of major Almograve kink band, based on D_2 conjugate shear zones;

C – Internal stress field of Abrantes kink band data using 2nd order kink-bands.

Although the stress fields obtained for the Late Variscan kink bands are similar for Almograve and Abrantes, the induced structural patterns originated by rotation and consequent layer parallel shortening are quite different (Fig. 16B and 16C). Flexural folds were formed in both cases, but they present distinct shapes due to the different rheology of the deformed multilayers. Indeed, in Almograve the folds were formed by dextral shear slip between adjacent layers (Fig. 11A) induced by the internal kink band rotation. The coeval layer parallel shortening was expressed, either by conjugate shear zones developed in the competent greywacke layers, or by orthorhombic folds found near the kink band boundaries (Dias et al. 2016b). In Abrantes, the layer parallel shortening on homogeneous lithological successions generates 2nd order conjugate kink bands.

X.2.5. Shortening Quantification in Almograve and Abrantes Kink Bands

The frequent complex structural pattern of kink bands and the existence of different genetical processes difficult the estimation of the shortening induced by rotation during their formation. However, when the genetical mechanism is known, it is possible to approach such distortion.

The projection of angular values of Abrantes and Almograve kink bands (table II) in the Srivastava et al. (1998) triangular diagram (Fig. 17), shows the clear predominance of the fixed hinge mechanisms (type III). Such classification is compatible with the field data for both regions, where their boundaries seem to have been stable during the deformation, sometimes with evidences of simple shear along boundaries. The presence of shortening structures within kink band and the occurrence of interlayer slip in Almograve are also evidences of type III model. The dispersion of data towards type IV model could indicate, either a slight change of the kink band boundaries during layering rotation, or the variation of angular parameters during the deformation process, as could happen by layer parallel slip on internal foliation (Stewart and Alvarez, 1991).

Previous works developed a graphical method to evaluate the volume variation within kink bands (Dewey, 1969; Suppe, 1985). Such approach was adapted to fixed hinge type III model assuming the geometrical constraints typical of this model (Fig. 18). The shortening quantification assumes that the kink band boundaries are parallel and kink band width (W) remains invariable during the rotation of internal primary layering. During the deformation progress, the length of primary layering from its initial position (L_0) to its final position (L_1) varies, allowing the shortening measure (Fig. 18). During rigid rotation, the angular values relation presents variations, always obeying to equation 1.

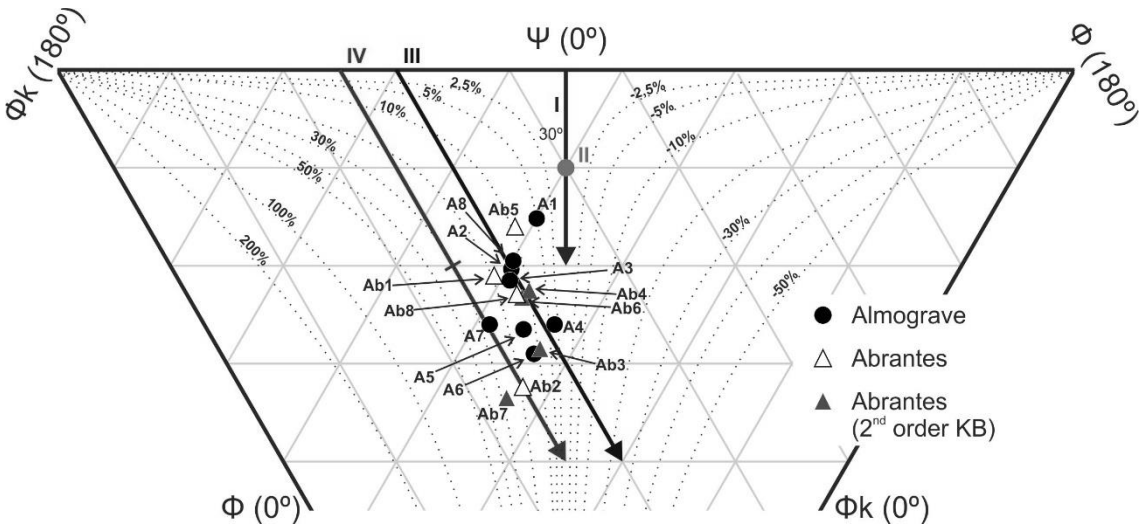

Figure 17 – Almograve and Abrantes data in Srivastava et al. (1998) triangular graphic of kink band types.

Table II – Angular parameters of Almograve and Abrantes kink bands (locations in figures 6 and 14).

		Φ	Φk	Ψ	Model type
Almograve	**A1**	69,5	80,5	30	near III
	A2	60	79	41	III
	A3	58,5	78,5	43	III
	A4	62	**66**	52	III
	A5	56	**61**	63	III
	A6	55,5	**66,5**	58	III
	A7	**50,5**	**67,5**	62	IV
	A8	61	80	39	III
Abrantes	**Ab1**	57,5	80,5	42	III
	Ab2	**50**	**65**	65	IV
	Ab3*	57	**66**	57	III
	Ab4*	61	74	45	III
	Ab5	65	83	32	near III
	Ab6*	59	74,5	46,5	III
	Ab7*	**47**	**66**	67	IV
	Ab8	58	76	46	III

* - 2nd order kink band

It was generated a predictive model based in a point matrix generated by multiple interactions for ϕ and ϕk angular values during the rotation. Associated with each (ϕk,ϕ) quoted point it was measured the stretching value ($S = L_1 / L_0$). All quoted points and respective S value are projected in bivariate graph, being generated a predictive model using the ordinary kriging as spatial interpolation method (Fig. 18A). When the ϕ angle is smaller than 30º a new kink band is not generated, since the shear reactivation of inhered primary layering are pervasive (Sibson, 2012).

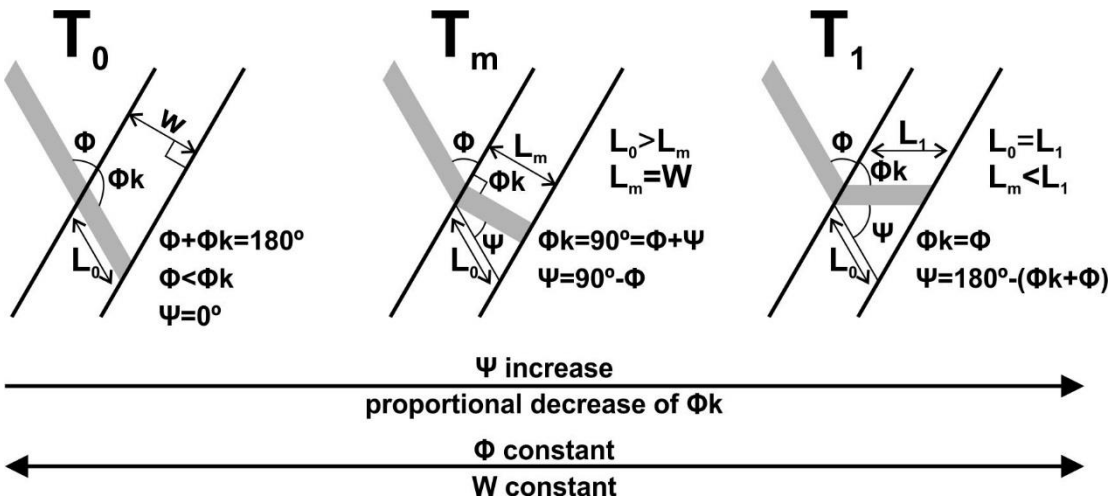

Figure 18 – Summary parameter conditions for graphic construction. Stretching parameter was obtained with the variation of length during rotation with constant kink-band width.

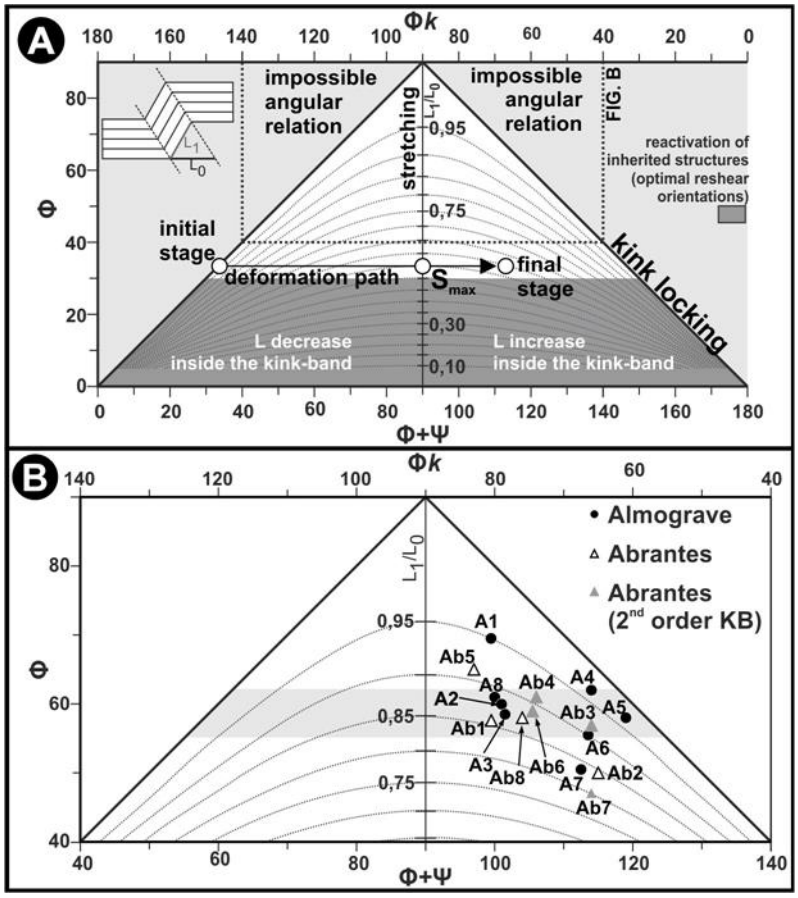

Figure 19 – Graphical estimation of stretching in type III fixed-hinge kink bands:

A – Proposal graphical method for shortening kink band analysis. The arrow represents an example of evolution of a kink band;

B – Projection of Almograve and Abrantes kink bands.

The use of this method in Almograve and Abrantes kink bands indicates a shortening ranging from 6 to 26% (Fig. 19B; table III). The projection of the data in the $\phi k > \phi$ field with $\phi k < 90º$ indicates a strong rotation of the kink bands during deformation, although lower than the theoretical maximum rotation (i.e. $\phi k = \phi$). The lower values of shortening is proportional to higher ϕ values, because the rotation until the orthogonal position is smaller.

Table III – Shortening values for Almograve and Abrantes kink bands (locations in figures 6 and 14).

		S max	Maximum shortening (%)	S actual position	S component (%)	$S_{\perp}$ Stewart and Alvarez (1991)
Almograve	**A1**	0,936	**6,4**	0,950	1,4	1,06
	A2	0,866	13,4	0,882	1,6	1,13
	A3	0,853	14,7	0,871	1,8	1,15
	A4	0,884	11,6	0,967	**8,3**	1,03
	A5	0,829	17,1	0,953	**12,4**	1,05
	A6	0,824	17,6	0,902	**7,8**	1,11
	A7	0,772	**22,8**	0,834	**6,2**	1,19
	A8	0,875	12,5	0,888	1,3	1,13
Abrantes	**Ab1**	0,843	15,7	0,855	1,2	1,17
	Ab2	0,766	**23,4**	0,845	**7,9**	1,18
	Ab3*	0,839	16,1	0,923	**8,4**	1,09
	Ab4*	0,875	12,5	0,910	3,5	1,10
	Ab5	0,906	**9,4**	0,913	0,7	1,10
	Ab6*	0,857	14,3	0,890	3,3	1,12
	Ab7*	0,732	**26,8**	0,803	**7,1**	1,25
	Ab8	0,848	15,2	0,875	2,7	1,14

These data emphasize some heterogeneity of the deformation. Indeed, in the Almograve main kink band (Fig. 6), four different shortening values were obtained (A4 to A8; Table III) ranging between 12% and 23%. This scatter could result from distinct displacements in the central and bordering areas of the same kink, which is compatible with lower shortening values closer to the boundaries where the rotation was smaller. However, the dispersion could also result from variation of ϕ values during deformation, like their decrease due to discrete slip along kink band boundaries. Evidences of sinistral slip along the boundaries are found both in Almograve (A7 kink band; Fig. 8A) and Abrantes kink bands (*e.g.* Ab7 kink band; Fig. $14C_2$).

Indeed, the three kink bands with higher values of shortening (A7, Ab2 and Ab7) fall in type IV field (Fig. 17), suggesting variation of ϕ during deformation. Concerning the obtained lower values of shortening (A1, A4 and Ab5) could be related with the increase of ϕ due to layer parallel slip in the external domains of the kink bands as already suggest (Stewart and Alvarez, 1991). In fact, there is evidences of slip in outer domains of kink band near A4 kink band, due the action of dextral shear related to kink-like fold (Fig. 6).

The Almograve and Abrantes kink bands always present ϕk lower than 90º which, for fixed kink boundaries, indicates that they already initiate a process of layer-parallel stretching (Fig. 19B). Nevertheless the extension rate in most cases is very small, (*i.e.* S component lower than 5%; table III), which means that some kink bands is almost orthogonal to kink band boundaries. Although in both regions the structural evidences of stretching within kink bands are not common, some localized C' shear zones in Almograve are compatible with layer parallel stretching (Fig. 11E). However, some care should be taken, because ϕk angle could also decrease due to slip of internal layering (Stewart and Alvarez, 1991), as sometimes observed in Almograve kink bands (Fig. 11A and 11B).

The strength of previous methodology could be accessed by comparing the graphical estimations with values obtained by independent approaches. In Abrantes, a thin quartz vein parallel to the main planar anisotropy and with a Ψ=46º (Fig. 20A_1; Ab8 sample) were reconstructed to its linear undeformed state (Fig. 20A_2). The comparison between the initial and final lengths shows that the kink band induced a 18% of shortening of the structure, which is quite similar to the 15,2% obtained by the graphical method and with the general range obtained to Abrantes type III kink-bands (13 to 17%; Table III). The widespread development of 2nd order conjugate contractional kink bands displacing the internal layering (Fig. 15B_2), shows that this shortening parallel to the layering was compensated by stretching in the orthogonal direction without evidences of vertical escape.

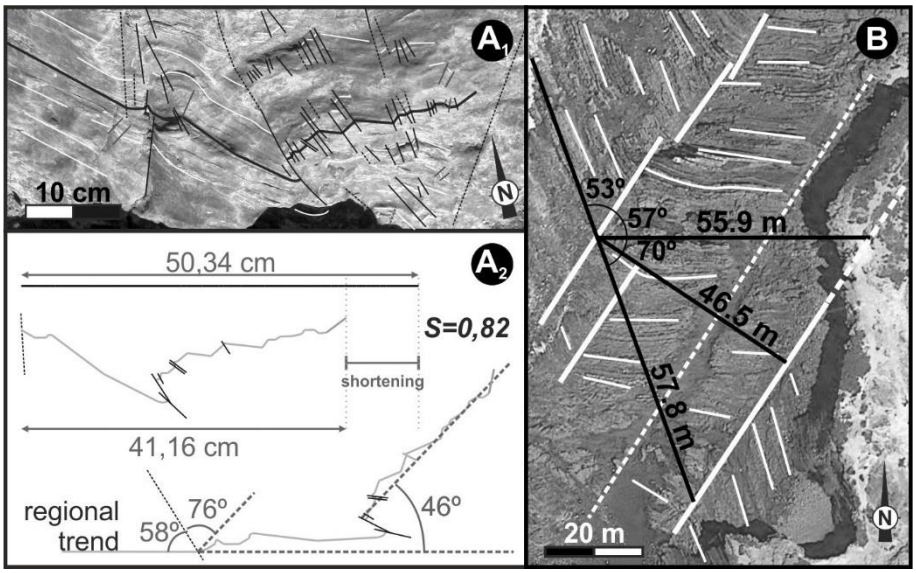

Figure 20 – Shortening estimation of kink band real cases:

A - The general pattern of Abrantes kink band (sample Ab8) using a quartz vein parallel to layering as strain marker (A_1) and the parameters used in the finite quantification (A_2).

B– General pattern and geometrical parameters of Almograve kink band.

Also in Almograve, the shortening was deduced by the geometry of a well exposed wave cut platform sinistral main kink band (Fig. 20B). Here, the total rotation ranges 70º and the maximum shortening is also circa of 19%. Taking into account the angular values (Fig. 21A), the proposal graph methodology estimate 20% of shortening. This value fits the Almograve estimations using the graphical approach that gave a maximum shortening usually ranging between 13 and 18% (table III and Fig. 19B).

The compatibility between the shortening estimations using the graphical methodology and the values obtained by detailed geometrical analysis of two previous examples, shows it is a good approach to estimate the distortion induced by kink band rotation. This is important because this method is fast and easy to use using only the measure of ϕk and ϕ values.

In the horizontal plane of the inner domain of Almograve kink band, several structures were developed due to this shortening. Some of these structures compensate this layer parallel shortening with extension orthogonal to the layering: conjugate shear zones in greywackes (Fig. 11D), orthorhombic folding near kink band boundaries (Fig. 8B) and monoclinic flexural folding due to the dextral reactivation of layering (Fig. 11A). However, the sparse development of these structures are not able to support the overall shortening. Nevertheless, the Almograve kink band is a particular situation where the initial and final lengths are very similar (57.8 m and 55.9 m; Fig. 20B), which give an almost negligible final shortening (*circa* 3%), compatible with the observed structures. Even so, during the intermediate state, where the minimum width was attained (46,5 m; Fig. 20B), some vertical escape is inevitable to compensate the 19% layer parallel maximum shortening. The lack of structures related to this subvertical thickening is due to the outcropping conditions (Almograve is mostly a subhorizontal wave cut platform), and the weakness of the effective stress field related to this subvertical escape.

Thus, it could be assumed a mechanism of rigid rotation of internal layering inside kink band coeval of vertical escape. This vertical variation is able to compensate, either the horizontal layer parallel shortening during the initial stages of kink band formation, or their extension in the latter stages. It should be noted that slickensides plunge also denotes a slightly oblique slip (Fig. 11B), compatible with the presence of a vertical escape component.

The data were also projected in Stewart and Alvarez (1991) graph (Fig. 21A). The data show, as expected, that if the shortening component is applied parallel to the layering, a stretch component is required in other orthogonal direction ($S_{\perp}$ in table III; vertical or parallel to kink band boundaries direction). So, all the Almograve and Abrantes kink bands are projected in $S>1$ field, which means that there is a bulk increase orthogonally to the layering.

The obtained values of streching parrallel and orthogonal to layering through both methods must to be complementar and a negative relationship is require (Fig. 21B). The projection of S_{MAX} vs $S\perp$ shows two distinct clusters are identified (Fig. $21B_1$):

- A1-A3, A8, Ab1, Ab4-Ab8 samples are disposed over or near the proportionality perfect curve (error < 2º), which indicates that both obtained S values are similar;
- A4-A7, Ab2-Ab3 samples are disposed below the proportionality curve (error > 2º) which means that the S component value parallel to layering is higher than the obtained orthogonal one.

The second cluster is coincident with the samples that have highly rotation to beyond the orthogonal position between kink band boundary and internal rotated layering, thus presenting a higher S component (table III). This discrepancy happens because the S_{MAX} parallel to layering is not the finite stretching in the actual position. The linear negative relationship is clearly visible when S in actual position and the S obtained in Stewart and Alvarez (1991) are projected, showing that the proposal method is a good approach (Fig. 21B2). The diference between both comparative graphs (Fig. 21B) corresponds to S component previously mentioned in Table III. The only exception is the sample Ab7, that according our method presents an higher S component. This fact could be related to an angular parameter change, namely decrease in ϕ, related to an intense slip along kink band boundary.

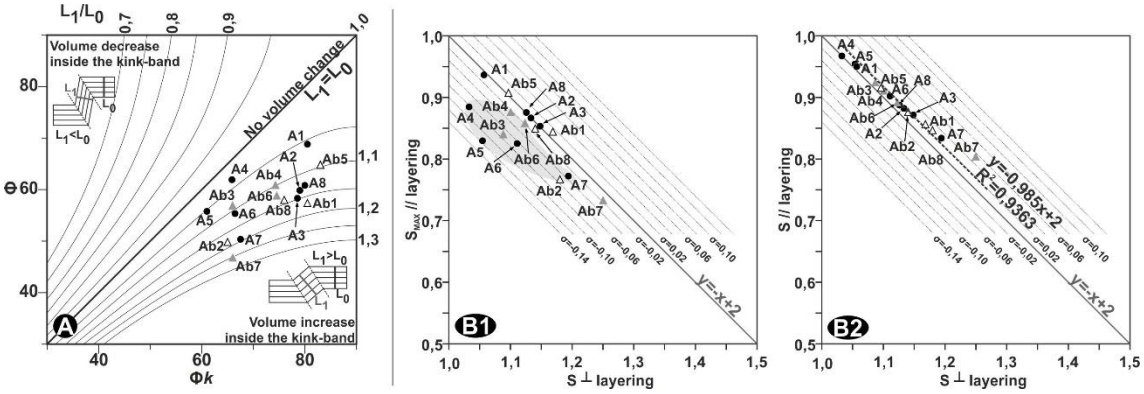

Figure 21 – (A) Thickening variation analysis within kink band using Stewart and Alvarez (1991) graphical method; (B) Comparison between stretching value obtained by proposal method (S // layering) and Stewart and Alvarez (1991) method (S ⊥ layering).

X.2.6. Layer Parallel Shortening and Layer Parallel Slip in Fixed-Hinge Models

The geometric and kinematic features of Almograve kink bands, and their spatial relation with NNE-SSW deformation bands, show this trend have a clear sinistral kinematics during Late Variscan times. The strong distortion induced by the rotation of the inner domain of the kink

band in relation to the outer NNW-SSE regional trend, superimposed on a highly anisotropic sequences, will gave rise to a strong heterogeneous deformation pattern.

In the WNW-ESE domains, the complexity of such deformation is expressed by the coexistence of two different sets of folds. An orthorhombic set of folds is common in the vicinity of sub-vertical kink band boundaries and could be explained by layer parallel shortening. The folds with monoclinic symmetry reflects the relation with dextral layer parallel slip along the subvertical WNW-ESE inner domain. Although both sets of folds are found in the same kink band, their different genetical mechanisms exclude their development in the same place. Nevertheless the absence of interference structures between them are compatible with the same sinistral simple shear along the NNE-SSW trend.

Also the rheology of deformed turbiditic sequences affects the final structural complexity. In the studied Carboniferous turbidites the rheology of more thicken greywackes layers difficult homogeneous folding, leading to the development of conjugate shear zones during layer parallel shortening. In some cases, the thicker greywackes package indents the less competent shales from the external domains distorting the kink band boundaries. The structural anomalies induced by indentation of thick competent layers on kink boundaries, which is a strong evidence to the presence of fixed boundaries, have been described in others tectonic environments (*e.g.* Coke et al., 2003).

The rigid rotation of previous structures are unable to accommodate all the deformation inside the kink band. As there is no evidences of considerable volume loss and the orthogonal shortening must be balanced, either by sub-horizontal or sub-vertical stretching. The deformation induced by layer parallel shortening is heterogeneously distributed, being stronger in the vicinity of the kink band sub-vertical boundaries.

The internal dextral layer parallel slip induced the formation of monoclinic flexural folds, which also have an important role in the dissipation of the layer parallel shortening component. Indeed, such folds thickening the sequence orthogonally to the layering, in sub-horizontal plane. The relation of these folds to low plunging slickensides the presence of some vertical escape component, which appears to be non-negligible in the horizontal shortening dissipation.

In Abrantes N20ºE kink band, the structural pattern is simpler, with the development of a conjugate set of 2nd order kink bands during layer parallel shortening. These structures induce an orthogonal sub-horizontal thickening inside kink band. In these case, there are no evidences of layer parallel-slip within kink-band.

The trend of the sinistral 2nd order structures presents a counterclockwise rotation (usually less than 45º) in relation to the main kink band. The geometric and kinematic features

of these structures are similar to the "shear crenulations" (Matte, 1969; Stubley, 1990) or strain-slip crenulations, if slip along kink band boundaries was present (Matte, 1969). During the deformation, the angle between these 2nd order structures and the main kink band decrease (Matte, 1969), which could explain the trend dispersion of these structure. Such dispersion could also be enhanced by the presence of simple shear along the main sinistral kink band, as highlighted in experimental works (Williams and Price, 1990). The shear crenulations are pervasive in wider kink bands and could result from different mechanisms (Stubley, 1990) as reorientation of stress field due to rotation in relation to external layering or rotation of main kink band direction and the presence of shortening parallel to internal foliation. The presence of conjugate 2nd order kink bands allows to calculate the internal stress field that is compatible with layer parallel shortening within kink band, as previously mentioned.

The 2nd order sinistral kink bands are considered structures developed during widening of pre-existing kink bands (Stubley, 1990). However, in the Abrantes kink band the angular data seems to indicate type III fixed boundaries and, consequently, fixed width. Thus, the 2nd order structures seem to result from continuous deformation process in simple shear regime related to the main kink band with diffuse boundaries.

X.2.7. Final Remarks

The Almograve and Abrantes kink bands show strong similarities in their deformation mechanisms, although with particular features. This particularities allows the better understanding of the late stages of the Variscan Orogeny dynamics. The observed sinistral non-coaxial deformation of NNE-SSW kink bands and its brittle to brittle-ductile behaviour are compatible to previous models for this deformation episode (Ribeiro, 2002; Dias et al, 2016b).

In fixed hinge kink bands, the rotation of the internal domains related to its genesis induces the distortion of previous structures. This distortion could be easily estimated using the proposal graph based in the classical kink band angles. The strength of this new methodology was assessed by comparing the graphical estimations with values obtained by independent methods for two particularly well exposed kink band examples.

Nevertheless, care should be taken in the interpretation of the estimated shortening value, because slightly variations in the angular values could be induced, either by slip along kink band boundaries or by layer parallel slip.

The studied field examples show that during the development of type III fixed hinge kink bands, the strain is localized within kink band due the internal rotation of primary layering and/or slip along the kink boundaries. Thus, some internal structures should be developed due

to the distortion induced by the kink folding mechanism. These structures are mostly controlled by the rheology and heterogeneity of deformed sequence, coupled with layer parallel shortening and layer parallel slip mechanisms.

References

Anderson, T. B. (1964). Kink bands and related geological structures. Nature, 202, 272–274.

Anderson, T.B. (1974). The relationship between kink bands and shear fractures in the experimental deformation of slate. Journal of the Geological Society, 130, 367–382.

Arthaud, F., Matte, Ph. (1977). Late Paleozoic strike-slip faulting in southern Europe and northern Africa: result of a righ-lateral shear zone between the Appalachians and the Urals. Geological Society of America Bulletin, 88, 1305-1320.

Babaie, H.A., Speed, R.C. (1990). Origin of kink bands in the Golconda allochthon, Toiyabe Range, Nevada. Geological Society of America Bulletin, 102, 315-321.

Borg, I., Handin, J. (1966). Experimental deformation of crystalline rocks. Tectonophysics, 3, 249–368.

Carreras, J. (2001). Zooming on Northern Cap the Creus Shear Zones, Journal of Structural Geology, 23, 1457-1486.

Choukhroune, P., Iglésias, M. (1980). Zonas de cisalla dúctil en el NW de la Peninsula Ibérica. Cadernos Laboratorio Xeolóxico de Laxe, 1, 163-164.

Carreras, J., Julivert, M., Santanach, P. (1980). Hercynian Mylonite Belts in the Eastern Pyrenees: an example of shear zones associated with late folding. Journal of Structural Geology, 2, 5-9.

Caroça, C., Dias, R. (2002). Deformação transcorrente nos sectores externos da zona Sul Portuguesa; os últimos incrementos da tectónica Varisca. Comunicações do Instituto Geológico e Mineiro, 89, 115-126.

Cobbold, P.R., Cosgrove, J.W., Summers, J.M. (1971). Development of internal structures in deformed anisotropic rocks. Tectonophysics, 12, 23–53.

Coke, C., Dias, R., Ribeiro, A. (2003). Rheologically induced structural anomalies in transpressive regimes, Journal of Structural Geology, 25(3), 409-420.

Collomb, P., Donzeau, M. (1974). Relations entre kink bands decametriques et fractures de socle dans l'Hercynien des Monts d'Ougarta (Sahara Occidental, Algerie). Tectonophysics, 24 (3), 213–242.

Davies, R.K., Pollard, D.D. (1986). Relations between left-lateral strike-slip faults and right-lateral monoclinal kink bands in granodiorite, Mt. Abbot quadrangle, Sierra Nevada, California. Pure and Applied Geophysics, 124, 177–201.

Denèle, Y., Laumonier, B., Paquette, J., Olivier, Ph., Gleizes, G., Barbey, P. (2014). Timing of granite emplacement, crustal flow and gneiss dome formation in the Variscan segment of the Pyrenees. In: Schulmann, K., Martínez Catalán, J.R., Lardeaux, J.M., Janousek, V., Oggiano, G. (Eds.) The Variscan Orogeny: Extent, Timescale and the Formation of the European Crust. Geological Society of London, 405, 265-287.

Dewey, J.F. (1965). Nature and origin of kink bands. Tectonophysics, 1, 459–494.

Dewey, J. F. (1969). The origin and development of kink bands in a foliated body. Geological Journal, 6, 193-216.

Dias, R., Basile, C. (2013). Estrutura dos Sectores Externos da Zona Sul Portuguesa; Implicações Geodinâmicas. In: Dias, R., Araújo, A., Terrinha, P., Kullberg, J.C. (Eds.), Geologia de Portugal, vol. I, Escolar Editora, 787-805.

Dias, R., Ribeiro, A., Coke, C., Pereira, E., Rodrigues, J., Castro, P., Moreira, N., Rebelo, J. (2013). Evolução estrutural dos sectores setentrionais do autóctone da Zona Centro-Ibérica. In: Dias, R., Araújo, A., Terrinha, P., Kullberg, J.C. (Eds.), Geologia de Portugal, vol. 1, Escolar Editora, 73-147.

Dias, R., Moreira, N., Ribeiro, A. (2015). Dextral strike-slip tectonics in Iberia and the Pangeia Assemblage; evidences of the Tardi-Variscan Deformation event in South Portuguese Zone. The Variscan belt: correlations and plate dinamics. Géologie de la France (Variscan 2015 special issue, Rennes), 2015(1), 50-51.

Dias, R., Ribeiro, A., Romão, J., Coke, C., Moreira, N. (2016a). A review of the arcuate structures in the Iberian Variscides; constraints and genetical models. Tectonophysics, 681, 170-194. DOI:10.1016/j.tecto.2016.04.01

Dias, R., Moreira, N., Ribeiro, A., Basile, C. (2016b). Late Variscan Deformation in the Iberian Peninsula; A late feature in the Laurentia-Gondwana Dextral Collision. International Journal of Earth Sciences (Geol Rundsch). DOI: 10.1007/s00531-016-1409-x

Donath, F.A. (1961). Experimental study of shear failure in anisotropic rocks, Geological Society of America Bulletin, 72, 985-990.

Donath, F.A. (1968). Experimental study of kink bands in Martinsburg slate. In: Baer, A.J., Norris, D. K., (Eds.) Researches in tectonics. Geological Survey of Canada, 68-52, 255–288.

Dunham, R.E., Crider, J.G., Burmester, R.F., Schermer, E.R., Housen, B.A. (2011). Geometry, microstructures, and magnetic fabrics of kink bands in Darrington Phyllite, northwestern Washington, USA: processes within fixed-hinge kinking. Journal of Structural Geology, 33, 1627–1638.

Gay, N. C., Weiss, L. E. (1974). The relationship between principal stress directions and the geometry of kinks in foliated rocks, Tectonophysics, 21, 287-300.

Gleizes, G., Leblanc, D., Bouchez, J. (1997). Variscan granites of the Pyrenees revisited: their role as syntectonic markers of the orogen. Terra Nova, 9, 38–41.

Goscombe, B.D., Findlay, R.H., Mcclenaghan, M.P., Everard, J. (1994). Multiscale kinking in northeast Tasmania – crustal shortening at shallow crustal levels. Journal of Structural Geology, 16, 1077–1092.

Goswami, T.K. (2013). Kink band microstructures in Mica in the Dafla Formation of the Siwalik Group of rocks, West Kameng District, Arunachal Pradesh. International Journal of Scientific Research, 2 (12).

Hanmer, S.K. (1982). Vein arrays as kinematic indicators in kinked anisotropic materials. Journal of Structural Geology, 4(2), 151-160.

Hanmer, S., Corrigan, D., Ganas, A. (1996). Orientation of nucleating faults in anisotropic media: insights from three-dimensional deformation experiments. Tectonophysics, 267, 275-290.

Iglesias, M., Ribeiro, A. (1981). Zones de cisaillement ductile dans l'arc ibéro-armoricain. Comunicações dos Serviços Geológicos de Portugal, 67, 85-87.

Jensen, H.M. (1999). Analysis of compressive failure of layered materials by kink band broadening. International Journal of Solids and Structures, 36, 3427-3441.

Kirschner, D.L., Teixell, A. (1996). Three-dimensional geometry of kink bands in slates and its relationship with finite strain. Tectonophysics, 262, 195-211.

Lourenço, J., Mateus, A., Coke, C., Ribeiro, A. (2002). A zona de falha Penacova-Régua-Verín na região de Telões (Vila Pouca de Aguiar); alguns elementos determinantes da sua evolução em tempos tardivariscos. Comunicações do Instituto Geológio e Mineiro, 89, 105-122.

Marques, F., Mateus, A., Tassinari, C. (2002). The Late-Variscan fault network in central-northern Portugal (NW Iberia): a re-evaluation. Tectonophysics, 359, 255-270.

Marques, F., Burg, J., Lechmann, S., Schmalholz, S. (2010). Fluid-assisted particulate flow of turbidites at very low temperature: A key to tight folding in a submarine Variscan foreland basin of SW Europe. Tectonics, 29. DOI: 10.1029/2008TC002439

Mateus, A., Noronha, F. (2010). Sistemas mineralizantes epigenéticos na zona Centro-Ibérica;. In: Cotelo Neiva, J.M., Ribeiro, A., Mendes Victor, L., Noronha F., Magalhães Ramalho, M., (Eds.). Ciências Geológicas. Associação Portuguesa de Geólogos, 2, 47-62.

Matte, Ph. (1969). Les kink bands-example de deformation tardive dam l'Hercynien du nord-ouest de l'Espagne. Tectonophysics, 7, 309-322.

Martins, H., Sant'Ovaia, H., Noronha, F. (2009). Genesis and emplacement of felsic Variscan plutons within a deep crustal lineation, the Penacova-Régua-Verín fault: An integrated geophysics and geochemical study (NW Iberian Peninsula). Lithos, 111, 142–155.

Misra, S., Burg, J.P. (2012). Mechanics of kink bands during torsion deformation of muscovite aggregate. Tectonophysics, 548–549, 22–33.

Moreira, N. (2012). Caracterização estrutural da zona de cisalhamento Tomar-Badajoz-Córdova no sector de Abrantes. MSc thesis (unpublished), Évora University, Portugal, 225 p.

Moreira, N., Dias, R., Coke, C., Búrcio M. (2010). Partição da deformação Varisca nos sectores de Peso da Régua e Vila Nova de Foz Côa (Autóctone da Zona Centro Ibérica); Implicações Geodinâmicas. Comunicações Geológicas, 97, 147-162.

Moreira, N., Araújo, A., Pedro, J.C., Dias, R. (2014). Evolução geodinâmica da Zona de Ossa-Morena no contexto do SW Ibérico durante o Ciclo Varisco. Comunicações Geológicas, 101, 275-278.

Moreira, N., Pedro, J., Romão, J., Dias, R., Araújo, A., Ribeiro A. (2015). The Neoproterozoic-Cambrian transition in Abrantes Region (Central Portugal); Litostratigraphic correlation with Cambrian Series of Ossa-Morena Zone. The Variscan belt: correlations and plate dinamics. Géologie de la France, 2015(1), 101-102.

Moreira, N., Romão, J., Pedro, J., Dias, R., Ribeiro, A. (2016). The Porto-Tomar-Ferreira do Alentejo Shear Zone tectonostratigraphy in Tomar-Abrantes sector (Portugal). Geo-Temas, 16(1), 85-88. ISSN 1576-5172.

Nance, R.D., Gutiérrez-Alonso, G., Keppie, J.D., Linnemann, U., Murphy, J.B., Quesada, C., Strachan, R.A., Woodcock, N.H. (2012). A brief history of the Rheic Ocean. Geoscience Frontiers, 3, 125-135.

Pachell, M., Evans, J.P., Lansing Taylor, W. (2003). Kilometer-scale kinking of crystalline rocks in a transpressive convergent setting, Central Sierra Nevada, California. GSA Bulletin, 115 (7), 817–831.

Paterson, M.S., Weiss, L.E. (1962). Experimental folding in rocks. Nature, 195, 1046–1048.

Paterson, M.S., Weiss, L.E. (1966). Experimental deformation and folding in phyllite. Geological Society of America Bulletin, 77, 343–374.

Peacock, D.C.P. (1993). The displacement-distance method for contractional kink bands. Tectonophysics, 220, 13-21.

Peacock, D.C.P., Sanderson, D. J. (1995). Strike-slip relay ramps. Journal of Structural Geology, 17, 1351-1360.

Pereira, E., Ribeiro A., Meireles, C. (1993). Cisalhamentos hercínicos e controlo das mineralizações de Sn-W, Au e U na Zona Centro-Ibérica, em Portugal. Cadernos Laboratorio Xeolóxico de Laxe, 18, 89-119.

Pereira, M., Castro, A., Chichorro, M., Fernández, C., Díaz-Alvarado, J., Martí, M., Rodríguez, C., (2014). Chronological link between deep-seated processes in magma chambers and eruptions: Permo-Carboniferous magmatism in the core of Pangaea (Southern Pyrenees). Gondwana Research, 25, 290–308.

Qiao, L., Winey, K.I. (2000). Evolution of Kink Bands and Tilt Boundaries in Block Copolymers at Large Shear Strains. Macromolecules, 33, 851-856

Ramsay, J.G. (1962). The geometry of conjugate fold systems: Geological Magazine, 99, 516-526.

Ramsay, J.G. (1967). Folding and fracturing of rocks. McGraw-Hill, New York, 568 p.

Ramsay, J.G., Huber, M. (1987). The Techniques of Modern Structural Geology, Vol. 2: Folds and Fractures. Academic Press.

Ribeiro, A. (2002). Soft Plate Tectonics. Springer-Verlag, 324 p.

Ribeiro, A., Munhá, J., Dias, R., Mateus, A., Pereira, E., Ribeiro, L., Fonseca, P., Araújo, A., Oliveira, T., Romão, J., Chaminé, H., Coke, C., Pedro, J. (2007). Geodynamic evolution of the SW Europe Variscides. Tectonics, 26, TC6009, DOI:10.1029/2006TC002058.

Romão, J., Moreira, N., Dias, R., Pedro, J., Mateus, A., Ribeiro, A. (2014). Tectonoestratigrafia do Terreno Ibérico no sector Tomar-Sardoal-Ferreira do Zêzere e relações com o Terreno Finisterra. Comunicações Geológicas, 101(I), 559-562.

Sant'Ovaia, H., Noronha, F. (2005). Gravimetric anomaly modelling of the post-tectonic granite pluton of Águas Frias-Chaves (Northern Portugal). Cadernos Laboratorio Xeolóxico de Laxe, 30, 75-86.

Sant'Ovaia, H., Bouchez, J.L., Noronha, F., Leblanc, D., Vigneresse, J.L. (2000). Composite-laccolith emplacement of the post-tectonic Vila Pouca de Aguiar granite pluton (northern Portugal): a combined AMS and gravity study. Transactions of the Royal Society of Edinburgh: Earth Sciences, 91, 123-137.

Sharma, B.K., Bhola, A.M. (2005). Kink bands in the Chamba region, Western Himalaya, India. Journal of Asian Earth Sciences, 25, 513–528.

Sibson, R.H. (2012). Reverse fault rupturing: competition between non-optimal and optimal fault orientations. Geological Society London, Special Publications, 367, 39-50.

Srivastava, D. C., Lisle, R. J., Imran, M., Kandpal, R. (1998). The kink band triangle: a triangular plot for paleostress analysis from kink bands. Journal of Structural Geology, 20(11), 1579-1586.

Starkey, J. (1968). The Geometry of Kink Bands in Crystals - A Simple Model. Contributions to Mineralogy and Petrology, 19, 133-141.

Stewart, K.G., Alvarez, W. (1991). Mobile-hinge kinking in layered rocks and models. Journal of Structural Geology, 13(3), 243-259.

Stubley, M.P. (1990). The geometry and kinematics of a suite of conjugate kink bands, southeastern Australia. Journal of Structural Geology, 12, 1019–1031.

Suppe, J. (1985). Principles of Structural Geology. Prentice-Hall, New Jersey.

Suppe, J., Sábat, F., Muñoz, J.A., Poblet, J., Roca, E., Vergés, J. (1997). Bed-by-bed fold growth by kink band migration: Sant Llorenç de Morunys, eastern Pyrenees. Journal of Structural Geology, 9(3-4), 443-461.

Tchalenko, J. S. (1968). The evolution of kink bands and the development of compression textures in sheared clays. Tectonophysics, 6, 159-174.

Tobisch, O. T., Fiske, R. S. (1976). Significance of conjugate folds and crenulations in the central Sierra Nevada, California. Geological Society of America Bulletin, 87, 1411-1420.

Twiss, R. J., Moores, E. M. (1992). Structural Geology. W. H. Freeman and Company, New York.

Verbeek, E. R. (1978). Kink bands in the Somport slates, west central Pyrenees, France and Spain. Geological Society of America Bulletin, 89, 814-824.

Wadee, M. A. Edmunds, R. (2005). Kink band propagation in layered structures. Journal of the Mechanics and Physics of Solids, 53(9), 2017–2035.

Wadee, M. A., Hunt, G. W., Peletier, M. A. (2003). Kink band instability in layered structures. Journal of the Mechanics and Physics of Solids, 52(5), 1071–1091.

Weiss, L. E. (1968). Flexural slip folding of foliated model materials. Canadian Geological Survey Paper, 68-52, 294-359.

Weiss, L. E. (1980). Nucleation and growth of kink bands. Tectonophysics, 65, 1-38.

Williams, H.R. (1987). Stick-slip model for kink band formation in shear zones and faults. Tectonophysics, 140, 327-331.

Williams, P. F., Price, G. P. (1990). Origin of kink bands and shearband cleavage in shear zones: an experimental study. Journal of Structural Geology, 12, 145-164.

XI

Conclusões gerais e Desenvolvimentos Futuros

Durante os estudos conducentes à obtenção do grau académico de doutor, os trabalhos realizados na região de Ferreira do Zêzere-Abrantes-Tomar mostram que as unidades e sucessões com afinidades à Zona de Ossa-Morena (ZOM) não se propagam para Norte desta região. A sucessão com semelhanças à sequência Paleozóica é definida na região de Abrantes, sendo que para Norte apenas afloram unidades que se consideram Neoproterozóicas (Romão *et al*., 2014). Na região de trabalho foram definidos dois domínios totalmente distintos no que respeita às suas características geológicas (metamórficas, estruturais, magmáticas e estratigráficas). Com efeito:

- Nos domínios mais a Este, esta região apresenta claras semelhanças com a ZOM. Na região de Abrantes definiu-se um conjunto de seis unidades que compõem uma sucessão com claras afinidades litoestratigráficas e geoquímicas com a transição Neoproterozóico-Câmbrico inferior da ZOM: três unidades atribuídas ao Neoproterozoico e três que mostram claras afinidades com a sucessão Câmbrica;
- No domínio a Oeste (entre Ferreira do Zêzere e Constância) foi identificada e caracterizada uma sequência com características tectonoestratigráficas, metamórficas e magmáticas próprias, incluindo-se no Terreno Finisterra (Ribeiro *et al*., 2007; 2013), limitado a Este pela Zona de Cisalhamento Porto-Tomar-Ferreira do Alentejo (ZCPTF). Esta zona de cisalhamento coloca em contacto este Terreno com as zonas paleogeográficas características do Terreno Ibérico, nomeadamente a ZOM no sector mais a sul (sector de Ferreira do Zêzere-Tomar-Abrantes) e com a Zona Centro Ibérica (ZCI) nos sectores mais a norte (sector de Coimbra e de Albergaria-a-Velha-Porto).

A sequência litoestratigráfica previamente descrita no domínio Este, e que Romão *et al*. (2010) interpretam como sendo composta pelos complexos Vulcano-Sedimentares Cadomianos e Paleozóicos pertencentes à ZOM, encontra-se sobreposta a granulitos e gneisses, que os mesmos autores interpretam como rochas crustais Cadomianas mais profundas. Estas unidades estão separadas entre si por acidentes tangenciais Variscos com cinemática inversa, com

transporte com topo para NE (Fig. 1). Toda esta sequência típica da ZOM encontra-se cavalgada sobre a ZCI, apresentando transporte semelhante.

A presença das rochas de alto grau metamórfico previamente referidas, com idades metamórficas em torno do 540 Ma (Henriques *et al*., 2015), e de um conjunto de unidades com idade Neoproterozóica, contendo rochas magmáticas com assinatura anorogénica, estão de acordo com o regime tectónico proposto para a ZOM durante o Neoproterozóio com o desenvolvimento de uma margem activa associada à subducção localizada no bordo norte da Gondwana (e.g. Linnemann *et al*., 2008; Sanchez-Lorda *et al*., 2014). Esta subducção origina um arco-vulcânico e uma bacia de back-arc, resultando daqui a génese das rochas anorogénicas supra mencionadas. Os processos extensivos associados à génese da bacia de back-arc podem ter gerado oceanização parcial na região onde hoje se localiza a ZCTBC, que é posteriormente reactivada durante o Ciclo Varisco como uma importante zona de cisalhamento intra-orogénica. Esta modelo conciliaria a interpretação de Eguiluz *et al* (2000), que define uma bacia de *back-arc* desenvolvida no domínio Norte da ZOM e sul da ZCI, com a de Ribeiro *et al*. (2009) que interpreta esta zona de cisalhamento como uma sutura cadomiana reactivada durante o Ciclo Varisco como um importante cisalhamento intraplaca.

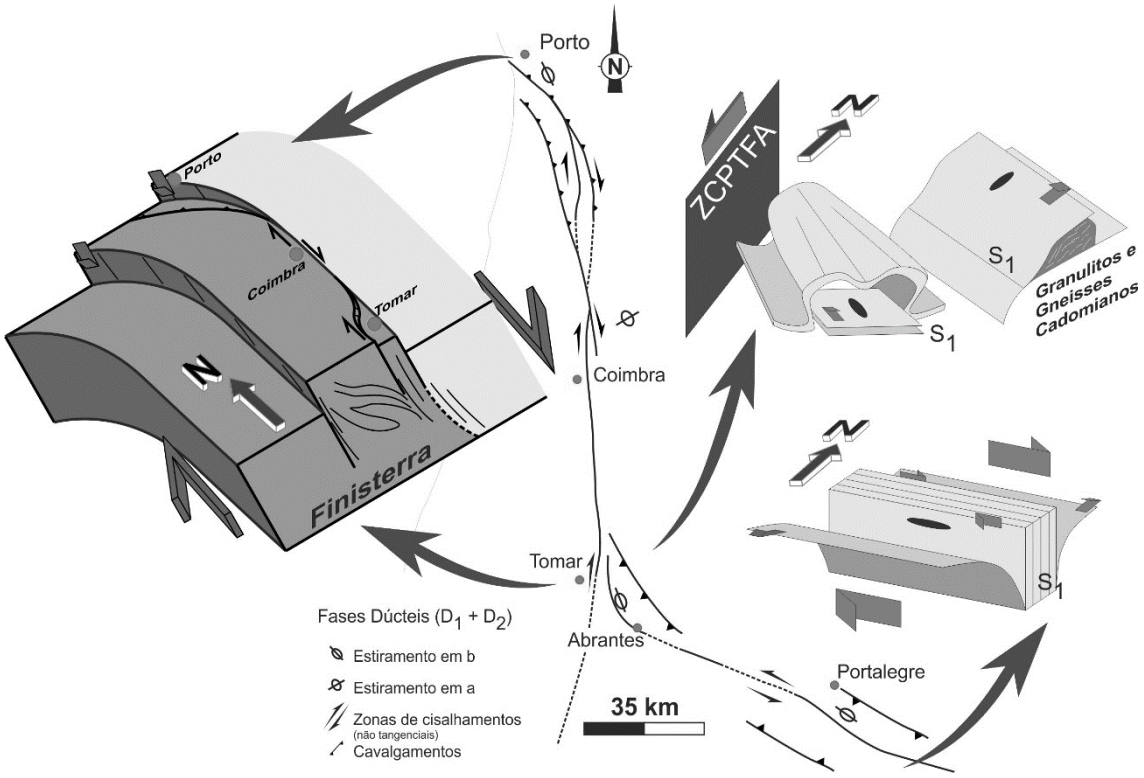

Figura 1 – Modelo estrutural esquemático para a interacção/interferência entre a ZCPTF e a ZCTBC.

Por sua vez, a sequência Câmbrica indicia e constrange os processos associados ao início do Ciclo Varisco durante o Paleozóico inferior. O conteúdo litoestratigráfico e o quimismo das rochas orto-derivadas contidas na sucessão câmbrica mostra o carácter sin-rift intra-continental das sucessões de Abrantes e de Vila Boim. A unidade basal, caracterizada pela presença de arcoses e microconglomerados, resulta da destruição da Cadeia Cadomiana, à qual se associam abundantes rochas félsicas resultantes da fusão da crusta cadomiana. Segue-se uma unidade carbonatada que denota a invasão marinha da bacia resultante do rifting intra-continental. A sequência Câmbrica definida para Abrantes mostra similaridades litoestratigráficas e geoquímicas inegáveis com a sucessão Câmbrica de Vila Boim As sucessões Câmbricas são relativamente homogéneas em toda a ZOM permitindo assim a correlação litoestratigráfica das unidades aqui definidas com os restantes sectores desta zona paleogeográfica do Terreno Ibérico. Tal facto é também evidenciado pela assinatura isotópica dos carbonatos câmbricos da ZOM. Com efeito, apesar da dispersão resultante dos processos metassomáticos do Paleozóico superior e da interacção com fluidos meteóricos (recentes?), as assinaturas obtidas são totalmente compatíveis com a assinatura de Sr da água do mar proposta para o Câmbrico.

No que respeita à estrutura do domínio Este, a existência de acidentes tangenciais com transporte com topo para NE nos domínios mais a NE é totalmente compatível com a presença de uma macro-dobra em bainha descrita por Ribeiro *et al*. (2009) e Moreira (2012) para a região de Abrantes. Esta estrutura apresenta uma zona axial onde se desenvolve o granito Neoproterozóico de Maiorga (ca. 570 Ma; Mateus *et al*., 2015) e que segue em direcção ao granito de Alverangel a norte (Romão *et al*., 2014) com idade Carbónica (U-PB em zircão, LA-ICP-MS; Pereira *et al*., 2010), apresentando também zircões detríticos de idade Neoproterozóica (ca. 600 Ma). Contudo, os autores mencionam que os zircões Carbónicos datados não têm boa qualidade, apesentando elevada concentração em U. As idades propostas para o Granito de Alverangel são indissociáveis da idade metamórfica obtida para a região Oeste (Pereira *et al*., 2010). Este metamorfismo resulta do evento de alta temperatura associado à ZCPTF, a qual afecta de forma clara o granito em causa, indicando que o granito deverá ser anterior à zona de cisalhamento e não contemporâneo. Assim, a idade obtida não está totalmente de acordo com os dados de campo, o que leva a considerar que este granito seja também ele Neoproterozóico. Contudo, serão necessários novos dados geocronológicos no granito em causa para que se possa confirmar a sua idade, sendo que a amostragem deverá ser realizada em locais onde o efeito da ZCPTF seja menos, nomeadamente no núcleo do granito (Romão *et al*., 2014).

A génese desta macro-dobra em bainha durante as fases precoces do Orógeno Varisco é interpretada como resultante do efeito de Barreira da ZCPTF à propagação para Oeste da Zona

de Cisalhamento Tomar-Badajoz-Córdoba (ZCTBC; Ribeiro *et al*., 2009; Moreira 2012). Este bloqueio gera durante as fases precoces do Ciclo Varisco a exumação das unidades infracrustais previamente referidas que são cavalgadas para NE sobre as sucessões de mais baixo grau da ZOM e estas sobre as sucessões típicas da ZCI.

Nos seus sectores mais centrais, na região de Portalegre (Fig. 1), a ZCTBC gera uma estrutura em flor compósita com uma zona axial verticalizada (Pereira, 1999), onde um metamorfismo com idades compreendidas entre o Devónico e o Carbónico se desenvolve (e.g. Dallmeyer e Quesada, 1992; Pereira *et al*., 2012), bordejado por sectores onde se desenvolvem estruturas tangenciais com vergências opostas, nomeadamente para SW no bordo SW e NE no bordo SW; estas estruturas tangenciais enraízam na zona axial da estrutura em flor (e.g. Abalos, 1992; Abalos e Cusí, 1995). Na região de Vila Boim as estruturas de primeira fase com cinemática tangencial para o quadrante SW, podem ser resultado da propagação do bordo sul da estrutura em flor, gerando assim a inversão da sequência câmbrica, com a génese de dobras deitadas com critérios de transporte para sul. Toda esta estruturação é compatível com a presença do Cavalgamento da Juromenha descrito por diversos autores como o limite sul do sector de Alter-do-Chão-Elvas (Oliveira *et al*., 1991; Araújo *et al*., 1994; 2013). Ao longo deste acidente surgem conglomerados *s.l.* interpretados quer como representativos da discordância Cambro-Ordovícica da ZOM, quer como um depósito sin-tectónico associado ao acidente da Juromenha (ver Oliveira *et al*., 1991 e Araújo *et al*., 1994; 2013 para uma discussão). Serão necessários trabalhos de detalhe ao longo do "Cavalgamento da Juromenha" para que se possa enfatizar a existência ou não desta estrutura, o que tem repercussões claras no modelo geodinâmico do NE Alentejano. Contudo, enfatiza-se que a presença de estruturas da primeira fase de deformação com vergência para Sul e a inversão da sucessão estratigráfica na região de Vila Boim são totalmente concordantes com a presença deste acidente de primeira ordem à escala da ZOM, localizado a sul do Sector de Alter-do-Chão-Elvas.

Este acidente propaga-se para o sector espanhol, onde acidentes tangenciais da primeira fase de deformação são também descritos (e.g. Expósito *et al*., 2002; Simancas *et al*., 2004), um dos quais volta a aflorar em Portugal nos domínios orientais de Barrancos (Cavalgamento do Cuco, Perdigão *et al*., 1982). Faz-se referência a estes acidentes, uma vez que os afloramentos de carbonatos de idades Silúrico-Devónica contidos no alinhamento Bencatel-Ferrarias-Cheles-Barrancos encontram-se sempre espacialmente associados à frente dos cavalgamentos de primeira fase.

Um dos pontos em aberto deixado durante a presente dissertação, embora não fosse um dos objectivos iniciais do trabalho, é a idade dos carbonatos contidos neste alinhamento e a sua relação com os mármores de Estremoz, problema que havia sido levantado por Piçarra (e.g.

Piçarra, 2000; Piçarra e Sarmiento, 2006). Do ponto de vista das suas litofácies, os Mármores de Estremoz são geralmente mais sacaroides e recristalizados, claramente distintos dos calcários deste alinhamento, menos metamórficos e muitas vezes fossilíferos. Uma excepção são os mármores de Cheles com litofácies similares aos carbonatos atribuídos aos mármores de Estremoz, bem como a alguns carbonatos dolomíticos que apresentam claras semelhanças com os calcários dolomíticos do câmbrico.

Na verdade, os carbonatos (dolomíticos e calcíticos) no sector de Barrancos foram incluídos dentro do Complexo Ígneo de Barrancos, encontrando-se geralmente associados a rochas magmáticas diversas (Piçarra 2000; Araújo *et al*., 2013). Também em Ferrarias, Bencatel, Villanueva del Fresno e Cheles tal associação é descrita. Estas rochas carbonatadas e magmáticas (vulcânicas e plutónicas) encontram-se por vezes associadas a brechas, como é claro em Barrancos, levantando-se assim a possibilidade destas rochas se encontrarem associadas a um depósito flyschóide de carácter sin-tectónico. Este depósito sin-tectónico seria gerado na frente dos acidentes de primeira fase de deformação, contendo olistólitos de carbonatados (Câmbricos e Silúricos?), bem como de rochas magmáticas. Estes depósitos resultariam da elevação e consequente erosão da cadeia Varisca que inicia o seu levantamento durante o Devónico. Esta hipótese explicaria a presença de litofácies (e idades) distintas de carbonatos num mesmo alinhamento, bem como a associação dos mesmos com abundantes rochas magmáticas e brechas. Neste caso, os mármores de Estremoz teriam uma génese distinta dos Carbonatos neste alinhamento.

Para além disso, os carbonatos deste alinhamento apresentam razões de Sr que não são totalmente esclarecedoras. Com efeito, as assinaturas dos carbonatos são compatíveis quer com as razões de Sr para o Câmbrico e para o Silúrico superior, nomeadamente do Pridoli, uma vez que as razões se sobrepõem parcialmente. A presença de conteúdo fossilífero nalguns dos carbonatos deste alinhamento indicam uma idade Silúrica Superior-Devónica Inferior (Piçarra e Sarmiento, 2006), é totalmente compatível com o modelo previamente exposto. Tendo em conta os episódios carbonatados da ZOM, estes carbonatos poderiam ser quer de idade Silúrica (Pridoli; Robardet e Gutierrez-Marco, 2004), quer do Devónico inferior (Emsiano), tendo sido remobilizados para uma bacia de carácter sin-orogénico. Contudo, é claro que estas assinaturas não são concordantes com as assinaturas Devónicas obtidas para os carbonatos do SW da ZOM (Emsiano-Givetiano; Machado *et al*., 2009; 2010) que apresentam claras similaridades com as curvas da razão de Sr propostas para a água do mar durante esse período. Desta forma, propõe-se que este alinhamento contenha carbonatos remobilizados (olistólitos e olistostromas) de diferentes idades (Câmbricas e Silúricas), o que também explicaria o padrão cartográfico altamente descontínuo e heterogéneo destes carbonatos.

Ainda no que respeita aos carbonatos Devónicos da ZOM, a presença de faunas diversificadas, algumas das quais com afinidades ao Maciço do Reno (Terreno Peri-Laurússico), leva a crer que durante o Devónico médio, a ZOM não estivesse geograficamente muito distante dos blocos continentais do Norte, nomeadamente da Laurússia, podendo haver trocas faunísticas entre a Gondwana e a Laurússia. Uma das linhas de investigação com bastante interesse e que permitiria perceber melhor a evolução da ZOM durante a passagem entre o Silúrico e o Devónico seria a comparação das faunas de conodontes e crinóides dos Calcários Devónicos do SW da ZOM com as faunas de outros carbonatos, nomeadamente:

- Os carbonatos Silúricos da ZOM que afloram nos sinclinais de Valle e Cerrón del Hornillo e se possível com os carbonatos Silúricos(?) do alinhamento Bencatel-Ferrarias-Cheles-Barrancos;
- Os olistólitos de Calcários de idade Frasniana (Devónico Superior) descritos por Boogard (1983) na Bacia de Cabrela;
- Os calcários das Formações de Escusa (Portalegre) e de Dornes (Ferreira do Zêzere) ambos de idade Devónica inferior (Gourvennec *et al*., 2008; 2010; Schemm-Gregory e Piçarra, 2013), mas com afinidade Centro-Ibérica;
- Os carbonatos de idade Devónica inferior a média de outros terrenos peri-Gondwanicos como seja o caso de Marrocos (e.g. El Hassani e Benfrika, 1995; Houicha *et al*., 2016).

Este estudo sistemático permitiria perceber a evolução espácio temporal da sedimentação carbonatada na ZOM, bem como a relação entre as faunas presentes na ZOM, nos restantes terrenos Peri-Gondwanicos e nos Terrenos Peri-Laurússicos. Esta metodologia permitiria afinar os modelos paleogeográficos para o Silúrico terminal e Devónico desta zona tectonoestratigráfica tanto à escala local como regional.

No que respeita ao Domínio a Oeste da ZCPTF na região de Abrantes, apesar das diversas dúvidas e questões que permanecem por responder, parece claro que este domínio apresenta uma evolução geodinâmica distinta dos sectores a Este, que apresentam claras afinidades com a ZOM e consequentemente com o Terreno Ibérico como referido previamente. O domínio Oeste apresenta uma tectonoestratigrafia própria, sendo que todas as unidades se apresentam uma orientação grosso modo N-S, seguindo o traçado geral da ZCPTF, o que leva a propor que a evolução geodinâmica destas unidades tectonoestratigráficas se encontra condicionada por esta zona de cisalhamento litosférica. Estas unidades apresentam características tectono-metamóficas próprias, com evidências da presença de um evento de alta temperatura (e alta pressão?; Fernandez *et al*., 2003) desenvolvido durante as fases precoces do Orógeno Varisco (Devónico), algo que a distingue dos restantes domínios do Maciço Ibérico. A presença de um

episódio magmático Silúrico-Devónico (Chaminé *et al*., 1998; Almeida, 2013) e a existência de uma unidade de baixo grau do Devónico superior-Carbónico, com faunas de acritarcas com afinidade à Laurússia (Machado *et al*., 2008), assente sobre as unidades de alto grau metamórfico na região compreendida entre Coimbra e o Porto, são também características únicas à escala do Maciço Ibérico, o que permite diferenciar um terreno tectonoestratgráfico com características próprias, o Terreno Finisterra. Contudo, importa referir que a idade das unidades de alto grau são discutíveis, embora sejam geralmente apresentadas como Proterozóicas. Contudo, a presença de zircões de idade câmbrica, ordovícica e silúrica nestas unidades (Almeida, 2013; Pereira *et al*., 2010) coloca a possibilidade destas unidades serem do Paleozóico inferior, tendo sofrido um episódio metamórfico de alto grau durante o Silúrico terminal-Devónico. Esta interpretação está de acordo com os dados geocronológicos obtidos para os ortogneisses da região de Albergaria-a-Velha-Porto (Chaminé *et al*., 1998) e para o evento metamórfico precoce nas Berlengas (Bento dos Santos *et al*., in press).

Desta forma, embora seja claro que a evolução geológica deste Terreno é, pelo menos em parte, distinta do Terreno Ibérico, são necessários trabalhos complementares, alguns dos quais já em curso. Com efeito, destaca-se desde logo a necessidade de uma caracterização pormenorizada dos episódios metamórficos, nomeadamente o episódio de alta temperatura idade Carbónica (ca. 340-320 Ma) associada à componente transcorrente direita da ZCPTF, mas também o episódio prévio, de idade Devónica, que já foi identificado nas Berlengas e que atinge a fácies granulítica (Bento dos Santos *et al*., *in press*). A caracterização do(s) episódios(s) metamórficos do Terreno Finisterra implicaria não só a caracterização dos percursos Pressão-Temperatura-Tempo para as unidades de alta temperatura, mas também as idade geocronológicas destes eventos. No que respeita à geocronologia isotópica pretende-se não só caracterizar a idade dos episódios metamórficos, mas também se possível a idade dos protólitos para- e orto-derivados contidos neste terreno; o trabalho em causa já se encontra em curso.

Outra das hipóteses a ser testada é a presença de um episódio de alta pressão Varisco no Terreno Finisterra. Este episódio está descrito quer no Mid-German Crystalline Rise (Alemanha; Scherer *et al*., 2002) quer no Bloco de Léon (França; Paquette *et al*., 1987), que se consideram terrenos equivalentes do ponto de vista da evolução geodinâmica do Orógeno Varisco Europeu. Na Finisterra evidências de alta pressão estão identificadas na região de Espinho, onde surgem micaxistos com granadas estiradas, mas também nas Berlengas. Este metamorfismo de alta pressão é caracterizado pela presença de rochas com características compatíveis com a fácies granulítica de alta pressão, sendo esta prévia ao evento de alta temperatura de idade Carbónica (Fernandez *et al*., 2003; Bento dos Santos *et al*., in press); contudo a idade deste evento é discutível.

Como referido anteriormente, estas unidades tectonoestratigráficas contidas no Terreno Finisterra apresentam um conjunto de litótipos ortoderivados (máficos e félsicos). A caracterização geoquímica destes litótipos é essencial para a compreensão dos processos activos durante o ciclo Varisco neste Terreno, tanto mais que surgem rochas ultramáficas contidas no Terreno Finisterra (Anfibolitos Olivínicos da Pedreira do Engenho Novo; Montenegro Andrade, 1977). A presença destas rochas pode resultar do processo de estiramento crustal resultante do regime geodinâmico geral descrito para as fases iniciais do Ciclo Varisco. Estes estudos de geoquímica de rocha total deveriam ser acompanhados de estudos de geocronologia isotópica com intuído de constranger temporalmente os processos de estiramento crustal presentes na Finisterra.

No que respeita à estrutura e relações geométricas entre as unidades definidas no Terreno Finisterra, os dados parecem indicar que a ZCPTF está activa desde as fases iniciais do orógeno, (algo que já havia sido enfatizado por Dias e Ribeiro, 1993), até às fases mais tardias, onde se geram zonas de cisalhamento direitas com cataclase associada. Os dados existentes parecem indicar a presença de uma importante anisotropia crustal separando dois terrenos tectonoestratigráficos distintos. Esta zona de cisalhamento é polifásica, sendo que durante as fases precoces o controlo da estrutura é escasso. Neste sentido, seria importante a cartografia estrutural sistemática e de pormenor dos sectores mais a Oeste do Terreno Finisterra, nomeadamente as ilhas das Berlengas e Farilhões, onde a influência da ZCPTF seria menor (ou mesmo inexistente), possibilitando assim a percepção da estrutura relacionada com as fases de deformação precoces deste terreno e que se relacionam com o evento metamórfico precoce. Os dados existentes para a região de S. Pedro de Tomar – Constância mostram a presença de dobras deitadas associadas a uma foliação pouco inclinada desenvolvida em gneisses e migmatitos de alta temperatura (e alta pressão?), podendo esta fase estar associada à exumação destas rochas. A segunda fase de deformação está claramente associada à transcorrência direita que caracteriza esta zona de cisalhamento. O diacronismo entre estas duas fases não está excluído, embora a segunda fase só se desenvolva junto da ZCPTF e afecte as unidades de alto grau metamórfico.

Apesar da existência de estruturas que parecem mostrar critérios com cinemática oblíqua direita-normal na região entre Ferreira do Zêzere e Abrantes, não existem evidências para que esta zona de cisalhamento funcione como um cisalhamento transtensivo durante o Ciclo Varisco. Aliás, as estruturas mais frágeis e tardias (estruturas em dominó) descritas na região de Abrantes parecem ser totalmente compatíveis com um regime transpressivo associado à componente direita. Com efeito, na região entre Albergaria-a-Velha e Porto (Fig. 1) os dados estruturais mostram a presença de um *restraining bend* associado à transcorrência direita desta

zona de cisalhamento, resultante da inflexão da direcção geral de N-S para NW-SE, enquanto na região de Ferreira do Zêzere-Abrantes a componente transcorrente direita é claramente dominante. A exumação das unidades de mais alto grau a Oeste, e a presença de uma foliação de segunda fase mergulhante para Este na região de Ferreira do Zêzere-Abrantes, denota a presença de uma subida do bloco Oeste (Terreno Finisterra) relativamente ao bloco Este (Terreno Ibérico). Embora sejam necessários mais dados, principalmente dos sectores norte, tal geometria e cinemática podem ser explicadas com um regime de transpressão triclínica de paredes inclinadas para Este (Dewey *et al*., 1998; Lin *et al*., 1998), com a subida de um bloco central em regime transpressivo direito, explicando assim a presença de rochas de alta temperatura na Finisterra (Fig. 1).

A análise dos dados obtidos e publicados e dos modelos propostos para a ZOM permitiram uma percepção global dos processos geológicos actuantes nesta zona paleogeográfica durante o Ciclo Varisco. Os processos actuantes durante o Paleozóico inferior levam à génese de uma sucessão estratigráfica que se pode separar numa sucessão sin-rift intracontinental que culmina com a abertura do Oceano Varisco (Rheic?) durante o Ordovícico, iniciando-se então a fase de deriva (*drift*). Esta transição *rift-drift* é evidente na presença de uma discordância/paraconformidade de idade Câmbrica superior e que se faz acompanhar por intenso magmatismo na transição Câmbrico-Ordovícico. As primeiras evidências geológicas que mostram o início das fases convergentes do Ciclo Varisco são do Devónico. O processo de subducção activa com início do levantamento da cadeia permanecem activos durante todo o Devónico prolongando-se até ao Carbónico, altura em que se iniciam os processos de colisão.

A presença de uma componente transcorrente esquerda paralela à direcção geral do Orógeno Varisco é geralmente aceite em todo o Maciço Ibérico (e.g. Araújo e Ribeiro, 1995; Dias e Ribeiro, 1995; Ribeiro *et al*., 2007; Moreira *et al*., 2010; Araújo *et al*., 2013; Dias *et al*., 2013; Perez-Cáceres *et al*., 2016). Esta componente esquerda parece ser geralmente mais intensa nas fases precoces do Orógeno diminuindo de intensidade durante as fases mais tardias. Esta situação está de acordo com a presença desta componente esquerda nas zonas mais internas da Zona Sul Portuguesa e a sua ausência nos domínios mais externos, a sul, onde o processo de colisão frontal passa a dominar (Dias e Basile, 2013).

A presença desta componente não-coaxial esquerda desde as fases precoces do Varisco Ibérico contrasta com o que acontece no Maciço Armoricano onde a componente dextrógira é de idade carbónica, sendo síncrona do evento magmático principal; aqui a componente frontal é anterior à componente transcorrente direita (Audren *et al*., 1976; Dias e Ribeiro, 1995). Em qualquer modelo de génese do arco este constrangimento temporal e estrutural deve ser tido

em atenção, algo que não tem sido tido em atenção nos modelos mais recentes para a génese do Arco Ibero-Armoricano (e.g. Gutierrez-Alonso *et al*., 2011; Shaw *et al*., 2012). Para além disso, os modelos mais recentes propõem ainda a existência de uma outra estrutura arqueada na Ibéria, o Arco Centro-Ibérico (e.g. Martinez-Catalan, 2011; Shaw *et al*., 2012; Johnson *et al*., 2013).

A discussão dos dados publicados para a Ibéria mostram que os modelos de delaminação crustal, implicando o *buckling* litosférico, não explicam satisfatoriamente as características geométricas, cinemáticas e dinâmicas do Arco-Ibero Armoricano. Estes modelos consideram o arco totalmente tardio (Carbónico) relativamente à edificação do orógeno, o que como vimos está em contradição com a componente esquerda presente desde as fases precoces do Orógeno Varisco na Ibéria. Para além disso, a análise dos dados de cariz multidisciplinar mostram que o Arco Centro-Ibérico é contestável (Dias *et al*., 2014; 2016). Este arco, quer na sua versão "curta" (Martinez-Catalan, 2011) quer na "estendida" (e.g. Shaw *et al*., 2012; Johnston *et al*., 2013), não só não tem em atenção as características estruturais e litoestratigráficas gerais, como contraria o zonamento interno do Maciço Ibérico colocado em evidência desde os trabalhos de Lotze (1945). Consequentemente apresenta-se na presente dissertação um modelo de indentação como proposta de modelo para a génese do Arco Ibero-Armoricano, reformulando/fortalecendo os modelos propostos em trabalhos anteriores (e.g. Ribeiro *et al*., 1995; Dias e Ribeiro, 1995), propondo-se um modelo evolutivo desde o Devónico até ao Carbonífero terminal–Pérmico. Após o processo de colisão entre os blocos continentais que dão origem à Pangeia, associado a um processo de transcorrência direita entre estes blocos continentais, inicia-se um último episódio de deformação associado ao Ciclo Varisco na Ibéria, geralmente designado de Tardi-Varisco (Ribeiro, 2002).

No que respeita à deformação Tardi-Varisca, apesar dos modelos existentes apresentarem cinemáticas diametralmente opostas para os cisalhamentos NNE-SSW (esquerdas – Ribeiro *et al*., 1979; direitas – Marques *et al*., 2002) que afectam todo o Maciço Ibérico, os dados agora apresentados mostram que a cinemática Tardi-Varisca é claramente esquerda. A maior abundância destas estruturas na ZCI pode resultar da presença de estruturas prévias de direcção N-S a NNE-SSW da terceira fase de deformação, que são reativadas durante o episódio tardi-varisco como cisalhamentos esquerdos (Ribeiro, 1974), estruturas estas que não são comuns nas restantes zonas paleogeográficas.

Os dados existentes para Abrantes e Vila Boim mostravam uma cinemática esquerda clara para os cisalhamentos NNE-SSW, contudo dúvidas permaneciam quanto à idade destes cisalhamentos. O estudo das bandas *kink* da Zona Sul Portuguesa não só mostram uma cinemática esquerda inegável das estruturas NNE-SSW, controlando a orientação geral da costa

Oeste Algarvia e Alentejana, como mostram também o desenvolvimento pontual de estruturas com o mesmo estilo de deformação e com uma relação espacial inequívoca, estas de orientação próxima do E-W e com cinemática direita. Na Zona Sul Portuguesa é possível datar este episódio de deformação como sendo Carbónico terminal a Pérmico, uma vez que estas estruturas frágeis(-dúctil) afectam os depósitos flyschóides da Formação da Brejeira de idade máxima Westefaliano D (Pereira *et al*., 2007), mas não afectam os depósitos sedimentares Triássicos que selam temporalmente este episódio.

O estudo pormenorizado das bandas *kink* Tardi-Variscas de Abrantes e Almograve permitiram ainda perceber os mecanismos de deformação associados à génese das bandas *kink*. Desta forma, foi possível perceber que os processos de *layer parallel shortening* e *layer parallel slip* controlam e acomodam a deformação interna das bandas *kink*. Considerando que as fronteiras das bandas *kink* se mantêm fixas durante o processo de deformação, o que está de acordo com os dados de campo, mas também com as características angulares ostentadas pelas bandas *kink* (Srivastava *et al*., 1998), foi possível propor um gráfico de uso simples onde a projecção dos valores angulares, previamente definidos por outros autores, permite calcular o valor de encurtamento interno teórico associado às bandas *kink*.

Referências

Abalos, B. (1992). Variscan shear-zone deformation of a late Precambrian basement in SW Ibéria: implications for Circum-Atlantic Pre-Mesozoic tectonics. Journal of Structural Geology, 14(7), 807-823.

Abalos, B., Cusí, J. D. (1995). Correlation between seismic anisotropy and major geological structures in SW Iberia: a case study on continental lithosphere deformation. Tectonics, 14, 1021-1040.

Almeida, N. (2013). Novos dados geocronológicos do Terreno Finisterra no Sector entre Espinho e Albergaria-a-Velha, Portugal. MsC Thesis (unpublished). University of São Paulo, 98 p.

Araújo, A., Ribeiro, A. (1995). angencial transpressive strain regime in Évora-Aracena Domain (Ossa-Morena Zone). Boletín Geológico y Minero, 106(2), 111-117.

Araújo, A., Lopes, L., Pereira, M.F., Gonçalves, F., Silva, J.B., Ribeiro, A (1994). Novos elementos sobre o carreamento de Juromenha (Elvas). Anais da Universidade de Évora, 4, 105-110.

Araújo, A., Piçarra, J.M., Borrego, J., Pedro, J., Oliveira, J.T. (2013). As regiões central e sul da Zona de Ossa-Morena, in: Dias, R., Araújo, A., Terrinha, P., Kullberg, J.C. (Eds.), Geologia de Portugal (Vol. I), Escolar Editora, Lisboa, 509-549.

Audren, C., Brun, J., Cobbold, P., Cogné, J., Iglésias, M., Jegouzo, P., Le Corre, C., Le Metour, J., Le Théoff, B. and Rabu, D. (1976). Données complémentaires sur la géometrie du plissement et sur les variations de forme et d'orientation de l'ellipsoide de d6formation dans l'arc hercynien ibero-armorican. Bol. Soc. Geol. Fr., 18, 757-762.

Bento dos Santos, T., Valverde Vaquero, P., Ribeiro, M. L., Solá, A. R., Clavijo, E. G., Díez Montes, A. Dias da Silva, I. (*in press*). The Farilhões Anatectic Complex (Berlengas Archipelago). In Quesada, C., Oliveira, J.T. (Eds.), The Geology of Iberia: a geodynamic approach. Springer (Berlin), Regional Geology Review series.

Boogard, M. (1983). Conodont faunas from Portugal and southwestern Spain. Part 7. A Frasnian conodont fauna near the Estação de Cabrela (Portugal). Scripta Geologica, 69, 1-17.

Chaminé, H. I., Leterrier, J., Fonseca, P. E., Ribeiro, A., Lemos de Sousa, M. J., (1998). Geocronologia U/Pb em zircoes e monazites de rochas ortoderivadas do sector Espinho–Albergaria--a-Velha (Zona de Ossa Morena, NW de Portugal). In: Azeredo, A. (Eds). Actas V Congresso Nacional de Geologia. Comun. Inst. Geol. Min., 84 (1), B115-B118

Dallmeyer, R.D., Quesada, C. (1992). Cadomian vs. Variscan evolution of the Ossa-Morena Zone (SW Iberia): field and 40Ar/39Ar mineral age constraints. Tectonophysics, 216, 339-364.

Dewey, J.F., Holdsworth, R.E., Strachan, R.A. (1998). Transpression and transtension zones. In: Holdsworth, R.E., Strachan, R.A., Dewey, J.F. (Eds.), Continental Transpression and Transtension Tectonics. Geological Society, London, Special Publication, 135, 1–14.

Dias, R., Ribeiro, A. (1993). Porto-Tomar shear zone, a major structure since the begining of the Variscan orogeny. Comun. Serv. Geol. Portugal, 79, 29–38.

Dias, R., Ribeiro, A. (1995). The Ibero-Armorican arc: a collisional effect against an irregular continent? Tectonophysics, 246 (1–3), 113–128.

Dias, R., Basile, C. (2013). Estrutura dos sectores externos da Zona Sul Portuguesa; implicações geodinâmicas. In: Dias, R., Araújo, A., Terrinha, P., Kullberg, J.C. (Eds.), Geologia de Portugal (vol. 1) Escolar Editora, 787–807.

Dias, R., Ribeiro, A., Coke, C., Pereira, E., Rodrigues, J., Castro, P., Moreira, N., Rebelo, J. (2013). Evolução estrutural dos sectores setentrionais do autóctone da Zona Centro-Ibérica. In: Dias, R., Araújo, A., Terrinha, P., Kullberg, J.C. (Eds.), Geologia de Portugal (vol. 1), Escolar Editora, 73–147.

Dias, R., Ribeiro, A., Coke, C., Moreira, N., Romão, J. (2014). Arco Ibero-Armoricano; indentação versus auto-subducção. Comunicações geológicas, 101 (Vol. Especial I), 261-264.

Dias, R., Ribeiro, A., Romão, J., Coke, C., Moreira, N. (2016). A review of the Arcuate Structures in the Iberian Variscides; Constraints and Genetic Models. In: J.B. Murphy, R.D. Nance and S.T. Johnston (eds.), Tectonic evolution of the Iberian margin of Gondwana and of correlative regions: A celebration of the career of Cecilio Quesada, Tectonophysics, 681C, 170-194. DOI: 10.1016/j.tecto.2016.04.011

Eguiluz, L., Gil Ibarguchi, J. I., Abalos B., Apraiz, A. (2000). Superposed Hercynian and Cadomian orogenic cycles in the Ossa-Morena Zone and related areas of the Iberian Massif. Geological Society of America Bulletin, 112(9), 1398-1413.

El Hassani, A., Benfrika, E.M. (1995). Biostratigraphy and correlations of the Devonian of the Moroccan Meseta: a synopsis. Bulletin de l'Institut Scientifique, 19, 29-44.

Expósito, I., Simancas, J. F., González Lodeiro, F., Azor, A., Martínez Poyatos D. J. (2002). Estructura de la mitad septentrional de la zona de Ossa-Morena: Deformación en el bloque inferior de un cabalgamiento cortical de evolución compleja. Rev. Soc. Geol. Esp. 15, 3–14.

Fernández, F. J.; Chaminé, H. I.; Fonseca, P. E.; Munhá, J. M.; Ribeiro, A.; Aller, J.; Fuertes-Fuentes, M., Borges, F. S. (2003). HT-fabrics in a garnet-bearing quartzite from Western Portugal: geodynamic implications for the Iberian Variscan Belt. Terra Nova, 15 (2), 96-103. DOI: 10.1046/j.1365-3121.2003.00472.x

Gourvennec, R., Plusquellec, Y., Pereira, Z., Piçarra, J.M, Le Menn, J., Oliveira, J.T., Romão, J., Robardet, M. (2008). A reassessment of the Lochkovian (Lower Devonian) benthic faunas and palynomorphs from the Dornes region (southern Central Iberian Zone, Portugal). Comunicações Geológicas, 95, 5-25.

Gourvennec, R., Piçarra, J.M, Plusquellec, Y., Pereira, Z., Oliveira, J.T., Robardet, M. (2010). Lower Devonian faunas and palynomorphs from the Dornes Syncline (Central Iberian Zone, Portugal): stratigraphical and

paleogeographical implications. Carnets de Géologie / Notebooks on Geology - Article 2010/09 (CG2010_A09).

Gutiérrez-Alonso, G., Murphy, B., Fernández-Suárez, J., Weil, A., Franco, M., Gonzalo, J. (2011). Lithospheric delamination in the core of Pangea: Sm–Nd insights from the Iberian mantle. Geology, 39(2), 155–158.

Henriques, S.B.A., Neiva, A.M.R., Ribeiro, M.L., Dunning, G.R., Tajčmanová, L. (2015). Evolution of a Neoproterozoic suture in the Iberian Massif, Central Portugal: New U-Pb ages of igneous and metamorphic events at the contact between the Ossa Morena Zone and Central Iberian Zone. Lithos, 220-233, 43-59.

Houicha, M., Aboussalam, Z.S., Rodríguez, S., Chopin, F., Jouhari, A., Schulmann, K., Ghienne, J-F., Becker, R.T. (2016). Discovery of Eifelian-Frasnian corals in metamorphic rocks from the Rehamna massif (Western Meseta, Moroccan Variscan belt): biostratigraphic and paleogeographic implications. Abstract book of Geological Days of Morocco, Rabat (Morroco).

Johnston, S., Weil, A., Gutiérrez-Alonso, G. (2013). Oroclines: thick and thin. Geol. Soc. Am. Bull., 125 (5–6), 643–663.

Linnemann, U., Pereira, M.F., Jeffries, T., Drost, K., Gerdes, A. (2008). Cadomian Orogeny and the opening of the Rheic Ocean: new insights in the diacrony of geotectonic processes constrained by LA–ICP–MS U–Pb zircon dating (Ossa-Morena and Saxo-Thuringian Zones, Iberian and Bohemian Massifs). Tectonophysics, 461, 21–43.

Lin, S., Jiang, D., Williams, P.F. (1998). Transpression (or transtension) zones of triclinic symmetry: natural example and theoretical modeling. In: Holdsworth, R.E., Strachan, R.A., Dewey, J.F. (Eds.), Continental Transpression and Transtension Tectonics. Geological Society, London, Special Publication, 135, 41–57.

Lotze, F. (1945). Zur Gliederung der Varisziden der Iberischen Meseta. Geotekt. Forsch, 6, 78–92.

Machado, G., Vavrdová, M., Fonseca, P.E., Chaminé, H., Rocha, F. (2008). Overview of the Stratigraphy and initial quantittive Biogeocgraphical results from the Devoniano f the Albergaria-a-Velha Unit (Ossa-Morena zone, W Portugal). Acta Musei Nationalis Pragae, 64(2-4), 109-113.

Machado, G., Hladil, J., Koptíková, L., Fonseca, P., Rocha, F. T., Galle, A. (2009). The Odivelas Limestone: Evidence for a Middle Devonian reef system in western Ossa-Morena Zone. Geologica Carpathica, 60 (2), 121-137.

Machado, G., Hladil, J., Slavík, L., Koptíková, L., Moreira, N., Fonseca, M., Fonseca, P. E. (2010). An Emsian-Eifelian Calciturbidite sequence and the possible correlatable pattern of the Basal Choteč event in Western Ossa-Morena Zone, Portugal (Odivelas Limestone). Geologica Belgica, 13 (4), 431-446.

Marques, F., Mateus, A., Tassinari, C. (2002). The Late-Variscan fault network in central-northern Portugal (NW Iberia): a re-evaluation. Tectonophysics, 359, 255-270. DOI:10.1016/S0040-1951(02)00514-0

Martínez Catalán, J. (2011). The Central Iberian arc: implications for the Iberian Massif. Geogaceta, 50 (1), 7–10.

Mateus, A., Mata, J., Tassinari, C., Rodrigues, P., Ribeiro, A., Romão, J., Moreira, N., (2015). Conciliating U-Pb SHRIMP Zircon Dating with Zircon Saturation and Ti-in-Zircon Thermometry in the Maiorga and Endreiros Granites (Ossa-Morena Zone, Portugal). X Congresso Ibérico de Geoquímica, Laboratório Nacional de Energia e Geologia, Lisboa, 38-41.

Montenegro de Andrade, M. (1977). O Anfibolito olivínico do Engenho Novo (Vila da Feira). Comunicações dos Serviços Geológicos de Portugal, 61, 43-61.

Moreira, N. (2012). Caracterização estrutural da zona de cisalhamento Tomar - Badajoz - Córdova no sector de Abrantes. MSc thesis (unpublished), University of Évora, Portugal, 225 p.

Moreira, N., Búrcio, M., Dias, R., Coke, C. (2010). Partição da deformação Varisca nos sectores de Peso da Régua e Vila Nova de Foz Côa (Autóctone da Zona Centro Ibérica). Comun. Geol. 97, 147–162.

Oliveira, J.T., Oliveira, V., Piçarra, J.M. (1991). Traços gerais da evolução tectono-estratigráfica da Zona de Ossa Morena, em Portugal: síntese crítica do estado actual dos conhecimentos. Comun. Serv. Geol. Port. 77, 3-26.

Paquette, J.L., Balé, P., Ballèvre, M., Georget, Y. (1987). Géochronologie et géochimie des éclogites du Léon: nouvelles contraintes sur l'évolution géodynamique du Nord-Ouest du Massif armoricain. Bulletin de Minéralogie, 110, 683-696.

Perdigão, J.C., Oliveira, J.T., Ribeiro, A. (1982). Notícia Explicativa da Folha 44-B (Barrancos) da Carta Geológica de Portugal à escala 1:50 000, Serviços Geológicos de Portugal, Lisboa.

Pereira, M.F. (1999). Caracterização da estructura dos domínios setentrionais d Zona de Ossa-Morena e seu limite com a Zona Centro-Ibérica, no Nordeste Alentejano. PhD Thesis (unpublished), University of Évora, Portugal, 115p.

Pereira, M.F., Silva, J.B., Chichorro, M., Ordóñez-Casado, B., Lee, J.K.W., Williams, I.S. (2012). Early Carboniferous wrenching, exhumation of high-grade metamorphic rocks and basin instability in SW Iberia: constraints derived from structural geology and U-Pb and ^{40}Ar-^{39}Ar geochronology. Tectonophysics, 558-559, 28-44.

Pereira, M.F., Silva, J.B., Drost, K., Chichorro, M., Apraiz, A. (2010). Relative timing of the transcurrent displacements in northern Gondwana: U-Pb laser ablation ICP-MS zircon and monazite geochronology of gneisses and sheared granites from the western Iberian Massif (Portugal). Gondwana Research, 17(2-3), 461-481. DOI: 10.1016/j.gr.2009.08.006

Pereira, Z., Matos, J., Fernandes, P., Oliveira, J. T. (2007). Devonian and Carboniferous palynostratigraphy of the South Portuguese Zone, Portugal – An overview. Comunicações Geológicas, 94, 53-79.

Pérez-Cáceres, I., Simancas, J.F., Martínez Poyatos, D., Azor, A., Lodeiro, F.G. (2016), Oblique collision and deformation partitioning in the SW Iberian Variscides. Solid Earth, 7, 857–872. DOI:10.5194/se-7-857-2016

Piçarra, J.M. (2000). Estudo estratigráfico do sector de Estremoz-Barrancos, Zona de Ossa Morena, Portugal. Vol. I - .Litoestratigrafia do intervalo Câmbrico médio?-Devónico inferior, Vol. II - Bioestratigrafia do intervalo Ordovícico-Devónico inferior. PhD Thesis (unpublished), Évora University, Portugal.

Piçarra, J.M., Sarmiento, G. (2006). Problemas de posicionamento estratigráfico dos Calcários Paleozóicos da Zona de Ossa Morena (Portugal). In: Abstract of the VII Congresso Nacional de Geologia, vol. II, 657-660.

Ribeiro, A. (1974). Contribution à l'étude tectonique de Trás-os-Montes Oriental. Mem. Serv. Geol. Portugal, 24, 168 p.

Ribeiro, A. (2002). Soft plate tectonics. Springer, Berlin.

Ribeiro, A., Antunes, M.T., Ferreira, M.P., Rocha, R.B., Soares, A.F., Zbyszewski, G., Moitinho de Almeida, F., Carvalho, D., Monteiro, J.H. (1979). Introduction à la Géologie Générale du Portugal. Serviços Geológicos de Portugal.

Ribeiro, A., Dias, R., Silva, J.B. (1995). Genesis of the Ibero-Armorican arc. Geodin. Acta, 8 (2), 173–184.

Ribeiro, A., Munhá, J., Dias, R., Mateus, A., Pereira, E., Ribeiro, L., Fonseca, P., Araújo, A., Oliveira, T., Romão, J., Chaminé, H., Coke, C., Pedro, J. (2007). Geodynamic evolution of SW Europe Variscides. Tectonics, 26, 1–24.

Ribeiro, A., Munhá, J., Mateus, A., Fonseca, P., Pereira, E., Noronha, F., Romão, J., Rodrigues, J.F., Castro, P., Meireles, C., Ferreira, N. (2009). Mechanics of thick-skinned Variscan overprinting of Cadomian basement (Iberian Variscides). Comptes Rendus Geoscience, 341(2-3), 127-139.

Ribeiro, A., Romão, J., Munhá, J., Rodrigues, J., Pereira, E., Mateus, A., Araújo, A. (2013). Relações tectonostratigráficas e fronteiras entre a Zona Centro-Ibérica e a Zona Ossa-Morena do Terreno Ibérico e do Terreno Finisterra. In: Dias, R., Araújo, A., Terrinha, P., Kullberg, J.C. (Eds.), Geologia de Portugal, vol. 1, Escolar Editora, 439-481.

Robardet, M., Gutiérrez-Marco, J.C. (2004). The Ordovician, Silurian and Devonian sedimentary rocks of the Ossa-Morena Zone (SW Iberian Peninsula, Spain). J Iber Geol, 30, 73-92.

Romão, J., Moreira, N., Dias, R., Pedro, J., Mateus, A., Ribeiro, A. (2014). Tectonoestratigrafia do Terreno Ibérico no sector Tomar-Sardoal-Ferreira do Zêzere e relações com o Terreno Finisterra. Comunicações Geológicas 101(I), 559-562.

Romão, J., Ribeiro, A., Munhá, J., Ribeiro, L. (2010). Basement nappes on the NE boundary the Ossa-Morena Zone (SW Iberian Variscides). European Geosciences Union, General Assembly, Vienna, Austria (Abstract).

Sanchez-Lorda, M.E., Sarrionandia, F., Ábalos, B., Carrracedo, M., Eguíluz, L., Gil Ibarguchi, J.I. (2014). Geochemistry and paleotectonic setting of Ediacaran metabasites from the Ossa-Morena Zone (SW Iberia). Int J Earth Sci (Geol Rundsch), 103, 1263–1286. DOI:10.1007/s00531-013-0937-x

Schemm-Gregory, M., Piçarra, J.M. (2013). Astraelenia Saomamedensis N. Sp. - a new gigantic Rhynchonellid species and its palaeobiogeographical implications for the Portalegre syncline (Central Portugal). Rivista Italiana di Paleontologia e Sratigrafia, 119(3), 247-256.

Scherer, E.E., Mezger, K., Münker, C. (2002). Lu-Hf ages of high pressure metamorphism in the Variscan fold belt of southern Germany. Goldschmidt Conference Abstract 2002. Geochimica et Cosmochimica Acta Suppl., 66, A677.

Shaw, J., Johnston, S., Gutierrez-Alonso, G., Weil, A. (2012). Oroclines of the Variscan orogen of Iberia: paleocurrent analysis and paleogeographic implications. Earth Planet. Sci. Lett., 329 (330), 60–70.

Simancas, J.F, Carbonell, R., González Lodeiro, F., Pérez Estaún, A., Juhlin, C., Ayarza, P., Azor, A., Martínez Poyatos, D., Almodóvar, G.R., Pascual, E., Sáez, R., Kashubin, A., Alonso, F., Álvarez Marrón, J., Bohoyo, F., Castillo, S., Donaire, T., Expósito, I., Flecha, I., Galadí, E., Galindo Zaldívar, J., González, F., González Cuadra, P., Macías, I., Martí, D., Martín, A., Martín Parra, L.M., Nieto, J. M., Palm, H., Ruano, P., Ruiz, M., Toscano, M. (2004). The seismic crustal structure of the Ossa Morena Zone and its geological interpretation. Journal of Iberian Geology, 30, 133-142.

ANEXO I

Dados de Geoquímica de Rocha Total utilizados no Capítulo II.2

TABLE I - Geochemical data from Abrantes (ActLabs - 4LITHORES (11+))

TABLE II - Geochemical data from Vila Boim (ActLabs - 4LITHORES (11+))

TABLE I - Geochemical data from Abrantes (ActLabs - 4LITHORES (11+))

				Abrantes Cemetery Pelites and Quartzwackes				*Abrantes Dam Amphibolites*		*Abrantes Castle Felsics*				*S. Miguel do Rio Torto Carbonates*				*Camelas Upper Detrital series*	
Classification according to Le Maitre et al. (1989)				Basalt dyke	Dacite	Dacite	Basalt	Basalt	Basalt	Rhyolite	Rhyolite	Rhyolite	Basalt	Basalt	Basalt	Basalt	Trachy-basalt	Basalt	Basalt
Analyte Symbol	Unit Symbol	Detection Limit	Analysis Method	GQAB 14	GQAB 16	GQAB 18	GQAB 20	GQAB 5A	GQAB 5B	GQAB 17	GQAB 26	GQAB 28	AB 41	AB 40	AB 48	AB 77-A	GQAB 19	AB 46	GQAB 25
SiO2	%	0,01	FUS-ICP	50,08	67,63	65,54	49,97	50,85	47,05	75,97	79,46	81,5	48,51	45,99	47,94	49,38	48,12	47,81	47,49
Al2O3	%	0,01	FUS-ICP	14,13	14,94	16,66	14,77	13,38	15,24	9,92	10,99	9,85	15,96	13,59	14,85	14,63	14,19	16,11	14,21
Fe2O3(T)	%	0,01	FUS-ICP	13,01	5,17	6,93	16,11	13,47	14,57	3,17	0,88	1,8	11,59	9,98	10,54	11,39	15,72	12,07	13,29
MnO	%	0,001	FUS-ICP	0,21	0,072	0,256	0,176	0,184	0,2	0,061	0,03	0,01	0,28	0,078	0,054	0,128	0,057	0,092	0,208
MgO	%	0,01	FUS-ICP	5,82	2,19	0,67	3,67	7,09	4,87	0,1	0,93	0,25	7,89	9,71	8,94	6,94	4,5	6,82	6,81
CaO	%	0,01	FUS-ICP	8,85	2,25	2,89	7,39	9,74	9,45	3,1	1,27	0,2	8,89	9,63	10,52	10,16	5,01	8,65	9,31
Na2O	%	0,01	FUS-ICP	3,29	4,1	4,84	2,46	2,67	3,46	3,34	5,65	2,31	2,16	2,37	2,83	3,02	3,69	4,3	2,97
K2O	%	0,01	FUS-ICP	0,76	2,28	0,71	0,3	0,25	0,41	2,17	0,07	3,21	1,12	0,9	0,45	0,5	3,05	0,24	0,54
TiO2	%	0,001	FUS-ICP	2,576	0,71	0,531	3,502	1,794	3,851	0,496	0,506	0,254	1,732	2,498	2,279	2,17	3,624	2,907	2,211
P2O5	%	0,01	FUS-ICP	0,25	0,19	0,15	0,85	0,15	0,65	0,09	0,15	0,08	0,18	0,28	0,25	0,23	0,54	0,4	0,25
LOI	%		FUS-ICP	1,22	1,05	0,43	0,56	0,96	0,64	0,75	0,66	1,13	2,01	5,31	1,72	1,95	1,45	1,36	1,36
Total	%	0,01	FUS-ICP	100,2	100,6	99,61	99,76	100,5	100,4	99,18	100,6	100,6	100,3	100,3	100,4	100,5	99,94	100,8	98,65
Sc	ppm	1	FUS-ICP	43	12	14	29	47	36	6	6	3	44	29	30	39	24	33	42
Be	ppm	1	FUS-ICP	1	3	7	3	< 1	2	< 1	1	1	2	2	1	1	2	2	1
V	ppm	5	FUS-ICP	368	77	12	229	397	334	54	38	30	277	249	233	288	326	325	334
Cr	ppm	20	FUS-MS	130	80	30	< 20	100	60	40	50	20	130	450	270	120	< 20	290	150
Co	ppm	1	FUS-MS	33	11	5	29	44	37	1	< 1	3	41	32	46	35	34	40	42
Ni	ppm	20	FUS-MS	40	30	< 20	< 20	60	60	< 20	< 20	< 20	70	150	130	50	< 20	70	70
Cu	ppm	10	FUS-MS	20	20	30	80	10	20	< 10	< 10	< 10	< 10	20	160	< 10	20	< 10	< 10
Zn	ppm	30	FUS-MS	60	40	< 30	70	80	80	< 30	< 30	< 30	40	130	80	90	80	50	70
Ga	ppm	1	FUS-MS	21	20	39	32	19	26	13	12	10	20	19	19	21	26	24	20
Ge	ppm	0,5	FUS-MS	2	1,6	2,3	2,1	2	1,8	1,7	1,2	1,4	1,9	1,9	1,5	1,6	2,1	1,6	1,6
As	ppm	5	FUS-MS	< 5	< 5	< 5	< 5	< 5	< 5	17	< 5	6	< 5	< 5	< 5	< 5	< 5	< 5	< 5
Rb	ppm	1	FUS-MS	23	106	16	4	3	4	51	< 1	81	38	18	4	9	272	2	15
Sr	ppm	2	FUS-ICP	249	155	309	184	240	405	65	142	139	207	1749	2764	835	384	698	282
Y	ppm	0,5	FUS-MS	53,2	20,9	86,1	51,3	44,5	63,5	31	19,7	17,6	30,8	17,3	16,8	31,9	38,3	24,8	37,8
Zr	ppm	1	FUS-ICP	183	210	1223	393	104	371	178	274	121	149	187	173	168	293	237	136
Nb	ppm	0,2	FUS-MS	6,8	11,3	75,1	46,4	1,6	25	7,9	8,9	4,2	4,2	20,8	16,6	6,6	37,2	22,2	4,3
Mo	ppm	2	FUS-MS	< 2	< 2	4	3	< 2	2	< 2	< 2	< 2	< 2	< 2	< 2	< 2	< 2	< 2	< 2
Ag	ppm	0,5	FUS-MS	< 0.5	< 0.5		< 0.5	< 0.5	0,6	< 0.5	< 0.5	< 0.5	< 0.5	< 0.5	< 0.5	< 0.5	< 0.5	< 0.5	< 0.5
In	ppm	0,1	FUS-MS	0,2	< 0.1	< 0.1	0,3	0,1	0,2	< 0.1	< 0.1	< 0.1	< 0.1	< 0.1	< 0.1	< 0.1	0,1	0,1	0,1
Sn	ppm	1	FUS-MS	2	2	< 1	11	2	3	2	2	1	3	2	2	2	20	2	1
Sb	ppm	0,2	FUS-MS	1	0,3	0,2	< 0.2	0,3	0,3	4,4	< 0.2	1	3,7	1,7	2,5	0,6	< 0.2	0,7	0,3
Cs	ppm	0,1	FUS-MS	1,4	6,7	0,3	< 0.1	0,2	0,1	0,7	< 0.1	1,9	0,7	2,4	0,4	0,7	60,3	0,3	0,4
Ba	ppm	3	FUS-ICP	440	533	220	84	46	75	405	40	1809	198	70	33	36	205	36	37
La	ppm	0,05	FUS-MS	13,8	27,3	75,8	44,1	3,33	25,5	22,9	21,1	18,1	7,06	16,8	12,9	10,3	33,3	20,7	7,44
Ce	ppm	0,05	FUS-MS	32,5	49,9	176	97,7	10,7	63,4	44,6	38,4	36,7	18,1	40,3	31,3	21,2	75,5	48,8	20,1
Pr	ppm	0,01	FUS-MS	4,95	6,66	19,9	12,1	1,95	8,78	5,65	4,98	4,62	2,66	5,22	4,12	3,6	9,5	5,98	3,08
Nd	ppm	0,05	FUS-MS	23,2	25	77,6	52	10,8	40,5	22,9	18,5	18	13	22,9	18,4	16,3	41	25,3	15,9
Sm	ppm	0,01	FUS-MS	7,01	5,05	17,3	11,9	4,27	10,6	5,57	3,65	3,88	3,59	5,09	4,38	4,64	10	5,97	4,5
Eu	ppm	0,005	FUS-MS	2,47	1,02	4,22	3,74	1,53	3,55	1,13	0,872	0,815	1,15	1,66	1,35	1,26	3,44	2,03	1,84
Gd	ppm	0,01	FUS-MS	8,67	4,01	15,4	11,3	5,84	11,7	5,3	3,26	3,3	4,79	4,5	4,15	5,47	10,3	5,68	6,18
Tb	ppm	0,01	FUS-MS	1,45	0,61	2,54	1,72	1,07	1,87	0,87	0,54	0,52	0,87	0,68	0,63	0,97	1,44	0,91	1,07
Dy	ppm	0,01	FUS-MS	9,52	3,69	15,9	9,97	7,49	11,6	5,33	3,45	3,25	5,72	3,8	3,59	6,23	8,25	5,27	6,57
Ho	ppm	0,01	FUS-MS	1,88	0,76	3,32	1,85	1,57	2,31	1,06	0,72	0,64	1,18	0,63	0,65	1,23	1,49	0,92	1,41
Er	ppm	0,01	FUS-MS	5,54	2,27	10,1	5,03	4,63	6,73	3,06	2,02	1,79	3,34	1,65	1,67	3,39	3,92	2,35	3,97
Tm	ppm	0,005	FUS-MS	0,785	0,363	1,5	0,683	0,683	0,916	0,458	0,288	0,255	0,504	0,219	0,214	0,494	0,518	0,322	0,554
Yb	ppm	0,01	FUS-MS	5,02	2,43	10,2	4,02	4,72	5,78	2,97	1,84	1,61	3,13	1,34	1,18	3,06	3,11	1,98	3,65
Lu	ppm	0,002	FUS-MS	0,75	0,389	1,64	0,653	0,742	0,915	0,417	0,274	0,272	0,463	0,185	0,159	0,441	0,462	0,272	0,572
Hf	ppm	0,1	FUS-MS	3,9	4,8	24,2	7,5	2,5	7,4	4,2	5,7	2,5	3,4	4,2	3,9	3,7	6,3	5,1	3
Ta	ppm	0,01	FUS-MS	0,52	0,95	5,28	2,96	0,11	1,68	0,82	0,94	0,46	0,25	1,45	1,2	0,37	2,56	1,75	0,32
W	ppm	0,5	FUS-MS	< 0.5	< 0.5	1	0,6	< 0.5	1,2	< 0.5	0,8	1,1	14,5	1,5	< 0.5	< 0.5	2,3	< 0.5	1,4
Tl	ppm	0,05	FUS-MS	0,12	0,46	< 0.05	0,06	< 0.05	< 0.05	0,15	< 0.05	0,25	< 0.05	< 0.05	< 0.05	< 0.05	1,82	< 0.05	< 0.05
Pb	ppm	5	FUS-MS	8	< 5	14	< 5	< 5	< 5	< 5	< 5	< 5	< 5	< 5	< 5	< 5	< 5	< 5	7
Bi	ppm	0,1	FUS-MS	0,2	0,1	< 0.1	0,2	< 0.1	< 0.1	< 0.1	< 0.1	< 0.1	0,1	< 0.1	< 0.1	< 0.1	1,1	< 0.1	< 0.1
Th	ppm	0,05	FUS-MS	1,69	10,6	11,3	3,83	0,13	2,09	8,59	12,3	5,28	0,16	1,32	1,02	0,24	2,85	1,67	0,57
U	ppm	0,01	FUS-MS	0,62	3,01	3,97	1,53	0,32	0,86	2,7	1,82	1,08	0,49	0,83	0,24	0,61	1,03	0,94	0,23

TABLE II - Geochemical data from Vila Boim (ActLabs - 4LITHORES (11+))

				Basal Cambrian Unit		*Elvas Carbonated Formation*				*Vila Boim Formation*
Classification according to Le Maitre et al. (1989)				Rhyolite	Rhyolite	Andesite	Tephrite-Basanite	Basalt	Basalt	Trachy-basalt
Analyte Symbol	Unit Symbol	Detection Limit	Analysis Method	VB 10	VB 11	VB 01	VB 05	VB 06	VB 07	VB 16
SiO2	%	0,01	FUS-ICP	76,71	74,29	52,18	39,74	46,92	42,65	44,62
Al2O3	%	0,01	FUS-ICP	13,22	14,19	15,33	13,02	15,3	13,44	13,79
Fe2O3(T)	%	0,01	FUS-ICP	0,7	0,76	6,16	10,89	12,51	14,01	13,39
MnO	%	0,001	FUS-ICP	0,008	0,005	0,028	0,136	0,147	0,105	0,256
MgO	%	0,01	FUS-ICP	0,05	0,67	4,62	4,06	6,48	4,49	4,93
CaO	%	0,01	FUS-ICP	0,36	0,59	6,53	11,92	10,97	7,59	6,7
Na2O	%	0,01	FUS-ICP	7,3	7,43	2,16	4,6	2,87	4,26	4,46
K2O	%	0,01	FUS-ICP	0,02	0,03	2,45	0,08	0,12	0,2	0,65
TiO2	%	0,001	FUS-ICP	0,663	0,448	0,579	3,838	2,197	4,135	2,773
P2O5	%	0,01	FUS-ICP	0,2	0,1	0,18	0,49	0,22	0,55	0,38
LOI	%		FUS-ICP	0,39	0,77	9,22	10,91	2,5	8,07	7,99
Total	%	0,01	FUS-ICP	99,63	99,3	99,44	99,68	100,2	99,49	99,94
Sc	ppm	1	FUS-ICP	3	4	18	30	42	33	38
Be	ppm	1	FUS-ICP	< 1	1	3	2	< 1	2	2
V	ppm	5	FUS-ICP	57	50	104	356	314	446	335
Cr	ppm	20	FUS-MS	70	50	220	70	110	60	90
Co	ppm	1	FUS-MS	1	5	12	42	36	45	48
Ni	ppm	20	FUS-MS	< 20	< 20	50	40	60	20	< 20
Cu	ppm	10	FUS-MS	< 10	20	< 10	50	30	< 10	< 10
Zn	ppm	30	FUS-MS	< 30	< 30	50	< 30	70	40	250
Ga	ppm	1	FUS-MS	16	13	19	20	22	23	23
Ge	ppm	0,5	FUS-MS	0,7	0,6	1,9	1,4	1,6	1,4	1,5
As	ppm	5	FUS-MS	< 5	< 5	< 5	< 5	< 5	< 5	< 5
Rb	ppm	1	FUS-MS	< 1	< 1	66	3	1	8	29
Sr	ppm	2	FUS-ICP	68	99	563	381	1547	347	335
Y	ppm	0,5	FUS-MS	26	9,2	18,7	44,8	34,7	64,4	46,8
Zr	ppm	1	FUS-ICP	622	195	198	273	160	323	298
Nb	ppm	0,2	FUS-MS	11,5	5,1	18	8,4	5,6	9,8	12,5
Mo	ppm	2	FUS-MS	< 2	< 2	< 2	< 2	< 2	< 2	< 2
Ag	ppm	0,5	FUS-MS	0,9	< 0.5	< 0.5	< 0.5	< 0.5	< 0.5	< 0.5
In	ppm	0,1	FUS-MS	< 0.1	< 0.1	< 0.1	0,1	0,1	0,1	0,1
Sn	ppm	1	FUS-MS	5	< 1	2	2	1	2	2
Sb	ppm	0,2	FUS-MS	0,8	0,3	1,4	0,9	1,3	2,1	1,8
Cs	ppm	0,1	FUS-MS	< 0.1	< 0.1	1,1	< 0.1	< 0.1	0,5	6,7
Ba	ppm	3	FUS-ICP	8	11	532	25	44	38	99
La	ppm	0,05	FUS-MS	6,99	15,9	34,6	17,8	9,13	25,5	16,8
Ce	ppm	0,05	FUS-MS	20,9	33,7	65,3	41,4	22,6	56,1	42,6
Pr	ppm	0,01	FUS-MS	3,13	3,73	7,24	5,64	3,43	7,69	5,7
Nd	ppm	0,05	FUS-MS	14,1	13,4	26,9	27,6	17,1	34,9	26
Sm	ppm	0,01	FUS-MS	3,28	2,36	5,65	7,51	4,98	10,1	6,84
Eu	ppm	0,005	FUS-MS	0,762	0,282	1,36	2,31	1,93	2,92	2,25
Gd	ppm	0,01	FUS-MS	3,76	2,03	5,11	8,94	6,18	11,1	8,1
Tb	ppm	0,01	FUS-MS	0,63	0,29	0,7	1,44	1	1,95	1,44
Dy	ppm	0,01	FUS-MS	3,93	1,59	3,78	8,66	6,32	12	9,1
Ho	ppm	0,01	FUS-MS	0,81	0,3	0,67	1,61	1,2	2,31	1,73
Er	ppm	0,01	FUS-MS	2,49	0,84	1,86	4,66	3,4	6,48	4,92
Tm	ppm	0,005	FUS-MS	0,378	0,123	0,277	0,698	0,494	0,973	0,716
Yb	ppm	0,01	FUS-MS	2,44	0,84	1,78	4,73	3,12	6,31	4,46
Lu	ppm	0,002	FUS-MS	0,332	0,123	0,257	0,695	0,451	0,923	0,624
Hf	ppm	0,1	FUS-MS	14,2	4,3	4,6	6,5	3,5	7,1	6,5
Ta	ppm	0,01	FUS-MS	1,2	0,42	1,32	0,57	0,33	0,68	0,87
W	ppm	0,5	FUS-MS	1,8	< 0.5	1,4	< 0.5	< 0.5	< 0.5	< 0.5
Tl	ppm	0,05	FUS-MS	< 0.05	< 0.05	< 0.05	< 0.05	< 0.05	< 0.05	< 0.05
Pb	ppm	5	FUS-MS	< 5	< 5	< 5	< 5	6	< 5	44
Bi	ppm	0,1	FUS-MS	< 0.1	< 0.1	< 0.1	< 0.1	< 0.1	< 0.1	< 0.1
Th	ppm	0,05	FUS-MS	20,4	6,22	9,97	1,08	0,23	1,26	1,78
U	ppm	0,01	FUS-MS	2,34	0,96	2,4	0,76	0,05	0,84	0,76

UNIVERSIDADE DE ÉVORA
INSTITUTO DE INVESTIGAÇÃO
E FORMAÇÃO AVANÇADA

Contactos:

Universidade de Évora

Instituto de Investigação e Formação Avançada - IIFA

Palácio do Vimioso | Largo Marquês de Marialva, Apart. 94

7002-554 Évora | Portugal

Tel: (+351) 266 706 581